Springer

Final Programme

Meet Europe

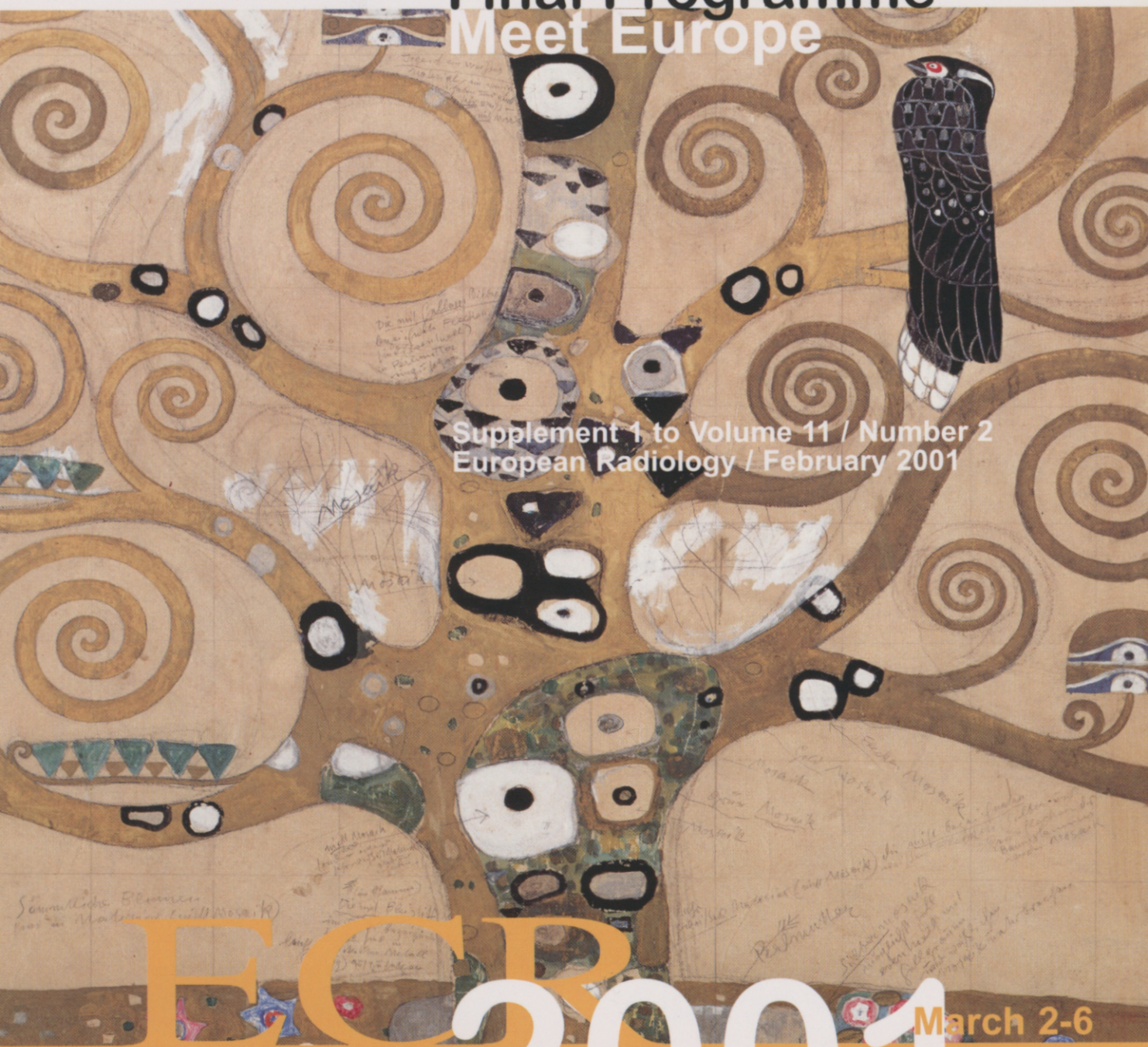

Supplement 1 to Volume 11 / Number 2
European Radiology / February 2001

ECR 2001

March 2-6

EUROPEAN CONGRESS OF RADIOLOGY

EUROPEAN RADIOLOGY ASSOCIATION & CONGRESS

Vienna
Austria

B

Scientific Sessions (SS)

Friday, March 2

	room A 2nd level	room B 2nd level	room C 2nd level	room E1 entr. level	room E2 entr. level	room F1 entr. level	room F2 entr. level	room G lower level	room H lower level	
08:30										08:30
09:00	**SA 1a**	**RC 110**	**CC 117**	**RC 101**	**SA 1b**	**RC 104**	**RC 111**	**RC 107**	**RC 109**	09:00
09:30										09:30
10:00										10:00
10:30	**CC 216**	**SS 210a** **Musculoskeletal** Shoulder imaging *(p. 105)*	**SS 201a** **Abdominal and Gastrointestinal** Pancreas: Malignant lesions *(p. 107)*	**SS 210b** **Musculoskeletal** New imaging devices *(p. 109)*	**SS 202** **Breast** Mammography and clinical breast imaging *(p. 111)*	**SS 204** **Chest** Thoracic neoplasm *(p. 113)*	**SS 211** **Neuro** Vascular - Interventional *(p. 115)*	**SS 201b** **Abdominal and Gastrointestinal** Colon and rectum (1) *(p. 117)*	**SS 209a** **Interventional Radiology** Aorto-iliac disease: Stents and stent grafts (1) *(p. 118)*	10:30
11:00										11:00
11:30										11:30
12:00										12:00
12:30	Opening Ceremony/ Inauguration Lecture & Honorary Member Awards									12:30
13:00										13:00
13:30										13:30
14:00	**CC 316**	**SS 310** **Musculoskeletal** Imaging of the knee-joint and cartilage *(p. 130)*	**SS 301a** **Abdominal and Gastrointestinal** Biliary tract *(p. 132)*	Schering Symposium	**SS 302** **Breast** Breast MRI *(p. 134)*	**SS 304** **Chest** Pulmonary and mediastinal blood vessels *(p. 136)*	**SS 311** **Neuro** Brain ageing/ Degenerative spectroscopy *(p. 138)*	**SS 301b** **Abdominal and Gastrointestinal** Colon and rectum (2) *(p. 140)*	**SS 309** **Interventional Radiology** Aorto-iliac disease: Stents and stent grafts (2) *(p. 142)*	14:00
14:30										14:30
15:00										15:00
15:30										15:30
16:00		**RC 410**	**CC 417**	**RC 401**	**RC 402**	**RC 404**	**RC 411**	**RC 407**	**RC 406**	16:00
16:30										16:30
17:00										17:00
17:30										17:30

	room I lower level	room K lower level	room L/M 1st level	room N/O 1st level	room P lower level	room X entr. level	room Y 1st level	room Z lower level	
08:30									08:30
09:00	**WS 118**	**RC 103**	**SS 106** **Contrast Media** New trends (1) *(p. 102)*	**RC 114**	**SS 115** **Vascular** Peripheral arteries (1) *(p. 103)*				09:00
09:30									09:30
10:00									10:00
10:30	**SS 201c** **Abdominal and Gastrointestinal** Abdominal imaging (1) *(p. 120)*	**SS 209b** **Interventional Radiology** MR-guided thermal tumor ablation *(p. 122)*	**SS 208** **Head and Neck** Neck lymph nodes/ Thyroid gland *(p. 124)*	**SS 203** **Cardiac** Coronary arteries: CT/MRI *(p. 126)*	**SS 215** **Vascular** Pulmonary arteries/ Miscellaneous *(p. 128)*				10:30
11:00									11:00
11:30									11:30
12:00									12:00
12:30									12:30
13:00									13:00
13:30									13:30
14:00	**SS 301c** **Abdominal and Gastrointestinal** Abdominal imaging (2) *(p. 144)*	**SS 306** **Contrast Media** New trends (2) *(p. 146)*	**SS 308** **Head and Neck** Head and neck cancer *(p. 148)*	**SS 307** **Genitourinary** Ureters *(p. 150)*	**SS 315** **Vascular** Ultrasound/ Vascular wall *(p. 152)*				14:00
14:30									14:30
15:00									15:00
15:30									15:30
16:00					**SS 415** **Vascular** Veins *(p. 153)*				16:00
16:30	**WS 418**	**RC 403**	**RC 408**	**RC 414**					16:30
17:00									17:00
17:30									17:30

08:30–10:00 **Room L/M**

Contrast Media

SS 106

New trends (1)

Chairpersons:
F. Caseiro-Alves (Coimbra/PT)
E. Fanucci (Rome/IT)

B-0001 08:30

Assessment of focal liver mass by biphasic contrast enhanced sonography

A.V. Zoubarev, I. Kalenova; *Moscow/RU*

Purpose: To study diagnostic possibilities of Biphasic Contrast Enhanced Sonography (BCES) in the diagnosis of liver tumors.
Methods and materials: Using BCES 30 pts with focal liver mass were examined on HDI-5000 (ATL-Philips) and Elegra (Siemens) in Harmonic Imaging with Contrast Enhancement. After i/v bolus injections of Levovist at the dosage of 300 mg/ml two phases of enhancement were evaluated: 1st – vascular and 2nd – parenchymal phases of enhancement. All pts were examined with low and high MI on Power Harmonics and Phase Inversion Harmonic. Examinations were videotaped and reviewed by 2 radiologists. Findings were confirmed by CT, MRT and surgical operation.
Results: 10 pts had metastasis, 11 hemangiomas, 4 FNH, 2 hepatoma, 1 cholangiocarcinoma, 2 nodular cirrhosis. BCES revealed differences in vascularity types and enhancement pattern in the two phases. BCES demonstrated similar contrast enhancement behavior to CT in all cases. Furthermore, BCES additionally defined small lesions.

B-0002 08:40

Molecular and physiological basis of blood pool contrast media

U. Speck, W. Ebert, H.-J. Weinmann; *Berlin/DE*

Purpose: Most contrast media (CM) are small molecules which leave the blood rapidly by diffusion through pores in the capillary endothelium into the interstitial space of tissues. Larger molecules may be advantageous in

- indicating differences in capillary permeability otherwise not detectable
- allowing for more intense contrast of blood vessels for a prolonged period of time
- diminishing the early offset of contrast between blood vessels and tissue by leakage
- decreasing the complexity of processes during first pass perfusion thus supporting perfusion quantification.

It should be clarified what may be expected from different classes of CM.
Methods and materials: The basic anatomy and physiology of vascular permeability is briefly reviewed. CM of different molecular size up to nanoparticles will be presented including problems in tolerance and excretion. Early biodistribution due to vascular permeability were measured in a way allowing a direct comparison of molecules of different size.
Results: All currently available CM disappear from the blood to a certain extent within the first few minutes. Blood levels drop to about 30 % of the dose in blood for small urographic molecules, ~50 % for albumin bound small molecules, 40 – 70 % for polymers of different size and slower for particles. Excretion becomes a problem if the size of molecules surpasses about 40 kD.
Conclusions: The use of large molecules delays extravasation but does not prevent it. Only particles seem to provide long lasting blood-pool effects.

B-0003 08:50

Prevention of generalized reactions to contrast media: A consensus report and guidelines

H.S. Thomsen[1], S.K. Morcos[2], J.A.W. Webb[3],
SUR Contrast Media Safety Committee[1]; [1]*Copenhagen/DK*, [2]*Sheffield/GB*, [3]*London/GB*

Purpose: Using consensus methodology, to document current practice for prevention of generalized reactions to contrast media (CM), to identify areas where there is disagreement or confusion and to draw up guidelines.
Materials and methods: A document with 165 questions was mailed to 202 members of the European Society of Urogenital Radiology (ESUR). The questions covered risk factors and prophylactic measures for generalized CM reactions
Results: 34 % responded. The majority indicated that a history of moderate and severe reaction(s) to CM and asthma are important risk factors and that patients with risk factors should receive non-ionic CM. In patients at high risk of reaction, if the examination is deemed absolutely necessary, a resuscitation team should be available at the time of the procedure. 91 % used corticosteroid prophylaxis given at least 11 hours before CM to patients at increased risk of reaction. The frequency of the dosage varied from one to three times. 55 % also use antihistamine H1. Prophylactic drugs are given to patients with a history of moderate or severe generalized reaction to CM. In patients with asthma, opinion is divided with only half of the responders giving prophylactic drugs. Aspirin, b-blockers, interleukin-2 and non-steroid anti-inflammatory drugs are not considered risk factors and therefore are not stopped before injection of CM.
Conclusion: The survey showed some variability in rating the risk factors for generalized CM reactions, and marked variability in the prophylactic measures used. There remain major areas of uncertainty. Some simple guidelines for prophylaxis of generalized CM reactions are proposed.

B-0004 09:00

Contrast media dose reduction in chest CT by means of multidetector helical CT

T. Doi, M. Kadota, Y. Yamashita, Y. Nakayama, J. Nishi, S. Tomiguchi,
M. Takahashi; *Kumamoto/JP*

Purpose: The purpose of this study was to assess whether diagnostic mediastinal and hilar vascular enhancement can be obtained with a low dosage of contrast material.
Materials and methods: Sixty patients who referred for chest CT examination with suspicion of either primary or metastatic lung tumor were included in these studies. All studies were performed by multidetector helical CT. They were randomly assigned to following five protocols (contrast medium concentration, dose, injection rate, injection duration): protocol 1: 300 mgI/ml, 100 ml, 2 ml/s, variable (standard dose); protocol 2: 300 mgI/ml, 1 ml/kg, 2 ml/s, variable; protocol 3: 300 mgI/ml, 1 ml/kg, variable, 30 s; protocol 4: 150 mgI/ml, 2 ml/kg, variable, 30 s; protocol 5: 150 mgI/ml, 2 ml/kg, 4 ml/s, variable In each protocol, regions of interest were measured: within pulmonary trunk, pulmonary artery and aorta. A composite profile of time versus CT value was generated in each group. Visual evaluation of major vessel was graded on five-point scale.
Results: The mean CT values and visual evaluation of protocols 2 and 3 were significantly lower than other protocols. Protocol 5 resulted in highest diagnostic capability, similar to protocol 1.
Conclusion: Iodine dose can be reduced without loss of diagnostic quality by means of multidetector helical CT. 150 mgI/ml with high injection rate resulted in highest diagnostic capability.

B-0005 09:10

Detection of renal artery stenosis by time-intensity analysis of renal enhancement curve at harmonic power Doppler imaging: Results of a pilot clinical study

R. Lencioni[1], S. Pinto[1], D. Cioni[1], F. Donati[1], L. Crocetti[1], D. Bokor[2], A. Salvetti[1],
C. Bartolozzi[1]; [1]*Pisa/IT*, [2]*Milan/IT*

Purpose: To investigate whether time-intensity analysis of renal enhancement curve at harmonic power Doppler imaging can predict the presence of significant (> 60 %) renal artery stenosis (RAS).
Materials and methods: Twenty patients with clinical suspicion of renovascular hypertension were enrolled in a pilot clinical study. The power Doppler examination was performed by injecting a 0.6 ml bolus of a microbubble contrast agent (BR1; Bracco, Milan, Italy) and by performing continous axial imaging of the kidney, in the harmonic mode, for 5 minutes. The renal enhancement curve showing the variation of the average pixel power inside the color box over time was automatically provided by a dedicated software implemented the US system (AU5; Esaote Biomedica, Genoa, Italy). Two curves were obtained for each kidney. Gold standard was provided by findings at digital subtraction angiography (n = 13) or breath-hold 3D contrast-enhanced magnetic resonance angiography (n = 7).
Results: Angiographic studies revealed renal artery occlusion in 2 kidneys, significant RAS in 13, nonsignificant RAS in 9, and normal arteries in 16. Analysis of time-intensity renal enhancement curves showed that the area under the curve and the maximum peak concentration were significantly greater ($p < 0.001$ and $p < 0.002$, respectively) in kidneys with significant RAS than in kidneys with nonsignificant RAS or normal arteries. No statistically significant differences were demonstrated by the analysis of variance (ANOVA test) between curves obtained in the same kidney.
Conclusion: Time-intensity analysis of renal enhancement curve at harmonic power Doppler imaging is a new promising method to detect significant RAS.

B-0006 09:20

Upper extremity venography using dota gadolinium as contrast agent

M. Tassart, O. Geoffroy, M. Bazot, A. Le Blanche, F. Boudghène, J. Rossert, J. Bigot; *Paris/FR*

Purpose: To evaluate the feasability and potential role of DOTA Gadolinium as contrast agent for phlebography of the upper extremity in patients with renal failure.

Materials and methods: Between April 1998 and March 2000, 60 consecutive patients with severe renal failure, not yet dialysed, were referred to our institution prior predialysis fistula placement. Digital subtraction venography (Multistar top Siemens), using 35 ml DOTA Gadolinium as contrast agent was performed with automatic injector. Images were rated by 2 experienced angiographers. Quality of the opacification (good, moderate but sufficient, or poor) was evaluated with a Kappa interobserver test.

Results: Vein's opacification was considered as good or sufficient in all cases on the fore arm and the arm. In 20 % of cases, insufficient opacification of vena Cava was efficiently completed by MRA. No interobserver discordance on superficial veins, no pain following injection or renal degradation were noted. In the first 40 cases, a good correlation with surgical findings and fistula's clinical development was demonstrated.

Conclusion: No contrast induced acute renal failure was noted with DOTA Gadolinium in this high risk population. Therefore DOTA Gadolinium venography is recommended in patients with severe renal failure not yet dialysed prior predialysis fistula placement.

B-0007 09:30

Quantitation of real time perfusion with the microbubble optison using power pulse inversion mode in renal transplants

C. Harvey[1], M. Lynch[1], M.J.K. Blomley[1], D.O. Cosgrove[1], A. Warrens[1], M. Averkiou[2]; *[1]London/GB, [2]Bothell/US*

Purpose: Power Pulse Inversion mode (PPI) is a novel mode which allows real time perfusion imaging with microbubbles. PPI is a low MI mode which allows a colorized image of the harmonic bubble signal to be displayed on a background tissue image. The aim of this study was to measure perfusion in renal transplants using this mode.

Methods: 15 patients were studied. Using a HDI 5000 and a P4-2 scanhead (ATL, USA) three 1 ml bolus injections of Optison (Mallinckrodt) were given followed by a saline flush while scanning in PPI. A manual flash contrast imaging sequence was employed using a high MI pulse to destroy the bubbles followed by imaging in PPI to capture the reperfusion phase. The sequence was repeated allowing the intensity to reach a steady state before another destructive pulse was administered. Using HDI Lab (ATL) regions of interest (ROIs) were drawn over the renal parenchyma and the intensity measured. A time intensity curve was plotted and a (1-exponential) fit applied. The curve plateau intensity; A (reflecting microvascular cross-sectional area) and B (reflecting the rate of rise of intensity; microbubble velocity) were derived. Renal blood flow (a measure of perfusion) was calculated from the product of A and B.

Results: Good correlations ($R > 0.7$) were obtained between A and B values in each patient.

Conclusions: Real time quantification of renal transplant blood flow can be derived using Power Pulse Inversion mode following an injection of microbubbles and may be of use in the assessment of renal dysfunction.

B-0008 09:40

Signal enhancement in the peripheral veins after intravenous application of Optison®

G.J. Schaffler, C. Kugler, G. Schreyer, G. Graber, M.M. Uggowitzer; *Graz/AT*

Purpose: Determination of the enhancement, duration and dynamics of Optison® effect in color Doppler sonographic studies of peripheral veins.

Material and methods: 24 healthy male volunters (mean age: 29, mean weight: 76 kg) underwent a prospective examination with color Doppler sonography (HDI 5000, ATL, Bothell, Washington, USA). All the volunteers were intravenously administered a bolus of 0.3 and 1.0 ml of a microspheres containing ultrasound contrast agent (Optison®). Measurements were always taken on the right femoral vein just underneath the inguinal ligament. Audiosignal enhancement was measured using audiointensiometric methods and correlated with a semiquantitatve classification of the color Doppler sonography.

Results: All the tests, showed a signal enhancement beginning after 25 to 30 seconds (mean time: 28 seconds) and a measurable audiosignal enhancement till the end of the examination. The maximum signal enhancement at a dose of 0.3 ml or 1.0 ml Optison® was on average 25.8 dB or 29 dB, respectively. All the examinations demonstrated a continous decrease in signal enhancement after reaching its maximum. The diagnostic window (< 7.5 ädB) for 0.3 ml and 1.0 ml Optison® was 9 and 18 minutes. The correlation between the quantitative audiointensitometric results and the semiquantitative classification of the color Doppler sonography revealed a clinically useable window of 6 and 13 minutes (0.3 ml versus 1.0 ml Optison®).

Conclusion: The intensity, duration and dynamics of the signal enhancement of Optison® was proven under clinical settings and the knowledge of these results may be helpful in the further planning of contrast enhanced ultrasound examinations.

B-0009 09:50

Unlicensed use of MR contrast agents: The medico-legal basis and issues

M.V. Knopp[1, 2], M. Lodemann[3], V. Runge[4]; *[1]Heidelberg/DE, [2]Bethesda, MD/US, [3]Radolfzell/DE, [4]Lexington, KY/US*

Purpose: The use of MRI contrast agents outside their labelled indications is routine. However, physicians feel frequently uneasey. It is the aim of this presentation to introduce the medical, judicial and billing relevant aspects in order to improve the knowledge on this topic.

Methods: Off-label refers to use of approved and marketed contrast agents outside of the labelled uses as printed on the package insert. Due to rapid advances in the field of MRI scientific evidence of new uses may substantial precede the labelling process.

Results: Use of approved and marketed MR-contrast agents outside of the labelled indications is possible, if the following requirements are satisfied: substantial scientific evidence reported in peer reviewed literature; the physician awareness of current literature on the indication; the manufacturer has not excluded the indication; there is a medical need for the indication; the patients informed consent has been obtained. The basis for off-label use is the physician's prerogative, which finds its roots in the "declaration of Helsinki". Off-label uses are allowed under special conditions, which do vary from country to country and might be even medical state of the art.

Conclusion: The necessity for off-label use will continue to increase for MR-contrast agents, as we are faced with the dilemma of rapid advances with new indications and the lengthy and quite costly regulatory process, which leads manufacturers to concentrate on essential, financially viable indications.

08:30–10:00 **Room P**

Vascular

SS 115

Peripheral arteries (1)

Chairpersons:
D. Fleischmann (Vienna/AT)
K. Schürmann (Aachen/DE)

B-0010 08:30

Contrast enhanced MR-angiography of lower extremities at 1.0 T

K.-P. Jungius[1], J. Hasselbach[2], J. Gaa[3], S. Freudenberg[3], R. Möckel[3]; *[1]Zürich/CH, [2]Berlin/DE, [3]Mannheim/DE*

Purpose: In a prospective study we evaluated contrast enhanced 3D MR-Angiography in floating table technique.

Methods: MRA has been performed in 63 patients suffering from arterial occlussive disease (AOD). All MRAs were performed at a Magnetom Harmony 1.0 T with the following parameters: TR 5.7 ms; TE 2.3 ms; AC 1; tMatrix size 192 × 512. After verifying circulation time (test bolus) Gd-DTPA (Magnevist) was applicated using an automatic injector (Spectris) in 0.2 mmol/kg body weight. Postprocessing was performed on a commercial available workstation. Images were evaluated by one radiologist and one vascular surgeon using a semiquantitative score system for 25 parts of the examed vascular structures. For stenosis evaluation source data have been available. In a second step MRAs were compared with corresponding DSAs.

Results: Depending on the coil technique (body or phased array) we found a adequate or good MRA quality in 82 – 100 % with respect to the iliacal, femoral and popliteal arteries, and in 75 – 76 % in the tibial and fibular arteries. With respect to stenosis grading in MRA we found overestimation in particular in high grade stenosis.

Conclusion: MRA seems suitable for screening patients with AOD and to plan further treatment (surgery; interventional) specially in the mainly interesting proximal arteries. Further development of MR equipment will lead to steady image quality in the shank arteries.

B-0011 08:40

Diagnosis of peripheral arterial occlusive disease by moving-bed magnetic resonance angiography on a 1.0 T system

C.M. Loewe, M. Grgurin, M. Cejna, M. Schoder, T. Rand, J. Sailer, J. Lammer, S.A. Thurnher; *Vienna/AT*

Purpose: To determine the efficacy of moving-bed contrast-enhanced Magnetic Resonance angiography (CE-MRA) on a 1.0 T magnet in the diagnosis of peripheral arterial occlusive disease (PAOD). The digital subtraction angiography DSA served as a standard of reference.

Materials and methods: 136 patients with known or suspected PAOD underwent CE-MRA and DSA within 14 days. MRA was performed before and after the administration of 40 ml contrast material on a 1.0 T unit. Every leg was divided into 14 vascular segments and scored in 4 categories of disease severity. A total of 2273 segments on 190 extremities were evaluated in comparison to the DSA.

Results: Out of the 136 patients, 2273 vessel segments were delineated by both techniques. All stenosis were delineated by MRA, and in 1962 (86 %) segments, there was full conformity in stenosis classification between the two methods. In 308 (13.6 %) segments, MRA overestimated a stenosis by one grade and in 21 by two classes.

Conclusion: Although the depiction of small vessel disease in the calf was sometimes hampered by venous overlay, correct diagnosis was possible in almost all patients. We conclude that moving-bed CE-MRA will play an important role in the diagnosis of PAOD in the next future.

B-0012 08:50

Moving-bed MR angiography on a 1.0 T system in the evaluation of peripheral bypass grafts

M. Grgurin, C.M. Loewe, T. Rand, M. Schoder, J. Lammer, S.A. Thurnher; *Vienna/AT*

Purpose: To assess the potential of moving-bed magnetic resonance angiography (MRA) on a 1.0 T system in the evaluation of peripheral bypass graft failure. Digital subtraction angiography (DSA) served as a standard of reference.

Materials and methods: 24 patients with previous peripheral vascular bypass graft surgery underwent DSA and contrast-enhanced MRA within two weeks. MRA was performed using a moving-bed imaging technique on a 1.0 T system. Every bypass graft was divided in three parts and every leg in fourteen vascular segments. Disease severity was scored in four categories. The MR angiographic findings were compared to those of the DSA. A total of 28 bypass grafts and 616 vessel segments on 39 extremities were classified.

Results: In 76 bypass segments the stenosis grading with both methods was corresponding, in 5 cases the stenosis was overestimated by MRA for one class. In 568 vascular segments there was conformity in graduation, but in 40 there was a difference of 1 grade and in 8 of 2 grades. 3 bypass segments could be not classified due to artefacts after surgery.

Conclusion: Moving-bed MRA on a 1.0 T system is feasible and a useful non-invasive tool in the detection of peripheral vascular bypass graft failure.

B-0013 08:55

Contrast-enhanced magnetic resonance angiography: When transfemoral subtraction angiography proves inadequate

E.M. Merkle, C. Wisianowski, J. Görich; *Ulm/DE*

Objective: Evaluation of contrast enhanced three-dimensional MRA as an alternative to a transbrachial approach for imaging of the femoro-iliac vessels in patients in whom transfemoral catheter subtraction angiography is inadequate.

Patients and methods: Nine patients underwent contrast enhanced three-dimensional MRA of the femoro-iliac vessels within 24 hours of an incomplete or inadequate attempt at transfemoral catheter angiography. Failure of transfemoral angiography was due to inability to create an adequate transfemoral access in 3 cases; in the remaining 6 patients, it was impossible to advance the catheter into the infrarenal abdominal aorta.

Results: Image quality of MRA was adequate in 8 of 9 cases to determine patients' subsequent management (no treatment, interventional, surgical). In one case, transbrachial catheter angiography was obtained as a supplemental examination in order to exclude a hemodynamically relevant stenosis of the infrarenal abdominal aorta, a finding at MRA which was later determined to be due to a susceptibility artifact caused by the presence of a surgically implanted metal clip. Patients' diagnoses included Leriche syndrome (n = 3), occlusion of the femoro-iliac vessels (n = 5) and an impassable anastomotic aneurysm in the iliac artery (n = 1).

Conclusion: Contrast enhanced three-dimensional MRA of the femoro-iliac vessels represents a diagnostic imaging method which is minimally invasive and generally free of complications. In most cases, findings obtained at MRA are adequate for determining patients' subsequent management in cases in which transfemoral catheter angiography is not feasible or incomplete. For this reason, three-dimensional MRA is preferable to transbrachial catheter angiography.

B-0014 09:05

Contrast enhanced peripheral MR angiography: Three step projection MR fluoro-angiography with operator controlled table movement

J. Bremerich, C.H. Buitrago-Tellez, M. Rausch, G.M. Bongartz; *Basle/CH*

Purpose/background: Contrast enhanced MR Angiography requires precise timing of contrast injection and data acquisition. The purpose of the current study is to assess a technique for peripheral 3 step MR Angiography which combines the following features: 1) Fluoroscopic Projection MR Angiography, and 2) operator controlled table movement.

Methods: Ten healthy volunteers and 3 patients with peripheral artery disease were studied in a 1.5 T Scanner (Siemens Symphony) with a standard body coil. During infusion of GdDOTA (0.2 mmol/kg; 2 ml/s) 2D Projection Angiograms were acquired at 3 steps (renal arteries to groin; thigh; lower limb). Imaging parameters of the turbo flash gradient echo sequence were: TR 5.3 ms; TE 2.0 ms; matrix 256 × 256; FOV 38 × 38 cm; acquisition time 1 s. Projection Angiograms were displayed immediately on the screen thus enabling real time visualisation of the contrast bolus and operator controlled table movement to the follwing step.

Results: Lower abdominal aorta, iliac, femoral and popliteal arteries were well visualized and occlusions depicted. Visualization of tibial and fibular arteries, however, was inconsistent.

Conclusion: Preliminary results of the 3 step Projection MR Fluoro-Angiography suggest feasibility of this technique. Direct visualization of the contrast bolus and operator controlled table movement may improve coincidence MR data acquisition when arterial enhancement is strongest, which helps to diminish venous overlay.

B-0015 09:15

Moving-table MRA of the peripheral run-off vessels: Comparison of a body coil and a dedicated phased-array coil system

A.M. Huber[1], B.J. Wintersperger[1], J. Scheidler[1], M. Schmidt[2], M. Requardt[2], T.K. Helmberger[1], A. Billing[1], M.F. Reiser[1]; [1]*Munich/DE*, [2]*Erlangen/DE*

Purpose: To compare the S/N ratio and diagnostic accuracy of moving table MRA in imaging the peripheral run-off vessels with a body-coil (BC) and a dedicated peripheral phased array-coil system (SC).

Methods and material: Fourty patients were examined with DSA and with moving table MRA at a 1.5 T MR system (Siemens Symphony). 20 patients were examined with a BC and 20 with a SC. The SC has 4 flexible wings and 8 coil elements. A care-bolus technique was used to determine the arrival of a 30 ml Gd-bolus. Unenhanced data sets were acquired at three stations and used as a mask, that was subtracted from the enhanced data sets.

Results: The S/N ratios were 56, 51 and 17 for the iliac, upper leg and lower leg arteries for the BC and 54, 74 and 64 for the SC, respectively. A high sensitivity and specificity in identifying stenosis (> 50 %) and occlusions were found for the iliac (100 % and 96 %) and upper leg arteries (100 % and 96 %) for the BC and for the SC (iliac arteries: 100 % and 96 %; upper leg arteries: 100 % and 98 %). However, a lower sensitivity and specificity was found in the lower leg with the BC (88 % and 85 %) compared to the SC (100 % and 97 %).

Conclusion: Moving table MRA has a high diagnostic accuracy. The dedicated peripheral coil system improves S/N ratio for the upper and lower leg and the diagnostic accuracy in the lower leg.

B-0016 09:25

Multislice spiral CT angiography vs. contrast enhanced MR angiography in the evaluation of patients with peripheral arterial disease

C. Catalano, A. Laghi, V. Panebianco, F. Pediconi, A. Napoli, F. Fraioli, R. Passariello; *Rome/IT*

Purpose: To compare multislice spiral CT Angiography (CTA) with contrast enhanced MR angiography (MRA) in the evaluation of patients with peripheral arterial disease.

Material and methods: 21 patients were examined with CTA and MRA. Four 2.5 mm thick slices per rotation were acquired with a volume extending from the aorta at the origin of the renal arteries to the the ankles after i.v. bolus administration of 140 ml of iodinated contrast agent, with a fixed delay of 25 seconds. Contrast enhanced MRA was performed using a 3D T1 weighted spoiled GRE se-

quence, with three different acquisition performed at the level of the abdominal aorta, thigh and knee-calf, each after i.v. injection of 20 ml of Gd-DTPA at 2 ml/s and with delay time obtained by means of a test bolus. In all cases DSA was also performed.
Results: Both modalities reached comparable values of overall sensitivity for lesion detection (CTA: 95 %; MRA: 93 %). Multislice CTA provided superior results in distal trifurcation vessels. CTA resulted superior in the assessment of the degree of stenosis, when axial images were also evaluated. Regarding the degree of stenosis both techniques were comparable, although CTA appeared superior in plaque morphology. In all severe stenosis at ce MRA the length of the stenosis appeared greater due to signal loss.
Conclusion: Multislice spiral CTA is a rapid technique for assessment of peripheral arterial disease, with a limited contrast agent dosage. MRA at the moment allows larger volumes to be studied, although examination time is still longer.

B-0017 09:35

CTA of the peripheral vascular tree using MDCT
A.M. Huber, B. von Rückmann, M. Matzko, R.D. Brüning, T.K. Helmberger, A. Billing, M.F. Reiser; *Munich/DE*

Purpose: The aim of this study was to visualize the arteries from the distal aorta to the ankle with contrast-enhanced MDCT angiography and to determine the accuracy in comparison to digital subtraction angiography.
Subjects and methods: Twenty-six patients with peripheral arterial occlusive disease underwent digital subtraction angiography and were examined at a MDCT (Siemens VZ) after intravenous contrast material application (300 mg/ml, 160 ml, flow rate 3.5 ml/s). We used a collimation of 4 × 2.5 mm, a pitch of 6, a slice thickness of 3 mm and an increment of 1.5 mm to cover a 110 – 130 cm FoV. The CTA angiographic results were compared with digital subtraction angiography by two blinded readers after reconstructrion of coronal MPRs. In addition, single slices were evaluated, when necessary.
Results: With digital subtraction angiography 77 hemodynamically significant stenoses and 35 occlusions were detected. For the assessment of stenoses in the pelvic region, the upper leg and the lower leg, a sensitivity of 97 %, 95 % and 88 % and a specificity of 96 %, 96 % and 87 % were found for CT angiography. For the assessment of occlusions a sensitivity of 100 %, 100 % and 97 % and a specificity of 100 %, 100 % and 95 % was found, respectively.
Conclusion: Contrast-enhanced MDCT angiography of the peripheral vascular tree proved to be reliable at identifiying arterial stenoses and occlusions.

B-0018 09:45

Postoperative evaluation of peripheral bypass grafts with multi-slice spiral CT
J.K. Willmann, J. Roos, P. Cassina, D. Weishaupt, B. Marincek, P.R. Hilfiker; *Zürich/CH*

Purpose: To assess the patency of peripheral bypass grafts with contrast-enhanced multi-slice spiral CT (MS-CT) in comparison with duplex sonography and angiography.
Materials and methods: MS-CT (collimation of 4 × 1 mm) was performed in a total of 20 patients with lower limb bypass grafts within the first week after surgery. Reconstruction was performed with 1.25 mm slice thickness, and 1 mm reconstruction increment. Image analysis was based on axial images and multiplanar reformations performed directly on a workstation. Two radiologists independently analyzed the results. The data were compared with the results from duplex sonography and angiography as gold standards in all patients.
Results: All parts of the bypass could be evaluated with MS-CT, including both, the proximal and distal anastomoses. There was a high correlation between the results of MS-CT and duplex sonography, as well as angiography. Anatomical localization of vessel pathologies was possible due to the overlap of soft tissue and bone structures. The high-resolution data sets allowed a multidimensional visualization of all parts of the bypass.
Conclusion: Contrast-enhanced MS-CT is a useful, non-invasive tool in the early postoperative evaluation of patients with peripheral bypass grafts.

B-0019 09:55

A novel vacuum device for extremity immobilization during digital subtraction angiography
R.J. Bale, M. Vogele, C. Lottersberger, A. Prassl, B. Czermak, P. Waldenberger, W. Jaschke; *Innsbruck/AT*

Purpose: To develop a non-invasive device for rigid immobilization during lower extremity angiography and to evaluate its feasibility and usefullness in a prospective study in 60 patients who underwent a digital subtraction angiography of the lower extremity. 60 patients were in the control group, which were not immobilized.
Methods and materials: The patented BodyFix immobilization device (Medical Intelligence, Schwabmünchen, Germany) consists of a vacuum pump connected to different types of cushions which are filled with tiny styrofoam balls and a plastic sheath that covers the body part to be immobilized. The patients extremity which needs to be immobilized is wrapped up with cushions, placed on the top of the therapy couch, and covered with the plastic sheath. When the vacuum pump is turned on, the air is evacuated. The cushion hardens and is sucked against the therapy couch resulting in immobilization of the patient's extremity.
Results: Immobilization with the novel device was well tolerated by all patients. The rigid immobilization resulted in a complete absence of motion artifacts in the majority of patients. Repeating of series could be avoided in all cases. In 10 out of the 60 patients in the control group series had to be repeated. A great increase in the quality of the images could be notified. Set-up of the device takes additional 1 – 2 minutes.
Conclusion: Vacuum immobilization allows for comfortable, effective extremity immobilization resulting in absence of motion artifacts. At our department the novel device has become an important tool in daily clinical routine.

10:30–12:00 **Room B**

Musculoskeletal

SS 210a

Shoulder imaging

Chairpersons:
R. Arkun (Izmir/TR)
H. Imhof (Vienna/AT)

B-0020 10:30

The painful shoulder: A new classification
R. Stramare, S. Puggina, L. Rubaltelli, F. Candiani, G. Feltrin; *Padova/IT*

Purpose: Painful shoulder syndrome is a common clinical finding. Recently ultrasonography has improved its accuracy in differentiating the causes of this syndrome. Shoulder ultrasound is an inexpensive, rapid, noninvasive method for evaluation of the integrity of the rotator cuff and to assess a medical or surgical treatment. On the other hand it is an operator-dependent technique and a long experience is needed. For this reason different shoulder pathologies were evaluated with ultrasound to suggest a simple and clear classification of rotator cuff tendons lesions.
Materials and methods: During a six years period about 1500 patients were evaluated with shoulder ultrasound. All the patients, moreover, were evaluated with X-ray examination and, in many cases, we had MR and surgical diagnostic verification. Rotator cuff tendons were studied with transverse, longitudinal and dynamical scannings. Only linear probes (10 – 13 MHz and 7.5 MHz – Esaote AU4 e General Electrics Logic 500) were utilized. Only experienced operators were included in the study. Supraspinatos, subscapularis and biceps tendons were evaluated.
Results: Common rotator cuff tendon lesions were: tendinosis, tendinitis, partial-thickness tear and full-thickness tear. Differential diagnosis was fundamental to suggest a correct therapy and follow up. Every lesions corresponded to a specific ultrasonographic pattern.
Conclusions: To easily compare shoulder examination of different operators and to correctly diagnose the different tendon lesions, we suggest a new classification of shoulder ultrasound findings.

B-0021 10:40

Normal anatomy and pathological conditions of the subscapularis muscle: US findings compared with surgery

T.V. Bartolotta[1], A. Iovane[1], M. Midiri[2], A. Carcione[1], R. Lagalla[1]; *[1]Palermo/IT, [2]Bari/IT*

Purpose: The aim of this work is to compare US results with those of surgery in the assessment of the subscapularis tendon.

Materials and methods: 1500 patients underwent US shoulder study (Esaote AU4 Idea and ATL Ultramark HDI 3000 – linear arrays 10 – 13 MHz transducers). Morphology, thickness and tendon echotexture were evaluated. US results of these patients were compared with those of surgery.

Results: US showed in 5 patients chronic degenerative tendon changes, in 4 patients focal tears, in 2 patients complete tendon tear, in 1 patient a bulky hematoma with coexhisting thickening and subtotal tear of the tendon. US findings were confirmerd at surgery in 10/12 patients. In the patient with hematoma the diagnosis was confirmed, but the subscapularis tendon was undamaged. Moreover, in 1 out of the 5 patients with US diagnosis of chronic degenerative tendon changes, a small focal tear of the tendon was found at surgery.

Conclusion: US is able to demonstrate early changes of the subscapularis tendon and nearby structures. Awareness of pitfalls might decrease the use of second level modalities such as CT arthrography and MRI, which on the other hand allow a better definition and assessment of the extent of the injury.

B-0022 10:50

Shoulder ultrasound: A reproducibility study

J.H. Miller jr., A. Richardson, F. Winter, S. Taylor, J. Rankine, W. Gibbon, P.J. O'Connor; *Leeds/GB*

Purpose: A prospective assessment of reproducibility and inter-observer agreement in the ultrasonic evaluation of the rotator cuff.

Materials and methods: Three musculoskeletal radiologists performed shoulder ultrasound on twenty-four consecutive patients. All scans were performed at the same visit with the findings recorded by independent observers. There were differing levels of radiologist experience (operator A had practiced musculoskeletal ultrasound for six months and operators B and C for six years). Normal or abnormal values were assigned to each diagnostic criterion (full thickness rotator cuff tear, tendon calcification, tendinosis of supraspinatus, subacromial fluid, subacromial synovial/bursal thickening, dynamic signs of impingement and long head of biceps tendon abnormality). Analysis was performed using Cohen's Kappa test.

Results: There was good agreement (Kappa > 0.6, $p < 0.01$) between the experienced operators for full thickness rotator cuff tear, tendon calcification, dynamic signs of impingement and long head of biceps tendon abnormality. There was no significant agreement for the less experienced sonologist in several categories including, most importantly, full thickness rotator cuff tears.

Conclusion: Ultrasound of the rotator cuff in experienced hands is a reproducible diagnostic test. There is poor agreement when there is a disparity between the experience levels of the operator. This suggests close attention should be paid to practical training and the definition of abnormality when examining the rotator cuff.

B-0023 11:00

SonoCT real time compound imaging in the evaluation of the supraspinatus tendon in subacromial impingement: Correlation with surgery

A. De Candia, S. Doratiotto, E. Segatto, E. Paschina, G. Giglio, M. Bazzocchi; *Udine/IT*

Purpose: To determine the value of SonoCT Real-Time compound imaging in the evaluation of supraspinatus tendon in subacromial impingement.

Methods and materials: Preoperative sonography was performed the day before surgery in 42 patients with clinical indication to acromion-plastica. The sonograms were obtained in static and dynamic examination using a commercially avaliable 5 – 12 MHz high frequency linear array transducer with compound elaboration of multiple frames from different viewing angles (ATL). The supraspinatus morfology was classified in absence of tears, partial thickness tears or full-thickness tears. In absence of tears the supraspinatus tendinopathy was classified in four classes in according with Neer stages. Sonographic findings were correlated with surgical inspection.

Results: Sonography demonstred 19 (95 %) of 20 full thickness tears, only one false negative in obese patient, and 4 (67 %) of 6 partial thickness. Sonography correctly showed 16 (100 %) of 16 rotator cuff absence of tears; in this patients sonographic patterns of tendinopathy were: homegeneously echogenic fibrillar pattern with thickened sub acromial-deltoid bursa (SADB) (19 %), diffusely hypoecoic and thickened tendon with normal SADB (12.5 %), diffusely hypoecoic and thickened tendon with thickened SADB (37.5 %), diffusely hypoecoic and narrowed tendon (31 %).

Conclusion: SonoCT Real-Time compound imaging provides outstanding definition of supraspinatus tendon patterns and improve accuracy of sonography (specifity of 100 %) for diagnosis of rotator cuff abnormalities in subacromial impingement.

B-0024 11:10

Normal arthro-MRI finding of the rotator interval of the shoulder

C. Faletti, G. Giudice, G. Regis, T. Robba; *Turin/IT*

Purpose: The rotator cuff interval is the space located between the superior edge of the subscapolaris tendon and the anterior edge of the supraspinatus tendon. This area is often involved in the pathology of the shoulder and its imaging is very complex.

Materials and methods: 6 patients, underwent MRI because of shoulder diseases different from rotator cuff interval alterations. We performed MRI examination after intra-articular injection of diluted paramagnetic contrast agent (arthroMRI). We made T1w and GE T2w axial and oblique sagittal sequences; the oblique sagittal plain was orientated along the long head of biceps tendon. Finally we correlated MRI results to arthroscopic findings about rotator cuff tendon.

Results: MRI and arthroscopic findings were strictly correlated. The arthroMRI proved to be very useful to show the edge of the structures of rotator interval and these structures. The oblique sagittal plane is the most specific in the study of the coraco-acromial ligament and the intra-articular portion of the biceps tendon; the axial plane is very useful to identify the superior gleno-humeral ligament and the insertion of the supraspinatus and subscapularis tendons.

Conclusions: ArthroMRI of the shoulder proved to be very useful in the axamination od rotator interval, with a strict correlation between MRI and arthroscopic findings.

B-0025 11:20

Supraspinatus tendon tears in asymptomatic patients without a history of trauma

N. Schibany, H. Zehetgruber, C. Wurnig, S. Trattnig, H. Imhof, A. Ba-Ssalamah, M.J. Breitenseher; *Vienna/AT*

Purpose: To investigate isolated rotator cuff tears in asymptomatic patients.

Methods and materials: 214 orthopedic inpatients (23 – 81 years, 109 males, 105 females) presenting with other complaints, but no symptoms and no history of trauma of the shoulder-joints, were prospectively examined with ultrasound (US) of the rotator cuff. The site of the tear and the number of tendons involved were assessed by US. In those patients where US showed a rotator cuff pathology, spring balance measurements in shoulder flexion with stretched ellbow according to Constant-score and magnetic resonance imaging (MRI) of the affected shoulder were obtained. MRI was performed at 1.0 T using a surface-coil. Paracoronal T2 TSE and T1 SE, paracoronal T2 TSE with SPIR and parasagittal T2 TSE sequences were obtained. We assessed size, site and specific tendons involved.

Results: US showed an isolated rupture of the supraspinatus tendon in 12 (58 – 79 years old, 8 males, 4 females) of 214 patients (5.6 %). In all 12 patients spring balance measurements revealed no significant loss of power in the affected shoulder. In 10 patients a MRI examination of the shoulder was obtained, 2 patients refused the MRI investigation. In correlation with US, MRI showed a partial rupture of the supraspinatus tendon in 1 patient and a complete rupture of the supraspinatus tendon in 9 patients, no other tendons were affected.

Conclusion: Supraspinatus tendon tears may occur also in asymptomatic patients with no history of trauma and are not associated with significant loss of power in the affected shoulder according to Constant-score. Nevertheless the typical US- and MRI-features are present.

B-0026 11:30

Dynamic MRI of the shoulder in patients with rotator cuff tears

W. Kenn, F. Gohlke, D. Boehm, D. Hahn; *Würzburg/DE*

Purpose: To evaluate pathological glenohumeral translation in patients with tears of the rotator cuff

Method/materials: Seventeen patients and 10 asypmtomatic volunteers underwent dynamic MR examination. 4 patients were suffering from incomplete tears, 6 patients had a tear of 1 tendon, 5 patients presented with a tear of 2 tendons (subscapularis and supraspinatus or supraspinatus and infraspinatus muscle tendon) and 2 patients did have a tear of more than 2 tendons. Axial and cranial glenohumeral translation were measured in 0° – 45° – 90° abduction with and without force (20 N) with a snapshot 2D Flash sequence (TR 37 ms TE 17 ms Siemens MR Open).

Results: For normal volunteers and patients suffering from incomplete or complete rotator cuff tear with involvement of 1 tendon there was no significant change of position of humeral head in respect to center of glenoid in rest and during abduction with and without force. For patients with a tear of 2 or more tendons there was a 3 mm average displacement of humeral head compared to the volunteer group at rest position, with a 1.5 mm increase during abduction
Conclusions: Our results demonstrated that exclusively rotator cuff tears involving 2 or more tendons lead to humeral displacement.

B-0027 11:40

Acquired instability of overstressed shoulder (AIOS): Arthro-MR evaluation vs. arthroscopy

F. Iannessi[1], C. Faletti[2], A. Castagna[3], A. Barile[1], V. Calvisi[1], C. Masciocchi[1]; *[1]L'Aquila/IT, [2]Turin/IT, [3]Milan/IT*

Purpose: To assess the diagnostic value of Arthro-MRI in the evaluation of acquired instability of overstressed shoulder (AIOS) respect to arthroscopy.
Methods and materials: We examined 23 patients, clinically suspected for non-traumatic shoulder instability. 18/23 patients performed sports activity. All patients underwent conventional plain film, standard MRI and Arthro-MRI. We employed SE T1w and FSE T2w sequence on standard MRI and SE T1w and fat-sat SE T1w after the intra-articular injection of 10 – 15 ml of contrast medium obtained from the diluition of 0.6 ml of Gd-DTPA in 250 ml of saline. Arthroscopy was considered as gold standard in all cases.
Results: Standard MRI showed 9 cases of supraspinatus tendon degeneration and 12 cases of flat-shaped glena (2/12 with paralabral cysts). Arthro-MRI evidenced 18 cases of antero-inferior capsular enlargement with also 7 supraspinatus tendinosis, 2 supraspinatus partial tear, 2 paralabral cysts and 6 capsular enlargement extended to the superior portion (rotator interval). In 1 of the 5 cases without capsular enlargement a Bouford complex was found. Arthroscopy confirmed arthro-MRI findings in all cases.
Conclusion: On the basis of our experience we postulated Arthro-MRI to be a worthy diagnostic mean in the evaluation of the acquired instability of overstressed shoulder.

B-0028 11:50

Low-field MR arthrography of the shoulder: Results of a prospective arthroscopically controlled study

K.-F. Kreitner, R. Loew, P. Kalden, M. Runkel, J. Zoellner, M. Thelen; *Mainz/DE*

Purpose: To define the diagnostic accuracy of an open low-field MR unit (Magnetom Open®, Siemens) for labral and rotator cuff pathologies of the shoulder.
Methods and materials: The MRIs of 82 patients were prospectively evaluated by two independent readers blinded to patients' data, clinical history and surgical results. The study protocol included a T1-weighted SE- and a STIR-sequence in the oblique coronal plane, and two T2*-weighted FI-2D-sequences in the oblique sagittal and axial planes. MRI was performed immediately after arthrography of the shoulder using a 2 mmolar solution of Gd-DTPA as contrast agent.
Results: Sensitivity and specificity for complete tears of the rotator cuff were 100 % each for both readers. For labral pathologies, both readers reached a sensitivity of 100 % and a specificity of 93 %, resepctively. Kappa values for interobserver agreement ranged between 1 (complete tears of the rotator cuff) and 0.63 (tendinitis of the supraspinatus tendon).
Conclusion: Using a time consuming examination protocol, low-field MR arthrography of the shoulder enables sufficient evaluation of the glenboid labrum and the rotator cuff. Thus, it can be recommended for routine clinical use.

10:30–12:00 **Room C**

Abdominal and Gastrointestinal

SS 201a

Pancreas: Malignant lesions

Chairpersons:
S.Z. Leszczynski (Warsaw/PL)
G. Mostbeck (Vienna/AT)

B-0029 10:30

Accuracy of MR tomography - MRCP in the diagnosis of pancreatic tumors

K. Liberopoulos, H. Margaris, E. Vardaki, Z. Nikolakopoulou, C. Manika, G. Papastratis, C. Samara, K. Stringaris; *Athens/GR*

Purpose: To evaluate the accuracy of magnetic resonance in detection and estimation of pancreatic tumors.
Method and material: 18 patients who were surgically treated for pancreatic or endopancreatic bile duct tumors, underwent preoperatively MR tomography and MRCP. MRI included the following sequences: T2-weighted TSE fat suppressed and T1-weighted TFE pre and post i.v. contrast material administration. Coronal 2D TSE raw data were transferred to a workstation and MRCP images were reconstructed. MRI and MRCP findings were compared to the macroscopic appearance of the histologic specimen and to the pathologic diagnosis.
Results: When MRI and histological results were compared we found that MRI had successfully detected a tumor in 16 of 18 patients and estimated the tumor size. There was a false positive answer in 1/18 patient who suffered from pancreatitis. There was an overestimation of the tumor's size in 1/18 patient who suffered from pancreatic tumor and concomitant pancreatitis.
Conclusion: According to our results MRI is a method of high accuracy in the detection and delineation of pancreatic tumor. This is extremely useful in the preoperative planning, especially in tumors with a very small size (less than 2.5 cm).

B-0030 10:40

Single-phase vs. dual-phase helical-CT in patients with suspected pancreatic cancer

M. Imbriaco, L. Camera, G. Selva, M. Romano, P. Mainenti, L. Pace, M. Salvatore; *Naples/IT*

Purpose: To compare single-phase (SP) vs dual-phase (DP) helical-CT in the detection and assessment of resectability of patients with suspicion of pancreatic carcinoma (PC).
Methods and material: 58 patients (30 F, 28 M; aged 62 ± 12 a) with a suspicious pancreatic mass underwent contrast-enhanced helical CT (5 mm collimation, 3 mm reconstruction intervals). Unenhanced scans were followed by either (Group A, n = 29) two separate set of scans performed at 20 – 25 and 60 – 80 s after the i.v. injection of contrast material (150 ml; 4 ml/s) or (Group B, n = 29) a single scan performed in a caudo-cranial fashion with a scan delay of 50 s from the uncinate process through the diaphragm. Images were blindly and independently analyzed by two readers who were asked to evaluate tumor detection and resectability using a three-point confidence scale.
Results: Histopatholgy showed 24 chronic pancreatitis and 34 PC. Of these, 27 were found to be unresectable at surgery. For both readers, SP protocol showed a comparable diagnostic accuracy to that of DP technique for assessment of tumor detection (86 % vs 90 %, p = n.s.). Assessment of resectability was impaired by the low number of resectable tumors (7). A high reproducibility was observed for SP helical-CT with an overall score agreement between the two readers of 83 % (k = 0.65).
Conclusion: SP and DP are equally effective in the diagnosis of PC. Due to the lower radiation burden and to the lower cost, SP helical-CT might be considered the protocol of choice when evaluating patients with suspicion of PC.

B-0031 10:50

Preoperative staging of ductal adenocarcinoma of the pancreas: The contribution of spiral CT

G.M. Carbognin[1], R. Graziani[1], C. Biasiutti[1], E. Bicego[2], F. Franzoso[1], C. Procacci[1]; *[1]Verona/IT, [2]Vicenza/IT*

Purpose: To assess the contribution of spiral CT in the preoperative staging of ductal adenocarcinoma of the pancreas.

Materials and method: The spiral CT examinations of 100 patients affected with pathologically proven ductal adenocarcinomas were reviewed. 37/100 patients did not undergo surgery, since unresectability was demonstrated. The remaining 63/100 patients underwent intervention: in 19/63 patients the tumor was resectable; in 44/63 patients was not. Initially, the assessment of resectability expressed on the basis of the spiral CT findings was considered. Subsequently, all the spiral CT examinations were retrospectively reviewed by two radiologist, aware of the final diagnosis. Discordant cases were solved by consensus.
Results: Among the surgically-verified cases (63 observations: 19 resectable and 44 unresectable), the prospective diagnosis of unresectability was correct in 30/44. In 14/44 cases a false negative assessment of resectability was made (missed recognition of local infiltration, peritoneal carcinomatosis, hepatic metastases, and vascular invasion). Among the 19/63 resected cases, CT correctly assessed resectability in 18/19 patients, while in 1/19 did not. During the retrospective evaluation, a correct assessment of unresectability was made in 37/44 cases, while in 7/44 cases an underestimation was made (missed recognition of hepatic metastases, local infiltration, vascular invasion). Among the 19/63 resected cases, CT made the correct diagnosis in 16/19 cases. It overestimated the diagnosis in 3/19 cases.
Conclusions: The careful demonstration and evaluation of the many signs of unresectability of pancreatic ductal adenocarcinoma reported in literature yield a better sensitivity in the diagnosis, associated with inevitable reduction of the specificity.

B-0032 11:00

Multidetector spiral CT in local staging of pancreatic carcinoma

A. Laghi, C. Catalano, V. Panebianco, I. Baeli, R. Iannaccone, R. Ferrari, R. Passariello; *Rome/IT*

Purpose: To evaluate the diagnostic accuracy of multidetector spiral CT in local staging of pancreatic carcinoma.
Materials and methods: Fifteen patients referred for suspected pancreatic carcinoma underwent multidetector spiral CT imaging using Somatom Plus 4 Volume Zoom (Siemens, G). Before imaging study water was administered in order to fill the duodenum. After non-enhanced CT scanning, cephalocaudad contrast-enhanced study (180 ml of 300 mgI/ml contrast medium; flow rate 3.0 ml/s) was begun during arterial (30 s delay) and portal venous (70 s delay) phase using 1.0 mm collimation, 500 ms rotation time, 1.25 mm reconstruction index. Images were evaluated by two observers in terms of lesion identification and conspicuity, infiltration of peri-pancreatic fat and vascular invasion of the coeliac trunk, SMA and SMV. Imaging findings were compared with surgical specimens in the resected tumors and with imaging follow-up in the remaining cases.
Results: Pancreatic carcinomas were identified in 12 of the 15 referred patients. In three cases no abnormalities were detected. Tumors were located in the head in 8 cases, in the isthmus in one case and in the tail in 3 cases. Peri-pancreatic spread was observed in 8 cases as thickening of peripancreatic fat tissue. Volume-rendered reconstructions on multiple planes correctly detected vascular encasement of the coeliac axis and the SMA in three cases, infiltration of the SMV in one case and encasement of the portal trunk in one case.
Conclusion: High resolution multidetector spiral CT images with multiplanar reconstructions are accurate in local staging of pancreatic carcinoma.

B-0033 11:10

Staging of pancreatic carcinoma: Comparison of three-phase spiral CT and MRI

B.J. Op de Beeck, B. Deboeck, K. Vanderdood, R. Luypaert, F. De Ridder, M. Osteaux; *Brussels/BE*

Purpose: To determine the accuracy of three-phasic spiral CT and MRI in preoperative staging of pancreatic carcinoma.
Materials and methods: 32 patients underwent spiral CT and MRI. 150 ml of iodinated contrast material was injected at 2 cc/s IV by an automated injector and a triphasic study was performed. MR technique consisted of MRCP and T2-weighted HASTE and T1-weighted SGE sequences in phase and with fat suppression and dynamic gadolinium enhanced evaluation. Tumor detection, peripancreatic invasion, vascular encasement and obliteration, adenopathies, liver metastases and general resectability were evaluated. 20 patients underwent surgery, 12 patients biopsy.
Results: The result for tumor detectability was 84.4 % for CT and 93.7 % for MRI with false positive and false negative values of respectively 6.2 % and 12.5 % for CT and 3.1 % and 3.1 % for MRI. Mean diameter of the tumor was 28.3 mm. Adenopathies of > 9 mm were seen in 50 % of the cases on CT and 43.7 % on MRI. Vascular encasement and obliteration was noticed on CT in respectively 12.5 % and 37.5 % and on MRI in 15.6 % and 37.5 %. Liver metastases were detected on CT in 21.9 % of the patients and in 25 % on MR. CT was false positive in 3.1 % and false negative in 6.2 %, MRI respectively 0 % and 3.1 %. For overall evaluation, MRI was preferred over CT in 57.9 %, equal in 21.0 % and inferior over CT in 21.0 %.
Conclusions: MRI with dynamic gadolinium enhanced imaging is superior to three-phasic spiral CT for detection and staging of pancreatic carcinoma.

B-0034 11:20

Role of spiral computed tomography (CT) and color Doppler ultrasonography (CDU) in pancreatic cancer

L. Calculli, M. Caputo, R. Casadei, F. Minni, M. Molinari, M. la Donna, D. Marrano, G. Gavelli; *Bologna/IT*

Purpose: Resection of pancreatic cancer is possible only at an early stage, when the tumor is localized to the pancreas without liver or peritoneal metastases or local extension to the portal-mesenteric trunk (PMT). Aim of this study was to evaluate the diagnostic accuracy of spiral CT and CDU in the detection of PMT involvement.
Materials and methods: 27 patients with pancreatic cancer were studied. Five vascular involvement grades were distinguished: Grade 0, no vascular involvement, normal flow; grade 1, loss of fat plane, normal flow; grade 2, slight irregularity of one side of the vessel, turbulent flow; grade 3, concentric infiltration, turbulent flow; grade 4, occluded vessel, no signal or reduced velocity flow and turbulent residual flow. During surgery, US was performed to confirm the preoperative results.
Results: Spiral CT showed 1 false negative and 3 false positives with high sensitivity (94.1 %); specificity was lower (70 %). Overall accuracy was 85.2 %, the positive predictive value was 84.2 % and its negative predictive value 87.5 %. CDU showed 2 false negatives and 3 false positives, sensitivity was 88.2 %, specificity 70 %, overall accuracy 81.5 %, positive predictive value 77.3 % and negative predictive value 83.3 %. Spiral CT and CDU were able to establish resectability of the tumor respectively in 87.5 % and 77.8 % of the patients with grade 0. Both techniques established non resectability in 100 % of cases with grade 3 or 4 avoiding exploratory laparotomy.
Conclusion: Spiral CT and CDU are useful in detecting PMT involvement and can improve the possibility to predict the resectability of pancreatic cancer.

B-0035 11:25

Colour Doppler semiquantitative evaluation of the vessel involvement in the assessment of pancreatic cancer resectability

M. Nowakowski, M. Pirski, A. Zapasnik, M. Studniarek; *Gdansk/PL*

Purpose: The study was made to establish the value of colour Doppler sonography in the evaluation of the extent of pancreatic cancer to choose optimal treatment.
Materials and methods: The research was carried out on 50 patients prior to ensuing surgery on pancreatic cancer by means of ultrasonography with colour Doppler option which was used to estimate the relation between the tumour and the nine nearby vessels. In two clinical groups of patients (resectable and non-resectable) direct and indirect features of vessel involvement were analysed for each of the 9 individual vessels and globally.
Results: A significant correlation between the resectability of pancreatic tumour and the vessel involvement of the splenic vein, the superior mesenteric vein and the confluence of the superior mesenteric and splenic veins was observed.
Conclusion: The overall analysis of the relation of the tumour and all vessel structures has significantly increased the accuracy of pre-operative estimation of the extent of the tumour. The sensitivity, specificity and accuracy of the test was 76 %, 95 % and 84 %, and the PPV and NPV values were 96 % and 74 % respectively.

B-0036 11:30

Dual phase helical CT in pancreatic cancer: Preoperative detection and assessment of resectability

C. Valls, O. Pozuelo, J. Quintero, J. Fabregat, E. Andia, T. Serrano; *Barcelona/ES*

Purpose: To prospectively evaluate helical CT in the preoperative diagnosis and assessment of resectabiliy in patients suspected to have pancreatic cancer.
Materials and methods: Preoperative evaluation and staging with dual-phase helical CT was performed in 46 patients with suspected pancreatic cancer. Iodinated contrast material was injected intravenously (170 ml; rate 4 ml/s); acquisition began at 40 s (pancreatic phase, 3 mm collimation) and 70 s (portal phase 5 mm collimation). Three radiologists prospectively evaluated CT findings to determine the presence of pancreatic tumor and unresectability signs (liver metasta-

sis, vascular encasement and regional lymph nodes). The degree of tumor-vessel contiguity was recorded (no contiguity with tumor, contiguity less than 50 %, contiguity more than 50 %).
Results: Helical CT results in the diagnosis of pancreatic adenocarcinoma were the following: overall detection rate 95 % (38 of 40 cases), positive predictive value (PPV) 95 % and false positive rate 5 % (2 of 40 findings). Thirty five patients were surgically explored and in 29 cases histologic diagnosis was adenocarcinoma. Curative resections were attempted in 25 cases and were successful in 17 instances. The sensitivity of helical CT to predict resectability was 68 % (17/25). Eight patients considered resectable by CT were unresectable at surgery because of liver metastases (n = 4), vascular encasement (n = 2) and lymph nodes metastases (n = 2). The overall accuracy of helical CT to determine resectability or unresectability of pancreatic adenocarcinoma was 72.4 % (21/29).
Conclusions: Dual phase helical CT is useful for preoperative diagnosis and staging of pancreatic cancer. The main limitation of CT is the detection of small hepatic metastasis.

B-0037 11:40

High resolution MSCT of pancreatic carcinoma: Assessment of vascular infiltration
U. Baum, A. Noemayr, M. Lell, S. Kastl, T. Brunner, M. Dobritz, W.A. Bautz; *Erlangen/DE*

Purpose: Value of coronal and sagittal MPR from high resolution isotropic MSCT data sets for the assessment of encasement of the peripancreatic vessels.
Methods and materials: 50 patients with suspected pancreatic carcinoma were examined with a biphasic MSCT protocol: slice collimation 4 × 1 mm (pancreatic phase) and 4 × 2.5 mm (portalvenous phase), pitch 1. After administration of 120 ml contrast medium and 50 ml NaCl with an flow rate of 4.0 ml/s the examination was started with a delay of 40 s (pancreatic phase) and 80 s (portalvenous phase). The encasement of the peripancreatic vessels was assessed with interactive MPR in axial, coronal, and sagittal plane in consensus of three readers experienced in abdominal radiology. 250 peripancreatic vessel (celiac trunc, hepatic artery, SMA, SMV, portal vein) were evaluated for the grade of encasement.
Results: Partial or total encasement of 85/250 peripancreatic vessels were assessed. In 30 cases the grade of encasement changed by using coronal and sagittal plane for the assessment of vascular encasement. Coronal and sagittal plane are superior to axial plane for the exact assessment of the encasement of celiac trunc, hepatic artery and portal vein, whereas for the assessment of the encasement of superior mesenteric artery and vein coronal images give additional information about the extent of the encasement. Changes of grade of encasement changed resectability in 5 patients.
Conclusions: High resolution multiplanar imaging of pancreatic carcinoma with MSCT is especially advantageous in defining critical relationships of the tumor to the adjacent vessels.

B-0038 11:50

Volume rendering of the vascular structures with MSHCT in patients suspected of pancreatic tumor: Initial experiences
M.G.J. Thomeer, D. Vanbeckevoort, D. Bielen, G. Marchal; *Leuven/BE*

Purpose: To evaluate the assessment of the anatomic variants and encasement of the vascular structures in patients with suspicion of pancreatic tumor.
Methods and materials: Multislice helical CT (Somaton Plus 4 Volume Zoom, Siemens, G) was performed in 15 patients suspected for pancreatic tumor. All studies were performed with a 1 mm collimation, a slice width of 1.5 mm and a reconstruction interval of 0.8 mm. Images were obtained in arterial and venous phase and evaluated with a volume rendering technique on an independent workstation (Virtuoso, Siemens Medical Systems, G).
Results: In all of the 15 patients an optimal visualization of the celiac and mesenteric arteries and their major branches was allowed. The porto-mesenteric confluence was reliably identified on all but one patient. Vascular encasement and invasion was routinely visualized and 3D reconstructions gave an excellent stereoscopic view of peripancreatic collaterals in case of tumor invasion. The major vascular branches could be identified on axial slices but volume rendering offered a better three dimensional interpretation of the vasculature (anatomy and collaterals).
Conclusion: Volume rendering tends to improve the interpretation of the vascular structures in case of pancreatic tumor.

Musculoskeletal

SS 210b

New imaging devices

Chairpersons:
F. Aparisi (Valencia/ES)
G. van Kaick (Heidelberg/DE)

B-0039 10:30

Imaging of extremities using a new flat-panel detector with and without a grid system: Intraindividual clinical comparison
P. Mildenberger, K. Dietrich, N. Vogel, S.C.A. Herber, M. Thelen; *Mainz/DE*

Purpose: To test the influence of a grid system on image quality using a new Digital Radiography System with a full-size, flat-panel x-ray detector.
Methods/materials: Patients who were recurrently scheduled for routine skeletal radiography were examined alternately with a new digital radiography unit (Philips Digital Diagnost) with and without a grid system. The flat-panel detector (Trixell Pixium 4600) uses a cesium iodide scintillator layer and a 3 k^2 amorphous silicon photodiode readout array with 0.14 mm pixels. Projections and radiation exposure were equal. In total, 80 clinical studies of routine diagnostic skeletal studies were included. Reading was done independently by 3 experienced radiologists in a blinded manner on a 2.5 × 2K dual monitor reporting station using optimized and standardized parameters (full resolution display mode, no individual image manipulation). Different criteria (presentation of cortex, matrix, soft tissue, detail resolution, noise, overall impression) were evaluated using a 4 point scale (1 … excellent to 4 … poor) and statistically analyzed.
Results: The hypothesis of this study was, that workflow could be improved using a grid in all examinations to avoid changes of the equipment and faulty operations. Intraindividual comparison of examinations with and without grid shows significant differences. The studies without grid are rated better for most criteria. The differences using the above mentioned scale are mostly about 10 %.
Conclusion: Digital radiography with Flat panel detectors (FD) produces high quality images for skeletal radiography, but there is still a difference in image quality with and without grid.

B-0040 10:40

Image quality and radiation exposure in abdominal and skeletal radiography with two different digital technologies
J. Deichen, M. Mechtel, R. Loose, M. Wucherer; *Nuremberg/DE*

Purpose: Comparison of image quality and radiation exposure in abdominal and skeletal radiography with storage phosphor and selenium technology
Material & methods: The impact of different physical and technical parameters on image quality and exposure was evaluated for abdominal and skeletal radiography. A storage phosphor system "ADC Compact" (Agfa) and a selenium based cylindric system "Thoravision" (Philips) with new software for abdominal/skeletal imaging were used. Radiographs of a physical test phantom, a humanoid abdominal/pelvic phantom and a human anatomical femur preparation were obtained using variable exposing parameters. The abdominal phantom was prepared with small mass leasions, the femoral phantom was prepared with drilled leasions of different diameter and depth to mimic osteolysis. The image quality was assessed by 4 experienced radiologists according to visual resolution, perceptability of test leasions and bone structures.
Results: Storage phosphor and selenium technique provide adequate image quality for abdominal and skeletal radiography. No significant difference of spatial resolution, detectability of simulated abdominal/pelvic masses and bony leasions were found.
Conclusions: The current test version of selenium technology with a cylinder provides adequate image quality comparable to established DLR techniques. In contrast to thoracic imaging, the current test version of the selenium technique has no advantage in radiation exposure compared to storage phosphor system.

B-0041 10:50

Storage phosphor radiography of wrist fractures: A subjective comparison of image quality at varying exposure levels

R. Peer, S. Peer, S.M. Giaccomuzzi, S. Pechlaner, K. Künzel, W. Jaschke; *Innsbruck/AT*

Purpose: Image quality of storage phosphor radiographs acquired at different exposure levels was compared to define the minimal radiation dose needed to achieve reliable results for the detection of wrist fractures.

Material and methods: In a study on fractured anatomical wrist specimens image quality of storage phosphor radiographs was assessed on a diagnostic PACS-workstation by three observers. Images were acquired at exposure levels corresponding to a speed class 100, 200, 400 and 800. Cortical bone surface, trabecular bone, soft tissues and fracture delineation were judged on a subjective basis. Image quality was rated according to a standard protocol and statistical evaluation was performed based on an analysis of variance (ANOVA).

Results: Only image quality achieved with an exposure dose equivalent to a speed class 100 and 200 was judged sufficient for detection of unknown fractures by all observers. In the ratings for different image features only images achieved with speed class 100 where judged as "good quality".

Conclusion: To achieve high quality storage phosphor radiographs, with image characteristics, that allow for a reliable evaluation of wrist fractures a minimum exposure dose of 9.5 mGy (equivalent to a speed class of 200) is needed, nevertheless observers are in favor of images acquired at an even higher exposure level.

B-0042 11:00

Direct digital radiography versus storage phosphor radiography of wrist fractures: A subjective comparison

S. Peer[1], U. Neitzel[2], S.M. Giacomuzzi[1], S. Pechlaner[1], R. Peer[1], I.E. Steingruber[1], E. Gassner[1], K. Künzel[1], W. Jaschke[1]; [1]*Innsbruck/AT,* [2]*Hamburg/DE*

Purpose: This study was undertaken to define the value of digital radiography with a clinical flat panel detector system for evaluation of wrist fractures and to compare presentation of anatomical image features with state of the art storage phosphor radiography.

Material and methods: In a study on fractured anatomical wrist specimens image quality of direct digital radiographs and storage phosphor radiographs was assessed by four observers. Hard copy images were acquired with the same exposure dose at a 400 speed level. Cortical bone surface, trabecular bone, soft tissues and fracture delineation were judged on a subjective basis. Image quality was rated according to a standard protocol and statistical evaluation was performed based on an analysis of variance (ANOVA).

Results: Image quality of radiographs acquired with the flat panel detector was rated significantly superior in respect of cortical and trabecular bone presentation as well as fracture evaluation while storage phosphor screen systems showed more soft tissue detail.

Conclusion: This study reveals that the image quality of direct digital radiographs using the cesium iodide/amorphous silicon technology is better suited for delineation and characterization of wrist fractures compared to storage phosphor screen systems.

B-0043 11:10

Volume rendering evaluation of soft tissues

G. Luccichenti, F. Cademartiri, V. Lucidi, M. Squarcia, L. Berti, P. Pavone; *Parma/IT*

Purpose: To evaluate accuracy limits and feasibility of volume rendering reconstructions of the soft tissues.

Materials and methods: This is a study performed on Spiral-CT scans of 22 patients with diagnosed thoracic and abdominal diseases. Images were acquired using the following protocols: collimation/table speed/reconstruction increment 3/4.5/1; 3/3/1 and 2/2/1. Images were sent to a HP workstation running on a NT platform. 3D images were generated with a volume rendering algorithm allowed by the software Vitrea 2.0 (Vital images, USA). Tissues were selectively visualized by modulating transparencies values, by trim and manual segmentation tools avaiable in the software. Two independent radiologists appraised image quality, the visibility and the fidelity of the reconstruction.

Results: Image quality was considered good. Small structures such as biliary ducts were not visible at all. An anomalous renal artery associated with a pieloureteral junction syndrome was found in one case. Two pancreatic lesions, two lung cancers, two renal cell carcinoma and several hepatic lesions such as metastasis and primary tumors were also well visualized particularly their relationships with contigous vascular and solid structures. Peritumoral tissue was also visible.

Conclusion: Volume rendering of soft tissues cannot be proposed as a routine technique although it allows a good representation of anatomic structures and can be proposed as a preoperative imaging modality.

B-0044 11:15

First experiences of multiplanar reconstruction (MPR) using multislice computed tomography (MS-CT) in complex joint fractures

M. Philipp, M. Funovics, M.H. Fuchsjäger, K. Kubin, D. Sandner, F. Grabenwöger, T. Müllner, W. Stoik, V. Metz; *Vienna/AT*

Purpose: In patients with complex joint fractures helical CT for operative planning can only be obtained in the axial plane. Multiplanar reconstructions (MPR) are frequently required for further treatment. However, with conventional spiral CT, multiplanar reconstructions are not always reliable due to a limited spatial resolution. Aim of this prospective study is to determine the value of isotropic multiplanar reconstructions obtained in MS-CT from patients with complex joint fractures.

Material and methods: Examinations are performed using a Siemens Volume Zoom unit (Siemens Medical Systems, Erlangen, Germany) with the following scan parameters: slice width 4 × 1 mm or 2 × 0.5mm, increment 6 mm or 1 mm, respectively. MPR-thickness is 0.5 – 1 mm and 2 mm for coronal reconstructions, and 3 – 4 mm for saggital reconstructions, respectively. This study includes the following fracture locations: face, spine, shoulder, acetabulum, knee and ancle. All examinations are evaluated by 4 experienced radiologists. Findings at subsequent surgery are used as gold-standard.

Results: MPR of MS-CT demonstrates very reliable results even for evaluation of thin fracture lines, dislocations of small fracture fragments and even occult fractures. In the examinations performed until now, MPR of MS-CT sensitivity and specificity are high.

Conclusion: MPR of MS-CT in patients with complex joint fractures is an important new diagnostic tool with high spatial resolution and very short exmaniation time.

B-0045 11:25

Volume rendering evaluation of soft tissues of the knee

G. Luccichenti, F. Cademartiri, F. Cusmano, V. Lucidi, M. Pedrazzini, P. Pavone; *Parma/IT*

Purpose: To evaluate accuracy limits and feasibility of volume rendering reconstructions of the soft tissues of healty knees.

Materials and methods: This is a retrospective study performed on Spiral-CT scans of 16 patients who were considered negative in the dismission hospital report and in the radiological report. Images were acquired using the following protocols: collimation/table speed/reconstruction increment 2/2/1. Images were sent to a HP workstation running on a NT platform. 3D images were generated with a volume rendering algorithm allowed by the software Vitrea 2.0 (Vital images, USA). Tissues were selectively visualized by modulating transparencies values, by trim and manual segmentation tools avaiable in the software. Two independent radiologists appraised image quality, the visibility and the fidelity of the reconstruction.

Results: Cruciate ligaments, menisci, muscles and tendons were correctly visualized. Collaterals ligaments, particularly the laterals ones were clearly visible in few patients due to the absence of an hypodense layer between them and the joint capsula. Time required for the reconstruction was 20 minutes per examination.

Conclusion: Volume rendering of soft tissues cannot be proposed as a routine technique although it allows a good representation of anatomic structures and can be proposed as a preoperative imaging modality of soft tissues of the knee.

B-0046 11:30

Lumbar spine: The influence of acquisition mode using multislice helical CT on patient radiation dose

T. Ludig, C. Marchal, A. Noel, F. Bresler, B. Corruble, A. Blum; *Nancy/FR*

Purpose: To evaluate patient radiation dose and image quality to optimize exploration protocols on lumbar spine using multislice spiral CT.

Method and materials: 48 patients underwent multislice spiral CT on lumbar spine (Somatom Plus 4 Volume Zoom, Siemens). Image protocol included a single helical acquisition from L3 to S1 without gantry inclination (4 × 1 mm, 2 mm thick MPR) and tilted helical acquisition on L3–L4, L4–L5 and L5–S1 (4 × 1 mm, 2/3 mm). Images were read by two independant radiologists. Disk, dural cul de sac, yellow ligaments and nerve roots were analysed. Each criterion was graded from

1 to 4 (poor, moderate, good, excellent); an average grade, ranging from 1 to 4, was calculated for each level. Skin dose was compared for twelve patients with 4 thermoluminescent dosimeters.
Results: Significant improvement in image quality was observed by the two readers for MPR obtained from single helical acquisition compared to tilted acquisition (reader 1: 2.60 vs 2.88 on L3/L4, 2.57 vs 2.90 on L4/L5 and 2.74 vs 3.18 on L5/S1; reader 2: 2.72 vs 3.15 on L3/L4, 2.66 vs 3.08 on L4/L5 and 2.84 vs 3.46 on L5/S1). The average length of single helical acquisition without gantry inclination was 13.5 cm and was 10 cm for helical blocs with gantry inclination.
Conclusion: The influence on normalized effective dose for each exploration will be discussed. A higher image quality is obtained with a single helical acquisition without gantry inclination which permits a decrease of the dose.

B-0047 11:40

Multidetector-row CT of the spine in plasmocytoma

A.H. Mahnken, J.E. Wildberger, U. Fabry, G. Gehbauer, T. Schmitz-Rode, R.W. Günther; *Aachen/DE*

Purpose: To compare multidetector-row CT (MDCT) and secondary reconstruction of the entire spine with conventional radiographs and MRI for bone lesion detection and evaluation of spinal instability in plasmocytoma.
Method and materials: Twelve patients, mean age 69.1 (62 – 79), suffering from plasmocytoma underwent MDCT (Somatom VZ, Siemens, Erlangen, Germany), conventional radiographs as well as MRI of the entire spine and were entered into a prospective trial. CT scanning was performed using a standard protocol (tube voltage 140 kV; tube current 250 mAs, slice collimation: thoracic and lumbar spine 4 × 2.5 mm, cervical spine 4 × 1 mm) without i.v. or oral contrast material. Overlapping coronal and sagittal MPR (maximum projection reformats) were exclusively used for establishing the diagnosis. Findings were compared to conventional radiographs and MRI.
Results: In all patients, coronal and sagittal MPR's depicted the extension of the osseous destruction, providing detailed information about potential bone instability. Compared to conventional radiographs additional lesions at risk for fracture were detected. However, bone marrow infiltration was best seen on MRI.
Conclusion: On the basis of our initial results, MDCT seems to be superior to conventional radiographs in the evaluation of bone destruction in plasmocytoma. In combination with MRI, detailed information for staging these tumors is obtained. To assess instability of the spine due to bone destruction MDCT seems to be the method of choice.

B-0048 11:50

Quality assessment and quality improvement in plain film musculoskeletal radiology

S.M.M. Metz-Schimmerl, L. Böck, M. Uffmann, M. Bauer, I. Loss, C.J. Herold; *Vienna/AT*

Purpose: To identify error sources of failed or borderline quality musculoskeletal radiographs, determine effective procedures in order to reduce costly and time consuming retakes, and improve the overall image quality in daily clinical work.
Method and materials: In a four-weeks period 1569 consecutive x-ray examinations of 32 anatomical projections were evaluated by two radiologists in terms of positioning and exposure settings. All examinations were rated according to three categories: Sufficient, borderline acceptable and non acceptable with need for a retake. Error sources in terms of positioning and technical parameters were identified in weekly meetings attended by both the radiographers and radiologists. Measures of improvement included optimisation of the examination protocols and training of radiographers. Two key joints (knee, shoulder) were reassessed in a second evaluation period.
Results: In the first evaluation period 6.7 % (n = 105) of 1569 examinations were classified as borderline and 4 % (n = 63) as non acceptable. Reasons for reduced or failed examination quality were patient condition, exposure settings, positioning and technical flaws. Frequent anatomical areas with reduced examination quality were nasal sinuses (borderline 14.5 %/non acceptable 2.9 %), shoulder (9.3 %/6.7 %), thoracic spine (1.7 %/5.1 %), lumbar spine (12.7 %/4.5 %) and knees (11.6 %/5.8 %). For the key anatomic regions a marked quality improvement was observed. During the reassessment period a significant reduction of borderline or non acceptable films was noted: Knee (4.5 %/2 %), shoulder (1 %/4 %).
Conclusion: Continuous reassessment of examination standards and self-appraisal in examination procedures improve efficiency and diagnostic quality in routine musculoskeletal radiography. In addition, a more respectful and satisfying working environment may evoke.

10:30–12:00 **Room E2**

Breast

SS 202

Mammography and clinical breast imaging

Chairpersons:
R. Holland (Nijmegen/NL)
H.H. Schild (Bonn/DE)

B-0049 10:30

Long-term outcomes in Swedish mammography trials

I.T. Andersson[1], N. Bjurstam[2], J. Frisell[3], B. Nordenskjöld[4], L. Nyström[5], L. Rutqvist[3], B. Vitak[4]; *[1]Malmö/SE, [2]Uddevalla/SE, [3]Stockholm/SE, [4]Linköping/SE, [5]Umeå/SE*

Purpose: To assess the long-term effects of mammographic screening on the breast cancer mortality.
Materials and methods: The trial populations in the screening studies in Göteborg, Malmö, Stockholm and Östergötland altogether 247.010 women (129.750 invited and 117.260 controls) were followed for more than 3.5 million woman years. The median trial time was 6.5 years (range 3.0 – 18.1) and the median follow-up time 15.8 years (range 2.8 – 20.2). Data on breast cancer diagnosis and cause of death were retrieved by record linkage to the Regional Oncologic Centers as well as to the Swedish Cause of Death Register.
Results: There was a significant 21 % reduction of the breast cancer mortality among women invited (RR 0.79; 95 % CI 0.70 – 0.89). The effect was greatest in the age group 60 – 69 years at entry (33 %). The Malmö and Göteborg trials which used predominantly 2-view mammography and a shorter screening interval showed a significantly higher screening benefit among women under age 50 compared with the other trials. The mortality reduction in women under 50 was statistically significant in both studies, RR 0.69 (95 % CI, 0.48 – 0.99) and 0.58 (95 % CI, 0.35 – 0.96) in Malmö and Göteborg respectively.
Conclusion: Breast cancer screening can reduce breast cancer mortality also in the long-term perspective. It is believed that the trials underestimate the effect of a continuous program due to few screening rounds, relatively long interval, single-view mammography (in 2 of the trials) and other factors.

B-0050 10:40

Breast screening program with multidisciplinary approach: One year results

B. Brancato, F. Caumo, M. Faroni, M. Tessari, C. Procacci, G.F. Pistolesi; *Verona/IT*

Purpose: To evaluate the effectiveness of a breast screening program in which further diagnostic assessments are performed in the same session.
Materials and method: In a time period of one year (1999 – 2000), 7590 women ranging in age between 50 – 69 years underwent a mammographic screening test performed in two projections, promptly read by the radiologist. When needed, further diagnostic assessment (additional radiograms, US, cytology, and core needle biopsy) and interdisciplinary consultations (pathologist and surgeon) were carried out in the same session.
Results: The rate of further diagnostic assessment (recall-rate, RR) was 10.9 % (826/7590). The majority of the diagnostic deepenings resulted negative (4.3 %, 237/826). A short-term follow-up was suggested to 153 women (2 %); 108 (1.4 %) women were sent to surgical intervention. Among the patients who accepted surgical intervention, the histologic examination demonstrated 86 (81.1 %) malignant and 20 (18.9 %) benign lesions, with a benign/malignant biopsies ratio of 0.23:1 and an identification rate (IR) of 11.3‰. The IR for tumors smaller than 1 cm was 4.9‰.
Conclusion: The global IR and that for tumors smaller than 1 cm were superior to that of all the other screening programs reported in literature with the exception of the Danish one. This result correlates with the high RR. In fact, if further diagnostic assessment would have not been performed in the cases of slight suspicion at the mammographic test, the RR would have reduced from 10.9 % to 3.0 %. Nevertheless, 10 tumors would not have been identified, so that the IR would have reduced from 11.3 % to 10 %.

B-0051 10:50

Accuracy of the breast center at the University of Erlangen-Nürnberg (1965-2000)

R.W.S. Schulz-Wendtland[1], U.G. Aichinger[1], S. Kraemer[1], L. Keilholz[1], M. Mitze[2], T. Kirchner[1], R. Sauer[1], N. Lang[1], W.A. Bautz[1]; *[1]Erlangen/DE, [2]Birmingham/GB*

Purpose: To evaluate the efficiency of interdisciplinary cooperation we analyzed the breast cancers which were histological verified at the breast center of the University of Erlangen-Nürnberg (since 1965) in 1999.

Materials and methods: At the breast center the radiology, gynecology, radiotherapy and pathology are closed together in one institution/building. From 01/99 to 12/99 12.365 patients were examined by clinic, ultrasound and mammography. At 4.4 % of the patients (20 – 96 years, mean age 57 years) (n = 548) we found suspicious lesions.

Results: In addition to the BI-RADS classification of ACR we received at the diagnosis BI-RADS 5 for the clinical examination a sensitivity of 35 % and a specificity of 99 %, the ultrasound 57 % resp. 92 % and the mammography 55 % resp. 90 %.

Conclusion: By institutions closed together in a breast center with double reading and interdisciplinary conferences weekly the efficiency in diagnostic and therapy of breast lesions will be better specially by the complementary mamma diagnostic (clinic, ultrasound, mammography).

B-0052 11:00

Mammographic pattern of microcalcifications: Histopathologic correlation

N. Piazza, G.M. Conti, G. Luccichenti, F. Cademartiri, C. D'Aloia, P. Pavone; *Parma/IT*

Purpose: To verify the most valid radiological pattern in the differential diagnosis of benign and malignant breast disease, evaluating number, density, configuration and pleomorphism of the lesions.

Material and methods: The authors retrospectively and blindly reviewed the mammograms of 200 consecutive patients whom had been subjected to surgical excision for microcalcifications. Microcalcifications were evaluated regarding their number, density, configuration and pleomorphism. These results were correlated with the pathologic findings.

Results: 100 % of linear branching calcifications and 80 % of linear calcifications were malignant. In 91 % of the cases, also the pleomorphic calcifications were associated with a malignant disease. The number of calcifications and the density were not useful to the differential diagnosis.

Conclusions: Configuration and pleomorphism of the microcalcifications are the most important parameters in differential diagnosis of benign and malignant breast disease.

B-0053 11:10

Radiological-pathological correlation of excised benign lesions during mammographic screening

I.G. Bilgen, E.E. Ustun, A. Memis; *Izmir/TR*

Purpose: Benign biopsies are an inevitable part of any screening programme. They add significantly to the psychological and financial "cost" of screening and so should be kept to a minimum. The purpose of this study was to identify possible means of reducing these false positive results.

Materials/methods: The mammographic features of the 245 histopathologically proven benign breast lesions detected in screening mammograms were retrospectively reviewed. All of the lesions were preoperatively localized by mammographically guided needle-wire system. Correlations were sought with the pathological findings.

Results: The mammographic abnormalities leading to benign biopsy were suspicious microcalcifications in 132 (53.8 %), well-defined mass in 82 (33.4 %), mass with microcalcifications in 5 (2 %), asymmetrical opacity with microcalcifications in 6 (2.4 %) and spiculated mass with architectural distorsion in 8 (3.2 %) cases. The histological correlates were; fibrocystic change (FCC) 48.9 % (n = 120), fibroadenoma (FA) 18.7 % (n = 46), FCC + FA 9.3 % (n = 23), sclerosing adenosis (SA) 7.7 % (n = 19), fat necrosis (FN) 3.2 % (n = 8), intraductal papilomatosis (IDP) 2.4 % (n = 6), FCC + IDP 2.8 % (n = 7), atypical ductal hyperplasia 1.6 % (n = 4), FA + FCC + SA 0.8 % (n = 2), radial scar 1.6 % (n = 4), FA + SA 1.2 % (n = 3), chronic nonspecific mastitis 0.4 % (n = 1), FN + mastitis 0.4 % (n = 1), chronic inflamated lymph node 0.4 % (n = 1).

Conclusion: A more selective approach is required in the final decision of mammographically guided biopsies considering the psychological and financial cost to the patient.

B-0054 11:20

Lesion detection and characterization after breast conservation therapy - a comparison of mammography, ultrasound and MRI

M. Müller-Schimpfle[1], S. Birrenbach[1], S. Miller[1], W. Stern[2], C. Belka[1], C.D. Claussen[1]; *[1]Tübingen/DE, [2]Schorndorf/DE*

Purpose: To assess lesion detection and lesion characterization within the first year after breast conservation therapy (BCT) using mammography (MX), ultrasound (US), or MR imaging (MRI).

Materials and methods: After breast conserving operation 20 patients were examined before and 6, 12, and 18 months after adjuvant radiotherapy (RT) with MX, US and dynamic contrast-enhanced MRI; US and MRI were additionally performed 3 months after RT. All 220 examinations between 0 – 12 months after RT were retrospectively read by two independent readers in a randomized order, blinded for the other examinations. The evaluation considered the confidence of lesion detection and lesion characterization for the treated and non-treated breast. All available informations including the examinations 18 months after RT were taken as gold standard. Kappa values were calculated to assess different reliabilities.

Results: Excluding a lesion with high confidence was achieved by MX/US/MRI in 30 %/5 %/43 % of all examinations ($p < 0.05$). Reliability between observers/time points/imaging methods was 0.496/0.411/0.215 for lesion detection, 0.303/0.282/0.091 for lesion characterization. Overall, true negative findings were observed in 90.4 %/82.5 %/94.4 % of all MX/US/MRI examinations ($p < 0.05$ for US vs. MRI).

Conclusion: Early after BCT, the influence of different imaging methods on the diagnostic outcome was greater than the influence of different observers or time points. MRI turned out to be the method of choice in excluding lesions with high confidence and gaining the highest true negative rate.

B-0055 11:30

Imaging modalities for detecting locally recurrent breast cancer: Results of a multi-center study (1977-1999)

U.G. Aichinger[1], U.-S. Albert[2], J. de Waal[3], V.F. Duda[2], J. Graesser[4], K. Rogenhofer[1], H. Sommer[4], R.W.S. Schulz-Wendtland[1], W.A. Bautz[1]; *[1]Erlangen/DE, [2]Marburg/DE, [3]Dachau/DE, [4]Munich/DE*

Purpose: Early detection of local recurrences after breast conserving therapy is associated with improved survival. This multicenter study was undertaken to determine the role of physical examination, mammography and ultrasound to detect breast cancer recurrences.

Material and method: Records of 434 women with histological proven recurrences were analysed retrospectively at four institutions. The primary cancer was treated with mastectomy in 209 cases, 225 patients have had breast conserving therapy (BCT). The sensitivity for each diagnostic method and for the combination of the methods were calculated.

Results: Breast cancer recurrences had been diagnosed in 434 cases female patients who had been surgically treated between July 1977 and March 1999. Mean age was 59 years, ranging from 31 to 98. Fifty-five cases (13 %) were detected by physical examination alone, seventeen cases (3 %) had been found as a result only of ultrasound and 35 (8 %) recurrences after breast conserving therapy were detected with mammography only. The remaining cases were detected with two or more modalities. Ultrasound led to an upgrading of the mammographic findings from benign to malignant in 19 % of the cases after BCT.

Conclusion: The results show that mammographic and sonographic follow-up is complementary to physical examination in the detection of local recurrences of breast cancer and leeds to an earlier detection and a better prognosis for the patient.

B-0056 11:40

Imaging modalities in the diagnosis of breast cancer: Diagnostic accuracy in 898 histological proven cases

U.G. Aichinger, R.W.S. Schulz-Wendtland, M. Dobritz, U.J. Wilhelmi, G. Faller, N. Lang, W.A. Bautz; *Erlangen/DE*

Purpose: The role of Ultrasound (US) in breast imaging is under discussion. It is proven, that sensitivity and specificity of multimodal mammadiagnosis is higher than of mammography alone. The purpose of this study was to determine the diagnostic value of US in breast lesions.

Patient and method: From 1–99 until 12–99 there were 898 breast biopsies at our gynaecologic department. All patients had a physical examination, ultrasound and mammography. The results of each modality alone and their combination were correlated with the histological outcome.

Results: The histological diagnosis of 345 (38 %) lesions was benign. 553 (62 %) lesions were malignant, 119 (22 %) DCIS, 275 (50 %) invasive ductal 88 (16 %) invasive lobular and 72 (13 %) other invasive cancer. The sensitivity of the physi-

cal examination was 25 % for pTis, 75 % for p1c and 90 % or more for tumors pT2 or higher. Ultrasound showed a low sensitivity of 30 % resp. 42 % for pTis/pT1a tumors, lesions pT1c and higher showed 93 % up to 100 % for T4 tumors. Mammography was the only method to detect Tis carcinoma at a sensitivity of over 90 %.
The combined sensitivity of mammography and ultrasound was much better than for each method alone, especially in women younger than forty. The results uprise here from 80 % to 93 %.
Conclusion: Ultrasound is a important adjunct to mammography and the physical examination in the work up of breast lesions. Especially in younger patients with dense breasts the sensitivity of a multimodal approach is higher.

B-0057 11:50

Diagnosis of invasive lobular breast cancer

K. Bock, V.F. Duda, N. Vetter, P. Hadji, J. Iwinska-Zelder, A. Ramaswamy, K.-D. Schulz; *Marburg/DE*

Purpose: Less than 10 % of all invasive breast cancers are of lobular origin. What is the value of clinical examination, mammography and sonography in predicting the diagnosis of lobular breast cancer and the size of the lesion which strongly influences the decision on breast conserving therapy?
Materials and methods: Retrospective evaluation of data of 38 patients diagnosed and treated for primary invasive lobular breast cancer at the women's hospital of the Philipps-University of Marburg during 1996 – 2000 (61 % pT1; 75 % pN0).
Results: Sensitivity of diagnosis of invasive malignancy: sonography 0.97, mammography 0.86, clinical examination 0.81. Correlation of histopathologic determined tumor size: sonography 6.17 (for tumors without desmoplastic reaction) and 5.75 respectively (for all tumors), clinical examination 5.88, mammography 4.68. Architectural distorsion as the only sign of a lesion on mammograms was observed in 24 %, corresponding to a poor correlation of size. Desmoplasia was found in another 24 % of tumors by sonography, thus also showing a worse correlation of size.
Conclusion: Sonography has to be recommended for improving the diagnosis of invasive lobular breast cancer as the most appropriate and accurate technique, although it normally is judged to be of additive value only. Nevertheless, the best results are achieved by a multimodal concept.

10:30–12:00 **Room F1**

Chest

SS 204

Thoracic neoplasm

Chairpersons:
A.A. Bankier (Vienna/AT)
T. Petsas (Patras/GR)

B-0058 10:30

Iatrogenic lesions to the lung during antitumoral chemotherapy: CT findings

G. Tognini, F. Ferrozzi, G. Luccichenti, G. Marchesi, M. Pedrazzini, P. Pavone; *Parma/IT*

Purpose: Toxic manifestations of antitumoral chemotherapy represent an important complication. The drug induced pulmonary injury demonstrates several interesting etiopathogenetic, pathologic, clinical and radiological characteristics. The aim of this study was to analyse the several models of lung injury relating the pathological and radiological findings with the mechanism of action.
Materials and methods: We reviewed thoracic CT examination of 1400 patients treated with antiblastic drugs. 23 patients (16 M, 7 F, mean age 57 years) demonstrated pulmonary findings subsequently proved to be jatrogenic. Therapeutic protocols included bleomycin, adriamycin, cyclophosphamide, vincristin, methotrexate, cis-platinum, ethoposide, busulfan, procarbazine, taxanes, arabinosyl-cytosine and interleukine-2, in variable combination. Diagnosis was proven by means of broncho-alveolar lavage, trans-bronchial biopsies or brushing with cytologic, biochemical and microbial analyses, as well as surgery, autopsies, or improvement after therapy.
Results: Bleomycin was found to be the most noxious molecule (14/21) with dose-related toxicity; also methotrexate (2/21) and arabinosyl-cytosine (2/21) both in association with cyclophosphamide were found to be responsible for jatrogenic damage. All the nodular lesions were associated with bleomycin administration, while methotrexate, arabinosyl-cytosine and interleukine-2 were associated with all cases of pulmonary edema. Taxanes were associated with edema and fibrosing evolution.
Conclusions: CT, especially if aided by high resolution technique allows for excellent characterization of structural pulmonary abnormalities related to chemotherapy.

B-0059 10:40

Evaluation of solitary pulmonary nodules with dynamic contrast-enhanced MRI

J.F. Schäfer, J. Vollmar, F. Schick, W. Luboldt, M.D. Seemann, M. Müller-Schimpfle, C.D. Claussen; *Tübingen/DE*

Purpose: To evaluate the performance of dynamic contrast-enhanced MRI in the differentiation between benign and malignant solitary pulmonary nodules (SPN).
Materials and methods: 40 Patients ranging in age from 25 to 86 years with SPN with a diameter of 7 mm to 45 mm underwent MRI at an 1.0 T scanner (Magnetom Expert, Siemens). Dynamic imaging (GRE: TR/TE/flip 20 ms/4.8 ms/70°) was performed in one sagittal plane following a bolus injection of contrast media every 10 s over a total period of 4 minutes. For all SPN peak percentage increase in signal intensity (peak SI %), the slope of the tumor's enhancement (SI %/t) and occurrence of wash-out kinetic were assessed. All 40 lesions (26 malignant, 14 benign) were confirmed with histologic examination after surgical resection, transthoracic or transbronchial biopsy.
Results: Malignant lesions showed a significantly higher peak SI % than benign ones (malignant: mean 130 ± 40 %; benign: mean 57 ± 45 %, $p < 0.00005$). Taking a threshold-value of 85 % for peak SI %, 25/26 malignant and 12/14 of the bening lesions were correctly rated (96 % Sensitivity, 86 % Specificity). Mean slope values were 6.1 ± 3.2 %/s and 2.2 ± 1.6 %/s for malignant and benign lesions, respectively. Wash-out kinetic was found in 13/26 malignant but none of the 14 benign nodules.
Conclusion: Dynamic contrast-enhanced MRI helps in the diagnostic work-up of SPN. Low peak SI % is indicative for benign nodules while high peak SI %, fast slope and wash-out-kinetic correlate with malignant lesions.

B-0060 10:50

Intraoperative sonography during thoracoscopic resection of pulmonary nodules

M. Piolanti, F. Coppola, F. Gruppioni, S. Papa, F. D'Ovidio, M. Di Simone, S. Mattioli, G. Gavelli; *Bologna/IT*

Purpose: This study evaluated the utility of ultrasonography in the intraoperative localization of lung nodules during video- assisted thoracoscopic surgery (VATS).
Materials and methods: This technique was firstly tested during thoracotomic surgery using a high frequency linear probe. Afterwards we performed ultrasonography during VATS using a laparoscopic multi frequence deflectable linear probe. 30 patients entered the study. Preoperative spiral CT diagnosed 38 lesions, with a mean average 17 mm diameter. PET diagnosed 2 lesions unrevealed at CT. Sonography was used in 10 cases via thoracotomy and in 20 cases during VATS.
Results: A complete lung collapse it's required to perform ultrasonography and it can be generally reached 40 minutes after selective lung ventilation exclusion. Air trapping in COPD patients was the major obstacle observed, although all lesions but one, preoperatively documented, were identified. Furthermore 2 occult lesion at preoperative evaluation were detected by ultrasonography. In total 42 lesions were resected. The smallest lesion detected was 4 mm in diameter.
Conclusion: Thoracoscopic ultrasonography is a useful tool to guide VATS resections, being highly efficient and with no related morbidity. Furthermore it may reveal preoperative occult lesions and determine surgical margins.

B-0061 11:00

Low-dose multislice-CT of the thorax in the follow-up of malignancies of extrathoracic or lymphatic origin

M. Sonnenschein, H.-P. Dinkel, P. Vock; *Berne/CH*

Purpose: Repetitive follow-up CT examinations of the thorax are needed in tumor patients. Especially in lymphoma, often young patients are affected and exposed to the risk of a new radiation induced tumor. We examined whether the radiation burden can be reduced safely by low-dose multislice-CT.
Methods: In 40 patients with follow-up of extrathoracic primaries and lymphoma low-dose multislice-CT was performed with 15 mAs/rotation, 120 kV, 0.75 s rotation, pitch 6, in 4 × 2 mm collimation (8 mm reconstruction interval) on a Asteion MS multislice scanner (Toshiba). All patients had a normal-dose spiral-CT of the thorax Siemens Somatom Plus 4 (120 kV, 200 – 300 mA, 0.75 s, pitch 1.5) within 3 – 12 months before. The quality of the present and past examinations was evalu-

ated by two independent readers and classified into the categories poor, satisfactory, good, excellent for different anatomic regions in lung and soft-tissue windows.
Results: Irrespective of body mass index the low-dose examinations were rated good or satisfactory in all patients by both readers. The ratings for the low-dose examinations were inferior (most often by one grade) but diagnostic in every patient. Even subtle lung pathologies as small as 3 mm were detected by low-dose MSCT. The mediastine could be assessed well by low-dose MSCT. In no case low-dose CT had to be repeated for increased image noise.
Conclusion: Low-dose multislice CT of the thorax is effective and sufficient for the follow-up of extrathoracic tumors and lymphoma. It potentially reduces the radiation dose by a factor of 10 – 20.

B-0062 11:10

Imaging of solitary pulmonary nodules with an open low-field MR scanner
J. Vollmar, J.F. Schäfer, F. Schick, C. König, W. Luboldt, M.D. Seemann, C.D. Claussen; *Tübingen/DE*

Purpose: To compare two breathhold sequences for imaging of solitary pulmonary nodules (SPN) at an open MR scanner.
Materials and methods: 12 patients ranging in age from 54 to 74 years with CT-detected SPN underwent MRI at an open 0.2 T scanner (Magnetom Open, Siemens) including a T1w spoiled gradient-echo sequence (2D-FLASH: TR/TE/flip 100 ms/7.4 ms/30°) and a T2w totally refocused gradient-echo sequence (true-FISP: TR/TE/flip 7.4 ms/3.5 ms/80°). Both sequences were compared for lesion depiction, reflection of the CT morphology and SNR as well as artifacts.
Results: On the 2D-FLASH all 12 lesions (8 malignant, 4 benign) ranging in size from 6 mm to 42 mm were visible whereas on the true-FISP two lesions (6 and 9 mm in size) were not visualized. The 2D-FLASH sequence was more accurate in reflecting the CT morphology than the true-FISP sequence. The mean SNR-value of the nodules was 13.6 for the 2D-FLASH and 3.6 for the true-FISP. The 2D-FLASH images showed less artifacts than the true-FISP.
Conclusion: The T1-weighted spoiled gradient echo sequence is superior to the true-FISP for imaging of pulmonary nodules at 0.2 T. MR-imaging of the lung at an open low field scanner seems to be feasible for follow-up exams of potentially benign lesions.

B-0063 11:20

Lymphoma of the lung: CT evaluation
M. Daskalogiannaki, A. Voloudaki, A. Athanassiou, G. Katrinakis, E. Magkanas, P.K. Prassopoulos, G. Eliopoulos, N. Gourtsoyiannis; *Iraklion/GR*

Purpose: To present CT appearances of lymphomatous lung involvement.
Materials and methods: The records of 194 patients with lymphoma, 66 (34 %) with Hodgkin disease (HD) and 128 (66 %) with non-Hodgkin's lymphoma (NHL) were evaluated. Chest CT examinations were assessed for micronodules, nodules, masses, infiltrates, ground glass areas, peribronchial thickening or thickening of interlobular septa and concomitant findings.
Results: Secondary lung involvement was identified in 15/194 (8 %) patients, 5/66 (7.5 %) with HD and 10/128 (7.8 %) with NHL. The lung was involved in 73 % of the patients at presentation and in 27 % with disease relapse. Micronodules were depicted in 12 (80 %) patients – 5 HD and 7 NHL – predominantly subpleurally (67 %), nodules in 4 (27 %), masses with or without air-bronchogram or cavitation in 8 (53 %) – 4 HD and 4 NHL – infiltrates in 2 (13 %) with NHL, and ground glass areas in one (7 %) patient with NHL. The majority of patients (67 %) had a combination of 2 or more CT findings, most commonly micronodules with masses (33 %). Three patients with NHL presented a diffuse interstitial pattern: either a combination of micronodules and peribronchial thickening mimicking sarcoidosis (n = 2), or micronodules and thickening of interlobular septa mimicking lymphangitic carcinomatosis (n = 1). In most cases lung involvement was bilateral (80 %) and affected more than one lobe (87 %).
Conclusion: Lymphomatous lung involvement demonstrates a variety of CT patterns, the most common being the presence of micronodules. The majority of cases presents a combination of findings and bilateral involvement.

B-0064 11:30

The use of multislice spiral CT of the chest in the staging of oncological patients: Scan protocol evaluation
E.M. Fallenberg[1], R. Fischbach[1], D. Maintz[1], P. Lange[2], K.U. Jürgens[1], J. Weßling[1], W. Heindel[1]; *[1]Münster/DE, [2]Munich/DE*

Purpose: To evaluate different spiral CT scanning protocols for routine staging examination of the chest using a multi-detector CT scanner.
Method/materials: 75 patients were examined on a Multislice-Spiral-CT (Somatom VolumeZoom, Siemens, Forchheim) using 140 kV, 90 mAs, 500 ms gantry rotation time and constant contrast injection parameters. Patients were assigned to 8 different spiral CT protocols resulting from combinations of table feet per rotation (pitch 3, 5, 7) and detector collimation (1 mm; 2.5 mm; 5 mm). Axial images with 5 mm slice width were independently assessed by 3 radiologists in a blinded fashion regarding overall image quality, anatomic detail, and artefacts.
Results: Overall image quality was regarded as optimal for images obtained with 1 mm detector collimation and 5 mm or 7 mm table feed. Images reconstructed from spiral data sets recorded with 4 × 2.5 mm detector collimation were of good diagnostic quality. Increasing pitch results in artefacts at borders of different tissue attenuation. It was even more pronounced using 5 mm collimation (pitch of 5 or 7). When comparing images obtained with equivalent scan time (24 s; 4 × 1 mm collimation and pitch 7 vs. 4 × 2.5 mm collimation and pitch 3) the narrow collimation images had a slightly better delineation of anatomic detail.
Conclusions: A narrow collimation with large pitch is superior to a wider collimation and a smaller pitch. Optimal image quality was achieved using a 4 × 1 mm detector collimation. 2.5 mm collimation and pitch 3 can be used with only minor, not significant decrease in image quality.

B-0065 11:40

Low dose spiral CT for screening of lung cancer
M. Bellomi, E. De Fiori, P. Arnaldi, U. Pastorino; *Milan/IT*

Purpose: Early detection of lung cancer could, in theory, reduce the mortality of the disease, due to the high rate of non-operable or late stage at diagnosis.
Methods and materials: The study, started in May 2000, aims to recruit 1000 volunteer subjects, over 50 and who have smoked over 146.000 cigarettes, to be submitted once a year, for 5 years, to low dose (140 kV, 40 mA) CT of the chest. Diagnostic work-up is performed by HRCT and nodule contrast enhancement in all lesions larger than 5 mm, followed, if necessary, by PET, FNAB and surgery.
Results: At September 2000, 230 volunteers were examined: lesions were detected in 21.5 % and 5 % (12) had nodules larger than 5 mm. 3 were false positive (pleural thickening and atelectasis); 2 were judged to be benign; 3 were followed-up at 3 months because non determinable (diameter 5.6 – 6.3 mm); and 4 were operated and confirmed as malignant (3 T1N0 and 1 T2N1).
Conclusion: It is early to draw any conclusion, but the number of detected lesions is similar to that of ELCAP study, while the cancer rate appears to be lower than that of American population. Contrast enhancement study and PET are promising in diagnostic work-up, reducing the number of FNAB with high risk in heavy smokers.

B-0066 11:50

Clinical impact of cerebral CT in the preoperative TNM classification of patients with bronchial carcinoma
H.B. Eggesbø, T. Flatabø, L. Vlatkovic, R. Dullerud; *Oslo/NO*

Purpose: To estimate the prevalence of cerebral metastases by CT in patients with bronchial carcinoma. Further, to assess the relation between cerebral metastases, TNM classification, and histology of the bronchial carcinoma to reveal other signs of inoperability in these patients.
Materials and methods: 128 patients with bronchial carcinoma (aged 33 – 85 years, mean 68 years; 50 females and 78 males) were TNM classified based on CT examination of the thorax, abdomen and brain, following the i.v. injection of 70 ml (300 mg I/ml) contrast medium. Cerebral and abdominal metastases as well as histology of the bronchial carcinoma were noted.
Results: Histologic examination revealed squamous cell carcinoma in 40 patients, small-cell carcinoma in 40, adenocarcinoma in 20, large-cell carcinoma in 12 and unclassified carcinoma in 16 patients. Metastases to the brain were demonstrated in 19 patients (15 %), liver 14 (11 %), adrenal glands 11 (9 %), other 11 (9 %). In 8/19 patients (2 squamous cell carcinoma, 3 adenocarcinoma and 3 small-cell carcinoma) cerebral metastases were the only sign of inoperability. 7/19 patients with cerebral metastases also had metastases to other organs, while 1/19 patients was classified as T4 and 3/19 as N3.
Conclusion: The finding of cerebral metastases as the only sign of inoperability in 8/128 patients with bronchial carcinoma justifies the routine imaging of the brain in these patients.

10:30–12:00 **Room F2**

Neuro

SS 211

Vascular - Interventional

Chairpersons:
J. Moret (Paris/FR)
L. Picard (Nancy/FR)

B-0067 10:30

"Fetal" configuration of posterior cerebral artery (fPCA) and anterior cerebral artery cross-flow (ACA-cf). Reciprocal correlation revealed on the basis of ^{99}Tc-HMPAO SPECT vs. angiography (DSA)

A. Piotrowski[1], E. Klemm[2], H. Urbach[2], L. Krolicki[1], H.J. Biersack[2]; *[1]Warsaw/PL, [2]Bonn/DE*

Objectives: FPCA may be revealed in 20 to 25 % of cases. The literature dealing with intracarotid amobarbital procedure (IAP) reports occurrence of ACA-cf in 30 % of patients. Recently, SPECT with intracarotid injection of ^{99}Tc-HMPAO has been used during IAP. This study aimed to investigate with both methods the correlation between ACA-cf and fPCA.
Methods: We evaluated retrospectively ninety-four DSA and SPECT studies performed during IAP in forty-seven patients (mean age: 29.9 a). After completion of DSA a mixture of 200 g amobarbital and 1 mCi ^{99}Tc-HMPAO was injected into ICA without catheter repositioning, with the same volume and injection rate. SPECT was performed with high-resolution γ camera.
Results: The ^{99}Tc-HMPAO uptake in the whole PCA territory was revealed in 13/94 (13.8 %) hemispheres and ACA-cf was revealed in 20 hemispheres (21.3 %). The whole PCA territory perfusion (including the hippocampus) was observed only in these cases in which no ^{99}Tc-HMPAO uptake appeared in the contralateral ACA territory ($p = 0.035$). This kind of correlation was not revealed on the basis of DSA ($p = 0.486$).
Conclusion: The hypothetical reason of the phenomenon revealed in the SPECT study may be a circulatory 'steal-shift' within the injected and contralateral hemisphere or it may have anatomical groundwork. Intracarotid ^{99}Tc-HMPAO SPECT deserves more consideration in respect of its importance in 'in vivo' investigation of some hemodynamic phenomena in the circle of Willis. We also suggest that comparison of both methods could be helpful for criteria definition enabling better interpretation of amobarbital distribution only on the basis of DSA study.

B-0068 10:40

Combined approach with CTA and dynamic MRA in pre-operative evaluation of carotid stenosis: An alternative to DSA in selected patients

M. Muto, A. Palmieri; *Naples/IT*

Purpose: To show the utility of the pre-operative association of CTA and dynamic MRA evaluating carotid stenosis, reducing the need of DSA.
Material and methods: 75 patients, with more than 60 % degree of carotid stenosis at US examination, were evaluated with CTA and dynamic MRA to confirm the US results and to evaluate the origin of epiaortic vessels and the intracranial segment of the ICA. (to exclude tandem lesions). In 10 cases a DSA was also performed. CTA was perfomed with spiral tecnique (Picker PQ 5000, 2 mm thickness, pitch 1.5) during automatic inj. of 110 cc non-ionic contrast media (Iopamiro, 3 ml/s) from C6 through skull base. Dynamic MRA was performed with 1.5 T Magnet (Picker Ellipse) with a 3D volumetric acquisition in 18' sec after a bolus inj by hand of 25 cc of Gd-DTPA (Dotarem, Guerbet) followed by 20 cc of saline solution.
Results: In 60 pts. we found the same data at US and CTA examinations; in 13 cases we had an overvalue by US examination in terms of stenosis or occlusion. Dynamic MRA also overmeasured the degree of stenosis in more the 75 % of cases (degree of carotid stenosis more than 70 %) but showed the presence of tandem lesions in 7 cases, confirmed also by DSA. In 2 patients the MRA examination was not diagnostic due to poor patient cooperation or to cardiac failure with incorrect bolus timing.
Conclusions: CTA and dynamic MRA reduce the need of DSA; CTA is usefull to confirm the degree of stenosis at carotid bifurcation while dynamic MRA can be usefull to visualize tandem lesions.

B-0069 10:50

Improved treatment planning of complex cerebral aneurysms with multislice CT angiography: A pilot study

C. Balassy, D. Fleischmann, G. Bavinzski, R. Mallek; *Vienna/AT*

Purpose: To evaluate if multislice CT angiography (CTA) with 3D image processing provides additional information over digital subtraction angiography (DSA) for treatment planning of complex cerebral aneurysms.
Materials and methods: Five patients (4 f/1 m) with eight untreated intracranial aneurysms and equivocal findings at DSA underwent cerebral CTA (2 × 0.5 mm detector configuration; 1 mm TI/rotation; 0.5 mm RI). Volume rendered images – targeted to the specific pretherapeutic questions – were read prospectively by a radiologist and the treating neurosurgeon and compared to surgical findings in three subjects.
Results: The location, shape and direction of all six aneurysms with surgical correlation were accurately shown at CTA. CTA correctly excluded an additional, angiographically suspected AcoA aneurysm in one patient. The origing of a small perforating artery from the base of an MCA aneurysm was correctly depicted with CTA, however, correlation with DSA was necessary to identify a neighbouring vessel as a vein. One patient unerwent successful endovascular treatment after CTA clearly demonstrated the neck of an AcoA aneurysm. In one patient with a 3 mm superior cerebellar aneurysm surgery was deferred because of it's topographic relation to the basilar artery and the skull base (as shown at CT), and unfavorable venous drainage (as shown at DSA).
Conclusion: CTA can provide additional, surgically relevant information in complex cerebral aneurysms when DSA findings are equivocal, but CTA cannot replace DSA.

B-0070 11:00

Comparison of volume rendering to other post-processing techniques in cerebral CT angiography

Z. Vikalo, J. Petrackova; *Decin/CZ*

Purpose: To compare Volume Rendering Technique (VRT) with Maximum Intensity Projection (MIP) and Shaded Surface Display (SSD) in cerebral CT angiography (CTA).
Methods and materials: Cerebral CTA was performed at thirty patients with clinically suspected intracranial aneurysm or SAH. Scan protocols were: slice 1 mm, pitch 2, increment 0.5 mm. Contrast medium: 120 – 140 ml, at 4 ml/s flow rate. Images were reconstructed on a VIRTUOSO-workstation. All patients who had an aneurysm or SAH underwent DSA or proceeded directly to Surgery. We compared the visibility of aneurysms for each technique using surgical finding or DSA as a gold standard. The visibility of atherosclerotic changes were compared too. In addition we compared the visibility of normal vessels and their contours under the maximum magnification. We also recorded the time required for post-processing and evaluation for each technique.
Results: The total of 14 aneurysms were diagnosed on CTA, all of them were confirmed either surgicaly or by DSA. For none of the patients, DSA detected any other aneurysms, and the localisation, size and shape also matched cerebral CTA. VRT required in average 14 minutes for post-processing and evaluation. The average time for SSD was 55 minutes. MIP required, in average 16 minutes, but the possibility of images manipulation and the visibility of normal and pathologic anatomy were considerably less. All statistics will be available later.
Conclusion: VRT requires a shorter time for post-processing and evaluation and provides better visibility of both pathological and normal vessels than MIP and SSD.

B-0071 11:10

MRI and MR angiography of intracranial aneurysms: Detection and characterization

Z. Merhemic, Z. Kadenic, G. Sulejmanpašic, M. Nikšic, A. Đuheric, F. Konjhodzic; *Sarajevo/BA*

Purpose: To assess 3DTOF angiography pre and post MIP algorithm for the detection and characterization of intracranial aneurysms using IADSAas the "gold standard" for the presence, location and size of aneurysm and the direction of the neck of aneurysm.
Methods and materials: Total 52 patients with nontraumatic intracranial hemorrhage were examined by 1.0 T unit using DUAL (PD; T2TSE) sequence, and 3DTOF MR angiography evaluating pre and post MIP algorithm, and they were correlated with IADSA.
Results: MR angiography and IADSA were in agreement both in positiv and negativ cases (32 and 20). 35 aneurysms were found by 32 patients; five 3 to 5 mm large. Size of aneurysms and direction of the neck were in agreement in all 5 with IA

DSA. 18 aneurysms were 6 to 12 mm large. Size of aneurysms were in agreement in all 18 in pre MIP evaluation, 17 in post MIP evaluation. The direction of the neck was in agreement with IADSA in all 18. 12 aneurysms were larger then 12 mm. The agreement in size were in all evaluating pre MIP algorithm, and in 7 post MIP. 4 of these had no neck. The direction of the neck were in agrement with IADSA in the rest in pre MIP, and only in 4 in post MIP 3DTOF.
Conclusion: 3DTOF MR angiography pre and post MIP algorithm is reliable tool in intracranial aneurysms evaluation. The evaluation of pre MIP algorithm 3DTOF MRA provide useful information about size of aneurysms and direction of the neck of aneurysms larger then 12 mm.

B-0072 11:15

Giant aneurysms: Preoperative evaluation with three-dimensional CT angiography
Z. Miloševiè, I. Kocijanèiè; *Ljubljana/SI*

Purpose: Three dimensional computed tomographic angiography (CTA) was developed as a screening tool for use in patients with suspected cerebrovascular disease. This imaging modality also has proven to be of value in surgical planning for patients with large or unusual vascular lesions of the brain.
Materials and methods: The three-dimensional CT angiograms obtained in 12 patients with giant intracranial aneurysms were analaysed. Using CTA we were evaluated the size and configuration of intracranial aneurysms, the presence and extent of intra-aneurysmal thrombus, the relationship of the vascular lesion to other cerebrovascular or skeletal structures, aneurysm wall thickness, and the presence and orientation of an aneurysm neck. The results were compared with conventional angiography and/or surgery.
Results: In our experience this imaging modality displays anatomical information that are not avaliable from conventional angiography and provides better details for surgical planning in patients with giant intracranial aneurysms.
Conclusion: Because three-dimensional reconstructions of intracranial vessels and vascular lesions offer anatomical imaging in the similar way as percepted with human vision, we can better understand the morphology of pathological proceses and its relations to surrounding structures.

B-0073 11:20

Treatment of arterio-venous malformations of the brain by percutaneous transarterial embolization with a low-concentration glue
M. Szajner, R. Pietura, M. Janczarek, M. Szczerbo-Trojanowska; *Lublin/PL*

Purpose: To evaluate the efficacy of embolization of brain AVMs with low-concentrated Histoacryl.
Materials and methods: 52 patients presenting with arterio-venous malformations of brain were treated in our Department between 1998 and 2000. There were: 22 angiomas of right hemispere, 14 angiomas of left hemispere, 16 patients with angiomas of cerebellum. The angioarchitecture of AVM nidus was: diffuse (d), compact (c), fistular (f) or mixed (m). We also distiguished complicated (co) or non-complicated (nc) AVMs. Nidus diameter > 3.5 cm was considered large (L), 1 – 3 cm medium (M) and < 1 cm small (S). The embolization was carried out with system of coaxial catheters: 5 F or 6 F guiding cath and microcatheters (1.5 F or 1.8 F) positioned in the AVM nidus. Before application of embolic material (Histoacryl/Lipiodol dilution: 16.6 – 25 %) supra-selective angiography was done. After injection of glue microcatheter was rapidly retrived and control angiography carried out.
Results: In our group of patients there were: GI – 14 (27 %) 100 % occlusion, GII – 25 (48 %) 90 – 95 % occlusion, GIII – 8 (15 %) between 60 – 90 % occlusion, GIV – 3 (6 %) less than 60 % occlusion and GV – 2 (4 %) technical failure. AVMs: GI – 9 S, 3 M, 2 L; 5 d, 6 c, 2 f; all nc. GII – 17 M, 3 S, 5 L; 11 m, 6 f, 5 c, 3 d. GIII – 5 L, 3 M; 6 d, 2 m; 6 co, 2 nc. GIV – 2 L, 1 M; 3 d; nc. GV – 2 L; d (teleangiectatic), nc. Minor complications – 3 patients. Major – 2 patients. Mortality – 0. 6 months follow up in 36 patients – 4 cases of reccurrence.
Conclusion: Embolization of arterio-venous malformation of brain with low-concentrated glue seems to be an effective treatment. Low-concentrated dilution of Histoacryl permits deep penetration into the AVM nidus as well as in venous drainage.

B-0074 11:25

Experience with the endovascular treatment of intracranial aneurysms
F. Charvat[1], V. Benes[1], P. Fencl[1], K. Antonin[2], J. Lacman[1]; [1]*Prague/CZ*, [2]*Hradec Kralove/CZ*

Purpose: The authors experience with the endovascular treatment of the intracranial aneurysms by Guglielmi detachable coils or by stenting is summarised.
Material and methods: Since January through June 2000 total of 54 patients has been treated. In 18 patients the clipping was the primarily chosen procedure. In 39 patients endovascular approach was the first step. In 7 patients only attempt at coiling was performed and after the failure to coil the aneurysm the patients were treated surgically. Totally 36 aneurysms in 32 patients was treated by endovascular methods. The parent vessel was occluded in 6 cases, the sack of the aneurysm was filled with GDCoils in 28 cases, in one fusiform aneurysm stent was introduced. The Hunt and Hess score (HH) in the serie was: HH0 in 9 patients, HH1/6, HH2/8, HH3/4, HH4/5, HH5/0 patient. HH was the single most important determinant of the outcome.
Results: Thirty-four aneurysms were closed completely and 2 partially. Mortality and morbidity rate of the series was 3 %. In the first follow up control one month after the procedure 30 aneurysms in 27 patients remained closed. Remnant of 1 ophtalmic aneurysm showed some growth.
Conclusion: The basic aim of any aneurysm treatment is to prevent rebleeding. Cons of the endovascular approach are: more frequent incomplete aneurysm occlusion and lesser stability of coils. Pros are: minimally invasive approach suitable for eldery patients and patients with higher HH score, and probably lower frequency of vasospasm.

B-0075 11:30

Local intra-arterial fibrinolysis with urokinase (LIF-U) in 14 patients with acute basilar artery thrombosis (BAT)
M. Voges[1], V. Jost[1], G. Brill[2], G. Fenzl[1], R. Eymann[1], J. Voges[1], J. Scheuermann[1], W. Reith[1]; [1]*Homburg a. d. Saar/DE*, [2]*Saarbrücken/DE*

Purpose: Observation of the following parameters: pre-therapeutic period (PRE-TP), duration of lysis, recanalization, income, outcome, complications, relationship between: outcome/PRE-TP and outcome/recanalization.
Material and methods: Examined: 14 patients (11 male, 3 female), average age 62.3 years ± 11.3 (range 33 – 81) with angiographically proven BAT, between 01.01.1995 and 31.12.1999. In all cases LIF-U followed angiography. Scaling of clinical process by Barthel Index points (BIP).
Results: Average PRE-TP: 7.5 ± 5.5 h (range 3 – 24). Average duration of lysis 35 ± 13.9 min (range 20 – 60). Average U-dose 600 000 ± 150 000 IU (range 250 000 – 900 000). Complete recanalization in 10 patients (71.4 %), incomplete in 3 patients (21.4 %), none in 1 patient (7.1 %). Average BIP-income: 6.4 ± 15.9. Death of 5 patients, all within the first month. Remaining 9 patients showed average improvement to 76.1 ± 37.3 BIP. No incidence of intracranial haemorrhage or other complications. A high correlation was found for outcome/PRE-TP and outcome/recanalization.
Conclusions: Our LIF-U results are comparable to other workgroups. A high correlation outcome/PRE-TP and outcome/recanalization is also described by other authors. A good outcome is decisively influenced by a short PRE-TP and a complete recanalization.

B-0076 11:40

Central retinal artery occlusion: Endovascular treatment
B.F. Schuknecht, K. Landau, A. Valavanis; *Zürich/CH*

Purpose: To analyse the results of endovascular fibrinolytic tx of 19 patients with acute central retinal artery occlusion (CRAO).
Patients and methods: 19 patients (11 m, 8 f, age range 33 – 77 years, mean 60.7) with acute (< 12 h) CRAO were retrospectively analysed with respect to angiographic findings and clinical outcome. Endovascular tx had been performed by superselective application of 1 Mio IU urokinase into the ophthalmic artery by means of a FasTracker Microcatheter (Boston Scientific).
Results: Angiographic findings consisted of nonopacification of the central retinal artery (CRA) in 6 patients, visualization in 13 patients. Following tx the CRA was seen in 4/6 patients and delineated to better advantage in 9/13 cases. The chorioretinal blush was demonstrated in 18/19 patients and was present following tx in every patient. Visual function improved in 15 patients (78.9 %) with full recovery of vision in 5/15 patients (33.3 %).
Conclusion: Endovascular tx may allow to regain full recovery of vision in a substantial proportion of patients which may be higher than peviously reported after conservative tx (5.8 – 9 %) or interventional tx (14 – 17.6 %).

B-0077 11:50

Extra axial cavernous haemangioma: MR imaging study
N. Chidambaranathan, S. Halbe, S. Kalyanaraman, S. Ghosh; *Chennai/IN*

Extra axial cavernous haemangioma is a rare entity, only 58 cases have been reported. Most of the extra axial cavernous haemangioma occur in the intracavernous location and are highly vascular. The clinical, radiological and

histological characteristics of these lesions are distinct from those of intracerebral haemangiomas. Due to lack of haemosiderin, they closely resemble "Meningiomas" in MR images and are often misdiagnosed.
Aim of the study: To analyse MRI findings of extra axial cavernous haemangioma and to distinguish them from other paracavernous neoplasms.
Materials: Four patients with histologically proven extraaxial cavernous haemangiomas were evaluated with CT, MR imaging and Cerebral angiogram. Complete resection was done in two cases, biopsy was done in two other cases as severe intraoperative bleeding precluded their total removal.
Method: CT .. MR: High resolution T1 (TR 400 ms, TE 15 ms); T2 (TR 2000 ms, TE 18 ms); Turbo FLAIR and Post gadolinium T1 weighted images in coronal and axial planes. Cerebral angiography.
Results: CT showed homogenous enhancing tumour similar to meningioma, yet lacking calcification or bony hyperostosis. MRI showed sharply defined lesions of very high signal intensity in T2 weighted scans, isointense in T1 weighted images and showing homogenous enhancement by gadolinium DTPA. Cerebral angiography showed no tumor vascularity, but two cases revealed mild tumor staining.
Conclusion: MR features help to predict this rare entity of cavernous sinus cavernoma, differentiate them from other paracavernous neoplasms, help in the pre operative assesment and to prevent unexpected intra operative complications.

10:30–12:00 **Room G**

Abdominal and Gastrointestinal

SS 201b

Colon and rectum (1)

Chairpersons:
W.A. Bautz (Erlangen/DE)
P.K. Prassopoulos (Iraklion/GR)

B-0078 10:30

First results in reduction of radiation exposure in double contrast barium enema with a state of the art digital fluororadiography system
K. Lomoschitz, G. Paertan, S. Newrkla, R. Mayrhofer, W. Hruby; *Vienna/AT*

Purpose: Since double contrast barium enema is the routine radiological method of examination of the colon, one major challenge is to keep radiation exposure as low as reasonably achievable. This paper reports dose reduction in barium enema resulting from technical development in Digital Flouroradiography Systems.
Materials and methods: Barium enema studies were performed in 70 consecutive patients using a new DFR-System (Siemens Iconos R200), capable of 10 bit gray levels and maximal resolution of 2K by 2K pixel matrix. Examinations were performed with pulsed fluoroscopy. Dose-area product, fluoroscopy time and number of images were compared to a control group (36 patients) investigated with an older system (Siemens siregraph D). Additional beam filtration (0.3 mm Cu) and kVp were equal in both systems. Examinations acquired with both systems were reported on PACS workstations. Image quality was assesed subjectively.
Results: Median DAP measured on the new system was 56 % below the values of the control group (580 vs. 1310 cGy·cm^2). Average number of acquired images was 16 in both groups, average fluoroscopy time was 251 s vs 102 s. Image quality with the DFR system was graded significantly superior compared to the older DFR system, although for the barium enema examination only 1K resolution was used with both systems.
Conclusions: With a new state of the art system, substantial dose reduction can be achieved (> 1/2 compared to lowest literature values, approximatly 1/10 to reference values) with better image quality. Therefore the new system is likely to be used in all fields of fluoroscopy examinations.

B-0079 10:40

Acute sigma diverticulitis: Diagnostic role of ultrasound examination in emergency
G. Moggio, L. Manfredonia, T. Donnianni, A. Mazzacca, G. Belfiore; *Caserta/IT*

Purpose: To describe the findings of abdomino-pelvic ultrasound (US) in the emergency evaluation of acute sigma diverticulitis (ASD), an inflammatory complication of the diverticular disease often leading to acute abdomen.
Materials and methods: 25 patients (17 M/8 F, age range: 50 – 75 years) were admitted to our hospital with clinically suspect ASD. All patients underwent abdominal X-ray, performed with supine and orthostatic anteroposterior views, US with a 3.5 MHz probe and empty bladder, and computed tomography (CT) after oral load of water-soluble contrast media.
Results: X-ray findings were not relevant for the diagnosis of ASD, except for 3 cases with perforation. US correctly detected ASD in 23 patients, showing increased wall thickness, diverticula, and increased echogenicity of the adjacent mesenteric sheets. As for complications, abscess was detected in 3 cases, perforation in 3, and peritonitis in 1. In 2 cases, US correctly located inflammation in the adjacent tuba. CT did not add relevant information versus US, except for an improved spatial evaluation in the complicated cases.
Conclusions: US allowed direct assessment of diverticula, optimal evaluation of wall thickening and detection of possible complications. In our experience, US resolved the diagnostic approach, making a CT scan necessary only in selected cases.

B-0080 10:50

Hydro-CT in preoperative diagnostic of acute diverticulitis: Too expensive or the method of choice?
A. Werner, S.J. Diehl, F. Graupe, M. Farag Soliman, C. Düber; *Mannheim/DE*

Purpose: Conventional colon contrast studies only allow examination of intraluminal structures. However, in acute sigma diverticulitis therapeutic decisions mainly depend on complications which are often extraluminally situated. This study evaluates the diagnostic efficiency of Hydro-CT in acute diverticulitis.
Materials and methods: 80 patients with a clinical diagnosis of acute sigma diverticulitis underwent a CT of the lower abdomen with iv contrast after rectal application of 1000 ml diluted iodic contrast. CT-results were compared with histopathologic, intraoperative, or endoscopic results.
Results: 21 % of the patients showed normal CT findings. They recovered rapidly and were discharged. 15 % of the patients exhibited a mild diverticulitis in the CT. At 48 % of the patients pericolitis with covered or free perforation, abscess formation, or stenosis was diagnosed in the CT. Among them 80 % were operated and the CT-diagnosis was confirmed in all cases. At 6 % the CT suggested colonic cancer which was confirmed in all cases with one exception. 10 % of the patients showed an extracolic reason for abdominal pain in the CT which always was confirmed operatively.
Conclusion: Hydro CT is not only reliable in detecting intraluminal signs of sigma diverticulitis but also reveals sensitively extracolic complications and other reasons for the clinical symptoms. It is therefore the method of choice to support the decision between conservative and operative therapeutic approaches.

B-0081 11:00

Rectal carcinoma: Multislice spiral CT imaging for preoperative staging
R. Ambrosini, A. Filippone, D. Genovesi, R. Basilico, L. Bonomo; *Chieti/IT*

Purpose: Preoperative staging of rectal carcinoma is critical for guiding therapy and prescribing the most appropriate treatment option. The purpose of this investigation was to evaluate the accuracy of multislice spiral CT in staging rectal cancer.
Materials and methods: Fifteen patients, referred with a diagnosis of rectal carcinoma, were examined. Multislice spiral CT scans (slice collimation 4 × 2.5 mm; table feed 12.5 mm/rotation; slice widht 3/5 mm; rotation time 0.5 s) were carried out after full colonic preparation, air insufflation and data were acquired in the prone position. CT scans were acquired 35 s and 70 s after injection of a bolus of contrast medium (130 ml, 3 ml/s, 400 mgI/ml). Analysis of the rectal wall and staging of the tumor were performed on axial CT sections and multiplanar informations. All patients underwent surgery and CT findings were compared to histopathological analysis.
Results: Good correlation between CT findings and postoperative staging was observed in all patients included in the study, with a sensitivity of 100 % and an overall staging accuracy of 95 %.
Conclusions: Multislice spiral CT can be useful and accurate in detecting and staging primary rectal carcinoma.

B-0082

withdrawn by author

B-0083 11:10

Endoanal ultrasound in the diagnosis of faecal incontinence: Comparison with anal manometry and operative findings

M.H. Fuchsjäger, J. Alt, M. Funovics, V. Metz, T. Filipitsch, G. Lechner, A. Maier; *Vienna/AT*

Purpose: The aim of this study was the evaluation of endoanal ultrasound in the diagnosis of faecal incontinence in comparison to anal manometry and operative findings. The presence and localisation of sphincter defects and therapeutic modalities were analysed.

Method and materials: Endoanal ultrasound was used to investigate 92 patients (85 female, 7 male; mean age 62 ± 13 years) with faecal incontinence in a 3 year period. The presence, localisation and the extent of anal sphincter defects were assessed. Results were compared with anal manometry in 81 cases.

Results: 27 (29 %) patients showed no sphincter defect, 18 (20 %) had an isolated internal sphincter defect, 13 (14 %) an isolated defect of the external sphincter and 34 (37 %) presented with a combined defect of internal and external sphincters. Manometric results correlated in 30 % with endoanal ultrasound. 13 patients underwent an operation. Endoanal ultrasound correlated in 100 % with operative findings and with manometry in 54 %. An obstetric history was most frequently related to faecal incontinence. In the group of combined sphincter defects, the percentage of operations was highest.

Conclusion: Endoanal ultrasound is the most sensitive diagnostic method for localizing anal sphincter defects and should be mandatory in the assessment of faecal incontinence.

B-0084 11:20

Is unenhanced CT useful when used as part of the staging protocol in patients with colorectal carcinoma?

M. Farrugia, S. Davitt, B. Sharma; *Romford/GB*

Purpose: To assess the utility of unenhanced spiral CT when used in conjunction with portal phase CT in the staging protocol for colorectal carcinoma.

Material and methods: We retrospectively reviewed the CT staging protocol in 85 patients with colorectal carcinoma as part of a clinical effectiveness and best practice audit. An unenhanced single-breathold volume from diaphragms to iliac crests (140 kV, 129 mA, 8 mm slice, pitch 1.5) and a portal phase acquisition from diaphragms to symphysis pubis (140 kV, 129 mA, 8 mm slice through liver, 10 mm slice through abdomen and pelvis, pitch 1.5, 100 mls Iopromide 300 mgI/ml, scan delay 60 seconds). The unenhanced and enhanced scans were reviewed individually and at random, blinded to patient details. The number, size, position and metastatic potential of any nodal or liver lesion detected was compared.

Results: All liver and nodal lesions identified on the unenhanced scans were more accurately delineated and characterised on the portal phase scans. No additional lesion or significant information was identified on the unenhanced scans that could have influenced the staging or clinical management in the patients analysed. Minor renal and pancreatic parenchymal calcification was more clearly identified on the unenhanced scans but this had no influence on staging or subsequent management.

Conclusion: Unenhanced liver spiral CT offered no significant additional information when used in conjunction with portal phase scans in the staging protocol in our series. The audit loop was closed with the introduction of a modified staging scan protocol including the portal phase scan only.

B-0085 11:30

Changes of the apparent diffusion coefficient measured with magnetic resonance imaging in patients with primary rectal carcinoma during a course of combined chemoradiation

C. Kremser[1], W. Judmaier[1], P. Hain[1], A. DeVries[1], J. Griebel[2], P. Lukas[1]; *[1]Innsbruck/AT, [2]Munich/DE*

Purpose: To study changes of the apparent diffusion coefficient (ADC) measured with magnetic resonance imaging (MRI) in patients with primary rectal carcinoma during a course of combined chemoradiation.

Materials and methods: The study was performed on patients (n = 7) with primary rectal carcinoma (cT3) undergoing preoperative chemoradiation. During therapy each patient underwent MRI on a weekly basis. For diffusion imaging EPI sequences with different diffusion weighting were applied. On the obtained ADC maps the tumor was segmented and the mean of the ADC values and ADC histograms were calculated. Subsequent resection of the tumors allowed for a correlation with pathological classification.

Results: In 4 patients tumor T-downstaging and in 3 patients no downstaging was observed. During the course of combined chemoradiation a sligth increase of the mean ADC values was seen within the first week after onset of therapy followed by a decrease between the first and third week and a slight reincrease during the fourth week. The final mean ADC value after therapy was significantly lower as the pre-therapy value. For the ADC histograms a slight difference between the patient group showing T-downstaging and the group without downstaging was observed before therapy. The difference disappeared during the course of therapy.

Conclusions: It could be shown that MR diffusion imaging is able to detect changes of tumor ADC values during the course of combined chemoradiation reflecting biological changes within the tumor tissue. Further studies will be necessary to prove the possible value of totally noninvasive ADC imaging on predicting therapy outcome.

B-0086 11:40

Value of high-resolution MRI in differentiation between local recurrency and scar tissue in patients with rectosigmoidal carcinoma

D. Dinter, S.J. Diehl, R. Hofheinz, J. Gaa, M. Georgi, C. Düber; *Mannheim/DE*

Purpose: Evaluation of high-resolution MRI in differentiation between local recurrence of carcinoma and scar tissue in patients with a history of rectosigmoid carcinoma.

Method and materials: During 24 months, 48 patients with suspected recurrence of rectosigmoid carcinoma were investigated in a 1.0 T scanner (Magnetom Harmony). The time interval between initial operation and MRI examination ranged from 12 to 174 months. Diagnosis was proven by resection or biopsy (n = 23) and by follow-up examination (n = 25). The MRI protocol consisted of T1w sequences with/without fat saturation before and after application of contrast media and T2w TSE sequences and turbo inversion recovery (TIRM) sequences using a high resolution technique (matrix of 512). Signal intensities of lesions in relation to muscle and fat were measured as well as the relative increase of the signal intensity after the application of contrast media.

Results: Local recurrence was found in 29 patients and scar tissue in 19 patients. T1w sequences before contrast application showed no significance differences between scar tissue and recurrence, whereas there was evidence of higher increase of signal intensity in recurrence after the application of contrast media (without FS: 93 %, with FS: 79 %) in relation to scar tissue (without FS: 81 %, with FS: 12 %). T2w images and TIRM images showed significantly higher signal intensity in local recurrence compared to scar tissue.

Conclusion: High resolution MRI using relative increase of signal intensity after application of contrast media and the relationship between signal intensity of lesion to muscle, is a useful examination for differentiation between local recurrence and scar tissue.

10:30–12:00 **Room H**

Interventional Radiology

SS 209a

Aorto-iliac disease: Stents and stent grafts (1)

Chairpersons:
A. Adam (London/GB)
B.M. Plavsic (New Orleans, LA/US)

B-0087 10:30

Early and mid-term results of endovascular stent treatment (EST) of thoracic aorta diseases

G. Napoli, G. Gavelli, P. Bertaccini, F. Fusco, M. Favali, L. Lovato, R. Fattori; *Bologna/IT*

Purpose: To state the reliability of endovascular procedure in the treatment of thoracic aorta diseases.

Materials and methods: The series reported consists of 40 patients (pts) who underwent endovascular stent treatment (EST) between July 1997 and September 2000. Different kinds of thoracic aorta pathology were treated: traumatic aortic rupture (13 pts), type B aortic dissection (11 pts), intramural hematoma (2 pts) and atherosclerotic aneurysm (14 pts). The mean age of the pts was 58.08 ± 15.3 years and 75 % of patients were classified into ASA class III – V. MRI and/or spiral CT scan were performed before the procedure, in order to define the anatomic characteristics of the lesions. Spiral CT was then performed at 1, 3, 6, 12 months and yearly thereafter to evaluate early and long term results.

Results: The procedure was successful in 39 pts. Nor death neither complications related to the procedures occurred. 4 cases of leakage was observed at first follow-up. One case was converted to surgery while the remaining three sealed spontaneusly at 3 months. A two years follow-up is complete in 20 cases showing the progressive reduction in size of the aneurysms.

Conclusions: Mid-term results indicate that EST can be considered a reliable therapeutic option in the management of patients with thoracic aorta diseases.

B-0088 10:40

Endoluminal treatment of AAA: Evaluation of complications in single center with 3 years follow-up

M. Chiesura Corona, E. Lot, G. Tropeano, D. Miotto, G. Feltrin; *Padova/IT*

Purpose: To evaluate the complications and clinical outcome associated with treating AAA treated with endoluminal endoprostheses.

Materials and methods: From 1997 to 2000, 43 patients with atherosclerotic AAA were treated. The mean dimensions of the aneurysms were: proximal neck diameter 22 mm (range 20 – 29), neck length 28 mm (10 – 45); aneurysm diameter 47 mm (38 – 80), aneurysm length 65 mm (35 – 130). 42 aorto-bifemoral endoprostheses and one aorto-aortic device from various materials were used. Follow up: CT at 7 days and at 3, 6 and every 12 months.

Results: Technical success 95 %. Primary patency 93 %. Two perioperative iliac limb thromboses occured; one was treated percutaneously and one surgically. An asymptomatic iliac limb thrombosis was detected at 12 months follow-up. The secondary assisted patency was 95 %. The aneurysm was excluded in in 37/40 patients (92 %). There were three endoleaks: one was a primary major leak in a patient not suitable for further treatment, who died at 18 months; one primary minor leak spontaneously resolved at three months; one secondary, PTCA-related leak was treated with iliac extension. There was one renal failure, after an implantation difficulty related to "C" arm rupture: one renal artery was occluded by the endoprosthesis; the contralateral artery was immediately stented, with progressive recovery. The periopertaive mortality (not device-related) was 5 %. In 30 patients with follow up longer than 6 months, AAA diameter reduction was observed in 15 patients (50 %).

Conclusions: Complications were observerd mainly during the first 15 implants, and are probably related to the learning curve. Perioperative mortality appears related to associated conditions. Mid-term aneurysmal sac exclusion, volume reduction and endoprosthesis patency are encouraging; long-term follow-up data and further device improvement are needed.

B-0089 10:50

Colour Doppler ultrasound in follow-up of AAA treated with stent-grafts

M. Szczerbo-Trojanowska, T. Jargiello, R. Pietura, J. Michalak, F. Brakowiecki, T. Zubilewicz; *Lublin/PL*

Purpose: To evaluate an efficacy of colour Doppler ultrasound in follow-up of AAA treated with stent-grafts in imaging of endoleaks, vessels patency and thrombus formation in the anerysmal sac.

Materials and methods: Twenty six male patients in the age of 49 – 78 years with aortic arteriosclerotic aneurysms were treated with endovascular stent grafting. All aneurysms were infrarenal. In 5 patients Vanguard II stent-grafts, in 11 patients Zenith stent-grafts and in the remaining 10 patients Endologix stent-grafts were implanted. Follow-up included clinical examination, Doppler USG, helical CT and angiography.

Results: Stent-grafts were placed successfully in all patients. There were no complications of the procedures. The follow-up ranges from 5 to 30 months. Endoleaks were diagnosed in 2 patients. In one there was a leak in a distal attachment side diagnosed with colour Doppler USG 2 days after procedure. Colour Doppler USG confirmed that it sealed spontaneously within one month. The other patient developed type II leak after a month which was followed with colour Doppler USG until its' spontaneous resolution in 2 months.

Conclusions: Colour Doppler USG proved useful, non-invasive tool in follow up of the patients subjected to abdominal aorta stent-grafting.

B-0090 11:00

Treatment of aortoiliac aneurysms with use of customized stent-grafts in 230 cases

P. Cluzel, F. Koskas, J.-D. Singland, C. Camiade, E. Kieffer, P.A. Grenier; *Paris/FR*

Purpose: To describe our experience with the use of a custom stent-graft for the treatment of abdominal aorto-iliac aneurysms.

Materials and methods: From January 1996 to September 2000, 230 aorto-iliac aneurysms were selected to be treated using custom stent-grafts of different design. Custom stent-grafts were constructed with Gianturco Z stents sutured together and covered with polyester (Twillweave, Vascutek, Innachinnan, Scotland). There were 2 occlusive devices, 39 tube stent-grafts, 5 bifurcated stent-grafts, 145 aorto-uni-iliac stent-grafts and 39 hybrid stent-grafts. In the last two cases, the contralateral iliac artery was occluded by a blocking device or a suture and a femoro-femoral bypass was performed.

Results: Seven patients (3 %) were converted to standard open repair. There were 27 primary endoleaks (11 %) seen on spiral CT before discharge and 8 secondary endoleaks (3 %). 10 of the 27 primary endoleaks sealed spontaneously, and 10 required a secondary procedure (8 embolizations and 2 additional covered stents). Eleven patients (5 %) died during the follow-up period, four by myocardial infarction and one by multi organe failure in the perioperative period, other deaths were not related to stent-graft placement.

Conclusion: Custom stent-grafts for the endovascular treatment of abdominal aorto-iliac aneurysms achieve good results. Longer follow-up is needed for the device.

B-0091 11:10

Endoluminal treatment of acute aortic dissections with stent-grafts

P. Schedlbauer, H.A. Deutschmann, P. Oberwalder, K. Tiesenhausen, J. Tauss, K.A. Hausegger; *Graz/AT*

Purpose: To evaluate the feasibility of endoluminal stent-grafts in the treatment of acute aortic dissection.

Material and methods: 5 patients with acute aortic type-B dissections and one with a type-A dissection were treated with endoluminal stent-grafts. In 4 patients the distance of the primary tear to the left subclavian artery (LSA) was < 0.5 cm and the covered portion of the stent-graft was placed across the origin of the LSA in these patients (1x transpositon of the left subclavian artery). Talent tube grafts and Excluder stent-grafts were used.

Results: Stent-graft insertion with sealing of the primary tear was successful in all patients. Left arm perfusion was preserved via a subclavian steel phenomenon in the patients in whom the stent-graft covered the origin of the LSA. Thrombosis of the false thoracic lumen occurred in all patients. In one patient the false lumen of the abdominal aorta thrombosed completely, in another diameter increased in size. In 4 patients the condition of the abdominal aorta remained unchanged. As complications we observed a segmental renal infarct in one and a secondary distal aneurysm in another patient.

Conclusion: Endoluminal treatment of acute type-B aortic dissections is feasible. However, further studies have to be done to evaluate its therapeutic potential fully.

B-0092 11:20

Retrograde lumbar embolization after endoluminal repair of AAA: Technique and results

R. Cioni, I. Bargellini, C. Vignali, P. Petruzzi, V. Napoli, P. Vagli, C. Bartolozzi; *Pisa/IT*

Purpose: To evaluate the role of lumbar embolization in the treatment of endoleaks occurring after endoluminal repair of abdominal aortic aneurysm (AAA).

Materials and methods: From November 1998 to July 2000, 68 patients underwent endoluminal repair of AAA. Follow-up included duplex sonography and CT Angiography (CTA). Endoleaks supplied by lumbar arteries were detected in 9 patients (13 %), either at discharge (n = 6) or after 6 – 12 months (n = 3). Embolization was performed in 5/9 patients (bilaterally in 2 cases). In 5 procedures, the feeding lumbar artery was selectively catheterized (coaxial microcatheter) with a retrograde approach through the hypogastric artery and embolized at the ostium. In 2 cases, collateral vessels of the iliolumbar artery were occluded from the hypogastric artery. After the procedure, all patients underwent CTA.

Results: Embolization was performed in all cases of late endoleaks (n = 3), and in case of early endoleaks persisting at 3 months follow-up (n = 2). Four patients were not treated because of spontaneous absorption of the leak (n = 2) or short follow-up (n = 2). Successful embolization was obtained in 5 procedures. In those cases (n = 2) in which selective catheterization of the lumbar artery could not be performed, requiring embolization of the afferent collateral vessels, a reduction of the leak was obtained, with complete absorption after 1 month in 1 case. No complications occurred after embolization.

Conclusions: Retrograde selective lumbar embolization represents a safe and effective treatment. Though less effective, embolization of hypogastric collateral vessels allows a reduction of the leak.

B-0093 11:30

Endoluminal repair of abdominal aortic aneurysm: Mid-term results

C. Vignali, I. Bargellini, R. Cioni, P. Petruzzi, E. Neri, A. Cicorelli, C. Bartolozzi; *Pisa/IT*

Purpose: To evaluate the role of endovascular repair in the treatment of abdominal aortic aneurysm (AAA).

Materials and methods: Between November 98 and August 2000, 70 patients (68 male, mean age 70) underwent endovascular repair of AAA. Preprocedurally, patients were evaluated by means of CT Angiography (CTA). Several types of prostheses were used; 64 were bifurcated and 6 straight. The procedure was performed in the surgical suite, in general anaesthesia, with a bilateral femoral approach. On follow-up, duplex sonography and CTA were performed at discharge, at 3, 6, and 12 months and annually thereafter.
Results: Technical success was achieved in 66/70 patients (3 immediate and 1 late surgical conversions). At discharge, endoleaks were detected in 14 patients: 4 spontaneously solved, 6 persisting on follow-up, not treated, 4 successfully treated (angioplasty in 1 case, IMA plus lumbar embolization in 2, IMA embolization plus angioplasty in 1). Late endoleaks occurred in 5 patients (1 at 6 months, 3 at 12 months), and were successfully treated (extender cuffs in 2 patients, lumbar embolization in 3). At 3 months follow-up, a stenosis of an iliac branch occurred in one patient, and was solved by angioplasty. At 1-year follow-up, a significant reduction of the aneurysmal sac diameter occurred in 28/32 patients (87.5 %).
Conclusions: Endoluminal repair of AAA represents an effective alternative to open surgery; relatively high rate of complications occurring on follow-up suggests that this procedure should be reserved to accurately selected high-risk patients and patients refusing surgical treatment.

B-0094 11:40

Renal infarction following "bare-spring"-overstenting after endovascular repair of abdominal aortic aneurysm
S. Krämer, J. Görich, H. Seifarth, R. Pamler, J. Bühring, H.-J. Brambs; *Ulm/DE*

Objective: The incidence of renal infarction after endovascular repair of aortic aneurysm has yet not drawn wide interest. Aim of the prospective evaluation was to determine the incidence of renal infarction after stent graft placement and to correlate it with "bare-spring" overstenting.
Materials and methods: 130 patients were treated by endovascular technique for exclusion of aortic aneurysm and followed prospectively by spiral-CT and clinical evaluation every 3 months for the first year and biannually thereafter. Included in the study were patients with infrarenal placement and a follow-up of at least 12 months (n = 99). Axial slices, MPR and MIP reconstructions were evaluated by two radiologists in consensus. Statistical analysis was performed by χ^2 testing. In patients with proven renal infarction pre- and postoperative kidney function was compared by retention parameters.
Results: 193 renal arteries could be evaluated in 99 patients (5 nephrectomies). Partial or complete "bare-spring" overstentig was found in 69 (35.75 %) compared to 124 renal arteries without covering (64.25 %). In 13 patients small renal infarctions were found. The incidence in the series of overstenting was 8.89 % and not significantly higher than 5.64 % in the collective without covering. In all patients with detected infarctions there were no alterations of kidney function.
Conclusion: "Bare-spring" overstenting does not rise the rate of renal infarctions after endovascular repair of aortic aneurysm compared to strict infrarenal placement. Transrenal placement therefore is possible in patients with few alternatives to the endovascular therapy. A possible cause for renal infarctions are manipulation and mircoemboli during the implantation procedure.

B-0095 11:50

CT angiography follow-up of abdominal aortic endoprostheses
I. Bargellini, E. Neri, C. Vignali, P. Petruzzi, R. Cioni, C. Bartolozzi; *Pisa/IT*

Purpose: We aimed to determine the outcome of abdominal aortic endoprostheses at 12 months follow-up with CT angiography (CTA).
Materials and methods: A series of 53 patients with abdominal aortic aneurysm treated percutaneously by means of stent-graft implantation, underwent single-slice CTA follow-up, 1 month (all cases), 3 months (42 cases), 6 months (36 cases) and 1 year (20 cases) after the procedure. Unenhanced, arterial and venous scan were obtained with 3 mm collimation and 1 mm reconstruction interval. CTA data sets were analyzed on independent workstation; multiplanar reformations (MPR) and maximum intensity projections (MIP) were used in addition to native images review. Angiography was additionally performed, in case of detected endoleaks at CTA.
Results: CTA revealed 13 cases (24 %) with endoleak, 7 cases (13 %) with air bubble into the aneurysmal sac, 1 case of stenosis of an iliac branch. All endoleaks were detected by CTA (sensitivity 100 %). In 1 case the arterial phase failed to demonstrate a small endoleak (1 false negative), revealed by the venous phase. CTA failed to demonstrate the type of endoleak in 3 cases (23 %); among these, 2 were classified as type II endoleaks, supplied by the inferior mesenteric artery; in both cases the endoleak was solved by means of angioplasty of the proximal neck (type I). In the other case, the endoleak was interpreted at CTA as a proximal type I, while the treatment was represented by the embolization of a lumbar artery (type II).
Conclusions: CTA can be proposed as the elective method on follow up of endoprostheses.

10:30–12:00 **Room I**

Abdominal and Gastrointestinal

SS 201c

Abdominal imaging (1)

Chairpersons:
M.S. Joshi (Mumbai/IN)
M. Kormano (Turku/FI)

B-0096 10:30

Multislice spiral CT of the abdomen: Comparison of different scan protocols for routine staging CT
J. Weßling, R. Fischbach, K. Ludwig, K.U. Jürgens, T. Link, W. Heindel; *Münster/DE*

Purpose: To evaluate different spiral CT scanning parameters for routine staging examination of the abdomen in oncologic patients using a multi-detector CT scanner with regard to radiation exposure.
Methods and materials: Examination of 40 patients in 4 groups on a multi-sclice CT scanner (Somatom volume Zoom, Siemens, Forchheim). Detector configuration (4 × 2.5, 4 × 5 mm) and pitch (3 and 5) were varied. Tube voltage (120 kV), effective tube current (160 mAs) and contrast injection parameters (1.5 ml/kg KM, flow 2.5 ml/s, scan delay 80 s) were kept constant. Axial images were assessed by 3 radiologists regarding spatial resolution, organ delineation, artifacts, and overall image quality. A score was calculated for each examination. Comparisons were performed using nonparametric tests.
Results: Image detail with 4 × 2.5 detector configuration and pitch 3 (scan time of 28 s) was found to be superior compared to pitch 5. However, subjective overall impression did not differ significantly for these protocols, while shortening the scan time to 17 s. Image scores were significantly higher for a 2.5 mm versus a 5 mm detector configuration (pitch 3: $p = 0.03$, pitch 5: $p = 0.02$). Significantly reduced image quality ($p < 0.05$) was observed using a 5 mm detector configuration with a pitch of 5 (scan time 9 s). The pitch independent average effective dose was 9 % higher using the smaller detector configuration (9.9 mSv vs. 10.9 mSv).
Conclusion: For routine staging CT of the abdomen use of a 4 × 2.5 mm detector configuration with a pitch between 3 and 5 is recommended.

B-0097 10:40

Retroperitoneal mesenchymoma: Imaging findings and criteria of malignancy
J.V. Sheikh, V.P. Kharchenko, P.M. Kotlyarov; *Moscow/RU*

Purpose: To determine criteria of malignancy on computed tomographic (CT), ultrasonographic (US), magnetic resonance (MR), and angiographic images of retroperitoneal mesenchymoma with emphasis on CT findings.
Materials and methods: 31 CT, 31 US, 15 MR and 16 angiography studies were obtained in 31 patients with pathologically proven retroperitoneal mesenchymoma (12 patients with malignant mesenchymoma).
Results: On CT and US images tumors were larger than 10 cm (17 %), heterogeneous and well-circumscribed (14 %) with heterogeneous enhancement on contrast-enhanced T scan (11 %). Tumors contained calcifications (n = 10 %). Tumors were hypointense on T1-weighted MR images (22 %) and heterogeneous on T2-weighted MR images (21 %).
Conclusions: The radiological criteria of malignancy of mesenchymoma are heteroechogenicity, multynodularity, poorly circumscribed border and signs of arterial blood flow on US images, heterogeneous enhancement on contrast-enhanced CT scan, heterogeneous hyperintensive appearance on T2-weighted MR images, dislocation and compression of major vessels and invasion of the liver and kidneys.

B-0098 10:50

Requests for body computed tomography: Increasing workload, increasing indications and increasing age

A.P. Toms, C.J.C. Cash, S.J. Linton, E. Hunt, B. Housden, A.K. Dixon; *Cambridge/GB*

Purpose: To examine changes in the age profile of patients referred to a department of radiology.
Materials and methods: Data was obtained from written and computerised records at Addenbrooke's Hospital, Cambridge, UK for the period 1988 to 2000.
Results: The total number of examinations has risen in all age groups. Between 1994 and 1999 there was a 6 % rise in workload (from 114 938 to 121 938 examinations per annum) in the under 60 s and a 16 % rise (from 51 869 to 60 337) in the over 60 s ($p < 0.001$). In particular between 1988 and 1998 there has been a 41 % rise from 1824 body CT examinations per annum in the under 60 s to 2568. This compares with a 130 % increase in the over 60 s from 1104 to 2544 ($p < 0.01$). The local demographic profile has not changed significantly over this period.
Conclusion: The considerable rise in the number of CT examinations in elderly patients refutes any suggestion of a discriminatory policy on the basis of age. Age alone is not a barrier to effective imaging. With increasingly effective intervention and therapy in the elderly the need for imaging in this group of patients is likely to continue to grow out of proportion to demographic changes. These factors need to be included when planning the provision of imaging services in the future.

B-0099 11:00

Castleman's disease: CT and MR features of 12 cases and review of the literature

S.-H. Shen; *Taipei/TW*

Purpose: To characterize and review the image features of Castleman's disease.
Materials and methods: Twelve patients were proved to have Castleman's disease during a period of nine years. Eight patients were of unicentric form and four of multicentric form. From the literature review, additional 29 cases with imaging studies were also enrolled. All the imaging and reports were reviewed for analysis.
Results: The unicentric form presented as well-defined soft tissue mass, most often located within the abdomen. Thirty six percent of them showed calcification. The calcification of the intraabdominal lesions was obvious with characteristic curvilinear or arborizing pattern. After contrast injection, 47 % of Hyaline-vascular type showed strikingly strong enhancement, which has never been observed in plasma cell type. MR imaging of unicentric form lesion revealed iso- or slightly high signal intensity on T1 weighted imaging and high signal intensity on T2 weighted imaging. In multicentric form, CT revealed generalized lymphadenopathy and hepatosplenomegaly.
Conclusion: The pattern of calcification and contrast enhancement are clues for the diagnosis of unicentric form of Castleman's disease. For these patients, CT is the best imaging modality since it can demonstrate calcification better than MR. Radiologically, the multicentric form Castleman's disease can not be distinguished from other lymphoproliferative disorders.

B-0100 11:05

The value of CT in blunt abdominal trauma management when the only finding is intra-peritoneal fluid

S. Deftereos, P. Argyropoulou, G. Alexiadis, S. Foutzitzi, J. Manavis; *Alexandroupolis/GR*

Purpose: The aim of this study was to estimate the clinical significance of intra-peritoneal fluid seen on CT scans in patients with otherwise normal findings.
Materials and methods: We retrospectively analyzed the CT examinations of 75 patients with blunt abdominal trauma with presence of intra-peritoneal fluid as a sole finding in CT. The amount and location of fluid were compared between the patients who required exploratory laparotomy and those who where managed conservatively.
Results: The location of fluid was determined and the amount in each location was categorized (minimal, moderate, marked). The total fluid volume in 62 (83 %) patients was small, in 9 (12 %) was intermediate and in the rest 4 patients was marked. 52 patients had fluid in one location, 15 in two and 8 in three locations. Patients requiring laparotomy had a higher total fluid volume score and larger amounts in the upper abdomen.
Conclusions: CT is a valuable technique for examining patients with blunt abdominal trauma as they enable rapid and accurate noninvasive diagnosis of visceral injuries and detection of intra-peritoneal fluid (e.g. hemoperitoneum). Patients with blunt abdominal trauma, who have small amount of intra-peritoneal fluid on CT (sole abnormality) may be treated conservatively. Patients with even a small quantity of mesenteric fluid may benefit from peritoneal lavage. Intermediate and large amounts of fluid have a higher likelihood of being associated with bowel or mesenteric injury.

B-0101 11:10

Comparison between tissue harmonic imaging and conventional US in the evaluation of abdomino-pelvic pathologic findings

D. Cioni, L. Crocetti, R. Lencioni, F. Donati, C. Franchini, M. Perri, C. Bartolozzi; *Pisa/IT*

Purpose: To compare tissue harmonic imaging (THI) with conventional US in the evaluation of abdomino-pelvic pathologic findings.
Material and methods: Sixty-eight abdominal or pelvic abnormalities detected in 42 consecutive patients were evaluated with both conventional US and THI. The examined pathologies included: nodular lesions of liver (n = 13), pancreas (n = 2), spleen (n = 2); fibromyoma of uterus (n = 3); abdominal or pelvic lymphoadenopaties (n = 7); cystic lesions of liver (n = 5), kidney (n = 12), pancreas (n = 2), ovary (n = 3); cholelithiasis and bile ducts lithiasis (n = 10), renal and ureteral stones (n = 6); bladder diverticula (n = 2), bladder tumor (n = 1). US examinations were performed with state-of-the art equipment and a 3.5 MHz probe. Conventional US and THI images were reviewed and overall image quality, lesion conspicuity, quality of lesion delineation and confidence in diagnosis were assessed on a 4-grade scale.
Results: The overall image quality of THI images was higher than that of conventional US (mean score, 3.19 vs 2.41). The highest difference between the two methods was observed in biliary and renal stones (3.59 vs 2.15). Lesion conspicuity and quality of lesion delineation reached a higher score in THI images (3.09) than in conventional US images (2.68). In contrast, confidence in diagnosis was similar in either THI or conventional US (3.15 vs 3.09).
Conclusions: THI is superior to conventional US in terms of overall image quality, lesion conspicuity and quality of lesion delineation.

B-0102 11:20

Cystic Fibrosis: Abdominal imaging findings

G. Tognini, F. Ferrozzi, M. Pedrazzini, S. Armaroli, P. Pavone; *Parma/IT*

Purpose: Cystic fibrosis (CF) is an autosomal recessive disorder characterized by an abnormal exocrine gland function. The lung represents the most frequently and seriously affected organ. The purpose of this study was to describe the spectrum of the abdominal involvement of CF.
Materials and methods: We reviewed US, CT and MRI examinations of 250 patients (143 M, 107 F, mean age 32 years) with cystic fibrosis. All patients were evaluated for pancreatic function. Pulmonary status was also evaluated in each patient by means of the Shwachman and Kulckzycki scoring scale.
Results: 212 patients showed pancreatic abnormalities: complete fatty replacement (105), focal fatty replacement (12), glandular atrophy (95). Hepatobiliary abnormalities were as follows: steatosis (130), hepatomegaly (125), biliary cirrhosis (2), litiasis (23), splenomegaly (60), portal hypertension (44). Gastrointestinal complications were demonstrated in 10 patients: meconium plug syndrome (3), intussusception (5), fibrosing colonopathy (2).
Conclusions: Diagnostic imaging demonstrated its validity in the clinical assessment of patients with cystic fibrosis.

B-0103 11:30

Diabetes mellitus: CT findings of unusual complications related to the disease

G. Tognini, F. Ferrozzi, M. Pedrazzini, E. Spaggiari, P. Pavone; *Parma/IT*

Purpose: The aim of our study was to assess the role of CT in characterizing unusual complications of diabetes.
Materials and methods: We retrospectively reviewed CT findings of 180 diabetic patients, among whom 27 patients (18 males, 9 females, mean age 67 years) showed complications. These were the complications and their distribution: subcapsular focal fatty liver (3), emphysematous cholecystitis (4), renal abscess (7), perirenal abscess (4), emphysematous pyelonephritis (4), emphysematous cystitis (1), gaseous gangrene (4).
Results: Subcapsular fatty infiltration of the liver is exclusively seen in insulin dependent diabetics receiving intraperitoneal insulin through peritoneal dialysis. Unenhanced CT showed a subcapsular area with negative HU numbers. In emphysematous cholecystitis CT demonstrated air in the gallbladder wall and lumen. In renal and perirenal abscesses CT showed round collections with low HU numbers and capsules demonstrating high attenuation numbers. In emphysematous pyelonephritis CT demonstrated the presence and the extension of perirenal gas.

In emphysematous cystitis CT showed gas in the bladder wall and lumen. In gaseous gangrene CT demonstrated necrotic tissue and gas in the soft tissues. In Fournier form the scrotum is involved with normal testes.
Conclusion: CT proved useful in characterizing some unusual complications related to diabetes.

B-0104 11:40

Diagnostics of the early displays of the metabolic syndrome
N.N. Kizimenko, I.V. Karetin, J.N. Kizimenko; *Krasnodar/RU*

Purpose: The use of computer tomography of the organs of the abdominal cavity for diagnostics of the latent display of metabolic syndrome.
Methods and materials: A standard examination of the organs of the abdominal cavity was carried out in 143 patients at the age of 25 – 55 years, among them were 64 women (44.7 %) and 79 men (55.2 %). We measured the cross-section area of the abdominal cavity and determined its average value on the 10 obtained scans. Then, using the function of subtraction from total density, we detected the areas appropriate to intra-abdominal adipose tissue, determined their total acres and struck the average on each of these sections. After determining the average percentage ratio of the area of intra-abdominal adipose tissue to the average cross-section area of the abdominal cavity we obtained different values: from 3 % to 26.4 %. Those patients who had this correlation more than 10 % were examined for insulin in blood.
Results: The rise of the insulin level in blood was detected in those patients who had the ratio of intra-abdominal adipose tissue acre to the cross-section of the body more than 14 %. There were 37 (25.8 %) such patients of the total amount.
Conclusion: Application of this method during the standard examination of the organs of the abdominal cavity can give additional information and be used as a screening method of diagnostics of the initial displays of the metabolic syndrome.

B-0105 11:50

Multislice computed tomography (MSCT): Value of a very early arteriographic acquisition for evaluating branches of the upper abdominal aorta as an adjunct to standard CT in patients with suspected liver disease
F. Zandrino[1], L. Benzi[1], L. Ferretti[1], M. Calabrese[2], F. Musante[1]; *[1]Alessandria/IT, [2]Genoa/IT*

Purpose: To assess the clinical value of an early arteriographic scan in the evaluation of patients with suspected primary or metastatic liver disease using MSCT.
Methods and materials: In 42 consecutive patients undergoing MSCT (Light Speed, General Electrics, Milwakee, WI/USA) for liver disease, a very early acquisition was performed before 25 s, 70 s, and delayed scans. Technical parameters: 2.5 mm collimation; table speed 15 mm/s; 120 kVp; 300 mAs; 10 s scan time; craniocaudal acquisition direction; 16 s delay after contrast injection. Acquisition volume was focused to image celiac trunk, hepatic, splenic, and superior mesenteric (SMA) arteries. 140 ml of iodinated contrast agent (Iomeron 350, Bracco, Milan, Italy) were injected i.v. at 4 ml/s. Axial, multiplanar reformatted, and maximum intensity projection images were evaluated.
Results: In 4/42 patients images were not diagnostic for delayed arterial enhancement. In 38/42 optimal image quality was obtained. In 8 patients vascular abnormalities were detected: 2 right hepatic arteries originating from the SMA; 2 stenoses of the SMA; 1 independent origin of the hepatic and splenic arteries; 1 large arteriovenous fistula; 1 stenosis of the celiak trunk; 1 aneurysm of the common hepatic artery.
Conclusion: This technique could add important diagnostic information to the surgeon or the interventional radiologist.

B-0106 11:55

Lipodystrophy syndrome in HIV-infected patients: Evaluation with helical CT
A. González-López, I. Pedrosa, R. Rodríguez, V. Estrada; *Madrid/ES*

Purpose: To evaluate changes in fat distribution in HIV patients with lipodystrophy syndrome (LD) after replacement of protease inhibitor (PI) therapy by Efavirenz (EFV).
Methods and materials: Inclusion criteria included: lipoatrophy phenotype, previous treatment for a minimum of 6 months with PI-containing regimen, viral load < 500 copies/ml, and CD4 > 150/mm^3. A helical CT study (5 slices at L5 level and 5 slices 20 cm distal to the femoral head) was performed with 5 mm collimation, and pitch 1, at the time of the change of PI treatment to EFV. A follow-up CT examination was performed in 26 patients after 6 months of EFV therapy. Total volume adipose tissue in the abdomen (TAT) and thigh (TF) was measured by applying a threshold in Hounsfield units (-50 to -150). Visceral adipose tissue (VAT) volume in the abdomen was calculated by subtracting subcutaneous fat (SAT) from TAT with a trackball.
Results: Thirty nine patients were included (33 male, 6 female) with average age of 44 years. HIV transmission was sexual in 29 patients (75 %). Measures in initial CT study were: TAT = 465 mm^3, VAT = 269 mm^3, VAT/TAT = 0.56 for the abdomen and TF = 57 mm^3 for the thigh. Measures in follow-up CT study were: TAT = 462 mm^3, VAT = 246 mm^3, VAT/TAT = 0.54 for the abdomen and TF = 67 mm^3 No statistical significant difference between initial and follow-up measures were found.
Conclusions: No differences in fat distribution after change in drug therapy were found. CT provides a practical method for measuring fat volume. Relation between visceral and subcutaneous adipose tissue was easily calculated.

10:30–12:00 **Room K**

Interventional Radiology

SS 209b

MR-guided thermal tumor ablation

Chairpersons:
G.W. Kauffmann (Heidelberg/DE)
C.L. Zollikofer (Winterthur/CH)

B-0107 10:30

Open MRI guided laser-induced interstitial thermotherapy of the liver with a temperature controlled diode laser
W.A. Wohlgemuth, G. Wamser, K. Bohndorf; *Augsburg/DE*

Purpose: The aim this prospective clinical study was to evaluate the safety and efficacy of LITT of liver metastases in an open MR-scanner, which allows for puncture and therapy monitoring in one session without the need for repositioning.
Patients and methods: Five patients with seven liver metastases were treated in 15 laser sessions. In each session, three to eight laser applications were performed with a standardized treatment protocol to a total of 91 applications. A diode laser with an incorporated temperature feedback loop and a diffuser-tip (1.8 mm cross section) was used. The intervention was performed in a superconducting, open MR scanner at 0.35 T.
Results: The procedure was technically successful in every case. The laser fibres were inserted safely and effectively under MR Fluoroscopy. Use of a temperature feedback loop successfully avaoided carbonization of liver tissue. The temperature distribution, however, was more difficult to image (signal loss was visualized in T1w images in 40 of 91 applications). Three minor complications occurred (one pleural effusion, one pericapsular liver hematoma, and one episode of fever).
Conclusions: This study demonstrates the clinical feasibility and safety of LITT of liver metastases with temperature-controlled diode laser under open MRI guidance. The procedure is safe, effective and reliable.

B-0108 10:40

MR-guided laser treatment of liver metastases of breast cancer
M.G. Mack, R. Straub, K. Eichler, S. Zangos, M. Böttger, K. Engelmann, D. Woitaschek, T.J. Vogl; *Frankfurt a. Main/DE*

Purpose: The goal of this evaluation was the analyses of the potential of MR-guided LITT for the treatment of liver metastases of breast cancer.
Methods and materials: A total of 127 consecutive patients with an average age of 54.0 years (range 28 to 79 years) was treated. The total number of treated metastases was n = 332, ablated in 250 treatment session between June 1993 and August 2000. Survival rates were calculated using the Kaplan-Meier method. We included patients with less than 5 metastases with a maximum diameter of 5 cm. 10.4 % of the patients had recurrent metastases after surgery, 49.6 % metastases in both liver lobes, 16.8 % refused surgical resection, and 24.2 % had metastases at difficult localization for surgery.
Results: All patients tolerated the treatment well under local anesthesia and on an outpatient basis. All lesions with a maximum diameter of 5 cm could be treated with safety margin of 5 – 10 mm around the lesion. Also lesions with relationship to the liver capsule, the gall bladder and major vessels were treatable. In patients treated with LITT for liver metastases of breast cancer the mean survival was 4.3 years (95 % confidence interval 3.6 – 5.0 years). The 1 year survival rate was 97 %, the 2 year survival rate was 75 %, the 3 year survival rate was 65 %, and the 5 year survival was 34 %.

Conclusion: MR-guided LITT means a safe and effective treatment protocol for oligonodular liver metastases of breast cancer with improved survival data.

B-0109 10:50

Laser-induced interstitial thermotherapy (LITT) of liver tumors: MR-morphology of laser-induced necrosis, success and recurrence criteria

R. Straub, M.G. Mack, K. Eichler, S. Zangos, D. Woitaschek, K. Engelmann, T.J. Vogl; *Frankfurt a. Main/DE*

Purpose: To describe imaging criterias for the evaluation of laser-induced necrosis after MR-guided LITT and the definition of a response and recurrence criteria.
Material and methods: 300 patients with liver metastases of different primary turmors were prospectively treated with MR-guided LITT using a Nd-YAG laser device, liquid irrigated power laser applicators and multiapplicator technique. Post interventional follow-up was performed with contrast enhanced MRI using T2- and T1w-SE- and GRE-sequences. 1056 lesions were evaluated in the 3- and 6-months-control studies and criteria for the definition of laser induced necrosis, scarring and demarcation of local tumor recurrence were defined.
Results: Successful LITT of treated liver metastases was defined as a sharply demarcation of the necrosis in the T2-w sequence with a low SI, surrounded by a rim with high SI in the 1 day post interventional control (95.7 %). T1w-images showed increased lesion SI with hypointense, sharp border line in 89.4 % of treated lesions. Geometric shape and no contrast enhancement were observed in 92 % of successful treated lesions. Regulary in the 3- to 6-months-control lesions presented with a decrease in size.
Conclusions: MR-guided laser treatment causes typical changes of SI in the T2- and T1w-sequences. Combined with changes of lesion size assessment of tumor recurrence is possible.

B-0110 11:00

Calibration of water proton chemical shift with temperature for MR thermography during RF ablation

S. Okuda[1], K. Kuroda[2], K. Oshio[1], H. Fujiwara[1], T. Kurata[1], Y. Yuasa[1], S. Kuribayashi[1]; *[1]Tokyo/JP, [2]Kanagawa/JP*

Purpose: MR based temperature measurement is a useful technique for monitoring thermal tumor ablation. However, the accuracy of calculated temperature is controversial because of uncertainty of thermal coefficient. The purpose of this study is to calibrate water proton chemical shift change with tissue temperature during RF ablation.
Materials and methods: RF ablation (RITA medical systems) with automatic power control was performed on extracted 6 calf livers using a MR-compatible probe. The chemical shift change measured with a phase-mapping method using spoiled GRASS (TR 40 ms, TE 7.4 ms, flip angle 30, matrix 256 × 128, field of view 12 cm) was compared with corresponding tissue temperature elevation directly measured with a copper-constantan thermocouple. The image acquisition time was 5 s for a single slice. The spacial resolution was 0.47 mm in the frequency-encoding direction and 0.94 mm in the phase-encoding direction. The RF ablation was paused during acquisition of MR images.
Results: Linear calibration with a regression coefficient of –0.0110 ppm/°C was obtained under 50 °C of absolute temperature. However, between 50 °C and 80 °C, temperature elevation (y) and chemical shift change (x) had different relationship ($y = -0.0016x - 0.2549$).
Conclusion: The relationship between temperature elevation and chemical shift change was changed around 50 °C. Temperature elevation above 50 °C should be calculated with different coefficient from one under 50 °C.

B-0111 11:05

Complications and management of complications of MR-guided laser-induced thermotherapy (LITT): Experience after 7184 laser applications in 1981 lesions

M.G. Mack, R. Straub, K. Eichler, K. Engelmann, S. Zangos, M. Böttger, T.J. Vogl; *Frankfurt a. Main/DE*

Purpose: To evaluate complications and local tumor control rate associated with MR-guided LITT of liver metastases.
Methods and materials: Between June 1993 and August 2000 a total of 7148 laser applications were performed in 1981 lesions in 705 consecutive patients in 1653 treatment sessions. The complications of the procedure were evaluated by clinical examination and MR/CT imaging. Local control of tumor was evaluated by unenhanced and contrast-enhanced follow-up using T1 and T2 weighted SE and GRE sequences at 3-monthintervals following treatment.
Results: The overall rate of complications was 7.5 %. The rate of clinically relevant complications was 1.3 %. The most common complication of LITT treatment was reactive pleural effusion (7.3 %), necessitating drainage in 0.9 %. Intrahepatic abscess was observed in 0.4 % and one pleura empyema in 0.1 %, both treated by drainage. Subcapsular hematoma was found in 3.1 %, intrahepatic bleeding in 0.1 % and intraabdominal bleeding in 0.2 %; none of these required treatment. Delayed complications: local infection in 0.2 % and bile duct injury in 0.1 %. Three patients died within 30 days, but in only one case was the death possibly LITT-related. MRI demonstrated that the local tumour control rates were 99.3 % at 3 months and 97.9 % at 6 months after laser treatment.
Conclusion: MR-guided LITT is a safe therapy method in patients with liver metastases, results in reliable local tumour control and improves clinical outcomes.

B-0112 11:15

MR-guided LITT in colorectal liver metastases: An alternative to surgery?

M.G. Mack, K. Eichler, R. Straub, S. Zangos, M. Böttger, D. Woitaschek, K. Engelmann, T.J. Vogl; *Frankfurt a. Main/DE*

Purpose: Evaluation of survival rates in patients with colorectal liver metastases treated with MR-guided laser induced thermotherapy (LITT) compared with historical surgical data.
Methods and materials: 1203 metastases were treated in 393 consecutive patients with an average age of 60.8 years were treated between June 1993 and August 2000. Survival rates were calculated using the Kaplan-Meier method. Analyses of complications was based on follow-up MR imaging and clinical examination
Results: After surgical resection of colorectal liver metastases show 5-year survival rate between 25 % and 35 %, one year survival between 71 and 88 %, and mean survival between 25 and 35 months. In patients treated with MR-guided LITT for unresectable colorectal liver metastases the mean survival was 41.8 months (95 % confidence interval 37.3 – 46.4 months). The 1 year survival rate was 93 %, the 2 year survival rate was 74 %, the 3 year survival rate was 50 %, and the 5 year survival was 30 %. While perioperative mortality in surgical patients ranges between 4.4 and 10 %. The overall rate of clinically relevant complications for LITT was 1.2 %. The 30-days mortality was 0.2 %, however only 0.06 % were possible LITT related.
Conclusion: MR-guided LITT means a safe and effective treatment protocol for oligonodular colorectal liver metastases, if there are not more than 5 metastases with a maximum diameter of 5 cm present. LITT proves comparable survival rates to surgical resection with a obvious lower complication rate thus forming the basis for a randomized trial of LITT versus liver resection in resectable liver metastases.

B-0113 11:25

MR-guided percutaneous brachytherapy of non-resectable liver metastasis: A pilot study

J. Kettenbach, S. Schamp, B. Pokrajac, R. Schmid, C. Fellner, J. Berger, W. Seitz, R. Pötter, J. Lammer; *Vienna/AT*

Purpose: To provide a palliative minimally invasive treatment of patients with non-resectable liver metastasis.
Material and methods: Six patients with unresectable liver metastases from colorectal cancer were treated using an open MR-system (0.2 T, Magnetom Open Viva, Siemens). Hepatospecific contrast agent and 2D-FLASH rapid gradient-echo sequences in a breathhold mode were applied for image guided placement of up to five brachytherapy-needles (14 G). High-dose rate irradiation with up to 20 Gy applied to tumor periphery was performed using a remote controlled ^{192}Iridium source.
Results: No major complication was observed. Four patients had to be retreated due to insufficient response or development of distant metastases following first treatment. Three patients with progressive metastases and extrahepatic disease showed only temporary response and died within up to 10 months following therapy. Patients with local disease showed a full response in 3 lesions, a partial response in 9 lesions, no response in 1 lesion.
Conclusion: MR-guided brachytherapy of liver metastasis is feasible and safe with the potential to ablate tumor tissue. Further clinical trials will have to determine the appropriate dose to improve tumor response rate.

B-0114 11:30

MR-guided laser-induced thermotherapy (LITT) in patients with oligonodular hepatocellular carcinoma

K. Eichler, M.G. Mack, R. Straub, D. Woitaschek, S. Zangos, M. Böttger, K. Engelmann, T.J. Vogl; *Frankfurt a. Main/DE*

Purpose: To prospectively evaluate the therapeutic potential of MR-guided laser-induced thermotherapy (LITT) in patients with oligonodular hepatocellular carcinoma.

Material and methods: 27 patients with 38 intrahepatic lesions were treated with MR-guided LITT. The Nd-YAG laser fiber was introduced with a percutaneously positioned cooled application set. Qualitative and quantitative MR parameters and clinical data were evaluated.

Results: All patients tolerated the procedure well under local anesthesia; no relevant clinical complications or side-effects were observed. The mean laser power was 25 W and the mean duration 25 min. Online MR thermometry allowed visualization of the volume of laser-induced changes and their relation to the neighboring anatomy. Lesions up to 2 cm in diameter could be efficiently treated with a single laser application, larger lesions were treated with a dual, triple and quattro simultaneous application. In 95 % we achieved a complete necrosis of the tumor and a 5 mm safety margin, resulting in a complete destruction of the tumor without local recurrences. Mean survival in this group was x = 3.53 years median: 5.41 years, (95 % confidence interval 2.46 – 4.59). The cumulative survival times were calculated using the Kaplan–Meier method.

Conclusion: In intrahepatic oligonodular involvement of hepatocellular carcinoma MR-guided laser-induced thermotherapy (LITT) appears to be an effective therapeutic procedure.

B-0115 11:40

Unresectable liver tumors: Repeated transarterial chemoembolization followed by MR-guided LITT (laser-induced thermotherapy)

S. Zangos, M.G. Mack, R. Straub, K. Eichler, D. Woitaschek, K. Engelmann, M. Böttger, T.J. Vogl; *Frankfurt a. Main/DE*

Purpose: To evaluate the clinical value and results of repeated transarterial chemoembolization (TACE) for patients with unresectable liver tumors initially unsuited for LITT (laser-induced thermotherapy).

Material and methods: 236 patients with different malignant liver tumors were evaluated between March 1999 and August 2000. The chemoembolization was performed with 50 mg/m² mitomycin C, 10 ml/m² lipiodol and microspheres. The tumor volume was measured by MR-imaging. Lipiodol retention and perfusion of the tumors were evaluated by CT and angiography. 37 patients (24 patients with metastases of colorectal cancer, 4 patients with metastases of breast cancer, 4 patients with metastases of different primary tumors and 5 patients with HCC) could be treated with MR-guided LITT4 to 6 weeks post embolization.

Results: Repeated TACE enabled a significant reduction in tumor size and tumor perfusion at 37 patients, forming the basis for the performance of MR-guided LITT-procedure for the complete ablation of the tumor. After 123 TACE (2 to 5 (mean: 3.4)) and 71 laser interventions (1 to 5 (mean: 1.9)) we archived a complete tumor ablation of the treated leasions. MR-thermometry revealed a more rapidity developing signal loss during LITT versus non embolized lesions.

Conclusion: Repeated TACE alteres the size and structure of primary unresectable tumors and expands the indication for MR-guided LITT.

B-0116 11:50

Potential use of Gadobutrol for positive contrast of necrosis induced by laser-induced thermotherapy

C. Stroszczynski, N. Hosten, U. Speck, P.M. Schlag, R. Puls, G. Gaffke, A. Grabig, R. Felix; *Berlin/DE*

Purpose: The aim of the study was to investigate the potential use of gadobutrol for the positive contrast enhancement of necrosis induced by laser induced thermotherapy.

Methods: In a preclinical phase, MR (1.5 T) was performed 1 – 7 days after induction of seven thermal lesions of liver and pancreas in domestic pigs before and after i.v. administration of 0.3 ml/kg b.w. gadobutrol (Gadovist®, Schering AG, Berlin, DE). In 18 patients with different malignancies of different organs (liver metastases (n = 6), hepatocellular carcinoma (n = 2), osteoidosteoma (n = 4), pancreatic cancer (n = 3), breast carcinoma (n = 1), granulosa cell tumor (n = 1), local recurrent rectum carcinoma (n = 1)), MR was performed 1 – 3 days after LITT.

Results: Animal experience: All thermal induced lesions appeared hypointense on early enhanced T1-weighted images but hyperintense on late T1-weighted images (6 h after gadobutrol). Lesion size by early scans correlated well with actual postmortem lesion size and histological necrotic area but overestimated necrosis (28.4 ± 7.3 versus 2.1 ± 5.8 mm, r = 0.92, P < 0.05). On late T1-weighted images, extension of necrosis was better visualized (2.2 ± 6.4 mm, r = 0.95, P < 0.05). Clinical applications: All thermal induced lesions demonstrated an up to six fold percental enhancement on T1-weighted images 4 – 8 hours after i.v. application of gadobutrol. Dependent on applied energy (4.2 - 25 W), lesions were homogeneous (n = 10) or target-like (n = 8) with a sharply demarcation line.

Conclusion: Gadobutrol appears to be a promising MRI contrast agent for detection and quantification of necrosis after thermal ablation of tumors.

10:30–12:00 **Room L/M**

Head and Neck

SS 208

Neck lymph nodes/Thyroid gland

Chairpersons:
G. Schroth (Berne/CH)
F. Torrinha (Lisbon/PT)

B-0117 10:30

Digital image fusion of CT and PET data sets in suspected cervical malignancies: Potential clinical value

G.J. Schaffler, R. Groell, H. Schoellnast, D. Kriegl, A.J. Ruppert-Kohlmayr, T. Schwarz, R.M. Aigner; *Graz/AT*

Background and purpose: We investigated the clinical value of digital image fusion of spiral computed tomography (CT) and 2-[^{18}F]-flouro-2-deoxy-D-glucose (18F-FDG) positron emission tomography (PET) studies in patients with suspected cervical malignancies.

Materials and methods: Due to suspected cervical malignancies 22 patients underwent CT and 18F-FDG PET studies during their pretherapeutic tumor staging. A digital workstation was used to fuse the data sets of both modalities by automatic adaptation of pixel size and slice interval and by semiautomatic adaptation of different body axes.

Results: Reviewing the CT studies there was a total of 42 pathologically enlarged cervical lymph nodes in four patients [Group A]. In two additional patients the CT scans revealed a group of at least three borderline lymph nodes suspicious for metastatic disease in each patient [Group B]. 18F-FDG PET studies of the neck revealed pathologically increased 18F-FDG uptake in 6 patients [Groups A and B]. Digital image fusion improved the localization of pathologically increased 18F-FDG uptake in 4 out of 6 patients [Groups A and B] with morphologically suspected cervical malignancies.

Conclusion: Digital image fusion of CT and 18F-FDG PET studies is a possible application in the daily routine. Improved localization of increased FDG uptake within enlarged lymph nodes will be particulary helpful in selected patients to guide further diagnostic and therapeutic procedures.

B-0118 10:40

Cervical lymph node characterisation using electrical impedance scanning (EIS) as an adjunct to ultrasound

A. Malich, M. Facius, T. Azhari, M. Fleck, M.G. Freesmeyer, W.A. Kaiser; *Jena/DE*

Introduction: Sonographic differentiation between inflammatory and malignant lymph nodes is difficult, due in part to almost unchanged morphology of small lymph node relapses. However, as cancer cells exhibit altered dielectric properties, measurement of local electrical field distortions may be useful in detection of malignancy. In this study, we evaluated the accuracy of Electrical Impedance Scanning (EIS) for differentiation of cervically-located sonographically equivocal lymph nodes.

Methods: 70 patients with 106 sonographically suspicious lymph nodes, cervically located, mean size 20 × 13 × 13 mm, mean depth 8 mm, were examined using TransScan TS2000 (Siemens, Erlangen, Germany; manufactured by TransScan R&D Co. Ltd., Israel). Included in the study were perivascular (64), location close to bones (32) and nuchal/supraclavicular (10) nodes. EIS results were compared to histopathological (n = 100) and serological (n = 6) findings.

Results: 62/64 malignant lymph nodes were correctly detected using EIS; 19/42 inflammatory/benign lymph nodes were correctly identified as benign (sensitivity 96.9 %, specificity 45.2 %; NPV 90.5 %, PPV 59.6 %).

Conclusion: The high sensitivity achieved in this study suggests EIS may be of value as an adjunctive technique in differentiation of cervically-located sonographically equivocal lesions. Software changes to reduce the high number of false positive markers would be necessary in order that the technique would be practical for evaluation in a regular clinical routine.

B-0119 10:50

Color flow Doppler sonography (CDS) in estimating the patterns most predictive of the metastatic infiltration of cervical lymph nodes

V. Summaria, T. Tartaglione, A. Costantini, D. Catanzaro, A. Medoro, G. Maresca; *Rome/IT*

Purpose: To assess the efficacy of both B-mode and color Doppler patterns in predicting the metastatic infiltration of the cervical lymph nodes (LN).
Materials and methods: Color Doppler Sonography (CDS) was performed in 37 consecutive patients with carcinomas of head and neck, before surgery, evaluating the most predictive CDS signs of metastatic infiltration in 65 suspected LN. The sonographic signs of metastatic infiltration were considered: longitudinal/transversal ratio (L/T < 2); absence of the hilum; cortical enlargement with heterogeneous echogenicity. The presence of metastatic changes of the intranodal angioarchitecture [cortical vascularity with focal perfusion defects or vessels displacement; subcapsular vessels; aberrant course of central vessels; intranodal artery with high resistance flow (PI > 1.5)] were also evaluated. The results were correlated with the histological findings and statistically evaluated with χ^2 test.
Results: On histology 29/65 LN were diagnosed as metastatic and 36/65 as benign. Using CDS 55 LN were classified correctly (specificity 78 %; sensitivity 93 %). On B-mode US, the most predictive signs of metastatic infiltration were cortical enlargement with heterogeneous echogenicity (specificity 94 %), and the combination of cortical enlargement with heterogeneous echogenicity/absence of the hilum (specificity 67 %). On color Doppler examination intranodal angioarchitecture changes showed an high specificity (91 %) but a low sensitivity (62 %); PI > 1.5 was the most predictive sign (specificity 95 %; PPV 93 %; sensitivity 86 %).
Conclusion: CDS has a good efficacy in the diagnosis of the cervical metastatic LN. If the CDS shows a change in the intranodal angioarchitecture with high resistance flow (PI > 1.5), an higher malignant predictivity is obtained.

B-0120 11:00

Ultrasonic color Doppler investigation in differential diagnosis of cervical lymph node metastases

V. Protsyk, T. Golovko, I. Dykan; *Kiev/UA*

Purpose: Lymph node status is crucial in evaluation of prognosis and in treatment planning in patients with primary malignant tumors of the head and neck.
Methods and materials: The investigation of the neck, including colored Doppler ultrasonography, routine ultrasonography, 3D-reconstruction vessels map, clinical and morphological methods, was accomplished in 93 male and female patients age 19 – 78 years old. The patients were pathologically and clinically confirmed to have metastasis (n = 34), lymphoma (n = 26) and benign reactive lymphadenitis (n = 33).
Results: Criteria of changes in lymph nodes for differential diagnosis in benign and malignant disease were elaborated. As for malignant processes the signs are lymph nodes with no differentiation structure, rounded and abnormal patterns of vascularity: absence of central, hilar or peripheral vascularity and appearance of chaotic hypervascularisation. The accuracy was 89.2 %, sensitivity 90.0 %, and specificity 87.8 %.
Conclusion: Color Doppler ultrasonography has great potentials in detecting metastases of cervical lymph nodes.

B-0121 11:05

Intra-observer variability and reliability of three-dimensional ultrasound in thyroid volume measurement

A. Lychtchik[1], V. Drozd[1], E. Demidchik[1], E. Werner[2], J. Terekhova[2], C. Reiners[2]; *[1]Minsk/BY, [2]Würzburg/DE*

Purpose: The reconstruction of a three-dimensional model from a sequence of two-dimensional ultrasound images is very useful in medical image analysis. 3D sonography allows calculation of thyroid volume without assumption of its geometry. Purpose of this study was to compare the sonographic measurement of thyroid volume, using either the conventional ellipsoid model with 2D images or manual planimetry of 3D images.
Methods & materials: The images of 48 children with thyroid nodular pathology who were refered for ultrasound examinations and surgery for thyroid were evaluated prospectively. 2D images were acquired by Hewlett Packard "ImagePoint" scanner with 7.5 MHz linear probe. 3D data sets were created using an 3D system "Freescan" (EchoTech, Germany). For each patient thyroid volume was measured three times using both 2D and 3D methods. True volume of thyroid was estimated after surgery.
Results: Mean error (m ± SD) of 2D US method in thyroid volume estimation was –1.02 ± 13.6 %, mean error of 3D US method was 0.89 ± 5.6 %. Intra-observer thyroid volume estimates have 17.0 % variability and 89.5 % reliability for 2D US and 6.6 % variability and 96.1 % reliability for 3D US.
Conclusion: Our data show that, 3D ultrasound methods have a high accuracy and precision in thyroid volume estimation.

B-0122 11:15

Power Doppler imaging of thyroid cancer in children

A. Lychtchik, V. Drozd; *Minsk/BY*

Purpose of this study was to describe the Power Doppler sonography findings in children with thyroid cancer.
Methods & materials: The images of 30 patients who were refered for ultrasound examinations and surgery for thyroid cancer were evaluated prospectively. Mean age of the patients was 14.8 years, male/female ratio 1/3.5. Studies were performed using Hewlett Packard "ImagePoint" scanner with 7.5 MHz linear probe. Power-Doppler patterns of thyroid node vascularisation were classified into three types: I – nodules without vascularisation, II – nodules with perinodular vascularisation, III – nodules with intra- and perinodular vascularisation. Pathological correlation was available in all cases. There were 29 cases of papillary and 1 of follicular carcinoma.
Results: All three types of vascularisation of the thyroid nodule were observed using Power-Doppler sonography. In cases of carcinoma pattern I of node vascularisation was found in 23 % cases, pattern II in 3 % cases and more often pattern III (in 74 % cases).
Conclusion: Our results suggest that Power Doppler sonography is necessary for initial diagnosis and can be used to improve diagnostic accuracy in thyroid carcinomas detecting.

B-0123 11:25

The ultrasound findings of postradiation changes of the thyroid gland in patients with Hodgkin's and non-Hodgkin's lymphoma

A.T. Balashov, I.V. Drobacha, A.A. Myasnikov; *Petrozavodsk/RU*

Purpose: Estimation of the postradiation changes in the thyroid gland in patients with malignant lymphomas after radical radiotherapy.
Materials and methods: Thyroid gland ultrasound investigations were acquired from 57 patients who underwent neck irradiation (32 with Hodgkin's disease and 25 with non'Hodgkin lymphomas). The integral neck dose was from 28 to 46 Gy. We used Shimadsu 350A unit, 8.5 MHz transducer. Every patient also had a thyroid status based on radioimmunological assay.
Results: There were changes in 49 (85.9 %) out of 57 patients. 43 out of 49 (group 1) had multiple focal, linear and point fragments alternated normal thyroid tissue. This was considered as postradiation thyroiditis. The other 6 patients (group 2) had hyperechogenic focuses alternating with hypoechogenic fragments (cellular infiltrates consisting of different lymphocytes). This was considered as autoimmune thyroiditis. The integral dose in group 1 was 32 – 46 Gy (average 38.5), in group 2 28 – 32 Gy (average 30.5). In group 1 we found isolated TTG increase in 11 patients (25.5 %) different time after the irradiation (average 3.2 years after the treatment). In group 2 we found 3 patients with isolated TTG increase and 1 with TTG increase and simultaneously T4 decrease, total 4 patients (66.7 %) within the first year after the treatment.
Conclusion: US thyroid gland examination reveals direct tissue injury by the effects of the irradiation. That could be postradiation dose dependent thyroiditis (mostly late after the irradiation) and typical autoimmune dose undependent thyroiditis frequently with thyroid gland function disorder.

B-0124 11:35

Colour Doppler in the differential diagnosis of thyrotoxicosis

G. Vagapova, F. Hamzina, M. Mikhailov; *Kazan/RU*

Purpose: To determine the use of Colour Doppler in the distinction of different forms of thyrotoxicosis.
Method and materials: 15 patients with hyperthyroidism were examined. The diagnosis were confirmed by high Free Thyroxine 30.5 ± 3.3 pmol/l in presense of suppressed Thyrotropin 0.12 ± 0.05 IU/l, by the data of sonography, fine needle aspiration biopsy, scintigraphy. Sonography with Colour Doppler was performed on Acuson 128 x P110. Peak flow velocities (PFV), resistive index (RI), pulsatility index (PI) were measured in parenchymal thyroid vessels (PTV) and in inferior thyroid artery (ITA).

Results: Patients with Graves disease (5 cases) showed pronounsed hypervascularisation of parenchyma basically due to increasion of the number of small vessels. PFV in ITA was 1.36 ± 0.19 m/s, RI ± 0.76, PI ± 1.44. Patients with Hashitoxicosis (4 cases) showed diffuse enhancement of parenchymal vascularisation with the prevalence of arterial signal around the zones of lymphoplasmocytal infiltration. PFV in ITA was 1.2 ± 0.18 m/s, RI ± 0.7, PI ± 1.25. Patients with thyrotoxicosis due to subacute thyroiditis (3 cases) showed the absence of vascularisation inside zones of lymphocytic infiltration and poor around them. PFV in PTV near inflammative zones was 0.85 ± 0.1 m/s, RI ± 0.67, PI ± 1.13. PFV in ITA on side of inflammation was 0.99 ± 0.1 m/s, RI ± 0.54, PI ± 0.78.
Conclusion: Colour Doppler can provide important data to enable differentation of various forms of thyrotoxicosis even before laboratory tests.

B-0125 11:45

Color dynamic US examination of thyroid nodules: Comparative findings of clinical and laboratory tests
V. Panaritis, E. Koukou, E. Papoulia; *Amfissa/GR*

Purpose: The aim of this study is to evaluate the color Doppler US as a supplementary method for the evaluation of thyroid nodes as compared with clinical examination and hormonal laboratory tests (T3, T4, TSH).
Materials and method: 30 female subjects were clinically examined and all exhibited thyroid nodes. They were all referred for US test and hormonal laboratory checks (T3, T4, TSH).
Results: Independent of node-size we had the following results

- In 10 patients with indicative values of hyperthyroidism the dynamic US Color Doppler showed an increased peripheral and central hematosis of the nodes.
- In the remaining 20 cases, where no pathological hormonal values were obtained the, US Doppler showed normal hematosis of the nodes.
- No hormonal findings compatible with hypothyroidism were obtained in any one of the cases examined.
- We did not employ scanning tests in any one of the cases.

Conclusion: The dynamic US Color Doppler seems to be a sensitive and specific method for the evaluation of node activity (D.D. warm-cold nodes). However, due to the small sample size a further confirmation is needed using a larger sample.

B-0126 11:50

Grading thyroid vascularity in diffuse thyroid disease: Interobserver agreement using different power Doppler pattern classifications
P. Raudvere, P. Ross, E. Purde, M. Meldre, K. Kivimäe, S. Nazarenko; *Tallinn/EE*

Purpose: Severity of thyroid hypervascularisation has been found useful in characterizing Graves' disease. Our aim was to determine interobserver agreement (IOA) in grading thyroid hypervascularity of diffuse thyroid disease using Power Doppler (PD).
Materials and methods: According to vascularity, 74 PD images of 54 patients were retrospectively classified into four and three grades by consensus of two radiologists with previous experience in thyroid vascularity assessment (TVA). After short instruction three observers (radiologists without previous experience in TVA) were asked to group images into four and three grades according to vascularity. IOA characteristic κ was calculated for every observer versus consensus for both classifications and separately for each grade in both classifications. Kappa was interpreted according to Landis and Koch (1977).
Results: IOA for grouping images into four grades was moderate to substantial (0.55 – 0.71), into three grades – substantial to almost perfect (0.79 – 0.87). Detailed analysis in four grades shows good IOA in grade 1, less IOA in grades 2 – 4, in three grades – substantial to almost perfect in all grades.
Conclusion: Having better IOA, grading thyroid vascularity into three grades is superior than into four grades.

10:30–12:00 **Room N/O**

Cardiac

SS 203

Coronary arteries: CT/MRI

Chairpersons:
A. de Roos (Leiden/NL)
G.K. von Schulthess (Zürich/CH)

B-0127 10:30

Breath-hold 3D MR coronary angiography with a new intravascular contrast agent (feruglose)
J.J.W. Sandstede[1], T. Pabst[1], C. Wacker[1], F. Wiesmann[1], V. Hoffmann[2], M. Beer[1], W. Kenn[1], W. Bauer[1], D. Hahn[1]; *[1]Würzburg/DE, [2]Ismaning/DE*

Objective: Demonstration of the initial results of breath-hold 3D MR coronary angiography with patients using a new intravascular contrast agent (feruglose).
Subjects and methods: Contrast-enhanced 3D MR-coronary angiography was performed in 5 patients with coronary artery disease after administration of feruglose in three different doses (0.5 (n = 3), 2, 5 mg Fe/kg body weight for each patient). MR coronary angiography was performed with an ECG-triggered 3D-FLASH-sequence during breath-hold at 1.5 T (TR 6.8 ms, TE 2.5 ms, flip-angle 30°). To reduce data acquisition time, only the two anterior elements of the phased-array body coil were activated. The data acquisition window within the cardiac cycle ranged between 217 – 326 ms depending on the matrix. Signal-to-noise (SNR) and contrast-to-noise ratios (CNR) of the coronary arteries were analyzed, and the results for the detection of coronary artery stenoses were compared with those obtained by conventional coronary angiography.
Results: SNR and CNR revealed an improved image quality at a dose of 2 mg Fe/kg compared with the lower dose, but no further improvement was obtained by rising the dose to 5 mg Fe/kg. Except for the left circumflex artery of one patient, at minimum the proximal parts of all four main coronary arteries could be imaged for all patients. Within the visible parts of the coronary arteries, six of eight significant coronary stenoses were identified correctly.
Conclusions: Imaging of the proximal parts of the coronary arteries including detection of stenoses is possible during breath-hold using an intravascular contrast agent.

B-0128 10:40

Multislice breath-hold spiral coronary MR angiography in combination with a intravascular contrast medium CLARISCAN (NC100150 Injection)
P.R. Knuesel, D. Nanz, G.K. von Schulthess, B. Marincek, J. Schwitter; *Zürich/CH*

Purpose: A multislice breathhold MR spiral approach in combination with an intravascular contrast medium (CM) CLARISCAN™ (NC100150 Injection) was evaluated for the detection of coronary artery stenoses.
Material and methods: In 11 patient one or more target vessel were evaluated by MR prior to CM administration and at cumulative doses of 0.25, 0.5, and 0.75 mg/kg of CLARISCAN™. In all patients quantitative coronary angiography (QCA) was performed. The spiral sequence acquired 4 slices (4 mm thick overlapping by 2 mm) within 16 heart beats (acquisition window: 29 ms; in plane resolution of 1.3 x 1.3 mm²). Vessel disease was graded as 1 – 3: mild (50 – 75 %), severe stenosis (76 – 99 %), or occlusion, respectively, by two observers. In addition, confidence was rated as grade 1 – 5: not present, probably not present, intermediate, probably present, definitely present, respectively.
Results: 11 diseased vessels were identified by QCA (stenosis > 50 %). Ten stenoses were correctly detected by native MR (Sensitivity: 91 %). In the 3 vessels without disease by QCA, MR suggested mild stenosis in one case (specificity 66 %). Confidence in diagnosis of stenosis was high in the segments evaluated (grade 4.6 ± 0.4). There was a tendency toward underestimation of stenosis severity by MR (grade: 1.55 vs 1.64 by QCA; p = ns). For the 3 CM dosages used, no increase in sensitivity and specificity for diagnosing diseased vessels was found.
Conclusions: Overlapping slices acquired with multislice spiral MR coronary angiography improves spatial coverage and detects stenoses with high confidence. In this small sample size no additional benefit was observed when combined with an intravascular CM.

B-0129 10:50

Cardiac gated multislice breath-hold sequences: Comparison of segmented turbo-flash and 3D true-fisp in demonstration of coronary arteries

A. Kluge, C. Müller, T. Dill, W. Ricken, C. Hamm, G.F. Bachmann; *Bad Nauheim/DE*

Purpose: To develop, evaluate and optimize the use of cardiac gated breath hold multislice-sequences for morphologic orientation and for locating coronary arteries in order to choose the orientation for subsequent contrast-enhanced angiography.

Materials and methods: Two cardiac-gated breath-hold multislice-sequences were compared on a 1.5 T MR-Scanner (Sonata, Siemens): a segmented turbo-flash multislice sequence of 3, 5, 7 and 9 slices and a modified 3d true-fisp-sequence. Spatial resolution, contrast, and depiction of the coronary arteries were investigated on 7 healthy volunteers and 25 patients of whom 14 had been examined by coronary angiography.

Results: The proximal RCA was visualized on 28 of 32 examinations (87.5 %), the middle part of the right coronary artery (RCA) was depicted on 25 examinations (78.1 %). The numbers for the left coronary artery (LCA) were 27 of 32 (84.3 %) and 22 of 32 (68.75 %), respectively. While both sequences permitted cardiac gated multislice-imaging in a single breath hold, but ghost artifacts initially hampered the depiction of coronary arteries in 3d true-fisp-sequences. The turbo-flash-sequence had to be optimized in order to allow acquisition in less than 22 seconds while preserving an anatomic resolution better than 2 mm^3.

Conclusion: Both segmented turbo-flash and 3d true-fisp sequences allowed visualization of coronary arteries on a routinely manner, but careful selection of parameters is mandatory for acceptable results.

B-0130 11:00

Assessment of flow reserve in coronary bypass grafts: Noninvasive measurement with breath-hold phase-contrast MR imaging

K.-F. Kreitner, T. Voigtländer, T. Wittlinger, P. Kalden, S.E. Petersen, J. Meyer, M. Thelen; *Mainz/DE*

Purpose: To measure vasodilator reserve in coronary bypass grafts with breath-hold phase-contrast MR imaging.

Methods and materials: 36 patients with 51 coronary bypass grafts (14 mammaria and 37 venous grafts) underwent MR imaging at 1.5 T. For flow measurement, we used a velocity-encoded k-space segmented gradient echo sequence with a temporal resolution 110 or 125 ms, respectively, before and after iv administration of adenosine (140 µg/kg BW/min). Further analysis comprised the calculation of mean flow, mean and peak velocity, and their vasodilator reserve. Coronary angiography (CA) served as the gold standard for detection of severly stenosed (> 75 % of vessel lumen) grafts.

Results: Measurements were successful in 48 grafts. According to CA, there were 13 stenosed and 35 competent grafts. There were statistically higher vasodilator reserves with respect to mean flow, mean velocity and peak velocity ($p < 0.001$, $p < 0.001$ and $p = 0.018$, respectively) in competent compared to stenosed grafts. The vasodilator reserve of mean velocity proved to be the best parameter for discriminating between competent and stenosed bypass grafts.

Conclusion: The determination of vasodilator reserves with breath-hold phase-contrast MR imaging allows for identification of severly stenosed bypass grafts with a high sensitivity.

B-0131 11:10

Evaluation of arterial and venous coronary artery by-pass grafting: Diagnostic value of contrast-enhanced ECG-gated multidetector spiral CT in the assessment of overall patency

M. De Santis, F. Manganaro, A. Pimpinella, T. Celano, R. Passariello; *Rome/IT*

Purpose: To assess the diagnostic value of contrast-enhanced ECG-gated multidetector spiral CT (MDSCT) in the evaluation of saphenous and internal mammary artery (IMA) by-pass grafts compared with conventional coronary angiography (CCA).

Materials and methods: Twentyseven patients with 82 coronary artery by-pass grafts (55 venous, 27 IMA) underwent contrast-enhanced spiral cardio-CT examination with retrospective ECG gating following bolus testing 5 – 22 days after 1 year follow-up CCA. All CT data sets were double-blinded reconstructed (2D and 3D MIP-MPR-Volume rendering) and reviewed by means of standard cath lab reporting charts for a) overall course patency, b) grafting anastomoses visualization, c) grafting anatomoses patency.

Results: Course patency rates were 92.6 % on CCA and 90.2 % on MDSCT. Visualization of grafting anastomoses was accomplished in all cases with both techniques and the anastomoses patency assessment obtained on MDSCT was considered optimal in 52/55 venous and 23/27 IMA grafts (overall 75/82 – 91.4 %).

Conclusions: Thanks to the interactive 2D-3D viewing options offered by standard reconstruction algorithms, contrast-enhanced ECG-gated MDSCT represents a reliable and cost-effective approach in CABG assessment.

B-0132 11:20

Non-invasive investigation of coronary artery bypass grafts using contrast-enhanced retrospectively ECG-gated multislice spiral CT

E. Wenkel, U. Baum, C. Schulte, S. Ulzheimer, M. Kachelrieß, D. Ropers, S. Achenbach, T. Giesler, W.A. Bautz; *Erlangen/DE*

Purpose: ECG-gated multi-slice spiral computed tomography (MSCT) is an interesting new approach for non-invasive coronary angiography. We investigated the ability to visualize coronary artery bypass graft patency and to detect high-grade bypass stenoses.

Materials and methods: 15 patients with 43 grafts were investigated by MSCT (Somatom Plus 4 Volume Zoom, Siemens, Germany) 1 to 192 months after bypass operation. During intravenous injection of contrast agent (160 ml at 4 ml/s), a volume data set of the heart was acquired (4 × 1 mm slice thickness, 500 ms rotation time, table feed 1.5 mm/360°). Contiguous cross-sections of 1.3 to 1.5 mm slice thickness were reconstructed using the retrospectively ECG-gated algorithm "180° MCI". Based Multiplanar reconstructions and shaded surface display reconstructions were rendered and evaluated regarding the patency and presence of high-grade stenoses (= 70 % diameter reduction) in coronary artery bypass grafts. Results were compared to selective coronary bypass angiography performed 1 to 3 days after the MSCT investigation.

Results: MSCT permitted detection of bypass occlusions with 100 % sensitivity (7/7) and 97 % specificity (35/36). Mainly due to artifacts caused by metal clips, only 18 of 36 patent grafts (50 %) could be evaluated regarding the presence of stenoses. In evaluable grafts, only 1 of 4 high-grade bypass stenoses was correctly detected by MSCT. In 12 of 14 bypass grafts high-grade bypass stenoses were correctly ruled out.

Conclusion: Retrospectively ECG-gated multi-slice spiral CT permits non-invasive assessment of bypass graft patency. Reliable examination of significant bypass graft stenoses is restricted due to metal clip artifacts.

B-0133 11:25

Coronary calcification detected by electron-beam CT and coronary heart disease: The Rotterdam study

R. Vliegenthart[1], M. Oudkerk[1], J.C. de Groot[1], H.-H. Oei[2], P.J. de Feyter[2], D.A.M. van der Kuip[2], A. Hofman[2], J.C.M. Witteman[2]; *[1]Groningen/NL, [2]Rotterdam/NL*

Objective: In an elderly population of men and women, we studied the association between coronary calcifications detected by electron-beam computed tomography (EBT) and the presence of myocardial infarction.

Methods: We performed a population-based cross-sectional study among elderly subjects. Baseline data were collected in 1990 – 1993. During the third examination phase (1998 – 2000), subjects were invited for EBT scanning for detection of coronary calcifications. Quantification of calcifications was performed using Agatston's method and resulted in a calcium score. Calcium scores were available for 1874 of 2263 subjects who underwent EBT scanning (46.8 % men, mean age (SD), 71.3 (5.7)). Myocardial infarction was considered present if a myocardial infarction had occurred before baseline (1990 – 1993) or during follow-up but before EBT scanning.

Results: Compared to the lowest calcium score category 0 – 100, the age-adjusted odds ratio for myocardial infarction in subjects with calcium score > 2000 was 9.2 (95 % confidence interval 4.7 – 18.3) for men, and 10.0 (3.4 – 29.8) for women. Additional adjustment for cardiovascular risk factors hardly changed the estimates. The association remained present in subjects above 70 years of age.

Conclusions: In this population-based study, a strong association between coronary calcification and myocardial infarction was present in both men and women, which remained present at higher age. Although prospective data in unselected populations have to be awaited, this study suggests that EBT is a promising tool for the detection of subjects at high-risk of coronary events in the general population.

B-0134 11:35

Coronary calcification detected by electron-beam CT and non-coronary indices of atherosclerosis: The Rotterdam study

R. Vliegenthart[1], M. Oudkerk[1], J.C. de Groot[1], H.-H. Oei[2], M. Bots[3], A. Hofman[2], J.C.M. Witteman[2], P.J. de Feyter[2]; *[1]Groningen/NL, [2]Rotterdam/NL, [3]Utrecht/NL*

Objective: Coronary calcification detected by electron-beam computed tomography (EBT) is a measure of coronary atherosclerosis. We investigated whether coronary calcification is associated with non-coronary measures of atherosclerosis.

Methods: We performed a population-based cross-sectional study among elderly subjects. Subjects were invited for EBT scanning to detection coronary calcifications. Quantification of coronary calcifications was performed using Agatston's method, and resulted in a calcium score. Calcium scores were available for 1874 of 2263 subjects who underwent EBT scanning (46.8 % men, mean age (SD), 71.3 (5.7)). Three calcium score categories were considered: 0 – 100, 101 – 500, and > 500. Measures of non-coronary atherosclerosis included presence of aorta calcification detected by X-ray, presence of plaques in carotid arteries and intima-media thickness of the common carotid artery, both detected by ultrasonography, and ankle to brachial blood pressure index as a measure of peripheral arterial disease.

Results: Using logistic regression analysis, age and sex adjusted odds ratios for carotid plaques were 2.4 in subjects with calcium score 101 – 500 (95 % confidence interval, 1.6 – 3.5) and 5.8 in subjects with calcium score > 500 (3.9 – 8.6), when compared to the lowest calcium score category. The corresponding odds ratios for aorta calcification were 3.2 (2.0 – 5.2) and 12.0 (7.6 – 18.9). With increasing calcium score category, the mean intima-media thickness increased, and the mean ankle to brachial blood pressure index decreased.

Conclusions: These results indicate that known measures of non-coronary atherosclerosis are strongly related to coronary atherosclerosis, as measured by EBT calcium.

B-0135 11:45

Variability of Agatston score and volumetric 3D Ca-scoring using multislice spiral CT with retrospective gating for quantification of coronary artery calcium

R. Fischbach[1], E. Fallenberg[1], B. Ohnesorge[2], T. Wichter[1], M. Nattermann[1], G. Assmann[1], W. Heindel[1]; *[1]Münster/DE, [2]Forchheim/DE*

Purpose: To compare reproducibility of coronary artery calcium scores obtained by the Agatston method (AgS) and volumetric measurement (VM) using overlapping and non-overlapping image reconstruction from multislice cardiac CT with retrospective gating.

Material and methods: Persons with symptomatic coronary artery disease (n = 14) and presymptomatic CAD (n = 16) underwent a cardiac multislice CT (Somatom VolumeZoom, Siemens) with retrospective ECG gating. Images were reconstructed using a dedicated cardiac algorithm (ACV, Siemens) without and with 50 % overlap. An additional couple of image sets was reconstructed with an offset of 2 mm to simulate repositioning of the patient. Calcium quantification was performed for each image set using the Agatston score and a volumetric method. Differences in variability were compared using the Wilcoxon test.

Results: Mean Agatston calcium scores for symptomatic (367 ± 456) and asymptomatic patients (196 ± 300) showed a significant difference. The variability of the Agatston score was 31 % for the volume method 18 % using non-overlapping images ($p < 0.05$). Overlapping image reconstruction achieved a significant decrease in variability: Agatston score 10 %, Volume measurement 7 %, ($p < 0.05$).

Conclusions: Spiral MSCT with overlapping image reconstruction significantly improves simulated interscan variability for coronary calcium scoring. Reproducibility of calcium quantification can be further improved using volumetric measurement.

B-0136 11:55

Progression of coronary artery disease. The value of quantitative coronary arteriography in the analysis of the natural history of coronary artery lesions. Our experience

J.D. Saponjski, M. Ostojic, V. Vukcevic, B. Beleslin, M. Nedeljkovic, S. Stojkovic, D. Orlic; *Belgrade/YU*

Purpose: The objective of this study was to evaluate the natural history of coronary artery lesions using quantitative coronary arteriography, including analysis of lesion morphology. The influence of coronary risk factors on history of coronary artery diseases was also evaluated.

Methods and materials: Study population included 108 patients (87 male, 21 female, mean age 52 ± 14 years) with 145 lesions in who repeated coronarography was performed in the period of 3 – 36 months. By quantitative coronary arteriography we have observed changes in obstruction diameter (OD) and % diameter stenosis (DS). Morphology of coronary lesions was assessed by Ambrose classification. Following coronary risk factors were observed: cholesterol, triglycerides, smoking, hypertension, diabetes, and family history.

Results: Progression of coronary lesions was more pronounced in coronary lesions with DS < 50 % (33 % to 53 %, OD: 1.7 to 1.3 mm, $p < 0.05$) than in significant coronary lesions (66 % to 68 %, OD: 0.9 to 0.9 mm, p = ns). In addition, progression to total coronary occlusion was also observed more in nonsignificant coronary lesions (DS < 50 % – 42 %; DS > 50 % – 29 %, $p < 0.05$). Progression of coronary artery disease was associated with transitions of coronary lesions to complex morphology type. Progression of coronary artery disease was associated with high cholesterol, hypertension, and smoking ($p < 0.05$) but not with other coronary artery disease risk factors.

Conclusion: In conclusion, in this group of recoronarography patients progression of coronary artery disease, even to total obstruction, was more pronounced in nonsignificant coronary artery lesions with transition to complex type of morphology. Progression of coronary artery disease was associated with high cholesterol, hypertension, and smoking.

10:30–12:00 **Room P**

Vascular

SS 215

Pulmonary arteries/Miscellaneous

Chairpersons:
M. Prokop (Vienna/AT)
D. Tsetis (Iraklion/GR)

B-0137 10:30

Ultrafast 3D MR angiography of the pulmonary arteries

M. Goyen[1], S.G. Rühm[1], J. Barkhausen[1], T. Lauenstein[1], G. Laub[2], J.F. Debatin[1]; *[1]Essen/DE, [2]Chicago, IL/US*

Purpose: To evaluate an ultrafast dynamic MRA-technique permitting the acquisition of a 3D data set of the pulmonary vasculature in under 4 seconds.

Materials and methods: MRA of the pulmonary vasculature was performed in 3 healthy volunteers and 30 patients referred with suspicion of PE. Imaging was performed on a 1.5 T MR-scanner (Sonata, Siemens, Germany). Sequence parameters: coronal plae, TR: 1.6 ms, TE: 0.6 ms, flip: 15°, slab thickness: 110 mm, slice thickness: 2.75 mm, 40 interpolated partitions, FOV: 360 mm, matrix: 140 × 256, partial k-space coverage. 20 ml of paramagnetic contrast agent was administered at a flow rate of 4 ml/s with an automated injector. Data collection was commenced 8 s following initiation of the contrast injection. Scintigraphy (n = 28) and CT (n = 7) were used as reference standard.

Results: All 3 healthy volunteers but only 13 of the 30 evaluated patients were able to hold their breath over the entire data acquisition period (5 data sets collected over 19 s). All patients were able to hold their breath for at least 8 s, during which the first two data sets were collected. PE was demonstrated by MRA in 19 of the 30 patients. In one patient atelectasis of the right lung with an elevation of the diaphragm mimicking a perfusion defect in scintigraphy was identified. MRA diagnosis correlated with the corroborating tests in all but one patient, resulting in a positive predictive value of 100 %.

Conclusion: MRA of the pulmonary vasculature has become possible even in severly dyspneic patients.

B-0138 10:40

Diagnostic accuracy of different post-processing techniques for assessing 3D pulmonary MR angiography (PMRA) data sets

U. Fronz, M. Goyen, S.G. Rühm, J. Barkhausen, J.F. Debatin; *Essen/DE*

Purpose: Traditionally the assessment of contrast-enhanced 3D MRA of the pulmonary arteries relies on inspection of rotated maximum intensity projections (MIP) and multiplanar reformations (MPR). Recently a new volume rendering method which allows stereo-viewing has become available. The purpose of this study was to evaluate stereo viewing in comparison to combined MIP and MPR assessments.

Materials and methods: PMRA was performed in 18 patients referred with suspicion of pulmonary emboli (PE). All imaging was performed on a 1.5 T MR scanner (Sonata, Siemens), equipped with high-performance gradients. Interpretation was

performed by a board certified radiologist on a workstation (Virtuoso, Siemens) once based on a combination of MIP and MPRs, and a second time based on stereo viewing. Data sets were analyzed on a 'per lobe' basis using a 5-point confidence scale from 'PE definitely present' to 'PE definitely not present'. In addition, the time required to reach the diagnosis was documented.
Results: Both methods revealed PEs in 21 lobes. For all anatomic regions, diagnostic confidence regarding the presence/absence of PE was significantly higher using stereo-viewing resulting in a greater area under the ROC curve ($p < 0.05$). There was no statistically significant difference concerning the time needed to reach the diagnosis ($p > 0.05$).
Conclusion: Stereo-viewing is an effective and accurate tool for assessing the complex pulmonary arterial tree in 3D MRA and provides more diagnostic confidence compared to the combination of common post-processing techniques (MIP + MPR).

B-0139 10:50

Visualization of pulmonary arteries in piglets using a Gadomer-17-enhanced navigator-angiography

N. Abolmaali[1], V. Hietschold[2], S. Appold[2], R. Hammerstingl[1], J. Balzer[1], T. Vogl[1]; *[1]Frankfurt a. Main/DE, [2]Dresden/DE*

Purpose: Evaluation of detectability of the pulmonary arteries with a modified and contrast-enhanced navigator-angiography (ce-Nav) in piglets. Could this technique be utilized to visualize the pulmonary arteries in patients with severe dyspnea? To which extend are the pulmonary arteries visible?
Material and methods: Five sedated piglets were examined with a modified 3d navigator-angiography in a clinical 1.5 T system (Magnetom Vision, Siemens). After application of intravascular contrast material (Gadomer-17, Schering; 0.05 mmol/kg) the entire thorax was scanned in one measurement (Slab 144 mm) with ECG-triggering and retrospective respiratory gating. Slice thickness was 3 mm, pixel size was 2.4 × 1.8 mm², dependent on heart-frequency measurements took 7 to 13 minutes. Pulmonary arteries were reformated in orthogonal planes, with curved-MPR and in MIP.
Results: 20 to 24 segmental arteries were detectable in any pig. Subsegmental arteries were visualized up to 8 mm towards the pleura. Maximum diameter of the main pulmonary arteries was 18 mm. Central and peripheral pulmonary arteries were clearly visualized. Expected suscebtibility artifacts did not disturb image qualitiy.
Conclusion: Ce-Nav might get an alternative imaging modality in detection of pulmonary embolism if a sufficient breath-hold is not possible. Further evaluation on detectablity of emboli is mandatory.

B-0140 10:55

Assessment of vascular anomalies of the pulmonary vasculature by breath-hold MR techniques

S. Ley, C. Dueber, S.E. Petersen, T. Voigtlaender, K.-F. Kreitner; *Mainz/DE*

Purpose: To evaluate different MR techniques for assessment of vascular anomalies of the pulmonary vasculature.
Method/materials: 9 patients aged from 12 to 60 years with different vascular anomalies of the pulmonary vasculature (1 patient with scimitar syndrome, 4 patients with arteriovenous malformations, 4 patients with anomalous pulmonary venous drainage associated with ASDs) underwent MR imaging at 1.5 T.
For morphological assessment, a 3D-Flash-sequence after application of 20 ml of Gd-DTPA (3D-contrast-enhanced MR angiography) was performed. Segmented cine-GRE- and velocity-encoded GRE-seqences (temporal resolution 50 and 110 ms, respectively) were used for delineation of cardiac septum defects and for determination of systemic left-to-right or intrapulmonary shunt volumes.
Results: MR angiography allowed for anatomic depiction of the vascular abnormalities. Flow measurements performed in the pulmonary arteries and in the ascending aorta enabled determination of systemic left-to-right shunting. The correlation with invasive oxymetry was good ($r = 0.91$, $p < 0.001$).
Additional GRE-sepuences clearly depicted associated cardiac shunt defects. In case of arteriovenous malformations, 3D MR angiography provided a preembolization road map. Flow measurements in the feeder arteries allowed for estimation of intrapulmonary shunt volumes; they correlated well with shunt volumes determined by nuclear medicine.
Conclusions: Breath-hold MR techniques allow for morphological and functional characterization of vascular anomalies of the pulmonary vasculature. Thus, it seems to be the non-invasive method of choice for planning further treatment.

B-0141 11:05

Demonstration of patency of segmental and subsegmental pulmonary arteries, thrombotic wall thickening and intraluminal webs in chronic thromboembolic pulmonary hypertension: Value of contrast-enhanced MR angiography and helical CT angiography

S. Ley, H.-U. Kauczor, K.-F. Kreitner, E. Mayer, M. Thelen; *Mainz/DE*

Purpose: To evaluate the potential of helical CT angiography (CTA) and contrast-enhanced MR angiography (MRA) of the pulmonary arteries in patients with chronic thromboembolic pulmonary hypertension (CTEPH).
Method/materials: The studies of 32 patients (21 m, 11 f, mean age 54 years) were included in this retrospective evaluation. MRA was done by using a contrast-enhanced 3D FLASH sequence (voxel size 1.58 × 0.78 × 1.8 mm³) in a 23 – 27 s breath-hold. CTA was performed with 3 mm collimation, pitch 2, increment 2 mm, with a mean breath-hold period of 32 s. Image quality was scored by two independent blinded observers as excellent, good, moderate or poor. Data sets were assessed for number of patent lobar/segmental and subsegmental arteries as well as number of vascular segments with thrombotic wall thickening, abnormal proximal-to-distal tapering and number of intraluminal webs.
Results: Image quality for MRA/CTA was scored excellent in 16/16, good in 14/11, moderate in 2/5 and poor in 0/0 examinations. MRA/CTA showed 366/357 patent lobar/segmental arteries and 627/834 patent subsegmental arteries. CTA was superior to MRA in visualization of thrombotic wall thickening: (339 vs. 164) and of intraluminal webs (257 vs. 162). In joint assessment of direct and indirect signs, MRA and CTA were equally effective (353 vs. 355).
Conclusions: MRA and CTA are equally effective in the detection of lobar and segmental occlusions of the pulmonary arteries in CTEPH. CTA is superior for the depiction of patent subsegmental arteries, of intraluminal webs and for the direct demonstration of thrombotic wall thickening.

B-0142 11:15

Advantages of volume-rendering in 3D reconstructions of MR angiography images: Comparison with MIP reconstructions

A. Laghi, C. Catalano, V. Panebianco, I. Baeli, A. Napoli, R. Ferrari, R. Passariello; *Rome/IT*

Purpose: To assess the potential advantages of real-time interactive volume-rendering algorithm in the evaluation of MR angiography images and to compare interactive volume-rendering with Maximum Intensity Projection (MIP).
Materials and methods: Thirty-six patients underwent MRA study on1.5 T superconductive magnet (Magnetom Vision Plus, Siemens, Erlangen, DE) with 23 mT/m gradients and 600 ms rise time equipped with phased-array multicoil. Different anatomical districts (carotid arteries; epiaortic vessels; abdominal aorta) were evaluated, using contrast-enhanced 3D FLASH sequence acquired during automatic injection of 0.2 mmol/kg of Gd-DTPA. Images were blindly reviewed after rendering with MIP and volume-rendering algorithms. Vessels visualization and identification of vascular anomalies were analyzed.
Results: Volume-rendered MRA images provided real-time interactive evaluation with 3D data set as opposed to MIP tecnhique requiring 2 to 3 minutes to produce images. Real-time interactive volume-rendering provided better 3D effects compared with standard MIP, with more precise evaluation of tortuous vessels. No statistically significant differences were observed in identification of vascular pathology (dilatation and/or stenosis) as well as in the evaluation of degree of stenosis. Endoscopic view provided no advantages in terms of diagnostic accuracy.
Conclusion: Real time perspective volume rendering is an efficient technique for generation of 3D reconstructions from MR data sets. It provides an easier and faster reconstruction of the vessels with a better comprehension of the vascular anatomy especially in tortuous vessels. A further possibility is represented by the abitlity to produce endoluminal views of the vessels (virtual angioscopy).

B-0143 11:25

Intraindividual comparison of three contrast agents for multiphasic MR angiography: A blinded reader analysis of Gd-DTPA, Gd-BOPTA, Gd-BT-DO3A

M.V. Knopp[1,2], H. von Tengg-Kobligk[1], F. Floemer[1], F.L. Giesel[1], S.O. Schoenberg[1], M. Bock[1]; *[1]Heidelberg/DE, [2]Bethesda, MD/US*

Purpose: To compare three contrast agents for time resolved MRA.
Methods/materials: An intraindividual, double blinded randomized, crossover comparison was performed in five healthy volunteers. The agents were used at a dose of 0.15 mmol/kg bw at 3 ml/s; Gd-DTPA 0.5 mol (DT) (Magnevist/Schering), Gd-BOPTA 0.5 mol (BO) (Multihance/Bracco) and Gd-DO3A-butriol 1.0 mol (BU) (Gadovist/Schering) with a minimum of 48 hrs between exams. A 1.5 T clinical MR using a fast 3D GE sequence (TR 3.2, TE 1.1, α 40°, acq. time 6.4 s) enabled

5 sequential abdominal image sets within breathhold. Blinded reader analysis using quantitative (ROI's) and qualitative data (continuous scale +5 (excellent) to -5 (unacceptable)) was performed.
Results: Quantitative assessment revealed significant ($p < 0.03$) differences between the three agents. Arterial peak enhancement (aorta) was for DT 356, BO 551, BU 328; BO was significant ($p << 0.05$) higher than the other two. Venous peak enhancement (cava) was for DT 233, BO 295, BU 160; BU was significant ($p < 0.05$) lower than BO. The qualitative assessment found for overall image quality scores of DT 3.6, BO 4.8, BU 3.5; BO was therefore found to be significant ($p < 0.01$) preferential than the other two. Visualisation scores of the portovenous system were DT 2.6, BO 3.9, BU 2.9 confirming the higher venous signal of BO.
Conclusions: This intraindividual comparison confirmed enhancement differences indicating that optimized MRA procedures need to consider the characteristics of the specific agent. Gd-BOPTA presents higher arterial and venous signal, while the higher concentrated Gd-DO3A-butriol presented lower venous enhancement compared also to Gd-DTPA.

B-0144 11:35

High resolution contrast-enhanced MR-angiography of the hand arteries
U. Krause, P. Meier, T. Pabst, W. Kenn, D. Hahn; *Würzburg/DE*

Purpose: The purpose of this study is to develop and to assess a high resolution 3d-contrast-enhanced MRA-technique concerning delineation of hand arteries.
Methods and materials: MRA examinations were performed on a 1.5 T system (Siemens Vision) equipped with a flexible surface coil. A modified 3d FLASH-sequence (TR 15 ms, TE 4.9 ms, FA 30°) with a non selective rf-pulse was applicated. By using a field of view of 100 mm × 200 mm and a 256 × 512 matrix a pixel size of 0.4 mm could be realized. To achieve an aquisition time of < 40 s slice interpolation, asymmetric echoes and a gradient booster were used. Contrast agent (Gd-DTPA, 0.4 mmol/kg, flow-rate 2 ml/s) was applicated by an injector system (MEDRAD). To obtain optimal arterial enhancement without venous overlay transit time calculation by using a test bolus (Gd-DTPA, 5 ml, flow-rate 2 ml/s) was performed. Maximum intensity projection was employed for postprocessing. 15 healthy volunteers and 9 patients were examinated. An additional intra-arterial-DSA was performed in one patient.
Results: Delineation of palmar arches, common palmar digital arteries and digital arteries was possible in all healthy volunteers. In one patient i.a.-DSA and MRA showed an excellent correlation. Pathologic findings which were seen in the other 8 patients had a good correlation to the symptoms of the patients.
Conclusions: High resolution contrast-enhanced MRA of the hand-arteries is a noninvasive and fast procedure with promising preliminary results.

B-0145 11:40

Value of gadolinium-enhanced elliptically reordered 3D pulse sequence MR angiography in the preoperative assessment of hand circulation before radial artery harvest for coronary artery bypass grafting
J.T. Winterer[1], U. Rosendahl[2], O. Schäfer[1], K. Scheffler[1], J. Laubenberger[1], J. Ennker[2], M. Langer[1]; [1]*Freiburg/DE*, [2]*Lahr/DE*

Purpose: The radial artery has been shown to provide excellent long-term results in coronary bypass grafting during the recent years. The value of high-resolution bilateral contrast-enhanced MRA of both hands was compared with Doppler studies in the preoperative assessment for radial artery harvesting.
Methods and materials: Prior to coronary bypass grafting hand circulation in 20 patients (40 hand studies) was examined with both, Doppler study and bilateral Gd-BOPTA-enhanced-MRA using an elliptical reordered ultrafast GRE-sequence with a 1.5 T scanner. Doppler and MRA studies were evaluated independently by two investigators regarding the presence and extent of collaterals between radial and ulnar artery vasculature. Completeness of the superficial palmar arch (SPA) was analyzed using targeted-MIP and MPR.
Results: 2/20 patients displayed non-sufficient ulnar collateral flow. MRA showed occlusion/hypoplasia of the ulnar artery and SPA in these cases. In the patients with sufficient ulnar collateral flow MRA displayed great variations in the formation of the palmar arch and arterial supply of the digits. The deep palmar arch was complete in 35/40 hand studies, the SPA was complete in only 3/40 studies. However, MRA showed frequent distal anastomoses between palmar metacarpal and palmar digital branches.
Conclusion: The presence and extent of collaterals between the radial and ulnar artery supply can be correlated with anastomoses that exist classically between the palmar arches but more frequently are found between the distal palmar and metacarpal branches. In the preoperative assessment bilateral MRA provides excellent information about the hand vasculature completing the data obtained from established Doppler studies.

B-0146 11:50

Unexpected similarities in the MR-angiographic appearances of the normal and dysfunctioning pancreatic allograft
R. Wolf, T. Kok, W.J. Sluiter, R.L. Kamman, J.J. Homan van der Heide, R.J. Ploeg, W.J. Boeve; *Groningen/NL*

Purpose: To evaluate the MR-angiographic appearance of the dysfunctioning and normal pancreatic allograft.
Materials and methods: 12 contrast-enhanced MRA examinations were performed in 9 patients with allograft dysfunction (group I) and 12 examinations in 12 patients without dysfunction (group II). An 18 s, breathhold 3D-Flash fat-suppressing pulse-sequence (TR/TE: 4.0/1.4, $\alpha = 30°$, Vision, Siemens, Erlangen) with slice-interpolation technique was repeated 4 times with 12 s breathing intervals. Allograft arterial Y-graft, splenic artery (sa) and SMA were evaluated for patency: (0) indeterminable, (1) no stenosis, (2) 1 – 19 %, (3) 20 – 49 %, (4) 50 – 79 %, (5) 80 – 99 % stenosis, (6) occlusion.
Perfusion was evaluated by determining complete or incomplete enhancement and calculating 'mean percentage of parenchymal enhancement' (MPPE) in head and tail.
Venous outflow was scored indeterminable, patent or occluded.
Results: Arterial anatomy could be assessed in all examinations. The following abnormalities (i.e. stenosis or occlusion) were scored:
Group I: Y-graft: 1 × (5), 1 × (6); sa: 1 × (4), 2 × (5), 5 × (6); SMA: 1 × (5), 4 × (6)
Group II: Y-graft: 2 × (2), 1 × (3); sa: 2 × (3), 3 × (6); SMA: 2 × (2), 1 × (3), 1 × (4), 1 × (6).
Three examinations demonstrated complete arterial occlusion with no or delayed enhancement. 21 examinations demonstrated complete pancreatic enhancement with maximum MPPE on scan 2 in 17/21 cases (head) and in 20/21 cases (tail). In 21/24 cases, venous anatomy was patent, 3/24 indeterminable. Statistical analysis showed no differences between group I and group II for arterial anatomy. (Yates-Cochran: sa $p = 0.5$, SMA $p = 0.99$).
Conclusion: Irreversible dysfunction of the pancreatic allograft cannot be attributed to occlusion or (severe) stenosis of one of the two supplying arteries. Parenchymal perfusion is not influenced by occlusion or stenosis of one of the two arteries.

14:00–15:30 **Room B**

Musculoskeletal

SS 310

Imaging of the knee-joint and cartilage

Chairpersons:
F. Kainberger (Vienna/AT)
C. Masciocchi (L'Aquila/IT)

B-0147 14:00

The radiographic axial view of the patellofemoral joint: Examination in the supine or standing position?
N. Egund; *Århus/DK*

Purpose: To compare the axial radiographic view of the patellofemoral (PF) joint obtained in the supine and standing position with regard to the position of the patella relative to the femoral condyles and (PF) osteoarthrosis (OA).
Patients and methods: Forty consecutive patients admitted for radiographic evaluation of (OA) of the knee and 15 patients with PF OA confirmed at previous standing axial radiographs. Males/females 21/34 aged 58 years (39 – 72 years). Both supine and standing/weightbearing axial radiographs of both PF joints (one knee in 3 patients).
Results: In 68 knees with normal PF joint spaces at both the supine and standing examination there were a significant medial displacement of the patella in the standing position compared to that obtained in the supine position. In 27 PF joints with reduction of the lateral PF joint space (OA) and lateral displacement of the patella, there were no difference between supine and standing. In 12 knees with moderate to advanced OA of the medial PF joint space and medial displacement of the patella in the standing position, only two was could be registered in the supine position.
Conclusion: Radiographic evaluation of the knee joint should include a standing radiographic view of the PF joint. Supported by the literature, the relevance of supine imaging of the PF joint for performance in the standing position may be of speculative nature only.

B-0148 14:10

Knee ACL reconstruction using the quadriceps tendon: MRI evaluation

V.M. Maffey, A. Chichiarelli, F. Franceschi, A.M. Mulap, B. Beomonte Zobel; *Rome/IT*

Purpose: To evaluate knee ACL reconstruction with quadriceps tendon, using MRI.

Methods and materials: Between March 1999 and July 2000, 23 patients were submitted to MRI evaluation of the knee after ACL surgical reconstruction with quadriceps tendon and notch plasty. In 9 cases partial meniscectomy was associated. MRI was performed 2.5 and 8 months after surgery, employing 1.0 T equipment, using FSE T1, T2 and GRE T2 weighted sequences, also with Fat-Saturation technique, on sagittal, coronal and axial scan planes (slice thickness 3 – 5 mm). Coronal scan planes along the tendon graft were also used.

Results: The homogeneous signal hypo-intensity of tendon graft was always depicted, distinguishing in 17 cases its two different components. In 3 patients the residual meniscus was irregular. The residual quadriceps tendon and its repair evolution, associated to fluid reaction, were well defined. The condition of patellar tendon and Hoffa's fat pad were demonstrated; in 6 patients a synovial reaction was present. The tunnel and the bioreabsorbable screws were depicted.

Conclusion: Also using this surgical technique, MRI allows obtaining information about the tendon graft, the impingement sites, and the tunnel and screws position. Moreover, it is always possible to evaluate the residual quadriceps tendon.

B-0149 14:20

Dynamic evaluation of PCL tears and related instability with MRI

M. Mastantuono, P. Mariani, E. Bassetti, L. Di Giorgio, F. Trenta, A. Napoli, R. Passariello; *Rome/IT*

Purpose: Even if Magnetic Resonance Imaging (MRI) with its high contrast and spatial resolution has proven to be an effective technique in the study of ligamentous tears there are limitations in the evaluation of instability patterns. In our preliminary experience we investigate the diagnostic potential of dynamic MRI in the evaluation of the instability related to PCL tears and the improvement of the instability after surgical reconstruction of the PCL.

Materials and methods: 15 patients with PCL tears and 4 patients after PCL reconstruction were studied with a low field permanent magnet (E-Scan Esaote Biomedica) during passive and active motion. The images obtained were related with the MRI examination performed in 21 healthy volunteers examined with the same technique.

Results: A good correlation beetween clinical data and dynamic MRI findings was obtained in all the patients. A significant difference exists between healthy volunteers and the patients with a PCL tear. The measurements perfomed after the MRI examination permit the evaluation of PCL incompetence and help to assess the influence of the other associated ligamentous tears

Discussion and conclusions: Our dynamic protocol, that is easy to perform and to repeat, allows a simple demonstration and documentation of instability related to PCL lesions.

B-0150 14:30

MRI of articular cartilage of the knee: Comparison between optimized sequences using a "dedicated" MRI unit (3D-contrast-enhanced gradient-echo sequence) and a 1.5 T whole body system (3D-FSPGR sequence) vs. arthroscopy

G. Cerone, A. Barile, M. Caulo, A.V. Giordano, V. Calvisi, C. Masciocchi; *L'Aquila/IT*

Purpose: To assess the sensibility and specificity of 3D contrast-enhanced gradient-echo sequence and 3D FSPGR sequence in the evaluation of cartilage disease of the knee, having arthroscopy as gold standard.

Methods and materials: Forty-two patients were examined using both dedicated MRI unit and 1.5 T whole body system. All patients were affected by different knee pathologies, previously detected by CT or MRI, and so candidate to arthroscopic procedure. The sequences employed were 3D "contrast-enhanced" gradient-echo for the dedicated system (E-Scan, ESAOTE, Italy) and 3D FSPGR for the whole body system (GE, Signa, Horizon). We classified chondral pathology following a grading system: grade 0, normal cartilage; grade 1, edema; grade 2, softening or swelling; grade 3, mild surface fibrillation; grade 4, severe surface fibrillation; grade 5, subchondral bone exposure. For low grade chondral lesions Arthro-MRI was performed.

Results: In all cases we found a significant correlation between dedicated and whole body units. Arthro-MR showed higher sensibility for grade 2 (1 case) and 3 (3 cases) lesions. All cases classified as grade 4 and 5 lesions (13 cases) were confirmed at the arthroscopy: in 7/13 cases MRI examinations showed a signal alteration of subchondral bone. In 5 patients with low grade chondropathy both MRI and Arthro-MRI examinations resulted less sensitive compared to arthroscopy.

Conclusion: The new optimized 3D contrast enhanced gradient-echo sequence performed on dedicated MRI unit showed a diagnostic accuracy equivalent to 3D FSPGR performed on 1.5 T unit. However they both underestimate low grade chondral lesions respect to arthroscopy.

B-0151 14:40

Anterior synovial impingement of the knee: Diagnostic value of static and dynamic MRI vs. arthroscopy

M. Caulo, F. Iannessi, A.V. Giordano, V. Calvisi, A. Barile, C. Masciocchi; *L'Aquila/IT*

Purpose: This work aims to retrospectively evaluate 30 patients affected by anterior knee pain comparing dedicated and whole body MR units imaging to arthroscopy.

Materials and methods: 30 patients entered this study. MR examination was performed using 0.2 T dedicated and 1.5 T whole body MR units. Dedicated MR unit allowed kinematics evaluation at three different degrees of flexion. In 20 cases i.v. injection of contrast media was performed. All the patients underwent arthroscopy.

Results: In all cases MRI revealed a region of altered signal intensity in the superior aspect of the Hoffa's body. Arthroscopy revealed the presence of synovial thickening in 15 cases and enlargement of the patello-femoral synovial recess in 10 cases. In 8 cases of synovial thickening infused MRI showed contrast enhancement meaning acute stage of inflammation and in 2 cases no contrast enhancement was found due to the presence of fibrous tissue. In 5 cases of histologically proved villonodular synovitis SE T2W sequences showed a region of high signal intensity with spots of low signal intensity inside. In all the patients showing synovial thickening kinematics MR revealed impingement of the Hoffa's body apex with the femoro-patellar joint.

Conclusion: We experienced three major pathological condition affecting the superior aspect of the Hoffa's body: enlargement of the patello-femoral synovial recess, synovial thickening and villonodular synovitis. Despite MR findings revealed not complete specificity we consider useful to compare imaging to arthroscopyc in order to establish criteria for diagnosis.

B-0152 14:50

Articular cartilage lesions: In vitro evaluation of T1-weighted MR imaging after Gd-DTPA^{2-} diffusion

K. Woertler[1], J. Moeller[2], H. Buerger[2], E.J. Rummeny[1]; [1]*Munich/DE*, [2]*Münster/DE*

Purpose: To evaluate contrast-enhanced T1-weighted MR imaging after Gd-DTPA^{2-} diffusion in the diagnosis of articular cartilage lesions with histopathological correlation.

Methods and materials: MR imaging was performed in 8 human patella specimens immediately (t_0) and 4 hours (t_4) after placement into a vessel filled with Gd-DTPA^{2-} solution (2.5 mmol/l), using T1-w SE and TSTIR-sequences with nulled cartilage signal (TI 300 ms). In a total of 128 articular cartilage areas MR imaging findings were correlated with macroscopic and histopathologic sections.

Results: Histopathology demonstrated 67 areas of normal articular cartilage (grade 0), 34 grades 1 and 2 lesions, and 32 grades 3 and 4 lesions. All grades 3 and 4 lesions (100 %) could be identified on t_0T1wSE, t_4T1wSE, t_0TSTIR, as well as t_4TSTIR images. Grades 1 and 2 lesions were identified as areas of decreased contrast enhancement on t_4T1wSE as well as t_4TSTIR images in 94 %. t_0T1-w SE and t_0TSTIR images demonstrated abnormal signal intensity in only 9 % and 12 %, respectively. Areas of decreased contrast enhancement were best visualized on t_4T1wSE and subtraction ($t_4 - t_0$) images.

Conclusion: In this experimental setting T1-weighted MR imaging after Gd-DTPA^{2-} diffusion provided excellent demonstration of articular cartilage surface lesions as well as early stages of cartilage degradation.

B-0153 15:00

MR imaging of the knee after arthroscopic treatment with osteocartilaginous autografts in cases of osteochondritis dissecans

C. Wisianowsky, S. Pokar, O. Kolokythas, A. Schütz, E.M. Merkle, H.-J. Brambs; *Ulm/DE*

Purpose: To evaluate the efficacy of MR imaging of the knee after arthroscopic treatment with osteochondral autografts in cases of osteochondritis dissecans compared with surgical scoring of clinical exploration.

Material and methods: 24 Patients were examined with 1.5 T MRI two years after surgical treatment. T2- and T1-weighted SE and T2-weighted GRE sequences with fat suppression were acquired. Application of contrast media was obsolete. The evaluation of MRI was made by two independent observers about edema of bone marrow, consolidation and vitality of the bone graft, status and vitality of the cartilaginous graft compared with a clinical scoring performed by surgeon after MR eamination.
Results: In all cases there was a good correlation between the findings of the two independent observers concerning the above mentioned criterias. A difference between radiological and clinical findings was not found.
Conclusion: MRI is an excellent non-invasive method in long-term monitoring of arthroscopic osteocartilaginous autograft of the knee.

B-0154 15:10

Longitudinal follow-up of early osteoarthritis of the knee with MRI
C.R. Krestan, M.J. Breitenseher, M.T. Schmook, F. Lomoschitz, S. Trattnig; *Vienna/AT*

Purpose: To evaluate the progression of early osteoarthritis of the knee joint by MRI.
Material and methods: Thirtytwo knees of 32 patients (mean age 43.6 ± 13.6 years) were selected from 978 MRI exams between 1/96 and 6/98. The inclusion criteria were grade 1 (intrachondral abnormality) or grade 2 (< 50 % loss of cartilage thickness) osteoarthritis in at least one compartment of the knee joint. Follow-up MRI scans were done 22 – 51 months later with the same protocol: sagittal T2-TSE; sagittal 3D-EPI with fat saturation on a 1.0 T MRI unit. Readers were blinded to date of scan and patient name. Cartilage lesions were assessed using a 4-grade classification. A total score was calculated from the sum of grades of each compartement.
Results: Total scores reached from 1 – 11 at baseline to 1 – 14 at time of follow-up exam. The mean difference of the total score between baseline and the second MRI scan was 0.96; $p < 0.05$ for all patients and 2.6; $p < 0.05$ for patients with progressive disease. Seventeen patients were stable, 15 showed progressive osteoarthritis.
Conclusion: Fortyseven % of patients with early osteoarthritis of the knee joint had a significant progressive cartilage destruction during a mean follow-up time of 31.4 months.

B-0155

withdrawn by author

B-0156 15:15

Nodular fasciitis: A comparative study of MRI findings and whole specimen histopathology
X. Wang, A.M.A. De Schepper, H. De Raeve, L.H.L. De Beuckeleer, J. Gielen, J. Somville; *Antwerp/BE*

Purpose: To compare histology of nodular fasciitis with MRI findings in order to define an MRI prototype of this lesion.
Materials and methods: Four patients who presented with some similar MRI findings were histologically diagnosed as nodular fasciitis. Findings of whole specimen sections in two patients were compared with the appearances on MRI.
Results: Two lesions presented with a peripheral component with higher SI than that of muscle on T1-WI and isointense to fat on T2-WI. The central parts were isointense to muscle and to water on T1- and T2-WI, respectively. The other two lesions showed relatively homogeneous SI, isointense to muscle on T1-WI, and overall high SI with central low SI areas on T2-WI. After contrast injection, there was marked enhancement at the periphery and no obvious enhancement in central areas in three cases. Whole specimen sections showed higher vascularity, more collagen and hyalin fibrosis, less cellularity and less fluid-filled spaces at the periphery than in the center in one lesion of half-year duration. In the second of two-month duration there was one component with rich myxoid stroma, and a second with abundant fluid-filled spaces.
Conclusion: Findings on MRI can be well explained by histopathological study, but time-related processes correlating with definite SI changes hamper the definition of a prototype presention of nodular fasciitis on MRI.

14:00–15:30 **Room C**

Abdominal and Gastrointestinal

SS 301a

Biliary tract

Chairpersons:
F. Arredondo (Miami, FL/US)
N. Elmas (Izmir/TR)

B-0157 14:00

Ultrasonographic monitoring of the effect of UDCA on the gallbladder motility in nonlithiasic patients with chronic hepatitis
D.L. Dumitrascu, M. Acalovschi, C. Pojoga, D.I. Dumitrascu; *Cluj/RO*

Background and aim: The ursodeoxycholic acid (UDCA) has been recently introduced in the management of chronic hepatitis (CH). There are contradictory data on its effect on gallbladder motility (GBM) in this group of patients. We looked for the effect of UDCA on the ultrasonographic parameters of GBM in patients with CH.
Methods: 16 patients were studied. They received either 200 mg UDCA t.i.d. (n = 9) or a conventional therapy including vitamins (n = 7, the control group). A high resolution 3.5 MHz sectorial transducer was used. The volume of the gallbladder was measured in fasting condition and at 0, 15, 30, 45, 60, 75, 90 min post cibum. The test meal was mixed and included 465 kcal, 14 g fat. GBM was measured from the following parameters: fasting volume (FV), residual volume (RV), ejection fraction (EF), AUC and T/2 of the gallbladder emptying curve. The protocol was repeated identically after 3 weeks of therapy.
Results: FV was increased by UDCA from 28.7 ± 14.9 to 41.8 ± 18.3 ml ($p = 0.027$). In the control group FV remained constant. RV, EF and AUC were not changed by UDCA and in the control group. T/2 was significantly lower in the group with UDCA compared to the control at the end of the trial (15.9 ± 7.5 vs. 33.4 ± 9.9 min ($p = 0.03$).
Conclusion: This is the first report on the diverging effects of UDCA on GBM in CH: the drug increases the fasting volumes but reduces the T/2 of the gallbladder emptying curve.

B-0158 14:10

Gallbladder varices in extrahepatic portal venous obstruction: Demonstration by intravenous CT portography
M.S. Gulati, S.B. Paul, N.K. Arora, M. Berry; *New Delhi/IN*

Purpose: We performed a prospective study to determine frequency of presence of gallbladder varices (GBV) by intravenous CT portography (CTP) in patients with extrahepatic portal venous obstruction (EHPVO).
Methods and materials: 90 patients (age range: 2 – 55 years) with EHPVO (initially diagnosed on abdominal sonography) underwent CTP using a subsecond helical CT scanner. Axial overlapping sections of 2 mm were obtained with collimation 3 mm and table speed 4.5 mm/s (pitch 1.5). Presence and patterns of GBV were studied.
Results: CTP demonstrated GBV in 54 (60 %) of 90 patients. GBV were said to be present when one or more of following findings were seen: diffuse wall enhancement (26/90), pinpoint areas of enhancement in GB wall (33/90), obvious large collaterals in GB wall (8/90) and pericholecystic collaterals (49/90). Presence of GBV did not correlate with the site and extent of EHPVO. Contiguous intrahepatic collaterals extending from GB bed to intrahepatic portal vein branches were seen in 41 of 54 (76 %) of patients with GBV, suggesting the role of GBV serving as bridging porto-portal collaterals. Hepatic perfusion defects were seen in 5/54 patients with GBV and were not seen in remaining 36/90 patients of EHPVO. GB calculi were seen in only 4/54 cases with GBV (as determined on sonography) suggesting no increase in risk for cholelithiasis.
Conclusions: GBV commonly develop as bridging collaterals in patients with EHPVO. CTP is very useful in detecting these varices and planning biliary surgery, given the frequency of iatrogenic surgical bleeding in these patients.

B-0159 14:20

Lymphatic spreading pathways of gallbladder carcinoma: Spiral CT demonstration
B. Song, Z.H. Yan, X.P. Zhou, P.Q. Min, X. Chen, Z.Y. Liu, J. Xu; *Chengdu/CN*

Purpose: To investigate the lymphatic spreading patterns of gallbladder carcinoma by spiral CT scanning.

Materials and methods: 35 histopathologically proven cases of gallbladder carcinoma were retrospectively included into the study. Contrast-enhanced spiral CT scanning of the upper abdomen was performed for all cases. CT images were jointly evaluated by three radiologists. A minimal anteroposterior diameter of 10 mm was used as the CT criteria for positive lymphadenopathy and the presence of malignancy within the enlarged lymph nodes was confirmed during surgical procedures. The location and CT visualization rates of lymphadenopathy were recorded for analysis.
Results: Three major groups of enlarged malignant lymph nodes from gallbladder carcinoma could be recognized on CT images: (1). Cholecystoretropancreatic group; (2). Cholecystoceliac group; (3). Cholecystomesenteric group. The spiral CT visualization rates of above nodal groups were 88.5 % (31/35), 71.4 % (25/35) and 57.1 % (20/35) respectively.
Conclusion: Three distinctive lymphatic spreading pathways can be observed in patients with gallbladder carcinoma, among which the cholecystoretropancreatic nodal group is the primary route.

B-0160 14:30

Frank intrabiliary rupture of hepatic hydatid cyst: Evaluation with MRI and MR cholangiography

I. Tsitouridis, N. Krokos, G. Kouklakis, D. Melidis, M. Emmanouilidou, F. Goutsaridou; *Thessaloniki/GR*

Purpose: To determine the accuracy of MRI and MR Cholangiography in the evaluation of obstructive intrabiliary rupture of hepatic hydatid cyst.
Materials and methods: Over a period of five years we studied with MRI and MR Cholangiography, 10 cases with proven intrabiliary rupture of hepatic hydatid cyst. Axial T2WI, axial pre-contrast T1WI were obtained using 1 T (Siemens Expert plus Scanner). MR Cholangiography was performed using a HASTE sequence with different slice thickness and different positional angles.
Results: In our study the incidence of intrabiliary rupture causing biliary obstruction was only 1.1 %. We depicted hydatid material in the biliary tract and dilatation in all cases. There was also a dilated biliary radicle in close proximity with the ruptured hydatid cyst. All the hepatic hydatid cysts were complicated unilocular or multicular cysts.
Conclusion: A combined study of MRI and MR Cholangiography is mandatory for proper preoperative evaluation of the intrabiliary rupture of hepatic hydatid cyst.

B-0161 14:40

Multislice CT cholangiography without biliary contrast agent: Technique and clinical applications

F. Zandrino[1], L. Benzi[1], L. Ferretti[1], M. Calabrese[2], F. Musante[1]; [1]*Alessandria/IT*, [2]*Genoa/IT*

Purpose: To describe our technique for CT cholangiography with multislice CT and to present our preliminary experience.
Methods and materials: Thirty-nine consecutive patients with suspected pancreatico-biliary disease were studied. A multislice CT unit was used (High Speed, General Electrics, Milwakee, WI) with the following technical parameters: 2.5 mm collimation; 7.5 mm/s table speed; 0.8 s rotation time; 200 mAs; 120 kVp; 18 – 24 s scantime; scan volume ranging from the hepatic dome to below the pancreatic head; 60 s delay after injection of 140 ml of iodinated contrast agent (Iomeron 350, Bracco, Milan, Italy) at 4 ml/s; no biliary contrast agent; oral iodined contrast agent to opacify stomach and small bowel loops; axial, multiplanar reformatted, and minimum intensity projection images were evaluated. Biliary ducts appeared as low density structures within the enhanced liver parenchyma.
Results: In 25 patients endoscopic retrograde cholangiography, percutaneous transhepatic cholangiography, or surgery were performed within 5 days after CT-cholangiography. CT cholangiography demonstrated 32/39 patients with biliary tree dilatation: 23/32 with malignant stenosis/obstruction, 9/32 with benign stenosis/obstruction; 3 patients with non obstructing lesions; 4 patient with normal findings. In the 32 patients with stenosis/obstruction further diagnostic or surgical procedures confirmed CT diagnosis.
Conclusion: Multislice CT cholangiography seem to be a promising diagnostic tool; it could be considered as a possible alternative to magnetic resonance cholangiography.

B-0162 14:45

Post-cholecystectomy syndrome, evaluation with helical-CT cholangiography and "Volume Rendering" reconstructions

A. Scardapane, A.A. Stabile Ianora, M. Midiri, M. Memeo, A. Rotondo, G. Angelelli; *Bari/IT*

Purpose: Aim of our work is to point out the helpful contribution of helical CT cholangiography with "Volume Rendering" reconstructions in patients with post cholecystectomy syndrome.
Methods and materials: 4 men and 9 women with post-cholecistectomy syndrome were studied. In 5 patients cholecystectomy was performed by laparotomic access and in 8 cases by videolaparoscopy. Cholangio-MRI could not be performed in any of the patient for the following reasons: claustrofobia in 2 patients, the presence of cardiac pace-makers, ferromagnetic vascular and surgical clips in 11 cases. Helical-CT scans were performed after oral administration of 6 g of iopanoic acid with the following parameters: thickness 5 mm, image index 2 mm, pitch factor 1.5, standard algorithm, with a minimum of 130 kV and 125 mA. All the images were trasferred to a workstation (Voxel Q, Picker) and reconstrucetd using the "Volume Rendering" software.
Results: The common bile duct was evident in all patients. Right and left hepatic ducts were visualized in 11 of 13 patients (84 %), second order intrahepatic branches in 9 of 13 (70 %) patients, third order intrahepatic branches in 4 of 13 (38 %) cases. Volume rendered reconstructions allowed the evaluation of the course of the main biliary duct, the morphology of cystic duct stump, the positioning of surgical clips and the presence of stones in the biliary tree in all patients.
Conclusion: Cholangio-CT has been found satisfactory for the study of the biliary tract in cholecystecomized patients who cannot be sujected to cholangio-MRI, or as a preliminary to ERCP.

B-0163 14:50

MRCP before interventional ERCP: A prospective study in pancreatobiliary disease

K.J. Hellerhoff, H. Helmberger, T. Roesch, M. Settles, T.M. Link, M. Classen, E.J. Rummeny; *Munich/DE*

Purpose: To determine the accuracy of MRCP preceeding therapeutic interventions with ERCP.
Methods: 45 patients (20 female, 25 male, 58.6 a) with obstructive jaundice or chronic pancreatitis scheduled for endoscopic/percutaneous therapy were included. The following information was required before ERCP: extent of hilar strictures and therapeutic options, number and size of bile duct stones, need of therapeutic procedures in symptomatic patients with bilioenteric anastomoses (BEA) or chronic pancreatitis (strictures or concrements?). MRCP was performed at 1.5 T (Philips ACS NT) using single shot, 2D multi slice- and 3D-TSE. ERCP was performed within one day of MRCP.
Results: The following diagnoses were found: Hilar strictures (HS) n = 8, bile duct lithiasis (BL) n = 3, obstruction in bilioenteric anastomoses (BEA) n = 9, chronic pancreatitis (CP) n = 25. In 89 % of all cases MRCP provided the required information for therapeutic planning. Results in subgroups: 100 % in BL, 63 % in HS, 100 % in BEA, 92 % in CP.
Conclusion: MRCP is a reliable method for the follow-up of chronic pancreatitis. In all patients with bilioenteric anastomosis, MRCP was able to specify the obstruction (stricture /stone) and to give further information for therapeutic approach. Hilar strictures are reliably detected and correctly classified. The number and location of dilated segments was better evaluated with MRCP, whereas in ERCP some dilated segments were overlooked. However, MRCP cannot yet provide reliable information concerning feasibility and efficacy of drainage.

B-0164 15:00

Bile duct obstructions caused by solid masses: MRI in differential diagnosis and prognosis for endoscopic treatment

T. Gorycki, M. Studniarek, P. Jagodzinski, M. Nowakowski, A. Zapasnik; *Gdansk/PL*

Purpose: To compare MRCP images and mean SIR of benign versus malignant lesions around bile duct strictures and to correlate them with size of endoprothesis.
Material and methods: Standard non-breathhold MR images encompassing the hepatico – pancreatic region and MRCP images were acquired from 80 patients (40 men, 40 women, mid. age 58). Mean signal intensity ratio and MRCP linear measurements were compared between benign and malignant conditions and in two groups including size of endoprothesis (< 10 F <) from 51 cases in which ERCP was performed. The significance of observed differences was determined by Kruskal Wallis test.

Results: Significantly higher mean SIR were counted in malignant lesions on T2W ($r = 0.0003$) and SPIRT2W images ($r = 0.0002$) and they were also associated with longer strictures ($r = 0.0071$) and larger diameter of biliary duct proximaly to obstruction ($r = 0.0024$). When grouping condition was size of endoprothesis significantly distinguishing features were: mean SIR on SPIRT2W images and stricture length on MRCP images. These relations were also estimated with ROC curves.
Conclusions: Probability of malignancy was higher with higher SIR on T2W images and with longer strictures. Inserting of larger endoprothesis was more probable with higher SIR on SPIRT2W images and in shorter strictures.

B-0165 15:10

Accuracy of different T2-w sequences for evaluation of intraductal pancreatic stones

P. Steiner, M. Bonacker, L.-U. Kühne, R. Maas, P. Nam, G. Adam; *Hamburg/DE*

Purpose: To compare the diagnostic accuracy of three different T2-w sequences for visualisation of intraductal pancreatic stones.
Material and methods: 20 patients with chronic pancreatitis and intraductal stones as shown by ERCP and CT underwent 1.5 T MR imaging. 10 patients with other pancreatic diseases and no intraductal stones served as control. Transversal and coronal HASTE, paracoronal RARE and thin-slice HASTE (TS-HASTE) in paracoronal orientation were performed. Prospective evaluation based on qualitative (5-point scale) and ROC-analysis performed by two observers. Sensitivity, specificity and interobserver variability were calculated.
Results: Qualitative analysis revealed no significant difference between RARE, HASTE and TS-HASTE (3.4; 3.5; 3.2). Areas under the curve (Az) of the ROC-analysis were 0.74; 0.66 and 0.60 for the first and 0.87, 0.93 and 0.82 for the second observer. Differences between Az were not significant. Interobserver variability was moderate to good (0.4 – 0.7) depending on MR-sequence. Sensitivity for detecting ductal stones was highest for the combination of transv. and coronal HASTE (82 %) followed by RARE (73 % and 63 %) and TS-HASTE (43 % and 52 %). Difference between the latter two being significant ($p < 0.01$). HASTE also revealed highest specificity (90 %) followed by TS-HASTE (80 %, 90 %) and RARE (77 %, 88 %).
Conclusion: All three T2-w sequences enable reliable detection of intraductal pancreatic stones. Interestingly, HASTE-imaging outperformed so-called MRCP sequences like RARE or TS-HASTE.

B-0166 15:20

Quadruple phase spiral computed tomography in the evaluation of peripheral type cholangiocarcinoma

M.G. Panteleli, E. Zafiriadou, G. Anastasiou, A. Anastasiou, G. Grollios, T. Tzormpatzoglou, K. Natsiopoulos, V. Sigounas; *Thessaloniki/GR*

Purpose: To define the hemodynamic features of the peripheral type cholangiocarcinoma by using quadruple phase spiral Computed Tomography (CT) of the liver.
Material and methods: Helical CT of the liver was performed in 29 patients with peripheral type cholangiocarcinoma, proved by needle (25) or surgical biopsy (4). 21 are men and 8 are women; age range 36 – 72 years, mean age of 61.055 years. Scans were obtained before i.v. contrast enhancement, 24 s, 60 s and 2 min after the start of acquisition.
Results: In 27 (93 %) patients there was a thick peripheral zone of enhancement of the tumor during the arterial and portal venous phase when the center of the tumor remain hypo attenuated. The border of the tumor with the normal hepatic parenchyma is irregular and lacy. 15 (55.5 %) of these tumors become homogeneous hypo attenuated on the delayed scans. 12 (44.4 %) demonstrate a "reversed" enhancement pattern on the delayed images, with enhancement of the previous hypo attenuated center and hypo attenuated, the previously enhancing, peripheral zone. In 2 (6.8 %) cases, the tumor enhances homogenously during the portal phase and the enhancement remains during the delayed phase; small distended ducts observed within the tumor.
Conclusion: Delayed scans are useful in characterization of liver neoplasms when helical CT is obtained.

B-0167 15:25

MR cholangiography: Evaluation of fat saturated T2-TSE in the axial plane for the diagnosis of choledocholithiasis

J.M. Alustiza, C. Gervás, E. Garciarena; *San Sebastian/ES*

Purpose: To evaluate the diagnostic accuracy of fat saturated T2-TSE weighted sequence with thin slices in the axial plane for the diagnosis of choledocholithiasis.
Materials and methods: Retrospective analysis of the MR-cholangiography images of 24 patients by two experienced radiologists blinded to each other and to the result of retrograde cholangio-pancreatography or intraoperative cholangiography considered as the "goald standards". The latter were positive in 12 patients. Patients were imaged in 1.5 T Philips MR system with the body coil. Imaging parameters of the sequence evaluated, fat suppressed T2-TSE in the axial plane, were as follows: echo time 100 ms, TR 1800 ms, turbo factor 23, fov 375, 228 – 256 matrix, respiratory compensation, contiguous slices, slice thickness 3 mm, number of slices 35, scan duration 5'40". Fat saturation achieved by means of Spectral Presaturation with Inversion Recovery pulse (SPIR).
Sensibility, specificity, and concordance between readers were calculated.
Results: Sensibility 91 %, specificity 86 % (2 false positive and 1 false negative), concordance between readers was 96 %.
Conclusion: Fat suppressed T2-TSE with thin slices (3 mm) in the axial plane has a high accuracy for the diagnosis of choledocholithiasis and is highly observer independent.

14:00–15:30 **Room E2**

Breast

SS 302

Breast MRI

Chairpersons:
Y. Grumbach (Amiens/FR)
W.A. Kaiser (Jena/DE)

B-0168 14:00

Breast lesions exclusively detected by MR: Correlation of quantitative signal parameters with malignancy

K.C. Siegmann, M. Müller-Schimpfle, S. Dannert, N. Fersis, U. Vogel, C.D. Claussen; *Tübingen/DE*

Purpose: To decrease the number of false-positive biopsies in exclusively MR-detected breast lesions by a better differentiation of benign and malignant by quantitative analysis of signal parameters in contrast enhanced (CE) dynamic MRI.
Materials and methods: The study included 51 exclusively MR-detectable lesions in 45 patients. All patients had undergone a dynamic CE MRI (0.16 mmol Gd-DTPA/kg) of the breast at 1.0/1.5 T (n = 36/15). Dynamic T1-weighted FLASH 3D (TR 13/9 ms, TE 6/4 ms, FA 50°) in coronar orientation and T2-weighted TIRM (TR 6200/5600 ms, TE 60 ms, FA 150/180°) were used for data acquisition. The following signal parameters were calculated for each lesion: (1) Time from contrast medium application to signal intensity peak (Tp); (2) Maximum slope of signal intensity curve (Smax); (3) Early enhancement (pre-contrast to first post-contrast; En1); (4) Wash out (fist to last post-contrast; En2-L); (5)Relative water content (RWC). Malignant and benign lesions were compared by t-test.
Results: 37 % (19/51) of the lesions have been malignant. The mean signal intensity peak has been reached faster in malignant lesions ($p = 0.16$) and mean loss of enhancement (wash out) from first to last post-contrast measurement has been stronger than in benign lesions ($p = 0.1$). But there is a considerable overlap of both parameters. En1, Smax and RWC show even less differences in malignant and benign changings.
Conclusion: Quantitative signal intensity parameters of exclusively MR-detected breast lesions do not correlate significantly with malignancy. However, malignancies show a tendency towards stronger wash-out and faster time to signal intensity peak.

B-0169 14:10

Evaluation of heterogeneity of breast tumors utilizing MR-elastography

J. Lorenzen, R. Sinkus, D. Schrader, C. Leussler, M. Dargatz, P. Roeschmann; *Hamburg/DE*

Purpose: Visualization and characterization of breast lesions by means of MR-Elastography
Materials and methods: MR-Elastography is a novel imaging technique to assess the in-vivo distribution of tissue elasticity. A transducer attached to the breast excites low-frequency sinusoidal mechanical waves, which are measured by a motion-sensitized spin-echo MR-sequence. Those measurements allow to reconstruct locally the elasticity tensor, from which tissue features such as anisotropy and local heterogeneity can be estimated. 10 patients with carcinoma, 5 patients with fibroadenoma and 10 volunteers were examined.

Results: All carcinoma could be visualized by MRE as regions of increased stiffness. However, local areas of increased elasticity were detected also in case of fibroadenoma and healthy volunteers. The analysis of the anisotropy yields an improved specificity. Still, the degree of local heterogeneity of the elasticity tensor seems as the most promissing parameter for the differential diagnosis.
Conclusions: MR-Elastography for breast lesion detection is feasible. The sole stiffness of the tumor is not sufficient to properly characterize pathology. The local heterogeneity of the tensor distribution holds promisses to increase specificity.

B-0170 14:15

Contrast enhancement in dynamic MR imaging of DCIS

P. Viehweg, D. Lampe; *Halle a. d. Saale/DE*

Purpose: In contrast to previous assumptions c.e. MRI is able to visualize DCIS. This study was undertaken to analyze the morphologic and dynamic features of pure DCIS and DCIS with microinvasion and to correlate these features with histopathology.
Material and methods: Retrospectively 90 cases were analyzed including 59 pure DCIS and 31 DCIS associated with microinvasion.
Results: Enhancement in DCIS was focal (70 %), diffuse (10 %) or ductal (16 %). No enhancement occurred in 4 %. Speed of enhancement was delayed in 62 %. There was a tendency toward a more ill-defined enhancement pattern in high grade DCIS and a more ductal in comedo type DCIS. However, no significant differences could be shown between high and non high grade DCIS, nor between comedo and non comedo type DCIS. No significant differences were noted between pure and microinvasive DCIS.
Conclusion: The enhancement behaviour was typical of malignancy (strong, early, focal ill-circumscribed or ductal) in only about 50 % of DCIS. Little or no enhancement does not allow reliable exclusion of non-invasive malignancy. This is of particular importance in cases with mammographically suspicious microcalcifications.

B-0171 14:25

MRI of the breast in patients with carcinoma of unknown primary origin

D. Roncaglia, M. De Santis, R. Romagnoli; *Modena/IT*

Purpose: To assess the utility of Magnetic Resonance Imaging of the breast in patient with Carcinoma of Unknown Primary (CUP).
Materials and methods: 8 patients presenting with metastatic disease compatible with breast cancer (axillary lymph node metastases n = 6, intramammary lymph node metastases n = 1, bone and brain metastases n = 1) who had negative X-ray mammograms and ultrasound underwent bilateral dynamic breast MR Imaging at 1.5 T (General Electric, Milwaukee, Wis., USA).
MRI was performed with 3D FSPGR. Six sequences were acquired, one before and five after intravenous bolus injection of gadopentate dimeglumine (DOTA Guerbet Aulnay-Sous-Bois, FRANCE).
The postprocessing included subtracted images, maximum intensity projection, multiplanar reconstruction and enhancement amplitude, calculated as percentage of signal intensity in the postcontrast phase.
Results: 5/8 patients showed lesions with enhancement amplitude typical of malignancy; in 3 cases MR images had corresponding tumor at surgery, 1 patient died one month later but autopsy was not performed and in the other one no tumor was detected after mastectomy. In 3/8 patients MR Imaging showed no abnormality and the primary lesion is still unknown.
Conclusion: MRI of the breast is an important procedure in patient population with Carcinoma of Unknown Primary and negative X-ray mammograms and ultrasound.

B-0172 14:35

3D non-rigid matching of contrast-enhanced MRI to assess chemotherapy response in breast cancer

N. Moore, C. Behrenbruch, C. Hardingham, P. Armitage, M. Brady; *Oxford/GB*

Purpose: 3D non-rigid registration between pre- and post-chemotherapy contrast-enhanced breast MRI acquisitions together with a pharmacokinetic model of contrast uptake, enables accurate and quantitative evaluation of the change in tumour vascularity.
Materials and methods: 13 women (mean age 48.2 a, range 40 – 62 a) were examined using either a 2D acquisition (9 cases) or a 3D acquisition (4 cases) dynamic gadolinium enhanced MRI study. Examinations were performed before and after three courses of chemotherapy. Enhancing lesions were segmented using a pharmacokinetic model and the two acquisitions non-rigidly deformed to the same geometry. The enhancement characteristics were compared automatically on a voxel-by-voxel basis. The computer analysis was compared with a radiological assessment of treatment response.
Results: Large (mean size 8.5 cm^2) tumours were confirmed in all patients; bilateral in 1, multifocal in 4 and multicentric in 4 women. The computer-based analysis corroborated with the radiologist's impression of no response in 1, partial response in 9 and complete response in 3 women.
Conclusion: Despite the difficulty of validating non-rigid registration algorithms, the preliminary results are encouraging. The long-term objective is to assess the effects of neo-adjuvant chemotherapy, rapidly and accurately.

B-0173 14:45

Examination of changes in size of malignant breast tumors during neoadjuvant chemotherapy using contrast enhanced dynamic MRI

K. Wasser, S.-K. Klein, S. Delorme, P. Sinn, H. Junkermann, I. Zuna, G. van Kaick; *Heidelberg/DE*

Purpose: To assess changes in breast carcinomas during neoadjuvant chemotherapy using contrast enhanced dynamic MRI and to directly compare preoperative measurement with the pathologically determinated size.
Methods: 21 patients with advanced breast cancer underwent a 1.5 T MRI scan prior to and following neoadjuvant chemotherapy (4 cycles of Epirubicin and Paclitaxel). A fast TurboFlash Sequence was used for the dynamic examination. The contrast uptake was quantified using a two compartment model and color-mapped. Diameters were measured for the overall extent of the tumor and the invasion foci only.
Results: 14 patients responded to treatment. In these cases the median tumor size reduction was 15 % after the 1st cycle (n = 14, range: –100 – +69 %), 18 % after the 2nd (n = 8, range: –100 – +76 %), 33 % after the 3rd (n = 8, range: –83 – –14 %) and 50 % after the 4th (n = 14, range –100 – –37 %). The correlation between preoperative diameter of the overall tumors'extent in MRI and the pathologically determinated size in all patients was r = 0.61 (p = 0.0031).
Conclusion: Contrast enhanced dynamic MRI is suitable for monitoring tumor response during neoadjuvant chemotherapy. In patients who respond to treatment a clear tumor regression is observable in later follow-up examinations, i.e. after the third cycle of chemotherapy.

B-0174 14:55

Cost-effectiveness of MR-imaging in the preoperative work-up of suspicious breast lesions

K. Schmitt[1], T. Böhm[2], A. Malich[1], M. Fleck[1], W.A. Kaiser[1]; [1]*Jena/DE*, [2]*Zürich/CH*

Purpose: To assess economic consequences of preoperative MRM in patients with suspicious breast lesions.
Patients and methods: 447 patients with suspicious breast lesions treated during 8/1995 and 3/1999 at the University of Jena underwent mammography, ultrasound, MRM surgery and histologic assessment. Costs of surgery of malignant lesions were calculated based on case-related billing agreements. Costs of surgery of benign lesions were calculated using the per-day billing rate and average hospitalization time.
In 36 cases no surgery was performed due to negative MRM. 140 benign lesions were treated surgically despite negative MRM. The resulting costs were compared to the costs of preoperative MRM.
Results: Costs of one MRM are DEM 1 034. Costs for benign breast lesion work-up are DEM 2 960 (the per-day billing rate DEM 722; average hospitalzation time 4.1 d). Costs for surgery of malignant lesions varied between DEM 6 092 (breast conserving therapy) and DEM 8 520 (mastectomy with expander implantation). Costs for MRM in 140 cases amount to DEM 144 886, treatment costs for 140 benign lesions come to DEM 414 470. Total savings due to avoided hospitalization could sum up to DEM 269 584. In 11 cases only MRM showed false positive results causing costs of DEM 32 565. The real amount of economization was DEM 69 203, caused by 36 cases with benign breast MRM and no surgery.
Conclusion: MR imaging of the breast is a valuable tool for preoperative evaluation of suspicious breast lesions. Despite the currently high costs of MRM a severe cost reduction caused by prevention of unnecessary surgery can be achieved, avoiding additionally surgery and associated trauma for the patients.

B-0175 15:05

Preoperative localization and biopsy of non-palpable breast lesions with a special localization device on an open Scanner

C. Perlet, H. Sittek, P. Schneider, E. Linsmeier, M.F. Reiser; *Munich/DE*

Purpose: MRI-guided interventional maneuvers in the breast, when closed MRI scanners are employed are relatively complex and time consuming. The purpose of our investigations was to develop a special device for the localization and biopsy of breast lesions using an open low-field MRI Scanner (Magnetom Open, Siemens, Erlangen, Germany) permitting free access to the patient.

Method/materials: Due to its particular material and construction characteristics, a newly developed device for localization and biopsy of breast lesions is appropriate to remain within the magnetic field during the examination without degrading image quality. We performed 125 tests in a phantom and 31 investigations in patients including 26 wire-localizations and 5 biopsies.
Results: The interventional maneuvers in the phantom could be performed very precisely. In all 125 phantom studies, the needle (14 G coaxial biopsy cannula, Bard) was positioned close to the simulated lesion. In 25 out of 26 patients the needle was positioned within a distance less than 5 mm from the lesion. When using the 14 G coaxial biopsy cannula (Bard, Karlsruhe, Germany) the needle tip was found adjacent next to the lesion in all 12 cases (7 wire-localizations, 5 biopsies).
Conclusions: Our results indicate that our device allows very precise preoperative localization of breast lesions within the Magnetom Open. Using MRI-compatible, large-core needles, biopsy under direct MRI control resulted in good results.

B-0176 15:15

Clinical value of MR-guided biopsy: Experience of 210 vacuum biopsies
B. Amaya, A. Heinig, C. Nowbary, A. Große, R. Beck, J. Buchmann;
Halle a. d. Saale/DE

Purpose: Contrast-enhanced MRI allows to detect lesions, which are not or barely visible by other methods. We have used MR-guided vacuum biopsy for work-up of these lesions and have analysed the value of c-e-MRI and of MR-guided VB in 210 consecutive cases.
Materials and methods: 210 consecutive VB in 176 patients have been analysed as to indication of initial MRI, histology, and further treatment/follow-up.
Results: Major initial indications concerned: discrete mammographic change on one view only, status after breast conserving therapy, same or contralateral breast, genetic risk, scarring, etc. 61/210 lesions were malignant including 27 DCIS. 65 % of the lesions were < 1 cm and 20 % < 5 mm. Advantages of MR-VB concerned: correct diagnosis and localisation of malignancy, preoperative proof/exclusion of multicentricity or larger extent, avoidance of surgery of benign lesions.
Conclusion: MR-VB allows to solve problems with MR-detected lesions and improve therapeutic decisions.

B-0177 15:25

Contrast-enhanced MRI of the breast after silicone implant
R. Beck, D. Lampe, J. Buchmann; *Halle a. d. Saale/DE*

Purpose: After mastectomy and reconstruction using silicone implants exclusion and detection of recurrence may be impaired. C.e. MRI promises additional valuable information. Our experiences in 280 patients are reported.
Method/materials: C.e. MRI was performed using dynamic 3D-FLASH and 0.2 mmol Gd-DTPA/kg b.w. In addition mammography and 7.5 MHz ultrasound was performed.
Results: Later than 6 months. postoperatively enhancement within scarring was usually insignificant. Problems occurred in 8 % of the patients because of focally enhancing granulomas or diffusely enhancing reactive-inflammatory changes, but could in 9/21 patients be solved by follow-up. 19/20 recurrences were visible by MR, 9/20 recurrences were detected by MRI alone. 1/19 recurrences was visible in retrospect as 2 mm enhancing focus on an MRI study performed two years before and was therefore counted as false negative for all methods.
Conclusions: C.e. MRI is of high value in patients with silicone implants after mastectomy.

14:00–15:30 **Room F1**

Chest

SS 304

Pulmonary and mediastinal blood vessels

Chairpersons:
C. Schaefer-Prokop (Vienna/AT)
P. Vock (Berne/CH)

B-0178 14:00

Does multidetector CT (MDCT) allow analysis of peripheral pulmonary arteries beyond the subsegmental level? A comparative study with thin collimation single detector CT (SDCT)
B. Ghaye, D. Szapiro, V. Delannoy, I. Mastora, J. Rémy, M. Rémy-Jardin;
Lille/FR

Purpose: To determine the frequency and order of well-visualized peripheral pulmonary arteries with MDCT; To compare the results with those obtained with SDCT.
Materials and methods: Peripheral pulmonary arteries were evaluated in 30 consecutive patients devoid of pleuroparenchymal disease scanned with contrast-enhanced MDCT (collimation: 4 × 1 mm; pitch of 1.7 to 2; scan time: 0.5 s). From each MDCT data set, two series of scans were systematically reconstructed, 1.25 mm (Group 1) and 3 mm (Group 2) thick sections, leading to the analysis of 600 segmental, 1200 subsegmental, 2400 5th order and 4800 6th order pulmonary arteries in each group. Each artery was coded as analyzable when the vessel was depicted without partial volume effect from its proximal to its distal portion. Results were compared with those obtained in a matched population of 20 patients scanned with SDCT (Group 3) (collimation: 2 mm; pitch: 2; scan time: 0.75 s).
Results: MDCT with 1.25 mm thick reconstructed sections (Group 1) allowed analysis of a significantly higher percentage of subsegmental arteries compared with Group 3 (94 % vs 62 %; $p < 0.0001$) and Group 2 (94 % vs 82 %; $p < 0.0001$); and a significantly higher depiction of 5th and 6th order arteries compared with Group 2, respectively identified in 74 % and 35 % of cases in Group 1 and in 47 % and 16 % in Group 2 ($p < 0.0001$). The reasons for inadequate depiction of Group 1 were partial volume effect (43 %), anatomic variants (39 %), cardiac motion artifacts (17 %) and respiratory motion artifact (1 %).
Conclusion: MDCT with 1.25 mm thick reconstructed scans significantly improves evaluation of peripheral pulmonary arteries down to the 6th order.

B-0179 14:10

Early and late outcome of surgical replacement of the ascending aorta: Assessment by spiral CT
E. Neri, P. Sbragia, C. Gianni, P. Boraschi, C. Spinelli, C. Cappelli, F. Falaschi, C. Bartolozzi; *Pisa/IT*

Purpose: We aimed to investigate the early and late outcome of surgical replacement of the ascending aorta by spiral CT.
Materials and methods: A series of 15 patients that underwent surgical repair of the acending aorta for Stanford type A dissection, were studied with spiral CT within 1 – 12 months from intervention. Unenhanced and enhanced spiral CT was performed with 5 mm collimation (2.5 mm reconstructions spacing) and pitch range 1.4 – 1.8. Images were analyzed at independent workstation (Advantage Windows 3.1; GE Medical Systems); multiplanar reconstructions and maximum intensity projections were always used. No patients underwent re-intervention. Aortography was used as standard of reference.
Results: Spiral CT revealed the occurrence of complications in 7 (47 %) patients. Five pseudoaneurysms occurred in 4 patients (27 %), located at the level of the proximal surgical anastomoses in 4 cases, and distal in 1 case. Two (13 %) re-dissections occurred at the level of the surgical anastomosis. Spiral CT correctly identify the signs of aortic rupture in 1 case (6 %). Spiral CT had 1 false positive case (1 artifact mimicking dissection), and no false negative (sensitivity 100 %, specificity 87 %).
Conclusions: In our experience the occurrence of pseudoaneurysm at the level of the surgical anastomoses was the most frequent complication. Spiral CT proved to be effective in excluding complications after surgery of the ascending aorta.

B-0180 14:20

Efficacy of embolisation for hemoptysis in 64 patients: Are there indicators predictive of recurrence?

R. Maroldi, G. Battaglia, F. Mossi, D. Farina, P. Maculotti; *Brescia/IT*

Purpose: To investigate the parameters related to the underlying bronchopulmonary diseases, to the characteristic of the hemorrhage and to the abnormal vascularisation that can predict relapse of the hemoptysis.
Materials and methods: Sixty-four out of 88 patients with hemoptysis have been embolised by mean of PVA particles. Forty-three patients (67.2 %) had no more hemorrhage; 9/21 recurrences underwent a second embolisation; 4/9 had a third procedure, in 2/4 it was successful (secondary success 70.3 %). Six patients were subsequently treated by surgery; 12 were controlled by medication; 3 patients died of hemorrhage. Follow up ranges from 8 to 79 months (avg. 47).
Results: Among the different parameters analysed, the following six resulted statistically significant: underlying bronchopulmonary disease ($p = 0.045$); combination of a micetoma and/or BT ($p = 0.0008$); time from hemoptysis-to-embolisation ($p = 0.01$); number of abnormal bronchial arteries ($p = 0.01$); exclusively ipsilateral abnormal vascularisation (bronchial or/and parietal arteries) ($p = 0.03$); demonstration of systemic-to-pulmonary shunts ($p = 0.02$).
Conclusions: This study suggests that the efficacy of particle embolisation for hemoptysis depends more on the type of the pulmonary lesion rather than on the simple presence of a well known pulmonary disease. As recurrences tend to develop from lesions that are fed exclusively by ipsilateral arteries and/or in the presence of a detectable systemic-to-pulmonary shunt, the hemodynamic features of the lesion seems to be significant for predicting the outcome of treatment.

B-0181 14:30

Segmental and subsegmental pulmonary embolism (PE): Improved detection with thin-collimation multislice CT (MSCT)

U.J. Schöpf, C. Rieger, N. Holzknecht, T.K. Helmberger, C. Hong, D.N. Exarhos, M.F. Reiser; *Munich/DE*

Purpose: To test MSCT of the chest with 1 mm collimation and reconstruction of thin slices for improving the detection of peripheral PE.
Materials and methods: We use MSCT (VolumeZoom, Siemens) to scan the entire chest with 500 ms/rotation and 1 mm collimation within one breath-hold. In 17 patients with central (> lobar) PE the data was used to perform 1 mm, 2 mm, and 3 mm reconstructions. Each set of images was monitor-read by three radiologists to determine the detection rates of emboli in segmental and subsegmental pulmonary arteries.
Results: 340 segmental and 680 subsegmental arteries were evaluated with 1, 2, and 3 mm section thickness by each reader (9180 observations). In segmental arteries, use of 1 mm sections resulted in a 32 % ($p < 0.01$) increase in the detection rate of emboli versus use of 3 mm sections, and an 8 % increase versus use of 2 mm sections. For the detection of emboli in subsegmental arteries, use of 1 mm sections yielded a 40 % ($p < 0.01$) increase versus use of 3 mm sections, and a 14 % ($p < 0.01$) increase versus use of 2 mm sections. With use of 1 mm sections versus 3 mm sections the number of indeterminate cases decreased by 67 % for segmental and by 76 % for subsegmental arteries. Overall interobserver agreement for the total number of emboli in subsegmental arteries was $r = 0.87$ with use of 1 mm sections, $r = 0.79$ with use of 2 mm sections and $r = 0.68$ for 3 mm sections.
Conclusions: MSCT scanning of the chest with 1 mm collimation and reconstruction of thin sections improves the detection of pulmonary emboli in segmental and subsegmental pulmonary arteries.

B-0182 14:40

Spiral CT angiography of pulmonary embolism: Impact of multislice CT (MSCT) on the frequency of indeterminate examinations

D. Szapiro, B. Ghaye, I. Mastora, A. Duhamel, J. Rémy, M. Rémy-Jardin; *Lille/FR*

Purpose: To evaluate the impact of multislice CT (MSCT) on image quality and diagnostic value of spiral CT angiograms indicated for pulmonary embolism (PE).
Materials and methods: 109 consecutive patients suspected of acute PE underwent MSCT (collimation: 4 × 1 mm; pitch: 2; scan time: 0.5 s) (Group 1). Image quality and diagnostic results in Group 1 were compared with those obtained in a population of 284 consecutive patients evaluated with thin collimation single slice CT (SSCT) (collimation: 2 mm; pitch: 2, scan time: 0.75 s) (Group 2), with similar injection protocols (120 ml of a 24 % or 30 % contrast agent; flow rate: 4 ml/s).
Results: For a significantly longer mean z-axis coverage (Group 1: 154 mm; Group 2: 113 mm; $p < 0.001$), the mean (± SD) duration of data acquisition was significantly shorter with MSCT (Group 1: 15.5 ± 4.7 s; Group 2: 22 ± 2.8 s; $p < 0.0001$) and the frequency of respiratory motion artifacts significantly reduced (Group 1: n = 29; 27 %; Group 2: n = 148; 52 %; $p < 0.0001$). No statistically significant difference between the two groups was found in the quality of arterial enhancement, mainly graded as good or excellent (Group 1: n = 109; 100 %; Group 2: n = 277; 97 %). Considering the absence of technical failures in Group 1 (Group 2: n = 10; 3.5 %), the number of spiral CT angiograms coded as technically adequate for the evaluation of PE was sigificantly higher in Group 1 (n = 109; 100 %) than in Group 2 (n = 274; 95.5 %) ($p < 0.05$).
Conclusion: Improvement in image quality provided with MSCT accounts for significant reduction in the number of indeterminate examinations in routine clinical practice.

B-0183 14:50

CT phlebography and CT angiography of the pulmonary arteries in the diagnosis of acute lung embolism

L. Jonetz-Mentzel, S. Basche, C. Eger; *Erfurt/DE*

Purpose: With the Multiple Detector Spiral CT we have a method which enables us to realize a CTA of the pulmonal arteries and a CT phlebography.
Method: During 7 month we performed a CTA of the pulmonal arteries in combination with a CT phlebography of the V. cava/V. iliaca/proximal V. femoralis and the V. poplitea down to the proximal shank veins on 70 patients with an assumed diagnosis of acute lung emboly.
Results: In 27 of 70 cases, the assumed diagnosis lung emboly was confirmed. In 8 of 11 central lung embolies, a thrombosis of the V. cava/V. iliaca/V. femoralis was found with the CT phlebography, in 1 of 11 a doubled V. cava. In 9 of 11 cases, an additional phlebography had been performed on both sides which showed in 2 further cases a thrombosis of the V. poplitea or of the shank veins. In 3 of 16 lung embolies, a thrombosis of the V. femoralis was found. In 6 of 53 patients without lung embolies, deep thromboses could be detected with the CT phlebography. In one case, we found a retroaortal left kidney vein.
Conclusions: Using contrast medium applications of the CTA, CT phlebograhy helped us detect therapy relevant thromboses of the V. cava/V. iliaca/proximal V. femoralis with high sensitivity. For the detection of thromboses in the popliteal veins and shank veins, an extension of the survey volume can be realized by Multi Detector Spiral CT.

B-0184 15:00

Severity of acute pulmonary embolism: Evaluation of a new spiral CT angiographic score in correlation with echocardiographic data

I. Mastora, P. Masson, E. Galland, V. Delannoy, A. Duhamel, C. Thery, J. Rémy, M. Rémy-Jardin; *Lille/FR*

Purpose: To investigate whether the severity of acute pulmonary embolism (PE) could be quantitatively assessed with spiral CT angiography (SCTA).
Materials and methods: 36 patients with a high clinical suspicion of PE underwent prospectively thin-collimation SCTA and echocardiography at the time of the initial diagnosis (T1) and after initial therapy (T2). The CT severity score was based on the percentage of obstructed surface of each central and peripheral pulmonary arterial section using a 5-point scale (1: < 25 %; 2: 25 – 49 %; 3: 50 – 74 %; 4: 75 – 99 %; 5: 100 %). The sum of the detailed scores attributed to 11 central (5 mediastinal and 6 lobar) (range: 0 – 55) and 20 segmental (range: 0 – 100) arteries per patient led to the determination of central, peripheral and global CT severity scores and subsequent quantification of percentages of obstruction of the pulmonary circulation. Echocardiographic severity criteria included the presence of signs of acute cor pulmonale and/or systolic pulmonary hypertension (> 40 mmHg).
Results: SCTA depicted acute PE in all patients at T1 (central PE: 34/36) with complete resolution of endovascular clots in 10 patients at T2. A significant correlation was found between the presence of echocardiographic signs of severity at T1 and the global, central and peripheral CT scores at T1 ($p < 0.005$). Reduction in the CT scores between T2 and T1 was significantly correlated with resolution of echocardiographic signs of severity ($p < 0.003$).
Conclusion: The CT severity score evaluated in the present study enables an accurate quantitative assessment of acute pulmonary embolism severity on SCTA, readily applicable in routine clinical practice.

B-0185 15:10

Rapid ELISA assay for plasma D-dimer in the diagnosis of segmental and subsegmental pulmonary embolism

P.E. Sijens[1], M. Oudkerk[1], H.E. van Ingen[2], E.J.R. van Beek[3], A. Berghout[2]; *[1]Groningen/NL, [2]Rotterdam/NL, [3]Sheffield/GB*

Purpose: To assess the accuracy of a rapid ELISA D-dimer assay for the exclusion of pulmonary embolism (PE) in patients suspected of PE, using pulmonary angiography alone as reference method rather than a diagnostic strategy including lung scintigraphy and leg vein ultrasonography.
Materials and methods: In 342 patients who were examined by pulmonary angiography to diagnose or exclude PE, the accuracy of the quantitative rapid VIDAS D-dimer test for the exclusion of PE was evaluated retrospectively. D-dimer levels were assayed in frozen samples collected during the diagnostic work-up at the time of pulmonary angiography while on treatment with unfractionated heparin for 1 – 2 days.
Results: Mean plasma D-dimer concentrations were increased in patients with angiographic evidence of PE ($P < 0.0001$). The sensitivity of D-dimer for segmental PE was 98 %, its accuracy in excluding segmental PE was 99 %, higher than the respective figures for subsegmental PE (76 % and 94 %; $P < 0.01$, both). For both forms of PE combined the sensitivity was 90 % and the negative predictive value 94 %.
Conclusion: The sensitivity and negative predictive values reported here, are low compared with previous studies using the same rapid ELISA D-dimer assay. This probably reflects an overlooking of mild cases of subsegmental PE in previous studies, although a reduction of D-dimer levels by the heparin pretreatment may have contributed to part of the discrepancy. Prospective studies are needed to clarify this issue.

B-0186 15:20

Prospective comparison of spiral CT and real-time MR imaging with radial scanning in suspected pulmonary embolism

P. Haage[1], A. Bücker[1], S. Krüger[1], G.B. Adam[1], G. Krombach[1], J. Wildberger[1], W. Piroth[1], T. Schäffter[2], R. Günther[1]; *[1]Aachen/DE, [2]Hamburg/DE*

Purpose: To evaluate the accuracy of real-time radial MR scanning without respiratory control in the diagnosis of pulmonary embolism.
Materials and methods: Twenty patients with suspected pulmonary embolism underwent both spiral CT angiography and radial MR angiography. Gradient echo images (TR 16 ms, TE 4 ms, FA 18°) were obtained with a 1.5 T MR imager after i.v. application of Gd-DTPA at a dose of 0.2 mmol/kg body weight. A combination of radial scanning and the sliding window reconstruction technique was applied, allowing data reconstruction in real-time with a frame rate of 20 images per second. Scanning was performed during free breathing. All images were reviewed with regard to the presence or absence of intravascular filling defects.
Results: Pulmonary embolism was detected by spiral CT in 9 of the 20 patients. All outflow tract and lobar emboli and > 90 % of segmental emboli as demonstrated by spiral CT were also identified on radial MR images.
Conclusion: In the diagnostic work-up of pulmonary embolism image acquisition without respiratory control by implementing real-time radial scanning is possible. The quantitative results using the described angiographic technique for depiction of and differentiation between the normal and pathologic pulmonary vasculature are promising.

14:00–15:30 **Room F2**

Neuro

SS 311

Brain ageing/Degenerative spectroscopy

Chairpersons:
A.G. Osborn (Salt Lake City, UT/US)
C.A. Raybaud (Marseille/FR)

B-0187 14:00

Brain MR spectroscopy in ageing women and men

P.E. Sijens[1], T. den Heijer[2], S.E. Vermeer[2], M.M.B. Breteler[2], A. Hofman[2], M. Oudkerk[1]; *[1]Groningen/NL, [2]Rotterdam/NL*

Purpose: To assess the effect of aging on the proportions of choline, creatine and N-acetyl aspartate in the brains of elderly women and men.
Materials and methods: Magnetic resonance spectroscopy was used to map the plane above the ventricles of the brain. The examinations were performed in 271 healthy elderly persons in 1995 – 1996 and were repeated four years later (1999 – 2000). Ratios of choline, creatine and N-acetyl aspartate were calculated and compared between women and men.
Results: In 1995 – 1996, at mean age 73, the proportions of choline, creatine and N-acetyl aspartate were identical in men and women. Four years later reduced choline/creatine and N-acetyl aspartate/creatine ratios were observed in both sexes, reduced choline to N-acetyl aspartate in women only ($P < 0.02$, both).
Conclusion: The proportions of choline, creatine and N-acetyl aspartate, while identical in healthy men compared to women at a mean age of 73 years, change substantially with further aging and differently in women and men.

B-0188 14:10

Quantitative approach for evaluating ageing peculiarities of human brain metabolism by ^{1}H MRS

V.A. Rogozhyn, Z.Z. Rozhkova, V.V. Kuznetsov; *Kiev/UA*

Purpose: Our goal is to investigate regional differences in cerebral metabolite concentrations with age by quantitative ^{1}H MRS.
Methods and materials: 45 volunteers (24 healthy mails and 21 femails ranged from 25 to 75 years old) were examined by ^{1}H MRS with 1.5 T Magnetom Vision Plus System (SIEMENS). Two locations with potentially different sensitivity to ageing pecularities are chosen: one is in the occipital gray matter (GM) of posterior parietal lobes (above the calcarine fissure and across the midline), and the other is in the parietal white matter (WM). All spectra are recorded with the STEAM sequence (VOI 8 cm^3; NS 128, 256; TR/TE 1365/135, 30; 1500/270).
Results: From analysis of the MRS spectra we find the metabolite concentrations C (mmol) in WM: NAA/Cr/Cho = $(7.60 \pm 1.54)/(4.32 \pm 0.87)/(1.87 \pm 0.23)$ and in GM: NAA/Cr/Cho = $(8.22 \pm 1.72)/(5.65 \pm 0.98)/(1.69 \pm 0.43)$. The ratio Cho/Cr decreases for %GM with age. The ratio Cr/NAA increases for %GM with age. Correlations between Cho/Cr and ageing, and Cr/NAA and ageing in WM are not established.
Conclusion: The results of our study show that ageing effects on metabolite ratios are more pronounced in the GM regions of the brain. In contrast in the WM, there is no significant change in the metabolite ratios with ageing. These observations are important for differentiating normal effects of ageing from changes due to brain diseases (such as degenerative or vascular disorders) which typically occur in elderly patientes.

B-0189 14:20

Age related changes in fMRI using 3D-PRESTO multi-shot EPI

V. Hesselmann, O. Zaro Weber, O.W. Schulte, B. Krug, H. Kugel, K. Lackner; *Cologne/DE*

Purpose: Assessing age related decline of BOLD signal change during finger tapping using a 3D-PRESTO multi-shot EPI sequence for functional MRI
Methods and materials: 110 right handed healthy volunteers (age 19 to 80 years) underwent fMRI-examinations on a 1.5 T imaging system (Gyroscan ACS NT, Philips, Best, NL). BOLD images were obtained using a three dimensional multi shot EPI sequence with shifted echo (PRESTO). Finger tapping of the right hand was used as task for motor stimulation. Absolute and relative signal differences and cluster sizes of activation for the left motor cortex were obtained using a scanner software postprocessing tool (ACT, Philips). In addition, Z-Score, pooled Z-score and cross correlation activation maps were calculated and matched with high resolution anatomic images.
Results: A significant decrease with age could be detected for absolute and relative signal intensity differences. Age related reduction of BOLD-activation can be assumed for signal loss. CC- and z-values decreased accordingly.
Conclusions: The BOLD Signal changes durin finger tapping decline with age. This corresponds to PET-studies and should be considered in clinical application of fMRI.

B-0190 14:30

Correlation of MRSI and neuropsychological tests in patients with Alzheimer's disease

O.W. Schulte, H. Kugel, B. Krug, B. Naumann, R. Mielke, K. Lackner; *Cologne/DE*

Purpose: Since MR spectroscopic studies have shown decreased NAA/Cr and NAA/Cho in gray matter and increased Cho/Cr in white matter in patients with Alzheimer's desease (AD), we aimed to determine whether there is a correlation in neuropsychological tests used to evaluate AD patients.

Methods and materials: 17 patients with probable AD according to NINCDS-ADRDA criteria underwent MRSI (using PRESS). The degree of dementia was assessed by different psychometric tests (MMST, Memo-1, Memo-2, DSST, FBT-1, FBT-2, FAS). 8 healthy, age-matched volunteers were examined as a control. Signal intensities for Cho, Cr and NAA were determined in 7 brain regions. Correlations between signal intensity ratios and neuropsychological tests were calculated with ANOVA and SAS statistical software.
Results: The increase of NAA/Cr correlated with the score on the Memo-1 test in the paravisual cortex ($r = 0.67$) and in the temporoparietal association cortex ($r = 0.52$). There was a significant decrease of NAA/Cr related to age in the visual ($r = -0.57$) and in the temporoparietal association cortex ($r = -0.58$).
Conclusion: The reduction found in NAA/Cr and NAA/Cho in AD patients is consistent with earlier investigations. The degree of metabolic alterations varies in different regions of the brain. Memo-1 test scores correlate with a decrease of NAA/Cr in the paravisual and the frontoparietal association cortex.

B-0191 14:40

Assessment of SPET brain semi-quantitative data using Benford's or the semi-logarithmic law

J.P. Coffey; *Manchester/GB*

Introduction: Benford's or semilogarithmic law is a phenomenological law stating that in numerical data acquired in a semi-random method the probability of the first digit being D, is given by the logarithmic distribution; $\ln(D + 1/D)/\ln 10$. The law is sensitive to biasing or tampering of data, in which case the frequency of the digit 1 differs from the predicted 30.1 % and an increased frequency of digits 5 and 6 in particular, is noticed. This phenomenon is independent of a numerical base and applies to data that are not dimensionless. To date its use has not been reported in evaluating data in medical research.
Purpose: To assess compliance of semi-quantitative data from single photon emission tomographic SPET brain perfusion scans with Benford's law.
Method: Total counts from 3561 regions of interest from the cortical ribbon of 90 SPET axial and coronal brain scans, (76 subjects; 14 had repeated scans) were obtained and the frequency of the first digit recorded. Each count reading had at least three digits. 10 subjects were normal volunteers and the remainder had diagnoses of probable Alzheimer (63 subjects) or multi-infarct or other dementing disorders (3 subjects).
Result: The frequencies of digits 1, 3, 4, 5, and 6 as first digits were 29.1 %, 12 %, 8.7 %, 6.1 % and 6.77 % and closely matched their predicted frequencies of 30.1 %, 12 %, 9.6 %, 7.9 %and 6.6 %.
Conclusion: This suggests that semi-quantitative SPET numerical data comply with Benford's law and that examining numerical data in this way may be useful in assessing data for the presence of bias in audit or research.

B-0192 14:50

Different patterns of ^{18}FDG-metabolism in patients with DLB vs. Alzheimer's disease

S. Mirzaei, P. Knoll, T. Bruecke, H. Koehn; *Vienna/AT*

The second most common cause of degenerative dementia is diffuse Lewy body disease (DLB) with progressive cognitive deterioration, fluctuation of cognitive and motoric functions and psychotic symptoms. It is characterized histologically by the occurrence of Lewy bodies in cortical and subcortical structures. Four patients with clinically suspected diagnosis of diffuse Lewy body disease were studied with 18-FDG PET and compared to 8 healthy control subjects. PET studies of the head was performed by a Siemens ECAT-ART PET-scanner with attenuation correction using 137-Cs point sources and iterative reconstruction applying OSEM-algorithm. In all the patients the same distribution pattern of diffuse glucose hypometabolism in the entire cortical region sparing the primary somatomotor cortex, but also in the occipital cortex was found, which was significantly differernt from those of control group. This characteristic pattern of cortical hypometabolism has been suggested as a result of diaschisis due to disruption of intracortical connections. The few cases reported in the literature so far describe similar findings. The pattern of diffuse FDG-hypometabolism in the entire cortex including the occipital region seems to be a typical scintigraphic feature of DLB that is distinctive from dementia of Alzheimer's disease.

B-0193 14:55

Sensitivity of PD sequence for lesion detection in Wilson's disease and Hallervorden–Spatz disease

D. Kozic[1], S. Popovic[1], S. Stojanovic-Kecojevic[2], O. Nikolic[2], J. Ostojic[1], R. Semnic[1]; *[1]Sremska Kamenica/YU, [2]Novi Sad/YU*

Purpose: The aim of the study was to perform retrospective evaluation of concrete importance of PD sequence application for lesion detection in Wilson's disease and Hallervorden–Spatz disease.
Methods: Sensitivity of PD-W spin-echo (SE) or turbo-spin-echo (TSE) and T2-W sequence for lesion detection was compared in 44 patients with Wilson's disease and in 3 patients with Hallervorden–Spatz disease.
Results: Putaminal lesions with a pattern of symmetric, bilateral and concentric PD/T2-W hypertensities, indicated to be typical in for Wilson's disaese were revealed in 54 % of patients. In 50 % of them only PD seqeuence demonstrated high sensitivity for lesion detection, while T2-W was either completely inconclusive or revealed much smaller zones of gliosis or dismyelination. In 3 patients with Hallervorden–Spatz disease T2-W sequence better demonstrated obvious symmetric deposits in globus pallidus and pars compacta of the substantia nigra, while PD-W sequence was much more sensitive for detection of the "eye of the tiger" sign typical for this disorder.
Conclusion: Application of only T1-W and T2W SE or TSE (single echo) without PD-W in order to be "time effective" for adult brain examination decreases possibility for lesion detection in some neurodegenerative disorders. "Modern" screening protocol in which turbo-FLAIR and single-echo T2-W sequences are combined as a replacement for traditional dual echo PD-W and T2W sequences should be strongly proven.

B-0194 15:00

MRI of mannosidosis

M. Patlas, M.Y. Shapira, J.M. Gomori; *Jerusalem/IL*

Purpose: Report the MRI findings of mannosidosis.
Methods and materials: Three patients with α-mannosidosis confirmed by leukocyte assay of acid-α-mannosidase activity were studied with conventional MRI of the brain. Two of the patients were brothers.
Results: All patients had widening of the diploic spaces with underdevelopment of the paranasal sinuses and two (unrelated) had prominent Virchow-Robin spaces. The two brothers had a tight foramen magnum with upward displacement of the brain stem without tonsillar descent. One of these brothers also had a C2–4 syrinx, and dilated perioptic nerve sheath CSF spaces associated with papilledema.
Conclusions: Tight foramen magnum and its associated findings have not been previously described in α-mannosidosis. Its appearance in the two brothers suggests that it might be a different subtype of α-mannosidosis. It is probably secondary to dysplasia of skull base.

B-0195 15:05

Correlation between brain MRI abnormalities and blood and urine 24-hour levels of Mn and Cu in patients with hepatic encephalopathy

T. Kodua, I. Diasamidze, F. Todua; *Tbilisi/GE*

Purpose: Recently "Manganeze Theory" for HE pathogenesis has been suggested. The aim of this study was to review correlation between pallidar index (PI) and levels of Mn and Cu in the blood and urine in patients with HE.
Material and methods: 42 patients with HE (26 with alcoholic hepatitis, 14 postviral hepatitis and 2 patients with Wilson disease) and 12 healthy volunteers were studied by MRI of abdomen and brain before and after treatment. Levels of Mn and Cu in the blood and urine were studied by atomic absorbtion method.
Results: PI of the patients directly correlated with 24 hour levels of Mn in the urine before and after treatment and correlated with 24 hour levels of Mn in the blood before treatment.
Conclusion: Correlation between brain MRI changes and Mn levels in the urine allows the recommendation of treatment with Zn-sulphate in the complex treatment of HE.

B-0196 15:10

Periventricular leukomalacia and parasagittal injury

N. Erdogan, S. Kumandas, A. Coskun, S. Isýn; *Kayseri/TR*

Purpose: Parasagittal injury is defined as wedge shaped injury of parasagittal cerebral cortex and subcortical white matter, whereas periventricular leukomalacia is the focal necrosis of periventricular deep white matter. Since both lesions are dominantly seen in the parietooccipital region, we tried to define the auxillary MR findings to differentiate these two entities.

Methods and materials: Thirtyseven patients with cerebral palsy underwent MR evalution with T1 axial, T2 axial, T1 sagittal and T2 coronal images obtained by Philips Gyroscan 1.5 T. In cooperation with the Pediatric Neurology clinician, 6 cases were diagnosed as parasagittal injury and 5 cases were diagnosed as periventricular leukomalacia.
Results: Auxillary signs other than diagnostic criteria were T2 hyperintensities extending into the subcortical white matter (100 %), presence of subcortical cysts (80 %) and ulegyrias (60 %) in patients with parasagittal injury. Undulation of lateral ventricular walls were observed in 50 % of cases with periventricular leukomalacia. Atrophic changes in body and splenium of corpus callosum were common in both groups.
Conclusion: T2 hyperintensities extending into the subcortical region, the presence of subcortical cysts and ulegyria greatly favors the diagnosis of parasagittal injury, whereas undulation of ventricular walls due to deep white matter atrophy was more frequently observed in periventricular leukomalacia.

B-0197 15:20

Correlation between MR imaging and neuro-endoscopy in supratentorial hydrocephalus: Preliminary results
E. Tedeschi, C. Iaccarino, A. Bellotti, M. Schonauer, G. Belfiore; *Caserta/IT*

Purpose: In patients with supratentorial hydrocephalus due to different etiologies, brain Magnetic Resonance Imaging (MRI) findings were used to plan and follow-up Neuro-Endoscopic (NE) intervention, a low-invasivity procedure which permits intraventricular exploration, intracranial shunting and biopsies of lesions bulging in the ventricular system.
Materials and methods: In the past 12 months, 7 patients with triventricular hydrocephalus of different origin (suprasellar archnoid cysts, neoplasms of the pineal region or III ventricle, normal-pressure-hydrocephalus) were studied with contrast-enhanced MRI at 0.5 T before and after NE, performed in general anaesthesia using a rigid, 6 mm diameter, Zeppelin device.
Results: In all cases, MRI defined the etiology of hydrocephalus, depicted the anatomy of the diencefalo-hypothalamic region, and pointed the target for biopsy in neoplastic cases. Most useful information included size, shape and position of Monro foramina, presence of masses or deformation of the III ventricle, and the position of tuber cinereum, mamillary bodies and basilar artery for planning a III ventricle-cisternostomy. Further, patency of intracranial shunts could be assessed at follow-up.
Conclusions: Brain MRI is necessary both for planning NE, especially if intracranial shunting or brain biopsies are considered, and for follow-up after intracranial shunting in supratentorial hydrocephalus.

B-0198 15:25

Measurements of supratentorial ventricular volumes using a stereotactic approach: Application to MR studies in schizophrenia
M. Quarantelli, M. Larobina, U. Volpe, G. Amati, A. Ciarmiello, A. Brunetti, M. Salvatore; *Naples/IT*

Aim of the study: To apply the Talairach 3D proportional grid to segmented brain MR images to measure volumes of supratentorial ventricular structures and to compare the results with those obtained by manual assessment.
Material and methods: A software for automated identification of third and lateral ventricles boundaries according to Talairach atlas was developed (automated method) and applied to 8 brain MR studies from schizophrenic patients, with different degrees of ventricular enlargement and asymmetry, thus obtaining automated measurements of the third and lateral ventricles volumes. The same subregions were manually outlined on original axial MR images to obtain measures of corresponding volumes (manual method, gold standard). Asymmetry of the lateral ventricles was expressed as difference/average of the two ventricles (asymmetry index).
Results: The automated method required 10 minutes per study. Automated technique significantly correlated with manual measurements for both lateral ($R = 0.997$) and third ventricles ($R = 0.85$), mean absolute difference between the volumes measured with the two techniques being 0.9 ml, with a maximum difference of 1.2 ml. Mean difference between asymmetry indexes as measured with the two techniques was 8.9 % (maximum 13.5 %), and significant correlation was present between these two measures ($R = 0.994$).
Conclusion: These results suggest that using a stereotactic approach is possible to automatically identify supratentorial ventricular boundaries. This method can be used to measure corresponding volumes from segmented MR brain image, when large data sets need to be analyzed.

14:00–15:30 **Room G**

Abdominal and Gastrointestinal

SS 301b

Colon and rectum (2)

Chairpersons:
P. Schnyder (Lausanne/CH)
P.J. Shorvon (London/GB)

B-0199 14:00

Activity assessment in ulcerative colitis: A comparison between hydro-MRI and endoscopy
K. Schunk, S. Reiter, N. Vogel, O. Rieker, T. Orth; *Mainz/DE*

Purpose: To assess the accuracy of hydro-MRI in the assessment of the activity in ulcerative colitis (UC).
Material and methods: After an oral bowel opacification using 1000 ml of a 2.5 % mannitol solution and a rectal bowel opacification using 250 – 500 ml of an 0.9 % saline solution, axial and coronal breathhold sequences (T2W HASTE ± FS, contrast-enhanced T1W FLASH ± FS) were acquired in 12 patients with UC. The enhancement of the bowel wall as well as morphological MRI findings were correlated with the colitis activity index (CAI) and the results of colonoscopy including biopsy specimens.
Results: The length of the affected bowel (MRI) correlated with the histopathologic index ($r = 0.62$; $p = 0.02$) and the colitis activity index (CAI) ($r = 0.56$; $p = 0.03$). The contrast enhancement of the inflamed bowel wall as well as the other MRI parameters did not correlate with the endoscopic/histopathologic indices.
Conclusions: In contrast to the transmural inflammation of Crohn's disease, the UC is limited to the mucosa. For that reason, the spatial resolution of MRI seems to be inadequate for the depiction of the morphologic and functional (contrast enhancement) changes, which indicate activity in UC.

B-0200 14:10

Timing of bowel preparation for colon examination: A prospective, randomised single blind study
F.-T. Fork, E. Tóth; *Malmö/SE*

Purpose: The efficacy and tolerance of a low volume sodium phosphate solution was compared with our standard high volume oral lavage solution in patients scheduled for colon examination during early morning and midday.
Methods and material: The purgative effect of phosphosoda (NaP) (Phosphoral®, Ferring, Sweden) and polyethyleneglycol (PEG) (Laxabon®, Tika, Sweden) was studied in 320 randomised patients. The patients were allocated to early morning and daytime examinations. The cleansing effect was scored on a scale of seven steps for each of four sections of the colon.
Results: The treatment regimens produced overall good cleansing effects in 51 – 63 % in the right colon and 70 – 80 % in the rectum. Best cleansing results were achieved with PEG alone, scoring 10 percentiles higher in the right colon and equal to NaP in the left colon and rectum. The cleansing effect improved by 5 – 40 percentiles by initiating the treatment at home and finalising it at the X-ray department in the morning after a night's rest. The taste and effects of the cleansing regimens were tolerated favourably by more than 61 %. The patients in 47 – 66 % registered no side effects and major ones were seen in up to 5 %.
Conclusions: PEG alone achieved the overall highest cleansing results, NaP being on par in the left colon and rectum and slightly inferior in the right colon. Irrespective of treatment group the best results were noticed in patients allocated to complete their pre-treatment at the Radiology department and examined later in the day.

B-0201 14:20

Acute colon obstruction: Comparison of spiral CT with water soluble enema and surgical findings
B. Twohig, E.J.R. van Beek, A. Blakeborough, R.A. Nakielny, A. Heseltine, M.C. Collins; *Sheffield/GB*

Purpose: To assess the potential value of contrast-enhanced spiral CT, as compared with water soluble enema and surgical findings in patients with suspected large bowel obstruction.

Materials/methods: A prospective study of consecutive patients with suspected large bowel obstruction as shown by plain abdominal X-ray. Patients with air in the bowel wall were excluded. Contrast-enhanced spiral CT was performed prior to water soluble enema, and read blinded for other results. Findings of enema and surgery were used as reference method.
Results: Since October 1999, 17 patients were included: 10 female, mean age 75.6 yrs (57 – 86). Water soluble enema demonstrated obstruction in 14 of 17 patients. CT correctly identified the site of obstruction in all 14 patients. The cause was identified in 12 patients, while 2 showed change in calibre only. Additional information was obtained in 75 % of patients, such as local extension 60 %), air in bowel wall (42 %), metastatic disease 40 %) and ureteric obstruction (8 %).
The management was affected in 75 % of patients, resulting in (less extensive) palliative surgery or expedition of surgery.
Conclusion: These preliminary results indicate that CT can identify obstruction and has additional value for the management of patients with suspected colonic obstruction. It seems likely that spiral CT will replace water soluble enema.

B-0202 14:30

Evaluation of CT in identifying colo-rectal carcinoma in the frail elderly patient

C. Ng, T. Doyle, H. Courtney, R. Bull, E. Pinto, T. Prevost, A. Freeman, A.K. Dixon; *Cambridge/GB*

Objective: Frail, elderly and immobile patients frequently have difficulty in tolerating formal colonic investigations. The aim of this study was to evaluate the accuracy of CT (merely with prolonged oral contrast medium) in identifying colo-rectal carcinoma in the frail/elderly population.
Materials and methods: The CT technique involved helical acquisition (10 – 15 mm collimation, 1.5 pitch) following two days of preparation with oral contrast medium. The outcome of four years experience (1995 – 99) have been reviewed. The gold-standards were pathological and cancer registration records, together with colonoscopy and barium enema, with a minimum of 15 months follow-up.
Results: 1104 CT studies in 1058 patients (mean age 78 years) were evaluated. CT correctly identified 85 of the 100 colo-rectal carcinomas in this group (sensitivity 85 %), but missed 15 cases (false negative rate 15 %; specificity 91 %). The overall positive predictive value (PPV), including weak as well as strong "calls", was 50 %. Abnormalities outside the colon, considered valuable to overall patient management, were identified in 173 patients (16 %).
Conclusions: CT has a valuable role in the investigation of frail/elderly patients with symptoms suspicious for a colonic neoplasm. Although interpretation can be difficult, the technique is able to exclude malignancy with fair confidence. Furthermore CT is able to identify otherwise occult extra-colonic diseases.

B-0203 14:40

Can MRI predict the circumferential resection margin in rectal cancer surgery?

R.G.H. Beets-Tan, G.L. Beets, R.F.A. Vliegen, A.G.H. Kessels, H. van Boven, A. De Bruine, M.F. Von Meyenfeldt, C.G.M.I. Baeten, J.M.A. van Engelshoven; *Maastricht/NL*

Purpose: To evaluate the accuracy of MRI with a phased array coil for preoperative staging of rectal cancer and predicting circumferential resection margin (CRM) in total mesorectal excision.
Methods: 76 patients with primary rectal cancer were evaluated with MRI at 1.5 T. Two observers scored tumor for T stage and measured the CRM. MR findings were compared with final histology.
Results: MR T stage agreed with histological stage in 83 % (κ 0.77) for observer 1, and in 67 % (κ 0.52) for observer 2. The intraobserver agreement on the T stage was good (κ 0.80) for observer 1 but moderate (κ 0.49) for observer 2. The interobserver agreement was moderate (κ 0.53). In 12 patients with a T4 tumor a CRM of 0 mm was correctly predicted. In 29 patients with histological CRM more than 1 cm, observer 1 predicted in 28 patients a CRM of at least 10 mm and observer 2 in 27 patients. Regression curve analysis (95 % confidence interval) of the remaining 35 patients revealed that a CRM of at least 1 mm can be predicted accurate when distance measured on MR is at least 5 mm. The intra- and interobserver reliability of CRM measurements was very high.
Conclusions: MRI shows moderately accuracy and reproducibility for predicting T stage. Clinically more important CRM can be predicted with high accuracy and consistency. This allows preoperative identification of patients at risk for a recurrence who will benefit from preoperative radiotherapy.

B-0204 14:50

Accuracy of MRI with phased array coil in local staging of rectal cancer

A. Laghi, C. Catalano, I. Baeli, V. Panebianco, F.G. Assael, R. Iannaccone, R. Passariello; *Rome/IT*

Purpose: To assess the accuracy of MR imaging with phased-array coil in local staging of rectal carcinoma.
Subjects and methods: Twenty-two patients (17 males; 5 females; mean age: 64 a) with known rectal cancer were studied using a 1.5 T magnet (Magnetom Vision Plus; Siemens, Erlangen, Germany) with phased-array coil. All patients underwent rectal enema of positive (nr. 10; 1:100 solution of Gd-DTPA, Magnevist, Schering) contrast agent. MR protocols included the following sequences: nonbreathhold, high resolution T2w Turbo spin-echo (TR/TE/ETL/matrix/acq.t.: 4055 ms/132 ms/33/390 × 512/3 min 26 s) and fat-suppressed T1w FLASH (TR/TE/matrix/acq.t.: 156 ms/2.3 ms/131 × 256/23 s) before and after administration of contrast medium acquired on multiple planes. Diagnostic confirmation was obtained at surgery in all the cases (17 anterior resections and 5 abdomino-peritoneal resections). MR data were compared with histological specimens.
Results: On T2w images rectal wall layers were visible in all the cases; no differentiation between mucosa and submucosa was possible. Sensitivity of MR imaging in T staging was 85 %, specificity was 89 % and overall diagnostic accuracy was 86 %. Accuracy was 89 % for T1-T2 lesions, 80 % for T3 and 100 % for T4. Sensitivity of MR imaging in N staging was 100 %, specificity was 60 % and overall diagnostic accuracy was 75 %.
Conclusion: The use of phased array coil provides good evaluation of rectal wall layers and T staging of rectal cancer with less patients discomfort compared with endorectal coil; a further advantage is in the evaluation of stenosing lesions and tumors of the recto-sigmoid junction. Poor results are obtained for N staging.

B-0205 15:00

Anal canal cancer: Diagnosis and follow-up with TRUS and color Doppler

F.M. Drudi, F. Trippa, F. Cascone, P. Ricci, A. Righi, P. Marziale, R. Passariello; *Rome/IT*

Purpose: To define the role of transrectal ultrasound and colour doppler in the evaluation, staging and management of patients with histologically diagnosed anal canal cancer.
Method and materials: 43 patients underwent digital rectal examination, anoscopy, abdomino-pelvic computed tomography, inguinal and transrectal ultrasound and colour doppler. 31 patients received combined chemoradiotherapy, while 12 received radiotherapy only due to clinical contraindications. Before and after therapy, UT and TNM staging was compared. Colour doppler was performed to assess the presence/absence of blood flow within the lesion. In patients with complete response to therapy, transrectal ultrasound sensitivity was compared to colour doppler in the differentiation of residual tumour from post-radiation fibrosis. Ultrasound examination was carried out to assess inguinal lymph node involvement, and computed tomography to detect abdominal lymph nodes.
Results: In all stages, except stage 4, there were differences between TNM and UT staging, as TNM is often understaged. After treatment, ultrasound showed a sensitivity of 71 % in the differentiation of fibrosis from residual tumour, of 93 and 95 % in the identification of perirectal and inguinal lymph nodes respectively. Before treatment, colour doppler showed colour signal in 91 % of patients. After treatment, colour doppler reached a sensitivity of 96 % in the differentiation of post-radiation fibrosis from residual tumour. All results were confirmed histologically.
Conclusion: Transrectal ultrasound is useful in the staging and follow-up of anal canal carcinoma. The combination of ultrasound and colour Doppler is useful in the distinction of fibrosis from residual tumour after therapy and as biopsy guidance.

B-0206 15:10

Clostridium difficile colitis: Value of CT findings

D. Geukens, J.H. Pringot, E. Ketelslegers, B.E. Van Beers, M. Delmee; *Brussels/BE*

Objective: To assess the sensitivity and specificity of CT findings in Clostridium difficile colitis.
Material and methods: 86 patients who underwent abdominal CT and toxin in stool assay within 3 days were divided into Group A (positive for toxin in stool) and Group B (negative for toxin in stool). In both groups, we studied the colonic wall thickening and 3 associated signs, i.e. halo, hyperintense inner layer, and accordion pattern. Sensitivity and specificity were assessed in 4 categories of features: colonic wall thickening > 4 mm, idem plus one of the associated signs, colonic wall thickening > 10 mm, idem plus one of the associated signs.

Results: In Group A (31 patients, 35 procedures) values for sensitivity were respectively 69, 40, 46, and 31 %. In Group B (55 patients, 61 procedures), values for specificity were 77.88, and 92 %.
Conclusion: In patients with colonic wall thickening > 10 mm, specificity of CT reaches 88 % and sensitivity 46 %. In patients with colonic wall thickening > 4 mm, sensitivity is 69 % but specificity remains high only when associated signs are taken into account.

B-0207 15:20

Colonic cancer screening in Russia: Retrospective analysis of 5-years experience

L.M. Portnoi, L.B. Denisova, G.A. Stashuk, V.A. Isakov, V.O. Nefedova, A.A. Kaluzhski, B.M. Turovski; *Moscow/RU*

Aim of the study was to evaluate the efficacy of colonic cancer screening program in Moscow region performed by radiology department of MONIKI.
Materials and methods: Screening was performed by annual photofluorography with double contrast barium enema in selected risk groups of local population. Risk groups were formed according to criteria developed on a basis of combination of main risk factors for colon cancer (age, dietary habits, hereditary etc). Colonoscopy was performed in all patients in whom barium study was abnormal and for polypectomy if it was necessary. In difficult cases CT-scan and MRI were performed for the staging of the tumor.
Results: Among the 6000 examined patients 189 colon cancers were found. In 272 patients benign polyps were found, in 358 diverticulosis, in 112 ulcerative colitis, in 1405 functional disorders of large intestine, in 222 other diseases, and in 3442 patients no disease was found. More than in 50 % benign diseases were diagnosed for the first time. Based on the estimated incidence of colonic cancer in Russia, we calculated that in our risk groups we found 2.5 – 3.0 times more colonic cancers than could be found in corresponding age- and sex-matched control groups in general population.
Conclusion: Colonic cancer screening based on barium enema photofluorography of selected risk groups of patients is efficient, as it allows to reveal majority of cases of colonic cancer and a lot of cases of benign diseases.

14:00–15:30 **Room H**

Interventional Radiology

SS 309

Aorto-iliac disease: Stents and stent grafts (2)

Chairpersons:
W. Cwikiel (Lund/SE)
G.M.L. Guerrero Avendaño (Mexico City/MX)

B-0208 14:00

Postoperative follow-up of thoracic aorta diseases treated by endovascular covered stents

V. Chabbert, P. Otal, P. Chemla, P. Soula, T. Smayra, P. Concina, F. Joffre, H. Rousseau; *Toulouse/FR*

Purpose: Stent grafting is emerging as a new treatment for several pathological conditions involving the thoracic aorta. We studied the outcome of thoracic aortas repaired with covered stents by CT scan and MRA.
Materials and methods: From January 1996 to june 2000, forty patients (36 men, mean age, 60.5 years) underwent stent grafting of the thoracic aorta: 15 traumatic aortic ruptures, 16 descending aortic aneurysms, 3 false aneurysms and 6 type B aortic dissections. The postoperative follow-up was performed with X-Rays, CT scans and/or MRA (1 week to 3.5 years; mean 9.7 months).
Results: Rates of residual leaks, complications and death were respectively 15 %, 15 %and 10 %. All the traumatic aneuryms were excluded, with shrinkage of the thrombus around the stent graft in 53.3 %. Aneurysms were completely excluded in 75 % of cases, there were residual leaks in 25 %; the aorta diameter was equal in 56.2 %, decreased in 31.2 % and increased in 12.5 % with leaks. All the false aneurysms were excluded with decreasing of the aorta diameter in 75 %. The false lumen of the dissections were completely clotted in 66.6 % of cases with significant reduction in size of the false lumen and increase of the true lumen in 66.6 %, the diameter increased with residual flow in 16.6 %.
Conclusion: Stent gafting is an effective alternative to open surgery for the treatment of thoracic aorta diseases. The follow-up must be regular. Increasing in size of the aorta suggests a leak or a residual flow in the false lumen.

B-0209 14:10

Volumetric analysis of the aneurysmal sac after endovascular repair of abdominal aortic aneurysms

I. Bargellini, E. Neri, C. Vignali, R. Cioni, P. Petruzzi, C. Bartolozzi; *Pisa/IT*

Purpose: We aimed to determine the value and the degree of volumetric change of the aneurysmal sac after abdominal aortic endografting.
Materials and methods: A series of 25 patients that underwent endovascular repair of abdominal aortic aneurysm was evaluated with CT angiography (CTA) 1, 3, 6 and 12 months after treatment. CTA data sets were evaluated on a dedicated workstation (Advantage Windows 3.1; GEMS). A region growing method was used to isolate the aneurysmal sac and endograft; thereby volume measurements could be obtained automatically by the software. Volume variations were determined for each patient and a comparison was made between patients with and without endoleaks. Endoleaks occurred in 5 patients, at discharge in 3, and 1 year after treatment in 2.
Results: In patients without endoleaks the average volume reduction was 5 %, 3.7 % and 2.8 % at 3, 6 & 12 months follow up respectively, with 12 % total reduction of the initial volume. In patients with endoleaks the mean reduction of the volume was null with mean size variations of 6 %, –1.5 % and –1.9 % at 3, 6, and 12 months follow-up. In patients with endoleaks that occurred at 12 months from the procedure the volume reduction was significant at 3 & 6 months (mean reduction size 5 %) accordingly. The difference of the mean variation of the volume size was statistically significant between the two groups ($p < 0.01$).
Conclusion: The precise volumetric assessment of the aneurysmal sac is a reliable method for the assessment of treatment outcome. In our study, no significant reduction of the aneurysmal sac occurred in patients with endoleaks.

B-0210 14:20

The role of computed tomography angiography (CTA) in the management of proximal renal artery stenoses (RAS). Part I: Pre-therapeutic lesion characterization

V. Chabbert, P. Otal, S. Musso, P. Chemla, H. Rousseau, F. Joffre; *Toulouse/FR*

Purpose: To evaluate and compare with digital substraction angiography (DSA) the anatomical information yielded by CTA in the pre-therapeutical assessment of proximal RAS.
Materials and methods: 84 consecutive patients presenting with an atherosclerotic stenosis located in the first centimeter of a renal artery were prospectively evaluated by CTA over a 16 months period. The analysis of the renal artery was focused on: the position of the ostium, the orientation and course of the origin of the renal artery, the characteristics of the stenosis (degree, calcification, location) and the importance of the involvement of aorta by the atherosclerotic process (plaques, calcification). The information yielded by CTA was compared with DSA, when performed (n = 64).
Results: 197 renal arteries were analysed. Comparison with DSA demonstrated the superiority of CTA over DSA in terms of determination of the renal artery in the axial plane, detection of calcification (55 versus 23 %) and depiction of para-ostial aortic plaques. CTA allowed the classification of RAS into 3 categories: truncal (type I), pseudo-truncal (type II) and ostial (type III) lesions.
Conclusion: When compared with DSA, CTA brings more precise information about the anatomical characteristics of RAS, that may influence endovascular treatment.

B-0211 14:30

The role of computed tomography angiography (CTA) in the management of proximal renal artery stenoses (RAS). Part II: Its impact on endovascular treatment

V. Chabbert, P. Otal, S. Musso, P. Chemla, H. Rousseau, F. Joffre; *Toulouse/FR*

Purpose: To evaluate the influence of CTA characterization of proximal RAS on the procedure and outcomes of percutaneous transluminal renal angioplasty (PTRA).
Materials and methods: Among 84 consecutive patients that were prospectively included in this series, 55 underwent PTRA. The decision for endovascular treatment, its feasibility, the rate of immediate success, the morbi-mortality and clinical outcomes were correlated to the CTA classification of the lesions into 3 types: I (truncal), II (pseudo-truncal) and III (ostial).
Results: The decision not to perform a PTRA was taken, according to the depiction by CTA of complex lesions, in 5 patients considered at high risk of angioplasty. The rate of failure (14.6 %), of technical difficulties (27 %), of complications (19 %), the need for endoprosthesis were correlated with the lesion type and its degree of calcification. Most of these events occurred in type II and III groups. 100 % of type III, 50 % of type II and 8 % of type I lesions required a stent placement.

Conclusion: CTA yields morphological information that are not available from angiography and may influence therapeutic strategy. CTA is a useful imaging modality when PTRA is planned.

B-0212 14:40

Endovascular treatment of acute and chronic type B dissection and penetrating ulcer with commercially available stent-graft in 11 patients

J. Sailer, P.L. Peloschek, M. Grabenwöger, T. Rand, S.A. Thurnher, J. Lammer; *Vienna/AT*

Purpose: To report clinical experience with endovascular repair of acute and chronic type B dissections and penetrating ulcers using stent-grafts.
Methods: We investigated efficiency of transluminal endovascular stent-graft insertion in 7 patients with descending (type B) aortic dissection and in 4 patients with penetrating ulcer using the Thoracic GORE-EXCLUDER Endoprothesis. We evaluated extend of the dissection, the distance between entry tear and left subclavian artery and the diameter of the true and false lumen using cross-sectional CT scans over a median follow-up period of 254 days.
Results: Stent-graft deployment was successful in all cases. In 8 patients deployment of two stent-grafts was necessary to exclude residual flow into the false lumen. The mean length of the typical type B dissections (n = 7) was 22.31 ± 24.59 cm and 3.28 ± 1.14 cm for the penetrating ulcers (n = 4). The mean distance between the origin of the left subclavian artery and the entry tear was 5.24 ± 3.74 cm (n = 11). We observed one major complication: a retroperitoneal haematoma, requiring surgical treatment. During follow up the mean diameter of the false lumen in dissecting aneurysms decreased from 2.34 ± 0.58 cm to 1.0 ± 0.36 cm (–58 %), the true lumen increased form 1.56 ± 0.5 cm to 3.5 ± 0.84 cm (+124 %). For penetration ulcer the equivalent data was from 1.08 ± 0.67 cm to 0.37 ± 0.32 cm (–65 %) and from 3.88 ± 1.52 cm to 4.53 ± 1.01 cm (+16 %). In 8 patients total thrombosis of the false lumen was achieved.
Conclusion: Stent-graft placement is considered as a potential alternative in the treatment of aortic type B dissection or ulcer-like penetrations.

B-0213 14:50

Stent angioplasty for managing renovascular complications of acute aortic dissection

M. Takahashi, M. Uder, D. Gohl, G.K. Schneider, B. Kramann; *Homburg a. d. Saar/DE*

Purpose: To describe the appropriateness of stent angioplasty in renovascular complication associated with acute aortic dissection.
Materials and methods: Three patients with acute aortic dissection developed unilateral renal artery strictures. All the patients complained abdominal pain and therefore underwent diagnostic catheter angiography in order that mesenteric ischemia could be surely ruled out. At the time of angiography both renal function and general condition were stable in two patients and deteriorating in one patient. The former received the stent placement in affected renal arteries at the same time, while in the latter generalized ischemia of abdominal organs were controlled at first with a percutaneous balloon fenestration. The stent placement in the latter patient was performed on later day. All the procedures were attempted with mild pre-dilatation followed by a uniquely thin pre-mounted stent system *(HERCULINK14; Guidant)*.
Results: In two patients, false aortic lumens totally perfused affected renal arteries and in one patient, a true lumen did. Every procedure was successfully performed via the true aortic lumen. Neither residual strictures nor complications were observed.
Conclusion: The emergency or sub-emergency stent angioplasty could properly resolve renal artery stricture associated with acute aortic dissection, probably resulting in salvage of blood supply to the kidneys.

B-0214 15:00

Multicenter clinical evaluation of a new endovascular stent (Za-Stent®)

R.F. Dondelinger[1], H. Rousseau[2], T. Jargiello[3], L. Stockx[4], K.A. Hausegger[5], D. Vorwerk[6], G. Trotteur[1], D. Henroteaux[1], M. Sapoval[7], D. Tsetis[8]; *[1]Liège/BE, [2]Toulouse/FR, [3]Lublin/PL, [4]Leuven/BE, [5]Graz/AT, [6]Ingolstadt/DE, [7]Paris/FR, [8]Iraklion/GR*

Purpose: To evaluate Za-Stent® in the treatment of primary and secondary stenosis or occlusion of the iliac artery.
Material and methods: The Za-Stent® is a selfexpanding Nitinol stent. A 12 month study was conducted. Seventy-five patients were included, 63 male, 12 female, aged 41 – 81 years (mean: 58). Onset of symptoms was 1 – 120 months (mean: 13, median 6). Forty percent of patients were classified Rutherford class 2, and 41 % class 3. Ninety lesions were treated. Fifty-two percent of the lesions were located in the common iliac arteries. Iliac occlusion was present in 16 % of the cases. Length of lesion was 10 – 29 mm in 47 %, 30 – 69 mm in 39 % and 70 – 89 mm in 5 %. Evaluation was obtained by clinical follow-up and Doppler examination at day 1; and 1, 3 and 6 months after stenting.
Results: Hundred stents were implanted in 90 lesions; 96 stents were placed as planned. Deployed stents were poorly visible in 80 %, stent markers were well identified in 75. The procedure was qualified 100 % successful in 87 %. 100 % stent expansion was reached in 70, 90 – 99 % in 26, and 80 – 89 % in 4 stents. All stents were patent at Doppler; 52, 38 and 13 stents at 1, 3 and 6 months follow-up. One occlusion of the superficial femoral artery and one groin hematoma occurred. One stent protruded in the aorta.
Conclusion: Treatment of iliac stenosis and occlusion with Za-stent® is effective and safe.

B-0215 15:10

Aortobiiliacal stenting in chronic iliac artery occlusions: Early and late follow-up in 21 patients

C. Müller-Leisse, K.-L. Hajeck, R. Janßen, F. Korsten, U. Kamphausen; *Mönchengladbach/DE*

Purpose: To determine the outcome of aortobiiliacal stenting in atherosclerotic iliac artery disease.
Material and methods: We evaluated retrospectively the data obtained in 21 patients with common iliac artery occlusion on one side and common iliac artery stenosis contralaterally, who had presented at our department over a six 6-year period. Occlusion of the common iliac artery alone was seen in 19, occlusion of the common and external iliac arteries in two. The recanalization procedure was performed with wire and catheter techniques using a retrograde (preferred) or an antegrade approach. Both sides were stented simultaneously. In 16 patients CT was performed after stenting either because of pain during balloon-dilatation (n = 4) or in order to check the position of the stents and their degree of expansion (n = 12).
Results: Technical success was seen in 20 of 21 patients (95.2 %). In the three patients with pain during balloon-dilatation, CT revealed incomplete expansion of the stent. Early reocclusion caused by stenosis proximal to the stent was seen in two patients (4.8 %). Late reocclusions were observed in three patients, one of which had already had early reocclusion, and another one of which had residual stenosis after primary intervention. In five patients restenosis developed within 30 months. Embolism was observed in two patients.
Conclusion: Aortobiiliac stenting may be an appropriate alternative to surgical Y-prostheses. Restenosis is one of the main reasons for reocclusions. CT is recommended after the stenting procedure in complicated cases.

B-0216 15:20

Long femoral and iliac artery occlusions: Recanalization and outcome

C. Müller-Leisse, K.-L. Hajeck, R. Janßen, A. Kippels; *Mönchengladbach/DE*

Purpose: To determine the feasibility of recanalization of long iliac artery occlusions and to establish its patency.
Material and methods: We retrospectively evaluated the data of 23 patients with long occlusions of either the common iliac artery (CIA) (n = 3), the external iliac artery (EIA) (n = 12) or both CIA and EIA (n = 7). In one patient all three vessels, the common femoral artery included, were involved. The mean length of the occlusions was 12.6 cm. The recanalization procedure was performed with wire and catheter from retrograde (preferred) or antegrade and stent-pta was performed.
Results: Technical success was seen in 20 of 23 patients (87 %). There was one acute thrombosis. We saw 4 early reocclusions (17 %), one because of insufficient run off, the other three because of insufficient dilatation. Late reocclusions were observed in 4 (17 %), one of which had already had early reocclusion, another one demonstrated stent breakage, no reason was found in the other two. In 3 patients, who were readmitted to our department within 30 months stenosis was diagnosed and successfully treated by ballondilatation or stent. Embolism was observed in 6 patients (26 %), in five on the ipsilateral, in one on the contralateral side of the occlusion.
Conclusion: Recanalization of even long iliac artery occlusions is feasible. As we mainly used one type of stent, the high rate of reocclusion and embolism may be due to the type of stent used.

14:00–15:30 Room I

Abdominal and Gastrointestinal

SS 301c

Abdominal imaging (2)

Chairpersons:
C. Evans (Cardiff/GB)
C. Stoupis (Athens/GR)

B-0217 14:00

Continuous ambulatory peritoneal dialysis: Assessment of complications with CT peritoneography

O.I. Karahan, H. Taskapan, C. Utas, A. Coskun, M. Gulec; *Kayseri/TR*

Purpose: To assess the effectiveness of CT peritoneography in detecting the complications of continuous ambulatory peritoneal dialysis (CAPD).
Materials and methods: We examined 64 patients with chronic renal insufficiency who were on CAPD treatment. Patients consisted of 39 males and 25 females (mean 44 years; range, 13 – 71 years). CT peritoneography was performed by adding 50 ml of 60 % meglumine diatrizoate to each liter of dialysis fluid one hour before the examination. Shimadzu CT/SCT-7000 TX scanner was used to get axial 10 mm thick slices through the abdomen and pelvis.
Results: Based on the presence of symptoms related to CAPD applications, the patients were divided into symptomatic (Group I) and asymptomatic (Group II). Group I consisted of 28 cases (44 %) and Group II consisted of 36 cases (56 %). At least one complication was detected in 19 (68 %) cases in Group I and in 8 cases (22 %) in Group II. In symptomatic group, complications were localized fluid collection in one (4 %), peritoneal adhesions in one (4 %), dialysis leakage in 13 (46 %) and abdominal hernias in 14 (50 %). Complications in asymptomatic group were leakage along the catheter tunnel in 6 (17 %), umbilical hernia in one (3 %) and peritoneal adhesions in one (3 %). In 27 cases with CAPD complications, clinical management was changed in 21 cases (78 %).
Conclusion: CT peritoneography is useful for detecting the complications related to CAPD. In patients without symptoms related to CAPD treatment, CT peritoneography at regular intervals may help to detect the complications in early period.

B-0218 14:10

Spiral CT findings of peritoneal carcinomatosis: GI vs. GYN origin?

S. Lee, O. Woo, C. Park, I. Cheong, K. Kim, I. Cha; *Seoul/KR*

Purpose: To assess it is possible to differentiate peritoneal carcinomatosis (PC) from gastrointestinal (GI) and gynecologic (GY) origin on the basis of spiral CT findings.
Materials and methods: Spiral CT findings of twenty eight patients (17 men, 12 women) of peritoneal carcinomatosis were evaluated retrospectively. PC from twenty two GI origin were 18 gastric, 2 colon, 1 peripheral cholangiocarcinoma, and 1 pancreas carcinoma. PC from seven GY origin were 4 mucinous adenocarcinoma and 4 serous cystadenocarcinoma. Spiral CT findings evaluated were (1) amount of ascites (no ascites, small amount, large amount), including the lesser sac, (2) thickening or contrast enhancement of parietal peritoneum, (3) mesenteric nodule, (4) omental thickening, (5) paraaortic lymphnode enlargement, (6) hydronephrosis, (7) intestinal dilatation.
Results: Large amount of ascites was seen in both groups of PC, but no case GY origin shows small amount of ascites. Abnormal findings of parietal peritoneum and mesentery were noted on 17 cases (78 %) of GI origin, and 7 cases (100 %) of GY origin. Omental thickening was seen in 12 cases (52 %) and 5 case (71 %), respectively. Paraaortic lymphnode enlargement was noted in 5 cases of GI origin (1 above renal vessel, 4 infrarenal) and 1 case (infrarenal) of GY origin. Hydronephrosis was seen only in GI origin, 3 in right, 2 in left, 3 in both kidneys. Intestinal dilatation was noted in 4 cases of GI origin.
Conclusion: PC from GY origin showed more amount of ascites, and tendency to involve the parietal peritoneum and mesentery than GI origin. Hydronephrosis was more frequent in GI origin.

B-0219 14:20

Systematic CT evaluation of thoracic and abdominal blunt trauma: Immediate vs. delayed film reading

P. Deleuse, J.H. Boverie, B. Ghaye, R.F. Dondelinger; *Liège/BE*

Purpose: To evaluate retrospectively systematic CT at admission in thoracic and abdominal blunt trauma patients and immediate vs delayed film reading.
Materials and methods: Three-hundred-eight trauma patients (233 male, 75 female) aged 2 to 98 years (mean 36.2) were admitted from 1997 to 1999. 98 % of patients had sustained blunt trauma. Two-hundred-seventy CT studies were obtained immediately after resuscitation. Intravenous contrast was given in 98.5 %, oral contrast in 0.4 %. In 82 %, thorax and abdomen were investigated, in 17 % abdomen alone, in 1 % thorax alone. 75 examinations were obtained between 6 and 12 p.m., 25 % between 0 and 8 a.m. Results of immediate vs delayed film reading were compared.
Results: 197 (73 %) examinations were abnormal. Pulmonary contusion was found in 51 %, hemothorax in 37 %, thoracic fractures in 32 %, hemomediastinum in 15 % and pneumomediastinum in 5 %. Thoracic aortic rupture was seen in 1 %. Hemoperitoneum was present in 19 %; splenic, hepatic, renal, and pancreatic contusion were seen in 8 %, 7 %, 3 % and 1 %. Injury to the GI tract was seen in 1 %. In 4 %, significant visceral contusion was present without hemoperitoneum. Pelvic bone or spine fractures were seen in 26 %. Extravasation of contrast material was documented in 4 %. Arterial hemostatic embolization was obtained immediately after CT examination, when necessary. Immediate film reading had a SE, SP, NPV, PPV of 86.2 %, 99.8 %, 98.7 %, 97.8 %, and delayed interpretation 97.0 %, 100 %, 99.7 %, 100 %.
Conclusion: CT is a reliable test in the evaluation of blunt polytrauma patients. Secondary reading does not improve results.

B-0220 14:30

T2-weighted MR-images for screening of the upper abdomen in pelvic malignant disease

V. Järv[1], L. Blomqvist[2]; [1]*Tartu/EE*, [2]*Stockholm/SE*

Purpose: To explore the efficacy of axial T2- weighted MR imaging for screening of metastases in the upper abdomen.
Materials and methods: Retrospective blinded review of MR images in 111 patients with pelvic malignant disease was performed. After high resolution pelvic MRI on a 1.5 T system with a multicoil array, all patients were additionally examined with T2-weighted fast spin echo (FSE) images of the upper abdomen using body coil.
Results: MR imaging was able to give additive diagnostic information (previously unknown metastases, progress of the malignant disease, confirmation or rejection of suspected metastases) in 21 from 111 studied patients. 79 from 86 (92 %) patients considered metastases-free on axial T2-weighted images maintained this status during for a minimum of 1.5 year follow-up. Nine patients 2 – 23 (median 8.2) months later developed liver or lymph node metastases. Average prolongation of the MR study for performing one additional sequence was 6.6 min.
Conclusion: Axial T2-weighted FSE MR imaging is in our experience reasonably effective way of screening the upper abdomen using scanners which do not have ultra-fast imaging techniques that potentially enable complete protocols covering both the upper and lower abdomen in one examination.

B-0221 14:35

CT findings of appendicitis resulting in small bowel obstruction

S.-W. Yoon, K. Kim, J.-S. Yu, H. Kim, M.-S. Park; *Seoul/KR*

Purpose: To evaluate the CT findings of appendicitis resulting in small bowel obstruction.
Materials and methods: Through a review of CT images of 144 surgically verified appendicitis, 6 cases accompanied with mechanical obstruction of the small bowel were identified. CT findings of six patients were analyzed into identification of the appendix, presence of appendicolith, periappendiceal fluid collection, periappendiceal fat stranding, and location of appendiceal tip. All the CT findings were compared to surgical findings.
Results: Five (83 %) of 6 cases showed dilated appendiceal lumen with periappendiceal fat stranding on CT. The diameter of the dilated appendiceal lumen were ranged from 1 cm to 2 cm (mean 1.44 cm). Appendicolith was identified in 3 (50 %). Periappendiceal fluid collections suggesting complicated appendicitis were seen in 5 cases (83 %) including 1 periappendiceal abscess formation. The appendiceal tip adhered to small bowel loop was identified on CT, and verified surgically in 4 cases (67 %).
Conclusion: Appendicitis can induce small bowel obstruction by means of inflammatory adhesion to the small bowel loop. Identification of adhesion site including the typical findings of appendicitis in CT can be crucial for early diagnosis and proper treatment of appendicitis resulting in small bowel obstruction.

B-0222 14:40

CT findings of surgically proved nine isolated mesenteric desmoid tumors: Radiologic-pathologic correlation

S.-W. Yoon, K. Kim, J.-S. Yu, H. Kim, H.-C. Shin, Y. Kim, M.-S. Park, S.-I. Lee; *Seoul/KR*

Purpose: To document the CT findings of isolated mesenteric desmoid tumors (not associated with Gardner syndrome) compared to the pathologic findings.
Materials and methods: Seven unenhanced and 9 contrast-enhanced CT images of surgically proved isolated mesenteric desmoid tumors in nine patients were subjected. CT findings of tumors were analyzed into the mass contour (round vs. oval), marginal smoothness, infiltration to the adjacent bowel, and the pattern of contrast enhancement. CT findings were correlated with surgical and pathologic findings.
Results: The tumors were measured from 5 cm to 9 cm in diameter (mean 6.9 cm). Among the 9 lesions, 5 (56 %) were oval and the others (44 %) were round. Two (22 %) cases showed lobulated contour. Six (67 %) were well-marginated, and 2 (22 %) showed perilesional fat stranding less than 30 % of their margin. The rest 1 (11 %) was poorly marginated. In 6 (67 %) of 9 cases, the presence of infiltration to the adjacent bowel was suggested on CT and verified surgically. All cases showed high attenuation in contrast-enhanced CT with inhomogeneous enhancement pattern in 8 (89 %). The component of myxoid degeneration (n = 3), hemorrhage (n = 1), hyalinization (n = 1), fat (n = 2) as well as tumor vascularity (n = 1) in the pathologic specimen were correlated with low attenuation densities considerably on CT.
Conclusion: Isolated mesenteric desmoid tumors are large, well-marginated mass in the most of cases on CT. Inhomogeneous contrast enhancement pattern of these tumors are determined by myxoid degeneration, hemorrhage, hyalinization, fat or tumor vascularity.

B-0223 14:45

Multislice-CT for immediate whole body examination in polytraumatized patients

M. Rieger, R.J. Bale, A. Mallouhi, A. Kathrein, C. Fink, B. Czermak, W. Jaschke; *Innsbruck/AT*

Purpose: Whole body multislice-CT (MSCT) offers the potential of fast and reliable primary diagnostic in patients with multiple trauma. However, the role of MSCT in emergency diagnostic is still uncertain. We evaluated the potential of MSCT in primary emergency diagnostic.
Materials and methods: A MSCT, installed next to the emergency room allows for fast volume acquisition and generation of high resolution multiplanar- (MPR's) and 3D-reconstructions. To improve initial management of multiple trauma we designed following comprehensive algorithm for in-hospital trauma care: (A) initial assessment of immediate life-threatening disorders, (B) chest X-ray and sonography to detect free fluid, (C) after stabilization and maintenance of vital functions performance of a whole body MSCT, (D) additional plain films if necessary. The results of 400 CT-examinations were reported. Additional radiological examinations and changes of diagnoses were documented. The number of recognized and non-recognized important CT-findings and the scanning duration were evaluated. Time saving was calculated by the number of examinations, which were not necessary due to the use of MSCT.
Results: Early use of MSCT instead of conventional radiographs saves time (1 – 2 hours per patient). Life-threatening injuries (skeletal fractures, thoracal and abdominal trauma, vessel injuries) can be reliably diagnosed (sensitivity 100 %). Diagnostic angiography can be supplemented by MSCT.
Conclusion: MSCT is a reliable and fast diagnostic method for management of severely injured patients.

B-0224 14:55

Causes of sonographic overdiagnosis in the radiology department of a university hospital

B. Krug, U. Wolters, H. Stützer, K. Lackner; *Cologne/DE*

Purpose: To establish why 16 % of all 1045 patients undergoing abdominal and/or vascular surgery who were referred to the Central Department of Radiology for a B-image sonogram for the first time over the period of one year had stated that they had imaging tests of the same regions of the body that had been conducted or scheduled over the last 6 weeks without changing the clinical findings.
Methods: One senior resident in radiology and one resident in surgery retrospectively reviewed the medical records of the patients reporting pre- and parallel tests.
Results: 108 of the 171 medical records (63 %) were available. Double-diagnosis was found on 14 report forms (13 %). There were 10 (9 %) parallel sonograms, 4 (4 %) parallel computed tomograms and 2 (2 %) parallel MR tomograms not mentioned in the patient reports. In total, 121 sonograms, 39 computed tomograms and 10 MR tomograms were evaluated. 41 of the 55 (75 %) preliminary sonograms performed by general practitioners and specialists in private practice were not documented in the medical records. Double-diagnosis was performed in 2 patients due to justified doubts about the accuracy of the preliminary findings. Even though a record existed of clinically plausible findings, 36 of the 43 (84 %) preliminary sonograms performed by doctors in the university hospital were repeated to verify the diagnosis without any diagnostic benefit.
Conclusions: A cross-specialty consensus about the diagnostic value of B-image sonography and management of the findings obtained is of paramount importance.

B-0225 15:05

3D FLASH sequence and volume-rendered reconstructions in MR imaging evaluation of upper abdomen

A. Laghi, C. Catalano, V. Panebianco, I. Baeli, I. Sansoni, R. Passariello; *Rome/IT*

Purpose: The aim of our study was to evaluate potential advantages of T1-weighted 3D GRE sequence for magnetic resonance imaging evaluation of the upper abdomen using volume-rendering as recostruction algorithm.
Materials and methods: Thirty-one consecutive patients underwent MR imaging of the upper abdomen using 1.5 T supeconductive magnet with 25 mT/m gradients, 600 ms rise time, equipped with phased-array multicoil. Imaging protocol included breath-hold sequences: T2w HASTE (TEeff/echo spacing/Nex/acq.t.: 90 ms/4.1 ms/1/20 s); unenhanced fat-suppressed T1w FLASH (TR/TE/matrix/acq.t.: 156 ms/2.3 ms/131 × 256/23 s) and unenhanced and dynamic contrast-enhanced fat-suppressed T1-weighted 3D GRE (TR/TE/matrix/acq.t.: 4.2 ms/1.8 ms/256 × 256/20 s) following i.v. injection of 0.1 mmol/kg of gadodiamide, acquired during arterial and portal phases. Images were interactively evaluated on a dedicated workstation using volume-rendering algorithm.
Results: Images of diagnostic quality were obtained in all the cases. Normal findings were observed in 12 cases. Hepatocellular carcinomas were detected in 6 cases, hepatic hydatid cysts in 6 cases, liver metastases in 3 cases and pancreatic carcinomas in the remaining 4 cases. Three-dimensional GRE images provided the correct diagnosis in all cases. The use of multiplanar reconstructions on different planes provided additional information on lesion localization and relationship with contiguous structures. MIP images from arterial phase provided visualization of arterial vessels demonstrating vascular encasement in three pancreatic carcinomas.
Conclusions: The use of T1-weighted 3D GRE sequence for the evaluation of the upper abdomen has the same diagnostic accuracy as 2D images. Further diagnostic advantages are represented by 3D data elaboration, providing thin and thick slab multiplanar views of the lesions and selective visualization of vascular structures.

B-0226 15:15

Herniography and inguinal pain: Correlation with surgery over a 5 year period

J. Jones, A. Mitchelmore; *Bristol/GB*

Purpose: To assess the sensitivity, specificity and safety of herniography when used in the clinical management of inguinal and peri-inguinal pain in the presence of a normal clinical examination.
Materials and methods: This retrospective study correlated case histories and examinations with the radiological and surgical findings over a five year period.
Results: Herniography was performed on 112 patients (74 men, 38 women). There were 3 false negative results and 2 false positive results giving a sensitivity of 84 % and specificity of 97.5 %. There were no significant complications of herniography.
Conclusion: Herniography is a sensitive, specific and safe investigation for the management of groin pain.

B-0227 15:20

Value of CT after laparoscopic repair of postsurgical ventral hernia

K.I. Gossios, A. Zikou, C. Tsompanlioti, P. Vazakas, A. Glantzouni, G. Glantzounis, D. Kontogiannis, E. Tsimoyiannis; *Ioannina/GR*

Purpose: To describe CT findings after laparoscopic repair of postsurgical ventral hernia.
Materials and methods: Ten patients underwent laparoscopic repair of postsurgical ventral hernia. After introduction of laparoscopic instruments through small trocar ports the herniated bowel loops were dissected free and reduced into the peritoneal cavity without resecting the hernia sac which was cauterized. The Gore-

Tex DualMesh Biomaterial patch was sized and placed over the abdominal defect. The mesh was secured onto the underlying fascia with unabsorbable sutures and clips. CT of the abdomen was performed the 1st and the 15th day after laparoscopic repair and according to clinical findings. Scanning was performed by a conventional equipment. The CT findings were correlated with the operative reports.
Results: Scans of two patients showed the presence of small collections within the abdominal wall between the hernia sac and the mesh. The rest of the patients did not have remarkable CT findings.
Conclusion: CT is a useful imaging tool in patients with laparoscopic repair of postsurgical ventral hernia showing the correct site of the mesh and complications such as collections in the abdominal wall even they are not palpable.

B-0228 15:25

Helical CT in the diagnosis of acute appendicitis
L. Laufer, L. Duhanu, I. Shelef, E. Sokolovsky, Y. Hertzanu; *Beer-Sheva/IL*

Purpose: To demonstrate the role of helical CT in the diagnosis of acute appendicitis.
Materials and methods: In the last year, 150 patients underwent appendectomy. 21 of them admitted with RLQ pain and inconclusive physical examinations were referred for helical CT examination. The bowel was opacified with diluted contrast material in 20 patients. IV contrast was injected in 19 patients.
Results: The appendix was visualized in 20 patients, while wall thickening was presented in 18/20. Homogenous wall enhancement was present in eight patients. Periappendicular fluid was seen in 12 cases and free fluid in another four. Periappendicular phlegmon or abscess was detected in four patients. Cecal or small bowel involvement by an inflammatory process was present in 12 patients. Appendicolith was found in one case, extraluminal air (1 patient), and arrow sign (1 patient) were demonstrated. The preoperative correct diagnosis was established in 18 patients and missed in 3 patients.
Conclusion: Helical CT with bowel opacification and IV contrast is a good tool in the diagnosis of appendicitis, but is associated with a learning curve.

14:00–15:30 **Room K**

Contrast Media

SS 306

New trends (2)

Chairpersons:
M. Langer (Freiburg/DE)
K. Verstraete (Gent/BE)

B-0229 14:00

Contrast enhanced US harmonic imaging in pancreatic masses
A.V. Zoubarev, I. Kalenova; *Moscow/RU*

Purpose: To study diagnostic possibilities of Contrast Enhanced Harmonic Imaging (CEHI) with Levovist in assessment neovascularity of pancreatic mass and evaluation of vascular involvement.
Methods and materials: 17 pts with pancreatic mass were examined on HDI-5000 (ATL-Philips), Elegra (Siemens) and Power Vision 6000 (Toshiba). Assessment of vascular involvement was performed to differentiate pancreatic cancer from local chronic pancreatitis. Vascular involvement was detected in the cases of narrowing, thrombosis and non visualization of major splanchnic vessels by PD. Tumor vascularity was revealed with CEHI after i/v bolus injections of Levovist at the dosage of 300 mg/ml. Findings were confirmed by surgical operation, biopsy and histopathological findings.
Results: 10 pts had pancreatic cancer, 7 pts had chronic pancreatitis. In 5 cases total vascular involvement revealed by CEHI was confirmed by CT and pts were referred to conservative treatment. In one case right diagnosis of resectability of pancreatic cancer on CEHI was established and the patient underwent pancreatectomy. In 4 patients with suspected vascular involvement in pancreatic cancer on CEHI surgical operation revealed unresectability. In all cases of pancreatic cancer CEHI with Levovist showed tumor neovascularity in arterial phase of enhancement. Contrary in chronic pancreatitis neovascularization of the mass was not detected.
Conclusion: We can conclude that CEHI is useful in detection of resectability of pancreatic cancer. CEHI may be useful tool to differentiate pancreatic cancer and local chronic pancreatitis.

B-0230 14:10

Contrast-enhanced MRA: Do contrast agents with enhanced relaxitivity improve the visualization of carotid artery stenoses?
S. Friese, H. Krapf, M. Fetter, M. Skalej, W. Küker; *Tübingen/DE*

Purpose: CE-MRA is a powerful tool for the non-invasive evaluation of cartoid artery occlusve disease. However, because of certain drawbacks, it has not completely replaced DSA. The purpose of this study was to evaluate if Gd-BOPTA, a contast agent with high relaxitivity, may increase the diagnositic accuracy of CE-MRA.
Material and methods: The CE-MRA examinations of 54 patients were evaluated retrospectively by two experienced radiologists, independently. 27 patients received contrast enhancement either with 20 ml Gd-BOPTA or with 20 ml Gd-DTPA. The reviewers were blinded to the contrast agent chosen and to the ultrasound results. They rated overall image quality and the degree of the ICA stenoses.
Results: For the estimation of the degree of the ICA stenoses there was high observer correlation. In comparison to the ultrasound findings 3 of 19 high-degree stenoses were underestimated as moderate stenoses. In one of seven sonographically occluded vessels MRA revealed residual patency in the vessel lumen. It was not possible to identify the contrast agent which was used for a study. Subjective estimation of the image quality (arterial contrast of the ICA, contrast of the other vessels, and general impression) did not significantly change with the contrast agent used.
Conclusion: The diagnostic accuracy of CE-MRA for the evaluation of intranal carotid artery stenoses is not improved by Gd-BOPTA. The potential of this contrast agent may be the reduction of the amount of contrast without loss of diagnostic information.

B-0231 14:20

MnDPDP-enhanced MRI vs. dual-phase spiral CT in the detection of hepatocellular carcinoma in cirrhosis
F. Donati, R. Lencioni, D. Cioni, L. Crocetti, C. Franchini, M. Perri, C. Bartolozzi; *Pisa/IT*

Purpose: To assess safety and tolerability of MnDPDP, and to investigate the sensitivity of MnDPDP-enhanced MRI, in comparison with dual-phase spiral CT, in the detection of hepatocellular carcinoma (HCC).
Subjects and methods: Fifty patients with histologically-proven HCC were enrolled in a prospective phase III B clinical trial. All patients underwent dual-phase spiral CT and precontrast and postcontrast MRI. MR examination protocol included SE and GRE T1-wi acquired before and after administration of MnDPDP (Teslascan); and precontrast fast SE T2-wi. Gold standard was provided by Lipiodol CT and follow-up CT studies repeated at 4-month intervals over a 10 to 27 month [mean ± SD, 20.1 ± 5.1 months] period.
Results: No serious adverse event occured. Eighty tumors 0.8 – 9.1 cm in diameter (mean ± SD, 3.2 ± 2.4 cm) were detected by Lipiodol CT or confirmed as cancerous foci by follow-up CT studies. Precontrast MRI detected 38/80 lesions (48 %); MnDPDP-enhanced MRI, 65/80 lesions (81 %); precontrast plus postcontrast MRI, 69/80 lesions (86 %); and CT, 64/80 lesions (80 %). The difference between unenhanced and MnDPDP-enhanced MRI was statistically significant ($p < 0.001$). The difference between MRI (precontrast plus postcontrast) and CT was not statistically significant ($p = 0.33$). The confidence in the final diagnosis was significantly higher for MRI as compared with CT ($p < 0.001$).
Conclusion: MnDPDP is a safe and well tolerated MR contrast agent. MnDPDP-enhanced MRI is significantly more sensitive than unenhanced MRI and as good as CT for detection of HCC in cirrhosis.

B-0232 14:30

The diagnostic accuracy of measuring enhancement pattern of ultrasound contrast agent: Intra- and interindividual variability in young healthy volunteers
A. Hochmuth[1], W.A. Kaiser[2]; [1]*Freiburg/DE*, [2]*Jena/DE*

Purpose: To clarify, whether the enhancement pattern after i.v.-administration of ultrasound contrast-agent is reproducible and can be used as a diagnostic tool.
Material/methods: 17 young, healthy volunteers (23.4 a mean age) with clinically and sonographically normal thyroid gland were examined repeatedly (four times) under standardized conditions using Power Doppler Sonography (ATL HDI 5000, ATL, Bothell, USA) while administration of contrast agent (Levovist, Schering, Berlin, Germany). The examinations were stored and evaluated using a dedicated PC-based system (Quanticon, Echotech, Hallbergmoos, Germany).
Results: All parameters (time-to-peak, gradient of enhancement, absolute values of enhancement etc.) showed a wide intra- and interindividual variability (f.e. time-to-peak 6.3 s to 11.7 s intraindividually, 6.3 s to 22.4 s interindividually).

Conclusions: The parameters that describe the enhancement after i.v.-administration of ultrasound contrast-agent showed impressive intra-/interindividual differences even in examinations of a healthy and homogeneous population under standardized conditions. Therefore, the correct interpretation of enhancement pattern in patients may be even more difficult.

B-0233 14:35

Paramagnetic vs. superparamagnetic contrast enhanced liver MRI in the same patient

C. Stoupis[1], P. Vock[2], E.N. Brountzos[1], K.S. Malagari[1], G. Malachias[1], D.A. Kelekis[1]; *[1]Athens/GR, [2]Berne/CH*

Purpose: To evaluate the use of either paramagnetic or superparamagnetic contrast agents in the detection and characterization of solitary or multiple benign liver lesion(s) in the same patient.

Material and methods: 20 non cirrhotic patients with 36 liver lesions were imaged at 1.5 T units. Paramagnetic (Dotarem or Omniscan) and superparamagnetic (Endorem) contrast enhanced MRI was performed within 15 days in all cases. Imaging protocol was done according to standard T1 and T2 sequences for each magnet system (Vision, Siemens and Signa, GE). Both breath hold and non-breath hold images were acquired. Qualitative and quantitative analyses were performed. Surgery, biopsy or follow up confirmed the diagnosis.

Results: All lesions were seen with either agent, however one lesion was masked by phase encoding artifact in paramagnetic agent. Cases of hemangioma (22) were characterized in both agents. Cases of FNH (12) were better characterized by superparamagnetic agent, with better appreciation of the central scar. Cases of adenoma (2) produced similar difficulties in characterization. Statistically, overall, non breath hold imaging using superparamagnetic contrast had better diagnostic confidence and patient comfort than breath hold paramagnetic contrast enhanced MRI.

Conclusion: Endorem enhanced MRI is a non breath hold technique that enables liver lesion detection and characterization without any technical fast imaging. Paramagnetic enhanced MRI is faster, however it requires high field units and curve analyses for characterization.

B-0234 14:45

Color-coded computed tomography: Principle and first clinical results

E. Hein, P. Rogalla, A. Lembcke, B.B. Hamm; *Berlin/DE*

Purpose: To develop a method for combining morphological and dynamic information in CT images.

Materials and methods: Multislice CT allows for scanning of large volumes within a few seconds. Instead of scanning organs during a single breathhold following intravenous contrast material administration, multiphasic scanning can be performed, each run with the respective fraction of radiation dose. Adding the partial series results in a morphologic image with standard detail resolution and image noise. By subtracting the partial series, a differential image can be calculated and color-coded, visualizing only dynamic information. Through weighted image-fusion of the addition and subtraction image, morphologic (gray values) and dynamic (color values) information can be merged in one picture. 13 patients underwent a biphasic liver CT during single breathhold (2 mm slice thickness, 30 s delay, 1. run (7 s), 12 s delay, 2. run (7 s) 26 s breathhold), 25 patients underwent a neck CT (1 mm slice thickness, 20 s delay, 1. run (13 s), 37 s delay, 2. run (13 s)).

Results: Portal venous branches, veins and arteries showed distinguishable color differences, depiction of morphology and image noise were not influenced. Cysts and solid liver lesion as well as tumors and muscle tissue differed in color. The total radiation exposure did not increase because the mA per spiral run was halved.

Conclusion: Color-coding represents a promising method through which differetiation of various tissues may be facilitated.

B-0235 14:55

Pulse inversion harmonic imaging vs. spio enhanced magnetic resonance in detection of liver metastases

C. Del Frate, A. De Candia, G. Como, V. Londero, C. Zuiani, M. Bazzocchi; *Udine/IT*

Purpose: To compare the sensitivity of pulse-inversion-harmonic-imaging (PIHI) with superparamagnetic-iron-oxide (SPIO) enhanced magnetic resonance (MR) in the detection of liver metastases.

Methods and materials: 14 consecutive patients, with primary malignacies, and suspicious liver metastases at conventional-US were examined with digital PIHI-ultrasound and SPIO-enhanced MR. MR was performed before- and after-SPIO infusion, using breath-hold GE T1W and TSESTIR T2W sequences. The PIHI technique was performed using a CSI-3 harmonic preset, low frame-rate (5 Hz), and high mechanical index (MI 1.1 – 1.3), before- and after-bolus injection of 10 cc of Levovist (400 mg/dl), in three delayed scans (respectively 20, 100 and 180 s). Two radiologist indipendently evaluated image quality, number, location and dimension of lesions in both techniques before- and after-contrast media. The 92 detected lesions were confirmed by intraoperative-ultrasound, percutaneous biopsy or follow-up.

Results: SPIO-enhanced MR detected 90 lesions, instead of 54 by unenhanced-MR (increasing: 40 %). The lesions detected only by SPIO-enhanced MR were small in diameter (average: 8.7 mm). Conventional ultrasound detected 49 lesions instead of 84 (increasing: 41.6 %) during the first scan, 92 (increasing: 46.7 %) during the second scan and 87 (increasing: 43.7 %) during the third scan in PIHI-ultrasound. The major conspicuity was obtained in livers with regular echogenicity while it was lower in hyperechoic livers or in lesions with basal high echogenicity.

Conclusions: PIHI-ultrasound is sensitive in liver metastases detection, and so is useful in screening, but inaccurate in their location and hard to repeat. SPIO-enhaced MR seems to be not replaceable in the follow-up of metastatic patient in medical treatement.

B-0236 15:05

Magnetic resonance perfusion imaging: Pros and cons of sophisticated image postprocessing

V. Hietschold, T. Kittner, D. Mucha; *Dresden/DE*

Purpose: To compare visualization methods in perfusion imaging concerning reliability and contrast-to-noise ratio (CNR).

Methods and materials: Perfusion measurements using EPI-FID and double-echo FLASH sequences were performed on enhancing and non-enhancing tissue in the regions of the head and neck. Difference images, time-to-peak maps and signal loss maps deconvoluted from the arterial input function were generated. In the case of enhancing lesions, a correction for signal increase due to contrast uptake was applied to the double echo data. Quantitative evaluations in regions of interest (ROI) prior to resp. after enhancement correction or deconvolution were also compared.

Results: Due to error propagation, the CNR for corrected images is generally worse – especially for postprocessing steps containing intensity ratios. In the case of quantitative ROI evaluations, due to the calculation of regional mean values prior to the correction steps, the results are considerably less disturbed by noise.

Conclusion: The calculation of parameter images is a valuable tool, especially since it allows for simple visual comparisons between lesions and normal tissue. Nevertheless, very simple postprocessing steps can visualize perfusion properties more impressive than parameter maps. As to be expected, evaluations of ROIs are significantly more robust against noise effects.

B-0237 15:15

Phase I clinical trial of G 792-12, a new blood pool agent for MRI

S. Gaillard, C. Kubiak, C. Stolz, B. Bonnemain, D. Chassard; *Roissy/FR*

Purpose: This study was designed to assess the safety and the kinetic of G 792-12, a new macrocyclic gadolinium blood pool MR contrast agent with a rapid renal elimination and a high R1 relaxivity (27.1 $mmol^{-1} \cdot s^{-1}$).

Materials and methods: 32 male subjects were prospectively enrolled into this single-blind, ascending dose and placebo controlled clinical trial. G 792-12 was injected as an IV bolus at doses of 0.0065 mmol, 0.013 mmol (clinical intended dose), 0.026 mmol and 0.039 mmol of gadolinium/kg body weight. Changes in vital signs (blood pressure and heart rate), ECG, clinical chemistry, hematology and urine analysis as well as adverse events report and tolerance at the site of injection were closely monitored.

Results: No serious adverse event occured within the 22 days period of observation following the administration of G 792-12 at either dose. No drop out was related to the study drug. No clinically relevant changes in vital signs, ECG prints or laboratory parameters and no side effect at the site of injection were reported. Only one non placebo subject presented 2 adverse events (hot flush and nausea) considered to be related to G 792-12.

Conclusions: The results of this first clinical study demonstrate that G 792-12 is safe when administered at doses up to 0.039 mmol gadolinium/kg (3 times the intended clinical dose) allowing further clinical evaluation in phase II studies.

B-0238 15:20

Interstitial MR lymphography with MS-325: Assessment in pigs and rabbits

T. Lauenstein, M. Goyen, S. Bosk, J.F. Debatin, S.G. Rühm; *Essen/DE*

Purpose: To evaluate the performance of MS-325, a macromolecular, Gd-based contrast agent, for the visualization of regional lymphatic vessels and lymph nodes in rabbits and pigs.
Materials and methods: Five white New Zealand rabbits and 2 pigs were used as animal model. The dorsal (n = 5) foot pads of the rabbits were subcutaneously injected with 0.5 ml undiluted MS-325; 4 ml undiluted MS-325 was injected subcutaneously into the mammary region of the pigs. Following the contrast administration the injection site was slightly and repeatedly massaged. Imaging was performed with a 3D spoiled gradient echo sequence. Image sets were obtained prior to as well as 5, 15, 30, and 60 min following the subcutaneous contrast injection.
Results: In the rabbits up to five successive lymph node groups including the thoracic duct could be visualized. Besides the visualization of lymphatic structures a faint contrast enhancement of vascular structures was present already after 5 to 15 min which facilitated anatomical classification of the various lymph node groups. In the pigs the draining mammary, mediastinal and cervical lymph nodes were displayed within a 15 minute period.
Conclusion: MS-325 allows depiction of the lymphatic system within less than 30 min following a small-volume subcutaneous injection The concomitant enhancement of vascular structures might facilitate possible future application such as preoperative MR guided sentinel node detection and marker placement or lymph node sampling in humans. The favorable safety profile of MS-325 warrants its use in human clinical trials.

14:00–15:30 **Room L/M**

Head and Neck

SS 308

Head and neck cancer

Chairpersons:
G. Moulin (Marseille/FR)
F.E. Zanella (Frankfurt a. Main/DE)

B-0239 14:00

Staging head and neck cancer: Is MRI really the method of choice?

D. Pickuth, G. Peters, H. Frimmel, M. Bloching, R. Spielmann;
Halle a. d. Saale/DE

Purpose: The aim of this study was to prospectively evaluate the accuracy of CT and MRI in staging head and neck tumours using a new standardized examination protocol and a clinically oriented reporting protocol. The protocols emphasize the specific information that needs to be conveyed to the referring otolaryngologist.
Patients and methods: 50 consecutive patients with head and neck cancer underwent both CT and MRI. Tumour volume, local extent, spread into soft tissues, invasion into bony structures, relationship to neurovascular bundles, extension across midline, and lymph node involvement (location, size, appearance) were determined in all patients. Images were reviewed by three radiologists and correlated with findings at subsequent operative resection.
Results: For T- and N-staging of head and neck tumours, the overall accuracy of CT was 86 % (MRI 82 %). CT was superior in the assessment of bone invasion. In contrast, MRI had a better soft tissue contrast than CT. Motion artifacts due to respiration movement or random patient movement (swallowing, coughing) degraded 10 % of the MRI studies. MRI findings caused an overestimation of tumour volume and invasion in 15 %.
Conclusion: In this era of cost concern, it is a good principle to perform one cross-sectional study that accurately stages the disease for the lowest price. Our results indicate that CT is the method of first choice for staging head and neck tumours. In some patients, an additional MRI study is needed to resolve specific issues that would have consequences for treatment (e.g. submucosal spread, muscle invasion).

B-0240 14:10

The relation of CT-determined tumour parameters and local and regional control of tonsillar cancer after definitive radiation treatment

K. Op de Beeck, R. Hermans, W. Van den Bogaert, A. Rijnders, L. Staelens, M. Feron, E. Bellon; *Leuven/BE*

Purpose: To investigate the value of CT-derived tumour parameters as predictor of local and regional outcome of tonsillar squamous cell carcinoma treated by definitive radiation therapy.
Materials and methods: The pretreatment CT studies of 112 patients with tonsillar squamous cell carcinoma were reviewed. After redigitizing the films, primary and nodal tumour volume was calculated with the summation-of-areas technique. The nodal CT-aspect was graded using a 3-point scale (homogenous, inhomogeneous, necrotic). Mean follow-up time was 33 months. Actuarial statistical analysis of local and regional outcome was done for each of the covariates; multivariate analysis was performed using Cox' proportional hazards model.
Results: In the actuarial analysis, CT-determined primary tumour volume was significantly correlated with local recurrence rate ($p < 0.05$) when all patients were considered, but primary tumour volume did not predict local control within the T2, T3 and T4-category. CT-determined nodal volume was significantly related with regional outcome ($p < 0.01$), but nodal density was not. Total tumour volume was not significantly related with locoregional outcome ($p = 0.1$). In the multivariate analysis, the T and N-category were the independent predictors of local, respectively regional outcome.
Conclusion: Compared to other head and neck sites, primary and nodal tumour volume have only marginal predictive value regarding local and regional outcome after radiation therapy in tonsillar cancer.

B-0241 14:20

Inter- and intraobserver reproducibility of CT examinations of oro- and hypopharyngeal carcinomas

M. Keberle, W. Kenn, H. Müller, D. Hahn; *Würzburg/DE*

Purpose: To evaluate the inter- and intraobserver reproducibilities of computed tomography (CT) in patients with oro- and hypopharyngeal carcinomas.
Methods: Two independent readers interpreted CT images of 41 patients with hypopharyngeal carcinomas, 45 patients with oropharyngeal carcinomas, and 23 patients without a tumor. All relevant subregional anatomic structures were evaluated for present tumor infiltration. Statistical analysis was done by using Cohen's κ and the Wilcoxon test.
Results: Mostly, moderate and substantial inter- and intraobserver reproducibilities were determined (range of the determined κ-values: 0.25 – 1.00). The κ-values of the intraobserver reproducibilities of both readers were not significantly different ($P < 0.2$). The κ-values of the intraobserver reproducibilities were in almost all the cases higher than the respective κ-values of the interobserver reproducibility ($P < 0.001$).
Conclusion: CT of oro- and hypopharyngeal carcinomas can be interpreted with clinically acceptable variability. A higher agreement can be achieved if repeated interpretation is done by a single person.

B-0242 14:25

Feasibility and reliability of "Rapid" SE MR sequences in the oncologic imaging of the oral cavity and oropharynx

D. Farina, G. Battaglia, P. Maculotti, A. Marconi, R. Maroldi; *Brescia/IT*

Purpose: To optimize "rapid" SE MR sequences and to assess their reliability in the study of oral cavity and oropharyngeal malignancies.
Materials and methods: Eighteen patients with SCC of the oral cavity and oropharynx were examined with 1.5 T MR. The protocol included, beyond conventional Turbo SET2 and SET1, *rapid* sequences: Turbo SET2: acquisition time (AT) 54 s, small FOV 175 × 200 mm, pixel size 0.80 × 0.39 mm; *rapid* SET1: AT 97 s, FOV 94 × 150 mm, pixel size 0.64 × 0.29 mm; *very rapid* SET1: AT 17 s, FOV 149 × 170 mm, pixel size 0.99 × 0.66 mm. To avoid aliasing due to the small FOV of the *very rapid* sequence, oversampling (60 %) was necessary. A score system was used to record motion artefacts (0 ... no artefacts, 1 ... < 50 % images degraded, 2 ... > 50 % images degraded). Tumour conspicuity was classified as excellent (0), good (1), poor (2). Mandibular infiltration was assessed by three blinded radiologists who analysed each a different set of SET1.
Results: Motion artefacts were relevant on conventional SET2 (44.4 % score 1 – 2) and SET1 (61.1 % score 1 – 2). A significant improvement was observed with modified SET1 sequences (16.7 % score 1 – 2 with very rapid SET1). Tumour conspicuity was excellent in more than 80 % of cases on all sequences adopted. Mandibular infiltration was correctly diagnosed in 3/4 cases on all enhanced sequences: 1/4 FP occured due to inflammation.

Conclusions: These preliminary results demonstrate a significant decrease of artefacts with *rapid* SET2 and SET1 sequence. This allows a better discrimination between tumour and normal structures. Identification of lesions and assessment of mandibular infiltration with rapid sequences are as accurate as with the conventional ones.

B-0243 14:35

Digital image fusion of early and delayed scans in dual-phase spiral CT of the head and neck

R. Groell, G. Wolf, W. Habermann, M. Wiltgen; *Graz/AT*

Purpose: To evaluate the feasibility of digital image fusion of different phases in spiral CT studies of the head and neck.

Materials and methods: Eight patients with squamous cell carcinomas of the head and neck underwent dual-phase spiral CT examinations using 100 ml of non-ionic contrast material. The scans started 30 s (early phase) and 3 – 5 minutes (late phase) after the start of contrast material injection. The images of the early phase (showing optimal vascular enhancement) were semi-automatically fused with the images of the late phase (showing optimal tumor conspicuity) on a digital image workstation.

Results: Digital image fusion of early and late scan sequences was possible in each patient within a time span of ten minutes per patient. The relationship between tumors and adjacent vessels was better visualized on the fused images than on the original source image. However, overall image quality was lower on the fused images than on the source images of the two different phases.

Conclusions: Digital image fusion of early and late phases enabled combined opacification of vessels and squamous cell carcinomas which facilitated the topographic assessment of the tumors' size and spread.

B-0244 14:40

Assessment of tumor vascularisation and bone involvement of head and neck tumors using spiral-CT and MR-angiography: Image fusion as a tool for diagnostic imaging

J. Hohmann, I. Ohnesorge, K.-J. Wolf; *Berlin/DE*

Purpose:

Previous studies showed that combination of 3D-Spiral-CT and 3D-MRI-datasets with Image Fusion provides better assessment of bone structures and surrounding softtissue in case of cystic maxillofacial tumors. Based upon these results further extension of the protocols was performed using MR-Angiography (MRA) to get more detailed information about vascularisation of tumors of head and neck, especially of tumors with an assumed hypervascularisation.

Materials and methods:

14 Patients with different tumors of head and neck where examined using Spiral-CT, MRI and MRA. Spiral-CT examinations were performed on a Siemens Somatom Plus 4 Q (SC/TF/RI 2/3/1 mm). MR examinations were performed on a Siemens Magnetom Vision using a T1-weighted 3D-MPRAGE and a 3D-Time-of-Flight (TOF)-Angiosequence. Image Fusion was performed on a SGI Workstation (O2) with the 3D-Reconstruction-Software 3D Virtuoso (Siemens Medical Systems, Erlangen, Germany). The evaluation consists of two steps. First the combination of Spiral-CT and MPRAGE-datasets for assessment of bone and softtissue structures in one dataset. Second the combination of the previous datasets with the MRA-dataset for assessement of the vascularisation of the tumor and surrounding anatomical structures.

Results: The recent findings are confirming the results of the previous studies. There is a significant improvement in the assessment of softtissue and envolvement of bone structures. In addition Image Fusion using the MRA-sequences allows a better evaluation of vessels concerning the hypervascularised tumors.

Conclusion:

Image Fusion of Spiral-CT/MRI and MRA-datasets improves significantly the assessment of tumor vascularisation and is a well accepted presentation tool for the maxillofacial surgeons in the preoperative work-up.

B-0245 14:50

Contrast-enhanced spiral CT of the head and neck: Improved conspicuity of squamous cell carcinomas on delayed scans

R. Groell, O. Doerfler, W. Habermann; *Graz/AT*

Purpose: To evaluate the impact of delayed scans on the conspicuity of squamous cell carcinomas in spiral CT of the head and neck.

Materials and methods: 27 patients with biopsy-proven squamous cell carcinomas of the head and neck underwent dual-phase spiral CT examinations using 100 ml of non-ionic contrast material. In all patients the early phase started 30 s after the commencement of injection. The patients were assigned to one of two groups in which the delayed phase started either 180 s (group A, n = 13) or 300 s (group B, n = 14) after the start of injection. The overall image quality including vascular opacification and the quality of lesion conspicuity were determined according to a scoring system (1 ... good, 2 ... medium, 3 ... bad).

Results: Overall image quality was scored better on the early scans (score: 1.4 ± 0.5) than on the late scans with 180 s (score: 1.6 ± 0.6, $p = 0.03$) or 300 s delay (score: 2.4 ± 0.5, $p = 0.002$). Tumor conspicuity was better scored on scans with 180 s delay (score: 1.4 ± 0.5) than on the scans with 30 s delay (score: 2.3 ± 0.7, $p = 0.02$) or on the scans with 300 s delay (score: 2.3 ± 0.7, $p = 0.03$). In 8/13 (62 %) patients in group A and in 6/14 (43 %) patients in group B the tumor was better delineated on the late scans than on the early scans.

Conclusions: Although early scans provide optimal vascular enhancement and are therefore necessary for spiral CT studies of the head and neck, additional delayed scans may improve lesion detection in patients with squamous cell carcinomas of the head and neck.

B-0246 15:00

MR guided interstitial photodynamic therapy in advanced head and neck tumours

H.R. Jäger, M.A.A. Suhr, J. Brookes, C. Hopper; *London/GB*

Purpose: To assess the feasibility and efficacy of MR-guided interstitial photodynamic therapy (iPDT) in advanced head and neck tumours. To determine the tissue reaction on early and delayed follow-up MRI scans.

Materials and methods: 8 patients with advanced head and neck tumours underwent iPDT using a 652 nm Laser light following i.v. injection of mTHC (Phoscan) as photosensitiser. The Laser light was delivered via optical fibres inserted through 18 G MR-compatible needles. These were positioned using a 0.2 T open MR system, avoiding close proximity to vital structures such as the carotid arteries, optic nerves and intracranial structures. Follow-up MRI scans were performed at 3 – 5 days and 6 weeks.

Results: There were no major complications or damage to vital structures. MR guidance allowed controlled needle placement ensuring overlap between the zones of illumination of each optic fibre. Contrast-enhanced MRI at 3 – 5 days showed areas of tissue necrosis of approximately 1 cm radius around each fibre track and correlated well with the amount of tissue necrosis seen at 6 weeks. Significant tumour reduction and palliation of symptoms was achieved in all but one case.

Conclusion: MR guided iPDT is a safe and promising new method of palliative treatment in advanced head and neck tumours.

B-0247 15:10

Radiation therapy combined with transcatheter intra-arterial infusion chemotherapy for advanced head and neck cancer: A preliminary report

M. Wakisaka, H. Mori, H. Odo, Y. Hori, T. Maeda, H. Mizuki, S. Yanagisawa; *Oita/JP*

Purpose: To evaluate the effectiveness of radiation therapy (RT) combined with transcatheter intra-arterial infusion chemotherapy (TAI) for the patients with advanced head and neck cancer.

Materials and methods: Eight patients (46 – 86 years old) with advanced head and neck cancers (tongue cancer 4, maxillary cancer 1, gingival cancer 2 and buccal mucosal cancer 1) received RT combined with TAI in Oita Medical University between 1997 and 1999. In total, 11 TAIs were performed by the Seldinger method in these eight patients. 4 French catheter was superselectively inserted to the feeding arteries of the tumors and CBDCA was infused. Tumor regression and adversed effect were retrospectively evaluated.

Results: Evaluation of tumor regression was done by CT or MRI. The cases with complete tumor regression were defined as CR, PR when there was more than 50 % but less than 100 % tumor regression, MR when there was more than 20 % but less than 50 % tumor regression, NC when there was less than 20 % tumor regression and PD when there was interval enlargement. CR was noted in 2 patients, PR in 4 patients, MR in 2 patient. No major complications were noted except for the nausea (Grade 1) in 1 patient and mucositis (Grade 1) in 1 patient. Two out of 4 PR patients were operated after the completion of the RT combined with TAI, but the resected specimen histopathologically revealed no tumor cells.

Conclusion: RT combined with TAI seemed to be very effective for the control of advanced head and neck cancers.

B-0248 15:20

Intraarterial infusion therapy for head and neck cancer: Evaluation of tumor perfusion with intraarterial dynamic CT during carotid arteriography with combined CT and angiography

A. Ishii, Y. Korogi, Y. Shigematsu, K. Kawanaka, M. Yamura, K. Yoshizumi, M. Takahashi; *Kumamoto/JP*

Purpose: To evaluate the perfusion in head and neck cancer with dynamic CT during intraarterial contrast-material infusion, and to compare the difference of perfusion between the good and poor response groups for intraarterial chemotherapy.

Materials and methods: Twenty consecutive patients underwent conventional angiography using a combined CT and angiography system. Relatively low-dose CDDP was injected through the microcatheter placed in each artery depending on tumor location. Dynamic CT images were obtained with a 15 s continuous scanning. Contrast material enhancement on dynamic CT images was evaluated qualitatively and including transfer index (k) using a Patlak plot method. The good and poor response groups for treatment were classified according to the modified Jakobsson's classification.

Results: In the qualitative evaluation, tumors showed early enhancement as well as rapid washout, and dynamic CT was useful for evaluation of the extent of the tumor. The mean values of quantitative parameters were not significantly different between the good and poor response groups.

Conclusion: Intraarterial dynamic CT was useful for evaluation of the extent of the tumor. However, quantitative data did not provide additional information in prediction of the treatment effect. This may indicates that the effectiveness of intraarterial chemotherapy is not directly affected by the perfusion of the head and neck cancers.

14:00–15:30 **Room N/O**

Genitourinary

SS 307

Ureters

Chairpersons:
E.K. Lang (New Orleans, LA/US)
J. Venâncio (Costa Caparica/PT)

B-0249 14:00

Vesicoureteral reflux: Diagnosis by contrast-enhanced ultrasonography

A. Klauser, C. Radmayr, L. Pallwein, F. Frauscher, G. Bartsch, D. zur Nedden; *Innsbruck/AT*

Purpose: The diagnosis of vesicoureteral reflux (VUR) is routinely performed by means of voiding cystourethrography (VCUG). With the development of ultrasound (US) echo-enhancing agents like Levovist (Schering, Germany) we assessed the diagnostic efficacy of those agents in the evaluation of vesicoureteral reflux (VUR).

Method/materials: 104 children, with a mean age of 5.4 years (± 4.8) were examined using echo-enhancing US. In the same examination session the VCUG was also performed. US of the urinary tract was followed by intravesical injection on Levovistregistered. The volume of the administered US contrast agent was 15 % of the bladder capacity. The diagnosis of VUR was made when microbubbles appeared in the ureters or renal pelvis. The sonographic findings were correlated with those obtained by VCUG.

Results: Out of the 208 kidney-ureter units investigated VUR was detected in 77 (37 %) by one (n = 8) or both (n = 71) techniques. All reflux grades could be identified. VUR was diagnosed in 5 cases only sonographically and in 3 cases only by VCUG. The specificity and sensitivity of the contrast reflux US were significantly high. The long contrast time of up to 30 minutes couples with high contrast effect result not only in convincing images but high level of diagnostic confidence.

Conclusions: Our preliminary results showed that the diagnostic accuracy of VUR by means of contrast enhanced US is comparable to the radiographic VCUG and therefore promises to reduce the number of children being exposed to ionising radiation.

B-0250 14:10

3D Virtual US in dilatated ureters

V.V. Gajonova, A.V. Zoubarev, G. Varentsov; *Moscow/RU*

Purpose: To evaluate the capabilities of 3D US in identification of ureteral obstruction.

Material and methods: 12 patients with hydroureteronephrosis were referred to conventional 2D and 3D US. 3D volumetric data were collected and 3D virtual reconstructions were performed to determine the level of obstruction and identify the etiology of hydronephrosis. All US results were confirmed by CT, urography, cystoscopy, surgery.

Results: 2D US was accurate in 25 % cases of proximal ureteral obstructions. 3D US revealed all proximal and 75 % of cases of distal level obstruction. 3D volumetric and rendered data of dilatated ureter showed anatomical relationships between ureter and different surrounding structures thus detecting the cause of obstruction in difficult cases (postoperative pelvic abscess, big adnexal tumor, postoperative fibrotic circular thickening of the ureter, deviation and dislocation of the proximal part of the ureter caused by interposition of inferior vena cava).

Conclusion: 3D US was superior to 2D in determination of the spatial relationships between dilatated ureter and different surrounding structures. Volumetric US reconstructions proved to be very helpful in preoperative planning. Our positive results showed that 3D US is a prospective non-invasive method for determination of the etiology of hydroureteronephrosis.

B-0251 14:20

Extended-field-of-view ultrasound imaging technology: Assessment in different urological diseases

L. Pallwein, A. Klauser, G. Helweg, G. Pinggera, F. Frauscher, G. Bartsch, D. zur Nedden; *Innsbruck/AT*

Purpose: The limited field-of-view (FOV) of a real-time ultrasound (US) scanner is a substantial disadvantage. The new US extended-FOV technology (SieScape™, Siemens, Germany) enables large resolution-preserved images up to 60 cm length. We investigated the value of this technique in different urological diseases.

Method/materials: The extended-FOV US imaging technology creates a panoramic image in real-time using an image-registration-based position-sensing technique. We examined 27 patients with nephroptosis, 6 patients with acute hydronephrosis, 17 patients with acute scrotal pain and 15 patients with urethral strictures. Extended-FOV images were correlated to standard real-time images.

Results: In patients with nephroptosis the downward displacement of the kidney in relation to surrounding structures could be easily demonstrated. The panoramic view enables an excellent delineation of hydronephrosis and hydroureter. In patients with scrotal pain, transverse extended-FOV images of both testicles were helpful in exact diagnostic evaluation and comparison of testicle size and echogenicity. The extent of urethral strictures was better evincible in comparison to the standard US scan.

Conclusions: The new extended-FOV US imaging technique was easily accomplished in all cases. This method provides a panoramic image which allows a better understanding of the topographic anatomy and expands diagnostic capabilities in diverse urological diseases.

B-0252 14:30

Distal ureteral calculi: Detection with 3D transrectal/transvaginal ultrasonography

F. Frauscher, A. Klauser, H. Volgger, L. Pallwein, G. Helweg, G. Bartsch, D. zur Nedden; *Innsbruck/AT*

Purpose: The detection of distal ureteral calculi by means of transabdominal ultrasonography and intravenous pyelography is often difficult. Therefore we evaluated the use of 3-D transrectal/transvaginal ultrasonography in identifying distal ureteral calculi.

Method/materials: Thirty-one patients (9 female, 22 male) with flank pain, hematuria and clinically suspected distal ureteral calculi underwent intravenous pyelography (IVP), abdominal and 3-D transrectal/transvaginal sonography. For the 3-D sonography we used an Kretz Combison 530 unit (Kretz, Austria). The transrectal 3-D sonographic findings were compared with the abdominal sonographic findings and the radiographic findings. The ureteral calculi were surgically confirmed by ureteroscopy.

Results: Distal ureteral calculi were found in all 31 patients by means of ureteroscopy. In all 31 patients 3-D transrectal/transvaginal sonograms demonstrated clearly a distal ureteral calculus; whereas in only 22 cases (71 %) the calculus was identified with IVP and in only 17 cases (55 %) the calculus was detected with transabdominal sonography. Distal hydroureter was identified with 3-D transrectal/transvaginal scanning in each patient but with abdominal scanning in only 16. Hydronephrosis was absent in six patients, mild in nine, and moderate in eleven patients with distal ureteral calculi. The mean examintion time for the 3-D transrectal/transvaginal sonography was 1.9 ± 0.6 minutes.

Conclusions: In symptomatic patients, use of 3-D transrectal/transvaginal sonography should be considered to evaluate the distal ureter for calculi. This technique showed to be superior to the IVP and the transabdominal ultrasonography. Furthermore 3-D transrectal/transvaginal sonography has the advantage of extremely short examination times.

B-0253 14:40

IVU or unenhanced helical CT in acute renal colic?

M.E. Hurley, W. Torreggiani, A. Twair, M. Guiney, S. Hamilton; *Dublin/IE*

Purpose: To evaluate the role of unenhanced helical CT in the diagnostic work-up of patients referred with a history of acute renal colic.

Methods and materials: A prospective study was performed over a one year period in our hospital. 52 patients were examined with unenhanced helical CT. Radiation exposure for helical CT and IVU were measured and compared. The CT images were read in double blind fashion by two radiologists.

Results: Mean patient age was 45 (range 17 – 69 a) and F:M ratio 1.2:1 (28 women and 24 men). The average radiation exposure of an unenhanced helical CT and an IVU were similar, 7.3 and 6.5 mSv respectively. Of the 52 CT examinations 45 (86 %) were diagnostic and 7 (13 %) indeterminate. The interobserver concordance was 92 % (48/52). The sensitivity was 95 % (19/20), the specificity 89 % (24/27) and the accuracy 93 % (42/45). Of the 18 patients who had a positive CT examination all showed an ureteral calculus; 56 % (10/18) had kidney asymmetry and/or cortical thickening; 72 % (13/18) had pelvicaliceal dilatation and 94 % (17/18) had ureteral dilatation; 72 % (13/18) had perinephric stranding and 56 % (10/18) periureteral oedema; none showed a tissue ring sign. Unenhanced helical CT was faster than IVU and required no contrast injection.

Conclusions:

1. Unenhanced CT did not expose the patient to a significantly increased radiation dose, versus IVU.
2. Phleboliths are a diagnostic problem in unenhanced CT.
3. KUB is not necessary when unenhanced CT is performed.
4. Helical CT is more comfortable for the patient.

B-0254 14:50

Central lucency of pelvic phleboliths: Comparison of plain radiographs and noncontrast helical CT

J. Kim, K. Han; *Daejeon/KR*

Purpose: Central lucency of pelvic phleboliths is frequently found on plain pelvic radiographs. When it is present on noncontrast helical CT, pelvic phleboliths may be easily diagnosed, with no suspicion of distal ureteral calculi. The objective of this study was to determine the frequency with which this phenomenon is seen on plain radiographs and noncontrast helical CT.

Materials and methods: During a recent two-year period, we identified 70 patients with renal colic who underwent both radiography and noncontrast helical CT scanning. Radiographs were obtained at 70 – 85 kVp and 30 – 40 mA. CT scans were preformed within one month of plain radiography with 120 kVp, 200 – 220 mA, 5-mm collimation, pitch of 1 – 1.6, soft tissue and bone window settings. With regard to the central lucency of pelvic phleboliths on both radiographs and CT, two radiologists reached a consensus.

Results: Among the 70 patients, a total of 150 pelvic phleboliths was found. In all cases except one, pelvic radiography and helical CT revealed the same number of phleboliths. The exception was a case in which one of two phleboliths demonstrated by CT was not seen on radiographs. Pelvic radiography revealed central lucency in 95 of 150 phleboliths (63 %), but CT failed to depict a hypodense center in any phlebolith.

Conclusion: Central lucency of pelvic phleboliths, as frequently seen on plain pelvic radiographs, was not revealed by noncontrast helical CT in any patient. The presence or absence of central lucency on CT cannot, therefore, be used to differentiate phleboliths from distal ureteral calculi.

B-0255 15:00

Magnetic resonance urography: The use of furosemide

J.T. Heverhagen, M. El-Sheik, T. Hartlieb, K.J. Klose; *Marburg/DE*

Purpose: The purpose of our study was the evaluation of the effectiveness of the use of furosemide in order to achieve magnetic resonance urograms in volunteers. Additionally, the optimal time point to acquire an MR urogram after the application of furosemide should be determined.

Method/materials: 40 volunteers (15 female/25 male; mean age: 23.2 ± 2.6 years) with no known disorders of the genitourinary tract were included in this study. Prior to the investigation they were hydrated drinking 750 ml water. Immediately before the investigation they had to void. Images were acquired using a single-shot turbo-spin-echo sequence (ssTSE; TR/TE: infinite/1100 ms; FA: 150°) with an acquisition time of 7 seconds. After obtaining a native image furosemide was applied in a standard dose of 5 mg. Post-furosemide images were acquired immediately after injection and subsequently every 30 seconds for a total imaging time of 20 minutes. Images were evaluated by three independent investigators with different grade of education.

Results: No volunteer presented a complete delineation of both urethers prior the application of furosemide. Complete single urethers were displayed in twelve volunteers. After i.v. application of furosemide both urethers could be visualized completely in all volunteers. Complete depiction of the urethers is achieved six to ten minutes after i.v. application of furosemide. During the twenty minute imaging period the normal filling of the bladder could be observed. A statistically significant difference between male and female volunteers was not demonstrated.

Conclusions: The use of furosemide improves respectively enables the delineation of the urethers of healthy volunteers.

B-0256 15:10

Diuretic-enhanced Gadolinium excretory MR urography: Comparison of different T1-weighted gradient-echo techniques

C.C.A. Nolte-Ernsting, J. Tacke, P. Haage, G.B. Adam, P. Jung, G. Jakse, R.W. Günther; *Aachen/DE*

Objective: To compare the value of different gadolinium-enhanced T1-weighted gradient-echo techniques for excretory MR urography.

Methods: MR urography was performed in 74 patients using various T1-weighted gradient-echo (GRE) sequences after injection of gadolinium-DTPA and low-dose furosemide. Examinations included conventional GRE sequences and echo-planar imaging (GRE-EPI), both of which were acquired using 3D data sets and 2D projection images. Breath-hold imaging was preferred.

Results: Complete MR urograms were obtained in 20 – 30 s using the conventional 3D GRE technique and in 14 – 20 s with 3D GRE-EPI sequences. Ghost artefacts caused by peristalsis of the ureters were frequently observed on conventional 3D GRE images and were almost entirely suppressed in GRE-EPI sequences. Susceptibility effects were more often visible on GRE-EPI MR urograms, which explained that calculi measured up to 20 % greater in diameter (mean: 10 %) than compared with conventional GRE sequences. The use of increased spatial resolution degraded the image quality only on GRE-EPI images. In projection MR urography, the entire upper urinary tract could be imaged without any postprocessing by acquisition of a fast single slice sequence. In projection imaging, the contrast-enhanced urinary tract morphology was more accurately visualized using the conventional 2D GRE sequence, which was significantly superior to the GRE-EPI technique.

Conclusion: Fast 3D GRE-EPI sequences improve the clinical practicability of excretory MR urography especially in old or critically ill patients who are unable to hold their breath for more than 20 s. The conventional GRE technique is superior in high-resolution detail MR urograms and in 2D projection imaging.

B-0257 15:20

Gd-BOPTA-enhanced excretory MR urography without application of diuretics

T. Allkemper, B. Tombach, W. Heindel; *Münster/DE*

Purpose: To evaluate the feasibility and clinical utility of Gd-BOPTA enhanced excretory magnetic resonance urography without additional application of diuretics in correlation with conventional urography.

Method: 15 preoperative patients with pelvic tumors were examined at 1.5 T using a breath-hold high-resolution 3D-FLASH sequence during first-pass as well as 5, 10, 15 min after iv. injection of 0.05 mmol/kg BW Gd-BOPTA (MultiHance®) without application of diuretics. Post-processed coronal and multiplanar MIP reconstructions were compared to conventional excretory urography with regard to morphologic accuracy, anatomic variability, filling defects, cause and level of obstruction or compression, tumor visibility, and time-effectiveness by two independent radiologists.

Results: Visualization of the urinary tract by MRU was comparable to conventional excretory urography in 14 of 15 cases. Caliceal fornices were better delineated on conventional urographies, whereas MRU was considered superior in the assessment of the inferior ureter sections, the urinary bladder and the extent of obstructive tumors. Examination times of both techniques were comparable.

Conclusion: The diagnostic value of non-diuretic Gd-BOPTA enhanced MRU is comparable to conventional excretory urography in preoperative assessment of pelvic tumors. Further improvements of this technique are expected by optimization of examination intervals and injection doses.

14:00–15:30 Room P

Vascular

SS 315

Ultrasound/Vascular wall

Chairpersons:
J.-M. Bigot (Paris/FR)
P. Landwehr (Hannover/DE)

B-0258 14:00

False aneurysms in drug addicts: Ultrasonic appearances

R. Mithalal IV, A. Garg sr., V. Chowdhury sr., A.K. Sarda sr.; *New Delhi/IN*

Purpose: To evaluate pulsatile masses of the thigh in intravenous drug abusers using high-resolution ultrasound (HRS), colour Doppler flow imaging (CDFI) and duplex Doppler.
Material and methods: Twenty patients who developed pulsatile masses in the thigh after administration of intravenous drugs were evaluated to assess the extent, nature and character of the masses.
Results: On HRS twelve masses were found to be anechoic, poorly defined lesions with echogenic walls and presence of swirling flow within them. The presence of red-blue hue on CDFI & To and fro sign on duplex Doppler confirmed these lesions to be false aneurysms. There was associated perilesional heteroechogenicity and comet tail shadowing due to the presence of focal abscess around the mass in 9 patients. This observation of ours is described as the DIRTY CYST sign which was not seen in cases of false aneurysms due to trauma or vascular catheterisation. Two patients had associated arteriovenous fistula. Eight patients had hyperechoic masses in the thigh with no discernible flow within it suggesting them to be haematoma.
Conclusion: The presence of red-blue hue with DIRTY CYST sign is a sensitive and accurate observation seen in patients of false aneurysms secondary to drug abuse.

B-0259 14:10

Role of color Doppler in the diagnosis of superior mesenteric artery ischemia

G. Moggio, A. Bencivenga, A. Mazzacca, G. Belfiore; *Caserta/IT*

Purpose: To assess sensitivity, specificity and diagnostic accuracy of EcoColorDoppler (ECD) in the diagnosis of acute and chronic superior mesenteric artery (SMA) ischemia.
Materials and methods: 73 patients (43 M/30 F, age range: 50 – 87 years) were admitted to our hospital with symptoms of small bowel ischemia, showing a clinical picture of acute (25 cases) or chronic (44 cases) ischemia. All patients underwent ECD examination of abdominal aorta and SMA, and, subsequently, digital subtraction aortography (DSA). Significant (> 70 %) SMA stenosis was considered critical with maximal velocity (Vmax) exceeding 220 cm/s, diastolic velocity (Vdias) exceeding 30 cm/s, and resistivity index (RI) exceeding 0.9.
Results: Sensitivity, specificity and diagnostic accuracy of ECD were 43 %, 100 % and 48 %, respectively, for acute SMA ischemia, and 92 %, 100 % and 97 % for the chronic cases. Positive and negative predictive values were 100 % and 13 %, respectively for the acute form, and 100 % and 62 % for the chronic form.
Conclusions: The high diagnostic accuracy of ECD in the diagnosis of chronic small bowel ischemia makes it the first-choice exam, when spiral CT is not available, thereby reducing the unnecessary utilization of DSA. Conversely, in our experience, a negative ECD examination in a suspect acute SMA ischemia should not prevent subsequent DSA.

B-0260 14:20

Imaging intraarterial hepatic port catheter systems by Power-Doppler using contrast media

R. Puls, N. Hosten, R. Felix; *Berlin/DE*

Purpose: This study was designed to determine whether intraarterial hepatic port catheter systems can be adequately detected by contrast-enhanced Power-Doppler.
Method: 15 patients with a liver port system were investigated before chemotherapy. Examinations were performed with short bolus-injections of the contrast media Levovist® in addition to angiographic imaging.
Results: Liver port systems were easily detected by contrast-enhanced Power Doppler method. In 11 out of 15 patients a correct flow of the contrast medium via port system was seen with both modalities. One partially occluded hepatic artery was not identified by Power Doppler despite correct flow of the contrast fluid. In one of three patients showing an incorrect flow of the contrast medium the blood circulated primarily through the splenic artery due to a dislocation of the catheter tip. Circulation through both the hepatic and splenic arteries was shown in a second patient and an occluded right hepatic artery was demonstrated in a third. All these findings were observed with both modalities.
Conclusion: Power-Doppler provides a reliable image the port catheter system. This method can be used as a follow-up-procedure to determine the state of the arterial hepatic circulation during chemotherapy.

B-0261 14:30

Quantification of intima-medial reflectivity to improve the descriminatory value of measuring common carotid artery intima-medial thickness for the assessment of atherosclerotic risk

P.S. Sidhu, S.M. Ellis, R.P. Naoumova, C.K. Neuwirth, R. Eckersley, D.O. Cosgrove; *London/GB*

Purpose: To quantify the intima-medial reflectivity (IMR) of the common carotid arterial wall as a means of improving the discriminatory value of measuring intima-medial thickness (IMT) in the assessment of risk of atherosclerotic disease.
Method/materials: Both common carotid arteries of 30 subjects with familial hypercholesterolaemia and 30 age matched controls were scanned using a 12 – 5 MHz linear array probe on an ATL HDI5000 ultrasound machine. Images with the arterial wall orientated parallel to the probe surface were analysed using 'HDI lab' a program designed to analyse raw ultrasound data. An IMR index (IMRI) was calculated as a ratio of the sub-intimal reflectivity 0.23 mm from the intima-medial interface (IMI) to the reflectivity at the IMI averaged over an 8 mm section of arterial wall within 1.5 cm of the carotid bulb. IMRI and IMT values of 0.69 and 0.75 mm were taken as the upper limit of normal. IMT values alone and IMT plus IMRI values separated the hypercholesterolaemic subjects into higher and lower risk groups based on cholesterol years score, an accepted measure of atherosclerotic risk. ($p = 0.0020$ for IMT alone and $p = 0.0015$ for IMT and IMR). In the control group 8 subjects had IMTs > 0.75 mm, high risk, but normal IMRI values identifying them as lower risk if both IMT and IMRI are considered
Conclusions: Results indicate that measurement of both IMT and IMRI is superior to measuring IMT alone when assessing changes in the IML with regard to atherosclerotic risk.

B-0262 14:40

High resolution 3T MR microscopy imaging of arterial walls and atherosclerotic plaques

J. Sailer, A. Berg, I. Sulzbacher, T. Hölzenbein, J. Lammer, T. Rand; *Vienna/AT*

Purpose: To achieve high resolution MR microscopic images of the inner structure of arteriosclerotic femoral arteries using a dedicated microscopic coil device and to compare the findings with those of histological images.
Method/materials: T2 weighted images (TR/TE: 3470 ms/30 ms) of the common femoral artery were obtained in 6 specimens using a 3 T MR unit (Medspec 30/80 Avance) in combination with a dedicated MR-microscopy system. Field of view (FOV) 1.2 cm, slice thickness 600 mm. Volume measurement and classification of intimal proliferations, thickness and morphology of the arterial walls was evaluated and compared with histological results. MR-measurement of the arterial tissue was undertaken directly after surgical sampling, followed by histological examination.
Results: We found significant correlation between MR images and histology for the morphology and extension of intimal proliferations and arterial wall components. We were able to differentiate fibrous and calcificated from lipid plaque components with different signal intensity. Furthermore we achieved high resolution in imaging of the arterial wall layers.
Conclusions: High resolution high field MR imaging of arterial walls may demonstrate morphological features as well as exact volume and extent of intimal proliferations. MR-microscopy allows visualization of arterial structure in vitro. Perspectives for in vivo application include differentiation of hard and soft plaques, decisive for further interventional or surgical strategy.

B-0263 14:45

Quantification of atherosclerosis with MRI and image processing in animal models

M. Hänni[1], H. Edvardsson[1], K. Pettersson[2], Ö. Smedby[3]; *[1]Uppsala/SE, [2]Mölndal/SE, [3]Linköping/SE*

Purpose: The aim was to find a non-invasive, reliable and quantitative method to assess atherosclerosis in vivo.

Material and methods: The abdominal aortas of 10 New Zealand White rabbits, fed with cholesterol-enriched diet for 12 weeks, and 6 spontanoeously atherosclerotic, Watanabe rabbits were investigated in a Philips ACS-NT 1.5 T scanner, using a knee coil. Two transverse sequences were performed; a 2D inflow angio (TOF) sequence and a proton-density-weighted (PDW) spin echo sequence. Using an active contour algorithm (gradient Vector Flow snakes) we identified the outer border and the inner border of the vessel wall in the PDW images and the angio images respectively and computed the vessel wall thickness. This was later compared with histopathology and serumcholesterol levels.
Results: For Watanabe rabbits the MRI-assessed wall thickness correlated well with histological intima-media thickness ($r = 0.884$). For cholesterol-fed rabbits, there were no correlations between MRI-assessed wall thickness, histopathology and serumcholesterol levels.
Conclusions: The proposed non-invasive method, combining MRI with modern image processing techniques, gave result in close agreement with histopathology when applied to spontaneously atherosclerotic rabbits. In our cholesterol-fed group, the amount of atherosclerosis was probably too small to be detected by either MRI or histopathology. The method may prove useful, in particular in future evaluations of new treatments, where animals are to be followed longitudinally.

B-0264 14:55

The effect of acute drop in estrogen level on the vessel wall: Evaluation with color Doppler ultrasound

I. Mihmanli, V. Mihmanli, S. Kurugoglu, G. Ogut, O. Cokyuksel; *Istanbul/TR*

Purpose: The aim of this study is to investigate the effect of acute drop in estrogen level on endothelium by color Doppler ultrasound (CDUS) in women with surgically induced menopause.
Material and methods: Forty women, aged 37 to 45 years were examined on 3rd preoperative and 7th postoperative day. All patients went through total abdominal hysterectomy and bilateral salpingo-oopherectomy. Aged matched healthy control group comprising of 15 women was also studied. Brachial artery was examined by CDUS. Peak systolic velocity, end-diastolic velocity, mean velocity, brachial artery diameter and volume flow were calculated.
After the baseline measurements, hyperemia was induced through the inflation of a blood pressure cuff to suprasystolic pressures for 5 minutes on the upper arm. To evaluate endothelium-dependent vasodilation, the brachial artery was viewed after the cuff was deflated and removed from the arm. The difference between the baseline and maximum value after the cuff deflation was calculated for each CDUS parameter.
Results: A significant difference was found between the serum estradiol levels during pre- and post-operative periods. No significant difference was found for serum estradiol levels between preoperative period and control subjects. Net changes found within each group during reactive hyperemia were statistically significant. However, no siginificant difference was found in values among pre, post-operative and control subjects.
Conclusion: Our study shows that acute drop in estrogen level does not seem to have tremendous effect on endothelium. We do believe that there is a lot to understand in the mechanism of effect of estrogen on vascular function.

B-0265 15:05

In-vivo carotid B-mode ultrasound compared with pathologic findings: Intima-media thickening, lumen diameter and cross-sectional area

G. Schulte-Altedorneburg[1], D.W. Droste[2], S. Felszeghy[3], V. Popa[3], K. Hegedüs[3], E.B. Ringelstein[2], L. Csiba[3]; *[1]Augsburg/DE, [2]Münster/DE, [3]Debrecen/HU*

Background: We wanted to determine the correlation of in-vivo transcutaneous B-mode ultrasound measurements of intima media thickening (IMT), lumen diameter and cross-sectional area of the common carotid area (CCA) with corresponding measurements obtained by gross pathology and histology.
Methods: Sixty-six moribund neurological patients (mean age 71 years) underwent B-mode ultrasound of the CCA a few days before death. During autopsy, carotid specimens were removed in toto. Carotids were ligated and cannulated for injection of an hydrophilic embedding material under standardised conditions. The carotid bifurcation was frozen and was cut manually in 3 mm cross slices. From the slices we performed planimetric analysis of the CCA's anatomic diameter and of the cross-sectional area. IMT was assessed by light microscope. Ultrasonic measurements and planimetric data were compared.
Results: Mean ultrasound measurements of lumen diameter and cross-sectional area were 7.13 ± 1.27 mm and 0.496 ± 0.167 cm^2 by ultrasound, and 7.81 ± 1.27 mm and 0.516 ± 0.194 cm^2 by planimetric analysis of the unfixed redistended carotids (correlation coefficients 0.623 and 0.705, both $p < 0.0001$). The mean IMT by ultrasound was 1.005 ± 0.267 mm and 0.67 ± 0.141 histologically, resulting in a difference of -31 % ($p < 0.001$), presumably due to shrinkage of the histological section.
Conclusion: Transcutaneous B-mode ultrasound provides a reliable approach for in-vivo measurements of the lumen diameter and the cross-sectional area and, less exactly, of the IMT of the CCA.

B-0266 15:15

Ultrasound detection of endothelial dysfunction used to diagnose vascular disease in patients with insulin resistance

M. O'Dowd, M.E. Hurley, C. Markham, D. McInerney, V. Maher; *Dublin/IE*

Purpose: The insulin resistance syndrome is strongly associated with cardiovascular disease. A simple, non-invasive test to detect early vascular disease in this condition would be of clinical value. This study examines the use of ultrasound in assessment of endothelial dysfunction.
Methods and materials: Ten patients with insulin resistance syndrome and ten control subjects were assessed noninvasively using high resolution ultrasound. Vessel diameter, flow velocity and resistive index in the brachial artery were measured at rest and in response to glyceryl trinitrate (GTN) and induced limb hyperaemia. Intima-media thickness of the carotid artery was also examined. Two-sample t tests were used to compare both groups. Descriptive statistics are expressed as mean and standard error and statistical significance is taken as $p < 0.05$.
Results: No significant difference was shown in response to GTN between the two groups. There was however a significant difference shown in induced hyperaemia response.
Conclusions: Ultrasound is capable of demonstrating early endothelial dysfunction in patients with features of insulin resistance. It may be used as a screening test for endothelial dysfunction in these patients as it can indicate the need for early treatment.

B-0267 15:25

Colour Doppler ultrasound of the nailbed: An objective tool for monitoring responses to vasodilatory treatment of connective tissue disorders?

M. Keberle, M. Jenett, C. Keßler, D. Hahn; *Würzburg/DE*

Purpose: Previously (ECR 1999), we have demonstrated that colour Doppler ultrasound (CDU) of the nailbed allows to assess microvascular changes in connective tissue disorders (CTD). Here, we applied this method to monitor the microvascular response to vasodilatory treatment.
Methods and materials: 13 symptomatic patients were treated with iloprost, a stable prostacyclin analogue. CDU (12 MHz Multi-D-array) was performed before and after treatment. The respective vascularities were quantified computer-aided and compared with the patients' subjective symptoms and the clinical status.
Results: CDU revealed that mean vascularities at baseline temperature ($P < 0.01$), after a cold ($P < 0.01$), and after a warm ($P < 0.05$) challenge significantly increased following iloprost treatment. Moreover, follow-up CDU-results correlated well with the patients' clinical responses to vasodilatory therapy ($P < 0.01$).
Conclusion: CDU holds promise to provide an objective tool for monitoring the effects of vasodilatory treatment in patients with CTD.

16:00–17:30 **Room P**

Vascular

SS 415

Veins

Chairpersons:
C. Rabbia (Turin/IT)
T. Schmitz-Rode (Aachen/DE)

B-0268 16:00

Anatomical variations of the deep venous system of the leg: Review of 624 venograms and implications for ultrasound assessment

P.S. Sidhu, R. Alikhan, D.J. Quinlan, P. Gishen; *London/GB*

Purpose: To exclude presence of thrombus on ultrasound (US), important anatomical variations need to be considered. We describe these variations as seen on contrast venography.
Method: Two pairs of observers familiar with venous contrast studies performed a retrospective review of 624 lower limb venograms. The venograms were evaluated for the presence, position and frequency of variations in the major lower limb veins.

Results: Two vessels were seen in the popliteal fossa in 251 (40 %) of 624 venograms, only 32 (5 %) were true duplicated popliteal veins. A duplicated superficial femoral vein (SFV), comprising of either a long or short segment of paired venous structure was present in 189 (30 %) with 12 (2 %) systems more complex. Of the 189 duplicated SFV 102 (54 %) began in the mid-thigh region and 61 (32 %) in the adductor canal region. The duplicated vessel was medial to main SFV in 97 (49 %) and lateral in 92 (51 %). Range of length of duplicated SFV was 1 – 35 cm, most common length 10 – 20 cm in 116 (61 %). There was no difference in the incidence of anatomical variations between genders or presence of multiple vessels in one leg and probability of occurrence in other leg.
Conclusion: Variations in lower limb venous anatomy are more common than previously thought. When performing US for the diagnosis of DVT it is important to look for two vessels in the popliteal fossa, and for a duplicated SFV, starting at the adductor canal and extending to the mid-thigh looking both medial and lateral of the main SFV.

B-0269 16:10

High resolution B-mode and power Doppler ultrasound: Useful diagnostic tools in the differential diagnosis of deep vein thrombosis

I.M. Barber jr., E.A. Gallardo sr., M.H. Martínez jr., N.G. Roson sr., X.C. Serres sr., X.C. Pruna sr.; *Granollers/ES*

Purpose: To describe pathologic entities that simulate deep venous thrombosis (DVT) and can be diagnosed by HRUS and Power Doppler (PD).
Methods and material: 363 patients with clinical DVT suspicious were evaluated with b-mode, CD and PD ultrasound in two years. Femoral, popliteal and tibioperoneal veins of the symptomatic leg were studied with multifrequency 7 – 9 and 10 – 13 MHz of a GE Logiq 700MR (Milwaukee, USA) linear probes.
Results: In 219 cases (60 %) DVT was not depicted. Subcutaneous fat cellulitis with or without superficial thrombophlebitis, complicated Baker cyst or venous insufficiency were demonstrated in 93 patients (42 %). In 14 patients (7 %) musculoskeletal pathology as fibrillar rupture, slackening of a knee prosthesis tibial sprout, infected hematoma, septic arthritis, osteomyleitis and bone and soft tissues tumorous pathology was settled. We also found arterial diseases in five cases (popliteal aneurysm and arteriovenous fistula).
Conclusion: A broad spectrum of disorders may clinically simulate DVT. HRUS and PD in addition to CD study are useful diagnostic tools in this entities.

B-0270 16:20

Thrombosis of the calf muscle veins: Frequency of isolated occurrence and the risk of pulmonary embolism: Evaluation with color Doppler sonography

T. Rettenbacher[1], A. Hollerweger[2], P. Macheiner[2], N. Gritzmann[2]; *[1]Innsbruck/AT, [2]Salzburg/AT*

Purpose: To determine the frequency of an isolated thrombosis of the calf veins or calf muscle veins. To evaluate the risk of pulmonary embolism with regard to the location of venous thrombosis of the lower extremities.
Materials and methods: In this study 357 consecutive adult patients (230 women, 127 men; age range: 17 – 94 years; mean age: 67 years) underwent a prospectively performed color Doppler sonographic examination of the deep veins of the lower extremities. Additional examinations for pulmonary embolism were performed in 184 of the patients.
Results: In 179 patients color Doppler sonography revealed a deep venous thrombosis of the lower extremities. The most common locations of thrombosis included the soleal muscle veins (n = 88), peroneal veins (n = 84), popliteal vein (n = 69), superficial femoral vein (n = 53), and the gastrocnemial muscle veins (n = 49). An isolated thrombosis of the calf veins was demonstrated in 47 % of patients (n = 85) and an isolated thrombosis of the calf muscle veins was shown in 25 % of patients (n = 45). The frequency of pulmonary embolism in patients with thrombosis of the lower extremities was 60 % (67/112), in patients with isolated thrombosis of the calf veins 48 % (26/54), and in patients with isolated thrombosis of calf muscle veins 50 % (16/32).
Conclusion: An isolated thrombosis of the calf veins or calf muscle veins occurs often and is frequently the source of pulmonary embolism. The calf veins and calf muscle veins should, therefore, always be investigated in patients submitted for the detection of deep venous thrombosis of the lower extremities.

B-0271 16:30

Detection of deep venous thrombosis (DVT) using multislice CT scans

M.A. Kessler, U.J. Schöpf, R.D. Brüning, M.F. Reiser; *Munich/DE*

Purpose of this study was to develop a method that allows to screen pulmonary embolism (PE) and deep venous thrombosis (DVT) in one image acquisition using multislice CT. Intravascular attenuation of contrast media, coincidence of PE and DVT and relevant additional or alternative findings were investigated. 45 Patients were scanned with Multislice CT (Siemens VolumeZoom). The chest was acquired with 0.5 s rotation time, 4 × 1 mm collimation, 180 mAs and pitch of 7. 120 ml Accupaque were injected at 4 cc/s with an empiric delay of 16 s. The deep venous system was acquired with 4 × 5 mm collimation, 180 mAs and pitch of 7 with a total delay of 150, 180 and 210 s (n = 15 in each group). Hounsfield units were measured in the popliteal, femoral, iliacal, and inferior vena cava in order to determine the density of contrast media depending on the used delay time. Additional or alternative pathological findings were recorded.
Results: PE was diagnosed in 15 patients. Four of these showed synchronous deeep venous thrombosis. Four patients showed DVT without PE. 6 Patients showed cystic or benign tumors. In three patients previously unknown malignant tumors or metastases were found. The mean contrast attenuation in the deep venous system was 104 with 150 s delay, 93 with 180 s delay, and 92 with 210 s delay.
Conclusion: Multislice CT is a valid modality to assess the entire scope of the clinical entity of venous thromboembolic disease. Valuable additional clinical information can be obtained in patients with suspected PE. The optimal delay time for performing scans of the deep venous venous system is 150 s for most patients.

B-0272

withdrawn by author

B-0273 16:40

Correlation between D-Dimer measurement and deep venous thrombosis assessed by ultrasound

I.M. Barber jr., E.A. Gallardo sr., N. Lopez sr., M.H. Martínez jr., F.E. Vilar sr., X.C. Pruna sr.; *Granollers/ES*

Purpose: The D-dimer (DD) is a specific degradation product of crosslinked fibrin. DD measurement in plasma is highly sensitive (but non-specific) to the presence of deep venous thrombosis (DVT) and/or pulmonary embolism (PE). The aim of our study is to establish the correlation between DD levels in plasma and the extension of DVT assessed by HRUS.
Methods and material: 66 patients were evaluated during the last 6 months. All patients had clinical suspicion of DVT and/or PE. Quantitative D-Dimer (ELISA technique) and B-mode and Colour Doppler ultrasonography (7 – 10 MHz linear probe) were performed the same day. Patients were divided in the following groups: (1) No DVT, (2) No DVT but superficial thrombosis, (3) DVT affecting tibioperoneal trunks and popliteal vein, (4) Complete DVT (including femoral veins). Average DD in each group was calculated and differences assessed with Student's t test.
Results: 28 patients were included in group 1 with an average DD of 845 ng/ml. Group 2: 8 patients, DD 594. Group 3: 10 patients, DD 2198. Group 4: 17 patients, DD 1561. Differences between groups 1 and 3 and between 2 and 3 were significant ($p < 0.005$). There was no significant difference between groups 3 and 4.
Conclusion: There is a significant difference in plasma DD levels when DVT is present. In this preliminary results there seems to be no correlation between the value of DD and the DVT extension. Exclusion of patients with concomitant diseases may be necessary because of the high rate of DD false positive results.

B-0274 16:45

Colour Doppler ultrasound assessment of stenosis in well-functioning arteriovenous fistulae for haemodialysis access

R. Pietura, M. Szajner, M. Szczerbo-Trojanowska; *Lublin/PL*

Well-functioning arteriovenous fistula is essential for the maintenance of haemodialysis in patients with chronic renal failure. Most causes of fistula failure are the results of stenosis leading to thrombosis.
Purpose: Limited data are available with regard to the well-functioning arteriovenous fistulae. The present study was conducted on completely asymptomatic arteriovenous fistulae to assess stenosis frequently in correct fistula.
Materials and methods: We studied 139 patients ranged in age from 19 to 79 years (mean 46.7 years) with end-stage renal disease receiving maintenance haemodialysis through 131 (94.2 %) arteriovenous fistulae and 8 (5.8 %) access grafts.

Results: Stenosis was detected in 89 (64 %) fistulae (one in 75 patient and two stenoses in 14 patients). 57 % stenoses were located in the anastomotic region (segment within 5 cm of the efferent vein close to anastomosis. 9 (10 %) stenoses were situated at the arterial anastomosis of graft, 17 (19 %) were located beside the aneurysm, and 14 % stenoses were in the remaining region of efferent vein. Mean maximum velocity in stenosis was 4.35 m/s, but accurate determination of this measurement was not possible because the maximum velocity has exceeded the upper limit of the scale. Perivascular colour artefacts were present at stenosis site of 60 (94 %) fistulae and were caused by perivascular vibration due to blood flow hitting the stenosis. There was no correlation between stenosis and fistula age. Central veins were not control because of limits of ultrasound examination.
Conclusions: We do conclude that stenosis is very frequent in well-functioning fistula.

B-0275 16:50

DOTA gadolinium as a contrast agent for upper extremity fistulography: Diagnosis and therapy

M. Tassart, A. Le Blanche, M. Bazot, O. Geoffroy, F. Boudghène, J. Bigot; *Paris/FR*

Purpose: Experience of DOTA gadolinium used as a contrast agent for fistulography in patients with contraindication to iodinated contrast agent (ICA).
Materials and methods: Between April 1998 and March 2000, 22 patients (16 F/ 6 M) with native dysfunctioning fistulas (17 humero-cephalic, 3 radio-cephalic, 2 humero-basilic), were referred with contraindication to ICA: Immature fistula not yet hemodialysed (14), allergy (4) or residual diuresis (4). Digital subtraction fistulography (Multistar top Siemens) was performed with 35 ml DOTA gadolinium. Clinical and renal tolerance was evaluated. Image quality of opacification (good, moderate or insufficient) of the veins was rated by 2 experienced angiographers.
Results: Correct imaging of anastomosis was obtained in only 45 % of cases but imaging was completed on MRA when necessary. The quality of upper extremity venograms was sufficient in all cases and superior vena cava in 82 %. 3 occlusions (1 on the innominate vein), 12 stenoses (cephalic vein and sub clavian vein), 1 anastomotic and 1 arterial stenosis were diagnosed. 5 cases were considered normal. No pain and no renal degradation in this high risk population were noticed. 2 interventional efficient procedures were performed.
Conclusion: Digital substracted fistulography using DOTA gadolinium as contrast agent is recommended in non hemodialysed patients with severe renal failure and dysfunctioning fistula and also when an interventional procedure is required.

B-0276 17:00

Thoracic outlet venous compression during postural manoeuvre: Prevalence in asymptomatic subjects on spiral CT venograms

I. Mastora, P. Masson, V. Delannoy, A. Duhamel, J. Rémy, M. Rémy-Jardin; *Lille/FR*

Purpose: To determine the prevalence of dynamically-induced thoracic outlet venous compression on spiral CT venograms (SCTV).
Materials and methods: 43 subjects referred for suspicion of unilateral thoracic outlet venous compression were prospectively evaluated with dynamic SCTV (3 mm collimation; pitch: 1; 4 – 6 % contrast agent; 4 ml/s). Functional anatomy of the asymptomatic side was evaluated on contiguous saggital reformations and 3D reconstructions generated from data sets acquired in the neutral position and after postural maneuver.
Results: In the neutral position, venous stenosis was depicted at the level of the prescalenic space in 4 cases (9 %) (> 50 %: 3/4), in the costoclavicular space in 13 cases (30 %) (< 50 %: 7/13) and in the subcoracoid tunnel in 4 cases (11 %) (> 50 %: 3/4). After postural maneuver, venous compression was found in 35 cases (81 %) in the prescalenic space (> 50 %: 21/35), in 39 cases (91 %) (> 50 %: 29/39) in the costoclavicular space and in 8 cases (19 %) (> 50 %: 5/8) in the subcoracoid tunnel in the absence of abnormal narrowness of these anatomical compartments. Postural maneuver induced significant reduction in the surfaces of the largest and smallest segments of the veins in each anatomical compartment with a mean reduction in the venous surface of 31 % in the prescalenic space, 62 % in the costoclavicular space and 76 % in the subcoracoid tunnel.
Conclusion: Venous stenosis is a frequent finding on dynamic SCTV of the thoracic outlet in asymptomatic subjects.

B-0277 17:10

Breath-hold 3D contrast-enhanced MR angiography of the portal venous system

E. Squillaci, G. Sodani, E. Fanucci, S. Masala, C. Mazzoleni, C. Pistolese, G. Simonetti; *Rome/IT*

Purpose: To evaluate the use of breath hold dynamic contrast-enhanced (CE) 3D MR Angiography (MRA) in the portal venous system.
Methods and materials: 30 patients with liver cirrhosis and portal hypertension were studied using MRA with a1.5 T magnet (NT15 Philips). Three breathold acquisitions (12 seconds each) were performed before, 30 and 50 s. after gadolinium injection (0.2 mmol/kg). Image evaluation included the source images, MIP and target MIP and subtraction images. The visibility of the normal and abnormal portal venous system was ranked on the scale from 1 (poor) – 4 (excellent) by 2 radiologists. The standard of reference was DSA.
Results: There was a complete agreement between MRA and DSA demonstrating SMA, SA and PV. Detectability of portosystemic collaterals was excellent in 21/30 patients, good in 5. No collaterals were evident in 4 patients. MRA correctly depicted thrombosis of the SMV (n = 3), of the splenic (n = 2) and portal vein (n = 5). In 2 patients with complete PV thrombosis a poor image quality was obtained due to complete absence of flow.
Conclusions: 3D dynamic gadolinium enhanced MRA is easy to performe with one contrast injection demonstrating the entire portal venous system. MRA gives excellent demonstration of normal anatomy and pathology.

B-0270 16:20

Thrombosis of the calf muscle veins: Frequency and the risk of pulmonary embolism. Evaluation with color Doppler sonography

T. Rettenbacher¹, A. Hollerweger², P. Macheiner², N. Gritzmann² ¹Innsbruck/AT, ²Salzburg/AT

Purpose: To determine the frequency of an isolated thrombosis of the calf veins or calf muscle veins. To evaluate the risk of pulmonary embolism with regard to the location of venous thrombosis of the lower extremities.

Materials and methods: In this study 357 consecutive patients (230 women, 127 men; age range: 17 – 94 years; mean age: 67 years) underwent a prospectively performed color Doppler sonographic examination of the deep veins of the lower extremities. Additional examinations for pulmonary embolism were performed in 184 of the patients.

Results: In 179 patients color Doppler sonography revealed a deep venous thrombosis of the lower extremities. The most common localizations of thrombosis included the soleal muscle veins (n = 68), peroneal veins (n = 64), popliteal vein (n = 59), superficial femoral vein (n = 53), and the gastrocnemial muscle veins (n = 49). An isolated thrombosis of the calf veins was demonstrated in 47 % of patients (n = 85) and an isolated thrombosis of the calf muscle veins was shown in 25 % of patients (n = 45). The frequency of pulmonary embolism in patients with thrombosis of the lower extremities was 60 % (67/112), in patients with isolated thrombosis of the calf veins 48 % (26/54), and in patients with isolated thrombosis of calf muscle veins 50 % (16/32).

Conclusion: An isolated thrombosis of the calf veins or calf muscle veins is often and is frequently the source of pulmonary embolism. The calf veins and calf muscle veins should, therefore, always be investigated in patients suspected for the detection of deep venous thrombosis of the lower extremities.

Saturday, March 3

	room A 2nd level	room B 2nd level	room C 2nd level	room E1 entr. level	room E2 entr. level	room F1 entr. level	room F2 entr. level	room G lower level	room H lower level	
08:30										08:30
09:00	**CC 516**	**SA 5**	**CC 517**	**RC 501**	**SF 5**	**RC 504**	**RC 511**	**WS 509a**	**WS 509b**	09:00
09:30										09:30
10:00										10:00
10:30										10:30
11:00	**CC 617**	**SS 610** **Musculoskeletal** Imaging of the hip-joint *(p. 160)*	**SS 601a** **Abdominal and Gastrointestinal** Liver: CT *(p. 161)*	Bracco Symposium 1	**SS 602** **Breast** Digital mammography (1) - Technique *(p. 163)*	**SS 604** **Chest** Chest imaging: Technical aspects and new developments *(p. 166)*	**SS 611** **Neuro** Functional MRI - Epilepsy *(p. 167)*	**SS 601b** **Abdominal and Gastrointestinal** CT/MR colonography *(p. 169)*	**SS 609a** **Interventional Radiology** Percutaneous tumor ablation *(p. 171)*	11:00
11:30										11:30
12:00										12:00
12:30	**HL 1**									12:30
13:00										13:00
13:30										13:30
14:00										14:00
14:30	**CC 716**	**SS 710** **Musculoskeletal** MRI of the foot and ankle *(p. 181)*	**SS 701** **Abdominal and Gastrointestinal** Pancreas *(p. 183)*	NICER Anniversary Symposium	**SS 702** **Breast** Digital mammography (2) *(p. 185)*	**SS 704** **Chest** Imaging and cardiopulmonary function *(p. 187)*	**SS 711** **Neuro** CNS infections - Demyelination/ Miscellaneous *(p. 189)*	**SS 705** **Computer Applications** Image processing and analysis *(p. 191)*	**SS 709a** **Interventional Radiology** Musculoskeletal intervention *(p. 193)*	15:00
15:30										15:30
16:00										16:00
16:30	**CC 816**	**RC 810**	**CC 817**	**SF 8**	**RC 802**	**RC 804**	**RC 808**	**RC 807**	**RC 806**	16:30
17:00										17:00
17:30										17:30

	room I lower level	room K lower level	room L/M 1st level	room N/O 1st level	room P lower level	room X entr. level	room Y 1st level	room Z lower level	
08:30								WS 19A	08:30
09:00	WS 518	RC 503	RC 508	RC 514					09:00
09:30								WS 19B1	09:30
10:00							WS 20A1		10:00
10:30	SS 601c Abdominal and Gastrointestinal Stomach *(p. 173)*	SS 609b Interventional Radiology Venous intervention and arterial access *(p. 175)*	SS 607 Genitourinary Obstetric imaging *(p. 177)*	SS 603 Cardiac Heart: CT *(p. 179)*		WS 19B2			10:30
11:00							WS 20A2		11:00
11:30									11:30
12:00					EFOMP Workshop		WS 20A3		12:00
12:30									12:30
13:00									13:00
13:30									13:30
14:00	SS 706 Contrast Media New trends (3) *(p. 194)*	SS 709b Interventional Radiology Hepatobiliary intervention *(p. 196)*	SS 708 Head and Neck Nose and paranasal sinuses *(p. 198)*	SS 707 Genitourinary Urinary bladder *(p. 200)*			WS 20B1		14:00
14:30						WS 19B3			14:30
15:00							WS 20B2		15:00
15:30									15:30
16:00							WS 20B3		16:00
16:30	WS 818	RC 803	RC 813	RC 814	SS 815 Vascular Carotid arteries *(p. 202)*				16:30
17:00									17:00
17:30									17:30

10:30–12:00 Room B

Musculoskeletal

SS 610

Imaging of the hip-joint

Chairpersons:
F.M. Sáez (Bilbao/ES)
D.J. Wilson (Oxford/GB)

B-0278 10:30

Three-dimensional CT reconstruction in the imaging of acetabular and pelvic fractures

A. Yotov, T. Deliversky; *Sofia/BG*

Purpose: To assay the relevance of 3D CT reconstruction in radiological assessment of problem pelvic and acetabular fractures.

Material and methods: For the period 1995 – 2000 3D reconstruction was performed in 86 patients with fractures of the acetabulum and pelvic ring. Plain radiographs and standard CT scan were obtained as well. There were 61 isolated acetabular fractures, 13 pevlic ring disruptions and 9 simultaneous acetabular-pelvic

Results: In 18 acetabular (26 %), 2 pelvic (15.3 %) and 5 combined (55 %) injuries additional lesions were detected after 3D reconstruction. In respect to acetabulum most of such features (N = 14, 23 %) were discovered in complex fracture patterns, in particular in anterior column/posterior hemitransversal and both column types. In 7 cases the preoperative planning was changed due to 3D findings. In pelvic ring fractures additional lesions revealed by 3D investigation did not affect the preliminary conclusions on fracture type and stability. In 4 of 5 combined injuries information obtained by 3D reconstruction concerned acetabular component. In all but one operatively treated fractures 3D information was proved during surgery.

Conclusion: 3D reconstruction is found to be of essential value in imaging of complex acetabular fractures and should be used routinely in evaluation of these injuries. Though in pelvic ring and simple acetabular fractures 3D imaging shows no considerable diagnostic advantages comparing to plain films and standard CT, it is helpful to clarify the stereometry of the injury and some fracture details and may be performed in selected cases.

B-0279 10:40

Painful syndromes of the hip with negative plain films: Diagnostic value of dynamic contrast enhanced MRI

G. Cerone, M. Caulo, A.V. Giordano, F. Iannessi, A. Barile, C. Masciocchi; *L'Aquila/IT*

Purpose: To verify the diagnostic potentialities of contrast-enhanced MRI in the evaluation of patients affected by painful syndrome of the hip with negative conventional plain film.

Methods and material: Twenty patients, with clinical evidence of hip pain and normal conventional radiographic examination, were studied by standard and contrast-enhanced MRI. Standard MRI was performed on 1.5 T unit using SE T1w and FSE T2w (with and without fat saturation) sequences. After i.v. injection of Gd-DTPA, SE T1w sequences, with and without fat saturation, on axial and coronal planes, were performed. In 6 cases a quantitative analysis of femoral head signal intensity, before and after contrast medium (c.m.) administration, was obtained. MRI follow-up of the lesions was performed in 16 patients after two months.

Results: At the first control, standard MRI showed in all cases anomalous signal intensity of the femoral head, related to bone marrow edema syndrome (BMES). After c.m. administration a homogeneous, diffuse enhancement, with normalization of signal intensity, in account of the presence of active vascularization, was observed in 17/20 cases; in the remaining 3 cases the persistence of small areas of low signal intensity after c.m. administration, related to an early process of bone necrosis, was evident. The follow-up confirmed the necrotic evolution of these last 3 cases and the recovery of the bone marrow edema in the other cases.

Conclusion: We propose the use of i.v. contrast medium in early differentiating small necrotic bone areas superimposed on BMES, when the conventional plain film is still negative.

B-0280 10:50

Collar osteophytes: A cause of false positive bone scans for hip fractures

J.U.V. Monu, V. Chengazi, G. Seo, B. Armandi, F. Garcia-Morales, M. Oka; *Rochester, NY/US*

Purpose: Radionuclide bone scans are often used to confirm cases of suspected hip fractures where plain films are negative or equivocal. Reasons for a false negative scan are well documented. Less well documented are the causes for a false positive scan. The management of a hip fracture is frequently operative. A precise and accurate diagnosis is essential if only to avoid an unnecessary surgery.

Materials and methods: From our radiographic patient database we identified patients who had positive bone scans for hip fractures and who also had MR studies. Those patients who MR studies were negative for hip fractures form the population for this study. The images including bone scan, plain films, CT and MR images were reviewed and correlated. The clinical charts were reviewed for clinical outcome on follow-up.

Results: Five patients (3 women and 2 men) were identified whose bone scans were positive for hip fractures and MR images were negative for hip fractures or significant soft tissue injuries. Review of the plain films, CT and MR revealed a ring of osteophytes around the femoral neck. This collar of osteophytes around the femoral is seen as linear focus of increased radio nuclide uptake on both planar and SPECT images.

Conclusion: Collar osteophytes are a cause of false diagnosis of hip fractures on bone scans. The presence of osteophyte should prompt CT or MRI correlation in cases of occult hip fractures that are positive on bone scans.

B-0281 11:00

Pattern of injuries seen on MRI of patients examined for suspected hip fractures

M. Oka, G. Seo, B. Armandi, J.U.V. Monu; *Rochester, NY/US*

Purpose: MRI is often used to confirm the presence of hip fractures. Other unsuspected injuries are often found in these studies. This study documents the pattern of abnormalities seen on patients who had MR imaging for clinical suspicion of hip fractures and negative X-rays.

Methods: From our radiology and clinical records we identified patients who were examined for suspected hip fractures over a three-year period (1997 – 1999). Their images and clinical records were reviewed for history of trauma, presence of fractures, patterns, extent and distributions of soft tissue abnormalities. Fifty-three patients, 16 males and 37 females, aged 14 years to 98 years qualified for this study.

Results: Thirty-one patients (M:F = 11:20) had bone trauma either in the femur or in the ipsilateral innominate bone. No bone abnormality was found in 22 patients (M:F = 5:17). 51 % of the patients had joint effusions. Abnormal signal was seen in the obturator externus muscle in 34 % of cases. Other muscles including the adductor brevis (21 %), obturator internus (15 %), gluteus medius (15 %), adductor magnus (15 %) showed abnormal signal indicating edema. In 13 % of cases there was evidence of trauma to the gluteus maximus, gluteus medius and adductor longus. Other muscles including the quadratus femoris, pectineus and ilio-psoas suffered trauma with less frequency.

Conclusion: Occult fractures are found at a higher frequency in males. Soft tissue injuries are common in cases of suspected hip fractures. These injuries need to be identified and the patient treated to reduce morbidity and assure proper rehabilitation.

B-0282 11:10

Imaging of pipkin injuries of the femoral head

T. Deliversky, A. Yotov; *Sofia/BG*

Purpose: To evaluate the reliability of image techniques in diagnosis of femoral head fractures (Pipkin injuries).

Methods and materials: Fourteen patients with Pipkin fracture-dislocations of the femoral head were reviewed in order to determine the optimal image diagnostic modality. There were 3 grade I, 3 grade II, 1 grade III and 6 grade IV injuries according to Pipkin classification. In all cases plain radiographs and standard CT scan were performed. In 9 fractures 3D CT reconstruction has been done for confirmation and of the diagnosis. Six fractures were operated subsequently.

Results: Eight injuries were properly diagnosed after conventional radiographs. In two cases fractures of the posterior acetabular wall were missed on the plain films and were detect on CT scans. In 2 injuried hip joints the femoral head fractures were recognized only after 3D assessment, whereas previous image investigation missed to visualize the lesions. In another two without 3D reconstruction the operation revealed suprafoveal expansion of the fracture, wrongly estimated previously as grade I injuries.

Conclusions: The conventional radiographs detect the Pipkin injury in most cases, but are unable to determine the fracture details especially in type IV lesions. The standard CT scan is helpful mostly to confirm and verify the posterior wall acetabular fractures in type IV injuries, whereas in transverse femoral head fractures coinciding with scanning plan it is of less value. The 3D reconstruction reveals the maximum details of injury pattern and in author's opinion is most valuable method for imaging of Pipkin fracture-dislocations.

B-0283 11:20

MRI assessment of pediatric hips: Normal and osteochondrotic hip in early and late childhood

M. Mastantuono, P. Milella, E. Bassetti, A. Scala, L. Di Giorgio, A. Napoli, R. Passariello; *Rome/IT*

Purpose: There are few MRI studies investigating the features of the normal hip and of the osteochondrotic hip in early and late childhood.
Materials and methods: The MRI examinations were performed with a low field dedicated equipment (E-Scan Esaote Biomedica) and with other open low field MRI units. One case was studied with a high field MRI unit (Siemens Vision Plus 1.5 T) The normal hips were studied in children aged 34 months to 6 years (11 patients). 9 patients with a unilateral Perthes disease of the same age were studied (6 with Catteral's third and fourth type and 3 with first and second type).
Results: In normal hips MRI allowed an exact definition of the anatomic cephalic profiles, the maturation of the ephyseal nucleus and its exact site in the cartilaginous epiphyseal hemisphere. In the 9 patients with infantile osteochondrosis hip MRI showed the structural changes of the ephiphyseal nucleus, usually missed with conventional radiology, and a early identification of the abnormal area and the recognition of growing disk. MRI demonstrated the alterations of the epiphyseal nucleus and differentiated osteochondritic evolution from recession.
Discussion and conclusions: MRI permitted a clear evaluation of the normal and osteochondritic hip, in childhood, clearly defining the cephalocotyloid relations, delineating the real anatomic edges of the head and its structural composition and investigating the cartilaginous cephalic extension and the positioning of the ossific nucleus.

B-0284 11:30

Radiologic evaluation of developmental dysplasia of the hip (DDH) in relation to outcome

I.W. McCall, S. Patel, V.N. Cassar-Pullicino, G.A. Evans; *Oswestry/GB*

Purpose: To evaluate the labrum at arthrography with relation to treatment and outcome in patients with persistent lateralisation following conservative treatment.
Method: We retrospectively reviewed patients with DDH referred for hip arthrography for persistent lateralisation despite conservative treatment between 1980 – 1986. Arthrograms were classified as subluxed or dislocated and the labrum graded (1) Rosethorn, (2) Flattened, (3) Cushion, (4) Inverted. Follow-up radiographs werefassessed with a series of geometric measurements for treatment outcome.
Results: 90 hips were evaluated with follow-up of 4 – 18 years (mean 12.9). 35 hips were subluxed and 55 dislocated. 28 hips were grade 1, of which 27 were subluxed. 26 were treated conservatively. 27 hips were grade 2 with 21 dislocated and 6 subluxed. 18 required surgery, 6 open reduction and 12 open reduction followed by salter osteotomy (SO). 9 were treated conservatively. 12 hips were Grade 3, 11 were dislocated and 1 subluxed. 4 had open reduction and 8 were treated conservatively. None required a SO. 23 hips were grade 4 of which 22 were dislocated and 1 subluxed. 19 underwent immediate open reduction and 4 were treated conservatively 3 subsequently requiring open reduction one of which had avascular necrosis. 8 had SO. Follow-up showed no significant difference between the grades for Sharps angle (42.5 – 46.6), acetabular depth (17.6 – 19), lateral displacement (7.5 – 9.6), and femoral head contour 85 – 89 %.
Conclusion: Grade 3 labrum can be treated conservatively if the hip is reasonably stable in flexion/abduction with no significant inferior capsular constriction. Treatment aided by arthrography produced a uniform outcome for all grades.

B-0285 11:40

A CT based 3-Dimensional analysis of femur geometry in cases of slipped capital femoral epiphysis (SCFE)

J. Kordelle[1], T.C. Mamisch[2], M. Das[2], R. Kikinis[3], F. Jolesz[3], R.M.M. Seibel[2]; *[1]Giessen/DE, [2]Mülheim a. d. Ruhr/DE, [3]Boston, MA/US*

Purpose: The goal of the presented study was to investigate the relation between the proximal femur and the orientation of the epiphysis and, furthermore, to determine if the acetabular development is influenced by the femoral neck orientation or the epiphyseal alignment.
Material/methods: Three-dimensional reconstructed models based on CT data sets of 22 patients with thirty SCFE were reviewed. Measurement of the hip joint geometry was performed by using a newly developed interactive software to determine projected angles. A phantom scan was performed to validate the accuracy of the tool. Mean error in a total of 24 measurements was 0.76 (Std.Dev. 0.61). The determination of the mentioned angles was performed three times.
Results: We found a significant positive correlation between the femur version and the version of the femoral epiphysis (P: 0.02, R: 0.41). Furthermore, there was a highly significant positive interdependence between the shaft-neck-angle and the shaft-epiphysis-angle (P: 0.001, R: 0.6). No correlation was detected between the femoral version and the acetabular anteversion (P: 0.11) or between the shaft-neck-angle and the acetabular inclination (P: 0.48). In addition, there was no correlation between the epiphyseal orientation and the anteversion (P: 0.14) and inclination (P: 0.35) of the acetabulum.
Conclusion: The three-dimensional measurement of the hip geometry in cases of SCFE demonstrates a significant correlation between the femoral orientation and the epiphyseal alignment. A correlation between the orientation of the acetabulum and the femoral neck, as well as between the alignment of the acetabulum and the epiphysis could not be observed.

B-0286 11:50

Intertrochanteric corrective osteotomy with moderate and severe cases of slipped capital femur epiphysiolysis (SCFE) based on 3D reconstruction of CT data

T.C. Mamisch[1], J. Kordelle[2], M. Das[1], J. Richolt[3], R.M.M. Seibel[1], R. Kikinis[3]; *[1]Mülheim a. d. Ruhr/DE, [2]Giessen/DE, [3]Boston, MA/US*

Purpose: Are comparable results to be obtained regarding the postoperative improvement of range of motion with flexionsosteotomie alone, or is this achieved by three-dimensional corrective osteotomy after Southwick?
Material and methods: 16 patients after epiphysiolysis were analyzed. A computer program for simulation of movement and osteotomy developed by the authors, served for study execution. According to 3D-reconstruction of the computer tomography data the physiological range (limits of bone to bone or bone to cartilage contact) was determined by flexion, abduktion and internal rotation, similar to the I neutral-null-method. The three-dimensional osteotomy after Southwick was compared with the flexionsosteotomy after Griffith. Both intertrochanteric osteotomietechniques were simulated and the improvements of the movement range assessed, and compared. The correction angles were chosen according to technique described by Southwick.
Results: The average slipping and thus correction angles measured inferior 25.5° (range: 7.5 – 51.0°) and posterior 52.0° (range: 29.0 – 78.5°). After the simulation of osteotomy by Southwick the angle of flexion was 61.3° (improvement: 41.4°), of abduction 60.3° (+42.9°) and interior rotation of 70.1° (+52.6°). The flexionsosteotomy after Griffith achieved a flexion of 66.7° (+46.8°), an abduction of 41.1° (+23.7°) and an internal rotation of 57.4° (+40.0°).
Conclusion: The improvement of the free movement range after flexion osteotomy is generally comparable, with three-dimensional osteotomy after Southwick with the exception of the abduction angle.

10:30–12:00 **Room C**

Abdominal and Gastrointestinal

SS 601a

Liver: CT

Chairpersons:
T.K. Helmberger (Munich/DE)
O. Matsui (Kanazawa/JP)

B-0287 10:30

3D visualisation of liver vessel anatomy and liver segment volumetry in living related liver transplantation: Correlation with intraoperative findings

F.C. Caldarone[1], B.B.J. Frericks[1], G. Stamm[1], B. Nashan[1], A. Schenk[2], D. Selle[2], H.-O. Peitgen[2], M. Galanski[1]; *[1]Hannover/DE, [2]Bremen/DE*

Purpose: In living related liver transplantation accurate knowledge of vessel variants and exact calculation of liver segment volume is required. The results of a new visualisation and volumetry software tool (MeVis) were compared with intraoperative findings.
Material and methods: Biphasic helical CT was performed in 24 potential donors of liver segments. Based on the volume data set all hepatic vessels were segmented using a threshold based region-growing algorithm. Liver parenchyma was

isolated semi-automatically with the 'live wire' algorithm. Combination of the separated liver and portal vein system using the nearest neighbour approach led to a Couinaud oriented liver segmentation and volume calculation. 3D results were presented interactively and discussed in an indication round. Intraoperatively the liver vessel anatomy was documented and the resected liver parts were weighted. Pre- and intraoperative results were compared.

Results: Calculated mean liver volumes ± SD were: total 1640 ± 260 ml, right lobe 1100 ± 180 ml, left lobe 530 ± 100 ml, segments II and III 270 ± 80 ml. Variants of hepatic vessels were found for arteries in 4, liver veins in 8 and portal veins in 3 cases. 5 potential donors were excluded from transplantation because of inadequate segment volumes or vascular architecture. Calculated volumes showed a mean deviation of 5 % from intraoperative values. In all transplanted cases vessel anatomy matched the preoperative findings.

Conclusion: This new image processing and visualisation technique allows a non-invasive accurate preoperative donor selection and precise surgical planning resulting in a minimised risk for recipients and donors.

B-0288 10:40

Prevalence and diameter of hepatic hemangioma in liver cirrhosis: Comparison with non-cirrhotic patients

H.j. Noh, A. Shin, C.K. Park, K. Kim, B. Kim, S. Cha, Y. Kim, K. Chung, I. Cha; *Seoul/KR*

Purpose: We evaluated the prevalence and diameter of hepatic hemangioma in liver cirrhosis.

Material and methods: Abdominal CT reports of 25 586 patients, which were made during recent 5 years, were retrospectively evaluated for the presence of hepatic hemangioma. The CT diagnosis of hepatic hemangioma was made on characteristic spiral CT findings or in combination with MRI findings. In cirrhotic group, diameter of the hemangioma was compared on the initial and follow-up CT scans.

Results: On CT reports, liver was normal (non-cirrhotic) in 24 386 patients, and 1 200 patients were cirrhotic. Hepatic hemangiomas were found in 2 503 (10.3 %) normal group, and six hemangiomas in 5 (0.4 %) cirrhotic patients. Mean diameter of hemangioma in cirrhotic group was 35 mm on initial CT, and 22 mm on 4 years follow-up CT scans.

Conclusion: In liver cirrhosis, the prevalence and diameter of the hepatic hemangioma are reduced, probably from progressive liver parenchymal fibrosis.

B-0289 10:50

Role of contrast-enhanced helical CT in the assessment of acute hepatic vascular abnormalities

M. Scaglione, A. Pinto, R. Grassi, F. Pinto, E. De Lutio, C. Acampora, L. D'anna, A. Ragozzino, L. Romano; *Naples/IT*

Purpose: To assess the capabilities and the limitations of contrast-enhanced helical CT in the diagnostic work-up of patients with acute hepatic vascular abnormalities.

Materials and methods: Monophasic contrast-enhanced helical CT examination was performed in 81 selected patients with potential acute hepatic vascular disease. Scans were performed at 70 seconds after intravenous injection of nonionic contrast material (3 ml/s rate for a total of 130 ml) administrered by a CT-power injector. Results were compared with color flow sonography, angiography and surgery.

Results: CT evidence of hepatic vascular disease was confirmed in all the cases. The morphology, the density and the different attenuation values of the abnormal hepatic parenchyma and vessels allowed the CT diagnosis of spontaneous rupture of hepatic neoplasms (27 patients), portal vein thrombosis within the main branches (19 patients), Budd–Chiari syndrome (14 patients), infarction (10 patients), artery aneurysms and pseudoaneurisms (7 patients), HELLP syndrome (4). CT findings were confirmed by color flow sonography in all the patients, angiography in 17 and by surgery in 32 patients.

Conclusion: Contrast-enhanced helical CT is the imaging modality for assessing hepatic vascular abnormalities in the acute clinical setting. Although CT may identify areas of hemorrhage, it usually does not differentiate arterial from venous bleeding and the evolution of the bleeding itself.

B-0290 11:00

CT angiography of the portal vein and hepatic vein: Techniques and clinical applications

D. Wang, W.S. Zhang, J.X. Xu; *Beijing/CN*

Purpose: To evaluate the technique and clinical application of helical CT angiography (CTA) in the portal vein and hepatic vein.

Materials and methods: Helical CT was performed with different colli-m[illegible]on, pitch, delay time and scan direction in 60 normal subjects and 70 [illegible]h diseases of portal vein and hepatic veins. Maximum inten-sit[illegible]) and shaded surface display (SSD) CTA of portal vein and [illegible]ere processed. The results were compared with findings f[illegible]ction angiography (DSA) or surgery.

Results: Both the optimal portal vein [illegible] CTA could be obtained using collimation 3.0 mm, pitch 1.[illegible] 45 – 50 seconds with the scan direction from feet to head[illegible] specificity and accuracy of MIP and SSD CTA in detecting[illegible]and hepatic vein abnormalities were 93 %, 92 %, 93 % and[illegible] %. SSD image was useful in demonstrating the relationsh[illegible]portal vein and hepatic vein and lesions such as tumor and[illegible]

C[illegible]TA can provide a three-dimensional image of portal vein and hepa[illegible]n diseases, and is a good complementary method of axial and MPR images.

B-0291 11:10

The natural history of indeterminate lesions at hepatic spiral CT

W.R. Lees, S. Punwani, A.R. Gillams; *London/GB*

Purpose: CT surveillance of patients with known liver metastases regularly demonstrates small < 1 cm lesions which are indeterminate by CT criteria. The purpose of this study was to determine what became of these lesions on sequential CT follow-up.

Methods and materials: The study cohort comprised 38 patients with known liver metastases treated by thermal ablation who underwent sequential CT scans. Five had breast and 33 colorectal liver metastases. Spiral CT was performed using a 5 mm collimation, 2.5 mm reconstruction interval, pitch < 1.7 following pump injection of 100 – 150 ml of iodinated contrast at 5 ml/s with a 48 s delay. All patients were scanned at 3 – 6 month intervals for a total follow-up period of 12 months. The scans were retrospectively reviewed to identify indeterminate lesions < 1 cm. An increase in size to > 1 cm, in conjunction with the typical appearance of a hypovascular metastasis was considered diagnostic.

Results: There were a total of 80 indeterminate lesions on 140 scans. Follow-up CT scans were available in 57/80, for a minimum of 3 months. 15 patients received chemotherapy during the follow-up period. There were 8 indeterminate lesions measuring 1 – 4 mm, 24, 5 – 7 mm, and 25, 8 – 10 mm. No lesion < 4 mm increased in size. 13/24 (54 %) in the 5 – 7 mm group became metastases and 17/25 (68 %) in the 8 – 10 mm group.

Conclusion: The overall probability of an 5 – 9 mm indeterminate lesion becoming a metastasis was 30/57 (52 %). The minimum detectable size for a metastasis was 5 mm.

B-0292 11:20

Focal hepatocellular carcinoma: Value of the delayed phase of helical-CT and a comparison with CT during arterial portography

C.R. Habermann, F. Weiss, C. Staedtler, M. Hillner, V. Schoder, J. Welger, P. Steiner, E. Bücheler; *Hamburg/DE*

Purpose: The aim of this study was to determine the value of the delayed-phase of helical CT in the detection of hepatocellular carcinoma (HCC) in cirrhotic liver and to compare the results with histology and helical CT during arterial portography (CTAP).

Material and methods: 51 patients with liver cirrhosis and suspected HCC were examined by triple-phase helical-CT (THCT). Images were obtained 25 seconds – arterial phase (AP), 60 – 70 seconds – portal-venous phase (PP), and 300 seconds – delayed phase (DP) after injection of 140 ml of intravenous nonionic contrast material. In 9 patients findings were correlated with CTAP within one month. In 17 patients histological work-up was performed, whereas in 34 patients clinical follow-up of at least 6 months was obtained.

Results: In 17 patients 49 lesions were detected by THCT. The arterial phase (AP) depicted 55 % of these lesions, whereas the portal-venous phase (PP) depicted 57 % and the delayed phase (DP) 78 %. DP showed a significant higher detection rate in comparison to the PP ($p = 0.008$). Nine lesions could only be detected with DP, eight only with AP. Combining AP with DP significantly more lesions were visualised than using AP and PP ($p = 0.031$). In nine patients 29 lesions were diagnosed by CTAP. In these patients 27 lesions were visualized by THCT.

Conclusion: The THCT shows comparable results to CTAP with DP increasing the sensitivity in detecting HCC which therefore should be performed when cirrhosis is present.

B-0293 11:30

Rare hepatic tumors in adults: CT findings

G. Tognini[1], F. Ferrozzi[1], G. Zuccoli[2], G. Marchesi[1], E. Spaggiari[1], P. Pavone[1]; *[1]Parma/IT, [2]Reggio Emilia/IT*

Purpose: To describe the CT pattern of rare hepatic tumors in adults and to investigate the capabilities and limitations in terms of characterization.

Materials and methods: We retrospectively reviewed CT scans of 29 patients (18 M, 11 F) with rare hepatic tumors between 1985 and 2000. 1 patient was affected by tuberous sclerosis, 1 had previous history of vinyl chloride exposure, 4 oral contraceptives therapy. All the lesions were pathologically proven. 5 cystadenomas, 3 cystadenocarcinomas, 2 cystic lymphangiomas, 2 lipomas, 2 angiolipomas, 3 hamartomas, 1 carcinoid tumor, 3 angiosarcomas, 1 embryonal sarcoma, 2 malignant fibrous histiocytomas, 2 primary lymphomas, 3 leiomyosarcomas, 2 hemangioendotheliomas were diagnosed.

Results: Cystadenoma, cystadenocarcinoma, embryonal sarcoma lymphangiomas and 2 hamartomas showed complex cystic appearance with liquid/paraliquid HU numbers, thickening of the walls, solid enhancing septa. 1 hamartoma showed solid necrotic appearance, lipomas showed homogeneously negative HU numbers, angiolipoma showed negative HU numbers with contrast enhancement (c.e.) of the vascular component. Lymphomas demonstrated hypodense nodules with little c.e. Angiosarcomas were large infiltrating lesions. Carcinoid showed non specific solid appearance with central hyperdensity in the portal phase. Histiocytomas were large infiltrating lesions with central hemorrhage. Hemangioendotheliomas demonstrated multiple nodules with capsular retraction and no calcifications. Leiomyosarcomas appeared as voluminous heterogeneously hypodense masses.

Conclusions: CT can provide virtually diagnostic informations (lipoma, angiolipoma). In the other tumors CT may be useful in narrowing the possible differential diagnoses.

B-0294 11:40

Focal nodular hyperplasia: CT findings in 78 patients with emphasis on multiphasic helical CT

G. Brancatelli[1], M.P. Federle[1], L. Grazioli[2], A. Blachar[1], M.S. Peterson[1], L. Thaete[1], K.M. Pealer[1], K. Menni[2]; *[1]Pittsburgh, PA/US, [2]Brescia/IT*

Purpose: To evaluate the CT imaging features of FNH on helical CT.

Material and methods: We reviewed the imaging findings in 78 patients (69 women, 9 men, mean age 37). Patients had either conventional (n = 9) or helical multiphase CT (n = 69). Diagnosis was based on complete resection (n = 20), biopsy (n = 42) or clinical and imaging follow up (n = 16). The number, sizes, location, margins, surface, homogeneity of enhancement, and the presence of a central scar, mass effect, exophytic growth, calcification, pseudocapsule or vessels feeding or draining the lesion were evaluated.

Results: 124 tumors (mean diameter 4.1 cm, range 1 – 11 cm) were depicted at CT. 62 tumors were considered small (less than 3 cm). The FNH were single in 60 patients (77 %), hypervascular and hyperattenuating on HAP (106 of 106, 100 %), isoattenuating on delayed images (82 of 89, 92 %), enhanced homogeneously (111 of 124, 90 %), had a smooth surface (109 of 124, 88 %), were subcapsular (101 of 124, 81 %), had ill-defined margins (89 of 124, 72 %) and a central scar (62 of 124, 50 %), more often in lesions larger than 3 cm (40 of 62, 65 %) than in small FNH (22 of 62, 35 %). FNH less frequently exerted mass effect (43 of 124, 35 %), had vessels around or within the lesion (42 of 124, 34 %), demonstrated exophytic growth (40 of 124, 32 %) or a pseudocapsule (10 of 124, 8 %). Only 1 FNH had calcifications.

Conclusion: Helical CT demonstrates characteristic features that may allow confident diagnosis of FNH. In typical cases neither biopsy nor further imaging is necessary.

B-0295 11:50

A scoring system based on liver-volume measurements using cross-sectional imaging data to assess the risk of postoperative liver failure in patients undergoing hepatic resections

M.A. Kessler, U.J. Schöpf, T.K. Helmberger, R.D. Brüning, H.G. Rau, M.F. Reiser; *Munich/DE*

Purpose: To determine the risk of postoperative liver failure in planned hepatic resection different parameters based on CT&MR data were evaluated. Parameters with predictive value were determined and a score system was developed to predict the risk of postoperative liver failure.

Material & methods: From 1990 to 1998 570 patients with hepatic neoplasms underwent liver resection. Preoperatively, the parenchymal hepatic resection rate (PHRR = resectedvolume - tumorvolume/livervolume - tumorvolume) was calculated from CT or MR data using manual planimetry (n = 486) or a custom-made software system for automated volumetry (n = 84). 10 clinical and laboratory tests with implications on liver function were performed preoperatively (bilirubin, c-aminopyrin-breath-test, g-GT, GOT, GPT, WBC, PCHE, PTT, thromboplastintime, serum-albumin). The correlation of these parameters to postoperative liver failure was tested using stepwise regressive multiple regression analysis. The determinants with significant correlation with postoperative liver failure were used to develop a scoring system to predict the postoperative outcome.

Results: Multiple regression analysis revealed only 2 determinants with significant correlation to postoperative outcome: PTT (p = 0.0014) and PHRR (p = 0.0007). PHRR alone and in combination with PTT, c-aminopyrine-breath-test, bilirubin and g-GT were subsequently included in our scoring sytem to assign each patient a preoperative risk score. Postoperatively 3.5 % of patients died due to liver failure. Major postoperative impairment of liver function occurred in 4.9 %. These events were correctly predicted based on our scoring system.

Conclusion: The PHRR as determined using axial imaging data is the most important predictor of postoperative liver failure. A score can be used to predict postoperative liver failure. In addition to providing diagnostic information and allowing surgical planning, cross sectional imaging techniques therefore are indispensable tools.

10:30–12:00 **Room E2**

Breast

SS 602

Digital mammography (1) - Technique

Chairpersons:
R. Rostagno (Buenos Aires/AR)
M.A.O. Thijssen (Nijmegen/NL)

B-0296 10:30

Optimizing radiation quality in full-field digital mammography for reducing the patient doses in comparison to screen-film mammography

K.-P. Hermann, U. Fischer, S. Obenauer, E. Grabbe; *Göttingen/DE*

Purpose: To compare radiation doses of full-field digital mammography (FFDM) with those dose levels used for conventional screen-film mammography (SFM). To evaluate the potential of radiation dose reduction in FFDM.

Materials and methods: Exposures of a PMMA phantom were made using a FFDM system and a state-of-the-art SFM system. The automatic mode controlled radiation and allowed the systems to select the acquisition parameters for different phantom thicknesses. FFDM was performed using a flat-panel X-ray detector based on a-Si technology. In the conventional system a dedicated mammographic screen-film combination was used. Both systems had a dual track X-ray tube with a molybdenum and a rhodium track on the anode and molybdenum or rhodium filtration. Entrance surface air kerma were measured free in air, the average glandular dose (AGD) were calculated by using published conversion factors. The effects of target/filtration and peak voltage settings on doses and signal-to-noise ratio (SNR) were evaluated.

Results: The dose values of FFDM were not significantly different from those of conventional SFM. Raising peak voltage by 2 kVp decreases AGD by 8 – 13 % for the same target/filter combination. Switching the target/filter material from Mo/Mo to Mo/Rh for 40 mm PMMA lowers AGD by approximately 25 %, while switching from Mo/Mo to Rh/Rh lowers the breast doses by approximately 40 % at the same peak voltage values. Exposures with lower doses results in low SNR, which is the limiting factor for further decrease in dose.

Conclusion: There is a technical potential of FFDM to decrease the currently used breast dose.

B-0297 10:40

Influence of anode-filter combinations Mo/Mo and Mo/Rh on image quality and radiation dose in mammography

G.M. García sr.; *Seville/ES*

Purpose: To evaluate how anode-filter combinations Mo/Mo and Mo/Rh influence image quality in and mean glandular dose to breast of different thicknesses and composition.

Material and methods:

- mamographic; mammomat 3000. (Siemens)
- a daylight processor (Agfa)
- a sufficient number of women (n = 400) were examinated.
- the oblique view was studied and kv fixed.

- the parameter were studied: breast thickness; mas and the breast parenchymal pattern of Wolfe.
- four radiologist specialist in mammography evaluated image quality.
- four tissues in the mammography were compared: glandular tissue; pectoral muscle; fine structural details and skin.
- the right mammogram was always the reference.
- the result were statistically evaluated with Montecarlo informatic programs.

Results:

- image quality.
  - N1P1 Mo/Mo better Mo/Rh.
  - P2DY Mo/Mo worse Mo/Rh.
- glandular dose.
  - N1P1 Mo/Mo higher Mo/Rh.
  - P2DY Mo/Mo higher Mo/Rh.
- thicknesses breast/dose.
  - 3 cm Mo/Mo higher Mo/Rh.
  - 4 cm Mo/Mo higher Mo/Rh.
  - 5 cm Mo/Mo higher Mo/Rh.

Conclusion: It was concluded from findings of all these studies that the image quality for thick or dense breast is higher and the dose statistically significantly lower when a Rh anode is used with a k-edge filter when a Mo anode is used with a Mo filter.

B-0298 10:45

Full-field digital mammography: Dose-dependant detectability of simulated breast lesions

S. Obenauer, K.-P. Hermann, E. Grabbe; *Göttingen/DE*

Objectives: The study compares contrast-detail-curves and microcalcification detectability of full-field digital mammography (FFDM) to conventional screen-film mammography (SFM) by using different doses in the digital technique.

Materials and methods: The examinations were performed with an FFDM system by using a digital flat-panel X-ray system based on amorphous silicon and a conventional SFM system proved on a contrast-detail-mammography phantom (CDMAM) and an anthropomorphic breast phantom with superimposed microcalcifications. The digital detector was exposed with standard dose of SFM and with a dose reduction of up to 75 %. Reading was performed by 3 radiologists. Contrast-detail-curves and correct-observation-ratio (COR) were performed for the CDMAM-phantom. ROC-analysis with a confidence level ranging from 1 to 5 was done with the anthropomorphic phantom.

Results: Digital mammography with the same dose revealed at least an equivalent or even higher detectability rate than conventional mammography. COR could be increased at about 10 – 25 %. The ROC-analysis yielded better results for the FFDM system. Same lesion detectability in digital mammography as in conventional was reached at a dose reduction of about 25 %, concerning spot views even at higher reduction. Dose reduction in the anthropomorphic phantom resulted in a continuous loss of detectability. The same detectability as in conventional mammography was reached, however, by a dose reduction of up to 50 %.

Conclusions: The results suggest that FFDM is at least equivalent or – as far as spot views are concerned – superior to conventional SFM concerning the detectability of simulated lesions. Thus, a potential of dose reduction is suggested.

B-0299 10:55

Contrast-detail resolution in full-field digital mammography by using lower doses in comparison to screen-film mammography

K.-P. Hermann, S. Obenauer, U. Fischer, E. Grabbe; *Göttingen/DE*

Purpose: Comparison of a full-field digital mammography system using a large-area amorphous silicon image receptor and a conventioanl screen-film mammography system with reagrd to lesion detection of low-contrast objects. Evaluation of the impact of a dose reduction with the digital flat-panel detector was of special interest.

Materials and methods: A cesium iodide coupled self-scanning flat-panel detector, based on amorphous silicon technology with 0.1 mm pixel size was used. The active imaging area was 19 cm × 23 cm. The theorectical limit of the spatial resolution was 5.0 lp/mm. A contrast-detail phantom containing gold disks from 0.1 – 3.2 mm in diameter and from 0.05 – 1.6 µm in thickness were exposed with a conventional mammography system using the automatic exposure control device. With the full-field digital mammography system the phantom was evaluated with the same exposure parameters and with dose reduction of 75 %, 50 %, and 25 %. Three readers examined each image. Contrast-detail curves were generated with the resulting data and compared.

Results: Images acquired with the full-field digital mammography system showed a significantly higher contrast-detail resolution than those acquired with the conventional screen-film mammography system at the same dose. The digital system showed superior lesion detection capabilities to the conventional system even at dose reduction of about 50 %.

Conclusion: The full-field digital mammography system used in this study is superior to the conventional screen-film system in detecting low-contrast objects.

B-0300 11:05

Comparison of 8 and 10 bit gray level display of mammograms

S. van Woudenberg[1], T. Roelofs[1], A. Boedicker[2], S. Bohnenkamp[2], D. Dechow[2], N. Karssemeijer[1]; *[1]Nijmegen/NL, [2]Bremen/DE*

Purpose: Is there a visual or diagnostic difference between an 8 and a 10 bit gray level representation of a mammogram in a soft copy reading environment?

Materials and methods: A set of 100 12 bit digitised analog high contrast MLO mammograms were presented in a 8 and 10 bit representation on high resolution monitors (BARCO MGD 521) using the same grayscale (8 or 10 bit) depth. Left and right breast were displayed simultaneously. The subject was free to toggle between 8 and 10 bit presentations and use an electronic magnifying glass. No window or levelling was possible during the session. There was no time limit. The 8 bit presentation was simulated on the 10 bit board (BARCO Medis 5MP1H) by resampling the 10 bit image using the Floyd-Steinberg error diffusion algorithm. Some 20 subjects took the test. About half of them were radiologists or radiographers, the other half comprised mainly physicists with some experience with radiological images. The medical workers were asked to identify the best images for diagnosis, others were requested to find the best image.

Results: There was no preference for either type of images, even when subjects took much time to decide.

Conclusion: The subjects score the same for 8 or 10 bit images. The more common, faster and cheaper 8 bit boards can be used in a softcopy reading environment without loss of quality when digitized mammograms are used. Comparison using direct digital mammograms is planned, but the same result is expected.

B-0301 11:15

Improved CAD of mammographic lesions by assigning non-uniform weight to different parameters

S.S. Buchbinder[1], R. Lederman[2], P. Bamberger[2], B. Novak[2], S. Fields[2], I. Leichter[2]; *[1]Bronx, NY/US, [2]Jerusalem/IL*

Purpose: To assess the potential of improving the performance of standard CAD for microcalcifications (MC), by means of non-uniform weighting of computer extracted features.

Method/materials: The CAD system automatically extracted from digitized mammograms, 13 quantitative features characterizing MC. Two hundred and sixty archival cases (age range 31 – 77) with known pathology (160 malignant, 100 benign) were analyzed. Stepwise Discriminant Analysis (SDA) selected the best features discriminating between benign and malignant MCs. A classification scheme, based on the optimized features, was constructed without weighting the features. Considering that certain features may potentially overwhelm in significance all other factors, a new scheme was constructed, which assigned a different weight to each feature, based on its predictive power. The performance of this new classifier was compared, by ROC analysis, with that of the non-weighted classifier.

Results: From the 13 variables extracted by the CAD system, 8 were selected by SDA for generating the classification scheme. The performance of the non-weighted scheme yielded a ROC curve with an Az of 0.81, resulting in a PPV of 67 % and an accuracy of 69 %, for 98 % sensitivity. The performance of the weighted scheme was significantly higher ($p < 0.0001$), with an Az of 0.90, a PPV of 79 % and an accuracy of 83 %, for 98 % sensitivity.

Conclusions: The performance of the weighted scheme was significantly higher than that of the non-weighted scheme. Since the contribution of each feature extracted by the CAD system to the classification of the MC is different, weighting should be included when constructing the classifier.

B-0302 11:25

Usefulness of a computer-aided detection (CAD)-system

M. Facius, A. Malich, C. Marx, M.G. Freesmeyer, M. Fleck, W.A. Kaiser; *Jena/DE*

Purpose: To determine the clinical usefulness of a CAD-system in the detection of highly suspicious microcalcifications by measuring sensitivity and the potential impact on biopsy rate.

Method and material: Mammograms from 108 breasts with highly suspicious microcalcifcations (Level of Suspicion, LOS category 4) were analyzed using the Second Look™ CAD-System (CADx Medical Systems, Quebec, Canada). All patients had microcalcificationes and underwent biopsy or surgical treatment (malignant, benign). Malignant microcalcifications, marked by the CAD-system in at least one of the two digital films were scored as true positive. Benign microcalcifications, marked in at least one film were scored as false positive.
Results: Of the 108 mammograms, 50 were biopsy proven cancer cases. 43/50 carcinomas were detected correctly (sensitivity 86 %). The remaining 58 cases had biopsy-proven benign microcalcifications and were correctly not marked in 25/58 cases, (specificity 43 %). The positive and negative predictive value were 57 % (43/76) and 78 % (25/32), respectively.
Conclusions: Used clinically, the Mammograph™ (CAD-printouts) would have efficiently and effectively directed the radiologists attention to the malignant lesions. The results indicate that the system could be used by a radiologist to potentially reduce the number of unnecessary biopsies of suspicious microcalcificatios. Therefore, the Second Look™ system is useful as a second reader of highly suspicious microcalcifications.

B-0303 11:30

3D real-time volume rendering of the breast using data from routine multislice spiral chest CT examinations

A. Stoeger, T. Frede, M. Daniaux, R. Frank, J. Loimayr, D. zur Nedden; *Innsbruck/AT*

Purpose: Evaluate the possibility of recognizing breast pathology on routine spiral CT examinations of the chest by post processing this as a region of interest and real-time rendering.
Material and methods: The data of 20 patients with suspected breast pathology (solid nodules or cysts n = 12, macro-calcifications n = 6, micro-calcifications n = 2), who had routine multislice spiral CT of the chest (4 × 2.5 mm, Pitch 6, Siemens Plus 4 Volume Zoom) was reconstructed to 3 mm slice thickness at 2 mm increments. This data was then real-time volume rendered on a 3D Virtuoso (Siemens Medical Systems) and the breast images were assessed interactively (clip plane editing, interactive change of rendering parameters).
Results: Solitary solid nodules > 1.5 cm were detected in 4 patients, single or multiple cysts > 5 mm in 8 and macro-calcifications > 3 mm in 6. Mammographically identified micro-calcifications could not be discerned. When contrast had been administered, enhancement aided in solid/cyst differentiation and in the assessment of cutaneous or muscular infiltration by tumors.
Conclusions: Interactive RTVR evaluation of the breast from post-processed volume CT data sets maximizes information of breast pathology contained in routine chest CT data. The limited spatial resolution does not allow for the assessment of micro-calcifications.

B-0304 11:35

A computer-assisted method for evaluating mammographic benign and malignant breast lesions

F. Grizzi[1], P.C. Muzzio[2], A. Di Maggio[2], N. Dioguardi[1]; [1]*Rozzano/IT,* [2]*Padova/IT*

Purpose: To investigate a computer-assisted method, based on the fractal dimension and the coefficient of roundness in order to measure the complex shape of benign and malignant mammographic lesions.
Materials and methods: Twenty-three digitized mammograms were classified as containing benign lesions (n = 12) or as containing malignant lesions (n = 11) on the basis of readings by two independent radiologists. Image and fractal analysis were automatically done by mean of a computer-assisted image analysis system.
Results: A significant increase ($p < 0.0007$) was obtained when the fractal dimension of benign versus malignant breast lesions and the coefficient of roundness of benign versus malignant mammographic lesions ($p < 0.00005$) were compared.
Conclusions: Benign and malignant breast lesions are characterized by complex morphologies. Complexity is the main property of all the biological systems, including human natural and pathological structures. This study shows that the fractal geometry allows the quantitative measure of the complex morphology of benign and malignant mammographic lesions. The coefficient of roundness represents the degree of irregularity of the lesion. The fractal dimension of the lesion's outline gives a measure of the increasing cells proliferation and their irregular invasion of the surrounding tissue. Furthermore, this mathematical approach may be of help for the study of the non-linear dynamical process involved in the breast cancerogenesis.

B-0305 11:40

Multimodal data fusion in breast imaging

C. Behrenbruch, N. Moore, K. Marias, P. Armitage, M. Brady, R. English, J. Clarke; *Oxford/GB*

Purpose: Non-rigid matching can relate pathological indicators between mammography and contrast-enhanced MRI. This is particularly useful for ductal carcinoma in-situ (DCIS) because calcifications visible mammographically may correspond to subtle, focal areas of enhancement that were not identified prospectively as abnormal.
Materials and methods: Fast Spoiled Gradient Echo (FSPGR) T1-weighted (TR/TE 8.9/4.2 ms, $\alpha = 10°$) acquisitions of the breast are segmented on the basis of a pharmacokinetic model of contrast (Gd-DTPA) uptake and projected in a simulated CC and MLO plane. The mammograms are then non-rigidly registered (matched) to the simulated projections, resulting in a geometrical correspondence between features in the two mammogram views and the 3D geometry of the MRI acquisition.
Results: MRI studies and standard two-view mammograms were compared in 12 women who had a range of benign and malignant diseases. The average error in the registration (based on evaluation of the centroid and extent of ROIs) was ~3.5 voxels with slightly higher error (~5 voxels) for large, poorly differentiated carcinomas. Correlating calcifications in the mammogram with the MRI data revealed subtle contrast enhancement, consistent with DCIS.
Conclusion: Matching (registration) between two mammogram views and CE-MRI can be used to correlate pathological indicators of various conditions, including DCIS.

B-0306 11:50

Mammatrainer: Web based training in mammography

U.G. Aichinger, M. Dobritz, R.W.S. Schulz-Wendtland, W.A. Bautz; *Erlangen/DE*

Purpose: Web based Training is expanding in the last few years in all fields of radiology. We present a new training program available since April 2000 with 90 cases in mammography and breast ultrasound.
Patients and method: In the Institute of Diagnostic Radiology, Gynecological Radiology, over 12 000 patients per year are examined clinically, with ultrasound and mammography. 10 % of these patients have suspect or malignant lesions and so we have many cases that can be used for a teaching program. 90 interesting cases are now prepared for the world wide web, the best way to give a wide group the opportunity to see these images.
Results: The program was tested at the 5th International Course of Mammography in Erlangen. 2000 partitions saw the cases there and gave there statements. 21 % had no experience with the internet, 46 % used the internet to get information's about medical problems and 33 % had used databases like this once before. 93 % said, that this was a good and effective way in training mammography.
Discussion: Internet training becomes now a fixed part in training of radiological modalities. Despite the problems of spatial resolution needed in mammography, with good image preparing it is possible to give a satisfying teaching file in breast imaging in the internet: www.gynrad.idr.med.uni-erlangen.de.

B-0307 11:55

Breast artery calcium and cardiovascular morbidity: Relationship in different age groups

P. Crystal[1], E. Crystal[1], M. Friger[1], S. Strano[2], J. Leor[3], G. Chudakov[1], Y. Hertzanu[1]; [1]*Beer-Sheva/IL,* [2]*Jerusalem/IL,* [3]*Tel-Aviv/IL*

Purpose: Cardiovascular disease (CVD) is a leading cause of death among women in the Israel. Early recognition of women in with occult cardiovascular disease has become a public health priority. Breast artery calcification (BAC) visible on mammography was proposed as a screening tool for detection of women in high cardiovascular risk. The aim of this study was to assess relationships between age, BAC, and CVD.
Materials and methods: The presence of BAC and CVD were analyzed in survey included 927 women referred for mammography. The patients were divided in to three age groups: < 55 a (group 1), 56 – 65 a (group 2), > 65 a (group 3).
Results: The mean age was 57 ± 10 years, with overall incidence of BAC 17 %. The incidence of BAC increased with age (from 3.6 % in Group 1, to 19.5 % in Group 2, and 43 % in Group 3). Clinical CVD increased from 5.7 % in group 1, to 11.8 % in group 2, and to 25.5 % in group 3. The positive predictive values of BAC for CVD in three study groups were respectively 12.5 %, 14.3 %, and 36 %. The negative predictive values were 94.6 %, 88.7 %, and 82.5 %. Multiple logistic regression analysis was performed for cardiovascular disease and BAC in all age groups. BAC was found as independent from age predictive factor for existence of cardiovascular disease.

Conclusion: Our findings suggest that mammography may be an effective and inexpensive screening tool for the detection of cardiovascular risk in women, especially in the age from 55 to 65 years.

10:30–12:00 **Room F1**

Chest

SS 604

Chest imaging: Technical aspects and new developments

Chairpersons:
T. Franquet (Barcelona/ES)
C.J. Herold (Vienna/AT)

B-0308 10:30

Clinical safety of SonoVue™, a new echocontrast agent, in healthy volunteers and in patients with chronic obstructive pulmonary disease

D. Bokor[1], J. Chambers[2], P. Rees[2], F. Luzzani[1], A. Spinazzi[1]; [1]*Milan/IT,* [2]*London/GB*

Purpose: To demonstrate the safety of SonoVue™ (Bracco S.p.A.), a new echocontrast agent, in healthy volunteers (HV) and in patients with chronic obstructive pulmonary disease (COPD).

Methods: (1) Two placebo-controlled phase I studies in 66 HV: 36 HV administered with a single intravenous ascending dose of SonoVue™ (from 0.003 ml/kg to 0.12 ml/kg) and 30 subjects given cumulative doses from 0.15 ml/kg to 0.6 ml/kg. (2) A phase II crossover, placebo-controlled study in 12 patients suffering from COPD administered with SonoVue™ at a dose of 4 ml (corresponding to 0.057 ml/kg in a 70 kg b.w.). Adverse events (AEs) monitoring up to 48 – 72 h post-dosing. All volunteers underwent extensive safety assessments (monitoring of vital signs, ECG, blood oxygen saturation, laboratory assessments and Mini-Mental Test) up to 24 – 72 hours post dose. In addition, COPD patients underwent specific lung function tests, such as forced expiratory volume (FEV1), forced vital capacity (FVC), and forced mid-expiratory flow (FEF 25 – 75 %).

Results: No serious AEs occurred throughout the study. All non-serious AEs were minor, mild in intensity and rapidly self-resolving. No difference in the incidence of AEs was observed among the various doses of SonoVue™ and between SonoVue™ and placebo. No clinically significant changes in any of the safety assessments. No statistically significant differences between SonoVue™ and placebo in mean FEV1, FVC or FEF–25 – 75 % levels.

Conclusions: SonoVue™ showed a good safety profile both in healthy subjects and in patients with chronic obstructive pulmonary disease.

B-0309

withdrawn by author

B-0310 10:40

MR evaluation of thoracic inflammatory and neoplastic disorders: Usefulness of ECG-gated breath-hold turbo-STIR imaging for lesion detection, size and characterization

M. De Santis, F. Manganaro, T. Celano, A. Pimpinella, R. Passariello; *Rome/IT*

Purpose: To assess the diagnostic value of ECG-gated breath-hold short-TI-inversion-recovery turbo-SE (turbo-STIR) MR imaging in the evaluation of thoracic inflammatory and neoplastic disorders.

Materials and methods: Sixtytwo patients with various thoracic disorders of inflammatory-neoplastic origin, i.e resected lung carcinoma followed by radiotherapy (21 pts.), esophageal carcinoma (13 pts.), lymphoma under chemotherapy (10 pts.), sarcoidosis (7 pts.), chest wall disorders (7 pts.), heart tumor (4 pts.) underwent composite turbo-SE MR chest examination (ECG-gated breath-hold pre-and post-Gd T1-weighted, T2-weighted and STIR imaging) for detection, sizing and characterization (viable-not viable) of primary and ancillary lesions (i.e. lymph nodes, soft tissues involvement, metastases etc.). Direct biopsy, pathology result and follow-up CT-MR examination served as reference.

Results: In comparison with T1- and T2-weighted turbo-SE imaging, turbo-STIR MR evaluation proved to be superior in the detection and characterization of both primary and ancillary lesions (92.6 % vs 73.5 %). 38 % of the lesions equally identifyed by both T1-T2 and STIR imaging displayed a greater size on the latter, owing to peripheral edema or microscopic tumor infiltration.

Conclusions: Coupling fat suppression and overall high signal intensity of active lesions due to the additive effect of T1 and T2 mechanisms on STIR imaging with the elimination of respiratory/cardiac motion offered by ECG-gated breath-hold turbo-SE sequences allows a reliable and cost-effective approach in the evaluation of inflammatory and/or neoplastic involvement of chest diseases, especially in the follow-up of cancer patients after surgical excision and/or radio-chemotherapy.

B-0311 10:50

Assessment of the localization and pleural relation of focal lung lesions with multislice CT: When are thin sections and multiplanar reformats necessary?

M. Uffmann, M. Prokop, C. Bas, C. Schäfer-Prokop, G.R. Strasser, C.J. Herold; *Vienna/AT*

Purpose: The amount of images increases substantially with thinly collimated multislice CT scans. Reviewing of multislice data is often preferred on thicker axial sections. Therefore, we wanted to identify those situations in which reconstructions of thin sections and multiplanar reformats are useful and do improve assessment of focal lung lesions.

Materials and methods: We examined 18 patients with suspected focal lung lesions. As a standard, we reconstructed 5 mm thick axial sections (mode A). From thin 1.25 mm axial sections (mode B) coronal (mode C) and sagittal reformats (mode D) were created. On a workstation we interactively reviewed images with respect to segmental localization of lesions, their relation to the pleural surfaces, and pleural retraction or infiltration. Reviewing started with mode A and progressed through mode D.

Results: In 16 of 18 patients, a total of 26 focal lung lesions was found, 9 of which had a close relation to the pleural surfaces. We noted pleural retraction in 14 lesions. Segmental localization of these lesions did change in 3 patients by multiplanar evaluation. Multiplanar data sets changed the assessment of infiltration into neighbouring segments in 4 cases. For all findings comparison of mode B to A revealed additional information in 7 patients, mode C to B in 5 and mode D to C in 2 patients.

Conclusion: Multiplanar reformats improve the assessment of focal lung lesions, especially of those related to horizontally aligned pleural surfaces. In such cases, thin section reconstructions and reformats from multislice data sets are advisable.

B-0312 11:00

Evaluation of pulmonary nodules with multislice CT: Comparison of routine axial slices with STS-MIPs and MPRs in three planes

R. Eibel, T. Tuerk, C. Kulinna, R.D. Brüning, M.F. Reiser; *Munich/DE*

Purpose: To evaluate the image quality of axial, coronal and sagittal reconstructions from breath-hold multislice CT (MSCT) of the chest to detect or exclude pulmonary nodules.

Methods and materials: 103 patients with suspected or known pulmonary nodules were scanned with 1 mm collimation and pitch 6 (Volume Zoom, Siemens, Germany). Two data sets were reconstructed: (a) contiguous axial images of 5 mm thickness, (b) 1 mm thin slices with 0.6 mm increment. From (b) axial, coronal and sagittal MPRs and STS-MIPs were reformatted with 5 mm slice thickness. Images were rated by three independent readers with regard to number of detected lesions and degree of confidence for their diagnosis using a three point scale (sure/relative/uncertain). Statistical significance was calculated by Mann–Whitney U-test.

Results: In consensus reading of all three planes of MPRs and MIPs, the number of detected nodules increased significantly ($p < 0.05$) compared to routine axial scans (mean values: 2.5 versus 1.5). Comparing the two reformation modalities, MIPs were superior to MPRs (2.7 versus 2.3, with $p < 0.05$) with the lowest level of uncertainty. 5 mm axial slices had the highest missing rate and the lowest reader confidence.

Conclusion: MPR- and especially MIP images of MSCT data sets are superior to routine axial images in the detection of pulmonary nodules and are therefore recommended as the routine diagnostic tool of choice.

B-0313 11:10

Value of single-slice and multi-slice spiral CT in the detection and characterization of pulmonary metastases

D. Pickuth, B. van Drünen, N. Kendzierski, R. Spielmann; *Halle a. d. Saale/DE*

Purpose: The aim of this study was to compare state-of-the-art single-slice (SSCT) and multi-slice spiral CT (MSCT) in the detection and characterization of lung metastases.

Patients and methods: 22 consecutive patients with 112 pulmonary metastases had contrast-enhanced scans of the lung with SSCT (SOMATOM Plus 4, Siemens) and subsequently with MSCT (SOMATOM Plus 4 Volume Zoom, Siemens) using lung, soft tissue and bone windowing. The number of pulmonary lesions, the overall lesion detection, and the characterization of lung metastases was evaluated by consensus. The diagnostic value of SSCT and MSCT was compared intraindividually.
Results: MSCT was superior to SSCT in detecting small parenchymal nodules, whereas MSCT and SSCT were equivalent for lesions > 5 mm. MSCT displayed the lesion shape and borders more precisely than SSCT. Furthermore, the widespread small connecting lines representing irregularly thickened interlobular septa in patients with lymphangitis carcinomatosa were better shown by MSCT.
Conclusion: MSCT is superior to SSCT in detecting and characterizing pulmonary metastases, because it can provide a narrower effective section thickness. Artifact-free image acquisition is feasible even in dyspnoeic or uncooperative patients. In comparison to SSCT, MSCT protocols of the lung should use a thinner collimation and a higher pitch to achieve the same length of coverage in a shorter scan time.

B-0314 11:20

Multidetector-row CT of the chest: Optimization of a scan protocol for routine studies

M.L. Storto, A. Guidotti, C. Ciccotosto, A.R. Larici, L. Bonomo; *Chieti/IT*

Purpose: To compare image quality and diagnostic efficiency of 3 different slice widths in routine examinations of the chest performed with a multidetector CT (MDCT) scanner.
Materials and methods: MDCT scans (4 × 2.5 mm collimation, 15 mm table feed/rotation, 0.5 s rotation time) were obtained in 50 patients with suspected pulmonary disease. Contiguous axial sections were reconstructed at 5, 7, and 10 mm slice width, using a standard algorithm. Images were evaluated by 2 chest radiologists for visibility of anatomic structures as well as the presence of pulmonary nodules and lymph nodes. Lesions were classified as definite, probable, or possible and their size was recorded.
Results: The mean number of axial sections were 27.2 ± 2.3, 38.4 ± 4, and 53.9 ± 4.7 at 10, 7, and 5 mm slice width, respectively. Visibility of anatomic structures was significantly better on 5 mm slice width images than on 7 and 10 mm images ($p > 0.05$).
Use of 7 mm slice width significantly improved the detection rate of pulmonary nodules (18.4 % increase) and lymph nodes (25.6 % increase) when compared to 10 mm slice width. Narrow slice width also yielded more definite and less possible lesions. Differences in lesion detectability between 5 and 7 mm slice width images were not significant.
Conclusion: Use of narrow slice widths in MDCT of the chest improves detection of pulmonary nodules and lymph nodes while enhancing confidence in the diagnosis. When using a collimation of 4 × 2.5 mm, reconstruction of images at 7 mm slice width represents a good compromise between the number of axial sections obtained and the diagnostic efficiency of the study.

B-0315 11:30

Multislice CT of the thorax with reduced volume of contrast material: A comparative study with single slice CT

M. Rémy-Jardin, I. Mastora, P. Masson, P. Campistron, A. Amara, J.-P. Guilliot, J. Rémy; *Lille/FR*

Purpose: The goal of this study was to assess whether diagnostic vascular enhancement can be obtained with multislice CT (MSCT) using lower amounts of nonionic contrast material than with single slice CT (SSCT).
Materials and methods: 120 patients with malignancies initially evaluated with SDCT and followed-up with MSCT were prospectively included in the study. The injection protocol with SSCT consisted of the administration of 120 ml of a 24 % contrast agent at a rate of 4 ml/s. A lower amount of the same contrast agent was injected when scanning the patients with MSCT. On SSCT and MSCT scans, arterial enhancement was graded on a 4-point scale: 1 ... poor; 2 ... fair; 3 ... good; and 4 ... excellent (grades 4 and 3 compatible with diagnostic examinations).
Results: The mean z-axis coverage of spiral CT angiograms was higher with MSCT compared with SSCT (256 mm vs 180 mm; $p < 0.001$). The mean volume of contrast material injected with MSCT was 80 ml (range: 50 – 90) at a rate of 3 ml/s, leading to a significant reduction in the mean amount of iodine administered (19 g vs 26 g with SSCT). On MSCT scans, overall quality of arterial enhancement was graded with a score of 4 (n = 78; 65 %), a score of 3 (n = 36; 30 %) and a score of 2 (n = 6; 5 %) with no significant difference in the number of diagnostic examinations compared with SSCT (n = 114; 95 % vs n = 110; 92 %).
Conclusion: Contrast-enhanced MSCT routinely enables a good opacification of mediastinal and hilar structures using 80 ml of a 24 % nonionic contrast agent.

B-0316 11:40

MR-imaging of lung parenchyma at 0.2 T: Preliminary results

N. Abolmaali[1], J. Schmitt[1], S. Krauss[1], R. Straub[1], V. Jacobi[1], M. Deimling[2], T. Vogl[1]; *[1]Frankfurt a. Main/DE, [2]Erlangen/DE*

Purpose: It has been shown that signal intensities in imaging of lung parenchyma at low B0 fields using multi-gradientecho sequences are superior to high field imaging due to lower susceptibility artifacts. We demonstrate our first experiences with three different sequences in patients in comparison to two-plane-radiographs.
Materials and methods: 43 patients with different lung diseases (e.g. cystic fibrosis, metastases, bronchogenic carcinoma, pneumonia, intrapulmonary bleeding) were examined with a conventional thoracic radiograph in two planes. MR-imaging was performed in a 0.2 T-system with high slew rates (Magnetom Open Viva, Siemens) using a body-spine-coil. Patients were examined with true-FISP- and 2d-CISS-sequences, both in breathhold-technique (Mx 256, FOV 450 mm, TR 6 ms, TE 3 ms) and 2d T1-SE with long term averaging. Acquired images were analyzed by two experienced radiologists to compare quality and diagnostic value of MR-imaging.
Results: In correlation to conventional radiographs major diagnosis was not changed in any case but additional clinical important information was achieved in one third of the patients. MR-imaging took 15 – 25 minutes, the breath-hold periods varied between 4 and 10 seconds. In contrast to closed-bore scanners even dypnoeic patients did not refuse full MR-examination.
Conclusion: Our preliminary results demonstrate that further research should be performed on fast low-field imaging of lung parenchyma especially in young patients who need many subsequent thoracic images for follow-up.

10:30–12:00 **Room F2**

Neuro

SS 611

Functional MRI - Epilepsy

Chairpersons:
K. Ericson (Stockholm/SE)
I. Isherwood (Manchester/GB)

B-0317 10:30

Identification of the pre- and postcentral gyrus by diffusion weighted imaging (DWI)

C. Fitzek[1], S. Fitzek[1], F. Rusch[2], P. Stoeter[2], H.-J. Mentzel[1], J.R. Reichenbach[1], W.A. Kaiser[1]; *[1]Jena/DE, [2]Mainz/DE*

Purpose: Imaging of the motor cortex is still a challenge and there are different ways to identify the central sulcus with a restricted reliability (20 % to 90 %) and analyse of multiple thin slices is necessary. Anisotropy of EPI-DWI can directly show white matter tracts.
Methods and materials: 20 healthy volunteers had an MRI after informed consent: EPI-DWI (TR/TE 4000/103 ms, b 1164 s/mm², 128 matrix, 20 slices, thickness 5 mm, 8 measuremts) and Flash-3D sequence (1 mm isovoxel). The sulcus centralis and the motor cortex was identified by two investigators by five typical signs in the 3D dataset. These signs were compared with the bright anisotropy signal of the in the EPI-DWI.
Results: In all 20 volunteers the central sulcus was seen in the 3D dataset with the standard signs. In all 20 volunteers the white matter tracts leading to the motror cortex and the primary sensory cortex showed anisotropy leading to exact identification of these regions in different slices.
Conclusion: With EPI-DWI it is possible to identify the motor cortex and the primary sensory cortex according to the anisotropy of the white matter tracts.

B-0318 10:40

Somatic/topographical localisation in the secondary somatosensory cortex studied by means of functional MRI and magnetoencephalography

A. Tartaro[1], C. Del Gratta[1], S. Della Penna[1], A. Ferretti[1], V. Pizzella[1], K. Torquati[1], L. Bonomo[1], G. Romani[1], P. Rossini[2]; *[1]Chieti/IT, [2]Brescia/IT*

Introduction: MEG and fMRI responses to median and tibial nerve stimulation were recorded in 4 healthy volunteers. The aim of this study was to delineate the topographical organisation of the human secondary somatosensory cortex and to compare results obtained by means of the two techniques.

Materials and methods: MEG recordings were performed via a 165-channel whole head neuromagnetometer operating in a magnetically shielded room. FMR images were acquired at 1.5 T with EPI sequence. Functional images were acquired according to a block paradigm. High resolution structural images were acquired as well, for data integration, and transformation into Talairach space. Stimuli were 0.2 ms rectangular pulses delivered unilaterally at the median nerve or at the tibial nerve. Stimulus frequency was 0.3 Hz in MEG recordings and 1.9 Hz in fMRI recordings. The latter figure was larger in order to increase the number of stimuli delivered between to consecutive fMRI volumes.

Results: In fMRI maps, activations were observed bilaterally in the SII cortices. Median and tibial nerve activation maps showed a clear somatotopic organisation. Median nerve representation was more anterior and inferior than the tibial nerve. Source locations, fitted from the SII time course in averaged data sets were consistent with fMRI activations.

Conclusions: Brain areas consistent with SII areas and associative areas are seen to activate bilaterally, in contrast to SI areas that are activated only contralaterally. Somatotopic organisation of SII was observed with both MEG and fMRI.

B-0319 10:50

The process of naming and the influence of different semantic categories: A fMRI study

G. Fesl, J. Ilmberger, T.A. Yousry; *Munich/DE*

Purpose: We used fMRI to identify cortical sites involved in the processing of semantic categories: tools and animals.

Material and methods: FMRI was performed with 16 subjects. In the naming task, drawings of tools and animals were presented and had to be named aloud. In the semantic task, in addition to naming the name of another member of the same semantic class had to be produced. Baseline stimuli consisted of a random dot pattern with no response required. Group-analysis was performed using SPM99.

Results: Group analysis showed the following corrected significant activations: naming tools: cingulate gyrus, superior frontal gyrus and supramarginal gyrus bilateral; naming animals: inferior temporal gyrus bilateral; When subtracting the naming condition from the semantic condition, left-sided activation was found in the medial frontal gyrus and the inferior parietal gyrus for both animals and tools.

Conclusion: When knowledge about animals is processed, a temporo-occipital activation is found in both hemispheres. The activation is stronger in the right hemisphere indicating a non-linguistic component. During the semantic generation task for both animal and tool conditions activation is found in left parietal and frontal areas. These additional activations may be due to semantic associations and working memory.

B-0320 11:00

FMRI of brainstem auditory structures using auditory click stimulation

V. Hesselmann, C. Wedekind, O.W. Schulte, O. Zaro Weber, H. Kugel, B. Krug, N. Klug, K. Lackner; *Cologne/DE*

Purpose: Functional MR brain imaging (fMRI) of brainstem auditory pathways

Materials and methods: Eighteen healthy volunteers (age 28 to 42 years) with normal hearing function underwent fMRI-examination on a 1.5 T imaging system (Philips, Best, NL) with periodic click stimulation. BOLD images were obtained using a three dimensional EPI sequence with shifted echo technique (PRESTO). Control scans without click stimulation were obtained in the identical setting. Cross correlation activation maps were calculated using the postprocessing tool "ACT" (Philips). They were matched with anatomic slices of identical orientation and thickness.

Results: Five of 18 subjects were excluded because of motion artifacts. In 4/13 subjects significant activation was observed at the root entry zone of the ipsilateral acoustic nerve corresponding to the cochlear nuclei. In 11/13 subjects, significant activation was found in the same sclice contralaterally close to the fourth ventricle, corresponding to the expected region of the superior olivary nucleus. Activation of the rostral parts of the auditory pathway (inferior colliculus, medial geniculate body) was not found. In the absence of the stimulus no activation occurred in these structures.

Conclusion: Activation of the brainstem auditory pathways by click stimuli can be visualized by fMRI.

B-0321 11:10

Electrically painful stimulation of cranial nerves: An event related fMRI study

C. Fitzek, S. Fitzek, R. Huonker, H.-J. Mentzel, J.R. Reichenbach, W.A. Kaiser; *Jena/DE*

Purpose: Recent functional brain imaging studies of pain using positron emission tomography (PET) and block designed fMRI showed activation of SII, contralateral and ipsilateral insular cortex, thalamus and cingulate cortex. We report the results of an event-related fMRI study to investigate electrically induced trigeminal pain.

Methods and material: 12 healthy right handed volunteers were included. Painful electrically stimulation of the first trigeminal branch was performed. We used an 1.5 T Magnetom Vision with an EPI booster. In an event related setting the following FMRI parameters were used: 20 slices, 3 mm thickness, isotropic voxel, 306 measurements with 54 randomized events. Statistical postprocessing was performed with SPM99.

Results: We observed activation of the contralateral SII and insular cortex as well as an ipsilateral activation of SII and a thalamic activation (T = 4.45, extending 15 voxels). 6 of the 12 volunteers also revealed activation of the cingulate cortex.

Conclusion: Event related fMRI with painful stimulation of the trigeminal nerve confirmed the suspected localisation of activation in the contralateral insular cortex, SII, thalamus and ipsilateral SII. In contrast to other studies activation of the cingulate cortex was not consistent.

B-0322 11:20

MR imaging in epilepsy that is refractory to medical therapy

S. Çakýrer, M. Basak, S.M. Ertürk, H. Yýldýrým, B. Çolakoglu; *Istanbul/TR*

Purpose: Epilepsy is a common neurological disorder, affecting 0.5 – 1 % of the population. 15 – 30 % of these patients have disease that is refractory to medical therapy. Surgery is the most effective method to control seizures in these patients if possible. Patients of this subtype were evaluated by MR examination for the etiologic work-up.

Materials and method: 73 patients with medically intractable epilepsy between the ages of 0 – 68 year old were evaluated by MR examination, using multiplanar imaging with T1 and T2 weighted sequences and if necessary with contrast enhanced sequences.

Results: Cerebralinfarct regions with atrophy and gliosis in 8 patients, dysembryoplastic neuroepithelial tumor in 1 patient, low grade cerebral glial tumors in 2 patients, metastases in 2 patients, hippocampal sclerosis in 16 patients, radial microbrain in 1 patient, cortical dysplasia in 3 patients, pachygyria in 2 patients, subcortical heterotopia in 2 patients, schizencephaly in 3 patients, cerebral hemiatrophy in 2 patients, herpes encephalitis in 2 patients, tuberous sclerosis in 1 patient, Rasmussen encephalitis in 1 patient, arteriovenous malformations in 2 patients, venous angioma in 1 patient, cavernomas in 2 patients and no abnormality in 22 patients were detected.

Conclusion: An important part of the epileptic patients are refractory to medical therapy. Structural brain abnormalities associated with this subtype of epilepsy can be detected with a high degree of sensitivity and specificity using MR imaging. In planning of the treatment, primarily surgical therapy, MR plays a primary role by detecting epileptogenic lesions.

B-0323 11:30

Value of MR volumetry of hippocampi in patients suffering from partial epilepsy

M.J. Krasun, C. Siemianowski, L. Krolicki, R. Andrysiak, K. Marach; *Warsaw/PL*

Purpose: To evaluate diagnostic value of MR volume measurment of hippocampi in comparison with conventional MRI. How the new method can improve evaluation of structural changes in CNS in epilepsy.

Subjects & methods: 38 patients (19 males and 19 females) aged 14 – 55 (mean age 28.9 a) with partial simple, partial complex and secondary generalized seizures. Mean frequency of partial seizures 72.4 per month and secondary generalized seizures – 7.8 per month. The period of observation – 6 months. All of patients underwent conventional MRI (5 mm transv and 4 mm coronal T2WI, 5 mm transv and 4 mm sagital T1WI) and MR volumetry of hippocampi (IR TR/TE 10/4,

eff.thk 1.4 mm) – the volumes were calculated with manual contouring from crura of fornix to the level of mammillary bodies. All patients underwent at least one EEG.

Results: Conventional MRI revealed relevant findings in 10 patients (26.3 %). MR volumetry revealed asymetry of hippocampi greater than 5 % in 22 cases (57.9 %). In patients with normal MRI (28 cases) asymetry of hippocampi greater than 5 % was revealed in 18 cases (64.3 %). The combination of conventional MR and volumetry revealed changes in 28 patients (73.7 %).

Conclusion: Results of this study show that sensitivity of MRI completed with measurment of hippocampal volume is greater than only conventional MRI. It seems that in many cases slightly decreased volume of specific cortical region is the only manifestation of epileptic lesion. Combination of hippocampal volumetry, MRI and other neurodiagnostic methods (EEG, SPECT, PET) allow to evaluate etiology of epilepsy and to lokalise epileptic lesions more precisely.

B-0324 11:40

Lateralization with MRSI in patients with temporal lobe epilepsy

S.E. Ekholm, B. Vikhoff-Baaz, K. Malmgren; *Gothenburg/SE*

Purpose: ^{1}H MR spectroscopy (^{1}H MRS) may contribute to the lateralization of the epileptic focus in temporal lobe epilepsy (TLE). The aim of this study was to investigate if metabolite concentration images from MRSI measurements could be used for lateralization of TLE patients.

Materials and methods: Nine consecutive TLE patients evaluated for epilepsy surgery, and nine neurologically healthy, age-matched volunteers were examined with MRSI. The volume-of-interest (VOI) was angled along the temporal horns in transverse and sagittal images, and symmetrically over the temporal lobes in coronal images. The metabolite concentration images of NAA and Cho + Cr were used for lateralization. Two methods for evaluation were compared: visual analysis of the images, and analysis from ROIs located in different positions, where the side-to-side differences of the NAA/(Cho + Cr) ratios were used for lateralization. The results from lateralization were compared with findings from the presurgical evaluation.

Results and conclusion: The metabolite concentration images were found useful for lateralization of TLE. Visual analysis can with high accuracy be used as routine evaluation. ROI analysis provides a useful tool to quantify the changes, which gives more quantitative information about the spatial distribution and the degree of signal loss.

B-0325 11:50

Amobarbital uptake (AmU) in the hippocampus is not critical for memory performance during Wada test. 94 hemispheres evaluated with ^{99}Tc-HMPAO SPECT and angiography (DSA)

A. Piotrowski[1], H. Klemm[2], H. Urbach[2], M. Kurthen[2], H.J. Biersack[2], C.E. Elger[2], L. Krolicki[1]; *[1]Warsaw/PL, [2]Bonn/DE*

Objectives: Amobarbital uptake (AmU) in the whole hippocampus was considered to be a precondition for transient memory impairment during Wada test. Its grade has a prognostic importance for patients undergoing partial temporal lobectomy. This study aimed to investigate both with DSA and SPECT study the relationship between AmU in the hippocampus ('fetal' configuration of PCA) and grade of memory deficit during non-selective intracarotid amobarbital procedure (IAP).

Methods: 94 hemispheres in forty-seven patients (mean age: 29.9 a) were investigated. After completing of DSA study 200 mg amobarbital and 1 mCi ^{99}Tc-HMPAO were co-injected without catheter repositioning. SPECT study was performed with high-resolution γ-camera. Memory assessment included 'pre-intra' and 'intra-post' memory testing.

Results: The hippocampal AmU was revealed with SPECT study only in 13/94 (13.8 %) hemispheres. DSA study disclosed 'fetal' configuration of PCA in 17/94 hemispheres. Both methods did not reveal any correlation between AmU in the hippocampus (or 'fetal' configuration of PCA) and grade of verbal and non-verbal memory impairment irrespective of the side of amobarbital injection. It was true both for 'pre-intra' ($p > 0.26$) and 'intra-post' memory testing ($p > 0.24$).

Conclusion: AmU in the whole hippocampus seems to be not necessary condition for valid assessment of memory during IAP. Most of the entorhinal and perirhinal cortex and the anterior part of the hippocampus are irrigated by ICA injection via anterior choroidal artery. Recent neuroanatomic studies have emphasized that not only the hippocampus but also related cortical stuctures (e.g. perirhinal, parahippocampal and entorhinal cortex) are critical for memory performance.

10:30–12:00 **Room G**

Abdominal and Gastrointestinal

SS 601b

CT/MR colonography

Chairpersons:
A.R. Gillams (London/GB)
D. zur Nedden (Innsbruck/AT)

B-0326 10:30

Protocol optimization for multislice CT colography

A.R. Gillams, R. Bhardwaj, W.R. Lees; *London/GB*

Purpose: Recent published figures for sensitivity of virtual colonoscopy were 75 % for polyps > 10 mm, 66 % for polyps 6 – 9 mm, 45 % for < 5 mm. Multislice technology with improved spatial and temporal resolution should improve accuracy. This study aims to identify the optimal protocol whilst keeping radiation dose to a minimum.

Methods and materials: Multiple polyps ranging in size from 4 – 13 mm were created within a fresh, cleaned, ex-vivo segment of pig's colon. Surgical sutures were used to produce polyps of different size and shape. The colon was distended and anchored within a water bath and multislice CT (Lightspeed Advantage, GE) performed. Acquisitions were made at 1.25, 2.5, 3.75 and 5 mm collimation using pitch from 1.5 – 6 and both HS and HQ algorithms. The water bath was rotated through 900 and 4 acquisitions repeated. Overlapping slices were reconstructed and 3D data sets interrogated using commercially available virtual colonoscopy software.

Results: The best compromise between dose and image quality lay with HS acquisition of 2.5 mm with table speed of 15 mm (pitch 6) or an HQ acquisition with 3.75 mm collimation at table speed 11.25 (pitch 3). The reduced pitch lessens Z directional. All polyps were detected on all sequences, but the 3 – 4 mm polyps were hard to identify on the 5 mm acquisitions even at pitch 1.5 and HQ mode. 1.25 mm collimation was optimal but not necessary.

Conclusion: The optimal balance between accuracy, artifact and radiation dose, was a 3.75 mm collimation with pitch 3 and HQ algorithm.

B-0327 10:40

CT colonography-bowel wall visualisation and impact of scanning in supine and prone positions

M.H. Svensson, E. Svensson, M. Hellström; *Gothenburg/SE*

Purpose: The aim was to evaluate the impact of supine and prone scanning on the degree of bowel wall visualisation at CT colonography.

Methods and materials: After bowel preparation, 111 patients underwent CT colonography in the supine and prone positions. The quality of air-distension, degree of fluid redistribution between supine and prone scans, possible influence of stool and degree of overall colon visualisation were evaluated using scales. The depth of fluid levels was also measured.

Results: The entire colon was air-filled in the supine and prone positions for 18 % and 46 % of the patients, respectively. All patients had intraluminal fluid and 70 patients had residual stool. On combination of supine and prone datasets, for all colon segments except the sigmoid, 95 – 99 % of the patients had complete air-filling, and except in the ascending colon and caecum, intraluminal fluid was completely redistributed in at least 90 % of the patients. On overall evaluation, 30 patients (27 %, n = 110) had complete visualisation of the colon wall and 52 (47 %) had subtotal visualisation affecting one or two colon segments and/or "partly disturbing" stool.

Conclusion: Supine and prone scanning allowed redistribution of intraluminal fluid and air, which was necessary for complete visualisation.

B-0328 10:50

CT colonography (virtual colonoscopy) is preferred to conventional colonoscopy

M.H. Svensson, E. Svensson, M. Hellström; *Gothenburg/SE*

Purpose: The aim was to prospectively evaluate patient-acceptance of CT colonography and conventional colonoscopy concerning the factors of importance in the patients' preference for examination.

Methods and materials: Questionnaires were administered to 111 patients undergoing CT colonography followed by colonoscopy. Problems associated with each examination were evaluated on self-rated scales, and after completion of both examinations the preference for examination was evaluated by comparative questions.
Results: Of the patients with a preference, 69 % ($p = 0.002$) considered the colonoscopy to be the most difficult examination in overall terms, and 82 % would prefer CT colonography ($p < 0.0001$).
Among 108 patients with an opinion on both examinations, 54 % graded pain higher after the colonoscopy than after the CT colonography ($p < 0.0001$). The CT colonography was not painful according to 62 patients and fairly or very painful according to six. Most patients (86 %) reported discomfort from air-filling during CT colonography and 80 % preferred scanning in the supine position.
Conclusion: CT colonography was less painful than colonoscopy and was the preferred examination. Discomfort from air-filling of the colon was the major problem associated with CT colonography, but pain seemed to be decisive in the choice of examination.

B-0329 11:00

Assessment of colorectal cancer with contrast-enhanced CT colonoscopy after an incomplete fiberoptic colonoscopy

E. Neri, P. Giusti, L. Battolla, P. Boraschi, P. Rondine, P. Vagli, F. Falaschi, D. Caramella, C. Bartolozzi; *Pisa/IT*

Purpose: We aimed to evaluate the impact of pre-operative contrast-enhanced CT colonoscopy (CE-CTC) after incomplete fibreoptic colonoscopy (FC) in the assessment of patients with clinical suspicion of colorectal cancer.
Method and materials: Thirty-four patients presenting with distal occlusive colorectal carcinoma identified at FC, were prospectively evaluated with CE-CTC. In all cases FC failed to explore the proximal colon. All patients underwent surgery. Contrast enhanced CT study was performed after pneumocolon in the prone and supine position and CE-CTC was obtained with perspective surface rendering.
Results: CE-CTC demonstrated 39 colorectal neoplasms, located in the sigmoid colon (n = 16), descending colon (n = 13), splenic flexure (n = 3), transverse colon (n = 3), hepatic flexure (n = 2) and ascending colon (n = 2). Five lesions were synchronous cancers and contrast enhanced abdominal CT allowed the detection of hepatic metastases in 9 cases. CE-CTC findings were all confirmed at surgery. On the basis of CE-CTC findings, the surgical approach was changed to a total colectomy in the 5 cases with synchronous cancer and intra-operative metastasis resection was performed in 7 cases, by hepatic segmentectomy in 5 and thermal ablation in 2.
Conclusion: CE-CTC is superior to FC in the pre-operative assessment of colorectal cancer, since in a single session it detects synchronous cancers and provides a liver study for accurate mapping of metastases.

B-0330 11:10

Virtual colonoscopy in detection of colorectal polyps and carcinoma: A comparison with conventional colonoscopy

A. Oto, A. Deger, V. Gelebek, B. Oguz, B. Sivri, E. Ozarslan, A. Baykal, O. Akhan, A. Besim; *Ankara/TR*

Purpose: To compare the efficacy of virtual colonoscopy in detection of colorectal polyps with conventional colonoscopy in patients at high risk of developing colorectal cancer.
Method and material: Virtual colonoscopy was performed on the same day following conventional colonoscopy in 29 patients at high risk of developing colorectal cancer. Patients were scanned both prone and supine. Intravenous contrast was administered prior to prone scan. Axial, 2D MPR and 3D colonoscopic images were interpreted by two radiologists for localization, number and size of detected polyps. Results of virtual colonoscopy and conventional colonoscopy were compared individually for each polyp.
Results: Seventeen of 21 endoscopically proved polypoid lesions were detected in virtual colonoscopy. Sensitivity of virtual colonoscopy for all polyps was 81 %, for polyps greater than 10 mm was 92 %, for polyps between 6 and 9 mm in diameter was 75 % and for polyps smaller than 5 mm in diameter was 50 %. In adenomatous polyps, sensitivity of virtual colonoscpy was 81 %, in adenocarcinoma it was 100 % and in hyperplastic polyps it was 66 %. Proximal colon of two patients, which could not be evaluated with conventional colonoscopy due to distal obstructing lesion could be successfully evaluated by virtual colonoscopy.
Conclusion: Virtual colonoscopy is found to be a sensitive and comparable method to conventional colonoscopy in detecting polypoid lesions in patients at greatest risk of developing colorectal cancer especially for the polyps greater than 10 mm. Virtual colonoscopy also provides evaluation of proximal colon in distally obstructing lesions.

B-0331 11:20

3D MR colonography after exclusive intravenous administration of a hepatobiliary contrast agent

M.V. Knopp[1,2], F.L. Giesel[1], H. von Tengg-Kobligk[1], J. Radeleff[1]; [1]*Heidelberg/DE*, [2]*Bethesda, MD/US*

Purpose: Cross-sectional imaging of the colon has been recently introduced as CT or MR colonography. All methods rely on the aboral or oral administration of a contrast agent, which does change the physiological function of the colon.
Method/materials: While performing studies using a partially hepatobiliary excreted contrast agent (reported 2 – 4 %), Gd-BOPTA (Multihance, Bracco) we noted substantial colonic contrast 24 h pi. We subsequently performed a prospective study at 0.1 mmol/kg bw in six volunteers to determine the intensity and extend of hepatobiliary excretion and detectable gastro-intestinal enhancement at 1, 12, 24, 36, 48, 70, and 105 h post injection. No further preparation of the subjects was done.
Results: Intense, homogenous contrast enhancement within the colon was observed within 24 h in all subjects. The bowel stools revealed homogenous enhancement within the lumen indicating thorough mixing of content comparable to bile acids. The signal intensity of the liver parenchyma and within the gallbladder decreased after the first hour with an initial halftime of 10 – 15 h. The highest signal intensity in the colon was detected at 16 – 50 h post injection. The quality of enhancement was sufficient to enable 3D processing for virtual colonoscopy.
Conclusions: We established the feasibility of MR colonography using only an intravenous MR contrast agent with partial hepatobiliary excretion. This new diagnostic procedure will enable not only morphologic assessment of the colon, but also patho-/physiological studies on the transport kinetics of bile and stool without any preparation of the patient.

B-0332 11:30

Fecal tagging in MR-colonography

T. Lauenstein, S.G. Rühm, D. Schoenfelder, S. Bosk, J.F. Debatin; *Essen/DE*

Purpose: Colon cancer continues to be the second most common cancer. The apparent failure of colonoscopy screening reflects limited patient acceptance. Patients are fearful of the pain associated with colonoscopy, and are put-off by the unpleasant protocols required to clean the colon. We evaluated different means to obviate the need for colonic cleansing prior to MR-colonography.
Materials and methods: Three volunteers received standardized low fiber meals laced with 15 ml 0.5 molar Gd-DOTA, 2 g lactulose and 0.4 g dimeticon. As a control a fourth volunteer ingested the same meals without the paramagnetic contrast. All volunteers were imaged the following morning. Stool samples were collected before and up to two days after the experiment. Subsequently 5 volunteers were assessed after filling the colon with unenhanced water. These volunteers had been given an oral contrast agent (Micropaque, Guerbet) to assure dark stool. The colon of all examined volunteers was examined with a fast T1-weighted 3D GRE sequence. The second set of volunteers were examined following the administration of intravenous contrast paramagnetic contrast (Gd-BOPTA, 0.2 mmol/kg).
Results: Both methods resulted in the ability to assess the colonic lumen without prior colonic cleansing. Administration of Gd caused bright stool, which was indistinguishable from the Gd-containing enema, thus permitting an unhibited fly-through. The administration of Micropaque on the other hand caused dark stool, which became indistinguishable from the water enema on T1-weighted images.
Conclusion: Virtual colonoscopy without prior colonic cleansing is feasible. Tagging the feces with oral Gd-DOTA or oral Micropaque is well tolerated.

B-0333 11:40

Multi-planar MR colonography for assessment of colo-rectal lesions

W. Schima, H. Ringl, C. Österreicher, A. Ferlitsch, E. Schober, A. Maier, R. Schoefl, R. Poetzi; *Vienna/AT*

Purpose: To evaluate the diagnostic yield of multi-planar MR colonography (MRC) for detection of colorectal lesions.
Method and materials: MRC was performed in 15 patients following an enema with 2 litres of Ringer's solution, spiked with Gd-DTPA-BMA (1:100). After filling to the caecum, a breath-hold T1w 3D-GRE sequence (TR 4.6, TE 1.8, matrix 200 × 512) was performed in the coronal plane in supine and prone positions and in the axial plane, covering only the rectum and sigmoid colon. Results were correlated with the findings of conventional colonoscopy, performed within one day.

Results: MRC detected 80 % of polyps > 10 mm, and 33 % of the polyps 6 – 10 mm, but none of the polyps ≤ 5 mm. Assessment of coronal supine images alone revealed in 93 % of patients colonic segments which could not be evaluated due to stool and/or air bubbles. Combination of supine and prone acquisitions allowed evaluation of all colonic segments in all patients. Addition of axial MRC images improved assessment of the sigmoid colon in 53 %.
Conclusion: Multi-planar MR colonography performed in supine and prone positions improves the confidence and accuracy of the reader for detection of colorectal abnormalities.

B-0334 11:50

Magnetic resonance colonography vs. virtual colonoscopy for the detection of colonic polyps
E. Casciani, G. Gualdi, E. Polettini, G. Pappalardo, F.M. Frattaroli; *Rome/IT*

Purpose: Prompted by the disadvantages of conventional colonoscopy (CC), we compared the diagnostic ability of MR Colonography (MRC) only, Virtual Colonoscopy (VC) only, and a combination of MRC and VC for detecting polyps.
Material and methods: Seventy consecutive patients referred for CC underwent preliminary MRC using a 3D TFFE sequence with spoiling gradients. For the VC reconstruction, the MRC data were downloaded to a voxel workstation. The diagnostic ability of these techniques in detecting colonic polyps was determined, compared with that of CC, and related to the findings from histologic examination.
Results: No statistically significant differences in the detection of polyps were found between the three techniques. However, the combination of MRC and VC resulted in polyps detection rates that were greater than those MRC or VC alone. In detecting polyps, the combination of MRC and VC achieved good diagnostic ability (53 true-positive; 2 false-negative; 14 true-negative, and 1 false-positive). This yielded high sensitivity (96 %) and specificity (93 %), a good positive predictive value (98 %) and a negative predictive value of 87.5 %.
Conclusion: The combination of MRC and VC provides the greatest rates of detection of polyps and VC improves the specificity helping to distinguish normal folds from fixed raised lesions that are suggestive of polyps.

10:30–12:00 **Room H**

Interventional Radiology

SS 609a

Percutaneous tumor ablation

Chairpersons:
R.D. Garcia-Mónaco (Buenos Aires/AR)
K. Hiramatsu (Tokyo/JP)

B-0335 10:30

Should thermal ablation be offered to patients with colorectal liver metastases who have been downstaged by chemotherapy?
A.R. Gillams, W.R. Lees; *London/GB*

Purpose: < 25 % of patients with colorectal liver tumors respond to chemotherapy but the response is temporary < 6 months. We studied outcome in chemotherapy responders who subsequently underwent thermal ablation.
Materials and methods: Since 1995 we have performed thermal ablation in 101 patients of whom 31 had responded to chemotherapy by a reduction in the size and/or number of liver metastases on CT. 29/31 received systemic and 2 intra-arterial chemotherapy. 30 received 5 FU, 25 with folinic acid and 5 with Irinotecan, Mitomycin or Oxaliplatin. The other patient received Tomudex, Irinotecan and Oxaliplatin sequentially. All subsequently underwent thermal ablation to their residual liver metastases. 9/31 patients had optimal disease extent < 5, < 5 cm tumors and no extra-hepatic disease. Patients were followed at regular intervals until death. Survival analysis was performed stratified for disease extent at the start of thermal ablation. Survival statistics were compared to the 70 other patients.
Results: Median survival from diagnosis of liver metastases was 44 months for chemotherapy responders with optimal extent of disease (n = 9) and 32 months for those with more extensive disease (n = 22). There was no significant difference in survival between chemotherapy responders and the remainder, allowing stratification for disease extent. Median survival for the remainder was 49 months in the optimal disease group (n = 36) and 21 months for the others (n = 34).
Conclusion: Thermal ablation should be offered to patients who respond sufficiently well to chemotherapy to fulfill standard thermal ablation acceptance criteria.

B-0336 10:40

Optimisation of treatment strategy using cooled-tip radiofrequency electrodes in ex-vivo liver
A.R. Gillams, W.R. Lees; *London/GB*

Purpose: Rises in impedance, restrict energy deposition and efficacy of radiofrequency ablation. Different techniques have been tried to circumvent this. We performed multiple treatments in ex-vivo pig liver to optimise treatment strategy.
Methods and materials: Treatments were performed with both single and triple cluster, cooled tip electrodes. We compared pulsing, incremental step down and cessation of treatment at the first impedance rise. Incremental step down involves re-introduction of power following impedance changes but to progressively lower power levels. Initial power settings were 40, 50, 75, 100, 150 and 180 W. Treatment times varied from 55 – 600 s. In another experiment a radiofrequency splitter was employed to allow simultaneous activation of 4 single electrodes. Different electrode configurations and electrode distances were studied. The diameter of induced necrosis was measured.
Results: The majority of induced necrosis occurs during peak power prior to impedance rise. Maximal necrosis was produced by maximum power > 170 W, for < 600 s. Pulsing after impedance changes produced only a small increment in necrosis. Incremental step down was more beneficial. An alternative strategy of moving the electrode to a new position after the first impedance rise will maximise necrosis, but may not be the preferred technique. Using the Rf splitter, maximal necrosis was obtained with four electrodes spaced at 1 cm intervals in a square configuration.
Conclusion: The incremental step down technique maximised necrosis, and is preferable if electrode repositioning is undesirable. Cluster electrodes with 1 cm spacing are optimal but the practicalities of easy deployment require smaller spacing.

B-0337 10:50

Radiofrequency (RF) ablation of liver tumors with the Le Veen probe: Is roll off predictive of response?
P. Cabassa, R. Cuomo, R. Piazza, F. Simeone, L. Grazioli, L. Matricardi; *Brescia/IT*

Purpose: The purpose of this study was to determine the relation of roll-off (the dramatic rise in impedance that occurs following the application of sufficient power for an appropriate period of time during RF ablation) to local control of hepatic tumors.
Methods and materials: 20 patients (16 M, 4 F) with hepatic tumors (16 HCC and 4 metastases) were treated. Lesions ranged from 1.6 – 7.5 cm in maximum diameter. The 15 gauge Le Veen needle electrode (Radiotherapeutics, Mt View, Ca) was inserted percutaneously or during laparotomy with the use of sonographic guidance. Tumours larger than 3 cm were treated with overlapping burns. Patients were followed with contrast-enhanced, triple-phase CT. Contrast enhancement within the tumour on arterial phase scanning was considered consistent with residual tumour.
Results: Roll-off was achieved in 12/20 lesions (60 %). No local failures occurred when roll-off was achieved. 4/8 lesions without roll-off were completely ablated. There were four residual tumors at treated sites. In all four of these lesions none of the burns resulted in roll-off.
Conclusion: Local failure occurred in 50 % of lesion without roll-off. Therefore the lack of roll-off during RF ablation does not necessarily represent a failure and does not reliably predict treatment outcome.

B-0338 11:00

Radiofrequency ablation of liver metastases: Ultrasound or CT guidance?
D. Pickuth, C. Achilles, W. Weiwad, J. Richter, S. Heywang-Köbrunner, R. Spielmann; *Halle a. d. Saale/DE*

Purpose: Radiofrequency ablation of liver neoplasms is usually performed by using US guidance. The purpose of this study was to prospectively evaluate the potential benefit of CT-guided treatment.
Patients and methods: 18 patients with metastatic tumours of the liver received a single treatment of both US- and CT-guided percutaneous radiofrequency ablation to 32 lesions (lesion size 1 – 4.5 cm; median 2.5 cm). For follow-up purposes, contrast enhancement of liver metastases was measured with CT by digitally subtracting tumour data acquired during a non-enhanced phase from data acquired in a portal-dominant phase.

Results: 22/32 lesions (69 %) were easier to identify and follow under CT guidance, this was particularly true for lesions < 2 cm. US and CT were equivalent for lesion delineation. Sonographically, radiofrequency lesions appeared as hyperechoic areas with blurred margins during and shortly after treatment. With CT, however, the actual size of necrosis and the extent of induced coagulation could safely be determined at all stages. In addition, multi-slice spiral CT minimizes patient motion artifacts that have hindered acceptance of digital subtraction CT in clinical practice.
Conclusion: Radiofrequency procedures should be performed with CT rather than US monitoring as this improves detection of liver lesions, guidance of electrode placement and monitoring of energy delivered. The degree of contrast enhancement of a tumour correlates with its vascularity and thus might be used to gauge its response to radiofrequency ablation.

B-0339 11:10

Thermal ablation of malignant hepatic lesions with assistance of a computerized CT guidance system

T.K. Helmberger, N. Holzknecht, U.J. Schöpf, A. Stäbler, M.F. Reiser; *Munich/DE*

Purpose: To evaluate the feasibility of a virtual guiding system (CTGuide, CTG; Ultraguide, Israel) for needle placement in thermo therapy of malignant liver lesions.
Material and methods: 52 patients with 123 lesions underwent percutaneous radiofrequency or laser induced thermo therapy. Because most of the lesions were hardly seen by US, CT was used for imaging where a lesion was depicted during one imaging phase at least (i.e. unenhanced, arterial, portal-venous phase). The CT images were transferred to the CTG system and were "3D correlated" with electromagnetic markers fixed at the patient and at the probe. The probe's movement was displayed as trajectory together with the current position of the needle tip virtually on the CT images. Thus, the puncture could be performed entirely outside of the gantry. Control scans were obtained for verification of the needle position.
Results: All needle placements succeeded with the virtual guidance. In 53 % of the lesions a double oblique approach was necessary because an in-plane or simple oblique approach was not possible (e.g. dome of the liver, area medial from the cava). Even with a skin-lesion distance of up to 20 cm in some cases the maximum needle deviation was only 1.5 cm from the target mostly caused by irregular breathing of the patient.
Conclusion: CTG proved to be a very helpful tool for accessing lesions at unfavorable locations. In comparison to placements done with CT-fluroscopy, CTG may preserve also the patients and interventionalists from radiation dose during the procedure.

B-0340 11:20

Thermal ablation of neuro-endocrine liver metastases

A.R. Gillams, W.R. Lees; *London/GB*

Purpose: There are few effective treatment options for patients with neuroendocrine liver metastases. We report our experience of thermal ablation in these patients.
Methods and materials: 17 patients were treated. The primary lesions were carcinoid 8, gastrinoma 4, insulinoma 1, adrenal 2, somatostatinoma 1 and vipoma 1. A total of 34 treatments were performed, 17 with interstitial laser therapy and 17 with radiofrequency. Lesion diameter was 1 – 8 cm. Six patients were treated to relieve symptoms secondary to hormone production.
Results: 4/6 patients treated for control of hormone production derived symptomatic benefit. Two did not, one with > 12 lesions and one with advanced carcinoid, pulmonary stenosis and right heart failure. This patient who was terminally ill if left untreated had an uneventful procedure but suffered a carcinoid crisis at 40 hours and did not recover. One patient with a cortisol secreting tumour became temporarily Addisonian. The patient with an insulinoma became hyperglycaemic (glucose 15 mmol/l) during the procedure but normal glucose homeostasis was spontaneously restored at 5 days. One patient with a bilioenteric anastomosis developed an abscess requiring percutaneous drainage. Two patients who initially presented with < 2 lesions developed > 20 metastases on follow-up. Local control of the extent of liver involvement was achieved in 7. 1 patient with a 5 cm, aggressive, poorly differentiated colonic carcinoid recurred such that further thermal ablation was not possible.
Conclusion: 4/6 patients derived significant clinical benefit from reduced hormone secretion. Control of the extent of liver disease was achieved in 7.

B-0341 11:30

Survival following thermal ablation: Does more complete ablation result in a survival advantage?

W.R. Lees, A.R. Gillams; *London/GB*

Purpose: Changing technology has resulted in improved technical success and more complete ablation of colorectal liver metastases. This study looks at the impact on patient survival.
Methods and materials: Since 1995, 101 patients with colorectal liver metastases have been treated with thermal ablation. 40 received interstitial laser photocoagulation (ILP), 22 received ILP followed by radiofrequency (RF) and 39 were treated with RF only. Tumour size and number were recorded. Kaplan Meier curves were generated for survival depending on disease extent. For the purposes of this analysis all those receiving RF ± ILP were considered together. All survival times are calculated from time of first thermal ablation.
Results: There was no significant difference in tumour size, number or length of follow-up between the two groups. Median survival for patients with tumours 0 – 3 cm in size was 34 months in the RF group (n = 16) and 24 months in the ILP group (n = 7), for tumours 3 – 4.5 cm, median survival was 31 months RF group (n = 16) and 23 months ILP group (n = 9) and for tumours > 4.5 cm 26 months RF group (n = 11) and 12 months ILP group. For patients with optimal disease extent ≤ 5 metastases, < 5 cm and no extra-hepatic disease the median survival was 34 months and the 3 year survival 48 % in the RF group (n = 28) and for the laser group the median was 23 months and 3 year survival 13 % (n = 16).
Conclusions: Improved technical efficacy has translated to improved survival for those without extrahepatic disease.

B-0342 11:40

Radiofrequency thermal ablation of liver malignancies: Assessment of treatment outcome by volume-rendered spiral CT

D. Cioni, R. Lencioni, E. Neri, L. Crocetti, P. Vagli, F. Donati, C. Franchini, M. Perri, C. Bartolozzi; *Pisa/IT*

Purpose: To investigate the usefulness of volume-rendered spiral CT in the assessment of the outcome of radiofrequency (RF) thermal ablation of liver malignancies.
Material and methods: Twenty patients with 26 liver tumors (18 hepatocellular carcinomas, HCC, and 8 colorectal metastases) ranging 1.8 – 4.9 cm in diameter underwent single session RF ablation. A 50 W generator and expandable electrode needles with 4 – 7 lateral-exit jackhooks (RITA, Medical System) were used. Spiral CT examinations included unenhanced and contrast-enhanced phases. Images obtained were volume-rendered by using a dedicated software tool (Advantage Windows 3.1; GE, Medical System) that allowed simultaneous visualization of liver parenchyma and vessels. A minimum follow up period of six months, including CT studies repeated at 3-months intervals, was used as term of reference in cases with complete ablation. CT guided percutaneous biopsy was performed in cases of suspected incomplete necrosis.
Results: Complete ablation was diagnosed by volume-rendered spiral CT in 16 of 18 HCC and 5 of 8 metastases and confirmed by percutaneous biopsy or follow-up studies in all cases. In cases of partial necrosis volume-rendered spiral CT enabled precise mapping of the area of viable tumor and demonstrated the relationship between tumor and surrounding vessels. These informations were used in the 5 cases of incomplete ablation to plan further RF treatment. Complete ablation was achieved in 4 of the 5 cases.
Conclusion: Volume-rendered spiral CT is an accurate tool for the assessment of the outcome of RF ablation of liver malignancies and enables precise retreatment in cases of incomplete ablation.

B-0343 11:50

A randomized comparison of percutaneous ethanol injection and radiofrequency thermal ablation for the treatment of small hepatocellular carcinoma

R. Lencioni[1], H.-P. Allgaier[2], D. Cioni[1], M. Olschewski[2], L. Crocetti[1], J. Laubenberger[2], A. Paolicchi[1], H. Blum[2], C. Bartolozzi[1]; *[1]Pisa/IT, [2]Freiburg/DE*

Purpose: The aim of this randomized study was to assess the efficacy of radiofrequency (RF) thermal ablation versus percutaneous ethanol injection (PEI) for the treatment of small hepatocellular carcinomas (HCC).
Material and methods: One hundred and two HCC patients with 141 tumor lesions were treated with either PEI (n = 50) or RF (n = 52). Treatment was considered successful in patients without viable HCC lesions detected by contrast-enhanced spiral CT.

Results: Complete tumor necrosis could be achieved in 83 % (60/72) of HCC lesions after 1 PEI cycle, and in 90 % (63/70) of HCC lesions after a single RF. Mean follow-up was 22.4 ± 8.6 months in the PEI group and 22.9 ± 9.4 months in the RF group, respectively. The 1- and 2-year survival rates were 96 % and 88 %, respectively, in the PEI-group and 100 % and 98 %, respectively, in the RF-group (univariate relative risk [RR] = 0.20, 95 % confidence interval [CI] (0.02 – 1.69), p = 0.138). One- and 2-year local recurrence free survival rates were 83 % and 62 %, respectively, in the PEI group as compared to 98 % and 96 %, respectively, in the RF group (univariate RR = 0.17, 95 % CI (0.06 – 0.51), p = 0.0016). One- and 2-year event free survival rates were 77 % and 43 %, respectively, for PEI patients and 86 % and 64 %, respectively, for RF patients (univariate RR = 0.48, 95 % CI (0.27 – 0.85), p = 0.012). No serious side effects or complications were observed in both treatment groups.
Conclusion: For the treatment of small HCCs RF is comparable to PEI with respect to early survival, but superior to PEI with respect to local recurrence free and event free survival.

10:30–12:00 **Room I**

Abdominal and Gastrointestinal

SS 601c

Stomach

Chairpersons:
F.-T. Fork (Malmö/SE)
A.H. Freeman (Cambridge/GB)

B-0344 10:30

Potential diagnostic importance of incidentally found gastrointestinal wall thickening at abdominal ultrasound
K. Kivimäe, P. Ross, P. Raudvere, E. Purde, M. Meldre, S. Nazarenko; *Tallinn/EE*

Purpose: Assessment of diagnostic importance of gastrointestinal (GI) tract wall thickening incidentally found at transabdominal ultrasound (US).
Methods and materials: A retrospective analysis of all transabdominal US examination reports (total 19 075) performed in our institution during the period from August 1998 to July 2000 was carried out. Out of 19075 cases a group of 30 (17 female and 13 male; age 52 – 87) patients was identified, who had uncharacteristic non-acute complaints, no clear diagnosis prior to US and in whom incidentally GI wall thickening of 7 – 20 mm was found. In all cases, transabdominal US had been the first radiological examination. In all cases, US findings were compared with histological results and with available radiological and endoscopic examinations.
Results: Further investigations revealed following diseases in observed 30 cases with GI tract wall thickening: malignant neoplasms (18 cases), lymphoma (1 case), benign neoplasms (2 cases), inflammatory bowel disease (5 cases), diverticulitis (2 cases) chronic gastritis (1 case) and peritoneal adhesions (1 case).
Conclusion: Diagnostic importance of abdominal US in detecting GI wall thickening should not be underestimated in clinical management of patients with uncharacteristic non-acute complaints and unclear diagnosis.

B-0345 10:40

Virtual gastroscopy: Technical features, clinical results and new developments
V. Panebianco, C. Catalano, A. Laghi, I. Sansoni, R. Alcetta, F. Fraioli, R. Passariello; *Rome/IT*

Purpose: To develop an examination protocol for virtual endoscopy (VE) of the stomach after CO_2 distention and to identify advanced gastric carcinoma, according to Borrmann's classification, based on tumour morphology.
Method and materials: 29 patients with gastric diseases underwent virtual endoscopy of the stomach. The stomach was distended with CO_2, by means of gas producing powder used for double contrast upper GI studies (Duogas, Bracco), after intra-muscular injection of 20 mg of hyoscine-n-butyl-bromide. All patients underwent a spiral CT volume zoom examination (120/130/2.5 mm/3 mm/15 mm/0.5 s/3 mm – Kv/Mas/slice coll/slice width/feed rot/rot time/incr). In 5 cases spiral CT was repeated in the prone position due to limited gastric distention by air. Fibreoptic endoscopy was performed within 1 week. We found good correlation with surgical specimens in 13 cases. Real time VE views were reconstructed using volume rendering technique with a dedicated workstation (Silicon Graphics O2) and specific software (Vitrea 2.1 – Vital Images), and interpreted together with axial images by two Radiologists.
Results: Image quality was graded as optimal in 27 cases. In 2 cases the stomach was not distended. VE correctly depicted intrinsic pathology (ulcerative lesions n = 14, vegetating lesions n = 10, benign lesions n = 3).
Conclusion: VE enables correct depiction of gastric lesions combining axial CT and VE images (perigastric tumour involvement, distant metastases). It has a potential role in replacing the barium study and for use in patients with surgical gastric exclusion.

B-0346 10:50

Radiological diagnosis in patients after adjustable gastric banding
R. Peer, H. Weiss, B. Labeck, S. Peer, F. Aigner, W. Jaschke; *Innsbruck/AT*

Purpose: Laparoscopic adjustable gastric banding is a well established low risk treatment option in patients with morbid obesity and has a high therapeutic efficiency. The value of the barium swallow in diagnosis of postoperative complications like leackage, pouch-dilatation, ulceration and migration of the band is presented.
Materials and methods: In the last two years 200 patients with morbid obesity were treated with adjustable gastric banding. Fluoroscopic controlls were obtained with a barium swallow at 6 and 12 months after the operation.
Results: In 8.5 % of patients complications were seen. 12 cases of port disconnection, 5 cases of band migration and 12 pouch dilatations were documented. In some patients a correlation with spiral CT of the esophagogastric junction was obtained.
Conclusion: With rising numbers of patients receiving an adjustable gastric band for treatment of morbid obesity, complications may rise also. The barium swallow proved to be an easily performed and cheap method for the recognition of early and late complications, which is necessary for institution of early minimally invasive surgical correction.

B-0347 11:00

Rare mesenchymal tumors of the stomach: CT findings
G. Tognini, F. Ferrozzi, G. Marchesi, S. Armaroli, P. Pavone; *Parma/IT*

Purpose: To evaluate the CT efficacy in characterizing rare mesenchymal gastric tumors.
Materials and methods: We reviewed CT scans of 67 patients (29 males, 38 females) with rare mesenchymal gastric tumors. We demonstrated 39 stromal tumors (31 myoid, 4 neural, 2 with both differentiation, 2 with no differentiation) 19 lipomatous tumors (14 lipomas, 1 angiolipoma, 3 liposarcomas, 1 teratoma) 6 sarcomas (5 Kaposi's sarcomas, 1 malignant fibrous histiocytoma), 2 vascular tumors (1 lymphangioma, 1 hemangiopericytoma), 1 plasmocytoma. Morphological and histopathologic parameters were compared.
Results: Benign myoid tumors showed sizes < 5 cm, intermediate forms had sizes between 6 and 10 cm, the malignant ones sizes > 10 cm; the Schwannomas were pseudocystic with peripheral enhancement, neurofibroma showed homogeneous hypovascular lesions; the malignant neurogen forms and the tumors with dual differentiation showed infiltrating growth. The lesion without differentiation showed "benign morphology". The lipomas showed homogeneous negative HU numbers, angiolipoma showed strong enhancement of its vascular component, teratoma was a solid mass with fatty cystic and calcified components, Kaposi's sarcomas showed non specific thickening of gastric wall, fibrous malignant histiocytoma showed mixed appearance with necrotic changes, lymphangioma was a small submucosal nodular lesion showing liquid/paraliquid HU numbers, plasmocytoma was a large lesion with non specific morphologic appearance, hemangiopericytoma was a large necrotic mass.
Conclusions: CT features may be useful in characterizing some rare mesenchymal gastric tumors.

B-0348 11:10

CT/MRI features of portacaval space metastases of gastric adenocarcinoma
P.Q. Min, L. Zhang; *Chengdu/CN*

Purpose: To evaluate CT/MRI features of portacaval space (PCS) metastases of gastric adenocarcinoma.
Materials and methods: We retrospectively reviewed CT/MRI images of 22 cases (CT 18, MRI 4) with PCS lymphadenopathy resulting from gastric adenocarcinoma metastases, and the correlations of the PCS abnomalities with the metastases occurring in the hepatogastric ligament (HGL), hepatoduodenal ligament (HDL) and the recurrent foci of the remanent stomach as well.
Results: The enlarged portacaval nodes (PCN) were shaped elliptical (15/22, 68 %) and irregular (7/22, 32 %), sized 14 – 65 mm (mean 36 mm) in their maximum diameter, located within (16/22, 73 %) or beside (6/22, 27 %) the PCS, soft tissue

density with rim enhancement on CT, low signal intensity in T1WI but a little high in T2WI on MRI. Lesions occurred in PCS, HGL and/or HDL and the recurrent foci of remanent stomach were shown as a continuum in 19/22 (86 %), while in the rest 3/22 (14 %) were separated.
Conclusion: The PCS lymphadenopathy can be a sign of CT/MRI images in metastases resulting from gastric adenocarcinoma, in which, the lesions mostly involve the PCS, HGL and/or HDL simutaneously, and may present with the recurrent foci of remanent stomach showing as a continuum.

B-0349 11:20

Preoperative staging of gastric cancer with multislice CT: Correlation with surgical and histopathological work-up. Preliminary results
A. Ba-Ssalamah, P. Pokieser, T.H. Helbich, M.T. Schmook, G. Bischof, F. Wrba, G. Lechner, M. Prokop; *Vienna/AT*

Purpose: To describe our preliminary results for staging of gastric cancer using multislice CT in comparison with post-operative histopathologic work-up.
Material and methods: Up to now, we examined 14 patients with endoscopically detected gastric cancer using a hydro-CT technique combined with multislice scanning. The stomach was distended by 1 – 1.5 l water immediately prior to the examination, and a spasmolytic agent was administered I.V. The upper abdomen was subjected to multislice scanning with 4 × 1 mm using an individually optimized biphasic contrast material injection protocol (testbolus injection). In addition to axial sections, thin coronal and sagittal images were reconstructed. CT findings were analyzed according to a standardized evaluation form and correlated with endoscopic, surgical and histopathologic results.
Results: All tumors were correctly detected and localized. None of the tumors was a T1 stage. A smooth gastric serosal surface predicted lack of infiltration of the perigastric fatty tissue (5 of 14 cases, T2). A markedly irregular serosal contour predicted fatty infiltration in 4 of 14 cases. Unsharp definition of the serosa, however, occurred in T2 tumors associated with lymphangitis and in T3 or T4 tumors (10 cases). Pathologic lymph nodes tended to be round with more enhancement in 36 of 47 pathologic nodes. N-staging with CT was correct in 7 of 9 patients in whom total gastrectomy was performed.
Conclusion: Our preliminary results suggest that there are highly specific findings on multislice CT that can help in staging of gastric cancer.

B-0350 11:30

Spiral CT evaluation following Whipple's operation: Improved visibility of the afferent loop after biliary contrast medium
P. Stumpp, R. Klöppel, T. Kahn; *Leipzig/DE*

Purpose: To improve CT-visibility of the afferent jejunal loop in patients who have undergone Whipple's operation by using biliary contrast medium and thereby allowing distinction between normal postoperative changes and local tumor recurrence.
Materials and methods: In a prospective study 15 patients received additional 100 ml biliary contrast medium (Biliscopin®) 30 – 60 minutes prior to a routine postoperative abdominal helical CT after Whipple's Operation. A qualitative and semiquantitative (no – weak – strong enhancement) evaluation of the enhancement of the jejunal loop was performed.
Results: In all patients biliary contrast medium could be successfully applied without complications. In all but one patients the afferent loop showed enhancement and allowed an easy identification. In two patients enhancement was visible but not very intense. Good enhancement was seen in all other patients.
Conclusion: Intraluminal enhancement after i.v.-application of biliary contrast medium allowed identification of the afferent jejunal loop, whereas unenhanced structures had to be further evaluated. Biliscopin® improved visibility of the afferent loop in almost all cases and thereby made distinction of normal postoperative changes from local tumor recurrence easier and more secure. For optimal enhancement CT-scans should follow about 30 to 60 minutes after i.v. application of Biliscopin®.

B-0351 11:40

Assessment of gastric carcinomas: Helical hydro-CT findings and pathologic correlation
M. Bankaoglu, M. Basak, M. Yilmazcan; *Istanbul/TR*

Purpose: To assess the diagnostic role of helical hydro-CT in patients with gastric cancers.
Method and materials: 31 patients with suspected gastric carcinomas on routine radiologic and gastroscopic examination were examined by helical hydro-CT preoperatively. All patients were evaluated by non-enhanced and contrast enhanced spiral CT. Water was given orally for gastric distention and hyoscine-n-butylbromide was used as an anti-peristaltic agent. TNM staging was performed in suspected lesions preoperatively.
Results: Hydro-CT was able to detect all lesions. 30 patients were positive for tumour by hydro-CT. 29 of the 30 cases had a histological diagnosis of cancer (96.5 %). One of the cases reported as suspicious was confirmed as an adenomatous polyp. One of our pathological cases was reported as a benign ulcer. Subgroups in N staging were considered separately for histopathologic correlation as we had detected a variety of lymph nodes in 20 of the 29 pathologic cases (68 %). Our TM staging was correct in 28 of the 30 cases (93.3 %).
Conclusion: Helical hydro-CT is more effective in staging gastric malignancies when performed with adequate technical parameters.

B-0352 11:45

Menetrier's disease in Childhood
S. Chakraborty, D. Casson, H.M.L. Carty; *Liverpool/GB*

Purpose: Menetrier's disease is a rare disorder in the paediatric population. We report three cases of Menetrier's disease to raise the awareness of this disease which might give rise to diagnostic confusion.
Materials and method: Three cases seen over a span of 20 years (males aged 3.5, 7 and 3 years) presented with generalised oedema, hypoalbuminaemia. All three had hypertrophic gastric rugae in barium studies. Two cases were confirmed by endoscopy. One case was followed up with ultrasound.
Discussion: Menetrier's disease in childhood is a shortlasting, self-limiting disease as compared with its adult counterpart. Its aetiology is unknown, though it is now thouhgt to be linked with CMV infection. The clinical presentation of all these cases suggested nephrotic syndrome. The absence of proteinuria lead to further investigations which revealed the diagnosis.
Conclusion: Childhood Menetrier's disease (also called protein losing gastropathy) is rare but it can give rise to considerable diagnostic confusion. Bowel ultrasound is a quick and easy way to rule out this condition. Ultrasound is also helpful in follow-up of these cases.

B-0353 11:50

Endoscopic ultrasonographical diagnosis of the myogenic submucosal tumor of the stomach: An interpretation experiment
H. Natori, K. Hirata, X. Sun, M. Mitani, H. Inomata, F. Shiramatsu, J. Teramoto; *Sapporo/JP*

Purpose: Evaluation of diagnostic ability of the endoscopic ultrasonography for differential diagnosis of the submucosal myogenic tumor was performed with interpretation experiment.
Methods and materials: 48 cases of pathologically proven submucosal myogenic tumors were studied by Olympus GFUM3 and GFUM20 endoscopic ultrasonograph. Maximal diameter, margin of the tumor, internal cyst, texture of internal echo were selected as findings for the score. Total reading score were compared with pathological diagnosis. Reading score were designated 0 for benign myoma, and to 6 for malignant myosarcoma. Results of the interpretation experiments by 16 interpreters were analyzed with Receiver Operating Characteristic (ROC) analysis.
Results: Result among 16 interpreters distributed sensitivity 70 to 100 % and specificity 57.9 to 86.8 % by the discrimination at the total reading score of 3. Experienced interpreters revealed better result than that of novice. However, few rotating doctors also have gotten good results. The design of reading sheet was suited for this study in differentiation of myosarcoma or myoma of the stomach.
Conclusion: Study on interpretation experiment in differential diagnosis of the submucosal myogenic tumor of the stomach revealed usefulness of the endoscopic ultrasonography.

B-0354 11:55

MR-Imaging of gastric emptying induced by Erythromycin
T. Lauenstein, S.G. Rühm, M. Goyen, J. Barkhausen, J.F. Debatin; *Essen/DE*

Purpose: Erythromycin, employed in small, non-antibiotic doses has been found to be a gastrointestinal prokinetic agent. The aim of this study was to assess the influence of Erythromycin on gastric emptying by using MR imaging.
Materials and methods: Five healthy volunteers with no history of gastrointestinal disorder ingested 500 ml of a high caloric, liquid nutrient, diluted with Gd-DTPA (1:50) after an eight hour fast. Gastric emptying was determined every 5 minutes after ingestion up to 30 minutes with a series of coronal, T1-weighted 3D GRE (TR/TE/flip 2.0/1.0/20°) scans. The examination was performed on two separate

days with and without i.v. application of 50 mg Erythromycin immediately after oral ingestion of the liquid. Gastric volumes and filling of the small bowel were quantified on the 3D data sets.
Results: The gastric lumen were fully imaged in all 10 exams. Initial gastric volumes with and without Erythromycin were identical. Administration of Erythromycin did result in a significantly faster decrease of gastric volume ($p < 0.05$). Similarly, Erythromycin resulted in vastly more small bowel filling of the liquid nutrient.
Conclusion: Gastric emptying is accelerated by i.v. application of Erythromycin. These results will be used as reference standards of MRI in prospective studies of gastric emptying in patients with gastric motility disorders. Furthermore, Erythromycin can be used to maximise contrast passage into the small bowel for subsequent imaging.

10:30–12:00 **Room K**

Interventional Radiology

SS 609b

Venous intervention and arterial access

Chairpersons:
R.F. Dondelinger (Liège/BE)
E. Zeitler (Nuremberg/DE)

B-0355 10:30

Mediastinal wallstents in malignant superior vena cava syndrome
H.-P. Dinkel, B. Mettke, D. Do, J. Triller; *Berne/CH*

Objective: Superior vena cava syndrome (SVCS) is the consequence of obstruction of blood flow through the superior caval vein which is due to a malignant tumor in most cases. We retrospectively evaluated the result of stent therapy in this entity
Material and methods: During a 9-year interval consecutive 51 patients with malignant SVCS (80 % due to bronchial carcinoma) were treated with wall stents ("rolling membrane" Schneider, Boston Scientific). 11 patients had complete occlusions, 40 partial obstructions. In 22 patients stents were bilaterally placed into the brachiocephalic vein. Clinical follow-up was 6 – 24 months.
Results: Primary technical success was achieved in 46 of 51 (90 %) cases. In 5 cases technical result was less than optimal (n = 2) or failed (n = 3). Complications were observed in 17 von 51 (33 %) patients. Minor complications were stent thrombosis (n = 7), stent dislocation n = 7, and tumor ingrowth (n = 2). These complications were treated by coaxial stenting successfully. One major complication happened (pericardial tamponade caused by stent migration through the caval vein).
Conclusion: Stent placement rapidly alleviates the symptoms of SVC syndrome and improves the patient's quality of life. The method is very successful with a relatively low complication rate. Recurrences can be treated with further radiographic interventions.

B-0356 10:40

Percutaneous angioplasty in venous stenosis and occlusion after thrombosis, trauma or iatrogenically enduced
K.-L. Hajeck, C. Müller-Leisse, R. Janßen, A. Kippels; *Mönchengladbach/DE*

Purpose: It was the aim of the following study to determine the feasibility of percutanous intervention in patients with chronic, traumatic or iatrogen venous stenosis or occlusion.
Material and methods: 10 patients with symtomatic lower extremity venous hemodynamics and stenosis or occlusion of either the femoral and/or iliacal vein were introduced in our institution between December 1997 and October 1999. Recanalization was achieved by wire and catheter in all. Angioplasty was performed with balloon dilatation and implantation of Wall-Stents in each, with an additional Palmaz-Stent in one. In 6 of the patients the stent was placed across the hip joint space. All patients were anticoagulated.
Results: The primary technical and clinical success rate was 100 %. Each patient had either improvement of his complaints or was free of symptoms. The stents, which had been placed across the joint space demonstrated no change in configuration even unter maximal hip flexion. At follow-up after 12 to 20 months 8 of 10 patients were still without symptoms and free venous drainage was documented. In one patient, in whom the Palmaz stent had been implanted, there was restenosis because deformation of the stent. A Wall stent was implanted and the restenosis was cured. In the other case reocclusion had happend because of derangement in coagulation.
Conclusion: Percutanous angioplasty of venous stenosis and occlusions in chronic, traumatic or iatrogenic disorders of the femoral and iliac veins is feasible if anticoagulation is appropriate. Flexible stents can be placed across the hip joint without complaints.

B-0357 10:50

Atypically high survival in critically ill (Child C) patients following TIPS for variceal haemorrhage
K. El-Haddad, T. Lacina, M. Williams, D. Patch, J. Tibballs, T. Watkinson; *London/GB*

Purpose: To evaluate the 30 day survival in critically ill patients following TIPS procedure in our institution and to redefine the indication and the prognostic variables.
Materials and methods: 249 TIPS procedures were performed at our institution between 1992 and 2000. We reviewed the results of 120 cases which were performed for acute or recurrent variceal bleeding in patients with Child C liver disease. 86 % (n = 103) were emergency procedures, with 50 % requiring assisted ventilation. Uncovered Nitinol stents were used and dilated to 8 mm. Further dilatation was only performed if variceal filling persisted or if the PSG remained above 15 mmHg.
Results: Our primary success rate (PSR) was 99 %. 30 % of the patients (n = 36) died within 30 days of the procedure due to re-bleeding or due to the underlying liver disease. In those patients who survive the first 30 days (70 %, n = 84) the primary patency rate was 86 %. Among those who survived the subsequent 6 months the secondray patency rate was 76 %. Of these 23 % (n = 27) required a total of 39 re-interventional procedures (18 stent stenosis and 9 stent occlusion).
Conclusion: TIPS is an effective treatment for uncontrolled variceal haemorrhage. Our 30 day survival rate of 70 % is considerably higher than that of 50 % qouted in the literature for this patient group. The PSR and PPR are not significantly different from those reported in more inhomogeneous patient groups. Peri-procedural assisted ventilation was not a significant predictor for poor outcome.

B-0358 11:00

The effects of endoluminal irradiation on the healing response of a PTFE-covered transjugular intrahepatic portosystemic shunt prosthesis
K.A. Hausegger, H. Portugaller, J. Tauss, P. Schedlbauer, H.A. Deutschmann, H. Stranzl, G. Stücklschweiger; *Graz/AT*

Purpose: To evaluate the performance of a PTFE-covered TIPS endoprosthesis in a swine-model.
Material and methods: The study was designed for 10 pigs. For TIPS creation a PTFE-covered-TIPS-endoprosthesis (Viatorr, Gore & Ass) was used. The animals were divided into 2 groups. Group 2 received intraluminal irradiation of 18 Gy with ^{192}Iridium. Group 1 served as the control group without irradiation. Angiographic evaluation of the TIPS was performed every 2 weeks, animals of both groups were sacrificed every 2 weeks and gross specimen, histological evaluation, and scanning electron-microscopy was performed.
Results: TIPS insertion was successful in all animals. 2 pigs died early due to procedural complications. One animal (group 1) developed encephalopathy and died 1 week too early (seventh week), 1 animal (group 2) scheduled for 6 week survival showed shunt occlusion after 2 weeks and was killed thereafter. The observation period was 8-weeks at maximum. All group 1 animals showed a patent TIPS. In group 2 one shunt occluded after 2 weeks, in another animal a 60 % midshunt stenosis was observed at the 2 week control. In group 1 all implants were firmly adhered to the liver tissue. The luminal surface gradually became covered by fibrous connective tissue which was covered by endothelium. In group 2 the implants were partially adhered or non-adhered to the liver and large thrombi were seen in 2 implants. Intimal necrosis in the host vessel was seen in one animal.
Conclusion: The endoprosthesis used in the study revealed good TIPS patency in a swine-model without radiation. Application of 18 Gy intraluminal irradiation with ^{192}Iridium seems to impare the natural healing process.

B-0359 11:10

Initial results of a newly designed e-PTFE covered stent-graft for TIPS
V. Chabbert, P. Otal, T. Smayra, P. Chemla, J.-P. Vinel, K. Barange, M.-I. Millan, F. Joffre, H. Rousseau; *Toulouse/FR*

Purpose: To assess the clinical and technical results obtained with the newly designed e-PTFE stent-graft (W.L. Gore) used for transjugular intrahepatic portosystemic shunts (TIPS).
Materials and methods: Twenty patients with cirrhosis (twelve of alcoholic aetiology, three from viral hepatitis C, two from both of these causes and three from other aetiologies) at Child-Pugh's class A (n = 8), B (n = 7), or C (n = 5), with a

history of oesophageal variceal bleeding (n = 11), refractory ascites (n = 5), or both (n = 4), were included in this prospective phase-I study. Six patients had recurrent stenosis of a previous TIPS. In the other 14 patients this was the first TIPS procedure. The stent-grafts were inserted under general anaesthesia, using a standard technique. The prostheses used had a 2 cm non-covered and a 4 – 10 cm e-PTFE-covered portion and extended from the portal vein to the ostium of the hepatic vein. Patency was assessed at discharge and follow up with doppler US was carried out at 1, 3, 6, 12 months. Venography with pressure gradient measurement was performed at six months and at other times when necessary.
Results: After TIPS placement, portosystemic pressure gradient dropped from 18 to 5 ± 4 mmHg. There was two cases of segmental liver infarction, one case of haemoperitoneum folowing hepatic vein injury and one case of encepholopathy. The devices are still patent.
Conclusion: The e-PTFE stent-graft can be deployed accurately in TIPS with 100 % immediate technical success.

B-0360 11:20

Aspiration of acute pulmonary embolism with a new aspiration device: First clinical results with the Oasis system
F. Bergen, Z. Puskas, M. Trompeter, P. Reimer; *Karlsruhe/DE*

Purpose: To study the utility of a new aspiration device for treatment of acute pulmonary embolism.
Method/materials: Aspiration procedures were performed in 8 patients (age 51 – 78 years) following diagnosis of acute pulmonary embolism with contrast-enhanced spiral-CT. Only patients with thrombotic material in the main pulmonary artery or first order branches were and clinical symptoms for less than two weeks were considered. A flexible 8 Fr introducer sheath was placed through the right internal jugular vein and positioned in the pulmonary trunk. The Oasis device (Boston Scientific) was advanced over a selectively placed 18″ steel wire (Hi-Torque, Mallinckrodt). Multiple passages (5 – 10) of the device with a flow rate of 2.5 ml/s with a total volume of 500 – 1000 ml saline were performed. The procedure time varied between 60 – 120 min. Patients were closely monitored for blood pressure, heart rate, and oxygenation.
Results: Oxygen saturation improved in all patients in the order of 5 – 10 %. A large amount of thrombotic material could be removed and pulmonary perfusion was significantly improved in all patients. Follow-up scintigraphy demonstrated an improvement in pulmonary ventilation and perfusion.
Conclusions: Aspiration of pulmonary embolism with the new Oasis aspiration device appears to be a clinically effective tool in this first series of patients. These initial results encourage treating further patients with this new device.

B-0361 11:25

Cost-benefit assessment of IVC filter placement (IVCFP) in cancer patients
P.Y.R. Marcy, N. Magné, P.Y. Bondiau, K. Benezery, B. Descamps; *Nice/FR*

Purpose: To evaluate the costs and benefits of IVCFP in advanced cancer patients.
Methods and materials: This retrospective study (1994 – 2000) analyzed the efficacy (absence of clinical recurrence of pulmonary embolism) of IVCFP for thirty cancer patients (mean age: 66 a), with a grade III or IV tumor (94 %) according to the AJCC classification. The reference strategy consisted of an estimation of cost-units by setting values for Relative Cost Indices (RCI). The cost ratio of IVCFP was obtained by dividing the cost of the procedure (= 53 RCI) by the mean cost of the hospital stay.
Results: IVCFP was successfully performed via a jugular (n = 12) or a femoral access. The mean follow-up was 162 days (range 2 – 651). The mortality rates were respectively 27 %, 44 %, 60 % at one, three and six months. Two major complications (suprarenal filter thrombosis with renal failure) and one groin hematoma occured. Invasive palliative procedures and chemotherapy courses were subsequently performed in 53 % of the patients. There was no evidence of recurrent pulmonary embolism. The relative cost of IVCFP represented 2 % of the entire cost of hospitalization.
Conclusion: IVCFP is effective and cost-effective. A low-thrombosis-rate device is especially advocated for extensive IVC thrombosis.

B-0362 11:35

In vitro testing of six modern vena cava filters
I. Battyány, T. Rostás, Z. Harmat, B. Gasztonyi, L. Horváth, J. Schubert; *Pécs/HU*

Introduction: The filtration capability of six widely used modern vena cava filters were evaluated using sizes of big clots to define the most efficient type of them.
Methods: A flow model was constructed to simulate the inferior caval vein in horizontal position. The experiments were performed using human blood and Dextran 40 solution. The clot-trapping rate of six cava filters – Günther, Günther Tulip, Greenfield Titanium, Bird's Nest, Simon Nitinol, TrapEase – were studied with 10 series of different blood clot sizes. The sizes of the emboli were 0.5, 1, 2 cm long and 0.8 cm in diameter. The pressure gradient caused by the filters was measured by Schiller digital monitoring system.
Results: The clot-capturing rate for each series of emboli was between 88 – 100 %, representing good filtering efficiency clinically. The Greenfield Titanium filter easily and frequently has moved from central to eccentric position having been resulted in the lowest clot-trapping capacity, but the degree of differences from zero in the drifting was significant ($P < 0.05$) only at capturing the 0.5 and 1 cm emboli. The other filters had no significant differences. As the result of these series of experiments the decreasing order is: SN = BN > G* > TE > GT > GF
Conclusion: This in vitro study justified that the tested modern IVC filters had a clinically appropriate protection in preventing recurrent major pulmonary embolisation, in spite of the fact that, today we have no optimal IVC filter available. The minimal differences are related to the number of the legs, the stability and the architecture of the filters.

B-0363 11:40

Intra-arterial chemotherapy in pancreatic cancer, delivered by Seldinger technique
N. Carlone, L. Miserocchi, M. Cantore, R. Caudana; *Mantova/IT*

Purpose: To assess a new intra-arterial chemotherapy regimen for patients with unresectable pancreatic cancer.
Patients and methods: 29 patients with unresectable pancreatic carcinoma were treated with intra-arterial chemotheraphy at three week intervals. The schedule used was FLEC 5-fluoracil 1000 mg/m², folinic acid 100 mg/m², carboplatin 300 mg/m² and epirubicin 60 mg/m².
Result: The overall response rates assessed with CT were: 15 % partial respose, 44 % stable disease, 17 % progressive disease. The overall medial survival was 9.9 months (10.6 months and 6.8 months for UICC stage III and IV respectively). Pain reduction occurrred in 42 % of patients. Weight gain > 7 % above baseline ocurred in 8 % of patients. A total of 341 courses of FLEC were administreted. One sudden death, a case of pre-infarction angina, and a transient ischaemic attack were observed. The only complication related to the angiographic procedure was an intimal dissection of the iliac artery.
Conclusion: The intra-arterial FLEC regimen was effective and well tolerated. It requires only one day of hospitalization.

B-0364 11:45

Complications in percutaneous transubclavian intraarterial permanent catheter implantation for local chemotherapy of liver tumors
M. Venturini, E. Angeli, M. Salvioni, P. Brambilla, F. De Cobelli, A. Del Maschio; *Milan/IT*

Purpose: To report our experience (technique and complications) of percutaneous catheter implantation for continuous local chemotherapy.
Materials and methods: From January 1996 to September 2000 in 167 patients with liver tumors (secondary in 92.4 %) a removable catheter was percutaneously transubclavian placed in proper (43.4 %) or in proximal tract of right (or left) hepatic artery (56.6 %). 122 gastroduodenal, 13 left hepatic, 6 accessories right hepatic, 5 pancreaticoduodenal and 2 piloric arteries were embolized. The catheter position was controlled before chemotherapy and one month later. Low-dose long term heparinization of the catheter was performed.
Results: The procedure was technically successfull in all patients. After one month, catheter dislodgment and consequent reimplantation of another catheter was necessary in 41/167 (24.5 %) patients (31/41 with the catheter in proper hepatic artery). Catheter removal and interruption of local chemotherapy was due to hepatic artery thrombosis (7.8 %), local sepsis (2.4 %) and general sepsis (0.6 %). In two cases hepatic artery thrombosis was successfully treated by local trombolysis. Other different complications occurred were: gastroduodenal ulcers (6.7 %), pneumothorax (0.6 %) and subclavian artery pseudoaneurysm (0.6 %). No revascularization of the arteries embolized were observed.
Conclusion: In liver tumors, percutaneous intraarterial catheter implantation is a good alternative to surgical placement (catheter removable and reimplantable), but with different type of complications: catheter dislodgment and arterial thrombosis can be reduced by surgical catheter tunnellization and long-term heparinization, respectively.

B-0365 11:55

Determinants of initial and early failure in superficial femoral artery angioplasty

A. Patsalides, M. Pomoni, C. Papadopoulos, A. Tsanis, N. Batakis; *Athens/GR*

Purpose: We present our experience regarding the initial and early success and durability of superficial femoral artery (SFA) angioplasty.
Materials and method: We retrospectively reviewed the results of 38 patients treated for 45 SFA lesions during the past two years. Mean age was 65 years and 70 % of the patients were diabetics. Results were analyzed with respect to initial and early (< 1 year) angiographic and clinical success. Indications for angioplasty were claudication (29), nonhealing ulcer (10) and rest pain (5). After the intial procedure patients were followed with serial color Doppler studies and in 11 cases with angiography. Mean follow up was 18.5 months (13 – 24 months).
Results: Initial failure occurred in one lesion. Minor complications occurred in 2 cases and a major complication occurred in one case, with no effect on technical success. Excluding the initial technical failure, overall patencies at 12 and 18 months respectively were 83 % and 77 % respectively. There 3 early failures which resulted in amputation in 2 cases.
Conclusions: Predictors of clinical failure were:

- initial: SFA occlusion, duration of interventional procedure, lesion length and eccentricity and
- early: age, SFA occlusion, degree of atherosclerosis, post PTA appearance, diffuse atherosclerotic cardiovascular disease, diabetes mellitus and tibial run off.

10:30–12:00 **Room L/M**

Genitourinary

SS 607

Obstetric imaging

Chairpersons:
J.M. McHugo (Birmingham/GB)
Y. Robert (Lille/FR)

B-0366 10:30

MR hysterosalpingography: An alternative techinque to HSG in the assessment of infertility?

A. Sias, V. Alvino, F. Lecca, C. Politi, G. Mallarini; *Cagliari/IT*

Introduction: The purpose is to establish whether MR hysterosalpingography has a role as alternative technology to HSG, "gold standard" technique in the visualization of fallopian tubes.
Materials and methods: We performed MR hysterosalpingography in 40 female patients with a diagnosis of infertility. The examination was performed on a 0.5 T scanner. We catheterized the uterus with a catheterization kit. A T1 weighted sequence was performed in 20 patients, after a 20 ml injection of diluted paramagnetic contrast. In another 20 patients we perfomed T2 weighted sequence, after a 20 ml saline injection. All patients underwent HSG to confirm the results of the MR hysterosalpingography.
Results: 98 % of the patients claimed that MR hysterosalpingography was less traumatic and painful then HSG. The fallopian tubes were visualized in 80 % of the patients, in the remaining 20 % only fluid in the lower abdomen was noted. HSG confirmed the results of the MR hysterosalpingography in 90 % of the patients in which the fallopian tubes were visualized.
Conclusion: MR hysterosalpingography provides a reliable tool to visualize the fallopian tubes. Its advantages include the lack of ionizing radiations, the clear visualization of pelvic organs. The examination seems also better tolerated by patients. Its disadvantages include the high cost and also that interventional procedures may not be carried out in the same setting as it happens with HSG. The possible role of MR hysterosalpingography is to visualize the patent fallopian tubes in most patients: thus these patients may avoid an unnecessary HSG and its inherent radiation dose.

B-0367 10:35

Magnetic resonance imaging of the uterus with the FLAIR sequence: Initial experience

A. Maubon[1], A.S. Thurmond[2], J.-P. Rouanet de Lavit[3]; [1]*Limoges/FR*, [2]*Portland, OR/US*, [3]*Montpellier/FR*

Purpose: Assessment of (1) feasibility of MRI hysterography (MRH), (2) value of the FLAIR sequence after MRH.
Materials and methods: The FLAIR sequence is a heavily T2 weighted inversion recovery sequence, with an inversion time of 2000 ms that nulls the signal of water. It is mainly used in brain and spine MRI for its high sensitivity. Ten female patients (25 – 76 years referred for endometrial or sub-endometrial abnormality detected at ultrasound underwent (1) pelvic MRI, (2) MRH performed at the magnet with intra-uterine injection of 20 cc saline, (3) pelvic MRI with the FLAIR sequence in the sagittal and axial planes after MRH. Endovaginal US, T1w, T2w, FLAIR and hysteroFLAIR sequences were compared.
Results: In all cases examination was well tolerated. No complication occurred. Images in FLAIR MRH were of diagnostic value. We describe a 4 layers uterine anatomy, instead of the 3 classically described: (1) low signal uterine cavity (saline, with its signal nulled by the FLAIR sequence), (2) high signal endometrium, (3) low signal junctional zone, (4) intermediate signal myometrium. Conspicuity of endometrial and subendometrial lesions was enhanced in 10/10 cases. A positive diagnosis, confirmed at pathology was possible in 8/10 cases (mucous polyp n = 3, endometrial hyperplasia n = 2, adenomyosis n = 1, sub mucous myoma n = 1, endometrial atrophy n = 1).
Conclusion: MRHysterography performed at the magnet is feasible. A novel zonal anatomy of the uterus is described. Use of the FLAIR sequence after MRH enhances conspicuity of endometrial and subendometrial lesions. Comparisons with endosonography are warranted.

B-0368 10:40

Three dimensional dynamic MR-hysterosalpingography (3D d-MR-HSG): A preliminary report

W. Wiesner[1], A. Kaim[1], S.G. Rühm[2], C. De Geyter[1], E. Reese[1], G. Bongartz[1]; [1]*Basle/CH*, [2]*Essen/DE*

Purpose: To evaluate the feasibility of 3D MR-hysterosalpingography (3D MR-HSG) for visualization of the cavum uteri and demonstration of bilateral fallopian tube patency as an alternative to conventional hysterosalpingography.
Material and methods: 5 infertile female patients underwent 3DMR-HSG prior to conventional hysterosalpingography. The MR-protocol consisted of an axial T1-w SE, axial/coronal T2-w FSE and a 3D MRA sequence before, during and after injection of a diluted gadolinium solution into the cavum uteri via a balloon catheter.
Results: Positioning of the catheter was feasible. In one patient the catheter slipped out during MRI and in one patient the catheter was placed far in the cavum uteri. In three patients catheter position was optimal at the level of the cervical canal. Evaluation of pelvic anatomy, myometrium and ovaries was possible in all patients using T1-w SE and T2-w FSE. Three dimensional visualization of the dilated cavum uteri was possible in 4 patients. In these 4 patients 3D MR-HSG also proved bilateral fallopian tube patency which was later on confirmed in each patient by conventional hysterosalpingography.
Conclusion: 3D MR-HSG is feasible and further research should be done to show if these new technique could evolve to an alternative to conventional hysterosalpingography with the advantages of lacking radiation, diminished contrast toxicity and additional visualization of the uterus wall and ovaries.

B-0369 10:45

Can hysterocontrast-sonography (HyCoSy) replace laparoscopy in the assessment of tubal patency?

F. Hild, V.F. Duda, K. Bock, P. Hadji, K.-D. Schulz; *Marburg/DE*

Purpose: Subfertility in women is mostly due to anatomical-mechanical reasons. Tubal patency should be evaluated prior to reproductive treatment. Up to now laparoscopy with dye represents the gold standard. Can it be replaced by HyCoSy?
Material and methods: Since 1997 altogether 252 fallopian tubes (126 patients) were examined with HyCoSy using Echovist®. 56 patients had an increased risk for tubal pathology (previous pelvic operations, endometriosis or pelvic inflammatory diseases). Laparoscopy was mostly performed in patients where HyCoSy revealed both fallopian tubes to be occluded.
Results: At HyCoSy 108 patients (46 with increased risk) were diagnosed to have at least one patent tube (187 patent, 29 occluded). In 14 patients laparoscopy was performed and confirmed the sonographic results in 13 cases. Both tubes were occluded in 18 patients. Among them 10 with increased risk underwent laparoscopy and showed equal results in 5 cases. Overall the laparoscopic evaluation showed an accuracy of 0.74 per tube.
Conclusion: In our hands HyCoSy showed good correlations to laparoscopic results. HyCoSy should be performed as first diagnostic method. Laparoscopy should be done in case of occluded tubes, delayed for 3 month in case of one patent tube and for 12 month in case of no abnormalities.

B-0370 10:55

Fluoroscopic transcervical fallopian tube catheterization and recanalization as a treatment of proximal tubal injection failure

A.A.G. Helmy, M.S. Guirguis, O.H. Omar, M.Y. Sabry; *Cairo/EG*

Purpose: Our work aims to study the efficacy of transcervical fallopian tube recanalizaion as alternative method for the relatively morbid and costly traditional surgical procedures.

Material and methods: Forty one fallopian tubes were studied in 25 patients, having age range between 23 and 41 years with either unilateral or bilateral proximal tubal obstruction diagnosed by H.S.G. Preliminary H.S.G. was done for all patients. This showed 12 patent tubes. Selective osteal salpingography was then done for the remaining obstructed tubes using the set manufactured by Laboratoire CCD, France. This showed an additional 8 patent tubes. Recanalization was performed in the remaining tubes.

Results: Technique succeeded in recanalization of the proximal part (proximal 3 cm) in 16 tubes of which 14 were patent distally and 2 tubes which showed distal occlusion. The procedure failed to recanalize 5 tubes. In follow up pregnancy occured in 8 patients, 2 via recanalized tubes, 4 in patients who had obstruction relieved by preliminary H.S.G., and 2 in patients with a previously patent tube who had successful recanalization of the second tube. Follow up H.S.G. of the other non pregnant patients revealed re-occlusion of 3 tubes in 2 patients.

Conclusion: Because of the high false positive rate of proximal tubal obstruction it is suggeted that a selective osteal salpingography should be performed as a next step to initial H.S.G. If obstruction is confirmed tubal recanalization can be attempted. It is a safe and effective alternative in selected patients compared with the relatively morbid and costly traditional surgical procedures.

B-0371 11:05

Roentgen and MRI pelvimetry comparison

V. Kulakov, S. Kurinov, A. Volobuev, V. Panov, E. Kulabukhova, M. Panova; *Moscow/RU*

Introduction: The aim of this investigation was to compare MRI pelvimetry (MRIP) data with roentgen pelvimetry.

Subjects & methods: All MRI were obtained on 1.0 T MRI system Magnetom Harmony (Siemens, Germany). T1W and T2W FSE and GRE images were obtained on 60 women (38 – 42 weeks of pregnancy) to define anatomical sizes of maternal bony pelvis, fetus head, placenta and umbilical cord: in sagittal plane – for sagittal diameters of pelvic inlet, wide part, midpelvis, outlet; in oblique axial plane – for widest transversal diameters of inlet, transversal diameter of wide part, interspinous and intertuberous diameters; in different planes – for fetus MRI in three orthogonal planes; in oblique coronal plane – for placenta examination. In all cases the low-dose digital roentgen pelvimetry (LDRP) also was used.

Results: In 45 cases the correlation between MRIP and LDRP data was: for sagittal diameters – pelvic inlet 0.96, wide part 0.97, midpelvis 0.97; for transversal diameters – pelvic inlet 0.90, wide part 0.89, interspinous 0.84, intertuberous 0.94. The difference between MRIP and LDRP data was not more than 8 %. In 4 cases (8.88 %) fetus head disorders were found. In 19 (42.22 %) an umbilical cord circumflex was shown. In 12 cases (20.0 %) it was not possible to make MRI (5 cases of vena cava inferior compression syndrome, 4 cases of claustrophobia, 3 cases of lumbar ache).

Conclusions: MRIP had enough accuracy in compare with LDRP but it is more safe, sensitive and specific method for pregnant women examination.

B-0372 11:10

Comparison of image quality and maternal acceptance of MR pelvimetry performed in 1.5 T and open low field systems

S.C.A. Michel, B. Marincek, A. Rake, L. Götzmann, K. Treiber, B. Seifert, R. Chaoui, R.A. Kubik-Huch; *Zürich/CH*

Purpose: MR pelvimetry is the imaging modality of choice to assess the maternal pelvis. The objective of this study was to compare image quality, measurements and patients acceptance of MR pelvimetry performed in open low field versus 1.5 T system.

Materials and methods: 22 women (9 pregnant; weight 71 ± 14 kg) referred for pelvimetry consented to participate. Examinations were performed in supine position in a 1.5 T system (TR 150, TE 1.9, 2 NEX) and an open 0.5 T GE system (TR 150, TE 8.6, 2 NEX, body flex coil); results of measurements were correlated. A questionnaire evaluating comfort and acceptance was filled out.

Results: One exam at the 1.5 T system had to be interrupted due to claustrophobia; in 2 cases with abdominal circumference exceeding 120 cm, interspinal and intertuberous diameters could not be assessed in the open system because of insufficient image quality. Pelvic measurements showed good reproducibility, although image quality was superior at 1.5 T. Examination time was 7.5 ± 2.2 min for the 0.5 T, 2.6 ± 1:5 min for the 1.5 T system. Women felt more claustrophobic (95 % vs. 58 %) in the 1.5 T system, but felt bothered by noise in both systems (60 % vs 65 %). Fear of harming the fetus was a problem in 21 %. 61 % preferred the open, 9 % the 1.5 T system, 30 % were equivocal.

Conclusion: Most women preferred MR pelvimetry performed in the open magnet. Although image quality is inferior, pelvimetric measurements in the open system are feasible as long as the abdominal circumference of the pregnant women does not exceed 120 cm.

B-0373 11:20

The effect of maternal posture on pelvic outlet MR measurements

S.C.A. Michel, B. Marincek, A. Rake, K. Treiber, B. Seifert, R. Chaoui, R.A. Kubik-Huch; *Zürich/CH*

Purpose: Different labor positions e.g. squatting, kneeling are offered for parturition according to the cultural background and recently even as "fashion". Changes in the pelvis under these conditions are anatomically not exactly known. MR pelvimetry is widely accepted as the imaging modality of choice to assess the maternal bony pelvis in obstetrics. The aim of our study was to investigate if measurements of the pelvic outlet are influenced by different positions.

Methods: MR pelvimetry was performed in 20 female non-pregnant volunteers (27 ± 3 a) in an open 0.5 T MR system in supine, hand-to-knee and squatting positions using a T1w FSPGR sequence in the axial and sagittal plane. Obstetric conjugate, transverse, outlet sagittal diameter, transverse interspinal and intertuberous diameters were measured and results of the different positions were correlated.

Results: In the hand-to-knee position a significant increase of the sagittal outlet (11.5 ± 1.1 cm) compared to the supine position (11.2 ± 1.1 cm) was observed ($p = 0.019$). Interspinal diameter was wider in hand-to-knee position (11.3 ± 0.9 cm, $p = 0.010$) and squatting (11.4 ± 0.6 cm, $p < 0.001$) compared to supine position (10.9 ± 0.7 cm). Intertuberous diameter was larger in squatting (12.5 ± 0.7 cm, $p = 0.019$) and hand-to-knee position (12.3 ± 0.8 cm, $p = 0.012$) than in supine position (12.1 ± 1.0 cm) and significantly increased in squatting vs. hand-to-knee position ($p = 0.011$). Obstetric conjugate and transverse diameter did not significantly change in the 3 different position.

Conclusion: Our results show that a difference in maternal posture can result in a considerable changes of pelvic bony distances and thus give a scientific evidence that changing position during labor can facilitate delivery.

B-0374 11:30

Impact of ultrasonography on management of early molar pregnancies

J. Czechowski, P. Deb, M.-U. Ahmed; *Al Ain/AE*

Purpose: To evaluate transabdominal ultrasonography in cases of early molar pregnancies with correlation to β-HCG levels and clinical disorders. Gestational trophoblastic disease is rare in the European population.

Materials and methods: Twelve patients of cosmopolitan orgin with an average age of 32.5 years (range 19 – 44) with gestation age of average 11 weeks (range 7 – 40) were examined by US using transabdominal technique with 5 MHz transducer (ATL and Toshiba) during 12 months as a part of our large study. The indication for US in the majority cases was vaginal bleeding and pain in 9 patients (75 %). β-HCG levels were determined in the day of US and 1 week later.

Results: In 10 cases (83 %) US were diagnostic showing distended uterine cavity with echogenic tissue containing multiple small cystic lesions due to early molar pregnancies. No typical text book picture of snow storm appearance was noted. In 2 cases US diagnosis of molar pregnancy was not correct. In those patients, retained products of conception were revealed (one case had a low and another high level of β-HCG). β-HCG levels were elevated in 11 cases ranging 54 690 – 200 000 IU/l (average 127 480 IU/l). All cases were confirmed by surgery and histology and in 10 cases complete mola were obtained. In this study we had one patient, who died with pulmonary embolism on 3rd day after evacuation of molar pregnancy, which is one of the rare complications.

Conclusions: US exanination gave an accurate diagnosis in 85 % of cases of early molar pregnancies There was good correlation with high elevated β HCG levels.

B-0375 11:35

Diagnosis of placenta adherent disorder by magnetic resonance imaging

C.H. Bruno sr.[1], J.M. Palacios Jaraquemada sr.[2]; [1]*Lomas de Zamora/AR*, [2]*Buenos Aires/AR*

Purpose: To demonstrate the utility of magnetic resonance imaging (MRI), enhanced and non-enhanced, in the diagnosis of placenta percreta.

Materials and methods: We studied 40 patients with multiple cesarean sections and ultrasound suspicion of placental adherent disorder. Patients were studied between 30 and 34 weeks of gestation. All patients consented to both magnetic resonance imaging (MRI) and contrast administration according to FDA recommendations. They underwent an enhanced MRI with gadolinium (0.1 mmol/kp) through Resonator 1.5 T, technique Spin echo, breath hold and Stir technique. Images were obtained from the three planes, at 60 and 90 s following contrast administration.
Results: The following results were obtained: 18 diagnoses of placenta percreta, 3 of placenta increta, and 13 of placenta accreta. In 6 patients of the latter group, MRI modified the extension of the adherent disorder diagnosed by ultrasound. We describes the typical images of placental invasion.
Conclusions: Enhanced MRI and Stir technique has proved to be useful for the differential diagnosis of placenta percreta. Its use is recommended for patients at high risk for placental adherent disorder, when ultrasound diagnosis is not clear or conclusive.

B-0376 11:45

Ultrafast magnetic resonance imaging of the fetus and utero-placental unit: 3-dimensional reconstruction and volumetric assessment: Feasiblity study

R.A. Kubik-Huch, S. Wildermuth, L. Cettuzzi, A. Rake, B. Seifert, R. Chaoui, B. Marincek; *Zürich/CH*

Purpose: To validate fetal volumetry based on 3D reconstructions of 2D single-shot fast spin-echo (SSFSE) MR data sets acquired in utero.
Materials and methods: 3D reconstruction was based on data sets of 22 fetuses acquired on a 1.5 system using T2w SSFSE imaging. 3D models were performed using a surface rendering technique running on a high-end Unix workstation. Fetuses, amniotic fluid, and placentae were segmented manually; volumes were calculated by ProVision software. Results were correlated to sonographic fetal biometry ($n = 22$) and birth weight ($n = 6$).
Results: MR estimates of fetal volume ranged from 109 to 3723 cm^3, placental volume from 58 to 1736 cm^3, and amniotic fluid volume from 101 to 2881 ml. MRI estimates of fetal weight (232 – 3958 g) correlated closely with sonography (166 – 4634 g) ($R2 = 0.97$). Six infants were delivered within 1 week of imaging; actual birth weight (3029 ± 592 g) was slightly overestimated by MRI (87 ± 112 g, NS) and sonography (353 ± 355 g, NS).
Conclusion: 3D reconstruction and volumetry of the fetus and utero-placental unit are feasible using ultrafast MRI data sets. MRI estimates correlated closely to sonographic fetal biometry and birth weight.

B-0377 11:55

MRI examinations in the diagnosis of pelvic hematomas in females

V. Kulakov, A. Volobuev, M. Panova, E. Kulabukhova, V. Panov; *Moscow/RU*

Introduction: Clinically silent haematomas of the female pelvis (especial in case of postpartum haematomas) are a diagnostic challenge. Possibilities and limitations of MRI in detecting and localizing clinically non-apparent female pelvic haematomas was the main aim of this investigation.
Subjects & methods: All MRI examinations were obtained on 1.0 T MRI system Magnetom Harmony (Siemens, Germany). T1- and T2-weighted FSE sequences, ordinary GRE and GRASE sequence images (without contrast enhancement) were performed on 12 women (2 after parturition) with pelvic pain and/or fullness following difficult vaginal deliveries. None of the patients had clinical or ultrasound evidence of haematoma.
Results: Haematomas in the pelvis were identified with GRE and FSE T1-weighted, GRASE and FSE T2-weighted images. Pelvic haematomas were found in contiguity with the vagina, cervix, and bladder, within the broad ligament, and in the presacral space. In two postpartum patients, haematomas were located in the perivaginal and pericervical regions. In 6 patients, a perivaginal haematoma extended into the perivesical space. In 2 cases, perivaginal haematomas extended between the double layers of the broad ligaments. In a further 2 patients, a haematoma was identified only within the presacral space. Based on MRI data, 9 patients were treated successfully with invasive means and 3 patients were managed successfully with conservative means.
Conclusion: Conclusions. MRI is very sensitive method in detection and localization of pelvic hematomas in comparison with clinical and/or ultrasound examinations. The risk for pelvic haemorrhage (including postpartum haematomas) following difficult vaginal deliveries is a clear indication for urgent MRI examination.

10:30–12:00 **Room N/O**

Cardiac

SS 603

Heart: CT

Chairpersons:
R. Rienmüller (Graz/AT)
V.E. Sinitsyn (Moscow/RU)

B-0378 10:30

Determination of cardiac stroke volumes with retrospectively ECG-gated spiral CT: An experimental validation

M.L. Bahner, J. Albers, J.M. Boese, J. Tremper, C.F. Vahl, G. van Kaick; *Heidelberg/DE*

Purpose: Aim of this study was to evaluate the accuracy of stroke volume measurement of the heart using retrospectively ECG-gated spiral CT in an experimental in vivo setting.
Methods and materials: Pigs ($n = 10$, weight 25 – 40 kg) were scanned on a Siemens SOMATOM Plus 4 scanner in spiral mode (slice 2 mm, pitch 0.5, rotation time 0.75 s, reconstruction increment 0.5 mm). Ventricular pacing with epimyocardial leads (90 bpm) was used. Blood flow was measured with a doppler probe placed at the ascending aorta. The self written reconstruction algorithm for CT data used 4 rotations for oversampling. Stroke volumes were determined with region growing from enddiastolic and endsystolic CT images.
Results: The temporal resolution achieved was 170 ms. With the chosen reconstruction increment isotropic volume datasets of the heart were available with 0.5 mm resolution allowing short axis reformations. The stroke volumes determined by CT correlated well with the invasively measured data ($r = 0.94$). The calculated volumes were underjudged by a mean of 1.75 ml in CT scanning.
Conclusion: Determination of cardiac stroke volume is possible with ECG-gated spiral CT. The measured results correlate well with true values determined by invasive measurement. The available temporal resolution is sufficient to offer the necessary image quality.

B-0379 10:40

A phantom study to validate image acquisition and reconstruction parameters in imaging of coronary stents using multislice spiral CT (MSCT) in vitro

C. Schulte, T. Giesler, U. Baum, E. Wenkel, R. Decker, D. Ropers, S. Achenbach, S. Ulzheimer, W.A. Bautz; *Erlangen/DE*

Purpose: It would be highly desirable to detect in-stent restenosis using multislice spiral CT (MSCT). However, imaging of stents is difficult due to metallic artifacts and partial volume effects. We evaluated the influence of image acquisition and reconstruction parameters on image quality of MSCT.
Methods: Using a MSCT (Siemens Somatom Volume Zoom) we examined 3 stent types (Palmaz–Schatz 15 mm, ACS RX Multilink 15 mm, NIR Primo 16 mm) of varying diameter (3.0 – 4.0 mm). Stents were placed in a water-filled phantom in 3 orientations (parallel to imaging plane, 45° and 90° angle) and a volume data set was acquired (rotation time 500 ms, pitch 1.5 mm/360°) using slice collimations of 2 × 0.5 mm, 4 × 1.0 mm, and 4 × 2.5 mm and tube currents of 200, 300 and 400 mAs. Image data sets with effective slice thickness of 0.65, 1.3 and 3.0 mm were created using an image reconstruction algorithm corresponding to ECG. Luminal signal-to-noise ratio and stent diameter determination were assessed in multiplanar reconstructions.
Results: We found a significant influence of stent orientation on the precision of diameter determination. The difference between real and measured diameter was 0.39 ± 0.12 mm in case orientation was parallel to the imaging plane, and 0.64 ± 0.21 and 0.74 ± 0.15 mm for orientations of 45° and 90° ($p < 0.01$). Signal-to-noise ratio remained uninfluenced by stent orientation. Slice collimation, tube current and reconstructed slice thickness showed no significant effect.
Conclusion: Image quality of stents in MSCT depends significantly on orientation of the stent relative to the imaging plane.

B-0380 10:50

Value and limits of CT-angiocardiography in coronary artery imaging: Correlation of different non-invasive visualization techniques with invasive angiocardiography

C. Herzog, K. Engelmann, T. Diebold, S. Dogan, T.J. Vogl; *Frankfurt a. Main/DE*

Objective: To determine the benefit of CT-angiocardiography in coronary artery imaging and to compare the value of four different visualization techniques.
Material and methods: 50 Patients underwent both Multislice CT and angiocardiography. All CT scans were performed at 4 × 1 mm collimation, pitch 1.5 and 500 ms rotation time. Using retrospective ecg-gating image reconstruction parameters were 1.5 mm slice thickness, 0.5 mm increment and kernel B30. Each patient's CT dataset subsequently has been explored applying axial, multiplanar, threedimensional and virtual endoscopic visualization modes.
Results: The highest sensitivity in the evaluation of stenoses has been achieved in axial reconstructions (66.7 %), followed by virtual endoscopy (55.9 %), multiplanar reconstructions (46.6 %) and threedimensional reconstructions (33.3 %). With regard to the detection of atheromatous plaques, axial scans (71.2 %), three-dimensional reconstructions (70.1 %) and virtual endoscopy (69.1 %) displayed a comparable sensitivity, whereas multiplanar reconstructions showed distinct lower results (55.6 %). In combining the four techniques a sensitivity of 74.2 % could be reached. The specifities of all four visualization techniques amounted to over 91.9 %.
Conclusion: In the detection of atherosclerotic plaques CT-angiocardiography does not achieve a sensibility comparable to angiocardiography and is restricted upon the main branches of the coronary arteries. Best results were observed at heart rates below 60 bpm. Of all four visualisation techniques axial scans showed the nearest correspondence in the quantification and qualification of atherosclerotic plaques.

B-0381 11:00

Multislice cardiac CT as a preoperative planning tool for total endoscopic coronary artery bypass

C. Herzog, S. Dogan, T. Diebold, K. Engelmann, G. Wimmer-Greinecker, A. Moritz, T.J. Vogl; *Frankfurt a. Main/DE*

Objective: To evaluate the benefit of CT-angiocardiography as a preoperative planning tool for totally endoscopic coronary artery bypass using computer enhanced robotic telemanipulation.
Methods: 20 patients with single vessel coronary artery disease scheduled for TECAB preoperatively underwent CT-angicardiography. Of each patient 2-and 3-dimensionally reconstructed images of the heart have been obtained. Examination criteria were the exact anatomic position relatively to the myocardium, the wall quality and the amount of atheromatous changes.
Results: In 10 cases an intramyocardial course of the LAD was diagnosed and later confirmed by surgery thus facilitating the localization of the target segment. In 10 patients the occluded LAD was displayed. CT based measurements revealed an individually optimized position for the TECAP that has intraoperatively been confirmed in all cases. In 3 patients the middle segment of the target vessel was predicted to consist of too many soft plaques, consequently making an anastomosis very difficult. These findings were confirmed intraoperatively and the TECAP procedure was successfully switched to a MICAP procedure.
Conclusion: Preoperative CT-angiocardiography showed a high correspondence to the surgical findings. It can succesfully be used as an preoperative planning tool facilitating the choice of the adequate operative technique. Applied before complex procedures such as totally endoscopic coronary artery bypass surgery it additionally helps to support the surgeons orientation.

B-0382 11:10

Retrograde ECG-gated MS-CT for preoperative assessment of the aortic valve

J.K. Willmann, J.E. Roos, D. Weishaupt, L. Haegeli, M. Lachat, B. Marincek, P.R. Hilfiker; *Zürich/CH*

Purpose: To evaluate retrograde ECG-gated MS-CT for preoperative assessment of the aortic valve.
Materials and methods: 25 patients with aortic valve disease were prospectively evaluated with contrast-enhanced MS-CT (collimation 4 × 1 mm; pitch 1.3 – 1.8) prior to surgery. The digital ECG signal was simultaneously recorded during the spiral scan and reconstruction was retrospectively performed with 250 ms/image temporal resolution, 1.25 mm slice thickness, and 0.8 mm reconstruction increment. Two radiologists analysed the data based on axial images and multiplanar reformations directly on a workstation. Calcifications, size, and morphology of the aortic valve, aortic sinus, coronary ostiae, and subaortic compartment were evaluated and compared to the intraoperative findings, preoperative echocardiography and angiography.
Results: Retrospective ECG-gated MS-CT allowed a motion-free visualization of the heart in all 25 patients. Evaluation of aortic valve morphology (bi- or tricuspid), location/extend of calcifications, and size measurements highly correlated between preoperative MS-CT and intraoperative situs. MS-CT evaluation of aortic sinus and coronary ostiae was confirmed by echocardiography and cardiac catheterization studies.
Conclusions: Retrospective ECG-gated MS-CT is a useful tool in the preoperative evaluation of patients with aortic valve disease, and widely used for operation planning by cardiovascular surgeons in our institution.

B-0383 11:20

Effects of heart rate on image quality of retrospectively ECG-gated coronary multislice CT angiography

C. Hong[1], C.R. Becker[1], A.M. Huber[1], U.J. Schöpf[1], B. Ohnesorge[2], R.D. Brüning[1], M.F. Reiser[1]; [1]*Munich/DE*, [2]*Forchheim/DE*

Purpose: To evaluate retrospectively ECG-gated reconstruction for coronary multislice CT angiography to reduce cardiac motion artifacts and to identify the influence of heart rate on image quality.
Materials and methods: Seventy-eight patients were studied with coronary CTA performed on a MSCT scanner using simultaneous acquisition of four 1 mm collimated slices. Helical raw data and digital ECG trace were used to retrospectively reconstruct axial images with a temporal resolution of 250 ms per slice. Slices at z-positions were reconstructed during end diastole at 30 % – 80 % of the RR-interval or 450 ms – 550 ms prior to the next R-wave. The heart rate, delay time and image quality were analyzed.
Results: The maximum of image quality was achieved using a trigger of 50 % for RCA and at a trigger of 60 % for RCx. The maximum of image quality for LAD was found for 50 % and 60 % of the cardiac cycle with equal mean values. A significant negative correlation between heart rate and image quality was observed ($p = 0.05$). The image quality decreased with an increasing heart rate for the majority of coronary arteries. Superior image quality could be achieved, if a heart rate was less than 70 beats/min ($p < 0.01$).
Conclusion: Retrospective gating is advantageous for coronary MSCT angiography. In order to achieve diagnostic image quality the heart rate of the patient needs to be sufficiently low. Selecting appropriate delay times and controlling heart rate will be important for reduction of cardiac motion artifacts.

B-0384 11:30

Correlation between coronary calcium score measured by electron-beam computed tomography and results of coronary angioplasty

M.B. Belkind, V.E. Sinitsyn, N.V. Gagarina, Y.G. Matchin, A.A. Lyakishev, V.G. Naumov; *Moscow/RU*

Purpose: Percutaneous transluminal coronary angioplasty (PTCA) is widely used in treatment for CAD. Main problems associated with clinical use of PTCA are complications and restenosis. The purpose of our study was to estimate the correlation between degree of coronary calcification measured by electron-beam computed tomography (EBCT) and outcomes of PTCA.
Material and methods: 80 patients with 96 coronary artery stenosis were subjected to balloon angioplasty. Before intervention all patients were examined with EBCT. The rate of complications and restenosis were estimated.
Results: The average coronary calcium score in the segments subjected to PTCA was 39.8. Complications during PTCA were registered in 24 (25 %) cases. Restenosis was detected in 22 (25 %) dilated segments. Among patients with restenosis the average calcium score in coronary segments subjected to PTCA was 74.5 comparing to the score of 22.9 in patients without restenosis ($p < 0.01$). Applying ROC-analysis we determined sensitivity and specificity of EBCT for forecasting complications and restenosis. The critical calcium score in segment of PTCA was 27 for restenosis (sensitivity 79 %, specificity 62 %), and 23 for complications (sensitivity 81 %, specificity 70 %). The patients were divided into two groups with significant and insignificant segments calcium score. The frequency of complications caused by PTCA and restenosis were notably higher in the groups with significant calcification ($p < 0.05$).
Conclusion: The high calcium score in a segment of coronary arteries subjected to PTCA is associated with increased risk of complications and restenosis. These observations may be important in selecting devices for endovascular therapy.

B-0385 11:40

A new CT ventriculography technique using 0.5 mm raw slice thickness and 0.5 second helical multidetector-row CT: Comparison of non-ECG gated and retrospective ECG-gated subsecond helical MDCT scans

S. Hamada[1], S. Yamamoto[1], H. Naito[1], H. Nakamura[1], S. Azemoto[2], T. Kanagawa[3]; *[1]Suita/JP, [2]Tokyo/JP, [3]Kobe/JP*

Purpose: The disadvantages of ECG-gated method are high radiation dose due to overlap scanning, and the need of ECG-gating apparatus. We propose a new method of cardiac helical multidetector-row CT (MDCT) without ECG-gating.
Methods and materials: With a single breath-hold, the patient's entire heart was scanned without ECG-gating (0.5 mm thick detector-row, pitch 5.5, and 0.5 s per rotation) by MDCT (Toshiba Aquilion). Reconstructed isotropic slices covered all cardiac phases periodically. Our new method is composed of the following four steps: (1) Coronal MPR image was created from all of these slices. (2) From MPR image, slices of convex (top) level as end-diastole and of concave (bottom) level as end-systole were re-extracted, respectively. (3) 3D-reconstruction of end-diastole slices and end-systole slices were performed, using interpolation. (4) Volume calculation. After moving phantom experinment, we applied this new method to the evaluation of cardiac function of the 20 patients. We also applied retrospective ECG-gated MDCT method to other 20 patients, and compared each method with conventional ventriculographic method.
Results: Close correlation between our method and conventional left Ventriculographic method was obtained ($r = 0.99$, 0.98, and 0.91, for end-diastolic volume, end-systolic volume, and left ventricular ejection fraction, respectively; $p < 0.05$ for all values). There was no significant difference between our method and retrospective ECG-gated method.
Conclusions: Our cardiac application of helical MDCT without ECG-gating provides a useful assessment of cardiac volumetry and function, and promises radiation dose reduction.
The presentation was supported in part by Voxar, England.

B-0386 11:50

Electron-beam CT in the pre-operative assessment of constrictive pericarditis

J.V. Sheikh[1], R. Groell[2], R. Rienmüller[2]; *[1]Moscow/RU, [2]Graz/AT*

Purpose: The clinical symptoms of constrictive pericarditis are often non-specific and may mimic those of restrictive cardiomyopathy. That is why the diagnosis of constrictive pericarditis has to rely on imaging studies. The purpose of this study was to determine the usefulness of electron-beam computed tomography (CT) for the diagnosis of constrictive pericarditis and to evaluate its implications for cardiac surgery.
Materials and methods: Electron-beam CT of the heart was performed in 27 patients with constrictive pericarditis in one of two different radiological centers. The appearance of the pericardium was evaluated and signs of cardiac congestion were documented.
Results: Pericardial calcifications which occurred in 23/27 patients (85 %) were precisely detected with electron-beam CT. Pericardial constriction was global in 15 (56 %), left-sided in 1 (4 %), right-sided in 4 (15 %), and annular in 6 (22 %) patients. Calcific invasion of the right or left ventricular myocardium was clearly visualized in 2 (7 %) or 3 (11 %) patients, respectively. Myocardial fibrosis or atrophy was present in 3 patients (11 %).
Conclusion: Due to the presence of calcifications in the majority of patients with constrictive pericarditis, CT still plays a dominant role in the diagnostic work-up of patients with suspected pericardial constriction. Detailed morphological information is essential for the surgeon to determine the optimal approach for pericardiectomy.

14:00–15:30 **Room B**

Musculoskeletal

SS 710

MRI of the foot and ankle

Chairpersons:
J. Hodler (Zürich/CH)
K. Jonsson (Lund/SE)

B-0387 14:00

MRI vs. arthroscopy in the evaluation of osteochondral pathology of the tibio-talar joint of the ankle

A.V. Giordano, F. Iannessi, M. Caulo, G. Cerone, A. Barile, C. Masciocchi; *L'Aquila/IT*

Purpose: This work aims to demonstrate the diagnostic accuracy of MRI in the evaluation of the osteochondral disease of the tibio-talar joint (TTJ) in comparison to arthroscopy.
Materials and method: Thirty patients affected by tibio-talar pain and swelling entered this study. In eighteen of them history of a previous inversion ankle sprain was present. All the patients were submitted to plain films and to MRI using dedicated and whole body MRI units; in three cases intra-articular injection of paramagnetic contrast media (5 – 10 ml of contrast medium obtained from the dilution of 0.6 ml of Gd-DTPA in 250 ml of saline) was performed. CT scan was performed in seven cases. All the patients underwent surgery.
Results: In 28 upon 30 cases arthroscopy confirmed the MR findings. 21 chondral disease were discovered by MR showing different degree of severity (5 low, 9 mild, 7 severe grade). In 2 of the 5 low grade conditions arthroscopy could not reveal the damage of the deepest aspect of the cartilage and subchondral drilling was performed on the base of MRI findings. In seven out of 28 cases athroscopy confirmed the MR and CT scan findings of dissecting osteochondritis. In the other two patients both imaging and arthroscopy could not reveal any pathological condition.
Conclusions: In our experience MR has to be considered the gold standard in the study of TTJ cartilage allowing evaulation of the full thickness and subchondral bone.

B-0388 14:10

Tibio-talar joint synovial impingement of the ankle: Contrast enhanced MRI vs. surgery

A. Barile, G. Cerone, M. Caulo, F. Iannessi, V. Calvisi, C. Masciocchi; *L'Aquila/IT*

Purpose: To establish the diagnostic accuracy of enhanced MRI in the evaluation of the tibio-talar joint (TTJ) synovial impingement compared to surgical findings.
Materials and method: Fifteen patients clinically suspected for tibio-talar joint impingement were submitted to infused MR examination using dedicated 0.2 T and whole body 1.5 T MR units. The sequences employed with the two different instrumentation were respectively: SE T1W, SE T2W, STIR on pre-contrastographic evaluation and TSE T2W, SE T1W and SE T1W with fat-saturation only after contrast media administration. The used scan planes were the axial, sagittal and coronal. All patients underwent arthroscopy after MRI evaluation.
Results: In seven cases MRI revealed the presence of anterior TTJ synovial impingement confirmed by arthroscopy; in three of these cases it was possible to appreciate contrast enhancement in the region of the synovial thickening. In four cases with history of remote sprain injury of the ankle arthroscopy confirmed the MRI finding of inferior tibio-peroneal ligament tear and the presence of concomitant synovial hypertrophy ("meniscoid syndrome"); contrast enhancement was present in two case. In four cases MRI was normal: arthroscopy in two cases confirmed the diagnosis while revealed the presence of anterior TTJ impingement in one case and "meniscoid syndrome" in the other case.
Conclusion: Infused MRI has high diagnostic accuracy in the diagnosis of TTJ impingement syndrome.

B-0389 14:20

Differential diagnosis of sportsman's talar pain: Role of magnetic resonance imaging

T.V. Bartolotta[1], A. Iovane[1], M. Midiri[2], A. Carcione[1], D. Macaluso[1], R. Lagalla[1]; *[1]Palermo/IT, [2]Bari/IT*

Purpose: To assess the outcome of MRI in the differential diagnosis of sportsman hindfoot pain.

Materials and methods: Fourtythree professional athletes affected by hindfoot pain underwent MRI. SET1W, GET2*, and fat suppression (STIR) images were acquired with a 0.5 T superconductive unit (Vectra, GE Medical System) and a dedicated extremities transmitter/receiver coil. The lesion seat, the presence of anatomic variants (os trigonum, Haglund's deformity), and signal intensity changes were evaluated.
Results: Tendinous abnormalities and inflammatory bursal involvement were frequently found (77 % of cases). Bone diseases (22 % of posterior talalgia alone) most of all involved heel (60 %). Cartilagineous diseases were present in 9 % of cases. In 60 % of cases an intra-articular osseous or cartilagineous displaced fragment coexisted, determinating joint locking. In 38 % of cases contemporary involvement of different articular structures was observed. Sagittal and axial planes were particularly well suited for the diagnosis and the assessement of disease extension. Furthermore GET2* and fat suppression images allow early disease detection, whereas hyperemia or fluid collection occur.
Conclusions: MRI is the most reliable technique in the identification of talalgia's causes – in relation to soft tissues (bursae, synovial or nervous structures), bone and articular diseases – providing a correct and effective pre-therapeutic planning.

B-0390 14:30

Painful syndromes of the forefoot: Evaluation with MRI
E. Bassetti, M. Mastantuono, M. Kvasnova, M. Francone, R. Passariello; *Rome/IT*

Purpose: Evaluate MRI usefulness in the study of pathological findings of forefoot in algic metatarsal syndromes.
Materials and methods: We used a permanent low field (0.2 T) MR equipment dedicated to the study of limbs. We studied 85 patients with clinical symptoms at the forefoot. All patients were studied using SE T1 and T2, G.E and STIR sequences. In 43 patients we administered intravenous contrast medium (Gd-DPTA) at 2 mmol/kg.
Results: Nodules at digit neurovascular complex were found in 27 patients (Civinini-Morton's neuroma). No other alterations of soft tissues were present in 14 patients. In 13 patients other sites in the space between the metatarsal heads were interested by the pathology, even though these were non specific.
In 17 patients there was a wide sclerosis of perineural connective tissue without evidence of primitive nervous involvement. Moreover, we documented different pathologies such as bursities, synovial cyst, inflammatory involvment of flexor tendons, osteochondral lesions and tendon degeneration.
Discussion/conclusions: The great number of anatomical details and the wide range of study make MR images highly useful both in the surgical and medical planning of metatarsal pathologies. In the evaluation of the metatarsal pathologies an important role may be played by dedicated magnets.

B-0391 14:40

Painful syndromes of the hindfoot: Evaluation with MRI
M. Mastantuono, E. Bassetti, L. Di Giorgio, R. Passariello; *Rome/IT*

Purpose: The painful syndromes in the hindfoot are always responsible of an high grade of disability for the affected patient. In our study we wanted to verify the possibility offered by MRI in the evaluation of the calcaneal region of the foot.
Materials and methods: We studied 55 patients (39 males and 16 females), sport trainees with pain localized at the level of the hindfoot. In 12 patients the pain was related with a trauma. MRI examinations were perfomed with a low field (0.2 T) dedicated equipment to the study of limbs (ARTOSCAN Esaote Biomedica) using S.E. T1 and Turbo-T2, G.E. and STIR sequences.
Results: 17 patients had a fluid collection at the level of the synovial bursae; 21 patients had a chronic or acute alteration at the level of the tendons, 8 patients presented an alteration localized at the level of the muskulo-aponeurotic structures with their insertion localized in front of the posterior process of the calcaneus. 4 patients presented bone or articular alterations, 5 patients had a focal inflammation that was responsible for disability.
Discussion and conclusions: In our experience MRI, due to its high spatial and contrast resolution gave an important contribution for a correct assessment of the alterations of the Achilles-calcaneo-plantar system of the foot.

B-0392 14:50

Diagnostic evaluation of coxa-pedis syndrome using MRI
F. Iannessi, A.V. Giordano, G. Cerone, A. Barile, C. Masciocchi; *L'Aquila/IT*

Purpose: The aim of this work was to evaluate the MR capabilities in the diagnosis of pathological conditions causing coxa-pedis syndrome.
Materials and methods: Thirty patients affected by coxa-pedis syndrome entered this study. MR examinations were carried on using dedicated and whole body MR units. All patients were previously submitted to plain film, in eight cases CT scan examination was also performed. MR examinations were carried on using 1.5 T whole body and 0.2 T dedicated MR units. The sequences employed were SE-T1W, GE-T2W and SE T2W with fat-saturation on sagittal and oblique-axial scan planes; the slice thickness was 3 – 4 mm. Five safe volunteers were previously submitted to MR examination to optimize MR sequences and scan planes.
Results: In one case MR showed complete spring ligament tear confirmed by surgery; in one case we observed a spring ligament tear with partial morphological recovery in a four months later MR examination. Posterior tibial tendon (PTT) disease was detected in twenty cases and associated condition of os tibiale was discovered in six cases. In the remaining eight cases talo-navicular chondropathy was detected by MR study.
Conclusion: In our experience tendonitis is the most common pathological condition affecting the coxa pedis. Talo-navicular chondropathy and spring ligament lesions are also involved in the field of the coxa pedis diseases. In all the cases MR has to be considered the method of choice in the evaluation of pathological conditions involving this complex anatomical structure.

B-0393 15:00

MR imaging of the foot and ankle: Prevalence and distribution of occult and palpable ganglia
D. Weishaupt[1], M.E. Schweitzer[2], W.B. Morrison[2], B. Marincek[1], K. Wapner[2]; *[1]Zürich/CH, [2]Philadelphia, PA/US*

Purpose: To evaluate prevalence and anatomic distribution of both occult and palpable ganglia of the foot and ankle.
Materials and methods: Within a 7-year period MR imaging of the ankle was performed on 2813 patients and MR imaging of the foot on 2277 patients using a 1.5 T magnet. 167 ganglia in 155 patients were detected. MR images of these patients were retrospectively reviewed by two observers with regard to prevalence and exact anatomic location and size of ganglia. Clinical findings and when available surgical reports were also reviewed.
Results: 157 ganglia in 145 patients were present on MR images of the ankle and 10 ganglia in 10 patients on MR images of the foot, resulting in a prevalence of 5.6 % in the ankle, and a prevalence of 0.4 % in the foot. The most common location was the sinus tarsi (34.1 %). However, only 4 of these (7 %) were palpable. The second most common location was around the Lisfranc joint (13.8 %) of which 11/23 [47.8 %] were clinically palpable. Palpable ganglia were statistically larger in size than occult ganglia measured in any of three diameters ($p = 0.01 - 0.002$). Ganglia of the foot and ankle represented 42 % of all clinically suspected soft-tissue masses.
Conclusion: Ganglia in the foot and ankle are an infrequent finding on routine MR imaging of the foot and ankle. Ganglia are most frequently located in the sinus tarsi where they are occult to clinical palpation.

B-0394 15:10

Osteosynthesis of talus fractures: Are metallic artifacts a drawback for MRI in the follow-up?
F. Lomoschitz, G.S. Pajenda, M.J. Breitenseher, U. Hoffmann, S. Grampp, S. Trattnig; *Vienna/AT*

Purpose: To evaluate the accuracy of MRI in the detection of longterm complications after osteosynthetic treatment of talus fractures.
Materials and methods: The study was based on 12 consecutive patients (m = 11/f = 1, 20 – 65 a) with displaced talus fractures treated with osteosynthetic reduction and internal fixation, respectively. MR examinations were performed 7 to 49 months after surgical treatment. Indications for MRI were decrease in function and consistent pain. MR studies were evaluated by two readers in consensus, who were unaware of the clinical extent of the condition. Metal induced artifacts were scored on a four-point scale (none/mild/moderate/severe). Findings assessed were necrosis in the central and subchondral portions of the talus, changes in the sinus tarsi, the talocrural and subtalar joints and the adjacent bones.
Results: In 7 (59 %) patients no metal induced artifacts were depicted. Mild artifacts due to metal implants were present in 3 (25 %), moderate in 1 (8 %) and severe in 1 (8 %) patient. Osteonecrosis was found in 8 (67 %), collapse of the talar dome in 6 (50 %) and non-union of the talar neck in 2 (17 %) patients. We found synovial enhancement in 6 (50 %) and alterations of the sinus tarsi in 5 (42 %) patients. Osteoarthritis was present in the talocrural joint in 5 (42 %), in the subtalar joint in 6 (50 %). 6 (50 %) patients showed posttraumatic changes in adjacent bones.

Conclusion: MRI is an accurate tool for diagnosis of posttraumatic complications in patients with osteosynthetic treatment of talus fractures. Metallic artifacts did not significantly influence the diagnostic yield.

B-0395 15:20

Chronic synovites of joints: The role of MRI for a correct differential diagnosis

E. Bassetti, M. Mastantuono, L. Lobina, F. Trenta, R. Passariello; *Rome/IT*

Purpose: The objective of our study is to assess the role of MRI to make a correct differential diagnosis in patients with chronic synovitis.
Materials and methods: We studied 31 patient with a non specific chronic synovitis of the knee or ankle. We used for the study a 0.2 T dedicated equipment and an high field MRI unit (1.5 T Siemens Vision Plus). In most patients we administered intravenous contrast media (Gd-DTPA).
Results: In 8 patients MRI confirmed the presence of chronic synovitis that was responsible of pain or of impingement. In 14 patients a villonodular synovitis was suspected and confirmed by histologic examination. In 7 patients the synovitis presented a hyperplastic appearance and was secondary to a rheumatic pathology. 2 patients had a synovial sarcoma.
Discussion and conclusions: The MRI examination permitted a correct assessment of chronic synovitis of the knee and ankle. In the patients with pigmented villonodular synovitis MRI showed the villous and the nodular formation in the joint. In patients with rheumatic disease MRI, expecially after the administration of intravenous contrast media, permitted evaluation of the hyperplastic pannus from the fluid. MRI for its high spatial and contrast resolution enabled the correct diagnosis to be made in patients with chronic synovitis.

14:00–15:30 **Room C**

Abdominal and Gastrointestinal

SS 701

Pancreas

Chairpersons:
Y. Itai (Ibaraki/JP)
P. Reimer (Karlsruhe/DE)

B-0396 14:00

Bowel wall lesions following acute pancreatitis: CT findings and impact on clinical follow up

W. Wiesner, U. Studler, T. Kocher, L. Degen, C.H. Buitrago-Tellez, W. Steinbrich; *Basle/CH*

Purpose: To determine the diagnostic value of spiral-CT for the detection of colonic wall thickening following acute pancreatitis and to evaluate the clinical impact of such CT-findings.
Material and methods: CT-examinations of 19 patients with acute pancreatitis were analyzed and divided into 3 groups: I (Balthazar C), II (Balthazar D), III (Balthazar E). Bowel wall thickening if present was assessed and clinical and laboratory findings, duration of hospital stay, the need for subsequent CT examinations, punctions or antibiotic therapy were documented and compared between and within each group.
Results: Patients with colonic wall thickening showed higher infectious parameters and a longer hospital stay than patients without bowel wall lesions. All patients with colonic wall thickening needed antibiotic therapy compared to only 1 of 4 patients from the same group without colonic wall thickening. In all patients with colonic wall thickening a second CT examination and in 4 of them even a CT guided punction was performed whereas no patient with a normal bowel wall needed a CT guided punction.
Discussion: Acute pancreatitis may be followed by ischemic bowel wall changes and patients who show a colonic wall thickening seem to be at risk for a complicated clinical course. Further prospective studies should address the issue whether patients with acute pancreatitis who show a colonic wall thickening at the initial CT should be regarded as a high risk group and if the presence of large bowel wall thickening should be included into the used CT grading scores for acute pancreatitis.

B-0397 14:10

Secretin stimulated CT in pancreatic disease

W.R. Lees, A.R. Gillams, A. Sadhev; *London/GB*

Purpose: Secretin has been used to stimulate pancreatic juice production for measurement of duct size for almost 20 years. It is currently widely used in MRCP but has not been used to improve CT pancreatic imaging to any significant extent.
Materials and methods: 27 patients suspected of duodenal, ampullary or periampullary tumours underwent secretin stimulated spiral CT and were compared with 15 cases using an identical protocol without secretin. After a large oral water load, arterial and portal phase scans were initiated 3 min after infusion of 1 U Secretin/kg bodyweight and duodenal paralysis. Thin section, high resolution scans were conventionally obtained.
Results: Secretin improved duodenal distension, ductal anatomy, lesion conspicuity and mucosal detail. Duodenal distension was rated excellent in 24/27 cases with secretin compared to 7/15 controls. There was good differentiation of mucosa and muscularis propria in 22/27. Lesion conspicuity was better in the secretin group. The anatomic resoution of the pancreatic duct system was improved. The accessory papilla was routinely visualised. There was only 1 complication, 1 patient with papillary stenosis following photodynamic therapy to an ampullary tumour developed acute abdominal pain which resolved after 2 hours.
Conclusion: Secretin dumps fluid into the duodenum exactly where and when it is needed for best contrast. Pancreatic blood flow is also stimulated improving lesion conspicuity. Conventional oral loads with paralysis frequently fail to provide adequate duodenal distension. Secretin should routinely be used in CT scanning of duodenal, ampullary or periampullary tumours.

B-0398 14:20

Collateral vessels secondary to pancreatogenic occlusion of splenic vein and superior mesenteric vein: Spiral CT features

X.P. Zhou, Z.H. Yan, B. Song, R. Liu, P.Q. Min, X. Chen; *Chengdu/CN*

Purpose: To investigate the spiral CT features of collateral vessels secondary to isolated splenic vein occlusion (ISVO) and isolated superior mesenteric vein occlusion (ISMVO) caused by pancreatic diseases.
Materials and methods: 19 cases with ISVO and 6 cases with ISMVO, in whom 21 cases were caused by pancreatic carcinoma and 4 chronic pancreatitis, underwent spiral CT scanning in portal venous phase with collimation of 8 mm, reconstruction interval of 6 mm and 100 ml contrast media injected at the rate of 2.5 ml/s. The spiral CT features were evaluated by two radiologists, with emphasis on the spiral CT visualization rates of perigastric collateral vessels.
Results: In the cases with ISVO, the CT visualization rates of the collateral vessels were as follows: gastric short vein (GSV) in 17 cases (17/19, 90 %), gastroepiploic vein (GEV) in 17 cases (17/19, 90 %), gastrocolic trunk (GCT) in 13 cases (13/19, 68 %), left gastric vein in 12 cases (12/19, 63 %), right superior colic vein (RSCV) in 12 cases (12/19, 63 %) and esophageal vein in 2 cases (2/19, 10 %). In the cases with ISMVO, the CT visualization rates of the collateral vessels were as follows: GCT and RSCV in 4 cases (4/6, 67 %) respectively, GEV and middle colic vein in 2 cases (2/6, 33 %) respectively.
Conclusion: In ISVO, the collateral vessels with the highest spiral CT visualization rates were GSV and GEV, while in ISMVO they were GCT and RSCV.

B-0399 14:30

Ability of MR in correctly classifying IPMT of the pancreas

G.M. Carbognin, A. Guarise, I. Piscioli, M. Ferrari, C. Procacci; *Verona/IT*

Purpose: To assess the ability of MR examination in adequately characterizing intraductal papillary mucinous tumor (IPMT) of the pancreas.
Methods and materials: 29 patients with suspected IPMT underwent MR examination. In 22/29 patients, the imaging protocol, besides the conventional sequences associated with the administration of gadolinium, comprehended an MRCP examination. A superparamagnetic contrast agent was orally given to all patients. The images were read by a radiologist, blinded about the pathological diagnosis. Type of the lesion, its site and the relationships with the main pancreatic duct were evaluated.
Results: Among the cases with complete MR examination (conventional, gadolinium-enhanced MR and MRCP), a correct diagnosis was achieved in 17/22 (77 %). The conventional MR examination, associated with gadolinium administration, led to the correct diagnosis in 5/7 (71 %) cases.
Conclusion: The complete MR examination represents the best single imaging modality in evaluating IPMT of the pancreas. Moreover, it suits perfectly in following-up the patients affected with this disease.

B-0400 14:40

Standardisation of imaging in neuroendocrine tumours: Results of a European consensus procedure

J. Ricke[1], K. Klose[2], M. Mignon[3], K. Oberg[4], B. Wiedenmann[1]; *[1]Berlin/DE, [2]Marburg/DE, [3]Paris/FR, [4]Uppsala/SE*

Purpose: To define workflow recommendations for diagnosis and monitoring of neurondocrine tumours.

Materials and methods: A delphi consensus procedure was performed over a period of 2 years. The procedure included four consecutive workshops of a European group of experts in neuroendocrine tumours as well as feedback given by specialists from the departments of radiology, nuclear medicine, surgery and internal medicine of the according home institutions.

Results: Workflow charts were developed covering 1. Non-functional and functional neuroendocrine tumours of the pancreas (except for insulinoma): assessment of unknown primary; 2. Assessment of unknown primary in suspected insulinoma; 3. Assessment of primary in ECL-Cell tumour; 4. Assessment of unknown primary in neuroendocrine tumour of the gut; 5. Assessment of metastases of neuroendocrine tumours.

Conclusions: Diverging approaches among the centres which became apparent during the discussion reflect a lack of controlled studies specifically for rare subgroups of neuroendocrine tumours. The results facilitate the handling of patients with neuroendocrine tumours as well as the design of controlled studies.

B-0401 14:50

MR, hydro-helical-CT, and endosonography in the diagnosis of pancreatic cancer: Verified by results of surgery or tumor free follow-up > 6 months

P. Gocke, S.G. Rühm, S. Bosk, M. Rünzi, J.F. Debatin; *Essen/DE*

Purpose: To optimize the diagnostic strategy for assessing patients with suspected pancreatic cancer. Breathheld, fast MR was compared to Hydro-Helical-CT and endo-sonography

Methods and materials: MRI was performed on a 1.5 T scanner (Sonata), equipped with high performance gradients. The protocol consisted of axial 2D T1-FLASH images collected prior/after iv injection of contrast; axial fatsat T2 HASTE, cor MRCP HASTE, and FLASH 3D Angio sequences. MRA data sets were collected following iv administration of Gd-BOPTA. The CT protocol included oral application of 1 l H_2O, a Buscopan®-induced hypotonia, a native spiral scan of the upper abdomen, and a double spiral scan (3/4.5/2 mm) of the pancreatic region after injection of 150 ml of contrast with a delay determined by bolus tracking and 70 s. EUS was done with a full circle radial scanner at 7.5 MHz.

Each exam was assessed by separate radiologists, blinded to the results of other exams and clinical data. The following criteria were assessed on a 5-point confidence scale: pancreatic lesion, vessel involvement, ductal dilatation, lymph nodes and extrapancreatic spread. Gold standard was surgery, or tumor free follow-up > 6 months.

Results: Regarding lesion detection EUS outperformed MR and CT. CT proved superior to MRI regarding lymph node status and extrapancreatic spread of tumor. MR was found superior to CT and US regarding vessel infiltration and superior to CT regarding ductal dilatation.

Conclusion: Our data suggests that a combination of MRI and EUS is the accurate strategy for assessing patients with suspected pancreatic cancer.

B-0402 15:00

Non-invasive detection of endothelial dysfunction by color Doppler ultrasound in islet-cells, kidney-pancreas, and kidney-alone diabetic transplanted patients

M. Venturini, P. Fiorina, E. Angeli, F. De Cobelli, A. Secchi, A. Del Maschio; *Milan/IT*

Purpose: To compare by CDU endothelial function in IC with KP and KA transplanted patients. Intraportal percutaneous transplantation of islets of Langherans is an alternative to pancreas transplantation. Diabetic uremic patients after KP transplantation, but not after KA, reach an insulin independence, and this seems to preserve them by cardiovascular diseases, determining a reversal of endothelial dysfunction.

Materials and methods: We examined with CDU (ATL HDI 5000/5 – 10 MHz. linear probe) the right brachial arteries of 20 IC (submitted also to kidney transplantation), 20 KP and 20 KA uremic patients, comparable for mean age, immunosoppressive treatment and time from onset of diabetes. Diameter and resistive index changes after ischemia (brachial compression) and after nitrates (sublingual administration) were evaluated to assess endothelial dependent and independent vasodilation and compared with a Control group (C) of 20 normal subjects.

Results: IC and KP showed an higher dependent vasodilation versus KA group. Specifically, increased diameter after ischemia was similar in IC and KP groups, comparable with C group and significantly lower in KA (IC = 2.28 ± 1.08 mm; KP = 2.55 ± 1.10 mm; KA = 0.14 ± 1.33 mm; C = 4.01 ± 1.20 mm). Furthermore the reduction of resistive index after ischemia was higher in IC and KP groups rather than in KA one, and was similar to control group. Vasodilation after nitrates was less evident.

Conclusion: CDU is a simple and non invasive method which allows to study endothelial function. Pancreas and islet-cells transplantation seem to determine a reversal of endothelial dysfunction and exert a protective role on cardiovascular diseases.

B-0403 15:10

Possibilities of power Doppler sonography in the follow-up study of acute pancreatitis

I. Kalenova, A.V. Zoubarev, V. Bashilov, N. Agafonov; *Moscow/RU*

Purpose: To determine the role of conventional grey-scale and Power Doppler Sonography (PDS) in monitoring parenchymal and vascular changes in acute pancreatitis.

Methods and materials: 31 patients with acute pancreatitis underwent US examination before, during and after treatment. Pancreatic size, echogenicity, echotexture and fluid collections were evaluated. The degree of intrapancreatic vascularity and detection of major splanchnic vessels were evaluated by PDS. US findings were confirmed by laboratory results, CT and at surgery.

Results: In 13 patients with severe necrotizing pancreatitis grey-scale US and PDS did not provide accurate information in the acute stage of the disease. However, acute fluid collections and pseudocysts were well detected. Changes in echogenicity, pancreatic enlargement and peripancreatic edema were observed in 18 patients with mild pancreatitis in the acute stage of the disease on grey-scale US. Reduction of the parenchymal vascularity was detected by PDS in the acute stage. During follow-up intraparenchymal vascularity was increased (from 2nd week up to 9 months after the 1st US examination). Changes in vascularity were better then grey-scale US in predicting patient outcome. US findings correlated with clinical, laboratory and CT data in all cases.

Conclusion: US is a useful method for monitoring the course of acute pancreatitis. Follow-up PDS provides additional information about intrapancreatic parenchymal vascularity which helps assess management. We believe, that PDS monitoring will exclude septic complications in patients with necrotizing pancreatitis.

B-0404 15:15

^{11}C-harmine as a potential PET tracer for ductal pancreas cancer: In vivo and in vitro studies

G. Herlin[1], B. Persson[1], M. Bergström[2], B. Långström[2], P. Aspelin[1], J. Karlsson[2]; *[1]Stockholm/SE, [2]Uppsala/SE*

Purpose: To find a tracer using PET which potentially could be of value in diagnosing pancreas cancer.

Materials and methods: Nine autoradiographies were performed with ^{11}C-harmine (a MAO-A-inhibitor) and unlabelled harmine for competitive inhibition. Tissue preparations used were from normal human pancreas and human pancreas cancer. For reference tissue preparations from ratbrain were used. The uptake of rat brain which has the highest uptake were set to 100 %. PET examinations with ^{11}C-harmine were also performed on two patients with histopathologically verified pancreascancer, of whom one also had liver metastases.

Results: In 16 samples from 5 different human pancreascancers 13 gave a significant difference ($p < 0.01$) between total binding of harmine and after competitive inhibition with unlabelled harmine. 4 human pancreascancers were compared to rat brain and the average uptake was 28.2 % (SD 11 %, N = 13 experiments). Normal human pancreas had an average uptake of 5.5 % (SD 0.8, N = 2) compared to rat brain. The specific binding in human pancreas cancer was higher than the binding from normal human pancreas. In the PET camera examinations the uptake of ^{11}C-harmine in the pancreas cancer in one patient was moderate and the liver metastases were also visible. In the other patient only a slight uptake was noticed in the pancreas cancer.

Conclusion: This study shows an uptake of ^{11}C-harmine in human pancreas cancer both in vitro and in vivo and this substance could potentially be of value in diagnosing pancreas cancer in patients using PET.

B-0405 15:20

Sonographic evaluation of pancreatic transplantation with portal venous and exocrine enteric drainage

B.H.J. Lin, M. Cihangiroglu, A.H. Dachman; *Chicago, IL/US*

Introduction: Pancreatic transplantation with portal venous drainage and enteric drainage of exocrine secretions is a new surgical technique with fewer complications reported compared to conventional technique. We sought to prospectively evaluate the ability of ultrasound to visualize the pancreatic allograft and its vasculature in order to avoid the nephrotoxicity associated with contrast enhanced CT.
Methods and materials: 29 patients were prospectively evaluated for a total of 39 sonographic examinations. Gland visualization, color flow (four point scale), and spectral Doppler evaluation of the arterial supply and draining vein were obtained.
Results: The gland was adequately visualized in 38/39 (97 %) scans and color flow could be graded in 28/37 (76 %) Doppler exams. The pancreatic duct was seen in 19 %. In 26 cases with adequate Spectral Doppler, all showed normal arterial wave forms, with mean peak systolic velocity 34 cm/s (12 – 121), resistive index 0.73 (0.63 – 0.9) and peak venous velocity in the draining vein of 15.5 cm/s. One patient with high peak systolic velocity (121 cm/s) developed infection and subsequent pseudoaneurysm.
Conclusion: Sonography is effective in evaluating the pancreatic allograft's vasculature, blood flow and size. Given the encouraging clinical results of this new approach to pancreas transplantation, radiologists may encounter these patients more frequently and should be aware of the post-operative anatomy and findings.

B-0406 15:25

3D CE MR angiography in simultaneous kidney and pancreas tranplantation: Initial experience

G. Carrafiello, A. Rampoldi, R. Corso, V. Tombini, F. Di Gennaro, A. Vanzulli; *Milan/IT*

Purpose: To evaluate the role of 3D CE MR angiography sequences in detection of vascular and parenchymal findings of kidney and pancreas in simultaneous transplantation.
Method and materials: 17 patients (13 male and 4 female), kidney and pancreas simultaneous recipients, were evaluated with 1.5 T Gyroscan Philips, using 3D contrast enhanced sequence (two consecutive, breath old acquisition of 15 seconds each) and a tardive axial sequence, after a MultiHance injection (20 ml with flow rate of 2.0 ml/s).
Results: The source images MIP and subs traction images were analysed. In all patients (100 %) we found high signal intensity in aorta, common iliac arteries and in main branches of transplanted arteries and also in IVC, common iliac veins and main branches of transplanted veins. In all patients was possible to evaluate parenchymal perfusion of kidney and pancreas transplanted.
Conclusion: 3D contrast enhanced sequence is useful and easy to evaluate, with one contrast injection, arterious and venous vascularization and parenchymal perfusion of kidney and pancreas transplanted. We belive that in future MRA will may develop a very useful to follow up kidney and pancreas simultaneous transplantation, because it is no invasive and because the contrast agent used not make worse renal function.

14:00–15:30 **Room E2**

Breast

SS 702

Digital mammography (2)

Chairpersons:
U. Fischer (Göttingen/DE)
A. Skjennald (Oslo/NO)

B-0407 14:00

Full-field digital mammography: Comparison of conventional and digital techniques in 100 patients

S. Obenauer, S. Luftner-Nagel, F. Baum, C. Schorn, D. von Heyden, E. Grabbe; *Göttingen/DE*

Purpose: To compare full-field digital mammography to screen-film mammography regarding image quality and lesion detectability by using images of the same patient from both systems.
Methods: Two mammography systems were used, one with a digital detector and the other one with a screen-film-system. Digital and conventional mammograms were performed of 50 patients with cytological or histological proven tumors on the same day. In addition, 50 digital mammograms and their corresponding screen-film mammograms not older than 1.5 years were reviewed in a random order with the mammograms of the tumor patients by three observers. Contrast, exposure and artifacts of the images were evaluated. Different details like skin, retromamillary space and parenchymal structures were jugded. The detectability of microcalcifications and lesions were compared and correlated to histology.
Results: Image contrast was jugded to be good in 76 %, satisfactory in 20 % and unsatisfactory in 4 % of screen-film mammograms. Digital mammograms were jugded to be good in 99 % and unsatisfactory in 1 %. Improper exposure in screen-film system occured in 18 % (10 % over-exposured, 8 % under-exposured). Digital mammograms were improperly exposed in 4 % of all cases, but of sufficient quality after post-processing. Artifacts were found in 78 % of conventional and none in digital mammograms. Different anatomical regions were better detectable in digital than in conventional mammography. Digital mammograms provided a slightly better lesion detection, the difference was not significant.
Conclusions: Digital mammography offers a consistent high image quality without artifacts. Lesion detection was equal or superior to conventional images.

B-0408 14:10

Intrapatient comparison of microcalcifications: Full-field digital mammography vs. screen-film mammography

U. Fischer; *Göttingen/DE*

Purpose: The goal of the study was to compare a full-field digital mammography system (FFDM) to a conventional film-screen mammography (FSM) system for the detection and characterization of microcalcifications.
Material and methods: Eighty-seven patients with 92 microcalcification clusters were evaluated with both, a FFDM system (Senographe 2000D, GE) and a FSM system (Senographe DMR, GE). A conventional film-screen mammogram and a digital contact mammogram were obtained in each patient. The image quality, the number, type and distribution and the characterization (BI-RADSTM 2 – 5) of microcalcifications were evaluated. The results were compared to histopathologic findings in 67 patients and follow-up in 20 patients.
Results: Histopathology revealed 28 benign lesions (sclerosing adenosis, dysplasia, hamartoma, radial scar) and 44 malignant tumors (in-situ carcinoma, invasive carcinoma). Twenty patients had benign changes verified by long-term follow-up. Image quality of FFDM was assessed superior to FSM in more than 50 % of the cases. FFDM depicted a significantly higher number of microcalcifications than FSM. Sensitivity, specificity and accuracy for FFDM vs FSM were 93 % vs 89 %, 55 % vs 45 % and 70 % vs 64 %, respectively.
Conclusions: In patients with mammographic microcalcifications, the FFDM system with a 100 µm pixel size provides better image quality, a higher detection rate and more accurate characterization of microcalcifications than FSM.

B-0409 14:20

Screen-film magnification mammography vs. digitized image display and processing in the detection of microcalcifications: A ROC study

K. Perisinakis, J. Damilakis, M. Kontoyiannis, N. Gourtsoyiannis; *Iraklion/GR*

Purpose: To compare the detectability of microcalcifications using the digitized mammographic view versus the magnification mammography film.
Materials and methods: Contact and magnification images of an ALVIM mammographic statistical phantom based on receiver operating characteristic (ROC) analysis were obtained using a GE Senographe DMR mammographic unit. The phantom simulates microcalcifications of various dimensions. Phantom images simulating breast with thickness 2.4, 3.3 and 4.2 cm were obtained. The contact and magnification mammograms of 27 patients presenting microcalcifications were also studied. All contact images were digitized using a film scanner with pixel size of 50 µm at 12 bit. The images were displayed to 3 observers for interpretation on the computer monitor and also presented as laser film hard copies on a film view box for comparison. Image Pro-Plus software package was used for digital image manipulations. Phantom images were evaluated with respect to the visualization of relevant structures. Patient images were evaluated on the basis of the information relevant to the (a) existence, (b) population and (c) form diversity of microcalcifications.
Results: Phantom lesion detectability did not differ significantly ($p > 0.05$) when the digitized film image or the magnification hardcopy film was used for all lesion dimensions and phantom thickness. Visualization of microcalcifications using the hardcopy magnification film was superior to digitized film however the difference was not significant ($p > 0.05$).
Conclusion: Computer-assisted visualization of the digitized mammogram may provide similar information to magnification mammographic view.

B-0410 14:30

Focal breast lesions: Digital mammography with computed radiography vs. conventional radiographic mammography

U.J. Wilhelmi, U.G. Aichinger, R.W.S. Schulz-Wendtland; *Erlangen/DE*

Purpose: In comparison to conventional radiograms digital mammography offers a greater dynamic range, reduction in radiation dose, the possibility of postprocessing images and using computer assisted diagnostic programms though spatial resolution is known to be lower in dm. The purpose of our study was to compare digital mammogaphy and conventional radiograms regarding detection and validation of dignity of breast lesions in clincal use.

Material and methods: For dm we used high resolution storage plates with a size of 24 × 30 cm² which allow a viewing rate of 10 pixel per mm in connection with a HQS which reach a spatial resolution of 8 light points per mm. The laserprinter has a line distance of 50 mm. Dm and cr of 48 patients were compared by three different examiners with regard to detection and validation of focal breast lesions.

Results: We found no significant difference between dm and cr in the detection and validation of focal breast lesions. Due to postprocessing the dm magnifying or repeating of the mammograms was not necessary which lead to smaller radition doses for the patient.

Conclusions: On the basis of our technical equipment and our results of this study we use dm in daily routine. In future dm, will probably become more common in the community due to its advantages such as dose reduction, importance of further archiving, cost-effectiveness, digital postprocessing and monitor diagnosis.

B-0411 14:40

Application of computer aided diagnosis (CAD) at digitalized mammograms: Detection of microcalcifications

I. Facecchia[1], U. Bottigli[2], P. Delogu[2], A. Marchi[2], V. Londero[1], S. Smania[1], M. Bazzocchi[1]; *[1]Udine/IT, [2]Pisa/IT*

Purpose: During mammographic screening programs indipendent double reading is essential in order to reduce the rate of false negative examinations of 5 – 15 %. The authors developed and applied a computer aided diagnosis (CAD) system. The aim of CAD is to support radiologists as a second reader.

Methods and material: Our database consists of 802 images corresponding to 213 patients. We performed traditional mammography and then we digitalized mammograms using a CCD linear scanner (pixel size of 85 × 85 µm², 12 bits). Images were evaluated by two radiologists with similar experience and then by CAD system. Our CAD searchs for microcalcifications by use of "ad hoc" algohoritms and artificial neural network (Sanger type).

Results: The number of clusters in our database is 141 corresponding to 140 images and 692 images are non pathological. The CAD system found 140 clusters with a mean number of 9 suspicious regions/image and 135 clusters with a mean number of 5 suspicious regions/image.

Conclusion: In the very next years the use of CAD will be easier and it could be applied in the every day practice especially in those centers in which digital mammography is performed. Thanks to the high sensitivity (> 82 %) of CAD, in spite of a quite low specificity (5 suspicious regions per image), CAD rappresents a concrete aid for the radiologists.

B-0412 14:50

Tumor detection rate with a new commercially available computer-aided detection (CAD) system

A. Malich, C. Marx, M. Facius, M. Fleck, T. Azhari, W.A. Kaiser; *Jena/DE*

Purpose: To determine the tumor detection rate and to assess the clinical usefulness of Second Look™, a mammographic computer-aided detection system.

Patients and methods: The CC and MLO images of 150 suspicious mammograms from 150 patients that were histologically proven to be malignant were analyzed using the Second Look™ computer-aided detection system (CADx Medical Systems, Quebec, Canada). Cases were selected randomly using the clinic's internal tumor case sampler. Correct marking of the malignant lesion in at least one view was scored as a true positive. Marks not at the location of the malignant lesion were scored as false positives.

Results: The 150 mammograms included 94 lesions that were suspicious due to masses, 26 due to microcalcifications and 30 showed both signs of malignancy. The overall sensitivity was 90.0 % (135/150). Sensitivity on subsets of the data was: 88.7 % (110/124) for masses and 98.2 % (55/56) for microcalcifications. The average numbers of false positive marks per image were 0.23 for microcalcifications and 0.74 for masses. 7/14 non marked masses had a size larger than 3.2 cm in diameter.

Conclusion: The CAD-system shows a high sensitivity with less than 1 false positive mark per image. Therefore, when used clinically, the Mammagraph™ (Second Look printout) would have effectively and efficiently directed the radiologist's attention to the malignant lesions. These results suggest that this system is clinically useful as a second reader of mammograms. A further reduction of FP marks, however, seems to be necessary to increase the clinical value of the system.

B-0413 15:00

Accuracy of computer assisted diagnosis in mammography: Experience with 200 proven cases

C. Balleyguier[1], S. Malan[1], P. Taourel[2], J. Fermanian[1], J. Chabriais[1], O. Hélénon[1], Y. Menu[1]; *[1]Paris/FR, [2]Montpellier/FR*

Computer Assisted Diagnosis (CAD) in mammography helps the radiologist for detection of breast masses and microcalcifications. The aim of this study was to evaluate the accuracy of this method in a cohort of 200 mammograms.

Material and methods: Among these mammograms, 100 were normal or showed benign lesions (cysts, adenofibroma, mastosis), and 100 corresponded to patients with biopsy-proven breast cancer, detected in a screening program. All mammograms were evaluated with a Second Look® system (CAD-X Medical System, Laval, Ca).

Results: Sensitivity and specificity for detection of malignancy were respectively 89 % and 16 %. Positive and negative predictive values were respectively 49 % and 59 %.

Conclusion: CAD mammograms carries a high sensitivity in the detection of malignancy, and may help the radiologist to find high risk areas. Medical expertise remains necessary due to low specificity. CAD mammography is a useful tool to improve the accuracy of mammogram interpretation.

B-0414 15:10

Computer assisted diagnosis in mammography: Does it help the junior and/or the senior radiologist?

C. Balleyguier[1], S. Malan[1], P. Taourel[2], J. Pujol[2], J. Fermanian[1], G. Djen[1], O. Hélénon[1], Y. Menu[1]; *[1]Paris/FR, [2]Montpellier/FR*

Computer Assisted Diagnosis (CAD) in mammography detects breast lesions with a high sensitivity. The aim of this study is to evaluate the improvement in breast cancer detection on mammograms by a junior and senior radiologist by using this system

Material and methods: 110 mammograms (97 normal or with benign lesions, 13 with biopsy proven cancer) were examined by a junior and a senior radiologist, without CAD system. Junior and senior radiologist read independently. In each session the radiologist read the mammography first without and then with CAD analysis. Both interpretations were recorded, and standardised according to the BIRADS classification.

Results: For the senior radiologist, sensitivity improved from 76.9 % to 84.6 % with the use of CAD analysis. Specificity, negative and positive predictive values did not change. For the junior radiologist sensitivity improved from 61.9 % to 84.6 %. Specificity did not change, but negative predictive value improved slightly

Conclusion: Even in a relatively small sample, CAD mammography proved very useful for the junior radiologist, improving dramatically sensitivity and to a lesser extent negative predictive value.

B-0415 15:20

Assessment of sono-CT vs. high resolution conventional B-mode US in the assessment of breast lesions and fibrotic breast tissue: Initial results in a blind study

A. Malich[1], C. Marx[1], M. Fleck[1], T. Böhm[2], W.A. Kaiser[1]; *[1]Jena/DE, [2]Zürich/CH*

Purpose: To test the ability of Sono-CT™ imaging to improve image quality in breast ultrasound of fibrotic tissue by suppressing image artifacts in comparison to conventional high resolution B-mode ultrasound.

Methods and materials: 60 breasts with very fibrotic tissue and corresponding shadow-artifacts underwent US examinations usin g HDI 5000 (ATL, USA) with and without Sono-CT™-usage in a clearly defined reproducible location (1 cm cranial of the nipple). Three independent observers scored the assessment of both US-examinations using a 3-grade score (1 … high image quality; 2 … normal image quality; 3 … rather poor image quality).

Results: In 55 % of the cases (mean value 32/60; 33/60; 34/60, respectively) the observers found an increased assessment of the structure using the new software modality. In the remaining cases no changes were visible. The scoring of the image quality increased from a mean of 2.27 (SD 0.46) using B-mode to 1.60 (SD 0.56) using the new modality.

Conclusion: Initial results suggest an increased assessment and a significantly increased image quality of fibrotic tissue when using Sono-CT™ software versus high resolution B-mode software.

14:00–15:30 **Room F1**

Chest

SS 704

Imaging and cardiopulmonary function

Chairpersons:
B. Ghaye (Liège/BE)
K. Malagari (Athens/GR)

B-0416 14:00

Magnetic resonance assessment of lung ventilation by mechanical delivery of aerosolized gadolinium-DTPA

P. Haage, G.B. Adam, S. Karaagac, R. Günther; *Aachen/DE*

Purpose: Analysis of a new technique using mechanical administration of aerosolized Gd-DTPA to visualize lung ventilation in MR imaging.
Materials and methods: Twelve experimental procedures were carried out in a domestic pig model. Gd-DTPA was aerosolized by a small particle generator. The intubated animals were mechanically aerosolized with the nebulized contrast agent. Imaging was performed before, during and after contrast administration on a 1.5 T MR imager using a T1-weighted turbo spin echo sequence with respiratory gating. Pulmonary signal intensity changes were calculated for corresponding regions of both lungs. Homogeneity of aerosol distribution was graded by two radiologists.
Results: After ventilation with the aerosolized Gd-DTPA, the signal intensity in both lungs increased significantly in all animals with mean values of 110 % above baseline. To achieve a comparable SI increase as attained in previous trials with manual aerosol delivery, a ventilation period of 20 minutes (formerly 30 minutes) was sufficient. Contrast distribution was rated homogeneous in all cases by the reviewers.
Conclusion: The feasibility of depicting pulmonary ventilation in large animals with aerosolized Gd-DTPA has been demonstrated before. The results of this refined technique sustain the potential of Gadolinium-based ventilation MR imaging by improving aerosol distribution and shortening of ventilation duration.

B-0417 14:10

Dynamic imaging of cardiopulmonary resuscitation (CPR) with contrast-enhanced EBCT in a porcine model

A. Schuster, W. Recheis, A. Kleinsasser, A. Loeckinger, R. Eder, P. Springer, T. Frede, C. Hoermann, D. zur Nedden; *Innsbruck/AT*

Purpose: To visualize the impact of reanimation forces on thoracic structures during automated cardiopulmonary resuscitation (CPR).
Methods: Four anesthetized and mechanically ventilated pigs were scanned during CPAP using an EBCT during automated reanimation by a programmable chest compression device. In the 50 ms scan mode four levels of the heart were scanned simultaneously at a rate of 13 images per second and a slice thickness of 7 mm with a gap of 4 mm. To get optimal contrast of heart cavities and vessels, a non-ionic contrast medium was administered at a flow rate of 2.0 ml/s (30 s start-delay). Cross-sectional areas and volumes were estimated on an external workstation.
Results: The 50 ms scan mode offered a direct access to the effects and dynamics of forces during cardiopulmonary resuscitation. The extent and chronology of changes to heart, central vessels, lung, tracheobronchial system and soft tissue could be cinematically visualized and quantified.
Conclusion: Intrathoracic effects of CPR could be visualized cinematically. This study contributes to a better understanding of the mechanics of CPR.

B-0418 14:15

Computerised detection and quantification of pulmonary emphysema: An improved algorithm

U. Tylén[1], O. Friman[2], M. Borga[2], J.-E. Angelhed[1]; [1]*Gothenburg/SE*, [2]*Linköping/SE*

Purpose: HRCT is the best method to diagnose pulmonary emphysema. It is so good that it may be used for long term studies provided there is a good method for quantification. Visual diagnosis of emphysema is accurate but inter- and intra-observer variation is large when it comes to quantification. Density mask technique may be adequate when the emphysema is extensive but is not specific enough for detection of early emphysematous lesions. We wanted to develop a more specific algorithm for quantification of early emphysematous lesions.
Methods: The sharp reconstruction algorithm used in HRCT, gravity and motion introduce artefacts making pixels get lower HU-values. Use of density mask technique then detects more pixels in the interval defined as emphysema. Thus the amount of emphysema in a slice may be overestimated. We have developed a computer programme which corrects the artefact mentioned. A group of 20 healthy volunteers were investigated, 10 with light emphysema and 10 without.
Results: With only density mask technique and a cut off at –950 HU persons without emphysema could not be separated from those with light emphysema. With our new algorithm the separation was very much improved. The algorithm is still sensitive for motion and will be improved further.
Conclusion: An improved algorithm has been developed which makes quantification of emphysema with density mask technique more accurate.

B-0419 14:25

A SCT study on the effect of CPAP during induction of general anesthesia on the development of pulmonary atelectasis

S. Wicky, S. Proietti, M. Rusca, P. Schnyder, L. Magnusson; *Lausanne/CH*

Purpose: The aim of this study is to assess if a CPAP applied during the induction of general anesthesia is efficient to reduce the development of pulmonary atelectasis.
Material and methods: Two groups of four volunteers, who underwent general anesthesia, were prospectively randomized. Before induction of general anesthesia, three SCT sections of 7 mm, in expirium, were acquired at the level of the interventricular septum. Group one (G1) consisted in volunteers to whom no CPAP was applied during induction of general anesthesia. In the group 2, pre-oxygenation was performed with a PEEP of 6 cm H_2O. General anesthesia was performed on the table of the SCT unit and after intubation, three SCT sections were acquired at the same level. With a threshold of –1000 to +100 Hounsfield Units, the surface of the pulmonary parenchyma was manually extracted from the SCT sections. The surface of pulmonary atelectasis was selected using a threshold of –100 to +100 Hounsfield Units and reported to the total pulmonary surface of the SCT sections.
Results: A statistically significant difference was observed in comparing G1 and G2 in the development of pulmonary atelectasis ($p = 0.0161$).
Conclusions: A CPAP applied during induction of general anesthesia allows reducing pulmonary atelectasis in volunteers.

B-0420 14:35

The impact of cardiopulmonary resuscitation (CPR) on lung aeration (air-tissue ratio): Porcine model with EBCT

W. Recheis, A. Schuster, A. Kleinsasser, A. Löckinger, C. Hörmann, D. zur Nedden; *Innsbruck/AT*

Purpose: To evaluate changes of air-tissue ratio in previously defined regions of interest after CPR.
Materials and methods: Four anesthetized and mechanically ventilated pigs were scanned before and 30 minutes after CPR at two constant PEEP levels (5 cm, 15 cm H_2O). Volume scans were obtained using an EBCT with 6 mm slices. After segmentation, the gray values of the lung were divided into steps of 100 HU to get access to the changes of air-tissue ratio. The air-tissue ratio was evaluated in the upper, intermediate and lower region of the lung.
Results: After CPR for 9 minutes, well aerated areas (–800 to –400 HU) became smaller, while highly aerated (–900 to –800 HU) and poorly aerated areas (–400 to –100 HU) grew.
The higher and intermediate regions of the lung showed more changes in the air-tissue ratio than the lower regions with previously poorer aeration. In total, the degree of atelectasis increased. Using the higher PEEP level, well aerated areas showed a marked increase in contrast to atelectatic areas.
Conclusion: After CPR, a redistribution of lung aeration could be detected. According to the impaired hemodynamics, the rate of well-aerated lung tissue decreased and the rate of highly and poorly aerated lung and atelectasis increased.

B-0421 14:45

Color-coded 3D visualization of lung aeration before and after cardiopulmonary resuscitation (CPR)

A. Schuster, W. Recheis, A. Kleinsasser, A. Loeckinger, R. Eder, P. Springer, T. Frede, C. Hoermann, D. zur Nedden; *Innsbruck/AT*

Purpose: To visualize the redistribution of lung aeration after CPR with color-coded volume-rendering: evaluation in a porcine model.

Methods: Four anesthetized and mechanically ventilated pigs were scanned before and 30 minutes after CPR at constant PEEP levels (5 cm and 15 cm H_2O). Volume scans were obtained using an EBCT with 6 mm slices. Post-processing was performed on a Siemens Virtuoso workstation. The Hounsfield range from –900 to 0 was divided into 9 intervals of 100 HU to quantify variances of the air-tissue ratio. Colors and opacity factors were assigned to each interval.
Results: After CPR for 9 minutes the antero-posterior and cranio-caudal lung attenuation gradients changed: well aerated areas (–800 to –400 HU) became smaller, while highly aerated (–900 to –800 HU) and poorly aerated areas (–400 to –100 HU) grew. By coloring 3D-data sets of lungs before and after CPR at two PEEP levels, the redistribution of well and poorly aerated areas could be impressively visualized.
Conclusion: Introducing color-coded volume rendering into lung tissue diagnostics proved to be a valuable device for a better visualization of lung aeration changes and could be a reasonable tool for the follow-up of patients suffering of impaired lung aeration.

B-0422 14:50

A SCT study on the effect of a low inspired concentration oxygen on postoperative pulmonary atelectasis in volunteers under general anesthesia
S. Wicky, B. Zilgia, L. Magnusson, P. Schnyder, S. Proietti; *Lausanne/CH*

Purpose: The aims of this study is to assess if under general anesthesia, a low inspired fraction of oxygen (FiO_2) prior to extubation is efficient to reduce postoperative pulmonary atelectasis.
Material and methods: Two groups of eight volunteers, who underwent general anesthesia, were prospectively randomized. Group one (G1) consisted in volunteers to whom one vital capacity maneuver (40 cm H_2O during 15 seconds) was performed, followed by a 100 % FiO_2 during 15 minutes prior to extubation. In the group 2, only 40 % FiO_2 was used during 15 minutes prior to extubation. After extubation, three SCT sections of 7 mm, in expirium, were acquired at the level of the interventricular septum. With a threshold of –1000 to +100 Hounsfield Units, the surface of the pulmonary parenchyma was manually extracted from one SCT section. The surface of pulmonary atelectasis was selected using a threshold of –100 to +100 Hounsfield Units and reported to the total pulmonary surface of the SCT section.
Results: Atelectasis was measured in 8.50 ± 6.23 % and 2.72 ± 1.05 % of the surface of the pulmonary parenchyma in G1 and G2, respectively ($p < 0.0139$).
Conclusions: A low FiO_2 of 40 % prior extubation allows reducing pulmonary atelectasis after general anesthesia in volunteers.

B-0423 15:00

Visualization of lung aeration dynamics: Comparing augmented and controlled mechanical ventilation with EBCT
W. Recheis, A. Schuster, A. Kleinsasser, A. Löckinger, C. Hoermann, D. zur Nedden; *Innsbruck/AT*

Purpose: To evaluate differences in changes of lung aeration (air-tissue ratio) between augmented and controlled mechanical ventilation in normal subjects.
Materials and methods: 5 volunteers, respirated with pressure controlled ventilation (PCV) and augmented ventilation (CPAP) via face mask, were scanned using the EBCT.
A software analyzed the respirator's digitized pressure and volume signals. Thus the EBCT was triggered at the onset of inspiration. In the 50 ms scan mode, 20 – 40 slices were acquired during the inspiratory phase at a level 1 cm above the diaphragm. Three degrees of pulmonary aeration were defined in order to visualize the dynamic changes: between –900 HU and –800 HU, between –800 HU and –700 HU and between –700 HU and –600 HU. The dynamic changes were evaluated in three separate areas: a ventral, an intermediate and a dorsal area.
Results: CPAP protocol results in an increase of air-tissue ratio in the dorsal lung area (ventral: 5 %, dorsal: 25 %) due to the active movement of the diaphragm, whereas PCV results in a more pronounced increase in air-tissue ratio of the ventral lung (ventral 25 %, dorsal 30 %) area.
Conclusion: This study gives further insight into the dynamic changes of the lung's biomechanics by comparing augmented and controlled mechanical ventilation in the healthy proband.

B-0424 15:10

Correlation of blood oxygenation and lung density in a porcine lavage ARDS-model: Use of dynamic multiscan CT
A. Bink, K. Markstaller, H.-U. Kauczor, B. Eberle, N. Weiler, M. Thelen; *Mainz/DE*

Purpose: To demonstrate physiological significance of different density ranges at dynamic multiscan CT in an ARDS-model and to correlate them to blood oxygenation.
Methods and materials: Six anaesthesized pressure-controlled ventilated pigs (inspiration:exspiration ratio = 1:1) were examined before and after induction of a surfactant-depletion ARDS-model induced by multiple lavages using saline. The airway pressure was increased stepwise (mean airway pressure 8, 13, 18, 23, 28, 33 and 38 mbar). On every step, dynamic multiscan CT was performed (CT technique: slice thickness 1 mm, high resolution algorithm, temporal increment 250 ms). The relative area of defined density ranges was measured planimetrically. The density range for ventilated alveolar space in healthy lungs was –910 to –700 HU, in ARDS it was –910 to –300 HU. Atelectasis was represented by the density range –300 to +200 HU. These areas were integrated over the whole ventilation cycle and fitted against time (% of mean lung area/s). Partial oxygen pressure and shunt perfusion were correlated with the mean area of ventilated alveolar airspaces and with atelectasis.
Results: Ventilated alveolar air spaces correlated with partial oxygen pressure: healthy lungs: $r = +0.85$; ARDS lungs: $r = +0.80$. Atelectasis showed a negative correlation: healthy lungs: $r = -0.73$; ARDS lungs: $r = -0.87$. Additionally, atelectasis showed a good correlation with the shunt perfusion fraction: healthy lungs: $r = +0.79$; ARDS lungs: $r = +0.89$.
Conclusion: Lung density ranges in dynamic multiscan CT can be used to estimate blood oxygenation and the amount of shunt perfusion in ARDS.

B-0425 15:20

Analysis of airspace size in healthy volunteers and single lung transplant recipients using the apparent diffusion coefficient at ^{3}He MRI
A. Bink, K. Gast, G. Hanisch, J. Lill, A. Vogel, E. Mayer, W. Schreiber, M. Thelen, H.-U. Kauczor; *Mainz/DE*

Purpose: To measure the apparent diffusion coefficient (ADC) of inhaled ^{3}He in healthy volunteers and lung transplant recipients as an MRI indicator of airspace size. The aim was to demonstrate gravity-dependence of ADC values and differences between healthy individuals and patients.
Methods and materials: 5 healthy volunteers and 7 patients after single lung transplantation (4 for fibrosis, 3 for emphysema), were examined in a 1.5 T MRI scanner. They inhaled 300 ml of ^{3}He (polarisation rate 45 %) administered by a PC-controlled delivery device. ^{3}He diffusive gas movement was measured by a two-dimensional FLASH sequence (TR/TE/α 15.5 ms/10 ms/< 3.5°, matrix size 64 × 64, FOV 320 mm, slice thickness 20 mm, 5 slices, acquisition time 20 s). From this data, ADC maps were calculated for each slice. For more detailed evaluation the lung was divided into the four quadrants.
Results: No anterior-posterior gradient of the ADC was found – neither in healthy nor in diseased lungs. Mean overall ADC of healthy individuals was 0.15 cm²/s (range: 0.13 – 0.17 cm²/s). In the transplanted lungs the mean ADC was 0.17 cm²/s (0.15 – 0.18 cm²/s). The native fibrotic lungs of the transplanted patients had a mean ADC of 0.23 cm²/s (0.22 – 0.25 cm²/s). The mean ADC of the native emphysematous lungs was 0.27 cm²/s (0.19 – 0.38 cm²/s).
Conclusion: Different airspace size is found in healthy and diseased lungs using ADC measurements at ^{3}He MRI.

14:00–15:30 Room F2

Neuro

SS 711

CNS infections - Demyelination/Miscellaneous

Chairpersons:
H.G. Becker (Hannover/DE)
E.M. Laasonen (Tampere/FI)

B-0426 14:00

Radiologic evaluation of the heavy eye phenomenon

B.H.J. Lin[1], H.Y. Lin[2], A.H. Wang[2]; *[1]Chicago, IL/US, [2]Taipei/TW*

Purpose: To describe the imaging characteristics and role of radiology in the evaluation of an ophthalmologic condition manifested by high myopia and restrictive esotropia.

Methods and materials: In a 4 year period, seven patients with chronic progressive high myopia presented to an ophthalmology clinic with bilateral or unilateral esodeviation. All patients were evaluated for endocrine and orbital pathology. All underwent non-contrast head CT examination. Three patients were evaluated with gadolinium enhanced MR of brain and orbits. Corrective surgery was performed in six patients.

Results: CT examinations revealed varying degrees of elongation in the longitudinal axis of globes, characteristic deviation of lens, and compression of the lateral rectus muscle. MRI examinations confirmed these findings with better detail. The imaging results were crucial for determination of surgical treatment by ophthalmologists. Six patients underwent myotomy and/or partial resection of rectus muscles. Pathologic evaluation of a resected specimen showed muscular atrophy and fibrosis.

Conclusion: Heavy eye phenomenon is receiving increasing recognition in the ophthalmology literature. Our experience with this cohort indicates that ophthalmologists rely substantially in the imaging findings for diagnosis and surgical planning of this uncommonly reported syndrome. Thus appropriate recognition and consultation from radiologists is important in the management of this entity.

B-0427 14:10

Brain MR in evaluation of SLE and other systemic connective tissue diseases

N. Bešenski, N. Èikeš, Z. Rumboldt, I. Boric, D. Pavic, M. Radoš, M. Lušic; *Zagreb/HR*

Purpose: To investigate the prevalence and extent of cerebral changes in patients with SLE by MR in clinically manifest and clinically silent brain lesion.

Material and methods: We examined 48 patients with SLE, (mean age 40 years) by MR. 29 patients (GROUP A) were clinically presented with major neurological manifestations (epileptic seizures, haemiparesis, stroke ect.). 21 patients were without major neurological manifestations of SLE (Group B). Clinical presentation in those patients were headache, dizzines and depression.

Results: MR was normal in 7 patients (4 Group A, 3 Group B). In 13 patients from Group A, MR showed multiple hyperintense small lesions in the WM. Diffuse brain atrophy was found in 6 and signs of vasculitis/cerebral infarctions in 5 cases. In 14 out of 19 asymptomatic patients (Group B) similar WM lesions were found and moderate diffuse brain atrophy in 7. In Group B ischaemic lesion was present in one. WM lesions dominated in frontoparietal, occipital and subcortical WM in both group FLAIR sequence was the most sensitive in patients with SLE. Using 3D TOF MRA dinamic flow changes were suspected in 3 patients in Group A, but in none from the group B. DWI did not showed signs of altered diffusion except in one pat. from group A.

Conclusion: Results showed that MR is also very sensitive in the detection of WM lesions in neurologically asymptomatic SLE patients. Whether this represents subclinical brain involvemnet remains unknown.

B-0428 14:20

Abnormal hyperintensity within the subarachnoid space evaluated by fast fluid-attenuated inversion-recovery MR imaging: A spectrum of central nervous system diseases

T. Ishii[1], M. Maeda[1], A. Yagishita[2], H. Sakuma[1], K. Takeda[1]; *[1]Tsu/JP, [2]Fuchu/JP*

Purpose: Fast fluid-attenuated inversion-recovery (FLAIR) MR imaging is routinely used on MR examinations of the brain in our hospital. Our purpose was to report various central nervous system diseases with abnormal hyperintensity within the subarachnoid space on fast FLAIR.

Methods and materials: We reviewed FLAIR MR images of the brain from all patients in a 20 month period. Special attention was paid to the abnormal hyperintensity within the subarachnoid space.

Results: There were various diseases that exhibited abnormal hyperintensity within the subarachnoid space on FLAIR images, including acute infarction, moyamoya disease, subarachnoid hemorrhage, inflammatory meningitis, and leptomeningeal spread of malignancy. The appearances of hyperintensity were tubular in acute infarction and moyamoya disease, and focal or diffuse in subarachnoid hemorrhage, meningitis, leptomeningeal spread, and moyamoya disease. The source of hyperintensity is thought to be from blood in subarachnoid hemorrhage and leptomeningeal spread of malignancy while it is probably due to a slow flow within the vessels in acute infarction and moyamoya disease.

Conclusion: There are various central nervous system diseases that can show abnormal hyperintensity within the subarachnoid space. This knowledge may help make a proper diagnosis.

B-0429 14:25

Highly active antiretroviral therapy (HAART) in patients with AIDS-related progressive multifocal leukoencephalopathy (PML): Effect on MR imaging findings and the clinical course

M.M. Thurnher[1], J.M. Donovan Post[2], A. Rieger[1], C. Kleibl-Popov[1], E. Schindler[1]; *[1]Vienna/AT, [2]Miami, FL/US*

Purpose: To estimate the changes in MR imaging findings in patients with AIDS-related progressive multifocal leukoencephalopathy (PML) after the highly active antiretroviral therapy (HAART).

Materials and methods: Initial and follow-up MR scans were performed in 4 consecutive AIDS patients with PML before and during the HAART. The clinical and virologic characteristics (CD4+ count, viral load, JCV in the CSF) at the baseline, and after the therapy were determined also, and compared with neuroradiological findings.

Results: Multifocal white matter lesions without contrast enhancement were found on MRI initially. Antiretroviral regimen consistent of nucleoside reverse-transcriptase inhibitors (NRTI), non-nucleoside reverse-transcriptase inhibiotors (NNRTI), and protease inhibitors (PI) was started. Two patients were "responders", improved clinically and immunologically after the HAART, and are still alive (survival period 1.5 and 3 years). Two patients died after 3 months ("non-responders"). On follow-up MR scans in responders group worsening was observed initially, followed by regression of the lesion size and subsequent atrophic changes of the involved brain areas. In one patient a temporary enhancement of the lesions was seen. Mass effect was present in both patientsThe white matter lesions on pre-treatment scans were more extensive in the non-responders.

Conclusion: Our results suggest that PML can show clinical and radiological response with HAART. Initial worsening of the MR imaging findings in "responders" was probably due to the effect of a posttreatment inflammatory reaction, and atrophic changes may represent burnt PML lesions. The persistent neurological deficit is rather due to the sequelae than to persistent disease.

B-0430 14:30

Echo-planar FLAIR imaging in depiction of white matter lesions: Comparison with fast spin-echo T2-weighted and fast FLAIR imaging

N. Tomura, K. Kato, S. Takahashi, R. Sashi, K. Sato, R. Kurosawa, J.-i. Izumi, J. Watarai; *Akita/JP*

Purpose: To compare a multi-shot echo-planar fluid-attenuated inversion-recovery (EPI-Flair) sequence with fast spin-echo Flair (F-Flair) and fast spin-echo T2-weighted (FSE-T2W) sequences in depiction of white matter lesions.

Methods and materials: Thirty-five patients with various white matter lesions were included in this prospective study. The protocol comprised three sequences: multi-shot EPI-Flair (TR/TE 8000/100, TI 2000, 22 slices, 8 shots), F-Flair (TR/TE 10000/150, TI 2200, ETL 22), and FSE-T2W (TR/TE 4000/100, ETL 16) sequences. The acquisition time of EPI-Flair, F-Flair and FSE-T2W was 1 minute 8 seconds, 4 minutes, and 2 minutes 24 seconds, respectively. In a blinded analysis, two independent readers for lesion detection compared sequences quantitatively. Virchow-Robin spaces were not considered lesions. In 22 patients, contrast was calculated between periventricular hyperintensity (PVH) and the cerebrospinal fluid (CSF).

Results: EPI-Flair showed more lesions (average number of lesions per patient 26.0) than T2W did (18.6) ($p < 0.01$). However, F-Flair showed more lesions (30.3) than EPI-Flair did ($p < 0.01$). For PVH-to-CSF contrast, EPI-Flair had significantly higher contrast (mean $\pm$ SD 16.6 ± 7.9) than FSE-T2W (0.3 ± 0.1). There were no differences in PVH-to-CSF contrast between EPI-Flair and F-Flair (18.6 ± 8.2).

Conclusion: This study shows that EPI-Flair has distinct advantages over FSE-T2W in depiction of white matter lesions. Although EPI-Flair saves imaging time and is more than 70 % faster relative to F-Flair, it cannot replace F-Flair for the detection of white matter lesions.

B-0431 14:40

Magnetization transfer ratio maps with different flip angles in evaluation of multiple sclerosis lesions

R.F. Bakhtiozin, V.L. Yarnykh, A.N. Boiko, A.A. Baev; *Moscow/RU*

Purpose: Evaluation of flip angle dependency of multiple sclerosis lesions contrast on magnetization transfer maps.

Methods and materials: Magnetization transfer (MT) images were obtained on 0.5 T whole body scanner (TOMICON S50, Bruker, Germany) with 3D MT-GRE pulse sequence (TR/TE 50/8 ms, MT pulse with Gaussian Shape, duration 20 ms, matrix 128 × 96 × 16, NEX 2, B1 5 μT, Δ = 2 kHz). For seven patients MT imaging was performed with two flip angles (FA): 6° and 20°. Additionally MT images for two healthy volunteers and one patient with multiple sclerosis (MS) were obtained with FA 5 – 45°. For all MS patients the conventional magnetic resonance images (MRI) with T1-, T2- weighted and fast FLAIR sequences were performed. 134 MS lesions in 8 patients were analyzed.

Results: The difference between magnetization transfer ratio (MTR) of normal appeared white matter (NAWM) and gray matter (GM) was the maximum at FA 30° The similar dependencies for different MS lesions was shown a maximum at FA 15 – 30°, therefore we have chosen the protocol with FA 20° for optimal. The protocol with higher FA provides much better contrast of lesions and GM (the sensitivity for FA 6° was 55 %, and for the protocol with FA 20° 94 %). This protocol was more informative for internal lesion structure evaluation.

Conclusion: The use of MT-GRE technique at optimal FA allows to increase significantly the sensitivity of MTR maps to the focal WM lesions.

B-0432 14:50

Value of cervical cord MRI in the differential diagnosis of cerebral white matter diseases vs. multiple sclerosis

M. Holtmannspötter[1], M. Rovaris[2], M. Inglese[2], M. Bozzali[2], M.A. Rocca[2], T.A. Yousry[1], M. Filippi[2]; *[1]Munich/DE, [2]Milan/IT*

Purpose: The current magnetic resonance (MRI) criteria to establish the diagnosis of multiple sclerosis (MS) mainly deal with cerebral lesions. In the present study, we investigated the role of cervical MRI abnormalities in establishing a diagnosis of MS.

Methods: Axial T2/PD-w scans of the brain and sagittal T2-w scans of the cervical spinal cord were obtained. Two groups of patients were included: MS-patients (106) and non-MS-patients (69: systemic immune mediated diseases [44], migraine [15], Leber's hereditary optic neuropathy [10]). The fullfillment of the criteria of Paty, Fazekas and Barkhof was determined.

Results: All three criteria were met in 86.8 % of the MS-patients and in none of the non-MS-patients. In 89.6 % of the MS patients, cervical lesion were also found. Only 1.8 % of MS patients had neither a cervical lesion nor did they fit all the three criteria based on brain MRI findings. 81.2 % of the non-MS patients did not fit any of the established MRI criteria for MS and none of them showed a lesion in the cervical cord.

Conclusions: The combination of MRI techniques in imaging the brain and the cervical cord increases the clinical certainty when making a diagnosis of MS.

B-0433 15:00

T2 relaxation: Differentiation of cysticerosis cysts and tuberculomas of the brain

P.N. Jayakumar, S.G. Srikanth, H.S. Chandrashekar, D.K. Subbakrishna; *Bangalore/IN*

Purpose: Ring-enhancing lesions of the brain are common imaging features in patients with seizures. Routine MR techniques have not been very successful in differentiating these lesions and the treatment of these lesions continues to be largely arbitrary in the absence of definite diagnosis. T2 relaxometry is an MR morphometric technique which provides a quantitative and objective means of comparing normal and pathological relaxation characteristics. We hypothesised that given the differences in the internal milieu of ring lesions, T2 relaxometry would differentiate such lesions in the brain. A prospective study using T2 relaxometry was performed to differentiate two common etiologies in the Indian Subcontinent; Tuberculomas and Cysticercal cysts.

Materials and methods: Fifty six ring enhancing lesions of the brain (Cysticercal cysts 33; Tuberculomas 23) in patients with focal seizures were studied for T2 relaxation times.

Results: The Mean T2 relaxation times of Cysticercal cysts was 552 ms (Range 240 – 956 ms; SD 149.7) and that of Tuberculomas 186 ms (Range 90 – 319 ms; SD 71.2) ($p = 0.001$, 95 % confidence). Ninety four percent of cysts and 100 % of Tuberculomas had T2 values within two standard deviations.

Conclusion: T2 relaxometry is a simple, reliable and valuable non-invasive MR technique to differentiate between intracranial Cysticercal cysts and Tuberculomas and may be incorporated in routine diagnostic protocols.

B-0434 15:10

MR-imaging of patients with primary anosmia

N. Abolmaali[1], V. Hietschold[2], T. Vogl[1], T. Hummel[2]; *[1]Frankfurt a. Main/DE, [2]Dresden/DE*

Purpose: To evaluate the appearance of frontal skullbase structures in patients with isolated congenital ansomia (ICA). To compare volume measurements of hypoplastic olfactory bulbs and measurements of olfcactory sulci in ICA-patients and normosmic volunteers.

Materials and methods: Data of 16 patients with ICA and 8 normosmic subjects were acquired. Imaging was performed in a 1.5 T system (Magnetom Vision) with a standard head coil. T1 SE sequences in a coronal plane perpendicular to the frontal skullbase (SL 3 – 4 mm, pixelsize 0.43 × 0.39 mm^2) and a T1w MP-RAGE with isometric voxels (1.0 mm^3) were performed. Volumes of normal and hypoplastic olfactory bulbs (OB) were calculated and lengths and depths of olfactory sulci (OS) were measured.

Results: Volumes of OBs in controls were 125 ± 17 mm^3. 8 patients had aplastic OBs, 8 patients had unilateral or bilateral hypoplasia of OBs. Neither absolute length nor maximal depth of OS showed any significant difference between anosmic and normosmic subjects even when related to head size. In a coronal plane through the dorsal edge of the eyeballs differences of OS between normosmics and anosmics with or without olfactory tracts (OT) were significant.

Conclusions: Structures of the frontal skullbase in ICA are clearly visualized with the performed sequences. A selected coronal imaging plane gives important information on the diagnosis of anosmia. Development of OT might change morphology of OS.

B-0435 15:20

T2 relaxation rate of basal ganglia and cortex in patients with α thalassemia major

M.I. Argyropoulou, Z. Metafratzi, D.N. Kiortsis, C. Tsampoulas, S.C. Efremidis; *Ioannina/GR*

Objective: In thalassemic patients neurophysiologic disturbances have been associated with high serum ferritin levels and deferoxamine therapy. Ferritin, the main iron storage protein, in the presence of a magnetic field induces a preferential decrease of the T2 relaxation time. The purpose of this study was to evaluate thalassemic patients for brain iron deposition by assessing the T2 relaxation rate (1/T2) of the grey matter.

Subjects and methods: Forty one thalassemic patients (age range 8.5 to 44 years, mean 24) and 58 age and sex matched controls were included in the study. The 1/T2 of the grey matter was evaluated, in a 1.5 T MR imager, using a multiecho SE sequence 2000/20, 40, 60, 80, 100, 120, 140, 160 (TR/TE). A contemporary assessment of the serum ferritin levels was also performed.

Results: The 1/T2 of the cortex (motor and temporal) (mean 0.0122 ms^{-1}; SD 0.0004), putamen (mean 0.0137 ms^{-1}; SD 0.0004) and caudate nucleus (mean 0.0132 ms^{-1}; SD 0.0003) was higher in patients compared to the controls (mean 0.0110 ms^{-1}; SD 0.0004), (mean 0.0120 ms^{-1}; SD 0.0005), (mean 0.0117 ms^{-1}; SD 0.0003) respectively ($p < 0.001$ for all parameters). No statistically significant differences were found in the globus pallidus. No correlation was found between 1/T2 and the serum ferritin.

Conclusion: The higher values of 1/T2 in the cortex, putamen and caudate nucleus of thalassemic patients probably reflect a higher iron deposition. The lack of differences in 1/T2 of the globus pallidus might suggest that even in thalassemic patients iron cannot exceed a saturation level.

14:00–15:30 **Room G**

Computer Applications

SS 705

Image processing and analysis

Chairpersons:
A. Skretting (Oslo/NO)
B.M. ter Haar Romeny (Utrecht/NL)

B-0436 14:00

A Jini service to reconstruct spect data

P. Knoll, S. Mirzaei, K. Koriska, H. Köhn; *Vienna/AT*

Purpose: Although the quality of iterative reconstructed SPECT slices is better than FBP slices, iterative algorithms are, due to their availability and longer reconstruction time, rarely used for clinical routine studies. In this work we used Jini, a new technology which is built on top of the Java programming language, to make iterative reconstruction algorithms available to all of our Jini community.
Methods and materials: Jini allows cooperating hardware devices and software services to access each other seamlessly. Jini clients find and access services which are available in the network by themselves, which simplifies the configuration and the access of Jini services in a network. We used Jini and a self-developed iterative reconstruction algorithm to develop a Jini reconstruction service. A physician selects the patient study from a database and a Jini client looks automatically in the department's Intranet for a registered Jini reconstruction service. If successful, the client downloads a proxy object of the registered Jini service, which is used to reconstruct the SPECT acquisition data. The reconstructed slices are visualized using a Java applet.
Results: Our Jini implementation of a reconstruction service functions on standard personal computers, but nevertheless, our Jini service reconstructs the patient study in approximately 20 seconds, because auxillary data, which are needed for our implementation of the reconstruction algorithm used, are loaded in advance.
Conclusions: Jini technology was applied to develop a robust reconstruction service for SPECT data, which can be used by members of our Jini community without installing software on client machines.

B-0437 14:10

Developing of a Java application for image analysis in radiology

A. Ferraris, G. Perron Cabus, L. Tettoni, S.D. Bianchi, M.C. Cassinis, G. Gandini; *Turin/IT*

Introduction: During last years, Java has been strongly improved; actually the most of the computer programmers, are Java developers. We have decided to develop a Java application, because it is a multiplatform application available for many Operating Systems.
Materials and methods: To develop this application, we used a Sun Java enviroment (ver 1.2) for Windows/OS; necessarily this application has been tested also under Linux/OS and Solaris/OS.
To manage DICOM images we have developed a dedicated library, to visualize them we used exclusively Java functions. We also create a very fast MPR module with opportunity to generate image slice on non ortogonals or curved planes.
Results: In our experience Java resulted a valid instruments of development with great image processing capability, the entire work will be soon free available on Internet.

B-0438 14:20

Teaching computer program in X-ray, ultrasound, MRI and radionuclide anatomy

M.B. Pervak, M.S. Kamenetsky, I.P. Vakulenko; *Donetsk/UA*

Purpose: Improvement of students' level of knowledge in X-ray, ultrasound, MRI, radionuclide anatomy.
Methods and materials: Teaching computer program developed consists of 10 sections in all human organism systems. Each section contains images received by conventional X-ray methods, angiography, CT, MRI, ultrasound and radionuclide methods. The images are provided with anatomical schemes coming through the images in a specific "semi-transparent" mode. The diagnostic images accompanied by textual, audio- and video information and animation contribute to moderate mastering of X-ray, ultrasound, MRI and radionuclide anatomy. Students use the program in preparation for classes in radiology.
Results: The thorough analysis made at the end of studying separate sections and the course of radiology as a whole demonstrated that the level of knowledge was higher in the students who utilized this program regularly. The form of information instruction and program service were positively assessed by students and colleagues from other departments and medical universities.
Conclusion: The use of corresponding computer programs contributes to enhancement of students' level of knowledge and facilitates their preparation for classes in radiology.

B-0439 14:25

Could electrical impedance scanning be useful for detection of metastases of malignant melanomas?

M. Facius[1], A. Malich[1], R. Anderson[2], M. Fleck[1], W.A. Kaiser[1]; [1]*Jena/DE*, [2]*Solna/SE*

Purpose: Electrical impedance scanning (EIS) is a relatively new non-invasive imaging modality for detecting cancer, based on inherent differences in the dielectric properties of normal versus malignant tissue. In this study, we tested the reliability and feasibility of impedance scanning (EIS) in the differentiation of superficial lesions suspicious for melanoma-metastases or -relapses.
Subjects and methods: 18 indeterminate lesions (chestwall, back, abdomen, inguinal, cervical, axilla, lower leg), highly suspicious for relapses/metastases of malignant melanomas were examined using ultrasound (B-Mode, Color Doppler, Power Doppler; ATL, HDI 5000, USA) and TransScan TS2000 (Siemens, Germany). A focal increase of conductance, which was not caused by an artifact constituted a positive EIS-finding and was consequently suspicious for malignancy. The lesions were surgically treated or identified by MRT.
Results: 13/18 malignancies were correctly detected as malignant (sensitivity 72 %), whereas 5 out of 18 were not detected by EIS.
Conclusions: Initial results suggest that EIS maybe useful as an adjunct to detect relapses of melanomas. However, higher sensitivity would be necessary and limitations have to be taken into account (large lesion size, lesion depth).

B-0440 14:30

Automatic detection of pulmonary nodules at spiral CT with a computer aided diagnosis system: Clinical experience

D. Wormanns[1], M. Fiebich[2], M. Saidi[1], S. Diederich[1], W. Heindel[1]; [1]*Münster/DE*, [2]*Giessen/DE*

Purpose: To evaluate a computer aided diagnosis (CAD) workstation with automatic detection of pulmonary nodules at low-dose spiral CT in a clinical setting for early detection of lung cancer.
Methods: 100 consecutive low-dose CT examinations were reported by two radiologists in consensus. A total of 138 nodules were detected (79 with diameters < 5 mm, 59 with diameters ≥ 5 mm). All examinations were reviewed using a UNIX-based CAD workstation with a self developed algorithm for automatic detection of pulmonary nodules. The algorithm is designed to detect nodules with diameters of at least 5 mm. The results of automatic nodule detection were compared to the consensus reporting of two radiologists as gold standard.
Results: CAD correctly identified 27 of 59 (46 %) nodules with diameters ≥ 5 mm detected by visual assessment by the radiologists. Only 24 % (36/138) of all nodules were detected due to the large amount of small (< 5 mm) nodules which can not be detected by the algorithm. In addition, 14 nodules were detected which were not mentioned in the radiologist's report but represent real nodules in retrospect, among them 11 (16 %) nodules with a diameter ≥ 5 mm. Analysis of reasons for non-detection of nodules by CAD included: exclusion because of morphological features (35 %), nodule density below the detection threshold (27 %), pleural contact (27 %), segmentation errors (5 %) and other reasons (5 %).
Conclusion: CAD significantly improves detection of pulmonary nodules at spiral CT and is a valuable second opinion in a clinical setting for lung cancer screening.

B-0441 14:40

An open source application for DICOM images with a plug-in interface

G. Perron Cabus, A. Ferraris, L. Tettoni, M.C. Cassinis, G. Gandini; *Turin/IT*

Introduction: If information technologies is increasing in radiology departments and there are many commercial applications available; although high costs are obstructing diffusion of these technologies. Moreover the applications seem not to be integrable. In our experience we wanted to create an OpenSource application to read DICOM images, analysis and to save images in JPEG format. With this application it is possible to integrate added functions by using a Plug-in interface.
Materials and methods: To develop this application we used a GTK (gimp tool kit) freely available on the net. This application has been written in "C" language. Thanks to the quality of the GTK libraries we could implement very complex func-

tions like image-sending and a Plug-in interface. DcmView has been developed on Linux/OS version 2.2.14, but it is also available in Windows/OS version and it can be easily transferred to other OS like Be-OS or Unix/OS.
Results: In our experience, DcmView is a good application for image analisys. The open structure of the system allows development and integration of functions separately developed.

B-0442 14:50

Image viewing, postprocessing and telemedicine by image viewing software Viewmed

D. Emmel, J. Ricke, A. Haderer, M. Pech, C. Gillessen, C. Zielinski, R. Felix; *Berlin/DE*

Purpose: To develop and implement a universal software for image viewing, postprocessing and telemedical image administration and communication.
Materials and methods: A Windows based viewing application was implemented optionally working as a helper application for internet browsers. The list of functionalities includes review of DICOM or other multimedia images, postprocessing of DICOM images including spatial frequency and contrast processing (β and γ curve correction), import, storage and export of DICOM and other multimedia images, import of scanned images, and synchronisation with an HL7 based RIS system.
Results: Viewmed serves as an integral part of our Intranet based PACS-system for image communication and image review on peripheral PCs such as located on wards or in outpatient clinics. Image postprocessing through β and γ curve correction significantly improves review of digital radiographs as proven by previous ROC analysis.
Conclusions: Viewmed may serve as a stand alone application for telemedical scenarios. It may also be used to satisfy image review and image communication demands of a digital archive accessible via web interface.

B-0443 15:00

The EU project IERAPSI: Integrated environment for rehearsal and planning of surgical interventions

E. Neri[1], D. Caramella[1], A. Jackson[2], N. John[2], S. Sellari Franceschini[1], N. Thacker[2], G. Alusi[3], G. Zanetti[4], C. Bartolozzi[1]; *[1]Pisa/IT, [2]Manchester/GB, [3]London/GB, [4]Cagliari/IT*

The three-years EU project IERAPSI (Integrated Environment for the Rehearsal and Planning of Surgical Interventions, IST-1999-12175), started on January 2000, is aimed to provide an interactive computerised environment for addressing surgery of the petrous bone.
The IERAPSI system will provide a group of image viewing and analysis tools, to allow the surgical review of CT, MRI and angiographic examinations in an interactive 3D manner, an integrated suite of image segmentation and visualisation, and a physics based surgical simulation system with visual and haptic feedback for training surgeons to perform operations on individual patient data.
Clinical trials will be performed in three universities (Pisa, Manchester and London) using a standard bank of clinical test data which will be read into the IERAPSI system and presented to ENT surgeons. The system will be developed by a series of "anatomical calibrations" on individual patients: definition of the areas of petrous bone that should be or should not be removed to obtain optimal clinical results, the presence of normal or aberrant blood vessels which must be avoided during the surgical procedure and the choice of optimal surgical approach. One specific task of the project is considered the identification of the facial nerve. The manual identification is considered necessary where anatomical deformation is present due to pathological processes.
The presentation will describe the different components of the IERAPSI system, with specific address to surgical planning of cochlear implantations.

B-0444 15:05

RheumaCoach: A computer-assisted approach to improve the scoring of rheumatoid arthritis

P.L. Peloschek, F. Kainberger, K. Bögl; *Vienna/AT*

Recently we developed the RheumaCoach software package for the radiological quantification of rheumatoid arthritis following the methods of Larsen and Rau. This software package includes a tutorial to explain the basic pathology of rheumatoid arthritis as well as the above mentioned scoring procdures. The interactive quantification is about 20 % faster than the conventional scoring procedure, without any loss of quality.
The RheumaCoach is not an image analysis system, but a computer-assistance for easier and less cumbersome scoring. It is a JAVA-stand-alone application and downloadable for free. We think that this software should be used for scoring rheumatoid arthritis.

B-0445 15:15

Fractal geometry: A useful tool in radiology

F. Grizzi[1], P.C. Muzzio[2], G. Brambilla[1], N. Dioguardi[1]; *[1]Rozzano/IT, [2]Padova/IT*

Purpose: The aim of this study were a) to investigate the fractal geometry in order to measure the complex and irregular shape of different biological systems observed by means of radiological imaging and b) to illustrate the fundamentals of fractal geometry.
Materials and methods: The fractal analysis was automatically done by means of a computer analysis system. 23 breast lesions, 54 lung and 30 liver parenchymal patterns have been taken as examples of irregular structures currently quantified in a subjective manner by physicians from different institutions.
Results: Fractal geometry is an accurate tool for studying the complex shape of biological systems. The use of the fractal dimension to measure the irregularity of biological structures may allow us the quantification of small structural changes due to some pathological processes. It has also been found that the fractal dimension measured using an image analysis system is fully reproducible and not subjective.
Conclusions: Irregularity and complexity are the main features of every biological system, including human tissues, cells and sub-cellular components. These two properties cannot be quantified by means of the classical Euclidean geometry, which is able to measure regular object, practically unknown in Nature. This study shows that the fractal geometry allows the quantitative measure of the complex morphology of different systems, such as breast lesions, lung and liver parenchymal patterns. Furthermore, this mathematical approach may be of help for the study of the non-linear dynamical process involved in many pathological processes.

B-0446 15:20

Evaluation of LC-Displays compared to a high-end monochrome and a standard color monitor

J. Ricke, J. Mulzer, U.K.M. Teichgräber, T. Ehrenstein, C. Gillessen, A. Haderer, R. Felix; *Berlin/DE*

Purpose: To evaluate the diagnostic accuracy of LC-Displays compared to monochrome and colour displays employing high and low frequency details in digital radiographs.
Materials and methods: LC Displays Pritech Desk Med II 20" and Sanyo LMU 18" were compared with a Philips 21CY9 monochrome and a Sony 20SE color monitor employing a ROC-analysis. After calibration of the monitors 4 similarly experienced radiologists rated the probability of the existence of 100 high frequency and 200 low frequency details in 600 predefined locations. Digital radiographs of statistical phantoms wer used simulating pneumothoraces, interstitial pneumonias and lung nodules. Statistical analysis was performed using Student's t-test.
Results: In high frequency details, the high-end monochrome monitor demonstrated significant advantages over LC-Displays. Compared to PC color monitor, true negatives were increased, though true negatives were decreased less significantly. For low contrast details, the monochrome monitor showed highest accuracy, followed by LC-Displays and PC color monitor.
Conclusion: Even though resolution was not different among the monitors, CRT technology showed advantages over LC-Displays. Variations between LC-Displays were significant with respect to low contrast details. Angle dependent variations of image contrast limit LCD technology.

14:00–15:30 **Room H**

Interventional Radiology

SS 709a

Musculoskeletal intervention

Chairpersons:
J. Earwaker (Brisbane/AU)
H. Zeumer (Hamburg/DE)

B-0447 14:00

Pelvic fractures: Clinical and radiological mid term results after CT-guided closed reduction and percutaneous screw fixation

H.G. Staedele, A.L. Jacob, N. Suhm, P. Regazzoni, W. Steinbrich, P. Messmer; *Basle/CH*

Purpose: To report clinical and radiological mid term results of pelvic ring fractures treated by CT-guided or CT-navigated closed reduction and percutaneous fixation (CRPF).
Methods and materials: An interdisciplinary team of radiologists and surgeons treated 67 patients with 81 pelvic ring fractures (AO/ASIF type C) with CRPF. Between 10/1993 and 10/1999 61 patients with 81 fractures fixed with a total of 161 screws had a mean clinical and radiological follow up of 26.5 month (3 to 74 month).
Results: 33/61 patients are painfree even after long mobilisation. 28/61 patients have little pain according to a standardized questionnaire. Radiological follow up showed precise reconstruction in all 3 planes. Persistant pain despite anatomical reconstruction, foraminal callus formation necessitating hemilaminectomy and superficial infection were observed in 1/67 patients each, loosening or breakage in 3/161 screws, persistent pain leading to screw removal in 2/161.
Conclusion: CT-guided and CT-navigated CRPF of the pelvis are minimally invasive and precise. Because of the low intraoperative trauma the number of early and mid term complications is low. A high percentage of patients has no or little pain.

B-0448 14:10

Overview of percutaneous vertebroplasty in Iran

H. Ghanaati, K. Firouznia; *Tehran/IR*

Purpose: To demonstrate our successful experience with percutaneous vebroplasty (P.V.)and to determine the outcome and complications of P.V. in our center.
Methods and materials: CT-guided cement injections have been done in 10 patients at a mean age of 58.9 years (32 – 68 years old, 6 female & 4 male). Four patients were suffering from metastasis, three from osteoporosis & three from hemangioma. Five patients had pathology in thoracic and five in lumbar region. The range of follow-up was from one to six months.
Results: One patient died of myocardial infarction two months after vertebroplasty. After one month according to our clinical scoring, six patients (60 %) had complete cure, two patients (20 %) showed significant and one patient (10 %) relative improvement. No complication was noted.
Conclusion: We concluded that percutaneous vertebroplasty can significantly prevent collapse of vertebral body to improve pain.

B-0449 14:20

Treatment of rotatory cuff calcification with an US-guided needle disruption aspiration technique

F. Calliada[1], A. Buvoli[1], D. Furiosi[1], M. Canepari[1], O. Bottinelli[2], R. Campani[2]; *[1]Lodi/IT, [2]Pavia/IT*

Purpose: To assess the value of US-guidance to treat calcifications in the rotatory cuff with needle disruption aspiration (NDA) technique.
Method and materials: Twenty-eight consecutive outpatients with shoulder pain lasting over 3 months and absence of adhesive capsulitis were submitted to NDA. Patients were clinically evaluated according to the Constant method and the size of the calcific deposits was recorded. NDA procedure was carried out after subacromial anaesthesia by inserting one 16 gauge needle within the calcification in the rotatory cuff under US guidance with 7 – 10 MHz probe. The calcifications were disrupted and aspirated by the needle and, at the end of the procedure 0.5 cc of steroid was injected within the residual calcification. The procedure was performed once in 26 cases and twice only in two cases.
Results: NDA was carried out without complications in 92.8 % of cases, hyperalgesic attack occurred in two cases. Constant average weight score moved from 54 % to 95 % and 89.2 % of the scores was over 85 points one month after the procedure. X-ray evaluation performed 4 weeks after NDA demonstrated that calcific deposits were almost disappeared in 71.4 % of cases and reduced in size of more than 50 % in 28.5 %.
Conclusions: US-guided NDA technique is successful to treat calcifications in the rotatory cuff. Follow-up controls demonstrated that results with US-guidance are comparable with those with fluoroscopy. Advantages over fluoroscopy include absence of radiation exposure and easier approach to small and low density calcific deposits.

B-0450 14:25

Extracorporal shock wave lithotripsy is highly effective in periarthritis humeroscapularis

J. Peters; *Frankfurt a. Main/DE*

Purpose: Extracorporal shock wave lithotripsy has been used for many years for the treatment of renal, urethral, gallbladder and salivary gland calculi. In recent years various orthopedic disorders have been treated with high energy shock waves. Humeroscapular periarthritis is a very painful and disabling disorder. Physical and drug therapy usually take a long time and frequently fail to relieve symptoms, leaving radiotherapy as the only remaining option. We have studied the effectiveness of extracorporal shock wave lithotripsy in the treatment of this condition.
Methods: Eleven patients with humeroscapular periarthritis, between 28 and 56 years in age, were treated with high-energy shock wave lithotripsy. All patients had calcium deposits in the supraspinatus tendon, up to 3 × 1 cm in diameter. They all had tried physical therapy with negligible success and were taking antiinflammatory drugs regularly. Mobility of the shoulder was limited.
Results: In nine patients a single treatment was sufficient for complete dissolution of the calcium deposits in the supraspinatus tendon, and the patients became asymptomatic within two days. In two patients a second treatment after an interval of 6 weeks was necessary ubefore complete resolution of calcium and pain were achieved. Full mobility of the shoulder was achieved in all patients. There was no correlation between the size of the calcium deposits and the number of necessary lithotripsy sessions.
Conclusions: Extracorporal shock wave lithotripsy is extremely effective in the treatment of humeroscapular periarthritis. This form of treatment is superior to physical and drug therapy. It may replace these treatments and make radiotherapy totally unnecessary.

B-0451 14:30

CT-guided percutaneous radiofrequency ablation of spinal tumors

A. Gevargez, M. Matysek, P.G. Kriener, G. Siepmann, M. Braun, D.H.W. Grönemeyer; *Bochum/DE*

Purpose: In the last few years there have been dramatic changes in the therapeutic approach to local tumor therapy. Radiofrequency ablation (RFA) has been reported as a method of liver tumor destruction. We have applied RFA modalities to the local therapy of spine metastases. Percutaneous local hyperthermia of spine metastases is indicated in patients where conventional cancer therapy is ineffective due to painful, severe, osteolytic bone metastases; high doses of opiates are necessary to control pain and rapid pain relief is necessary.
Materials and methods: Between September 1999 and August 2000, 17 patients with 35 unresectable spine metastases underwent RFA on tumors ranging from 1.5 to 9 cm in diameter. CT imaging was used to guide RFA and lesions were excised by applying temperatures of approximately 90° C for 8 minutes. Overlapping ablations were used for larger lesions. In patients with multiple lesions, RFA was performed in different locations. Subjective pain reduction was analyzed with the help of a visual analogue scale (VAS). RFA was undertaken percutaneously on an outpatient basis on 17 patients (35 lesions), with an average follow-up length of 2 months.
Results: Overall, there was a significant postoperative reduction of the local tumor pain as established with the help of a visible analogue scale (VAS). The comfortable and safe execution of the procedure allows the expectation of a promising response.
Conclusion: RFA is an effective alternative for the percutaneous ablation of unresectable bone metastases improving pain reduction and can, when used adjunctively, reduce morbidity.

B-0452 14:40

CT/MRI-guided percutaneous laser discs decompression (PLDD) using a minimally invasive highly flexible canula set

M. Braun, A. Gevargez, M. Matysek, D.H.W. Grönemeyer; *Bochum/DE*

Purpose: While using the diode laser for CT-guided PLDD a thin coaxially bent memory canula was developed and performed in clinical use.

Material and methods: The PLDD canula set was employed on 13 patients with herniated lumbar discs. The employed laser system is a diode laser, with a 980 + 30 nm wavelength (Ceralas D, CeramOptec®) and lightfibers with a 240 µm outside diameter. The straight positioned operating canula is placed vertically posterolateral up to the intervertebral foramen under CT-guidance. Once the mandrin is removed out of the operating canula, a lightfiber with a 240 µm outside diameter is placed in the disc. The lasering is performed in single shots lasting 0.1 – 1 seconds and 1 second breaks. Output is 4 W, 1800 – 4000 J were applied in each PLDD.
Results: 84 % (VAS) of the patients had excellent or good results and 16 % experienced fair or poor results since PLDD.
Conclusion: Optimal radial spread of laser energy is accomplished by reducing the angle of the operation canula intradiscally. This and the thin 20 gauge canula make this an excellent tool for CT guided PLDD in nonsequestered herniated discs and especially suitable for the therapy of segments L5/S1 and/or in the cervical- or thorax spine.

B-0453 14:50

Balloon dilatation of recurrent ostial occlusion of the frontal sinus
D. Göttmann, M. Strohm, E.-P. Strecker; *Karlsruhe/DE*

Purpose: In patients suffering from chronic frontal sinusitis there is a high incidence of repeated recurrent ostial stenosis causing acute inflammatory symptoms. Balloon dilatation representing a less invasive alternative to repeated surgery has been evaluated.
Patients and methods: 7 patients with recurrent chronic frontal sinusitis were operated previously 2 to 4 times without any permanent success. Using the endonasal access the ostium of the frontal sinus has been crossed with an angiographic catheter and a hydrophilic guidewire under fluoroscopic control. Then, the stenosed ostium has been dilated with a PTA high pressure balloon with a diameter of 5 mm initially, increasing to 8 mm. This procedure has been performed 2 to 8 times with intervals of 2 to 12 weeks.
Results: All procedures were technically successful, there were no complications. All patients are free of symptoms and have no evidence of recurrence as confirmed by endoscopy with a follow-up of 6 months to 5 years.
Conclusion: In patients with repeated frontal sinusitis balloon dilatation is a new, successful and far less invasive method for treatment of this painful disturbing disease.

B-0454 15:00

Lumbar sympathicolysis in diabetic patients
R. Moll, M. Fieger, P. Frühwald, J. Knüpffer, P. Range, A. Kraus, G. Schindler; *Würzburg/DE*

Purpose: To evaluate the potential of lumbar sympathicolysis in diabetic patients when there is no possibility of surgical or radiological reconstruction of the proximal arteries.
Methods and materials: 56 patients with ischemic disease of the lower limb underwent one to three CT-guided lumbar sympathicolysis in dorsal approach. Percutaneous neurolysis, using a 22 G fine needle, after a test block with contrast agent and local anesthetic, definitiv block with 10 – 15 ml of 95 % ethanol and 3 – 5 ml of local anesthetic in lumbar segment 3 and 4. 55 % (31/56) were diabetic patients. Success was defined as the prevention of amputation or the reduction/elimination of pain.
Results: Amputation rate of all patients was 44 %, of diabetic patients 48 % and of non-diabetic patients 40 %, but dependant on the state of the disease (III: 35 %, iV: 46 %). There was no mortality and no severe complication like bleeding, hydronephrosis, persistant neuralgia which were found with surgical sympathectomy. Two-segment technique and repetition of the intervention cannot improve success rate.
Conclusion: There is a good chance (more than 50 %) for diabetic patients to profit by lumbar sympathicolysis. The success rate is slightly lower than in non-diabetic patients, complication rate is similar and negligible.

B-0455 15:10

CT-guided periganglionic corticosteroid injection in sciatica: Follow-up study on 50 cases
A.V. Giordano, M. Gallucci, R. De Amicis, D. Erriquez, M. Caulo, C. Masciocchi; *L'Aquila/IT*

Purpose: CT-guided periganglionic injection of corticosteroids has demonstrated a long-term analgesic effect in patients with radicular sciatica. The aim of this work was to asses the long term efficacy of this combined therapy in cases of monoradicular sciatica, comparing cases of foraminal stenosis caused by arthritis or by intervertebral disk herniation.
Material and methods: Fifty patients with monoradicular sciatica underwent CT-guided periradicular corticosteroid therapy. In 25 cases the synptoms were caused by arthritic changes and in in the remaining 25 cases by radicular compression due to disk herniation. In all the cases the treatment involved the percutaneous introduction of 80 mg of Triamcinolone Acetonide into the intervertebral canal, using a 22 G needle.
Results: On clinical follow-up seven days after treatment there was symptomatic improvement in 23/25 cases of arthritic foraminal stenosis and in 22/25 cases of foraminal stenosis due to disk herniation. The improvement was present after six months in 12 patients with arthritic changes and in 20 patients affected by disk herniation.
Conclusion: Periganglionic corticosteroid injection provides useful therapeutic support in monoradicular compressive sciatica. It is more effective in patients with disk herniation, probably because of the high rate of spontaneous resolution of this pathology.

B-0456 15:20

Paravertebral nerve block in a high-field MR-system: Clinical evaluation of 63 patient series involving 261 punctures
E.K. Salomonowitz, M. Glatz; *St. Pölten/AT*

Purpose: Lumbar paravertebral nerve and facet joint blocks are simple interventional techniques that produce dramatic relief for patients suffering from pain involving groin, lower extremity, and the lumbar spine. We have developed a MR-guided puncture for a standard closed-bore magnet system to add safety and simplicity to this clinical pearl.
Materials and methods: Since 1997, 63 patients underwent a complete pain management series consisting of up to five consecutive MR-guided punctures with local perineural anestetic and steroid in the same location, according to the clinical presentation, at intervals of one to three weeks. The 63 sets involved 261 individual punctures. Indications were disc herniations with refusal to operate, and postoperative states. The precision of a puncture was evaluated by visual assessment of the location of the titanium needle tip, local contrast injection, and neurologic effect. The clinical results of treatment were evaluated by visual-analogue scaling and neurologic testing.
Results: 43 needles of the 261 punctures (16.5 %) had to be repositioned due to visible thecal contrast extravasation. 47 of the 63 patients (74.6 %) were cured, and nine (14.3 %) reported a change for the better. There were no side effects nor complications.
Conclusion: Interventional radiology is called upon to execute the notions of health economics and provide additional benefit to our patients. MR-guided pain management is simple and very effective and the crucial step for its implementation is not to contemplate its application but to simply start applying the procedure.

14:00–15:30 **Room I**

Contrast Media

SS 706

New trends (3)

Chairpersons:
G.P. Feltrin (Padova/IT)
S.K. Morcos (Sheffield/GB)

B-0457 14:00

Evaluation of focal liver lesion vascularity using color/power Doppler without and with echocontrast agent
L. Aiani, C. Borghi, F. Clarizia, A. Martegani; *Como/IT*

Purpose: To demonstrate that the use of an echocontrast agent (SonoVue™) with dedicated algorithm scans, allows the visualisation of macro and microvascular parenchyma characteristics.

Methods and materials: 20 patients with primary benign (hemangiomas) or malignant focal liver lesions and secondary (mets) hypo- and hypervascular lesions underwent ultrasound Color/Power Doppler examination without and with contrast agent, (SonoVue™, Bracco, Milan, Italy). Acuson Sequoia system equipped with 2 – 4 MHz probe and Contrast Coherent Imaging (CCI) at low mechanical index, was used. On a semiquantitative scale the capability, to show macrovascular structures and possible modifications of parenchyma during the basal arterial, portal and late phases using Color or Power Doppler with and without echocontrast administration, was evaluated.
Results and conclusions: Color/Power Doppler is widely used for the study of focal liver lesions. Its limitations in terms of sensitivity prevents the possibility of showing the microcirculation. This study demostrates that low MI-CCI and contrast enhancement allow the visualisation of both macrovascular and parenchymal circulation characteristics.

B-0458 14:10

Specific features of focal hepatic lesions on pulse inversion and intermittent imaging after ultrasound contrast agent bolus injection

F. Calliada[1], R. Campani[2], O. Bottinelli[2], M. Passamonti[1], A. Vercelli[2], A. Azzaretti[2]; [1]*Lodi/IT*, [2]*Pavia/IT*

Purpose: The purpose of this study is to determine the role of Pulse Inversion and Intermittent Imaging (PI&II) after bolus injection of Ultrasound (US) contrast agent for characterization of hepatic lesions.
Method and materials: 45 haemangiomas in the liver in 40 patients and 56 malignant hepatic tumors in 35 patients were evaluated with pulse inversion harmonic US using HDI-5000 scanner (ATL). US images were obtained after a bolus injection of 2.5 g of Levovist US contrast agent. The evaluation was performed with PI&II acquiring images in arterial, portal and late phases. The contrast enhancement pattern of 101 hepatic lesions was assessed. Dynamic contrast enhanced CT was performed in every patient.
Results: During the arterial phase of 45 haemangiomas, 39 revealed a peripheral enhancement filling-in centripetally in late phase, the remaining 6 (13.3 %) showed homogeneous enhancement. In 48 metastases, the enhancement was rim-like in 22 (45.8 %), homogeneous with early washout in 5 (10.4 %) and central stippled in 3 (6.2 %), and in the remaining 18 (37.5 %) no significant enhancement was seen. All the metastasis were hypohecoic in late phase. Hepatocellular carcinomas revealed rapid enhancement, in arterial phase heterogeneous in 4 (50 %) and homogeneous in 4 (50 %). CT results confirmed US enhancement pattern in 98 lesions (97 %).
Conclusions: Haemangiomas showed peripheral enhancement with centripetal fill-in (86.6 %) or homogeneous enhancement (13.3 %) in arterial phase with enhancement similar to liver parenchyma in late phase. PI&II seems to be highly specific for diagnosis of haemangiomas demonstrating characteristic enhancement features, equivalent to dynamic CT.

B-0459 14:15

MR imaging of a tetracycline controllable expression vector

H. Alfke, F. Nocken, H. Stöppler, J.T. Heverhagen, F. Czubayko, K.J. Klose; *Marburg/DE*

Purpose: MR imaging of a tetracycline controllable expression vector comprising the cDNA coding for human tyrosinase, a key enzyme in melanin synthesis.
Materials and methods: Followed by the stable transfection of a doxycyclin hydrochloride (Dox) dependent tyrosinase expression vector (Tet/off) into the human breast cancer cell line MCF-7 we established vector positive cell clones. The cell clones were analysed for tyrosinase expression by means of RT-PCR, immunhistochemical staining using tyrosinase specific antibodies, Melanin staining and MR imaging (T1 weighted high resolution SE and GE sequences) dependent on Dox treatment.
Results: Cell clones contained tyrosinase mRNA and were stained positively for tyrosinase and melanin only in the absence of Dox. Also the MR images distinctly detect more than 20 % higher signal intensity in untreated cells in comparison to treated ones.
Conclusion: The MRI enables the detection of adjustable gene expression vectors in living cells. This detection system could be an useful tool for the development of in vivo gene transfer strategies and offers a perspective of monitoring the persistence of gene expression.

B-0460 14:25

Pretreatment visualization of hepatic vasculature with contrast-enhanced MRA: 1M vs. 0.5M Gd-DTPA for contrast-enhanced MRA of the liver arteries for therapy planning in patients with HCC

M. Matzko, A.M. Huber, A. Huppertz, J. Scheidler, T.K. Helmberger, M.F. Reiser; *Munich/DE*

Purpose: To compare results of 3D dynamic MRA of the liver arteries in patients with HCC prior to therapy using a 1.0 molar Gd-DTPA contrast agent and a 0.5 molar Gd-DTPA contrast agent.
Methods and materials: 30 patients with HCC were examined on a 1.5 T unit with a fast gradient system (Symphony, Siemens, Germany) using a dynamic 3D MRA sequence (TR/TE/FA 3.3/1.37/250, 512 × 512 matrix, acquisition time 2 × 19 s breath hold) during arterial and portal venous phase. A 0.5 molar Gd-DTPA contrast agent (Magnevist, Schering, Germany, 15 patients) or 1.0 molar Gd-DTPA contrast agent (Gadovist, Schering, Germany, 15 patients) in a total amount of 30 ml contrast agent with a injection rate of 2 ml/s was applied. Image subtraction and MIP reconstruction were performed. Two radiologists evaluated the image quality with a six-point grading system (0 … poor, 5 … excellent). The image quality analysis included an evaluation of the arterial and portal venous S/N ratio and C/N ratio, and the visualisation of the main and peripheral branches of the liver artery and the portal vein.
Results: In the grading image quality of 1 mol enhanced MRA was superior to 0.5 mol enhanced examinations. In the 1 mol enhanced examinations there was a significant higher S/N (80.29) and C/N (79.79) than in the 0.5 mol enhanced examinations (S/N 43.56; C/N 42.84).
Conclusion: 3D dynamic MRA of the liver arteries with 1.0 mol Gd-DTPA is superior to enhancement with a 0.5 mol Gd-DTPA and offers a high quality road map for therapy planning in patients with HCC.

B-0461 14:35

Specific features of hepatic tumors on C3-mode bidimensional gray scale US technique with microbubble contrast agent

P. Ricci, M. Coniglio, A. Di Filippo, V. Cantisani, F. Arduini, R. Passariello; *Rome/IT*

Purpose: C3-Mode (Combined Contrast Chain mode – Esaote, Italy) is a recently developed real-time, high spatial resolution, bidimensional gray scale technique, which ensures high sensitivity in the depiction of the effect of contrast agents. This technique is based on a temporal correlation of successive echoes of the same scanned area. The purpose of this study is to determine the role of this technique in the characterization of focal liver neoplasms.
Methods and materials: Thirteen hepatic tumors (5 hemangiomas, 3 HCCs, 3 mets and 2 FNHs) in 13 patients were evaluated with C3-Mode using Technos scanner (Esaote, Genoa, Italy). US images were obtained before and after contrast administration of a bolus injection of the 4 g microbubble contrast agent Levovist (Schering, Berlin, Germany) with the incremental interval delay scanning technique.
Results: All the hemangiomas revealed initial peripheral enhancement, mainly globular, with progressive centripetal filling-in. The HCCs showed rapid enhancement in the arterial phase, with fast wash-out in the portal phase. Rim-like enhancement was present in 2 out 3 mets, while one revealed homogeneous enhancement with rapid wash-out. Both FNHs presented rapid arterial enhancement and homogeneous filling-in during the portal phase.
Conclusions: All liver neoplasms presented characteristics enhancement features at C3-Mode evaluation, equivalent to dynamic CT or MRI.

B-0462 14:45

USPIO-enhanced magnetic resonance imaging of atherosclerotic plaques

S.A. Schmitz, M. Taupitz, S. Wagner, K.-J. Wolf, D. Bayersdorff, B.B. Hamm; *Berlin/DE*

Purpose: Experimental data show accumulation of ultrasmall superparamagnetic iron oxide (USPIO) particles in atherosclerotic plaques. SPIO uptake occurred in plaques showing an increased endothelial permeability and macrophage phagocytosis as signs of inflammatory plaque activity. We incidentally observed USPIO uptake in aortic and arterial wall segments in patients who had originally received the MR contrast agent for staging lymph node metastases.
Materials and methods: Twenty patients, 19 male, 1 female, mean age 64 (29 – 78) years, with bladder or prostate cancer underwent MRI using a T2*-weighted high-resolution gradient-echo sequence prior to and 24 – 36 hours after intravenous injection of 2.6 mg Fe/kg of SPIO (Sinerem®). The aorta, both common, external and internal iliac, as well as both superficial femoral arteries were analyzed.

Results: One patient was excluded. A positive finding was defined as an area of pronounced signal loss on postcontrast images clearly confined to the arterial wall, which was absent in the precontrast examination or increased in size. Such a finding was observed in 1 – 3 arteries in 7 of the 19 patients.
Conclusions: The pronounced signal loss in the wall of the aorta and pelvic arteries seen in part of an elderly patient population after intravenous USPIO administration strongly suggests that this contrast agent accumulates in human atherosclerotic plaques.

B-0463 14:55

Optimization of test-bolus injection technique for accurate tailoring of arterial enhancement at CT-angiography: Is saline flushing necessary?
S. Schick, A. Gahleitner, K. Hittmaier, D. Fleischmann; *Vienna/AT*

Purpose: To assess the effect of combining test-bolus injections of contrast material with automated saline flushing of the venous system at CT-angiography.
Method/materials: 66 consecutive patients referred for CTA of the abdominal aorta underwent two test-bolus injections: In all patients, one of the test-boluses consisted of a saline pre-flush, 16 ml contrast medium, and a saline post-flush. The other test bolus was either a contrast injection without saline flushing (group A, n = 22), or a contrast injection with saline post-flushing only (group B, n = 22), or a contrast injection with saline pre-flushing only (group C, n = 22). The time-to-peak (TP), the peak enhancement (PE) and the area under the curve (AUC) were determined from the time-attenuation curves and compared within subjects of each group.
Results: PE and AUC was significantly higher in patients with saline pre and postflushing (85/400 HE in A and 87/400 HE in C) compared to no saline flushing in A (65/328 HE) and soley pre flushing in C (58/318 HE). PE and AUC were not significantly different between pre and post-flushing (88/444 HE) compared to soley post flushing (87/425 HE) in B.
Conclusions: If used for timing purposes alone, saline flushing of the venous system is not necessary. It is critical, however, if the time-attenuation response to the test injection is used quantitatively for calculating individually customized injection protocols.

B-0464 15:05

Hepatocellular carcinoma: Findings at Mn-DPDP MR imaging with histopathologic correlation after liver transplantation. Preliminary results
E. Casciani, G. Gualdi, E. Polettini, M.T. Lonardo, M. Rossi, I. Pecorella, U. Di Tondo; *Rome/IT*

Purpose: To compare lesions detection and characterization predicted by Mn-DPDP-enhanced MR imaging with histopathologic correlation after liver transplantation.
Material and methods: Ten patients with liver cirrhosis and high level of aFP underwent MR imaging before (T1-weighted SE, T1-weighted SE Fat Suppression, T2-weighted SE) and 40 minutes – 1 hour after the end of intravenous administration of 8 – 10 µmol/kg Mn-DPDP (T1-weighted SE, T1-weighted SE Fat Suppression). MR imaging findings were correlated with findings at 7 mm thick sections pathologic examination after liver transplantation.
Results: At macroscopic examination, 42 suspect (other that regenerative nodules) nodules were identified in 10 patients. MR depicted 4 of 18 (22 %) diameter inferior 1 cm nodules, 13 of 19 (68 %) diameter between 1 to 2 cm nodules and 5 of 5 (100 %) diameter superior 2 cm nodules. Microscopic examination revealed 37 HCC, 3 dysplastic nodules with subfocus of HCC, 1 adenoma and 1 complex cyst. Homogeneous enhancement was observed only in 4 nodules of HCC, while all the other focal liver lesions showed little or no tumor enhancement resulting in increased lesion conspicuity. However, some lesions were more readily detected in unenhanced MR images.
Conclusion: Mn-DPDP is a safe contrast agent for MR imaging of liver lesions. Mn-DPDP-enhanced images can improve detection and characterization of hepatocellular carcinoma. To obtain optimal diagnostic information of liver lesions T2-weighetd images are also essential.

B-0465 15:10

BisBOMEDTA-Manganate magnetic resonance imaging enhancement and comparison with MultiHance in rabbit liver
A. Tartaro[1], P. De Matthaeis[1], L. Calabi[2], F. Uggeri[2], L. Bonomo[1]; *[1]Chieti/IT, [2]Milan/IT*

Purpose: To compare the Magnetic Resonance Imaging (MRI) enhancement of different doses of bis (benziloxymethyl)EDTA-Manganate, dimeglumine salt [bisBOMEDTAMn] with a single dose of gadobenate dimeglumine (MultiHance), in rabbit liver.
Method and materials: Five rabbits were imaged, under anesthesya, by using a 1.5 T scanner and dedicated surface coil. Each animal was scanned before, 5 and 20 min after IV injection of three different doses of bisBOMEDTA-Mn (0.01 mmol/kg, 0.03 mmol/kg and 0.05 mmol/kg) and MultiHance (0.01 mmol/kg). Scan protocol included T1 weighted spin-echo (SE) sequences (parameters: TE 500, TR 12 and slice thickness 3 mm) and in-phase and out-phase fast low angle shot (FLASH) sequences. All images were acquired on axial plane. Signal enhancement was measured by drawing circular regions of interest (ROIs) in the right lobe of the liver. Relative enhancement (RE) was defined as the signal difference divided by the pre-contrast signal.
Results: The dose of 0.03 mmol/kg of bisBOMEDTA-Mn showed the highest RE in all sequences. As compared to MultiHance, a significant higher signal enhancement of bisBOMEDTA-Mn was calculated at 5 and 20 min after IV injection.
Conclusions: At 0.03 mmol/kg concentration, bisBOMEDTA-Mn showed the best liver imaging result. RE of bisBOMEDTA-Mn was always higher than RE of MultiHance.

B-0466 15:20

USPIO-enhanced direct thrombus MR imaging: Preclinical evaluation of a new technique
S.A. Schmitz, S. Winterhalter, S. Schiffler, R. Gust, S. Wagner, W. Semmler, S. Coupland, K.-J. Wolf; *Berlin/DE*

Purpose: To test the hypothesis that ultrasmall superparamagnetic iron oxide (USPIO) may diffuse into nonendothelialized fresh thrombi owing to the high intravascular concentration of this blood-pool MR contrast medium.
Materials and methods: Stagnation thrombi of different organizational stages (1, 3, 5, 7 or 9 days) were induced in the external jugular vein of 25 rabbits. Direct thrombus MR imaging was performed using a fatsat T1w gradient-echo sequence (3D-MPRAGE) before and 24 h after I.V. USPIO (DDM 43/34 from IDF, Berlin; particle size 25 nm, 200 µmol). The length of the thrombi demonstrated on 3D-reconstructions was compared to X-ray venography and histology. Agreement was determined using a length ratio (thrombus length at T1w MRI/true thrombus length). T2*w gradient-echo (3D-FLASH) images were generated and scored semiquantitatively.
Results: T1w 3D reconstructions visualized appeared as hyperintense structures. The mean length ratio increased significantly from pre- to post-contrast MRI at a thrombus age of 3 days (0.6 ± 0.4 to 0.8 ± 0.4), 5 days (0.1 ± 0.1 to 1.0 ± 0.1) and 7 days (0 to 0.6 ± 0.4), but not at 1 day (0.1 ± 0.3) or 9 days (0), $p < 0.05$. No signal change was observed on T2*w images.
Conclusions: USPIO enhances thrombi of a defined age on T1w MRI, but no signal change can be observed on T2*w images. USPIO-enhanced direct thrombus MR imaging may have a potential for the detection and age characterization of thrombi.

14:00–15:30 **Room K**

Interventional Radiology

SS 709b

Hepatobiliary intervention

Chairpersons:
N. Gourtsoyiannis (Iraklion/GR)
J. Lammer (Vienna/AT)

B-0467 14:00

Radiologic gastrostomy placement: Balloon- vs. mushroom-retained catheters
B. Funaki[1], R. Peirce[1], J. Lorenz[1], G. Zaleski[2], T. Van Ha[1], J. Rosenblum[1], J. Leef[1]; *[1]Chicago, IL/US, [2]Racine, WI/US*

Purpose: Two different types of percutaneous flouroscopic gastrostomy procedures were evaluated.
Materials and methods: Between July 8, 1999, and August 4, 2000, eighty percutaneous gastrostomy catheters were placed in eighty patients in eighty attempts. Twenty-five 16, 18, or 20 French balloon-retained catheters and fifty-five 20 French mushroom-retained catheters were inserted. Catheters were placed on the basis of operator preference, except balloon-retained tubes were preferentially placed in patients with obstructive head and neck or esophageal malignancies. Follow-up of these patients was conducted through chart reviews and telephone interviews. The technical success, procedural complications, and catheter complications were recorded. Chi-squared statistical analysis was performed.

Results: Technical success was 100 % (80/80) and there were no procedural complications. In patients who received balloon-retained catheters, the major complication rate was 0 %, the minor complication rate was 8 % (2/25), and the tube complication rate was 68 % (17/25). The following complications occurred: catheter dislodgement (n = 17), superficial cellulitis (n = 1), and bleeding gastric ulcers (n = 1). In patients who received mushroom-retained catheters, the major complication rate was 0 %, the minor complication rate was 4 % (2/55), and the tube complication rate was 4 % (2/55). The following complications occurred: superficial cellulitis (n = 2), tube occlusion (n = 1), and periostomal tube leakage (n = 1). There were no significant differences in major and minor complications between procedures. Balloon-retained catheters had a significantly higher rate of tube complications.
Conclusion: Compared with balloon-retained catheters, mushroom-retained gastrostomy catheters are significantly more durable and secure and are less prone to tube dysfunction. These catheters should be preferentially placed when possible.

B-0468 14:10

Percutaneous cholecystolithotomy in elderly patients with empyaema of gall bladder

S.K. Agarwal[1], G. Mackie[2], P. Jennings[1], R.G. Willis[1]; [1]*Carlisle/GB*, [2]*Dunfermline/GB*

Purpose: To use the principle of percutaneous nephrolithotomy (PCNL) in the treatment of gallstones with empyema of gall bladder in elderly patients unfit for surgery.
Materials and methods: Thirteen elderly patients with empyema of gall bladder presenting between september 1991 and october 1998 were included in the study. Seven were males and six were females aged between 58 and 93 years with a mean of 78 years. Two patients underwent emergency laparotomy which resulted in cholecystostomy as it was judged too dangerous to complete the planned cholecystectomy. Eleven patients with the clinical diagnosis of empyema of gall bladder were referred urgently for ultrasound guided percutaneous drainage (PJ). Percutaneous cholecystostomy was combined with track dilatation, lithotripsy and extraction of gall stones.
Results: Complete stone clearance was achieved in 12 patients (92.3 %). There were no immediate complications and no in-hospital or 30 day mortality. During a mean follow-up of 26 months, 11 patients underwent ultrasound scan; 8 remained stone free. On subjective evaluation 8 were asymptomatic (2 with recurrent stones).
Conclusion: In elderly patients presenting as an emergency with empyema of gall bladder, ultrasound guided percutaneous drainage followed by track dilatation and endoscopic extraction of gallstones appears to be a safe and satisfactory management plan in high-risk patients.

B-0469 14:20

Percutaneous cholecystostomy vs. conservative treatment for acute cholecystitis: What is preferable for high surgical risk patients?

A.A. Hatzidakis, E. Chrysos, P.K. Prassopoulos, I. Petinarakis, H. Sanidas, D. Tsiftsis, S. Vassilakis, N. Gourtsoyiannis; *Iraklion/GR*

Purpose: To compare the effectiveness of percutaneous cholecystostomy (PC) versus conservative treatment (CO) in high surgical risk patients with acute cholecystitis.
Materials and methods: One hundred twenty (120) high surgical risk patients were referred with acute cholecystitis. All patients fulfilled the ultrasonographic criteria of acute inflammation and had an APACHE II score > 10. Patients were randomized in two groups. PC was attempted in 63 cases. Sixty patients were successfully punctured under ultrasonographic or computer-tomographic guidance and comprised the PC-group. Fifty seven patients were treated conservatively and comprised, together with the 3 patients undergone unsuccessful puncture, the conservatively treated CO-group.
Results: In the PC-group, symptom resolution occurred in 44 patients, 9 of which were uneventfully operated following clinical improvement. Six patients were successfully operated in high risk because of persisting symptoms and/or catheter dislodgement while 10 patients died within 30 days either from underlying diseases (n = 7) or from ongoing sepsis (n = 3). In the CO-group, 8 patients died within 30 days from ongoing sepsis. Overall, 44/60 patients (73 %) benefited from PC while 52/60 (87 %) from conservative management.
Conclusion: In our experience, conservative management of high surgical risk patients with acute cholecystitis was more effective and exhibited lower mortality rates than PC.

B-0470 14:30

Percutaneous cholecystostomy in the management of acute cholecystitis

M. Patlas, I. Hadas-Halpern, D. Fisher, M. Knizhnik, I. Zaghal; *Jerusalem/IL*

Purpose: To evaluate the efficacy and safety of percutaneous cholecystostomy as the initial treatment of acute cholecystitis in high-risk patients.
Materials and methods: From 1994 – 1999 out of a total of 323 patients who suffered from acute cholecystitis, 80 patients (42 men, 38 women) aged 53 – 96 years underwent ultrasound-guided percutaneous cholecystostomy as the initial treatment. Sixty-three patients had acute calculous cholecystitis, four patients had acalculous cholecystitis, eleven patients had sepsis of unknown origin and two patients had biliary obstruction.
Results: Sixty-eight patients improved soon after percutaneous gallbladder drainage. Ten patients died due to other conditions disease and two patients died as a result of biliary peritonitis. Thirty-two patients had interval cholecystectomy (15 laparoscopic and 17 open) without complications. During a one year follow up four additional patients died from other conditions, 18 patients had no gallbladder symptoms, and 14 were lost to follow up.
Conclusion: Percutaneous cholecystostomy is an effective procedure with low morbidity and mortality and makes a significant contribution to the treatment of the acute cholecystitis in high risk patients.

B-0471 14:35

Metallic stents in the treatment of benign biliary strictures: 12-year follow-up

M. Bezzi, V. Cantisani, A. Zolovkins, G. Andreoli, F.M. Salvatori, P. Rossi; *Rome/IT*

Purpose: To determine the long-term efficacy of metallic stents in the treatment of recurrent benign biliary strictures (BBS).
Materials and method: From 1988 to 1999, 35 metallic stents were positioned in 29 patients (mean age 54 years, range 13 – 81 years) with BBS resistant to balloon dilatation who were not candidates to reconstructive surgery. Stricture level was at biliary-enteric anastomosis (n = 10), common bile duct (n = 8), and end-to-end choledocal anastomosis after liver transplantation (n = 11). Nineteen single and 13 double Z-stents were placed in 26 patients, 3 Angiomed stents were placed in 3 patients. Patency was assessed by life-table analysis. The longest follow-up period was 12 years (average 6 years; range 1 – 12 years).
Results: Technical success rate was 100 %, with no complications. The 1-year, 5-year and 10-year primary patency rates were 89 %, 60 % and 40 %, respectively. Reintervention due to epithelial hyperplasia associated with stones and sludge formation was necessary in 12 cases (41 %) (average 1.3 procedures/patient), and consisted in balloon dilatation, lithotripsy, and debris removal. The 5-year and 10-year secondary patency rates after reintervention were 80 %. Therapeutic results were better in patients with common bile duct strictures as compared with strictures at biliary-enteric anastomoses ($P < 0.5$).
Conclusions: Expandable metallic stents are effective in the treatment of BBS, as they improve the quality of life. Long-term patency can be achieved in a large number of cases by a limited number of reinterventions either radiological or endoscopic.

B-0472 14:45

Preliminary results of covered GORE biliary stent for malignant obstruction

P. Rossi, M. Bezzi, A. Zolovkins, F. Salvatori, M. Rossi; *Rome/IT*

Purpose of this study was to determine the safety, efficacy and performance of a new covered self-expanding stent in the treatment of malignant biliary obstruction.
Materials and methods: This pilot study included 15 patients with biliary stricture located in the CBD or CHD pancreatic carcinoma 13 pts, metastatic hilar nodes 2 pts). From January to August, 2000, 16 stents covered with non-porous ePTFE-FEP were placed percutaneously (diameter 8 and 10 mm, length 4, 8 and 10 cm). In 7 cases the biliary endoprostheses had transmural holes at proximal end to allow drainage of branch ducts. In 12 cases the distal end of the device was positioned in the duodenum and in 3 cases above the papilla. At 1, 3 and 6 months clinical assessment, serum bilirubin measurement and ultrasound were performed. At 3 and 6 months MRI and spiral CT examination were performed.
Results: Jaundice was relieved in 100 % of cases. No early stent-related complications occurred. The 30-days mortality rate was 7 % (non-correlated to implantation). The medium follow-up was 4.1 months (range 1 – 8). In 2 (13 %) stent occlusion occurred due to tumor overgrowth. In 2 pts acute cholecystitis occurred, which were treated by percutaneous drainage in one case and cholecystectomy in another. The average patency rate was 2.7 months (range 1 – 5.3).

Conclusion: Our initial results indicate that GORE biliary endoprosthesis was effective in achieving good palliative drainage. Percutaneous insertion of the device was easy and the fluoroscopic visibility was adequate.

B-0473 14:50

Should we stent the sphincter of Oddi in every case of malignant obstructive jaundice?

A.A. Hatzidakis, D.K. Tsetis, I. Tritou, A. Athanassiou, I. Stamouli, J. Romanos, J. Petrakis, N. Gourtsoyiannis; *Iraklion/GR*

Purpose: To evaluate the necessity of Oddi's sphincter metallic stenting for malignant obstructive jaundice treatment when tumor has > 2 cm distance from the Papilla.

Materials and methods: In 60 patients, self-expandable nitinol stents were placed. Ten Klatskin's tumors and 50 patients with extrahepatic lesions were present, with the tumor's distal margin having a distance > 2 cm from the Papilla of Vater. Hilar tumors were stented through the right bile ducts, without papilla stenting. Another 20 extrahepatic biliary tumors were stented above the sphincter (Group A). In the other 30 patients the stent crossed the papilla (Group B).

Results: In group A, 18 patients survived < 90 days and cholangitis occurred in 8 cases. In the other 12 patients with survival > 90 days, only one patient developed cholangitis. In Group B, 13 patients who survived < 90 days had no incidence of cholangitis and in the other 17 with survival > 90 days, cholangitis occurred in 3 cases. Klatskin's patients didn't develope cholangitis or stent dysfunction, although only the right bile ducts were drained.

Conclusion: Klatskin's tumors seem to be sufficient drained through the right biliary system. If patients have poor prognosis (< 3 months), Oddi's sphincter should be stented in order to reduce postprocedural morbidity.

B-0474 15:00

Percutaneous drainage of pancreatic pseudocyst into the stomach

P. Popovic, M. Surlan, M. Sever, D. Vidmar; *Ljubljana/SI*

Background: We report our experience with percutaneous ultrasonographically guided internal cystogastric drainage of symptomatic pancreatic pseudocysts using a double pig-tail catheter, performed under local anasthesia.

Methods: In the period from September 1995 to October 1999 percutaneous drainage of pancreatic pseudocysts was performed in 18 patients. There were 13 males and 5 females with an average age of 48 years. The medium diameter of the pseudocysts was 12 cm. The aetiology of pancreatitis was biliary in eleven cases, alcoholic in six cases, and unknown in one case. Fourteen patients had already undergone previous surgery for pancreatic pseudocyst. The catheter was removed endoscopically 4 – 14 months after the intervention.

Results: The procedure was technically successful in all 18 patients. Complications occurred in five patients. In three cases the pseudocyst recurred soon after catheter removal. In two of these three cases the catheter was introduced again in the same way with no sign of pseudocyst recurrence during further follow-up. Three patients underwent an operation, one because of pseudocyst recurrence and two because of early drainage complications. After five years, clinical and ultrasonographical follow-up in 15 patients confirmed successful treatment. In twelve patients the primary procedure was satisfactory whereas in three patients a second procedure was needed.

Conclusion: The method is minimally invasive, save and effective.

B-0475

withdrawn by author

B-0476 15:10

Echinococcus cysts of the kidney: Percutaneous treatment

G. Sjenicic, B. Putnik, S. Lukac, Z. Djordjevic, G.T. Petkovic, S. Kupresanin; *Belgrade/YU*

Materials and methods: We have treated five patients with echinococcal cysts of the kidney (four male, one female, 16 – 37 years old), with percutaneous drainage. All cysts were in the left kidney, all were solitary, and all were classified as type Gharby 4 or 5. All patients had intravenous urography, US, CT, TIF and TIH analysis, and diagnostic puncture. Before the puncture, all patients were treated with oral Albendazol. Percutaneous treatment was performed using the modified Seldinger technique, in three steps: 1. Puncture under the US guidance 2. Gradual dilatation of the drainage tract 3. Drainage with 16 – 20 Fr drainage catheters. The cyst was aspirated and the cavity was irrigated with Iodine. The cysts continued to drain for 30 – 60 days. The patients were hospitalized for the first seven days, and after that they were treated as outpatients.

Results: There was obliteration of the cyst cavity in all patients. This was followed by scaring of the kidney parenchyma, confirmed by IVU, US and CT. Morphological and functional preservation of the kidney was achieved in all cases. There were no complications or recurrences during the 3 – 18 month follow-up period.

Conclusion: Percutaneous treatment is a reliable, simple and safe procedure, which can achieve complete sterilization of the cyst with minimal renal trauma and greatly reduced treatment costs.

B-0477 15:15

Percutaneous peritoneovenous shunt for the treatment of benign and malignant refractory ascites

J. Park, J. Won, S. Park, D. Lee; *Seoul/KR*

Purpose: To evaluate the usefulness of percutaneously-placed peritoneovenous shunts (Denver shunts) in patients with benign and malignant ascites.

Methods: We placed peritoneovenous shunts in twelve patients (M:F = 9:3, mean age 50.2 years) with refractory ascites and symptoms of: extensive abdominal distension (n = 12), respiratory difficulty (n = 10), or bed-ridden status (n = 9). Seven patients had advanced malignant neoplasms: five had hepatocellular carcinoma, one had colonic cancer, and one had gastric cancer. Nine patients had liver cirrhosis of Childs classification B (n = 2) or C (n = 7). The peritoneovenous shunts were placed under ultrasound and fluoroscopic guidance.

Results: Symptomatic improvement was achieved in all patients. Two patients (16.7 %) are still alive with preserved shunt function. These patients were discharged from hospital. In ten patients who have died (83.3 %) the mean survival was 84 days (range 2 – 420 days). Five patients with esophageal varices died of upper gastrointestinal bleeding; their mean survival was 21 days. Other causes of death were hepatic failure (n = 1), rupture of hepatoma (n = 1), Disseminated Intravascular Coagulation (n = 1), pneumonia and sepsis (n = 2). Shunt function was preserved in nine of the patients until death (90.0 %). Of the ten patients who died, four had benign ascites, and six had malignant ascites

Conclusion: Peritoneovenous shunt placement is technically feasible under ultrasound and fluoroscopic guidance. It is useful in the control of intractable malignant and benign ascites.

14:00–15:30 **Room L/M**

Head and Neck

SS 708

Nose and paranasal sinuses

Chairpersons:
A. Chiesa (Brescia/IT)
U. Mödder (Düsseldorf/DE)

B-0478 14:00

Low dose CT of the paranasal sinuses with eye lens protection: Effect on image quality and radiation dose

E. Hein, P. Rogalla, R. Klingebiel, B.B. Hamm; *Berlin/DE*

Purpose: To assess the effect of lens protection on image quality in CT of the paranasal sinuses.

Material and method: In 127 patients referred to rule out sinusitis, an axial spiral CT with a lens protection shield placed on the patients eyes was obtained (1.5 mm slice thickness, 2 mm/s table feed, 1 mm reconstruction interval, 50 mAs, 120 kV). Coronal views were reconstructed at 5 mm interval. To quantify a subjective impression of image quality, 3 ROIs within the eye ball were plotted along a line perpendicular to the protection shield at 2, 5, and 9 mm beneath skin level on the axial images. Additionally, dose reduction of a Bismuth radioprotective latex (0.85 mg/cm^2) was measured using film dosimetry technique.

Results: The average eye ball density was 17.97 HU (SD 3.7). The relative increase in CT density was 180.6 (SD 17.7), 103.3 (SD 11.7), and 53.6 (SD 9.2), respectively. On coronal views, no diagnostic information loss was observed. The HU shift was practically invisible in bone window/level setting. The use of Bismuth radioprotective latex reduced skin radiation from 7.5 mGy to 4.5 mGy.

Conclusion: The use of a radioprotection shield to the lens is a suitable and effective means to reduce radiation dose to the lens by 40 % in paranasal CT.

B-0479 14:10

A scoring system for paranasal sinus CT findings as a diagnostic tool in cystic fibrosis

H.B. Eggesbø, S. Søvik, S. Dølvik, K. Eiklid, F. Kolmannskog; *Oslo/NO*

Purpose: Cystic fibrosis (CF) is diagnosed by clinical findings, sweat test, and genotyping. However, over-diagnosing of CF has been reported. In CF patients, paranasal sinus affection approaches 100 %. We designed a scoring system based on paranasal sinus findings to distinguish CF patients from other patients.
Materials and methods: 116 CF patients (3 – 54 years) and 136 control patients with inflammatory sinonasal disease (7 – 51 years). CF patients were grouped according to their number of confirmed CF mutations; CF–2 (70 patients), CF–1 (32 patients), or CF–0 (14 patients). Coronal CT scans of the paranasal sinuses were evaluated with respect to: (1) Frontal sinus aplasia, (2) Maxillary sinus hypoplasia, (3) Sphenoid sinus hypoplasia, (4) Advanced ethmomaxillary ipsilateral masses, (5) Medial bulging of the lateral nasal wall, and (6) Absence of pneumatization variants. Each criterion was given 0.5 point if unilateral and 1.0 if bilateral. Criterion 6 was scored as 0 or 1.
Results: Total score in controls and CF–2 patients showed little overlap. In the control group, 94 % had total score of ≤ 1.0 point, and all had ≤ 3.0 points. In the CF–2 group, 90 % had total score ≥ 3.0 points, and all had ≥ 1.5 points. The CF–1 and CF–0 groups consisted of two distinct populations, with total score overlapping the CF–2 group's and the control group's, respectively.
Conclusion: Genetically confirmed CF patients have characteristic paranasal sinus anatomy and inflammatory patterns. We propose that paranasal sinus CT scoring can be used as a diagnostic tool.

B-0480 14:20

MR findings of inverted papillomas: Comparison with nasosinusal malignant neoplasms

L. Palvarini, D. Farina, G. Battaglia, P. Maculotti, R. Piazza, R. Maroldi; *Brescia/IT*

Purpose: To evaluate whether the MR patterns of inverted papillomas (IP) permit to differentiate from nasosinusal malignant tumours (MT).
Materials and methods: MR examinations of 15 patients affected by IP (13 primary, 2 recurrent) and of 15 patients affected by MT (8 adenocarcinomas, 5 SCC, 2 neuroendocrine carcinomas) have been evaluated. Size of lesions was assessed. Bone involvement was graduated as: remodelling; focal (< 15 mm), extended (> 30 mm) or intermediate erosion. Signal intensities on SET2 and SET1 have been compared to muscles, enhancement to the nasal septum mucosa.
Results: Size of lesions significantly differed between IP and MT (avg. 34 mm vs 59 mm, p = 0.0003). Remodelling was observed in 14/15 IP, in 4 cases associated to focal (2) or intermediate (2) erosion. In all MT remodelling was also present but combined with focal (1/15) or extended (14/15) erosion. A relevant correlation (Pearson 0.89) was observed between histology and grade of erosion; conversely bone changes did not correlate with size of both IP or MT. The columnar pattern was detected on enhanced SET1 in all IP and in 1/15 MT which had also extended bone erosion. In this patient the pathological examination demonstrated several areas of IP associated to a SCC.
Conclusions: The columnar pattern is the most relevant sign (PPV = 93.7 %) for the diagnosis of IP. The combination of this sign with the absence of extended bone erosion permits to discriminate IP from MT.

B-0481 14:30

Effectiveness of imaging in detecting subclinical recurrence in the follow-up of 51 treated nasosinusal malignancies

D. Farina, G. Battaglia, P. Maculotti, A. Marconi, R. Maroldi; *Brescia/IT*

Purpose: To assess the accuracy of Imaging in detecting subclinical recurrences in patients treated by radical surgery for malignant nasosinusal neoplasms.
Material and methods: Fifty-one patients previously operated on with radical surgery (19/51 craniofacial resection) were considered; all were affected by nasosinusal malignancies (23 adenoca, 7 SCC, 6 adenoidcystic ca, 6 esthesioneuroblastoma, 9 mesenchymal sarcoma). Patients had a clinical and radiological follow-up longer than 12 months (avg. 58.4). Overall 214 examinations (CT 56/MR 158) were performed. Suspected relapses were confirmed by biopsy, FNAC or follow-up.
Results: Nineteen out of 51 patients (37.2 %) died of disease, 27/51 (52.9 %) are alive without disease (in 17/27 follow-up is longer than 5 years). Pathology and follow-up confirmed 34 recurrences (25 patients). Twelve relapsing lesions (35.3 %) in 10 patients, missed on the clinical examination, were detected only by CT or MR. Sensitivity of Imaging was superior to the clinical-endoscopic evaluation (89.7 % vs. 68.7 %). The NPV of CT and MR was relevant (95.1 %). Imaging yielded a higher rate of FP (4.7 % vs. 1.4 %). Although the accuracy of CT and MR resulted superior to clinical examination (92.1 % vs. 88.8 %), this difference did not reveal statistically significant ($\div^2$, $p > 0.3$).
Conclusions: In ten patients Imaging demonstrated 12 subclinical recurrences. Survival of these patients was better (4 alive, 2 NED) than in 15 patients with clinical recurrence (only one alive).

B-0482 14:40

CT and MR imaging of the lymphoma involving the pterygopalatine fossa

D. Haba[1], F. Veillon[2], S. Riehm[2], M.N. Redlich[2], B. Enachescu[3], J. Tongio[2]; *[1]Iasi/RO, [2]Strasbourg/FR, [3]Bucharest/RO*

Purpose: Study the role of CT and MRI in the assessment of the lymphomas of the pterygopalatine fossa.
Methods: 9 non-Hodgkin lymphomas of the pterygopalatine fossa were retrospectively studied with CT (Elscint 2400 Elite Plus, Siemens Somatom Plus) n = 9 and MRI (MR Max 0.5 T GE, Siemens Vision 1.5 T) n = 4 considering its size, bony walls and fatty content in 4 females, 5 men, aged between 17 and 82 years old.
Results: The pterygopalatine fossa was involved in all the patients with extension to the buccal space (n = 3), masticator space (n = 3 with 1 recurrence), retrostyloid (n = 1), external ear and parotid space (n = 1), orbit and maxillary sinus (n = 1). The fatty content disappear in all the patients with pterygopalatine fossa enlarged in 2 cases, and erosion of the pterygoid process in another 2 cases. MRI was better then CT in delimiting the infiltration along the mandibular or the masticator space but didn't add better information in the buccal space.
Conclusion: The infiltration of pterygopalatine fossa and several spaces with poor bony lesions (n = 2) may suggest the diagnosis of a lymphoma compared with a possible carcinoma. MRI is necessary if an infiltration of the cranial nerve is expected.

B-0483 14:45

Cranial fibrous displasia: MRI findings

A. Kocharyan; *Yerevan/AM*

Purpose: MRI criteria in osteofibrousdysplasia (OD) of skull.
Methods and materials: Based on results of MRI examination of 35 patients with intravenous contrast enhancement (0.5 T Picker, Magnevist 20 ml).
Results and conclusion: OD usually met in persons under 20 – 25 years of age and accompanied by "inflation" of the bone, caused by protein containing heterogeneous hyperintensive masses in T2. They do not contain admixtures of haemoglobin, make thinner but do not destroy the closure plasties. Cystic inclusions neither predominate nor reach big sizes, and contain osteoid and cartilaginoid inclusions. The obliteration of pneumatic sinuses is met quite often, the multicentral foci tend to junction, and the sutures, as distinct from synchondroses, do not make an obstacle. Possessing slow but progressive dynamics they tend to stabilisation with the elements of partial and "perverse" reparation at a more mature age. At the same time there appear vaguely partitioned areas of "intact" bone without infiltration growth. "Inflation" of the bone can be absent, and the closure plasty is hardly differentiated, as being thickened it merges with the total hypointensive signal. The signal in this case does not decrease up to its complete disappearance because of the presence of the fibrous component. No intraosseous oedema is observed, the hydrophilic property is not increased and no infiltration of the adjacent soft tissue structures is found. In intravenous contrast enhancement local shortening of relaxation time is not observed.

B-0484 14:50

MR follow-up examinations of maxillary sinus floor grafting

S. Youssefzadeh, C. Czerny, A. Gahleitner, G. Fürst, T. Bernhart, F. Kainberger; *Vienna/AT*

Purpose: To describe the MR findings of maxillary sinus floor grafting on follow-up examinations.
Materials and methods: 17 patients (14 female, 3 male) aged 24 to 56 years (mean age 45.8) underwent maxillary sinus augmentation with hydroxylapatite and allogenous bone (bilateral in 16 cases, unilateral in 2 cases). MR studies were done on a 1 T unit (Gyroscan T10-NT, Philips, Best, Netherlands) with a circular polarized head coil 2 months afterwards. In 12 patients a follow-up examination after 6 months was available. Axial and coronal T1- and T2 weighted sequences with and without SPIR were done before and after i.v. contrast application. Evaluation criteria included predominant signal intensity on T2- and T1-weighted sequences before and after contrast application and measurement of maximal height and width.

Results: 14/17 grafts displayed hypointensity on T2, 15/17 hypointensity on T1. Contrast uptake was low in 10/17 cases, moderate in 2/17 and high in 4/17. Follow-up examinations showed no changes before contrast application, but contrast uptake was moderate in 8/12 and high in 3/12 patients. Mean height was 18.9 mm, mean width 14.2 mm on the first examination, and 19 mm/15.6 mm on follow-up examinations, respectively.
Conclusion: MR follow-up examinations revealed vitality of the graft and progressive vascularization.

B-0485 15:00

The role of helical CT in high energy maxillofacial trauma
J. Czechowski, L. Seres, L. Borbely, A. Kovacs, L. Ekelund; *Al Ain/AE*

Purpose: To evaluate the usefulness of helical CT with 2D and 3D reformations in the management of facial bones fractures in road traffic accidents.
Methods and materials: Twenty five patients were examined using Helical CT (Sienens Somatom Plus 4), 1.5 pitch. All patients were examined in the axial plane and in 8 patients with additional coronal viewes. In all cases 3D reformations were performed routinely. Analyses were done by two radiologists and 3 oral surgeons. Most of the patients were drivers without seat belt during the accident. There were 21 men and 4 women with an average age of 25 years (range 2 – 60 years). Twenty three patients were operated by maxillofacial surgeons.
Results: High energy trauma of maxillofacial regions often resulted in difficultes in classical classification of injures, but majority opinion has been taken under consideration. The following complex fractures were diagnosed: Le Fort 1 (LF) – 2 cases, LF 2 – 4, LF 3 – 5, comminuted midface – 6, fronto-orbital – 4, naso-fronto-ethmoidal – 6, zygoma – 4, mandible – 7. 2D examinations showed more details, but 3D reformations were better to estimate topography of main fractures and location of fragments and permitted easier planning for surgery. Moreover 3D images were more proper for presentation to lay-persons like family members and medicolegal purposes.
Conclusions: Helical 3D CT is an essential accessory to 2D CT in the management of patients with high energy trauma of the maxillofacial region.

B-0486 15:05

Nasal midline destructive diseases: Is imaging able to discriminate cocaine abuse from Wegener granulomatosis?
R. Maroldi, M. Trimarchi, P. Nicolai, G. Gregorini, F. Facchetti, G. Battaglia; *Brescia/IT*

Purpose: To evaluate radiological features of patients with cocaine induced midline destructive lesions (CIMDL) in comparison to patients with nasal symptoms affected by Wegener Granulomatosis (WG).
Material and methods: Sixteen CIMDL underwent 24 examinations (7 CT, 17 MR); 16 WG were evaluated by CT (2) and MR (14). In all MR studies T2w and enhanced T1w sequences were acquired. All CT examinations were obtained without contrast enhancement. Septal destruction, its area, erosion of adjacent nasal structures (inferior, middle, superior turbinates), lateral nasal wall (medial antral wall, lamina papyracea) and the floor of the nasal cavity (hard and soft palate) were analysed. A score was obtained by counting one point for each involved structure.
Results: All CIMDL had septal perforation while it was present only in 2 WG patients ($\chi^2 = p < 0.0005$); the PPV being 88.89 %. Involvement of a second nasal structure, besides the septum, was observed in 75 % of CIMDL, whereas not present in any WG. A positive correlation between the extent of septal perforation and the number of nasal structures eroded (area vs score, Pearson 0.8, $p = 0.0002$) was observed. Moreover, the occurrence of hard palate perforation showed to be correlated to the destruction of both the inferior (Pearson 0.50, $p < 0.05$) or middle (Pearson 0.54, $p < 0.03$) turbinates.
Conclusion: Radiological findings suggest a more destructive localized diseas process in CIMDL compared to WG. The observed pattern of destruction supports the hypothesis of a centrifugal progression of destruction from the septum towards all nasal walls.

B-0487 15:15

Imaging findings in case of sinonasal cavity osteoma
K. Gordeladze, D. Miminoshvili; *Tbilisi/GE*

Purpose: 27 – 35 % of all bone-forming tumors are osteomas. They mostly occur in the skull bones.
Material and methods: We studied 19 patients with suspected skull bone lesions after X-ray examination. (12 men and 7 women). Age varied from 16 to 55 years. In all cases CT of the skull was performed.
Results: The most frequent presenting symptom was headache. In 7 cases a lesion of frontal bone and frontal sinuses was seen (3 cases bilateral, 4 cases unilateral) which was represented by thickening of the bone structures. In 5 cases osteoma of ethmoid bone and ethmoid sinus was seen, which spreaded towards the retrobulbal space. In 4 patients a sphenoid sinus lesion was detected and in all of these cases the sphenoid sinus was completely occupied by osseus structure. In 4 cases an osteoma was seen in the maxillary sinus. In 2 cases a bone density (200 – 300 HU) structure totally occupied the right maxillary sinus, and the right zygoma was also involved.
Discussion: The use of CT enables to get more information on the nature of bone lesions than X-ray examination. CT is very important in the differential diagnosis of bone-forming tumors.

B-0488 15:20

Is there any clinical role for ultrasonography in the evaluation of maxillary sinuses?
A. Athanassiou, P.K. Prassopoulos, G. Gavridakis, N. Papanikolaou, N. Charoulakis, A. Voloudaki, N. Gourtsoyiannis; *Iraklion/GR*

Purpose: To investigate a possible clinical role for ultrasonography (US) in the evaluation of the maxillary sinuses.
Methods and materials: Eighty one patients with abnormal findings on plain films, CT or MRI, were gathered into three groups (162 sinuses): group A ($n = 57$) with presence of fluid, group B ($n = 58$) with mucosal thickening cysts or polyps and group C ($n = 47$) with normal sinus appearance. Patients underwent US with a 4 MHz transducer and images were analyzed blindly to patient's history and findings of other modalities. Echogenicity and extent of posterior sinus wall (PSW) delineation were ranked on a 4-point grading scale.
Results: PSW was demonstrated in all group A cases with moderate to high echogenicity. In group B, PSW was delineated with low to moderate echogenicity in 47 cases while in 12 PSW was not identified. There was significant difference ($p < 0.0001$) in PSW echogenicity between groups A and B. The PSW was not demonstrated in any group C case. The sensitivity and specificity of US in determining the presence of fluid were 100 % and in excluding pathology in the sinuses were 89.5 % and 100 %, respectively. The extent of abnormalities detected did not differ between US and other modalities ($p = 0.085$).
Conclusion: US may be used as an initial imaging method in diagnosing or excluding the presence of fluid in the sinuses and selecting patients for further imaging work up, especially when radiation exposure should be avoided i.e. pregnant women, children.

14:00–15:30 **Room N/O**

Genitourinary

SS 707

Urinary bladder

Chairpersons:
C. Roy (Strasbourg/FR)
J.A.W. Webb (London/GB)

B-0489 14:00

Does clinical examination under dynamic MRI improve the preoperative diagnosis of female pelvic prolapse?
A. Maubon[1], M. DeGraef[2], M.-P. Boncoeur-Martel[1], C. Courtieu[2], P. Marès[3], J.-P. Rouanet de Lavit[2]; *[1]Limoges/FR, [2]Montpellier/FR, [3]Nîmes/FR*

Purpose: To assess the diagnostic input of clinical examination performed in the magnet, on preoperative dynamic MRI examination for female pelvic floor dysfunction.
Material and methods: Prospective study of 23 patients (39 – 78 years, mean 59 ± 6) referred for pelvic floor prolapse. Preoperative assessment included clinical examination by a gynecologist, static and dynamic MRI: dynamic T2w turbo-spin-echo sequences (contraction, at rest, straining), without and with examination valves successively placed in the anterior and posterior vaginal cul de sac by the radiologist. Comparison of diagnoses and of the extent of prolapses between static and dynamic MRI, and between dynamic MRI and dynamic MRI with examination valves.
Results: Dynamic MRI was superior to static MRI ($p < 0.003$ wilcoxon test) in tne detection of prolapses. The extent of each prolapse was not statistically different between dynamic MRI with or without valves for the urinary, genital or digestive

compartment (signed rank test). It was statistically superior for the peritoneal compartment (p = 0.03). Dynamic MRI with valves detected 5 cystoceles (p = 0.045), 4 periotneoceles (p = 0.025) and 4 rectoceles (p = 0.01) not detected without valves.
Conclusion: Clinical examination with valves in the magnet, coupled with dynamic MRI greatly improves the diagnostic performanceof MRI in the preoperative assessment of female pelvic floor prolapse.

B-0490 14:10

MRI in women with pelvic prolapse
V. Kulakov, A. Volobuev, M. Panova, E. Kulabukhova, V. Panov, M. Blinova; *Moscow/RU*

Introduction: Genitourinary prolapse (GP) is a diagnostic challenge in surgical and gynecological practice. The aim of this investigation was to determine possibilities and limitations of MRI diagnosis of genitourinary prolapse (GP).
Subjects & methods: All MRI were obtained on 1.0 T MRI system Magnetom Harmony (Siemens, Germany). T1W and T2W FSE images and GRE images with short TR 13 ms (full acquisition time – 5 s) were obtained on 37 women (25 healthy women and 12 with G). The GRE was used to make "dynamic" MRI ("bearing-down"). The following parameters were determined: levator muscles thickness and signal intensity; urethra-symphysis distance; proximal urethra diameter; vaginal wall thickness and configuration. These parameters were correlated with: patient's age and parity; global urodynamic parameters; clinical examination data and number and circumstances of deliveries.
Results: The "static" MRI findings in women with GP were: increase in the levator muscles relative contrast in 5 – 6 %; the abnormal configuration of the vagina. "Dynamic" MRI had reliably shown GP only in 4 cases. The severity of damage to the pelvic floor at delivery is determined by the traumatic event and not by the number of deliveries. The morphometry of the levator musculature, urethral diameter, urethra-symphysis distance and vaginal walls thickness did not differ between controls and women with GP. Urodynamic and functional clinical parameters do not correlate with the changes in the pelvic floor musculature.
Conclusions: MRI shows morphological changes clearly and supports clinical and ultrasound findings.

B-0491 14:15

Urinary bladder blood supply: Assessment of contrast-enhanced color Doppler ultrasound
F. Frauscher, A. Klauser, G. Hohlbrugger, G. Helweg, L. Pallwein, G. Bartsch, D. zur Nedden; *Innsbruck/AT*

Purpose: Evaluation of urinary bladder blood supply by contrast-enhanced color Doppler ultrasound (US) in normal human bladder.
Method/materials: Comparative cystometry (filling of the bladder with NaCl and 0.2 mol KCl solutions; filling rate 50 ml/min) was performed in 9 healthy volunteers. Contrast-enhanced US was performed using Levovist (300 mg/ml). Peak systolic velocity (PSV) and enddiastolic velocity (EDV) were measured in 3 intramural arteries at a filling volume of 50 ml and at maximal cystometry capacity (C_{max}) using a transrectal probe of 10 MHz (Acuson Sequioa 512). The resistive index (RI) was assessed. Afterwards Doppler comparison of the different fillings.
Results: In the presence of NaCl, mean PSV increased significantly ($p < 0.005$) with bladder distension (mean values: 9 cm/s at a volume of 50 ml; 17 cm/s at C_{max} (mean: 512 ml)). Compared with NaCl, filling with KCl induced a significantly higher mean PSV of 15 cm/s at a volume of 50 ml ($p < 0.001$). With increasing distension the rise in PSV observed with KCl filling (mean value: 478 ml) was nearly parallel to that obtained on NaCl filling (mean value: 22 cm/s). The RI values showed no significant changes ($p > 0.05$).
Conclusions: Contrast-enhanced US showed during bladder distension and intravesical KCl instillation a significant increase in PSV ($p < 0.001$). Unchanged RI indicates concomitant increases of vesical perfusion. Hence, the composition of urine (high potassium concentrations and hyperosmolarity) influences vesical circulation independently of cardiac output. These findings suggest the presence of prevesical arterio-venous shunts and of an autoregulatory mechanism in the bladder that controls vesical blood supply.

B-0492 14:25

Staging of bladder carcinomas with ultrasonography and Gd-DTPA-supported dynamic magnetic resonance tomography
A.K. Karpenko, V.Y. Startsev; *St. Petersburg/RU*

Purpose: In our studies we tried to evaluate the accuracy of ultrasonography (US), unenhanced T1- and T2-weighted magnetic resonance (MR) imaging, and dynamic gadolinium-enhanced spoiled gradient-echo MR imaging in the staging of bladder cancer.
Methods and materials: Thirty-two patients with histologically proven bladder cancer were prospectively examined with US and MR imaging before tumor resection. Histologic correlation was available in all cases. All patients were examined at the begining with routine T1- and T2-weighted MRI and late Gd-DTPA enhanced T1-weighted MRI. Dynamic study was performed without delay immediately after bolus intravenous injection of Gd-DTPA.
Results: All methods demonstrated tumors comparably well Staging accuracy with transabdominal and with transrectal US was about 40 % (13 of 32) and 62.5 % (20 of 32), respectively. It was the best visualization of carcinoma at the neck of bladder. Dynamic technique showed accuracy about 87.5 % (28 of 32), which was significantly better than conventional MR imaging – 68.7 % (22 of 32). The staging of the intramural extent of bladder tumors was thus improved with gadolinium-enhanced dynamic MR imaging. Overstaging was the most common error, and both US and MR imaging were more accurate for higher-staged tumors.
Conclusions: US and MR imaging perform well in the detection and in preoperative staging of tumors. The difference between dynamic gadolinium-enhanced MR imaging and transrectal US in staging of bladder carcinomas is not statistically significant.

B-0493 14:30

Tailored CT in the diagnosis of bladder lesions causing hematuria
E.K. Lang[1], G. Lechner[2], R. Thomas[1], F. Richter[3], R. Macchia[4], M. Marberger[2], R. Watson[3], B. Gayle[4], F. Mydlo [5], T.H. Helbich[2], K. Cho[3], A. Sabel[1]; *[1]New Orleans, LA/US, [2]Vienna/AT, [3]Newark, NJ/US, [4]Brooklyn, NY/US, [5]Philadelphia, PA/US*

Purpose: Identification of cause for microscopic haematuria.
Methods and materials: 186 patients with unexplained recurring microscopic haematuria were examined with spiral computed tomography (CT) performed according to the following protocol at 5 medical centers: (1) 3 mm pre enhancement spiral CT's from kidney to lower symphysis. (2) 2 mm arterial phase CT cuts (commencing 20 seconds after intravenous injection of 100 – 150 ml contrast medium) kidney and lower half of pelvis. (3) 3 mm CT cuts cortico-medullary phase kidney. (4) 3 mm spiral CT cuts during excretory phase (4 – 7 minutes after injection of intravenous contrast medium) from kidney to floor of the bladder. Appropriate follow-up studies to confirm and establish diagnosis of suggested abnormality.
Results: 23 abnormal patterns of bladder were found in 186 patients. Spiral CT diagnosed 5 bladder neoplasms, 1 urachal neoplasm, 2 invasive adjacent pelvic neoplasms, 5 inflammatory lesions and 1 telangiectasia secondary to prior radiation therapy. Follow-up examination confirmed the diagnosis in 15 patients. In 8 patients an abnormality was noted on the spiral CT without suggesting an etiology; 4 of these were attributed to oedema at the trigone on cystoscopy possibly secondary to passage of ureteral calculus.
Conclusions: The CT protocol designed for microscopic haematuria work-up identified 15 bladder lesions responsible for haematuria in 186 patients and is recommended as a cost effective, low complication rate technique.

B-0494 14:40

Virtual endoscopy of the urinary tract from T2-weighted and gadolinium-enhanced T1-weighted data-sets
A.J. Beer, B. Saar, T. Link, M. Settles, C. Drews, H. Schwaibold, E.J. Rummeny; *Munich/DE*

Purpose: To determine the diagnostic performance of T2-weighted (T2w) and gadolinium-enhanced T1-weighted (T1w-Gd-enhanced) MR-urographies for virtual endoscopy of the urinary tract.
Materials and methods: 36 patients with pathologies of the urinary tract underwent MR-urography at 1.5 T. In each patient a T2w (TSE 3D, TR 2911 ms, TE 650 ms, respiration triggered) and a T1w-Gd-enhanced sequence (T1 FFE, TR 4.5 ms, TE 1.2 ms, breathhold) were acquired. Furosemide and n-butylscopolamin were administered prior to the examination to enhance diuresis and reduce peristalsis. Data reconstruction was performed as maximum intensity projection (MIP) and virtual endoscopy (VE). The endoscopic and surgical findings served as a standard of reference.
Results: MIP and VE delineated 32 of 35 pathologies. One flat bladder tumor and 2 calculi smaller than 5 mm were missed.
83 % of intraluminal pathologies could only be depicted by VE and not by MIP. For the assessment of the renal pelvis, MIP was superior to VE in 60 %. Concerning the ureter, MIP was equal in 62 % and superior to VE in 38 %.
T2w data-sets were superior for virtual cystoscopy for 2 reasons: no contrast medium is required in cases of renal failure and sedimentation artifacts of the contrast medium can be avoided.
T1w-Gd-enhanced data-sets were superior for virtual ureterorenoscopy due to their higher temporal resolution.

Conclusion: Virtual endoscopy of the urinary tract is a useful tool for the depiction of intraluminal pathology. For virtual cystoscopy, T2w data-sets are preferrable, while T1w-Gd-enhanced data-sets are superior for virtual ureterorenoscopy.

B-0495 14:50

MRI-based virtual cystoscopy: A new method for the diagnosis of urinary bladder cancer

M. Lämmle, A. Beer, M. Settles, H. Schwaibold, C. Drews, C. Hannig, C. Hierholzer; *Munich/DE*

Purpose: The evaluation of virtual MRI endoscopy in patients with urinary bladder cancer and its potential clinical use.
Materials and methods: Twenty-five patients (20 men, 5 women, mean age 67.2 years, range 45 – 89 years) with urinary bladder cancer primarily diagnozed at conventional cystoscopy were subjected to MRI of the pelvis. Patients were examined without exterior bladder filling or application of any medication. All examinations were performed on a Philips Gyroscan ACS-NT 1.5 T scanner, using a T2 weighted 3D TSE sequence, TR 2911 ms, TE 500 ms. After reconstruction, location and size of tumors were individually determined and compared with results of conventional cystoscopy, to determine sensitivity and specificity of virtual MR endoscopy of the bladder, depending on the size of tumor. Advantages and disadvantages of virtual endoscopy should be clearly defined so that possible indications for clinical use can be identified.
Results: Range of tumor size was from 0.4 to 6.4 cm in diameter. Thirty out of 33 tumors detected in conventional cystoscopy were identified with virtual endoscopy, corresponding to an overall sensitivity of 90.9 %. Specificity was 100 %. Difficult conditions for conventional cystoscopy including hematuria, anterior wall involvement, diverticula and urethral strictures had no impact on virtual cystoscopy.
Conclusion: The results of this study suggest a high reliability in the diagnosis of bladder cancer by MRI-based virtual cystoscopy. Presently, this technique may be indicated when conventional cystoscopy is contraindicated or restricted in feasibility or interpretation or on risk of hemorrhage, perforation, infection or pain.

B-0496 15:00

MR virtual cystoscopy in the detection of neoplastic bladder lesions

V. Panebianco, A. Laghi, C. Catalano, I. Sansoni, R. Alcetta, A. Napoli, R. Passariello; *Rome/IT*

Purpose: To identify bladder lesions with MR-Cystoscopy protocols.
Methods and materials: 23 patients with suspected or known diagnosis of bladder tumor were submitted to MR cystoscopy. We used 2 different protocols for bladder distention: with 300 to 500 ml of a 1:100 solution of Gd-DTPA (0.5 molar) using Foley catheter or with natural contrast (urine) and monitoring bladder filling with 3DFLASH sequence with i.v. c.m. MRI examinations were performed on a 1.5 T Siemens Vision plus MR imager. We used: 3DSPGRE (TR: 4.6; FA: 30°; TE: 1.8; Slice thickness 2 mm; matrix 195 × 512; TA 23 s); 2D FSE on axial planes, with TR 4300, TE eff. 132, ETL 33, matrix 420 × 512, FOV 280, Phase oversampling 80 %; T1 weighted GRE sequence for bladder wall evaluation (FLASH 2D, TR 156, TE 2.3, Matrix 131 × 256). This sequence was repeated after i.v. injection of Gd-DTPA (0.0025 mmol/kg). VE images were reconstructed using volume rendering technique with dedicated workstation (Silicon graphics O2) and specific software (Vitrea 2.1, Vital Images).
Results: Image quality was considered optimal in all cases. A total of 18 lesions were detected and confirmed at biopsy. In 3 cases no lesion were evident at MRI and at conventional cystoscopy. All lesions were evident on morphological T1 and T2 weighted images, with size ranging between 8 and 20 mm. VE did not allow evidence of intramural end extravescival extension of the disease, whereas these findings were easily appreciated on morphological T1 – T2w images.
Conclusions: MR Virtual cystoscopy optimizes detection and staging of the bladder pathology by combining axial T1 – T2 weighted and VE.

B-0497 15:10

Pitfall: Pseudo-obstruction of the proximal urinary tract system after ileal bladder substitution

H.C. Thoeny, M. Sonnenschein, P. Vock, U.E. Studer; *Berne/CH*

Purpose: To differentiate urographic dilatation of the upper urinary tract caused by pseudo-obstruction from true obstruction after ileal bladder substitute surgery.
Material and methods: Between 1986 and 1993 47 patients (median age: 62, range: 44 – 80) underwent radical cystectomy for bladder cancer and received an ileal orthotopic bladder substitute. Urography was performed 1 and 6 months, 1, 3, 5, 7 and 10 years after surgery. By definition contrast medium in the pelvicalyceal system 10 minutes post injection was considered to exclude significant obstruction. Width of pyelon and calyceal necks as well as the appearance of the fornices (three grades: pointed, blunted and rounded) were analysed. 7 patients where excluded due to lack of follow-up studies over a 2 year period.
Results: Early postoperatively 75 % of all patients showed dilatation of the upper urinary tract at 10, 25 and 60. Among all patients 80 % (32/40) studied more than 1 year after surgery repeatedly showed dilatation of the upper urinary tract only at 25 minute films whereas at 5 and 60 minute films the upper tracts where not dilated. Out of the 8 remaining patients 3 presented with unilateral obstruction whereas 5 demonstrated normal findings throughout all studies.
Conclusion: While dilatation of the upper urinary tract at 10, 25 and 60 minutes after contrast medium administration is a common normal finding in the early postoperative phase, even on later studies dilatation limited to the 25 minute film should not be overinterpreted as obstruction.

B-0498 15:20

The long-term appearance of the upper urinary tract after orthotopic bladder substitution

H.C. Thoeny, M. Sonnenschein, P. Vock, U.E. Studer; *Berne/CH*

Purpose: Does orthotopic bladder substitute affect the proximal urinary tract system and function in the long term?
Material and methods: 47 consecutive male patients underwent radical cystectomy for bladder cancer and received an ileal orthotopic bladder substitute. Intravenous urography was performed at regular intervals (1 and 6 months, 1, 3, 5, 7 and 10 years after surgery). 7 patients were excluded due to follow-up being less than 2 years. 2 kidneys were lost due to nephrectomy for recurrent cancer. Kidney size and parenchymal thickness at superior and inferior poles as well as mid-level were measured pre- and postoperatively in the remaining 78 renoureteral units (10 % change threshold).
Results: After a median observation time of 70 months there was no alteration of renal size in 75 out of 78 kidneys; 3 decreased significantly in size: two with preoperatively pre-existing severe dilatation of the upper urinary tract, one with ureteroileal stenosis. In 72 out of 78 renoureteral units the parenchymal thickness at all levels remained unchanged; 6 decreased in parenchymal thickness: 5 with ureteroileal stenosis and one with recurrent cancer. Dilatation of the upper urinary tract in the early postoperative period at 10, 25 and 60 minutes was a common finding in 75 % and dilatation limited to the 25 minute films on later studies in 80 %. Obstruction due to ureteroileal stenosis occurred in 3 out of 78 (3.8 %).
Conclusion: Long-term follow-up after orthotopic bladder substitute demonstrates no significant morphological or functional change of the upper urinary tract.

16:00–17:30 **Room P**

Vascular

SS 815

Carotid arteries

Chairpersons:
P. Cluzel (Paris/FR)
C. Fugazzola (Varese/IT)

B-0499 16:00

Contrast enhanced turbo-MRA in the evaluation of carotid artery stenosis

C. Catalano, F. Fraioli, A. Laghi, F. Pediconi, A. Grossi, A. Napoli, R. Passariello; *Rome/IT*

Purpose: To determine the feasibility and accuracy of contrast enhanced Turbo-MRA (CE-MRA) in the evaluation of patients with carotid artery stenosis.
Material and methods: 53 patients with suspected carotid artery stenosis were examined with a 1.5 T magnet (Siemens Vision Plus) using a multiphase 3D T1 weighted spoiled GE (TR/TE/NEX: 3.8/1.4/1; TA 10 s; matrix 110 × 160) after i.v. administration with a power injector of 15 ml of Gd-DTPA at 2 ml/s. In all patients DSA, was also performed and considered the standard of reference. Measurements were performed according to the NASCET criteria by two blinded readers.
Results: CE-MRA was correct regarding the degree of stenosis in 14/15 mild stenoses, 15/17 discrete stenoses, 19/20 severe stenoses and 7/7 occlusions and correctly negative in 45 normal carotid arteries. The degree of stenosis was overestimated in 3 cases and underestimated in 2. CE MRA allowed to detect tandem lesions of the internal carotid arteries in 6 cases. Stenosis at the origin of the common carotid arteries were correctly detected in 9 cases.

Conclusion: CE-MRA is a rapid, reliable method to evaluate patients with suspected carotid artery stenosis. A further advantage is the large field of view allowing evaluation of the aortic arch, origin of the supraaortic vessels and carotid arteries up to the intracranial portion. In consideration of the excellent results of ce MRA, DSA should not be performed in the assessment of the carotid arteries.

B-0500 16:10

Dynamic contrast-enhanced MRA of the carotid arteries in comparison to i.a. X-ray angiography

R. Janka, F.A. Fellner, R. Wutke, C. Fellner, A. Schmid, W.A. Bautz; *Erlangen/DE*

Purpose: To determine the value of dynamic contrast-enhanced (CE) MRA of the carotid arteries in comparison to 3D time-of-flight (TOF) turbo MRA and i.a. x-ray angiography.

Material and methods: We examined 30 consecutive patients suffering from arteriosclerotic disease of the carotid arteries. All examinations were done on 1.5 T MR system (Magnetom Symphony, Siemens, Erlangen). Following MRA sequences were applied: (1) 3D TOF turbo MRA through the carotid bifurcation in transverse orientation. (2) Dynamic CE MRA through the whole vasculature from the aortic arch up to the circle of Willis in coronal orientation. Temporal resolution was 10 s per data set. 25 ml of Gd-DTPA (Magnevist, Schering, Berlin) were injected in each case with a flow of 2.0 ml/s. Selective i.a. x-ray angiography was performed in all patients.

Results: Dynamic CE MRA revealed excellent delineation of the aortic arch due to the short measurement time. However, accuracy of stenosis grading at the level of the carotid bifurcation was not satisfying, when compared with 3D TOF turbo MRA and selective i.a. x-ray angiography. This is probably due to the low spatial resolution of dynamic CE MRA. Venous overlap in the area of the intracranial vessels which could deteriorate evaluation of those small vessels was not relevant in dynamic CE MRA.

Conclusion: Dynamic CE MRA is an excellent method for delineation of the aortic arch. However, due to reduced accuracy in stenosis grading we do not recommend this technique as unique method for pretherapeutical visualization in patients with arteriosclerotic carotid artery disease.

B-0501 16:20

Fluoroscopically triggered ("CareBolus") contrast-enhanced (CE) 3D MRA of the carotid arteries in comparison to selective i.a. X-ray angiography

R. Wutke, F.A. Fellner, C. Fellner, R. Janka, A. Cavallaro, W. Lang, W.A. Bautz; *Erlangen/DE*

Purpose: To determine the value of fluoroscopically triggered CE-MRA of the carotid arteries in comparison to selective x-ray angiography (DSA) and high resolution 3D time-of-flight (TOF) turbo MRA.

Material and methods: 30 consecutive patients with arteriosclerotic carotid artery disease were included. MR-examinations were performed using a 1.5 T scanner (Magnetom Symphony, Siemens, Germany). 3D TOF turbo MRA was applied in transverse orientation restricted to the area of the carotid bifurcation. For CE MRA a 3D FLASH sequence in coronal orientation was performed from the aortic arch up to the circle of Willis.

Results: Concerning stenoses (grade I ... 0 – 30 %, II ... 40 – 60 %, III ... 70 – 90 %, IV ... occlusion) of the internal and external carotid arteries agreement between CE MRA and DSA was excellent (94 – 97 %). Regarding local stenosis grading in steps by 10 % 3D TOF turbo MRA is more accurate than CE MRA. CE MRA tended to overestimate stenoses in comparison to DSA and 3D TOF. All relevant stenoses of the common and internal carotid arteries up to the circle of Willis were correct detected by CE MRA. Problems with reduced delineation at the aotic arch may occur in adipose patients with long distance between vessels and coil.

Conclusions: CE MRA allows sufficient classification of stenoses of the carotid arteries. Exact stenosis measurement is a question of spatial resolution. At the moment, in borderline cases, 3D TOF turbo MRA is more accurate for this purpose. The combination of both techniques has meanwhile replaced x-ray angiography in our routinely clinical setting.

B-0502 16:30

Assessment of carotid artery stenosis with breath-hold high-resolution MR angiography in comparison to DSA: A single slab technique with a combined coil system

B.J. Wintersperger, A.M. Huber, G. Preissler, N. Holzknecht, T.K. Helmberger, A. Billing, J. Scheidler, M.F. Reiser; *Munich/DE*

Purpose: To compare high-resolution breath-hold contrast enhanced MR Angiography (CE-MRA) with digital subtraction angiography (DSA) in detecting carotid artery stenosis and to visualize the whole carotid system in a single slab technique.

Material and methods: 28 patients underwent breath-hold CE-MRA on a 1.5 T whole body system (Symphony Quantum; Siemens AG) equipped with a high performing gradient system (30 mT/m; 240 µs). Carotid arteries were imaged in a single slab including the aortic arch and the middle cerebral artery with a high-resolution technique. Contrast enhancement was provided by injection of 1.5 mmol/kg BW Gd-DTPA after transit time assessment. DSA was the standard of reference in all patients and stenoses graded according to NASCET criteria in both modalities.

Results: Sufficient image quality was achieved in all patients. DSA depicted 32 stenoses ≥ 30 % (26 ≥ 70 %). Overall sensitivity, specificity and negative predictive value for MRA in stenoses ≥ 70 % were 100 %. In stenoses ≥ 30 % sensitivity, specificity and negative predictive value for MRA were 100 %, 98 % and 91 %, respectively. MRA allowed for a reliable depiction of atheromatous pseudo-occlusions.

Conclusions: With recent scanner technologies a complete coverage of the carotid vasculature from the aortic arch to the middle cerebral artery is feasible in a single slab examination with submillimeter resolution. MRA allows for a reliable assessment of carotid artery stenosis including atheromatous pseudo-occlusion and can replace invasive DSA in judgement of carotid artery stenoses and screening for additional lesions.

B-0503 16:40

The role of MRA in the diagnosis of carotid artery diseases

D. Yararbas, M. Paryldar, A. Solak, S. Kalaycýoglu; *Izmir/TR*

Purpose: The aim of our study was to evaluate the effectiveness of MRA in detecting carotid artery stenosis and to compare the contrast enhanced and non-contrast enhanced MRA techniques.

Methods and materials: In this prospective study, 20 patients were examined using a 1.5 T MR unit (Philips Powertrak 6000 ACS-NT)with quadrature neck coil. MR angiographies were performed with and without contrast enhancement. The non-contrast sequence was a M2D inflow gated sweep gradient echo sequence (TR/TE/FA: 20/4.1/60) and the scan time was 10 minutes. The contrast enhanced sequence using 20 ml Gd-DOTA (Dotarem, Guerbet)was a bolus-trak application consisting of a real time 2D bolus tracking sequence (TR/TE/FA: 5.1.1.4/40) followed by a 18 second 3D gradient echo sequence (TR/TE/FA: 5.1.1.4/40; matrix: 512 × 512). The reference gold-standard technique was conventional angiography.

Results: The contrast enhanced and non-contrast MRA techniques were evaluated seperately and although contrast enhanced scans had some advantages like shorter scan time and better image quality with longer coverage, no statistically significant difference has been shown in detecting carotid artery stenosis ($p > 0.005$). When compared to conventional angiography, MRA in general, has a high sensitivity and specificity in detecting carotid artery stenosis.

Conclusion: MRA is a powerful tool for the non-invasive diagnosis of the carotid artery diseases and should be considered as an alternative test in pre-surgical evaluation of patients.

B-0504 16:50

Asymptomatic carotid artery stenosis - MR-imaging and color Doppler correlation

D. Gachechiladze, I. Diasamidze, D. Berulava; *Tbilisi/GE*

Purpose: The aim of our study was to analyze the relationship between Magnetic Resonance Imaging (MRI) findings and Carotid artery changes in patients with Carotid artery asymptomatic stenosis.

Materials and methods: 60 patients (mean age 56.8) with clinically asymptomatic Carotid artery stenosis > 50 % were investigated. All patients underwent standard neurological examination, MRI, MRA and Color Doppler (CD) of extracranial arteries, cardiologic examination to exclude cardiogenic embolism.

Results: MRI revealed presence of anterior circulation silent brain infarctions (SBI) in 14 (23 %) cases. SBIs were small and located as in basal ganglia and periventricular white metter, as in cortex. CD showed encrease of mean Common

Carotis artery Intima-Media Thickening – 1.12 ± 0.34 mm. In 28 (47 %) cases changes of IMT structure was marked. 48 (80 %) of ICA stenosis were moderate (50 – 75 %), 11 (18 %) critical, only in 1 (2 %) case-occlusion of ICA was diagnosted. The CA stenosis turned out bilateral in 46 (77 %) cases. From them 16 (27 %) cases were hemodinamically significant. The majority (32 (53 %)) of plaques were unstable (26 heterogenous, 6 "soft"). Such type of plaques appeared in 10 (71 %) cases of SBI.

Conclusion: This data show that patients with asymptomatic > 50 % CA stenosis in about 1/4 of cases present SBI. CA stenosis in majority cases is bilateral. The embolism from unstable plaque may be cause of SBI despite the absence of focal neurologic symptoms.

B-0505 17:00

Multidetector spiral CT angiography vs. time resolved contrast enhanced MR angiography in the assessment of carotid artery stenosis

C. Catalano, A. Laghi, R. Brillo, F. Fraioli, A. Napoli, F. Pediconi, R. Passariello; *Rome/IT*

Purpose: To compare multislice spiral CT angiography (CTA) with contrast enhanced MR Angiography (MRA) in patients with suspected carotid artery stenosis.

Material and methods: 16 patients with suspected carotid artery stenosis were examined within 4 days with CTA using a multislice spiral CT (Somatom Volume Zoom, Siemens) and MRA using a 1.5 T magnet (Vision plus, Siemens). Multislice spiral CTA was performed using a 4 × 1.5 collimation after bolus administration of 100 ml of contrast agent at 4.5 ml/s. Contrast enhanced MRA was performed using a multiphase sequence after bolus administration of 15 ml of Gd-DTPA at 2 ml/s. CTA images were reconstructed using a volume rendering algorithm on dedicated consoles, while MRA images using a standard MIP algorithm on the magnet console. The two techniques were compared for degree of stenosis and plaque morphology, using DSA as standard of reference.

Results: With both techniques images were diagnostic and free of artifact. In 1 case of calcified plaque CTA overestimated the degree of stenosis, which correctly appeared mild at MRA. No significant difference was seen in detecting ulcerated plaques. CTA resulted significantly more time consuming in image reconstruction.

Conclusion: Although multislice spiral CT encompasses most of the problems of spiral CTA (spatial and temporal resolution), contrast enhanced MRA provides in a simpler way comparable results, with well tolerated contrast agents and without ionizing radiations.

B-0506 17:10

Carotid artery stenosis: Multislice spiral CT (MSCT) vs. DSA

M. Lell, A. Noemayr, U. Baum, F.A. Fellner, R. Wutke, W. Lang, W.A. Bautz; *Erlangen/DE*

Purpose: To evaluate the potential of MSCT in the investigation of carotid artery (CA) stenosis in comparison with DSA.

Material and methods: 30 patients with different grade of CA stenosis were examined with MSCT (Somatom VZ, Siemens, Germany) and i.a. DSA. CA stenosis were graded according to the NASCET criteria as mild (0 – 29 %), moderate (30 – 69 %), severe (70 – 99 %) and occluded. MSCT (4 × 1 mm slice collimation, table feet 6 mm/rot., rotation time 0.5 s, 80 ml contrast material) results were compared with the results of DSA.

Results: 1 mm slice collimation proved to be sufficient for grading of CA stenosis with MSCT. The whole length of the CA from the aortic arch to the circle of Willis was assessed. All cases of occlusion were correctly identified with both methods. In 56 cases MSCT and DSA showed the same degree of stenosis. In 3 cases MSCT demonstrated higher stenosis grade, proved by surgery. 1 circular short range stenosis was missed with MSCT.

Conclusion: MSCT proved to be a robust and highly accurate non-invasive method in the preoperative evaluation of CA stenosis.

B-0507 17:20

Grading of carotid artery stenoses with multislice CT angiography: Comparison with US and DSA

S.H. Kreuzer, M. Prokop, M. Cejna, R. Ahmadi, A. Willfort, D. Fleischmann, S.A. Thurnher, M. Hörmann, C.M. Loewe; *Vienna/AT*

Purpose: To compare multislice-CT-angiography (MCTA) and color duplex ultrasound (US)for the grading of carotid artery stenoses and evaluation of vascular diseases.

Methods and materials: We studied 15 patients prior to carotid stenting (3 female, 12 male, 69 mean age) using MCTA (Somatom Volume Zoom, Siemens), US and digital subtraction angiography (DSA). With MCTA, the volume from the aortic arch to the sella was covered with 4 × 1 mm section thickness using a pitch of 5 – 7 and a 0.7 mm reconstruction increment. The application of intravenous contrast medium was tailored individually based on a test bolus injection. We used axial sections and curved planar reformats to classify stenoses according to the NASCET criteria; in US we employed flow velocity measurements. Severity of stenoses was graded in 10 % steps. DSA was used as the gold standard. Additional vascular findings were recorded.

Results: We found an excellent correlation ($r^2 = 0.91$) between the grading of stenoses using MCTA and DSA. The correlation between US and DSA grading was significantly worse ($r^2 = 0.80$, $p < 0.05$). As compared to DSA, MCTA tended to slightly underestimate the degree of stenoses (average –2 %, range –30 % to +10 %). US on average led to overestimation of stenoses (average +12 %, range – 10 % to +40 %). MCTA revealed a stenosis that was not detected with US and an intracranial aneurysm in another patient.

Conclusion: MCTA is similar to DSA and more accurate than US in the evaluation of carotid artery stenoses. In addition, intracranial abnormalities can be detected with MCTA.

Sunday, March 4

	room A 2nd level	room B 2nd level	room C 2nd level	room E1 entr. level	room E2 entr. level	room F1 entr. level	room F2 entr. level	room G lower level	room H lower level	
08:30										08:30
09:00	**CC 916**	**RC 910**	**CC 917**	**RC 901**	**SA 9**	**WS 915**	**SF 9**	**RC 908**	**WS 909**	09:00
09:30										09:30
10:00										10:00
10:30										10:30
11:00	**CC 1016**	**SS 1010** **Musculoskeletal** Interventional procedures/ Miscellaneous *(p. 210)*	**SS 1001a** **Abdominal and Gastrointestinal** Liver maging *(p. 211)*	Bracco Symposium 2	**SS 1002** **Breast** Breast ultrasound *(p. 213)*	**SS 1004** **Chest** Airway and lung disease *(p. 215)*	**SS 1011** **Neuro** Tumors - Advanced diagnostic techniques *(p. 217)*	**SS 1001b** **Abdominal and Gastrointestinal** Dynamic studies *(p. 219)*	**SS 1009** **Interventional Radiology** Arterial intervention (1) *(p. 221)*	11:00
11:30										11:30
12:00										12:00
12:30	**HL 2**									12:30
13:00	Gold Medalist Awards									13:00
13:30										13:30
14:00	Image Interpretation Session									14:00
14:30										14:30
15:00										15:00
15:30										15:30
16:00										16:00
16:30	**CC 1216**	**RC 1210**	**CC 1217**	**RC 1201**	**RC 1202**	**RC 1204**	**RC 1211**	**RC 1205**	**RC 1206**	16:30
17:00										17:00
17:30										17:30

	room I lower level	room K lower level	room L/M 1st level	room N/O 1st level	room P lower level	room X entr. level	room Y 1st level	room Z lower level	
08:30									08:30
09:00	**WS 918**	**RC 912**	**RC 913**	**RC 914**	**SS 906** **Contrast Media** New trends (4) *(p. 208)*				09:00
09:30									09:30
10:00									10:00
10:30							**WS 20C1**	**WS 19C1**	10:30
11:00	**SS 1001c** **Abdominal and Gastrointestinal** CT colonography *(p. 223)*	**SS 1012** **Pediatric** Genitourinary and central nervous system *(p. 225)*	**SS 1008** **Head and Neck** Larynx and pharynx *(p. 227)*	**SS 1003** **Cardiac** Heart: CT/MRI/MRS *(p. 229)*	**SS 1015** **Vascular** Supraaortic and renal vessels *(p. 231)*	**WS 19C2**	**WS 20C2**		11:00
11:30									11:30
12:00							**WS 20C3**		12:00
12:30									12:30
13:00									13:00
13:30									13:30
14:00						**WS 19C3**	**WS 20D1**		14:00
14:30									14:30
15:00							**WS 20D2**		15:00
15:30									15:30
16:00							**WS 20D3**		16:00
16:30	**RC 1212**	**WS 1215**	**RC 1208**	**RC 1203**	**RC 1213**				16:30
17:00									17:00
17:30									17:30

08:30–10:00 Room P

Contrast Media

SS 906

New trends (4)

Chairpersons:
M. Kormano (Turku/FI)
J. Pringot (Brussels/BE)

B-0508 08:30

Comparative assessment of monomer and dimer CM for spiral CT in surgical clinic

G.G. Karmazanovsky, V.D. Fedorov, E.B. Guzeeva; *Moscow/RU*

Purpose: Significance of monomer and dimer CM for differential diagnosis and virtual surgery.
Materials and methods: Spiral CT with bolus contrast enhancement was performed in 104 pts (100 ml, 3 ml/s): arterial and venous phases – 19 pts with monomer CM and 17 with dimer CM; only phase of the portal vein (PVP) was performed with Ultravist-300 in 16 pts – 100 ml and 17 pts – 50 ml. Vizipaque-270 was introduced in 16 pts – 100 ml and in 19 pts – 50 ml. The densitometry of aorta, VCI, stem of the portal vein, parenchyma of liver and pancreas, pathological formations in them were performed.
Results: Monomer CM in AP gave the density gradient from 23 HU between the hepatic parenchyma and VCI to 143 HU between the aorta and hepatic parenchyma. In VP – from 8 to 20 HU (respectively). In PVP – from 29 HU to 73 HU. Dimer CM gave gradients from 20 to 178 HU in AP and from 11 to 38 HU in VP, from 19 to 50 HU in PVP.
Conclusions: For 3D-reconstructions contrast enhancement monomer CM is the most optimal. For differencial diagnosis of surgical diseases the application of dimer CM is the most optimal, as parenchymatous organs accumilate CM quicker than other organs visualizing better all kind of lesions on their background.

B-0509 08:40

Assessment of the vascularization of neuroendocrine tumors by stimulated acoustic emissions of SH U 508A ultrasound contrast agent and color or power Doppler sonography

J. Ricke, E. Lopez Hänninen, H. Amthauer, R. Felix; *Berlin/DE*

Purpose: To assess the vascularization of neuroendocrine tumors by stimulated acoustic emissions (SAE) of SH U 508A during blood pool phase in comparison to contrast enhanced doppler sonography.
Materials and methods: Thirty-six patients with neuroendocrine tumors received contrast enhanced doppler sonography, 21 an additional SAE. To classify tumor perfusion in doppler sonography, a four-step rating score was introduced: (1) no, (2) one feeding or central vessel defined hypoperfusion; (3) some and (4) disseminated vessels defined hyperperfusion. Out of 36 patients, 1 pancreatic primary, 33 liver and 1 splenic metastases as well as 1 lymph node metastasis were examined. Results were correlated with biphasic spiral CT (n = 35) and angiography (n = 2).
Results: Arterial phase CT and DSA revealed 18 hyper- and 18 hypoperfused lesions. Contrast enhanced doppler classified 15/18 patients (83 %) with hyperperfused lesions correctly as well as 16/18 (89 %) hypoperfused tumors by applying the rating score. SAE identified 4 of 9 hyperperfused lesions correctly (44 %), 2 were isoperfused compared to normal liver tissue (22 %), 3 hypoperfused (33 %). Out of 12 hypoperfused lesions, 11 were classified correctly (92 %), 1 showed isoperfusion. Hence, the positive and negative predictive values for SAE were 80 and 69 %, respectively. For contrast enhanced doppler sonography, positive and negative predictive values were 88 and 84 %, respectively.
Conclusions: Blood pool SAE failed to determine subtle tumor perfusion correctly. The rating score for contrast enhanced doppler sonography characterized tumor perfusion with high accuracy. The use of contrast agent improved perfusion characterization significantly.

B-0510 08:50

The first phase I study of a novel ultrasound contrast agent (BR14): Assessment of safety and efficacy in liver and kidneys

R. Basilico[1], M.J.K. Blomley[2], D.O. Cosgrove[2], J. Llull[3], A. Broillet[3]; [1]*Chieti/IT,* [2]*London/GB,* [3]*Geneva/CH*

Purpose: BR14 (Bracco Research, Geneva) is a novel ultrasound contrast agent. We describe the first phase I study using pulse inversion harmonic imaging (PIH) of the liver and kidneys of healthy volunteers.
Materials and methods: 30 male subjects were studied using a single-blinded, placebo controlled methodology. Five single iv doses of BR14 were given; 4 subjects received BR14 and 2 were randomised to placebo at each dose. The left kidney was scanned using continuous PIH (HDI 5000 scanner, ATL, Bothell WA) from arrival to disappearance of contrast from main renal vessels (immediate phase). Five minutes later, brief 20 s duration scans of the liver/right kidney were stored as cine-loop digital files every 30 minutes until disappearance of contrast enhancement (late phase). Backscatter values for regions of interest (ROIs) in the liver/renal cortex were calculated using ATL proprietary software. In addition, subjective enhancement in both early and late phases was scored.
Results: No serious adverse events and no significant changes in vital signs and laboratory parameters was observed. Strong enhancement of main renal vessels and cortex during the immediate phase was seen in all subjects receiving BR14 with a dose dependent increase in main vessels enhancement duration (from 6.8 minutes to 26.9 minutes at the highest dose). Moreover, all the tested doses of BR14 produced a strong late phase liver parenchymal enhancement. Quantitative analysis showed evidence of delayed renal parenchymal phase at the highest three doses.
Conclusion: BR14 is a safe, effective US contrast agent showing late phase parenchymal enhancement in the liver and renal cortex.

B-0511 09:00

Iron oxides differentiate between hyperplastic hematopoetic marrow and bone marrow neoplasms

H.E. Daldrup-Link[1,2], B. Ihssen[2], T.M. Link[1], E.J. Rummeny[1]; [1]*Munich/DE,* [2]*Münster/DE*

Purpose: To compare the value of Ferumoxides and Ferumoxtran-enhanced MRI to characterize hematopoetic marrow and neoplastic infiltration of the spine in patients with malignant lymphomas.
Methods: 18 patients with plasmocytoma or other Non-Hodgkins lymphomas underwent MRI of the spine after infusion of either Ferumoxides (AMI-25, Endorem, n = 9) or Ferumoxtran (AMI-227, Sinerem, n = 9). All patients had suspected hypercellular bone marrow, diagnosed by iliac crest biopsies or estimated from previous treatment with GCSF (granulocyte colony stimulating factor) and all patients had suspected diffuse or multifocal bone marrow infiltration, based on clinical data and conventional radiographs. Pre- and postcontrast MRI pulse sequences comprised sagittal T1- and T2-weighted turbo spinecho (TSE) as well as STIR-sequences. Data were analysed by measuring pre- and postcontrast signal intensities of the hematopoietic marrow and tumor infiltrates.
Results: Hematopoetic bone marrow demonstrated a significantly stronger signal decrease after infusion of Ferumoxtran as compared to Ferumoxides on STIR-images ($p < 0.05$). The contrast between focal bone marrow lymphoma and hematopoetic marrow increased with both contrast agents. The iron oxide uptake in diffuse lymphomatous bone marrow infiltrates varied with the grade of tumor cell infiltration, but was decreased compared to hematopoietic marrow in most cases, while hyperplastic hematopoietic marrow demonstrated a markedly increased iron-oxide uptake.
Conclusion: Ferumoxtran is better suited than Ferumoxides for MRI of patients with suspected lymphomatous bone marrow infiltration. Iron oxide-enhanced MRI identifies focal and multifocal bone marrow infiltrates with malignant lymphomas and differentiates neoplastic infiltration and hyperplastic marrow after chemotherapy.

B-0512 09:10

MR-angiography with a new intravascular contrast agent (P 792): Assessment in rabbits

S.G. Rühm[1], C. Corot[2], K. Treiber[3], J.F. Debatin[1]; [1]*Essen/DE,* [2]*Aulnay-sous-Bois/FR,* [3]*Zürich/CH*

Purpose: To assess the performance of a newly developed Gd-based macromolecular intravascular contrast agent for MRA (P792; Laboratoire Guerbet) in rabbits.
Materials and methods: New Zealand rabbits served as the animal model. MR imaging was performed on a 1.5 T whole-body MR system with a 3D spoiled gradient recalled echo sequence The 3D acquisition was performed once prior to

application of the contrast agent, during the bolus phase as well as successively every minute thereafter up to 10 min. Dose relationship testing was performed with 3 doses of P792 (0.015, 0.03 and 0.045 mmol/kg) as well as a single dose of Gd-DOTA (0.1 mmol/kg). Experiments were repeated three times for each dose. To assess vascular contrast enhancement signal to noise and contrast to noise ratios were calculated in the aorta.
Results: With P792 at doses of 30 and 45 µmol/kg vascular enhancement was significantly higher in the 1 min post bolus phase compared to the bolus phase ($p < 0.05$). With P792 administered at a dose of 15 µmol/kg as well as Gd-DOTA at a dose of 0.1 mmol/kg peak enhancement was present in the bolus phase. In comparison with Gd-DOTA P792 showed higher and longer peak vascular enhancement for all three doses ($p < 0.05$).
Conclusion: Due to the excellent enhancement of vasculature without background enhancement P792 appears to be well suited for high quality first pass and equilibrium phase MRA. Since the agent is rapidly cleared by renal excretion repetitive perfusion imaging appears feasible.

B-0513 09:20

Static and dynamic MR imaging using iron oxide contrast agent for characterization and detection of focal liver lesions correlated with histopathologic findings

W. Schwarz[1], R. Hammerstingl[1], S. Blume[1], J.O. Balzer[1], T. Balzer[2], T.J. Vogl[1]; *[1]Frankfurt a. Main/DE, [2]Berlin/DE*

Purpose: To determinate the potential of iron oxide-enhanced dynamic and static MRI for detection and differentiation of liver lesions.
Materials and methods: 83 patients with known liver tumors (HCC n = 47, metastases n = 21, CCC n = 5, lymphoma n = 1, adenoma n = 1, FNH n = 2, hemangioma n = 2, regenerative nodules n = 4) were examined with T1-weighted, T2-weighted and dynamic sequences before and after bolus-application of iron oxides (Resovist). Imaging data were correlated with histopathology. Signal intensity of tumors, liver and spleen were measured in MR images.
Results: The results of measured signal intensity for the dynamic sequences yielded three different types of contrast enhancement for malignant liver lesions. Type 1 revealed no significant changes in signal intensity, type 2 demonstrated a drop out-phenomena (HCC n = 16, metastasis n = 1) and type 3 showed only a rapid decrease of signal intensity followed by a plateau phase (HCC n = 6). Liver and spleen demonstrated fast decrease of signal intensity after application of iron oxides in all patients. Decrease of signal intensity were also identified by FNH (PSIL = 44.3 %) and adenoma (PSIL = 22.6 %).
Conclusion: MRI of the liver with use of bolus-injectable iron oxides is superior to unenhanced MRI for detection of liver lesions. Iron oxide-enhanced MRI allows more confidence in the final diagnosis and higher quality of delineation of the lesions.

B-0514 09:30

Tissue-specific or non-specific contrast agents for hepatic MRI? A comparison of Gd-DTPA- and Ferumoxides-enhanced MRI in over 900 patients with focal hepatic disease

T.K. Helmberger, N. Holzknecht, S. Banac, B. Scher, B. Knuth, R. Stangl, J. Scheidler, M.F. Reiser; *Munich/DE*

Purpose: Comparison of the diagnostic value of unenhanced, Gd-DTPA (Gd), and Ferumoxides (Fe) enhanced MRI in a large patient population on suspicion of focal hepatic disease.
Material and methods: 919 patients (Gd-group 453, Fe-group 466 patients) were studied for staging with suspicion of extrahepatic malignancy in 48.1 %, suspicion of/known HCC in 24.7 %, incidental finding in other imaging tests in 24.4 % and "other" in 2.8 % of the cases (standard of reference: histology in 28.7 %, final report/consensus reading/12 month follow-up in 71.3 %). Imaging was performed on a 1.5 T system (Magnetom Vision, Siemens, Germany) using GRE-T1-, Fast-SE-T2-, HASTE-T2- and GRE-PD-weighted imaging pre/post Gd-administration (0.1 mmol Magnevist/kg bw) and Fe-administration (15 mmol Endorem/kg bw), respectively. Pre- and post contrast images were randomly assessed by two blinded readers (number of lesions, image quality, diagnostic confidence). Efficacy parameters were calculated based on the standard of reference.
Results: The post contrast imaging revealed significantly higher efficacy parameters than the pre contrast imaging without significant difference for the quality parameters. In HCC's the sensitivity (94 %) of Fe-enhanced MRI was significantly ($p < 0.05$) superior to Gd-enhanced imaging (89 %). The contrary was true for specificity and accuracy. In all other types of lesions Gd-enhanced MRI produced not significantly but slightly better efficacy parameters than Fe-enhanced MRI.
Conclusion: Without a specific patient selection Gd- and Fe-enhanced MRI are not differing significantly regarding their diagnostic efficacy. To our surprise, the "pure imaging of vascularization" in Gd-enhanced MRI provides the same diagnostic accuracy as tissue-specific contrast enhancement in FE-enhanced MRI.

B-0515 09:40

Characterisation of focal lesions in patients with liver cirrhosis using second generation contrast-enhanced (CE) wideband harmonic sonography (WBHS) in different enhancement phases

L. Solbiati, L. Cova, T. Ierace, P. Marelli, V. Osti; *Busto Arsizio/IT*

Purpose: To characterize focal lesions in liver cirrhosis using CE-WBHS in arterial (AP), portal (PP) and late (LP) phases.
Methods and materials: 47 focal lesions (0.9 – 4.6 cm) detected by unenhanced harmonic sonography in 32 patients with liver cirrhosis were studied after iv bolus 2.4 ml Sonovue™ (Bracco, Milan, Italy). Scans were obtained intermittently (every 10 seconds): 20 to 60 (AP); 90 (PP); 180 seconds (LP) post-injection using wideband B-mode phase inversion sonography. Tumors were assessed for enhancement pattern and overall vascularity. Triphasic helical-CT scans were obtained in all and fine-needle aspiration biopsy in 6 doubtful lesions. Final diagnoses were hepatocellular carcinoma (HCC) (35, 7 with daughter nodules), regenerative (5) or dysplastic (7) nodule.
Results: 29/35 HCCs and 7/7 daughter nodules showed marked homogeneous enhancement in AP, rapidly decreasing in PP; remaining 6 HCCs showed inhomogeneous enhancement in AP due to necrotic changes. All 5 regenerative and 7 dysplastic nodules showed no enhancement in AP, increasing progressively in PP. In LP all HCCs, dysplastic nodules and 2/5 regenerative nodules appeared as unenhanced lesions; remaining 3 regenerative lesions were undetectable (same brightness surrounding parenchyma). Six tiny (5 – 9 mm) unenhanced lesions undetected in previous phases were seen in LP and confirmed as HCCs by helical-CT. Helical-CT confirmed all 35 HCCs shown by CE-US, demonstrating 5 more HCCs (6 – 11 mm).
Conclusion: AP is crucial to differentiate HCCs from non-neoplastic lesions in liver cirrhosis and to detect daughter nodules. LP may allow detection but not characterization of additional lesions.

B-0516 09:50

Benign hepatic tumors: MRI features before and after superparamagnetic iron oxide (SPIO) administration

T.V. Bartolotta[1], M. Midiri[2], M. Finazzo[1], M. De Maria[1]; *[1]Palermo/IT, [2]Bari/IT*

Purpose: To assess the yield of superparamagnetic iron oxide (SPIO)-enhanced MRI in the detection and characterization of benign hepatic tumors.
Materials and methods: Eighteen patients underwent MRI before and after administration of SPIO. SE T1, DP, T2 and GE T2* images were acquired with a 0.5 T superconductive unit. MR diagnosis was bioptically proved in 12 patients and, in the remaining six – who had hemangiomas only – it was confirmed at least by means of two other imaging techniques, and both clinical and imaging follow-up.
Results: Thirhy-four tumors – 6 FNH, 6 adenomas, 22 hemangiomas – were detected on MRI: 29/34 (85.3 %) before and 33/34 (97 %) after SPIO administration. One adenoma was detected on baseline MRI only. Four lesions (3 adenomas, 1 FNH) were detected after SPIO administration only.
Conclusion: In our experience, although numerically limited, SPIO-enhanced MRI was clinically safe and more effective than unenhanced MRI both in the detection and characterization of benign hepatic tumors, providing useful clues to the diagnosis. It demonstrates well the central scar or septa. Nevertheless it is useful to compare baseline with SPIO-enhanced MRI. Indeed well differentiated lesions will uptake SPIO as well as normal hepatic parenchyma, becoming isointense and therefore undetectable.

10:30–12:00 **Room B**

Musculoskeletal

SS 1010

Interventional procedures/Miscellaneous

Chairpersons:
S. Grampp (Vienna/AT)
W.R. Obermann (Leiden/NL)

B-0517 10:30

Computer assisted interventional procedures using a novel vacuum immobilization device

R.J. Bale, M. Vogele, C. Hoser, C. Fink, R. Rosenberger, R. Franz, M. Rieger, W. Jaschke; *Innsbruck/AT*

Purpose: Frameless stereotactic interventional procedures require rigid immobilization of the patient.
Methods and materials: Our patented BodyFix immobilization device (Medical Intelligence, Schwabmünchen, Germany) consists of a vacuum pump connected to different types of cushions and a plastic sheath that covers the body part to be immobilized. For the CT scan the patient is wrapped up with one of these cushions, placed on the top of the therapy couch, and covered with the plastic sheath. When the vacuum pump is turned on, the air is evacuated from the cushion under the covering sheath. The cushion hardens and is sucked against the therapy couch resulting in immobilization of the patient. After the scan the targeting device is adjusted using the frameless stereotactic navigation system. After opening the plastic sheath at the skin entrance point and sterile draping the needle is advanced through the preadjusted aiming device to the preselected target.
Results: Immobilization was well tolerated by all patients. The novel technique was used for drilling of osteochondral lesions of the talus in 3 patients and bone tumors biopsies in 2 patients. In one patient a biopsy was taken from the disc space between L5 and S1. The accuracy of needle placement was within 2 – 3 mm in all patients.
Conclusion: Application of frameless stereotactic navigation systems in combination with the novel immobilization technique allows for accurate puncturing of different targets in the pelvis, the extremities and the spine for a variety of different purposes.

B-0518 10:40

Correlation between high-resolution ultrasound and microscopic anatomy in the evaluation of the biceps tendon disorders

E.A. Gallardo sr., I.M. Barber jr., A. Serrano sr., V.F. Garriga sr., X.C. Pruna sr., X.C. Serres sr.; *Granollers/ES*

Purpose: To evaluate the correlation between sonographic subtle abnormalities of the long head of biceps brachii tendon (LHBT) with the microscopic findings.
Material and methods: We performed transverse and longitudinal sonograms of LHBTs after their dissection in 30 consecutive necropsies, using a multifrequency linear probe of 9 – 13 MHz (Logiq 700 GE). We evaluated the synovial sheath thickness, the preservation of normal fibrillar pattern and the presence of ruptures. We correlated these findings with the histologic changes.
Results: The presence of synovial thickening in ultrasound (US) was correlated with inflammatory changes in the microscopic study. Both High Resolution US (HRUS) and histology demonstrated a superior involvement of the proximal tendinous area in most of the cases. The depiction of hypoechoic areas replacing the normal fibrillar pattern were related to myxoid degeneration and fibrous proliferation of the endotendineum in the microscopic study.
Conclusions: HRUS is very sensible in the depiction of subtle alterations of tendons. These findings may be used in current sonograms to improve the accuracy of the technique.

B-0519 10:50

Laser induced thermotherapy: Clinical experiences in treatment of bone tumors

C. Stroszczynski, N. Hosten, P. Tunn, G. Gaffke, R. Puls, P. Schlag, R. Felix; *Berlin/DE*

Aim: Laser induced thermotherapy (LITT) is a minimal invasive method for ablation of tumors. This paper reports on clinical results of the treatment of various bone tumors.
Patient and methods: 11 patients (13 – 83 years) were treated by LITT (5 osteoidosteoma, 6 bone metastases). LITT was performed under general anesthesia or local anesthesia. 1 – 2 internally cooled applicators were positioned into the tumor under CT/MR guidance. Control MR imaging was performed in all cases. Gadobutrol (0.3 ml/kg b.w.; Gadovist, Schering AG, Berlin, Germany) was used for visualization of thermal ablated tissue.
Results: All patients tolerated well the procedure without complications (follow up 6 – 45 weeks). Clinical symptoms disappeared in all patients with osteoidosteoma, successful ablation was performed in 4/6 patients with bone metastases. MR signs of successful ablation included hypointense bone marrow on both T1- (plain and enhanced) and T2-weighted images.
Conclusion: LITT is a promising method for minimal invasive ablation of bone tumors. Contrast enhanced MR enables postinterventional documentation of successful ablation.

B-0520 11:00

Interventional procedures in the evaluation of bone infections: Comparison of histological and microbiological results

L. Thanos, G. Papaioannou, A. Nikita, H. Koutrouvelis, A. Sissopoulos, D.A. Kelekis; *Athens/GR*

Purpose: To determine the optimal algorithm for the diagnostic approach of bone infections.
Materials & methods: The records of 62 patients with clinical and imaging findings of bone infections were reviewed. 53 patients presented clinical symptoms of infection and 62 local pain at the site of the affected bone. On CT examination, the patients presented osteolytic (47/62) and osteoporotic (15/62) lesions located in the lumbar spine (33/62), the thoracic spine (17/62), the hip joint (7/62), the iliac bones (4/62) and the cervical spine (1/62). CT-guided biopsy and fine needle aspiration (FNA) were performed in all patients. Using the bone biopsy set and/or automated biopsy needles 18 G multiple tissue samples suitable for histological evaluation were extracted. Following that, FNA was performed using spinal needles 18 G in order to yield material for microbiological culture.
Results: Histological study documented infection in 48/62 patients. Among them, FNA was positive only in 27 patients. In 14/62 patients both biopsy and FNA were negative. This result was false negative in 6/14 patients, as eventually proven by the open biopsy (2/6) and the clinical and imaging response of the lesion to antibiotics (4/6). There were no cases of negative biopsy and positive FNA. The sensitivity of FNA in detecting bone infections was 56.2 % while the combination of FNA and biopsy increased the sensitivity to 88.8 %.
Conclusion: Bone infections can be accessed safely and effectively with percutaneous CT-guided approach. It seems that the combination of FNA and biopsy increases the diagnostic yield of the procedure.

B-0521 11:10

Percutaneous treatment of osteoid osteoma

J. Serra, M. Rovira, E. de Lama, F. Portabella, M. Orduña, J. López-Moreno; *Barcelona/ES*

Purpose: Osteoid osteoma is a benign bone primary tumor responsible of a strong local pain. Standard therapy is surgical removal of the entire nidus. Our purpose is to review the results of percutaneous treatment by laser (2 patients) or radiofrequency (3 patients) in 5 patients with osteoid osteoma (2 tibial diaphysis, 1 femur diaphysis, 1 scaphoid and 1 illium).
Material and methods: The technique consists in introducing a needle (gauche 14 – 16) in the nidus guided by C.T. Once the trocar is correctly sited a filament is placed through the needle. Then we applied (laser or radiofrequency) necessary to ablate the tumor.
Results: In 4 cases the result was a completed relieve of the pain in all of them, 3 in the first hours and 1 within 2 days after treatment. In the remaining case (scaphoid) the percutaneous treatment (laser) was not successful, being necessary surgical therapy.
Conclusions: The percutaneous treatment of osteoid osteoma seems to be highly beneficious and should be considered as a treatment option.

B-0522 11:15

Percutaneous vertebroplasty (PVP) guided by CT-fluoroscopy

M. Rovira, J. Serra, A. Muntane, Y. Roca, A. Mejía, J. López-Moreno; *Barcelona/ES*

Introduction and purpose: PVP consists in a percutaneous injection inside a collapsed vertebral body of a biomaterial (polimethylmethacrylate) with the aim of reducing the pain and stabilising of the spine. The most common indications of

PVP are osteoporotic vertebral collapse, metastasis and aggressive hemangioma. We report our initial experience with PVP guided by CT-fluoroscopy in eight patients.

Material and methods: We have treated 8 patients with PVP, 5 with osteoporotic collapse, 2 with metastasis and 1 with aggressive hemangioma. The technique consists in the introduction of polimethylmethacrylate through one or two 14 – 16 gauge needles guided by CT-fluoroscopy inside the collapsed vertebral body. A transpedicular or posterolateral approach was used depending on the level of the affected vertebral body.

Results: In all our cases we obtained total or partial pain relief and consolidation of the vertebral body. We did not have any clinical complications although in two cases the cement has passed into the epidural venous plexus.

Conclusions: PVP is an effective method to treat the pain and the instability originated by a collapsed vertebral body (osteoporotic, metastasic or secondary to an aggressive hemangioma). It is essential to have proper selection of the patients for PVP. Long-term follow-up results are still not well known.

B-0523 11:20

In-vivo laser-induced interstitial thermotherapy of pig tibias with a diode laser: Histological and MRI correlation of thermal damage

G.R. Wamser[1], W.A. Wohlgemuth[1], A. Prescher[2], K. Bohndorf[1]; *[1]Augsburg/DE, [2]Aachen/DE*

Purpose: To evaluate the feasibility and efficacy of laser-induced thermotherapy of pig tibia with a temperature controlled diode laser.

Materials and methods: In 4 anaesthetized pigs the tibia was anatomically prepared for instrumental access. After drilling the cortex the flexible quartz fibre was advanced into the marrow. 6 applications were performed with a standardized protocol with a temperature controlled diode laser system at 3 different temperatures for 3 or 6 minutes. The removed bones were investigated in a 0.35 T open MRI scanner using T1w and T2w sequences. After demineralizing the bone samples were cut, stained and histologically evaluated. Lesions on MR-images were correlated with the macroscopic findings.

Results: There was no influence of lasing temperature or duration on the size of necrotic area. The lesions were larger within the hematopoetic marrow than within the fatty marrow with a mean of 0.4 cm in diameter. In T1w the lesions were not clearly visualized. On T2w images the lesions consist mainly of a hyperintense zone of coagulation, which corresponds well with the measured defect.

Conclusion: The temperature controlled diode laser provides reproducible necrosis within bone. Based on restricted laser absorption in bone the size of the necrotic defect is limited.

B-0524 11:30

Early sonographic detection of delayed union in endomedullary stabilised tibial fractures

E.A.M. Geusens, S. Nijs, H. Janzing; *Leuven/BE*

Purpose: After endomedullar stabilisation of tibial fractures, delayed healing is a common problem. The aim of this study was to see if ultrasound can predict delayed healing in an early stage, prior to conventionel x-rays.

Materials and methods: Twenty fractures in 19 patients were stabilised with endomedullary nails. Patients were followed at 3 weeks interval up to the 12th post-operative week with ultrasound, x-ray and clinical follow-up. Ultrasound was performed by a radiologist, blinded for clinical and radiographic data. At ultrasound, the visibility of the nail and the echogenicity of callus were evaluated in three planes. Visibility of the nail and hypoechoic callus were used as an indication of delayed healing.

Results: Of the 20 fractures, 14 healed and 6 did need a second procedure. At 9 and 12 weeks post-operative, there was a full match between ultrasound, x-ray and clinical data. At 6 weeks, there were 2 false positive ultrasound examinations predicting a delayed union, and at 3 weeks, there was no correlation with the later outcome. There were no false negative results.

Conclusion: At 9 and 12 weeks post-operative, there was a full match between the sonographic, clinical and radiological data, so ultrasound can be used for early detection of delayed union.

B-0525 11:40

MR imaging of the alar ligaments: Morphologic findings in 80 healthy subjects

K. Woertler[1], E. Urner-Schal[2], W.H.M. Castro[2], W. Heindel[2]; *[1]Munich/DE, [2]Münster/DE*

Purpose: To describe the MR morphology of the alar ligaments (AL) in healthy subjects.

Methods and materials: MR imaging of the craniocervical junction was performed in 80 volunteers (m: 46; f: 34; age range: 18 – 60 years). Exclusion criteria were a history of cervical spine trauma (incl. whiplash injury), surgery, rheumathoid arthritis, and relevant neck pain. The imaging protocol (1.5 T) included coronal T1wSE and T2wFSE, as well as axial/oblique T2wFSE sequences (section thickness: 2 mm). Image analysis was carried out with reference to course, shape, maximum length, thickness, and signal intensities of the AL, as well as position of the odontoid process relative to the intercondylar line (ICL).

Results: The AL could be depicted as symmetrical structures in all volunteers, most often showing a caudocranial (39 %) or horizontal (41 %) orientation in the coronal plane, an anteroposterior orientation (84 %) in the axial plane, and a fan-shaped configuration (97.5 %). A transverse occipital ligament was present in 9 % of cases. Mean values for maximum length and thickness of the AL were 0.97 ± 0.15 cm and 0.70 ± 0.14 cm, respectively. Typical signal intensities were intermediate on T1- and hypointense on T2-w images, with a "striated" appearance in 94 % and 100 %, respectively. The tip of the odontoid process was localized below, at, or above the level of the ICL in 28 %, 31 %, 41 % of cases.

Conclusion: MR imaging constantly provides depiction of the AL. Knowledge of normal findings and variants appears to be crucial for correct interpretation of MR studies following cervical spine trauma.

B-0526 11:50

The value of imaging in the diagnosis of nonsacral-vertebral chordoma

X. Wang[1], D. Smolders[1], K. Verstraete[2], F.M.H.M. Vanhoenacker[1], A.M.A. De Schepper[1]; *[1]Antwerp/BE, [2]Gent/BE*

Purpose: To define the imaging features of nonsacral-vertebral chordoma and to evaluate their specificity in the differential diagnosis with other spinal lesions.

Materials & methods: Four cases of pathologically proven chordoma were reviewed. Their location included the cervical spine (n = 2), thoracic spine (n = 1), and lumbar spine (n = 1). Patient age ranged between 35 and 58. The following imaging features were evaluated: lesion morphology, bone and soft-tissue involvement, signal intensity and enhancement pattern on magnetic resonance (MR) imaging, encasement of vascular structures, intralesional calcification, and multilevel involvement.

Results: The most common imaging features were: combined vertebral body and soft-tissue involvement (n = 4), multilevel involvement (n = 4), lobulated contour (n = 3), heterogeneity on all MR imaging sequences (n = 4), moderate to strong enhancement (n = 4) with ring-and-arc-like enhancement pattern (n = 2), hyperintensity on T2-weighted images (n = 3) with intralesional hypointense septa (n = 2), epidural tail sign (n = 3), neuroforamen enlargement (n = 2), and vascular encasement (n = 2). There was no posterior element and disk involvement or intralesional calcification in our cases.

Conclusion: MRI features of nonsacral-vertebral chordoma are helpful in diagnosis and differential diagnosis with other spinal lesions.

10:30–12:00 **Room C**

Abdominal and Gastrointestinal

SS 1001a

Liver maging

Chairpersons:
E.K. Makó (Budapest/HU)
F. Terrier (Geneva/CH)

B-0527 10:30

New method to exclude influence of cardiac output and other factors on enhancement-measurement of normal liver parenchyma or liver lesions

A.J. Ruppert-Kohlmayr, C. Kugler, T. Riepl, O. Doerfler, D. Zebedin, M.M. Uggowitzer; *Graz/AT*

Purpose: To find a way of enhancement-measurement of liver-parenchyma and liver lesions in multiphasic helical-CT that is not influenced by external factors like cardiac-output.

Method/materials: Multiphasic helical-CT was analysed in 26 patients with 37 histologically proven focal nodular hyperplasia (FNH) and 18 hepatocellular adenomas (HCA). CT-protocol: unenhanced (u), arterial (a) and portal-venous (pv) phase with flow of 4 ml/s, slice-thickness 8 mm, pitch 1.5 and reconstruction increment 4 mm. Measurements included: Density of liver parenchyma and lesions in all three phases. Additionally density in arterial and portal-venous phase was measured in aorta at the height of celiac trunk (TCa and TCpv). From all density values in aorta of both phases measured in our cohort mean-value (mTC) was

calculated. Measured density of liver-parenchyma and lesions was standardised by multiplying them with following standardisation-factor: mTC/TCa for arterial and mTC/TCpv for portal-venous phase.
Results: For arterial phase we got mTC-value of 250 HU and for portal venous phase of 130 HU. For all patients measured TCa- and TCpv-values were corrected to this mTC-value by the above described formula. The standardised density-values of liver-parenchyma were: (1) Arterial – mean-value (mv): 80.29 HU (range: 48.21 – 123.1), (2) portal-venous phase – mv: 105.43 HU (range: 73.41 – 146.8); of FNH: (1) mv: 117.91 HU (range: 86.3 – 147.6), (2) mv: 112.08 HU (61.4 – 123.75); of HCA: (1) mv: 80.09 HU (range: 61.78 – 94.9), (2) mv: 110.23 HU (73.28 – 126.8).
Conclusions: Our method is an appropriate method to exclude influence of external factors on density and enhancement-measurement of liver parenchyma and lesions, and it seems to be appliable also in other parenchymal organs and in helical-CT and multidetector-CT technology.

B-0528 10:40

Early enhancing hepatic pseudolesions on spiral CT
L. Romanini, E. Dettori, K. Menni, L. Palvarini, L. Rendina, L. Grazioli; *Brescia/IT*

Purpose: To evaluate frequency, morphologic features and vascular pattern of pseudolesions.
Methods and materials: 388 patients underwent consecutively multiphasic spiral CT: 248 patients affected by chronic hepatitis or cirrhosis (I group), 59 patients with suspected benign focal liver lesion (II group), 81 patients to search hypervascular metastases (III group). We considered pseudolesion a parenchymal area, peripheral, wedge-shaped, hyperdense on arterial phase, not evident on portal venous phase, with "dot light sign" (presence into the lesion of an hyperdense vessel on arterial phase). The area was not recognisable by US, without modifications at CT follow-up (12 – 18 months).
Results: 47 pseudolesions were identified in 27/388 (7 %), 42/45 in the I group. 80 % of pseudolesions was wedge-shaped and 20 % round or oval shaped; size ranged between 1 – 7 cm. The "dot light sign" was present in 71 %. Digital angiography performed in 14 patients with HCC, showed in the 33 % arterial-portal (AP) shunts in the areas corresponding to pseudolesions on CT images. This sign represents early portal venous drainage due to shunt. In II group 2 pseudolesions were detected, both with "dot light sign", next to small capillary hemangiomas. In III group 3 pseudolesions in 3 patients were identified, 2/3 with "dot light sign".
Conclusion: The most frequent detection of pseudolesions in hepatopatic patients seems to be well correlated with AP shunts. Morphologic features and their contrast behaviour allows differentiation from other hypervascular hepatic lesions.

B-0529 10:50

Multiphasic spiral CT and octreoscan in the staging of liver metastases from neuroendocrine tumors
D. Poretti, F. Orsi, R.F. Grasso, G. Bonomo, G. Gerli, M. Bellomi; *Milan/IT*

Purpose: To report our experience in CT and Nuclear imaging of liver metastases from carcinoid tumors.
Materials and methods: 26 patients affected by liver metastases from carcinoid tumors underwent three phase helical CT examination of the upper abdomen and Octreotide scintigraphic scans (18 patients) for the staging of their disease. CT examinations were reviewed to count liver metastases and classify them by their enhancement behaviour through the different CT phases. Likewise a Nuclear Medicine Specialist evaluated the distribution of the octreotide nucleotide thruoghout the liver on scintigraphic scans.
Results: We identified 432 metastases of which 59.6 % could be recognized on non-contrast scans, 67.6 % during arterial phase (16.4 % hyper, 51.2 % hypo), 94.2 % on parenchymal phase (5.8 % hyper and 88.4 % hypo) and 60 % on delayed phase. Arterial phase detected double the number of lesions than in parenchyma phase in 15.4 % of patients.
Conclusion: In our experience, only 16.4 % of lesions was hypervascular on the arterial phase. However multiphasic helical CT changed therapeutic work-up in 15.4 % of patients. Also the Octreoscan played a crucial role in diagnostic and therapeutic planning.

B-0530 11:00

Helical-CT in liver cirrhosis: Evaluation of attenuation patterns associated with the diagnosis of hepato-cellular carcinoma and the role of equilibrium imaging
L. Camera, M. Imbriaco, G. Selva, A. Di Giacomo, S. Daniele, L. Pace, M. Salvatore; *Naples/IT*

Purpose: To evaluate the contribution of equilibrium imaging in the diagnosis of hepato-cellular carcinoma (HCC) in patients with liver cirrhosis by means of helical-CT.
Materials and methods: Helical CT-findings in 40 patients (35 M, 5 F; aged 62 ± 9 years) with liver cirrhosis were retrospectively evaluated. All patients underwent tri-phasic helical CT with three separate set of scans (10 mm beam collimation, 7 mm recon. intervals, pitch 1.0, 120 kV, 200 – 250 mAs) performed at 25, 60 and 300 s after i.v. bolus injection of 120 cc of an iodinated contrast agent (I 300 mg/ml) at 4 ml/s. Previous data by ROC analysis (Radiology 213: 469, 1999) indicated arterial-phase and equilibrium imaging to be the more accurate for detection of HCC. Combining these phases, three different attenuation patterns (Hyper-Hypo, Hyper-Iso and Iso-Hypo) were identified and correlated with final diagnosis obtained by either aspiration biopsy (18 pts) or follow-up data (22 pts).
Results: A total of 54 nodules (0.6 – 4.5 cm) were identified in 31 patients. At final diagnosis, forty-six out 54 proved to be HCC. This was most likely associated with the hyper-hypo pattern (33/46, 71 %) followed by the hyper-iso (7/46, 15 %) and iso-hypo (6/46, 13 %) patterns. Six out of 13 nodules (46 %) who exhibit the hyper-iso pattern and 2 out 8 (25 %) nodules with the iso-hypo pattern were found not to be HCC. Overall, positive predictive values were 100 %, 75 % and 53 % for the hyper-hypo, iso-hypo and hyper-iso pattern, respectively.
Conclusion: In patients with liver cirrhosis evaluation of equilibrium phase increases the diagnostic accuracy of helical-CT.

B-0531 11:10

Diagnostic accuracy of standard CT, ^{111}In Octreotide and ^{123}I mIBG SPECT imaging in finding disseminated neuroendocrine tumours
J.B. Cwikla, J.R. Buscombe, W.A. Mielcarek, M.E. Caplin, A.J. Watkinson, A.J.W. Hilson; *London/GB*

Standard imaging modalities can underestimate presence/extent of disseminated neuroendocrine tumours (NET). Aim of this study was to assess diagnostic accuracy of triple-phase spiral CT and new approach using radioisotopes in patients with known NETs.
There were 27 patients, 18 with carcinoid, 4 carcinoid like NET's, 3 gastrinoma, single islet tumour and malignant paraganglioma. Twelve pts had primary tumours. Final diagnosis was confirmed by pathology.
SPECT imaging was performed using ^{111}I mIBG and ^{111}In octreotide. Each scan was reported on presence and extent of disease.
CT did not find NET in 3 patients, evaluates as normal or benign lesions. In 3 cases the result was equivocal. Others had evidence of tumour/s in CT. Only 2 patients had single lesions confirmed using others modalities and finally surgery. CT showed single lesion in 3 pts with disseminated tumours. Octreotide failed to demonstrate disease in single case. In 2 patients Octreotide underestimated extent of disease. mIBG studies which were performed in 21 patients. In 5 patients results were false negative. Additional single case was equivocal. In 6 patients mIBG underestimated extend of disease.
Our results confirm the recommendation of European NET group, that functional imaging should be performed in patients with suspected NET.

B-0532 11:20

Comparison of conventional sonography, contrast-enhanced pulse inversion sonography and dual phase spiral CT in the detection of hepatic metastases: Results of a multicentre study
T. Albrecht[1], M.J.K. Blomley[2], P.N. Burns[3], S. Wilson[3], E. Leen[4], M. Claudon[5], F. Calliada[6], J.-M. Correas[7], M. LaFortune[8]; *[1]Berlin/DE, [2]London/GB, [3]Toronto, ON/CA, [4]Glasgow/GB, [5]Nancy/FR, [6]Lodi/IT, [7]Paris/FR, [8]Montreal, PQ/CA*

Purpose: To determine whether assessment of hepatic metastases by ultrasonography is improved by the addition of pulse inversion imaging during the liver-specific phase of Levovist (Schering AG, Berlin, Germany).
Materials and methods: 128 patients were studied with conventional ultrasonography, pulse inversion harmonic contrast ultrasonography in the liver-specific late phase of Levovist using HDI5000 equipment (ATL, Bothell, USA) and dual-phase spiral-CT. The conspicuity and number of metastases on the conventional sonogram and the contrast-enhanced pulse inversion sonogram were compared using CT

as the reference. In a sub-group of 23 patients MR imaging, intraoperative ultrasonography or resection pathology were available as independent reference for comparison of pulse inversion ultrasonography and spiral-CT.
Results: Conspicuity of metastases was improved by contrast-enhanced pulse inversion in 87 % by a mean of 10.8 dB ($p < 0.0001$). In 47 patients more metastases were seen than on conventional ultrasonography, in 3 of which the conventional scan was normal. Using CT as the reference, contrast-enhanced pulse inversion improved the sensitivity for the detection of individual metastases from 71 % to 88 % ($p < 0.0001$). On a patient basis sensitivity improved from 94 % to 98 % (NS) and specificity from 59 % to 88 % ($p < 0.01$). In the 23 patients with independent references, 7 patients showed more confirmed metastases on contrast-enhanced ultrasonography than on CT.
Conclusion: Contrast-enhanced pulse inversion ultrasonography markedly improved the sensitivity and specificity in detecting hepatic metastases. It revealed metastases that were not detected by spiral-CT in selected cases. It could complement or replace CT for assessment of hepatic metastases.

B-0533 11:30

Study of focal liver lesions with SonoVue™ and contrast coherent imaging: Comparison with MRI
L. Aiani, C. Borghi, F. Clarizia, A. Martegani; *Como/IT*

Purpose: To compare the diagnostic potential of SonoVue and Coherent Contrast Imaging (CCI) in the evaluation of patients with primary and secondary liver lesions in comparison with Magnetic Resonance Imaging (MRI).
Methods and materials: Seventy five patients with malignant focal liver lesions underwent ultrasound examination without (baseline) and with contrast agent (SonoVue, Bracco, Milan, Italy). Post-contrast dynamic scans were obtained using an Acuson Sequoia System with CCI at medium (0.6 – 0.4) and low (0.1 – 0.2) MI during the arterial, portal and late phase. All patients were also studied with MRI with T1 and T2 sequences and bolus administration of a paramagnetic contrast agent within 1 week from the US examination. Statistical evaluation of the results was performed using the Wilcoxon test.
Results and conclusions: The contrast enhanced ultrasound examination showed a higher sensitivity in comparison with unhenhanced imaging and a diagnostic potential comparable to that of MRI in the diagnosis of primary and secondary liver lesions.

B-0534 11:40

Diagnosis of atypical hemangioma using contrast-enhanced wideband harmonic sonography (CE-WBHS)
L. Solbiati, L. Cova, T. Ierace, P. Marelli, S. Osti; *Busto Arsizio/IT*

Purpose: To assess the potential use of CE-WBHS for the diagnosis of hemangiomas with atypical presentation, due to non-hyperechoic sonographic pattern or diffuse changes of the surrounding liver.
Methods and materials: Seven atypical hemangiomas (1.5 – 6.5 cm) in 7 patients were studied: 4/7 lesions had hypo-anechoic echopattern, the remaining 3 were almost undistinguishable from the surrounding "bright" cirrhotic liver parenchyma. The lesions were studied with B-mode wideband, phase inversion harmonic imaging before and after bolus injection of 2.4 ml of Sonovue™ (Bracco, Milan, Italy). Arterial (20 – 60 s), portal (90 – 120 s) and very late phases (4 – 7 min) post-injection were examined for each case. Sonographic images were compared with helical CT scans achieved at arterial and portal phases.
Results: In the arterial phase, all the lesions showed only peripheral enhancement, either globular (4 cases) or thin, rim-like (3), remaining mostly unenhanced compared to the surrounding liver. In the portal and, mostly, late phases, progressive centripetal filling-in lasting up to 5 – 7 minutes was observed in all the lesions which became isoechoic and subsequently hyperechoic, allowing a confident sonographic diagnosis. Contrast-enhanced helical CT showed the same enhancement pattern in all the 7 lesions.
Conclusion: CE-WBHS can be very helpful for the diagnosis of atypical hemangioma, obviating the need for helical CT. All the three vascular phases are needed to achieve the final diagnosis. This method may prove also helpful to differentiate hemangiomas from hepatocellular carcinomas when doubtful nodules are detected in liver cirrhosis.

B-0535 11:50

Detection of focal liver lesions with the new US contrast agent NC100100: Results of an exploratory multicentre study
T. Albrecht[1], L. Needleman[2], M.J.K. Blomley[3], E. Leen[4], C. Harvey[3], B.B. Goldberg[2], D.O. Cosgrove[3], C.W. Hoffmann[1]; *[1]Berlin/DE, [2]Philadelphia, PA/US, [3]London/GB, [4]Glasgow/GB*

Purpose: To evaluate detection of focal liver lesions using pulse/phase inversion ultrasound (PIUS) during the vascular and liver-specific phases of NC100100 (Sonazoid, Nycomed-Amersham, Oslo, Norway).
Materials and methods: 52 patients from 4 centres (3 European, 1 US) with known focal liver lesions by a reference examination (contrast-enhanced MR or SCT) were studied. There were 23 with metastases, 12 with HCC, 9 with haemangioma, and 8 with other lesions. After a conventional baseline scan NC100100 was injected intravenously. It initially enhances the blood pool and then accumulates in normal liver due to Kupffer cell up-take and shows a strong harmonic response below the threshold to bubble destruction. PIUS was performed immediately (arterial phase) as well as 5, 10 and 15 min after injection.
Results: Contrast-enhancement was adequate in 84 %, partially adequate in 14 % and inadequate in 2 %. Continuous scanning at low mechanical indices (0.3 – 0.6) provided liver enhancement lasting 15 min without substantial bubble destruction. Metastases and HCCs showed a varying degree of arterial enhancement and appeared as sharply marginated enhancement defects on delayed PIUS. Lesion conspicuity improved in 76 % (delayed phase). The number of reference confirmed metastases increased from 68 (baseline) to 83 (PIUS), reference imaging showed 93 metastases, sensitivity improved from 73 % to 89 %.
Conclusions: NC100100-enhanced PIUS of the liver can be performed at continuous imaging over at least 15 min. It thus overcomes the limitations (i.e. short time window) of current microbubble contrast agents. It improves the detection of liver lesions compared to unenhanced sonography.

10:30–12:00 **Room E2**

Breast

SS 1002

Breast ultrasound

Chairpersons:
M. Müller-Schimpfle (Tübingen/DE)
P. Piperopoulos (Athens/GR)

B-0536 10:30

Documentation of 2D- vs. 3D-sonography of solid breast lesions: Observer variability of lesion description and evaluation
C.F. Weismann, P. Kainberger, A. Auer, L. Datz, A. Hollerweger, P. Macheiner; *Salzburg/AT*

Purpose: Is a 3D-sonography volume documentation superior compared with a typical 2D-sonography documentation of solid breast lesions? Influences a 3D sonography documentation the assessment of lesions dignity?
Materials and methods: The electronically stored 2D images and 3D volume datasets of 40 unselected and histologically proven solid breast lesions were retrospectively evaluated by 5 radiologists. The 3D volume datasets were acquired with a linear array small part volume probe (5 – 13 MHz, Voluson 530D, Kretztechnik, Austria). The 2D images were taken from the 3D datasets and were stored electronically. They provided the same quality such as the multiplanar 3D images and were investigated on the same screen under comparable conditions.
Results: The interobserver variability of sonographic criteria (lesion shape, margins, echogenicity, echotexture, transmission and pseudocapsule) were evaluated and compared with 2D and 3D image information. Each category was analyzed and measured using Cohen's κ statistic. An assessment of the breast lesions dignity (benign, indeterminate, malignant) with 2D documented image information and 3D volume information was performed and compared.
Conclusion: 3D volume documentation providing the additional coronal plane and the interactive analysis of complex lesion morphology is superior to typical 2D documentation and provides additional features for lesion assessment.

B-0537 10:40

3D power Doppler ultrasound of breast lesions with a microbubble ultrasound contrast agent

C.R. Krestan, T.H. Helbich, C. Riedl, M. Memarsadeghi, M. Rudas, G. Wolf; *Vienna/AT*

Purpose: To assess the enhancement of benign and malignant breast lesions after i.v. administration of an ultrasound contrast agent using 3D-power-Doppler ultrasound (3D-PDUS)

Methods and materials: 39 patients (mean age 48 ± 17 years) with 39 breast lesions (20 malignant, 19 benign) underwent 3D-PDUS (Voluson 530D, Kretz, Austria) before and 0.5, 1, 2, 3, 4 and 5 min after i.v. administration of (Levovist®). The colorpixel intensity described by the flowindex (FI) was calculated of each 3D-dataset.

Results: The precontrast FI in malignant lesions was 17.0 ± 13.3 and 23.3 ± 8.1 in benign lesions, respectively. The FI increased significantly ($p < 0.001$) after contrast administration in malignant lesions ($FI_{max} = 28.3$) compared to benign lesions ($FI_{max} = 27.2$) $p = 0.051$. Time from baseline to maximum FI was 2.1 min in malignant and 2.6 min in benign lesions.

Conclusion: After US contrast agent administration 3D-PDUS enables an improved assessment of the tumorvasculature. Malignant breast lesions enhance significantly stronger after microbubble contrast application than benign lesions, however there is a considerable overlap.

B-0538 10:50

Wash in - wash out characteristics of the echo-enhancing agent Levovist in the assessment of breast tumors

V.F. Duda, K. Bock, A. John, K.-D. Schulz; *Marburg/DE*

Purpose: The value of the echo-enhancing agent Levovist was tested to delineate specific wash in – wash out curve profiles for different types of breast tumors.

Materials and methods: 10 ml of Levovist (Schering) were applied by an intravenous injection of 300 mg/ml in 34 women with consecutive histologically proven breast masses (15 malignant and 19 benign lesions). The wash in – wash out curve characteristics of the first minute after the injeciton were registerd using an AU 5 Harmonic ultrasound scanner (10 – 13 MHz, linear transducer; Esaote Biomedica).

Results: The malignant breast tumors showed a more rapid echo-enhancement of their vessels, this was not so obvious in the benign lesions. To achieve clear and reproducible curve profiles an exact placement of the regions of interest was necessary. A wash in – wash out registration of more than one minute proved to be unreliable due to the fact that it was very difficult to fix the same region of interest in the necessary way. Being successful in the differentiation of several characteristic curve profiles, the overlap between these curves in benign and malignant breast masses, however, was to wide for a specific differentiation.

Conclusion: The possibility to achieve different profiles of wash in – wash out reactions was not usefull for the differentiation between benign and malignant breast masses. Nevertheless, ist might be promising in predicting the growth-dynamics of breast tumors.

B-0539 11:00

3D ultrasound imaging of breast tumour neovascularization: Work in progress

W.E. Svensson, K. Humphries, A. McBride, D. Barratt, P. Forouhi, P. Stanley, A. Welsh; *London/GB*

Purpose: To determine the potential of 3-dimensional ultrasound imaging techniques in the investigation of tumour vascularization.

Materials and methods: A series of colour Doppler volume data sets images have been obtained freehand from over 200 patients, using the 15 MHz transducer of the Acuson Sequoia system. 41 lesions have been processed, so far, using the VoxBlast 3D measurement and visualization software, to obtain 3-dimensional images of the transparent greyscale, haemodynamic and combined greyscale/colour views. The cases included 22 fibroadenomas, 9 cancers, 4 inflammatory masses, 2 lymph nodes, 2 cases of ANDI, 1 duct ectasia and 1 papilloma. The rendered images, using the dual volume rendering facility, show the 3D spatial relationship of the vascularization within and surrounding the tumour.

Results: Initial studies show that the vascular morphology is better demonstrated using 3D views of grey scale and vascular information than in either 2-D images or 3D vascular, only, images. The number of feeding vessels can be enumerated and internal and external vascular density estimated

Conclusions: These initial results already show that the 3-dimensional ultrasound angiographic techniques described have the potential to determine vascular morphology and quantify vessel density and distribution within, around and outside the lesion.

B-0540 11:10

The value of mammography and ultrasonography in the follow-up of breast carcinoma treated with neoadjuvant chemotherapy

I.G. Bilgen, A. Memis, E.E. Ustun; *Izmir/TR*

Purpose: To evaluate the changes in the mammographic and ultrasonographic features of breast carcinoma treated with neoadjuvant chemotherapy (NCT).

Materials/methods: Thirty-two patients, who underwent NCT because of either locally advanced breast carcinoma, inflammatory breast carcinoma or systemic disease preventing operation, were prospectively evaluated prior to and following NCT by physical examination, mammography (MG), and ultrasonography (US). Clinical and radiological findings were compared.

Results: Of the 31 cases, who had masses depicted on MG and US; the size of the mass, decreased in 16 (51.6 %), disappeared in 7 (22.5 %) and did not change in 8 (25.8 %). In the continuing follow-up mammograms, 1 of the 7 "disappeared masses", 3 of the 16 "shrinked masses", and 2 of the 8 "unchanged masses" showed increase in size. The microcalcifications did not change in 5 (50 %), became fainter and fewer in 3 (30 %) and resolved completely in 2 (20 %) cases. Of the 10 patients, who showed edema pattern on initial mammograms, the follow-up mammograms demonstrated decrease in edema in 6 (60 %), minimal increase in 1 (10 %), and no change in 2 (20 %). In one patient microcalcifications developed while edema pattern decreased.

Conclusion: In the evaluation of NCT response, MG and US provide information complementary to physical examination. The changes in mass size, microcalcifications and edema pattern is demonstrated objectively on MG and US, which is essential in the accurate assessment of the response to chemotherapy.

B-0541 11:20

Complex ultrasound investigation in monitoring the efficiency of treatment of local mastitis

T. Golovko, V.V. Medvedev; *Kiev/UA*

Purpose: To use color Doppler flow imaging to predict the response of treatment of local mastitis.

Methods and materials: The investigations of pathological formations of the breast including colored Doppler ultrasonography, routine ultrasonography, 3D-reconstruction vessels map, clinical and morphological methods were accomplished in 19 female patients 18 – 36 years old and were carried out on the US ATL HDI 3000 probe 7.5 – 12 MHz. Results were compared with the biopsy response.

Results: After treatment determined 9 respondents of good results and 10 poor results. Ultrasound criteria of good results were: decreasing of size, changes of structure including disappearance of the border of formations with appearance of more homogeneous tissues, disappearance of liquid insertions, decreased number of small disorderly vessels. Ultrasound criteria of good results were: increasing of size, forming of capsule and more non homogeneous structure, increased and more thick liquid insertions, increased number of vessels.

Conclusion: The usefulness of Complex ultrasound investigation in monitoring of efficiency treatment of local mastitis was proved. The advantage of this method is in its superior accuracy, noninvasive nature, availability and low cost.

B-0542 11:30

US-Guided needle biopsy in the diagnosis of breast lesions: Fine-needle aspiration vs. core biopsy

G. Esen, I. Mihmanli, S. Kurugoglu, N. Uygun, S. Ilvan, A. Altug; *Istanbul/TR*

Purpose: To compare the advantages and disadvantages of fine-needle aspiration biopsy (FNAB) and core needle biopsy (CNB) in the diagnosis of nonpalpable breast lesions.

Materials and methods: FNAB followed by CNB were performed in 74 lesions. A cytopathologist was present on site to evaluate the adequacy of the aspirated material in all procedures. All lesions with atypical or malignant findings in either biopsy method as well as those with suspicious radiological findings were operated (n: 52). The others were followed up for a minimum of 2 years.

Results: Twenty-one lesions were malignant and 53 were benign. Accuracy was 82.43 % in FNAB and 95.94 % in CNB. The biopsy material was inadequate for diagnosis in 7 FNABs and 1 CNB. In 2 lesions with a correct FNAB result, CNB

was false negative; while CNB revealed the correct diagnosis in 12 out of 13 lesions in which FNAB results were either insufficient or incorrect. Complication rate was 0 % for FNAB and 8.11 % for CNB.
Conclusion: FNAB is less invasive, more practical and less expensive than CNB, but yields more insufficient or false negative results. We think that FNAB should be combined with CNB in those cases that the aspirated material is inadequate or the biopsy result does not agree with the radiological findings.

B-0543 11:40

3D ultrasound in high speed core biopsy of breast lesions
M. Lell, U.G. Aichinger, R.W.S. Schulz-Wendtland, W.A. Bautz; *Erlangen/DE*

Purpose: To evaluate the potential of 3D ultrasound in free hand high speed core biopsy in solid breast lesions.
Material and methods: 33 ultrasound guided core biopsies were performed in 31 patients with solid breast lesions (BI-RADS 4 – 5) from 8/00 – 9/00. 5 specimen were taken from each lesion. A linear 3D US volume scanner (Voluson 530D MT, Kretztechnik, Austria) and a 11 G coaxial core needle system was used for the procedure. Localization of the lesion and placement of the needle was done under 2D US guidance. After core needle shot a 3D US volume acquisition was performed to correlate lesion and needle position (3D targeting). Accuracy of this 3D procedure was compared with the routine procedure performed on a 2D US system.
Results: No false negative results occurred in the 3D US group. In 5/33 lesions fibroadenoma, in 9/33 lesions fibrosis and in 19/33 lesions carcinoma was proved histologically. Mean diameter of the lesions was 23 mm (7 – 80 mm, median 18 mm). 3D US targeting revealed 16 central, 16 eccentric and 1 marginal hits. 3D US volume scanning is done within < 5 seconds (additional storage time 30 s). In a control group with 2D US core biopsy 2 % false negative results occurred.
Conclusion: 2D guidance and 3D US targeting is a fast and valuable tool in optimizing core biopsy of solid breast lesions. Higher confidence of appropriate needle placement within the lesion is gained. In large lesions, the reduced size of the 3D transducer in comparison with 7.5 MHz 2D transducers is disadvantageous.

B-0544 11:50

Focal fibrosis of the breast: Imaging features and follow up with fine needle aspiration biopsy
B.E. Dogan, S. Tükel, O. Aksu; *Ankara/TR*

Purpose: "Focal fibrosis" of the breast (focal fibrous mastopathy – FFM) is a lesion having common radiological findings with other benign breast pathologies, but is accepted as a distinct clinicopathological entity, its most definitive characteristic being stromal proliferation of the mammary glands. The aim of our study was to determine the significance of this distinct entitiy amongst the differential diagnosis of solid breast lesions as well as overview its radiological findings.
Materials and methods: Fine needle aspiration biopsy (FNAB) results obtained in one year period of 80 patients with a cytologic diagnosis of benign fibrous mastopathy of the breast were examined regarding morphologic and sonographic characteristics. Sonographic features were determined according to the Stavros criteria.
Results: Most of the patiens were under 50 years with a mean age of 44.83 ± 5.69. Statistical analysis revealed most lesions to be non palpable, hypoechoic with regular margins, not always visible by mammographic examination, appearing in those breasts with P2 and DY pattern.
Conclusion: FFM is a benign lesion with a possible involutionary etiology, differential diagnosis of which is possible by FNAB. Still, for thoe lesions with a strong clinical and radiological suspicion of malignancy it is advisable to perform excisional or core biopsy.

10:30–12:00 **Room F1**

Chest

SS 1004

Airway and lung disease

Chairpersons:
H.-U. Kauczor (Mainz/DE)
H. Özer (Izmir/TR)

B-0545 10:30

Virtual bronchoscopy using different representation models
M.D. Seemann[1], D.R.G. Schuhmann[2], J.F. Schäfer[1], W. Luboldt[1], C.D. Claussen[1]; *[1]Tübingen/DE, [2]Munich/DE*

Purpose: The purpose of this study was to demonstrate the possibilities, advantages and clinical application of a virtual bronchoscopic examination using several different representation models.
Materials and methods: We examined 13 patients with inoperable primary or metastatic lung tumors (n = 10) and transplantation of the lung (n = 3), including stent implantation (n = 2), using image data sets from thin-section spiral computed tomography (SCT). The tracheobronchial tree, the tumor lesions and the stents were segmented and visualized with a shaded-surface display (SSD) rendering method. Virtual bronchoscopy was performed with a shaded-surface model without color coding, with a transparent color-coded shaded-surface model and with a color-coded triangle-surface model.
Results: The shaded-surface model without color coding allowed only an assessment of the airway surface The transparent color-coded shaded-surface model enables the simultaneous visualization of the airways and the adjacent structures behind the tracheobronchial wall. The color-coded triangle-surface model allows a clear and detailed spatial representation of the dimensions of extraluminal anatomical and pathological, but it is of limited use for the depiction of an airway surface, since the lumen is less well defined.
Conclusions: Virtual bronchoscopic examinations of the tracheobronchial system with a transparent color-coded shaded-surface model obviate the need for time consuming detailed analysis and presentation of axial source images and offers a practical alternative to fiberoptic bronchoscopy.

B-0546 10:40

Multislice CT virtual bronchoscopy in central airway disease
H. Hoppe, H.-P. Dinkel, P. Vock; *Berne/CH*

Purpose: We examined the use of virtual bronchoscopy (VB) in the evaluation of central airway disease. The diagnostic value of VB was compared to fiberoptic bronchoscopy (FB) and pathological analysis of material obtained from surgery.
Methods: A consecutive cohort of 20 patients with various clinical indications for multislice computed tomography (MS-CT) scan was examined. VB was performed with patients after plastic reconstruction for tracheo-bronchial defects, bronchial tumors, bronchial stump insufficiency and bronchiectasis. Other 5 patients without central airway abnormalities were included as control subjects. The CT data were obtained on a Toshiba Asteion MS system in 4 × 1 mm or 4 × 2 mm collimated multislice spiral mode (100 – 180 mAs, 120 kV). Axial slices were reconstructed with an interval of 1 – 2 mm and transferred to a dedicated Advantage Windows 3.1 workstation (General Electric). VB was performed in a blinded fashion in all patients using the Navigator 1.3 software and correlated to FB findings later.
Results: VB was reliable in the assessment of central airway defects and was accurate in assessing stenosis as well excluding or visualizing other trachiobronchial pathology. Correlation of degree of stenosis between FB and VB was excellent (within a margin of error of 10 %). However, VB was impaired by mucous plugs and posttumoral atelectasis and could not detect superficially spreading epithelial growth.
Conclusions: VB is a useful diagnostic tool for the assessment of central airway pathology. However, evaluation of axial slices in combination with VB is mandatory. FB is necessary for obtaining histopathological information and for detecting subtle epithelial abnormalities.

B-0547 10:50

CT changes after fiber-endoscopic bronchoscopy
R. Groell, G. Ambrosch, A. Hermann; *Graz/AT*

Purpose: To determine which changes occur in computed tomography (CT) studies of the chest due to manipulations during fiber-endoscopic bronchoscopy.

Sunday

Materials and methods: High-resolution CT studies of the chest were performed in 11 patients 3 – 6 hours after fiber-endoscopic bronchoscopy. These studies were compared with CT studies acquired before bronchoscopy. During endoscopy either bronchioalveolar lavages, brushing or biopsies were performed. The CT findings were correlated with clinical data such as volume of fluid during lavages or endoscopically visible sites of bleeding.
Results: The CT findings after endoscopic procedures included ground-glass opacities, alveolar infiltrates and patchy consolidations. These findings correlated with the amount of fluid installed during bronchioalveolar lavages or with visible sites of bleeding. No patient developed pneumothorax.
Conclusion: Manipulations during fiber-endoscopic bronchoscopy cause characteristic findings on CT studies of the chest. The radiologist should be aware of these patterns to avoid their misinterpretation as primary pathologies.

B-0548 11:00

Disagreement between bronchoscopy and CT in the diagnosis of total bronchial occlusion

O. Woo, S. Lee, S. Lee, Y.-W. Oh, K. Kang, H. Seol, E.-Y. Kang; *Seoul/KR*

Purpose: To evaluate mismatched bronchial occlusions between bronchoscopy and CT, and to assess their causes.
Materials and methods: In patients with total bronchial occlusion at bronchoscopy, we selected 70 patients with available initial CT record. The interval between CT and bronchoscopy was 0 – 8 days. CT and bronchoscopic findings were reviewed retrospectively by two radiologists and one bronchoscopist in mismatched cases between bronchoscopy and initial CT record.
Results: 15 patients showed disagreement between initial CT records and bronchoscopic findings. Among these 15, 7 showed patent bronchi, 4 had disagreement in location, and 4 did not mention about bronchial anatomy at initial CT records. With retrospective study of CT; Among 7 showing patent bronchi at initial CT records, one showed bronchial occlusion and 6 again showed patent bronchi. In these 6, 2 performed bronchoscopy before CT, 3 showed bronchial narrowing, and 1 had bronchial compression. Among 4 showing mismatching in extent, 2 had bronchial narrowing and 2 corrected obstruction level by retrospective review of bronchoscopic findings. 4 without mention about bronchial occlusion showed matched occlusion with bronchoscopy.
Conclusion: CT scan often mismatched bronchial occlusion with bronchoscopy, and showed tendency to underestimate the extent and level of bronchial occlusion as comparing with bronchoscopy.

B-0549 11:05

Virtual bronchoscopy (VB) in the evaluation of patients with hemoptysis: Work-in-progress

V. Maniatis, S. Kourelea, K. Liberopoulos, T. Vontetsianos, S. Kavadias, A. Rigopoulou, K. Stringaris, G. Zois; *Athens/GR*

Purpose: To evaluate virtual bronchoscopy (VB) as a diagnostic tool for patients presented with hemoptysis and normal chest X-ray.
Methods and material: During a 6-month period 16 patients have been studied. 11 men and 5 women are included, 41 – 77 years old, 12 smokers and 4 non-smokers. They presented with hemoptysis as a symptom and their chest X-ray showed no abnormalities related to their clinical problem. All of them underwent: (a) fiberoptic bronchoscopy (FOB) and (b) spiral CT of the thorax (slice thickness: 3 mm, table feed: 5 mm/s, reconstruction undex: 2 mm) with intravenous injection of contrast medium. Raw axial images were transferred to a work-station where VB images were reconstructed.
Results: CT findings included: broncіectasies in 6 patients and consolidation in 5 (with bronchial narrowing as a VB finding in 2 of them). In the rest 5 patients both CT and VB were normal. FOB showed: (a) no endobronchial lesion in 10 patients (5 with normal CT and VB, 3 with consolidation and normal VB and 2 with broncіectasies), (b) submucosal oedema in 2 patients (bronchial narrowing was found in VB) and (c) non-specific mucosal changes in 4 patients (bronchiectasies were found on CT).
Conclusion: Although FOB is considered to be necessary in the evaluation of patients with hemoptysis, it didn't offer any additional information in our study group. According to our preliminary results, CT and VB may reliably replace FOB in these patients.

B-0550 11:10

Pulmonary cystic fibrosis: Evaluation with a new and extended HRCT scoring system

A. Economou[1], J. Manavis[2], P. Karagianni[1], E. Zafiriadou[1], G. Grollios[1], M. Badouraki[1], I. Tsanakas[1], S. Efremidis[1]; *[1]Thessaloniki/GR, [2]Alexandroupolis/GR*

Purpose: The aim of this study is to test the efficacy of a new and extended HRCT scoring system for the evaluation of the pulmonary status of patients with cystic fibrosis by comparing it with chest-X-ray, clinical status and spirometry.
Materials and methods: Fifty-eight patients with cystic fibrosis underwent chest-X-ray, lung HRCT, spirometric and clinical examination. HRCT findings were scored with a new scoring system including 13 parameters. The total score for each patient was correlated and compared with the chest-X-ray, spirometric and clinical score. Patient population was classified into three groups according to age and genotype and into two groups according to pseudomonas in the sputum.
Results: The most frequently detected HRCT abnormalities among the 58 patients were bronchiectasis in 54 (93.1 %), atelectasis-consolidation in 43 (74.13 %), bronchial wall thickening in 42 (72.41 %), tree-in-bud in 40 (68.96 %) and mucous plugging in 39 (67.24 %) patients. The overall HRCT score correlated significantly with the chest-X-ray score, pulmonary function tests and clinical status. Comparing HRCT scores with all the other indexes showed that HRCT classifies the pulmonary status in a worse rank than any other method. The severity of the HRCT score increased with age and was higher in the group with pseudomonas in the sputum. We did not find any correlation between genotype and HRCT scores.
Conclusion: HRCT can detect lung deterioration earlier than any other method and should therefore be incorporated as the imaging technique in a clinico-functional-radiological scoring system for the evaluation of the lung status in cystic fibrosis.

B-0551 11:20

Focal pulmonary fibrosis adjacent to thoracic vertebra: Do osteophytes cause focal fibrosis?

S. Otake[1], M. Takahashi[2], T. Ishigaki[3]; *[1]Toki/JP, [2]Otsu/JP, [3]Nagoya/JP*

Purpose: To evaluate the speculation that the osteophyte of the thoracic vertebra causes focal fibrosis in the adjacent pulmonary tissue.
Methods and materials: One hundred cases with the osteophyte of the thoracic vertebra and 100 cases without the osteophyte in the same age distribution were randomly selected and their chest CT images were retrospectively reviewed. Patients with active or chronic pulmonary diseases were excluded from this study.
Results: Focal pulmonary fibrosis was shown in 45 % of the cases with the osteophyte and none of cases without the osteophyte. The common location of fibrosis was the medial portion of the right lower lobe (azygo-esophageal recess). The patterns of fibrosis were reticular or linear. Fibrosis was seen in 37 % of the cases with the osteophyte of 5 – 9 mm thickness, 53 % with 10 – 14 mm thickness, and 100 % with more than 15 mm thickness. Statistical analysis showed a significant difference between the incidence of fibrosis and the thickness of the osteophyte. There was no relationship with age, sex, smoking, and past history.
Conclusion: The osteophyte of the thoracic vertebra can be one of the causal factors of focal pulmonary fibrosis in the adjacent pulmonary tissue.

B-0552 11:30

Radiological imaging as the basis for a simulation software to improve individualised inhalation therapies

S. Ley[1], D. Mayer[1], B.S. Brook[2], E.J.R. van Beek[2], C.P. Heussel[1], D. Rinck[1], K. Markstaller[1], N. Weiler[1], H.-U. Kauczor[1]; *[1]Mainz/DE, [2]Sheffield/GB*

Purpose: Inhalation therapies are increasingly used for airways and systemic diseases. For new developments a comprehensive model is essential, which takes into account the anatomy, delivery process, inhalation deposition and uptake of inhaled drugs. The purpose of this study is to implement CT and MRI as the foundation of a compartmental lung model.
Material/methods: Spiral-CT data and segmentations using automatic region-growing algorithms are implemented to provide detailed anatomic information of the tracheobronchial tree, pulmonary arteries and lung volumes. Paired inspiratory/expiratory HRCT scans, dynamic cine-CT and cine-MRI during continuous respiration demonstrate calibre changes of the trachea and central airways as well as density changes of the parenchyma during respiration. From these data the changing three-dimensional geometrical structure of elastic-wall airways is modelled using surface-meshes, and particle trajectory models within a computational fluid dynamics environment. The results are displayed with the volume rendering technique.

Results: From CT-data the tracheobronchial and the pulmonary arterial tree were automatically segmented down to the 5th level. Calibre changes of the trachea at dynamic CT- and MRI-studies were successfully used to model airflow using computational fluid dynamics. Lung volumes were automatically quantified. Density-based assessment of dynamic scans allowed for separation of pulmonary compartments exhibiting different functional characteristics. From dynamic CT time-constants were assigned to the different compartments.
Conclusion: CT and MRI represent the basis for a simulation program, which can assist in the development of new inhaled therapies. Refinements of this lung model are ongoing.
Supported by: European Commission (IST–1999–14004: "COPHIT") and the British Council.

B-0553 11:40

X-ray and CT in the evaluation of pulmonary echinococcosis
D. Akilova, A. Ikramov, N. Djouraeva; *Tashkent/UZ*

Purpose: The purpose of this study is to evaluate the need for CT of the chest after an initial X-ray study in patients with pulmonary echinococcosis.
Materials and methods: The chest X-ray and chest CT-studies of 38 patients (22 male, 16 female) with surgically verified echinococcosis of the lungs (10 male, 8 female) were retrospectively reviewed. Twelve of these patients had relapsed echinococcosis cysts (8 male, 4 female). P.a. and lateral standard chest X-ray were performed. CT was performed without contrast at midinspiration level in supine position (slice thickness 5 mm).
Results: The image analysis revealed in 31 of 38 patients no differences between X-ray and CT results. In only 2 patients the CT diagnosis of echinococcosis differed from the one made by surgery suggesting tuberculous cavern and malignant cystic tumor respectively. In 7 patients the X-ray results differed from those of CT. In 3 cases tuberculous cavern and in 4 cases tumours of the lungs were interpreted as echinococcosis. CT was correct in 5 of these cases. The surgically identified multiple cysts in both lungs (18 patients) were all seen by CT however by X-ray studies only when larger than 1 cm in diameter (7 patients).
Conclusion: CT study of the chest should follow a chest X-ray study in following situations: – numerous cysts in one or both lungs – sonographic appearance of complicated echinococcosis (suppuration, break through to bronchus or pleural cavity) – difficult interpretation of chest X-ray because of superimposed soft tissue – relapsed echinococcosis cysts.

B-0554 11:50

The periaortic "Crescent sign": Prevalence, significance and possible mechanisms
M. Uffmann, G.R. Strasser, C.J. Herold; *Vienna/AT*

Purpose: To determine the origin of a crescent-shaped density located laterodorsally to the descending aorta and potentially mimicking aortic dissection on contrast enhanced chest CT examinations.
Materials and methods: During a 3-months interval, consecutive contrast enhanced helical chest CT examinations of 502 patients were analysed by two radiologists. Assessment included the presence/absence of a crescent-shaped tissue adjacent to the descending aorta, contrast enhancement of the periaortic tissue, signs of dissection in other parts of the aorta, the maximum aortic diameter, and its relationship to the thoracic spine and the left lower lobe. Logistic regression was performed to evaluate the influence of patients age, aortic diameter, and mediastinal course of the aorta on the presence of contrast enhancing crescent shaped periaortic tissue.
Results: Crescent-shaped tissue adjacent to the aortic wall was found in 20 patients (3.9 %). It showed a uniform contrast enhancement which was classified visually as of equal (n = 12) or slightly lower density (n = 8) compared to the adjacent aorta, mimicking dissection. Acute dissection was ruled out clinically and by follow-up in all patients. At logistic regression analysis, the sign was more often found in increasing age (odds ratio 2.7), in increasing diameter of the aorta (odds ratio 1.6), and in increasing deviation of the aorta from its normal position into a low lateral paravertebral location (odds ratio 5.2).
Conclusion: A crescent-shaped contrast enhancing density adjacent to the descending aorta is not uncommon, may mimic intramural hematoma in dissection and probably reflects atelectasis due to aortic enlargement and abnormal position.

10:30–12:00 **Room F2**

Neuro

SS 1011

Tumors - Advanced diagnostic techniques

Chairpersons:
J.A. Castelijns (Amsterdam/NL)
G. Wilms (Leuven/BE)

B-0555 10:30

Brain metastases: Assessment of treatment response by means of dynamic susceptibility contrast enhanced MRI at 1.5 T
M. Essig[1], F. Wenz[1], J. Debus[1], R. Hentrich[2], M.V. Knopp[3]; [1]*Heidelberg/DE*, [2]*Constance/DE*, [3]*Columbus, OH/US*

Purpose: To assess if measurements of regional cerebral blood flow (rCBF) and volume (rCBV) are able to predict the response of brain metastases to radiation therapy and to assess the influence of radiosurgery on rCBV on brain metastases and normal surrounding tissue.
Patients and methods: 9 patients with brain metastases prior high dose radiosurgery were examined with conventional T1- and T2- weighted MRI and dynamic susceptibility contrast enhanced MRI (DSC MRI). For DSC MRI 55 T2*w GE images of two sections were acquired after bolus administration of 0.1 mmol/kg gadoteridol (Prohance, Bracco) for the simultaneous measurement of brain feeding arteries and brain tissue allowing an absolute quantification of rCBF and rCBV. Follow-up examinations are being performed 6 weeks and 3 month after radiotherapy and the acquired perfusion data were related to a 3 point scale of treatment outcome.
Results: DSC MRI successfully assessed perfusion data in all patients. Higher pretherapeutic rCBV seems to predict a poor treatment outcome. After radiosurgery patients with tumor remission and stable disease presented a decrease of rCBV over time regardless temporary tumor volume increase. Patients with tumor progression at the 3 month follow-up presented an increase of rCBV. Effects on normal surrounding tissue could not be observed.
Conclusion: DSC MRI using Gadoteridol allows the noninvasive assessment of rCBV and rCBF of brain metastases and its changes due to radiosurgery. The method may also be able to predict treatment outcome. Furthermore radiotherapeutic effects on surrounding unaffected tissue can be monitored.

B-0556 10:40

Imaging findings in cranial leptomeningeal carcinomatosis
R. del Carpio-O'Donovan, C. Torres; *Montreal, PQ/CA*

Purpose: Leptomeningeal carcinomatosis (L.C.) is a serious complication of cancer occurring in about 5 % of patients with this disease and resulting in significant mortality and morbidity. This disorder is being recognized with increasing frequency although the diagnosis remains elusive even with CSF analysis as patients live longer and as neuroimaging studies improve. We present the computed tomography (CT) and magnetic resonance imaging findings in 17 patients diagnosed with L.C. at the Montreal General Hospital (M.G.H.). The advantages of magnetization transfer modality are also reviewed.
Methods and materials: Seventeen symptomatic patients with several known primaries (breast, lung, stomach carcinoma, melanoma and lymphoma) had contrast CT and/or MRI of the brain and L.C. was diagnosed.
Results: The imaging findings consisted of linear or nodular enhancing lesions on the surface of the brain or in the depth of the sulci, nodular enhancing lesions within the Virchow–Robin spaces, ependymal enhancement, subepedymal enhancing nodules, cranial nerve enhancement and enlarged ventricles.
Conclusion: CT, and especially MR imaging are valuable tools in the diagnosis of L.C. in patients with known primaries and may allow the early recognition of this disease with improvement in the prognosis of this entity.

B-0557

withdrawn by author

B-0558 10:45

Comparison of Gd-enhanced MRI and ^{123}I-IMT-SPET in the preoperative grading of malignant gliomas

K. Papke, B. Riemann, B. Höss, O. Schober, H. Wassmann, W. Heindel; *Münster/DE*

Purpose: It was the aim of the study to compare Gd-enhanced magnetic resonance imaging (MRI) and ^{123}Iodine-a-methyl tyrosine (^{123}I-IMT) SPET in the non-invasive grading of malignant gliomas.

Material and methods: 48 patients with untreated gliomas were studied preoperatively using both Gd-enhanced MRI and ^{123}I-IMT SPET. For MRI assessment of tumor grading, a weighted scoring system of nine criteria was used (signal heterogeneity, cyst or necrosis, haemorrhage, crossing midline, edema and/or mass effect, border definition, flow void, degree and heterogeneity of contrast enhancement). SPET was performed using the triple-headed camera MULTISPECT 3, equipped with medium-energy collimators. ^{123}I-IMT uptake was quantified as the ratio between amino acid uptake in the tumor over that in the contralateral hemisphere. A threshold value of 1.9 was used for differentiation between low- and high-grade gliomas. The final tumor grading was proven histopathologically in all patients. 15 tumors were WHO grade II, 9 tumors grade III and 24 tumors grade IV.

Results: Sensitivity, specificity and accuracy in the differentiation between low- and high grade gliomas were 80 %, 91 % and 88 % for Gd-enhanced MRI and 67 %, 88 % and 81 % for ^{123}I-IMT SPET, respectively.

Conclusion: Gd-enhanced MRI and ^{123}I-IMT SPET showed similar accuracies in differentiating between low- and high-grade gliomas with a slight superiority of MRI. Therefore, ^{123}I-IMT SPET does not have to be performed routinely prior to therapy of malignant gliomas.

B-0559 10:55

Realtime fMRI for image guided neurosurgical intervention

C. Dannenberg, U. Quäschling, M. Biesold, C. Trantakis, D. Winkler, J. Dietrich, S. Kösling, T. Kahn; *Leipzig/DE*

Purpose: The indications for resection or biopsy of slow growing or rapid growing brain tumors in eloquent areas are difficult up to now. The aim of our study was to evaluate the use of realtime fMRI in neurosurgical planning.

Methods and materials: 13 praeoperative patients (52 ± 16 years) with cerebral tumors within or nearby the central sulcus; additionally 13 healthy volunteers. Active motor task fMRI; 1.5 T Magnetom Vision (Siemens, Germany): Head coil; EPI sequences (TR 4 s; TE 66 ms); 16 transversal slices; matrix 128 × 128; Siemens post processing software mripp. Data analysis: Visual analysis of EPI-BOLD images, ROI analysis of statistical t-maps.

Results: On the realtime images it was possible to watch the fMRI success during activation. Post processing for further motion correction lasted 11 minutes. Activation of sensorimotor cortex failed only in 1 patient because of motion artefacts. Activation level in tumor affected hemisphere was lower compared to control group. With respect to the distance of tumor edema to the activated area and the preoperative suspected histology the neurosurgical therapy was planned: In 5 patients complete tumor resection, in 4 cases nearly complete open MRI-guided resection, 4 patients were classified as none resectable. Postoperative outcome: Paresis did not occure in 6 cases, improved in 1 and did not change in 2 patients.

Conclusion: Realtime fMRI is a reliable, not time consuming support in planning of neurosurgical intervention.

B-0560 11:05

Curvilinear multiplanar reformatting (CMPR) from 3D MRI for the localization of the pre-central gyrus (preCG) in brain tumor disease

M. Caulo[1], D. Tampieri[2], A. Bastos[2], R. Brassard[2], D. Melançon[2]; *[1]L'Aquila/IT, [2]Montreal, PQ/CA*

Purpose: Despite the use of sophisticated imaging techniques the complexity of the brain surface in patients with space occupying lesions make it often difficult to recognize the preCG. The capability of a new technique of reformatting (CMPR) MR images for the identification of the preCG was analyzed.

Materials and method: 30 patients affected by intra and extra-axial tumors of the central region were retrospectively evaluated. Conventional MR examination and 3D Gradient-echo sequences were performed. Using a Power Macintosh workstation with an in-house developed software (Brainsight, Rogue Research. Montreal, Canada) symmetrical curved slices were generated from a manually delineated brain profile obtaining superficial curvilinear reconstruction of the brain at different depth levels. Three neuroradiologists read CMPReconstructions considering four different anatomical landmarks of the central region known from the literature for conventional MR cuts and adapted for CMPR. All the patients underwent surgery.

Results: Lesions included meningioma (8 patients), metastasis (5 patients), grade II astrocytoma and grade III oligodendroglioma (3 patients each), lymphoma and Grade II ependymoma (1 patient each), grade IV astrocytoma (7 patients), grade II oligodendroglioma (2 patients). In all the cases CMPR allowed to identify at least one anatomical landmark of the preCG allowing to exactly establish the relationship between the tumor and the preCG.

Conclusions: Using different anatomical landmarks and manipulating CMPReconstructions to reach the best projection it was always possible to localize the preCG and to establish its relationship with the tumor. CMPR is not an expensive technique and it requires short post-processing time.

B-0561 11:15

Automatic visualization of corticospinal tract displacement in patients with brain tumors from structural MRI

T.C. Mamisch[1], A. Nabavi[2], M. Kaus[3], S. Warfield[4], R.M.M. Seibel[1], R. Kikinis[4]; *[1]Mülheim a. d. Ruhr/DE, [2]Kiel/DE, [3]Hamburg/DE, [4]Boston, MA/US*

Purpose: Enhance the understanding of the spatial relationship understanding between the corticospinal tracts and an intracerebral lesion from structural MRI automatically by registration. of a standardized normal brain atlas to the individual pathologic anatomy of brain tumor patients.

Material/methods: The skin and the brain were segmented in the patient MRI volume. Subsequently a deformable volumetric atlas of a single normal subject was registered to the patient brain using affine and non-linear registration techniques. The estimated spatial correspondence between atlas and patient brain was used to warp the corticospinal tracts from the atlas onto the patient. The accuracy of the method was evaluated in 5 patients MRI with extrinsic tumors of different histopathology and location by comparing selected anatomical landmark structures from the projected atlas to their manually segmented counterpart in the patient.

Results: We have developed a method for the automated extraction of non-visible inherent information of a structural scan based on non-linear template matching of a brain atlas.

Conclusion: Our method enables the visualization of MRI-Datas with complex anatomy and pathology with minimal user interaction for routine surgical planning that would otherwise demand the acquisition of additional imaging modalities.

B-0562 11:25

A new concept of a unified approach in the treatment of brain tumors

R.J. Bale, R.A. Sweeney, M. Vogele, J. Burtscher, W. Eisner, R. Moncayo, E. Donnemiller, M. Rieger, W. Jaschke; *Innsbruck/AT*

Purpose: The fundamental idea is the application of the VBH mouthpiece as an individualized reference base for a unified, multidisciplinary diagnosis and therapy by allowing image fusion of CT/MR/SPECT/PET, and fixation for radiotherapy and neurosurgery. We report our first clinical experiences with this new device in various disciplines.

Methods and materials: The VBH mouthpiece is an individualized vacuum dental-cast, which is attached to the upper palate by underpressure. For immobilization of the patient's head the VBH mouthpiece (MP) is secured to a base plate by hydraulic arms. A frame provides external reference points for image fusion, computer aided surgery and radiotherapy. The diagnostic scans are performed with the VBH mouthpiece. Image-fusion is based on reference points on the frame. Biopsy is performed with frameless stereotactic navigation. If a surgical intervention is necessary, the image guided surgery relies on the fiducials on the frame, thus necessitating another additional scan. For radiotherapy the patient is repositioned with the original VBH mouthpiece, thus necessitating the fabrication of a mask. For follow-up subsequent image acquisitions are performed with the frame.

Results: The VBH head holder was successfully used for fractionated radiotherapy, brachytherapy, SPECT acquistion and computer assisted surgery. The VBH head holder offered rigid, accurate, and reproducible fixation and accurate external reference points for registration and image fusion.

Conclusion: Application of the mouthpiece is an important step towards unified, multidisciplinary diagnosis and therapy by allowing image fusion of CT/MR/SPECT/PET, use of imaging data, fixation for radiotherapy (external beam, brachytherapy, radiosurgery) and neurosurgical applications.

B-0563 11:35

CT-MRI-SPECT image fusion using external landmarks and a vacuum mouthpiece: A precise and simple method of combining diagnostic and functional imaging in the head region

R.J. Bale, R.A. Sweeney, R. Moncayo, E. Donnemiller, P. Helfer, S.R. Felber, J. Burtscher, M. Rieger, W. Jaschke; *Innsbruck/AT*

Purpose: CT, MR and SPECT/PET data can offer important information in diagnosis, treatment and follow-up of tumors. While methods of fusing CT and MRI have been developed and offer satisfactory results, the possibility of assigning functional information of SPECT/PET images to precisely defined anatomical structures is still a challenge. We present a simple and precise and method of combining all three modalities.

Materials and method: Imaging is performed with a reference frame (SIPLab Innsbruck Frame) with the respective image modality-specific markers in precisely defined positions. This frame is reproducibly connected to the VBH vacuum-mouthpiece, which allows objectively identical repositioning of the frame with respect to the head. The desired imaging modalities can then be fused (superimposed) to the desired extent in the axial, coronal and sagittal planes using the "pair-point matching" algorithm (Immerge, Sofamor Danek Ind.).

Results: CT und MR Datasets of 13 patients were fused with a mean RMS (mean root error) of 0.8 mm. SPECT – CT fusion on two patients gave a mean RMS of 2.3 mm. Fusion per data-pair requires from 5 – 10 minutes.

Discussion: The functional information of SPECT/PET superimposed on the anatomic regions in CT and MR gives important information on tumor response/activity. The same Mouthpiece can be used for frameless stereotactic neurosurgery and high precision fractionated radiotherapy, during which all three imaging modalities can be performed, if desired, not sacrificing repositioning.

B-0564 11:45

Accurate frameless stereotaxy using a non-invasive vacuum-affixed dental cast that acts as a reference base: A phantom study and initial applications in patients with trigeminal neuralgia

R.J. Bale, A. Martin, M. Rieger, M.S. Giacomuzzi, M. Vogele, J. Burtscher, C. Mayr, E. Ladner, W. Jaschke; *Innsbruck/AT*

Purpose: The authors present the results of a phantom study, a cadaver study and initial clinical experiences with frameless stereotactic localization of cranial targets using the VBH head holder (Medical Intelligence, Schwabmünchen, Germany).

Method and materials: A prosthesis of the upper dentition was glued to the underside of a test phantom and it's corresponding VBH vacuum-mouthpiece was created. CT scans with three different slice thicknesses were obtained. After mouthpiece-based registration the targeting device was adjusted with frameless stereotactic guidance. The phantom was repositioned and the needle was inserted producing impressions on an aluminium foil. Each of the 12 fiducials was targeted 30 times, 4 steps per scan totalling 270 punctures. A three-dimensional localization error vector was calculated for every attempt. In addition, the trigeminal ganglion was targeted through the foramen ovale in 3 cadavers (6 times) and in 7 patients with drug resistant trigeminal neuralgia.

Results: The mean localization error (MLE) was: 5 mm axial: MLE 1.84 mm, SD 0.96 mm, 3 mm axial: MLE 1.38 mm, SD 0.65 mm, 1 mm axial: MLE 1.31 mm, SD 0.67 mm. In addition, in all cadavers and in all patients the foramen ovale (5 to 3 mm in diameter) could be reached at the first attempt.

Conclusion: Our experiences indicate that frameless stereotaxy allows for accurate targeting of cranial structures, comparable to the accuracy achieved with common invasive stereotactic frames. Using the non-invasive reproducible VBH head holder image acquisition, adjustment of the targeting device and therapy can be separated in time and location.

10:30–12:00 **Room G**

Abdominal and Gastrointestinal

SS 1001b

Dynamic studies

Chairpersons:
O. Ekberg (Malmö/SE)
W.M. Gedroyc (London/GB)

B-0565 10:30

Oropharyngeal neurogenic dysphagia in patients after esophageal surgery

M. Memarsadeghi, P. Pokieser, M. Scharitzer, W. Schima, E. Schober; *Vienna/AT*

Purpose: Patients after oesophageal surgery may suffer from neurogenic dysphagia. The present study aimed at evaluating the frequency of neurogenic oropharyngeal dysphagia and associated symptoms after oesophageal surgery.

Method and materials: From 1989 to 2000 video-fluoroscopy of deglutition was performed in 4349 patients. There were 171 patients after oesophageal surgery, presenting with suspected aspiration (36 pts), dysphagia (92), globus sensation (8) and other symptoms of swallowing impairment (35). We calculated the frequencies of dynamic findings suggesting oropharyngeal neurogenic dysphagia for the post-surgical groups with different symptoms.

Results: Signs of oropharyngeal neurogenic dysphagia were found in 63 patients (37 %) after oesophageal surgery. They included 23 patients with suspected aspiration, 21 with dysphagia, 1 with globus sensation and 18 with other symptoms.

Conclusion: Oropharyngeal neurogenic impairment of deglutition seems to be frequent in patients after oesophageal surgery. The diagnosis of neurogenic dysphagia in patients after oesophageal surgery should be considered, especially when morphological abnormalities are absent.

B-0566 10:40

Videomanometry for the assessment of pharyngo-esophageal motor disorders

C. Bnà, S. Brusori, L. Braccaioli, A. Nocco, F. D'Ovidio, M.L. Lugaresi, S. Mattioli, G. Gavelli; *Bologna/IT*

Purpose: To evaluate the efficacy of simultaneous video-fluorography and manometry (video-manometry) assessment in pharyngo-oesophageal motor disorders.

Method and materials: Video-manometry was used to study 8 patients (age range 34 – 72) complaining of oro-pharyngeal dysphagia: 2 had pharyngo-oesophageal incoordination; 3 pharyngo-oesophageal incoordination and Zenker diverticulum; 3 patients Zenker diverticulum alone. Ten healthy volunteers (age range 24 – 73) served as controls. Two computerised and synchronised units were developed: one digital video-fluorographic unit with a remote control, connected to a video recorder and a manometric unit adopting an original 3 balloon sensor probe.

Results: Patients with oro-pharyngeal dysphagia compared to healthy volunteers had anticipated opening and closure of the upper oesophageal sphincter with reduced opening time and diameter (radiological parameters), and alteration of sphincter relaxation along with increment of the residual pressure (manometric parameters). These changes were compensated by hypopharyngeal intra-bolus pressure increment measurable only by combined video-manometric study.

Conclusion: With respect to video-fluorography, video-manometry improves diagnosis for the study of upper oesophageal sphincter disorders. It is also an excellent research tool for the pharyngo-oesophageal tract.

B-0567 10:50

Pharyngeal retention as a predictive factor of aspiration during videofluoroscopy in dysphagic patients

E. Eisenhuber, W. Schima, E. Schober, P. Pokieser, A. Stadler, M. Scharitzer, E. Oschatz; *Vienna/AT*

Purpose: To evaluate the clinical significance of pharyngeal retentions to predict aspiration in dysphagic patients.

Methods and materials: At videofluoroscopy, pharyngeal retentions were found in 53 (38 m, 15 f; mean age, 59 a) of 193 (28 %) patients with suspected deglutition disorder. Swallowing function was assessed videofluoroscopically. The amount of residual material in the valleculae and/or piriform sinuses pharyngeal retentions was graded as mild, moderate, or severe. The frequency, type, and grade of aspiration were assessed.

Results: Pharyngeal retention was caused by pharyngeal weakness in 91 %. In 35 patients (66 %) with pharyngeal retentions postdeglutitive overflow aspiration was found. Aspiration was more often found in patients, who had additional functional abnormalities, such as incomplete laryngeal closure or impaired epiglottic tilting. Postdeglutitive aspiration was diagnosed in 1 of 5 patients (20 %) with mild, in 6 of 18 patients (33 %) with moderate, and in 28 of 30 patients (93 %) with severe pharyngeal retentions.
Conclusion: Postdeglutitive overflow aspiration is a frequent finding in patients with pharyngeal retentions and increases markedly with the amount of residue. Functional abnormalities other than pharyngeal weakness, such as impaired laryngeal closure, may contribute to aspiration.

B-0568 11:00

Morphological abnormalities of the pharynx and esophagus detected by videofluoroscopy in patients with neurologic dysphagia

M. Scharitzer, P. Pokieser, E. Schober, W. Schima, M. Memarsadeghi; *Vienna/AT*

Purpose: To evaluate the frequency of morphological findings of the pharynx and esophagus in videofluoroscopic (VF) studies of symptomatic patients with neurological disorders.
Material and methods: Of 4349 patients referred for a VF-investigation between 01/1989 and 06/2000, VF studies of 911 symptomatic patients with neurological disorders were reviewed for morphological findings of the upper gastrointestinal tract. Neurological diseases included vascular disorders like stroke (419 pts), posttraumatic neurological disorders (n = 90), tumors of the central nervous system (n = 88), postoperative neurological patients (n = 66), Parkinson disease (n = 38) and others (n = 210).
Results: In 911 patients, 68 morphological findings in 64 pts (7 %) could be depicted, including: tumors of oral cavity, soft palate, epiglottis and hyoid/larynx (n = 2); pharynx: diverticula (n = 9), tumors (n = 5), other structural lesions (n = 5); upper esophageal sphincter: webs (n = 7), tumors (n = 3), others (n = 12); esophagus: diverticula (n = 2), webs/strictures (n = 13), others (n = 10).
Conclusion: Besides functional disorders VF can also reveal morphological abnormalities in neurologically impaired patients, which can be the cause of or contribute to impaired swallowing function.

B-0569 11:10

Visualization of swallowing using MR fluoroscopy with real-time TrueFISP

J. Barkhausen, T. Lauenstein, D. Arweiler-Harbeck, M.E. Ladd, S.G. Rühm, M. Goyen, J.F. Debatin; *Essen/DE*

Purpose: To evaluate the ability of different real-time True FISP sequences for the visualisation of swallowing.
Method and materials: Examinations were performed on a 1.5 T scanner (Magnetom Sonata, Siemens, Erlangen Germany) equipped with high performance gradients (amplitude 40 mT/m). Different real-time True FISP sequences (TR 2.2 – 3.0 ms, TE 1.1 – 1.5 ms, matrix 63 × 128 – 135 × 256, FOV 250 mm, acquisition time per image 139 – 405 ms) were evaluated for the visualisation of swallowing. The sequences were tested in 8 volunteers and 4 patients with dysphagia. Water, yogurt and semolina pudding were used as oral contrast agents.
Results: Functional exploration of the oropharyngeal apparatus was optimal using the fastest real-time True FISP sequence (TR 2.2 ms, TE 1.1 ms, matrix 63 × 128). Increased acquisition time resulted in blurring of the anatomical structures. As the image contrast of True FISP sequences depends on T2/T1 properties, all tested foodstuffs were well suited as contrast agents, but image quality was best using semolina pudding.
Conclusion: Real time visualisation of swallowing is possible using real-time True FISP sequences and oral contrast agents. For functional exploration of swallowing, high temporal resolution is more crucial than spatial resolution.

B-0570 11:20

Staging of esophageal cancer with optimized double-contrast spiral-CT

N.M. Hof, H. Helmberger, K. Lehner, K.H. Dittler, E.J. Rummeny; *Munich/DE*

Purpose: To assess the diagnostic accuracy of an optimized double-contrast (d-c) spiral-CT (SCT) protocol for T-staging of esophageal cancer in correlation with endosonography (EUS), bronchoscopy and histo-pathologic findings from surgical resection.
Method and materials: A total of 98 patients with different stages of esophageal cancer underwent preoperative helical CT. Intravenous injection of 40 mg Buscopan was followed by oral administration of a vanilla-flavored paraffin emulsion (200 ml). Nonionic contrast material was injected at a rate of 3 ml/s. Images were obtained in the arterial phase. The results were categorized according to TNM classification by 2 experienced radiologists in a blinded fashion and compared to EUS, bronchoscopy and intra operative as well as histo-pathologic findings.
Results: A differentiation of stage T1 and T2 was possible only by endoscopic ultrasound. Compared with histo-pathologic findings SCT showed an overall sensitivity of 86.3 % for T3 and T4 tumors. T stage was underestimated in 11 % of cases and overestimated in 18 % of cases. EUS was limited in predicting tumor infiltration to the tracheo-bronchial system, whereas an d-c SCT revealed a higher diagnostic value in demonstrating tumor extent in T4-tumors with surgical irresectability.
Conclusion: Optimized d-c SCT of the esophagus may be a suitable technique for the T staging of advanced esophageal tumors and provides additional information to EUS.

B-0571 11:30

Clinical experience after three years of open MR defecography

P.R. Hilfiker, K. Bertschinger, B. Marincek; *Zürich/CH*

Purpose: To demonstrate pathologies detected with MR defecography in the sitting position and to demonstrate the acceptance in a clinical setting
Method/materials: Since August 1997, 160 patients were referred for MR defecography. All imaging was performed in the sitting position on a 0.5 T open MR system (GE Medical Systems). After filling the rectum with mashed potatoes mixed with Gd-DTPA, T1w GRE images were acquired in a mid-sagittal plain every 2 seconds (TR 23.9/TE 11.3 ms). Image analysis was performed on a workstation in the cine mode.
Results: Whereas in 1997 all referals came from our hospital, 61 % of the patients today are sent by other hospitals or doctors in private praxis. 86 % were female, and 65 % had pelvic surgery in their past. Indication was obstipation (33 %), outlet disorders (29 %), pain (10 %), incontinence (10 %), organ prolaps (8 %) and others (10 %). The following disorders were diagnosed: rectoceles (n = 52), enteroceles (n = 40), descending perineal syndrome (n = 37), intussuceptions (n = 24), spastic pelvic floor (n = 16), organ prolapse (n = 9), and others (n = 9). 25 % were normal (n = 40).
Conclusions: Open MR defecography has completely replaced conventional defecography in our institution; the numbers of defecographies increased substantially since 1997. The method is widely accepted by clinicians and by patients.

B-0572 11:40

Dynamic MR defecography and defecography: Comparative study and interobserver agreement

J. Tunkel, J. Knuepffer, W. Kenn, D. Bussen, D. Hahn; *Würzburg/DE*

Purpose: To compare defaecography and dynamic MR-defaecography in patients with defaecation disorders.
Method and materials: 30 patients with defaecation disorders were studied with evacuation proctography (defaecography) and dynamic magnetic resonance (MR) defaecography performed with a superconducting system (Magnetom Vision). T1-weighted gradient-echo images were acquired every second in the midsagittal plane at rest, during straining and defaecation. Analysis of the anorectal angle and anorectal junction was performed by two independent observers in a blinded fashion for defaecography and MR defaecography.
Results: By regression analysis, there was moderate correlation ($r = 0.71$, $p < 0.01$) concerning descent of the anorectal junction and good correlation concerning the anorectal angle ($r = 0.89$, $p < 0.001$). Inter-observer variability of both methods was comparable concerning the anorectal angle (4.8 ± 3.5 % for MR defaecography versus 4.4 ± 4.1 % for defaecography), MR was superior concerning anorectal descent (8.7 ± 7.7 % versus 15.9 ± 26 %). Both methods revealed one intussusception and 24 rectocoeles. Dynamic MR defaecography did not identify one rectocoele seen on radiographic defaecography. There was a tendency to underestimate the size of rectocoeles in dynamic MR-defaecography.
Conclusion: Dynamic MR defaecography and defaecography yield moderate to good correlation concerning measurement of anorectal descent and the anorectal angle. Inter-observer variability of dynamic MR defaecography was superior concerning anorectal descent. The diagnostic accuracy of both methods was comparable for rectocoeles with a tendency for underestimation in MR defaecography.

B-0573 11:50

Spiral defeco-computed tomography: A new technique of evaluation of pelvic floor and anorectal dynamics

A. Salzano, V. Nocera, G. Cavallo, A. Nunziata, C. Bruno; *Naples/IT*

Purpose: To illustrate the use of spiral defeco-CT, that represents a new method of evaluation of anorectum and pelvic floor dynamics. To describe its role in detecting particular pathologies such as enteroceles, sigmoidoceles, perineal prolapse disorders and fecal incontinence findings, that can avoid at only defecographic examination.

Methods and materials: We report a study of sd-CT on 21 patients (17 females and 4 males, with mean age of 57 years range of 50 – 77 years); all subjects were previously undergone defecography. Spiral CT of low pelvis was carried out in different dynamic phases of pelvic floor. The contrast agent was prepared by ourselves and injected into ampulla and vagina; the bladder was not opacified because of urine filling.

Results: By sd-CT we observed 10 rectoceles, 8 cistoceles, 7 perineal descent syndromes, 5 of fecal incontinence, 3 external rectal prolapses; besides, 4 enteroceles and 3 sigmoidoceles (4 of them referred hysterctomy). CT signs of fecal incontinence appeared more expressive in comparision to defecography.

Conclusion: Sd-CT is an useful technique to diagnose pelvic floor disorders such as enterocele pathologies, that remain occulted using other methods as defecography; besides, sd-CT improves radiological findings of rectal disfunctions such as fecal incontinence and rectocele.

10:30–12:00 **Room H**

Interventional Radiology

SS 1009

Arterial intervention (1)

Chairpersons:
W.J. Huk (Erlangen/DE)
K. Ivancev (Malmö/SE)

B-0574 10:30

In vitro mechanical thrombectomy efficacy of the Amplatz thrombectomy device and the Cragg thrombolytic brush catheter

J. Grimm, S. Müller-Hülsbeck, M. Heller; *Kiel/DE*

Purpose: To determine the efficacy for mechanical thrombectomy of the 6F Amplatz thrombectomy device (ATD) and the 6F Cragg thrombolytic brush catheter (CBC) in a flow model.

Methods and materials: Thrombectomy of clots (n = 40) from porcine blood was performed with the ATD and CBC in a flow model (1000 ml/min) simulating a arteriovenous shunt (5 or 7 mm diameter). The effluent was weighted in a three step filter system (1000, 100, 10 µm) to evaluate embolized material, remaining thrombus and activation time were evaluated as well.

Results: No significant difference in the activation time was evaluated. The CBC produced significantly less emboli (0.003 % vs. 4.4 % in 5 mm and 0.5 % vs. 1.2 % in 7 mm model for CBC, ATD respectively). However, more thrombus remained if compared to the ATD (41.2 % vs. 1.0 % in 5 mm and 0.3 % vs. 61.8 % in 7 mm model for the CBC, ATD respectively).

Conclusion: The ATD is capable of removing almost all thrombus whereas the CBC only removes up to 60 %. The CBC produces less embolic particles in the size of > 10 µm than the ATD, optimal for the combined use of the CBC with thrombolytic agents as the area of interface between clot and lytic agent is enhanced. Due to the large amount of remaining thrombus the CBC should not be used without additional lytic agents. The ATD is capable of removing almost all thrombus, with a somewhat higher rate of embolization.

B-0575 10:40

Long-term results after femoral artery stent placement

K. Schürmann[1], A.H. Mahnken[1], P. Haage[1], J. Meyer[1], A. Kulisch[1], D. Vorwerk[2], R.W. Günther[1]; *[1]Aachen/DE, [2]Ingolstadt/DE*

Purpose: To report the long-term clinical course after stent placement into the femoral arteries.

Materials and methods: From 1987 to 1990, 20 patients (18 male, 2 female, median age 56.5 years) with femoral artery lesions were treated with Wallstents. Two patients had bilateral lesions. Sixteen lesions were occlusions, 6 stenoses. Most lesions were category 2 (SCVIR classification). Most patients were Fontaine stage 2b before and stage 1 after treatment. Patients were followed with AB-index measurements, colour duplex ultrasound, and clinical examination.

Ten years after treatment the clinical course of all patients was evaluated with telephone interviews and questionnaires. All patients were invited to a follow-up examination. The data collected was analyzed with the Kaplan-Meyer procedure.

Results: Two patients had died. Seventeen of the 22 lesions developed restenosis. The median interval to restenosis was 12 months (range 0.1 – 132 months). In the first year after stent insertion 10 restenoses occurred, in the next 10 years only 7. Ten of the 17 restenotic lesions were reopened, but 7 reoccluded again. Two patients had an amputation of the treated leg, and another patient had femoropopliteal bypass surgery within less than 1 year after stent insertion. The primary cumulative patency rate (Kaplan–Meyer) was 0.45 after 5, and 0.21 after 10 years.

Conclusion: The long-term patency rate after femoral artery stent placement is poor. Indications for stent placement into the femoral arteries should be restrictive. Our data indicates that the risk of restenosis decreases markedly if the stent remains patent during the first year after implantation.

B-0576 10:50

The kissing balloons technique in simultaneous dilatation of stenosed branches at the bifurcation of the renal artery

S. Baus, A. Chavan, J. Radermacher, M. Galanski; *Hannover/DE*

Purpose: Presentation of the Kissing Balloons Technique as a reliable and safe method for the dilatation of stenosed branches at the bifurcation of the renal artery.

Methods: Narrowing of the renal artery at its bifurcation with involvement of its segmental branches still poses a complex therapeutic problem. Substantial danger is posed by the risk of occlusion of one of the arteries while dilating the other. Long-term results of surgical reconstruction of a stenosed bifurcation are not saticfactory. Untreated stenoses bear the risk of intractable hypertension and impairment or loss of renal function.

Five patients with impaired renal function were diagnosed with segmental stenoses of the renal artery at its bifurcation. Using a bifemoral approach 2 balloons were placed at the origins of the renal artery branches and simultaneously inflated. All patients received follow-up examinations evaluating renal function parameters.

Results: All interventions were successful in terms of angiographic criteria, no segmental artery was sacrificed. All patients showed improvement in one or more of the following diagnostic criteria: serum creatinin levels, creatinin clearance, hypertension or need for medication.

Conclusion: This method provides an elegant and save method to save an endangered kidney.

B-0577 11:00

Early experience with a new stent-technique for treatment of renal artery stenosis

S. Müller-Hülsbeck, T. Jahnke, J. Grimm, J. Brossmann, M. Heller; *Kiel/DE*

Purpose: To determine the feasibility and security of a monorail-balloon-stent device for the treatment of renal artery stenosis.

Materials and methods: During a period of four months 22 patients (severe hypertension n = 19, renal insufficiency n = 3) with indications for renal artery stenting (calcified ostial lesion n = 20, insufficient PTA n = 1, dissection n = 1) were enrolled into the prospective evaluation. After pre-dilatation, stents (Rx-Herculink™ 5 mm – 4, 6 mm – 17, 7 mm – 1) were unfolded manometer-controlled with long-sheath technique (6 French) via femoral (n = 19) or brachial approach (n = 3). Parameters of hypertension and renal insufficiency were determined before and after the procedure up to 6 months. Restenosis rate was determined with colored-duplex-ultrasound).

Results: Renal artery stent placement (mean diameter 5.9 mm, mean length 16.2 mm) was technical successful in all cases (100 %). No complications occurred. Transstenotic pressure drop decreased from 88 mmHg before to 1 mmHg after stent placement. Follow-up data will be presented at the meeting.

Conclusions: Renal artery stent placement with the introduced monorail-system is technically superior. In combination with the long-sheath technique (6 French!) an adequate control of stent deployment is guaranteed during the whole procedure.

B-0578 11:10

Initial experience with the Duett sealing device to achieve arterial haemostasis

B. Burns, J. Phillips Hughes; *Oxford/GB*

Purpose: Reduction of puncture site complications and earlier patient ambulation are two current challenges facing interventional radiologists. A number of arterial closure devices are available although there are few clinical trials involving patients with peripheral vascular disease. The Duett is a new device which utilises a balloon catheter to create a temporary seal of the arterial puncture site whilst a procoagulant is delivered to effect a permanent seal. The balloon is deflated and removed. We report on the use of twenty Duett devices and comment on any actual or potential problems encountered.

Materials and method: Twenty Duett devices were deployed in 17 patients. All procedures employed the transfemoral approach. Any immediate complications were noted at time of deployment. The case notes were retrospectively reviewed for delayed complications.

Results: Duett devices were successfully deployed in 19 cases. No immediate complications were noted. Deployment was abandoned in one case where disease in the external iliac artery was felt to preclude safe delivery of the procoagulant. Two patients had successful repunctures within 2 months. Four patients had subsequent surgery without significant problems.

Conclusion: The Duett device is a relatively simple method of achieving haemostasis. In comparison with some of the other closure devices it has the advantage of allowing immediate repuncture and does not leave any residual intravascular component. However caution is required as arterial disease or intervention close to the puncture site may interfere with deployment. Larger studies would be necessary to evaluate puncture site complication rates and ambulation times.

B-0579 11:20

Percutaneous balloon pericardial window formation for patients with symptomatic pericardial effusion

L. García del Barrio[1], J.H. Morales[2], C. Delgado[1], T. Fernández-Villa[1], A. Benito[1], A. Martinez-Cuesta[1], I. González-Crespo[1], J. Larrache[1], J.I. Bilbao[1]; [1]*Pamplona/ES*, [2]*Bogotá/CO*

Purpose: To describe the technique and our experience in percutaneous creation of a pericardial window in patients with recurrent pericardial effusion.

Methods and material: Ten consecutive patients (8 male and 2 female; mean age 61; range 37 – 79 years) with recurrent pericardial effusion were treated from December 1994 to May 2000. Malignant effusion was the cause of cardiac tamponade in eight patients. The puncture of the pericardial space was performed under ultrasonographic and fluoroscopic guidance. Once a guidewire was safely positioned and the wall of the pericardium identified, it was dilated with an 18 mm balloon catheter. A temporary (1 – 3 day) 8 Fr pigtail catheter was inserted in order to stabilize the tract and aspirate the fluid.

Results: The goal of a pericardial tract was achieved in all patients. Two of them presented recurrence of pericardial effusion. One patient who had had a heart transplant required a surgical pericardial window. Another had a major complication because of an accidental puncture of the right ventricle wall. Three deaths owing to progression of the underlying disease occurred during the first two weeks after the procedure. The follow-up ranged from 6 days to 382 days, mean 128 days.

Conclusions: Percutaneous creation of a pericardial window is a safe therapeutic alternative for patients with symptomatic pericardial effusion, particularly those with a malignant condition.

B-0580 11:30

A randomized trial comparing ultrasound guidance with the conventional technique to puncture the femoral artery

J. Ricke, U.K.M. Teichgräber, P. Podrabsky, R. Sörensen; *Berlin/DE*

Purpose: To evaluate ultrasound guidance to puncture the femoral artery.

Materials and methods: A randomized controlled trail was performed comparing ultrasound guided with conventional puncture. Factors assessed included time until completion, number of attempts, complications, risk factors of peripheral arterial disease, intensity of the arterial pulse, previous unilateral puncture and diameter of the leg at the puncture site. For ultrasound guided puncture, a mechanical swivel arm was employed. 112 patients were randomized for ultrasound guided or conventional puncture performed by two experienced interventionalists.

Results: Comparing US and conventional method, risk factors for arteriosclerosis, history of peripheral arterial disease or previous punctures did not influence the mean number of attempts or the time for completion. However, there was a trend for decreased number of attempts in patients with a leg diameter of more than 55 cm. In patients with weak arterial pulse, a decreased number of attemps with US was significant, whereas the time for completion demonstrated a trend to be superior over the convetional method. In patients with strong pulse, US guided procedure significantly extended the time until completion, whereas the number of attemps was equivalent.

Conclusion: Ultrasound guidance for femoral artery puncture is recommended in obese patients and in patients with weak arterial pulse.

B-0581 11:40

Ultrasound-guided compression of postangiographic femoral artery pseudoaneurysms

J. Fernandez Sanchez[1], W. Bücklein[2], K. Bohndorf[2]; [1]*Stuttgart/DE*, [2]*Augsburg/DE*

Purpose: A pseudoaneurysm (PA) is an uncommon complication after femoral artery catheterization. The aim of this study was to evaluate the efficacy of US-guided compression of postangiographic femoral artery PA.

Methods and materials: In 21 patients with a femoral artery PA after transfemoral angiography a US-guided compression of the PA was performed. PA size, total time of compression, number of compression attempts, success or failure of the therapy and possible complications were evaluated. All patients underwent follow-up US examinations after succesful compression.

Results: US-guided compression was succesful in 17 of 21 PA (81 %). 4 patients without thrombosis of the PA after manual compression underwent surgery. The mean diameter of the PA was 2.9 cm. Mean compression duration was 30 minutes. A single compression attempt was performed in 17 patients. 3 patients were treated with two separate compressions. 1 patient underwent three compression attempts. A partial thrombosis of the common femoral vein after US-guided compression was detected in one case. There were no other complications.

Conclusion: US-guided compression is a safe, reliable, noninvasive and cost-effective alternative to surgical repair of postangiographic femoral artery PA.

B-0582 11:50

Combined local thrombolytic therapy and mechanical recanalization in chronic arterial occlusive disease of the lower extremities

R. Cioni, I. Bargellini, C. Vignali, P. Petruzzi, F. Donati, G. Campori, C. Bartolozzi; *Pisa/IT*

Purpose: To evaluate the efficacy (limb salvage) of percutaneous revascularization in patients with severe arterial occlusive disease of the lower limbs.

Materials and methods: Between February 2000 and August 2000, 12 patients (9 male, mean age 67) with severe and extensive occlusive disease of the peripheral arteries below the popliteal artery were treated, in order to avoid major leg amputation. All patients underwent multiple percutaneous angioplasties of the peroneal and tibial arteries (balloon catheters for small vessels), associated with local fibrinolysis (100 000 – 200 000 IU Urokinase) and vasodilators. Mean procedural time was 95 minutes. Following the procedure, infusional thrombolytic therapy was performed for 24 – 72 hours. On follow-up, patients were evaluated clinically and by means of duplex sonography, at discharge and at 1, 3, and 6 months.

Results: Immediate technical success (recanalization of at least 1 artery and/or improvement of distal circulation) was achieved in 10/12 patients (83.3 %); in 1 patient, thrombolytic therapy was interrupted because of retroperitoneal bleeding; in the other case, no improvement of distal circulation was achieved; in both cases amputation of the leg was required. No other complications occurred. On follow-up, improvement of circulation and clinical conditions was obtained in 10/10 patients (100 %) at discharge, 9/10 (90 %) at 1 month, 5/6 (83.3 %) at 3 months.

Conclusion: Although at high risk of complications, combined thrombolytic therapy and mechanical revascularization represent an effective treatment in patients with severe chronic arterial occlusive disease of the lower extremities, achieving at least temporary limb salvage. Longer follow-up and larger series are needed.

10:30–12:00 **Room I**

Abdominal and Gastrointestinal

SS 1001c

CT colonography

Chairpersons:
C.I. Bartram (Harrow/GB)
B. Marincek (Zürich/CH)

B-0583 10:30

Unravelling the colon using multirow detecor-CT: Technique and first experiments with technical and cadaveric phantoms

E. Sorantin[1], E. Balogh[2], G. Werkgartner[1], E. Spuller[1], K. Palagy[2], S. Loncaric[3], M. Subasic[3], R. Fotter[1]; *[1]Graz/AT, [2]Szeged/HU, [3]Zagreb/HR*

Virtual colonoscopy represents a challenging imaging modality for colonic polyp detection. A software tool, which enables, similar to the pathologist's table, a virtual cut along the colons's axis, would allow to inspect the oral and aboral side of folds simultaneously.

Purpose: To present a technique for unrevealing the colon as well as the appearance of colonic polyps on artificial and cadaveric phantoms on those views.

Material and methods: Two phantoms were created. Phantom A consisted of a plastic tube and polyps were simulated by knobs of plastilin. Phantom B was 50 cm long cadaveric colon, where 13 artificial polyps were created. After scanning the following steps were necessary for unrevealing: (1) segmentation of the inner surface, (2) extraction of the central axis using a skeletonisation algorithm, (3) computation of the cross sectional cuts orthogonal to the central axis, (4) remapping of the cross sectional cuts into a new orthogonal 3D data volume, (5) shaded surface rendering of the remapped data. The whole inner surface of the phantoms was displayed at one view, investigated for polyp occurrence and findings compared to real dissection of the phantom.

Results: Human interaction took less than 10 minutes for the segmentation step. Computation time was 2 hours. Simulated polyps appeared as bumps on phantom A and as bumps or as asymmetric broadening of the colon folds on phantom B.

Conclusion: Simulated polyps on artificial and cadaveric phantoms could be demonstrated on virtual views after unrevealing. Thus making these views a feasible display technique for virtual colonoscopy.

B-0584 10:40

Evaluation of patient acceptability for CT virtual colonoscopy after retrograde CO_2 insufflation

M.G.J. Thomeer, D. Vanbeckevoort, D. Bielen, A. Gevers, P. Rutgeerts, G. Marchal; *Leuven/BE*

Purpose: To evaluate patient acceptability for virtual colonoscopy (VC) using CO_2 in comparison with sedated colonoscopy (SC).

Methods and materials: 52 patients referred for SC underwent a virtual VC prior to the SC. All patients received a routine bowel preparation. Retrograde insufflation of CO_2 was performed to a degree the patient could tolerate. Buscopan was injected intravenously prior to the VC. Patient acceptability for the bowel preparation, VC en CC was assessed using a 10 point scale (0 ... highly acceptable, 10 ... not acceptable). Patient tolerance at different times (0 minutes, 10 minutes, 20 minutes) after CO_2 insufflation was also investigated with the same type of scale. Patients were also asked which procedure (VC, SC) they preferred if repeating would be necessary.

Results: Patients found VC (median score 10 vs 0: 2.4) more acceptable then SC (median score 10 vs 0: 3.4) and bowel preparation (median score 10 vs 0: 4.1) was clearly the most uncomfortable procedure though not unbearable. VC was the less pleasant directly after the CO_2 insufflation though the embarrassment decreased exponential over the first 20 minutes. 73 % of the patients preferred VC when they were asked which procedure they would choose in the future.

Conclusions: VC is likely more acceptable then SC when retrograde CO_2 insufflation is used.

B-0585 10:50

Fecal tagging in virtual CT colonoscopy

E. Hein, P. Rogalla, F. Vogel, B.B. Hamm; *Berlin/DE*

Purpose: To evaluate the diagnostic gain of fecal tagging for detection of colonic polyps.

Materials and methods: 132 patients (semi-screening population) underwent a virtual CT colonoscopy after standard bowel preparation using phosphosoda. 12 – 16 h before the CT examination, the patients were given 30 ml of iodined oral contrast material, and again 1 – 2 hours before scanning. Images were obtained in supine position only with 3 mm slice thickness, 5 mm/s table feed, and 2 mm reconstruction interval, and colonic distension with CO_2-gas rectally. Resulting virtual endoscopic fly-throughs were calculated: first with single thresholding (remaining fluid levels were seen as such, method 1), second, with dual thresholding (for air and contrast medium, method 2). The number of polyps detected were compared between both groups. If polyps or other intraluminal findings were seen, patients underwent subsequent colonoscopy.

Results: A total of 17 polyps (sizes: 5 – 13 mm) and 2 cancers (stage T2N0 and T3N1) were detected in 13 patients, all were confirmed on subsequent flexible colonoscopy. A total of 2 polyps were missed (4 and 5 mm) on both methods. 1 polyp was submerged under a contrast fluid level thus not seen with method 1, but seen with method 2. Fecal residue was selectively contrasted and thus did not carry the risk of being misinterpreted as vital tissue.

Conclusion: Fecal tagging with iodinated oral contrast medium is feasible and effective. However, in combination with optimal patient preparation, the additional diagnostic gain may be little.

B-0586 11:00

Optimization of multislice spiral computed tomography colonography: Study on a colonic phantom model

A. Laghi, C. Catalano, R. Iannaccone, V. Panebianco, I. Baeli, F. Iafrate, R. Passariello; *Rome/IT*

Purpose: To optimize scanning parameters for CT colonography using a multislice spiral CT scanner in a study on a colonic phantom model.

Materials and methods: A home-made colonic phantom, represented by a plastic tube containing 27 simulated lesions (12 polyps, 9 depressed lesions, and 6 flat lesions) was scanned in transverse, oblique (45°), and coronal planes in a water-filled plastic box. Four scanning protocols were tested using different collimation, slice width, and reconstruction index values. Each protocol was tested three times using different rotation feed values. Milli-Ampere/s values were set to 80. Images were interactively reviewed on a dedicated workstation using a software with volume-rendering capabilities (Vitrea 2.0, Vital Images, USA).

Results: Image quality was optimal for any protocol when evaluating axial 2D images. Three-dimensional endoluminal images were optimal for protocol nr 1, good for protocol nr 2, fair for protocol nr 3, and poor for protocol nr 4. Evaluation based on simultaneous assessment of 2D and 3D images demonstrated an average sensitivity for protocols nr 1, 2, 3 and 4 of respectively 100 %, 98 %, 94 %, and 85 %. The evaluation of three different rotation feed values tested for each of the four protocols did not show statistically significant differences in terms of sensitivity. In the assessment of 3D images, average sensitivity was 92 % for protocol nr 1, 85 % for protocol nr 2, 77 % for protocol nr 3 and 58 % for protocol nr 4.

Conclusions: The introduction of multislice technology in CT colonography provides improved spatial resolution and better image definition.

B-0587 11:10

Multislice spiral CT colonography: Initial clinical study with a high-resolution protocol

A. Laghi, C. Catalano, V. Panebianco, I. Baeli, J. Carbone, R. Iannaccone, R. Passariello; *Rome/IT*

Purpose: To evaluate the sensitivity detection rate of CT colonography for colorectal disorders using a multislice spiral CT scanner.

Materials and methods: Thirty-five patients (20 males; 15 females) with clinical indication for conventional colonoscopy or after unsuccessful performance of conventional colonoscopy were selected. Spiral CT (Somatom Plus 4, Siemens, G) examination was performed after standard oral colonoscopy preparation and colonic distension with room air. Images were obtained using 1 mm collimation, 1 mm reconstruction index, 8 mm/s rotation feed, and mAs 80. Supine and prone acquisitions were obtained in all patients. Images were interactively reviewed on a dedicated workstation using a software with volume-rendering capabilities (Vitrea 2.0, Vital Images, USA).

Results: Images of the distended colon were judged as optimal in all the cases, although artifacts were evident in 2D images due to low mAs value. Dose exposure never exceeded 9.12 mGy for each scan. All colorectal cancers were identified. Sensitivity for detecting polyps was 89 %, with 100 % for lesions larger than 10 mm.

Conclusions: The introduction of multislice technology in CT colonography has improved image quality and simultaneously reduced dose exposure. Larger clinical studies are necessary to assess its improvements in terms of diagnostic accuracy.

B-0588 11:20

Virtual colonoscopy: A painful procedure

D.A. Nicholson, R. Mehan, H. Burnett; *Salford/GB*

Purpose: Virtual colonoscopy (VC) is a new CT based method of large bowel visualisation. For VC to become established as a diagnostic test for colorectal polyp/cancer detection it must be well tolerated and accepted by patients.
Methods: Patients undergoing evaluation of colonic symptoms underwent VC prior to fibreoptic colonoscopy (FC). All patients had standard colonic cleansing/preparation. To perform VC a rectal tube is inserted followed by air insufflation after intravenous Buscopan in order to minimise colonic spasm. A spiral CT of the abdomen and pelvis is then performed. The whole examination generally takes less than 15 minutes. FC was performed using standard intravenous sedatives and muscle relaxants. Before and after both tests patients completed a questionnaire concerning their symptoms of discomfort/pain, abdominal bloating, anxiety and overall preference of techniques. The patients were asked to score each variable on a 100 point scale.
Results: To date 76 patients have been evaluated. Regarding symptoms of discomfort and pain; 35 % of patients experienced no difference with either technique. 48 % found FC more comfortable than VC with only 17 % tolerating VC better than FC. Regarding patient preference scores 21 % patients had no preference, only 21 % preferred FC whereas 54 % would prefer a VC in the future. These preliminary results from thisstudy has shown that patients experience more discomfort/pain with VC compared to FC. However patients prefer VC when asked to choose between these two techniques of colonic imaging. Full results from this on-going trial will be presented.

B-0589 11:25

Spiral CT colonography in postoperatory surveillance after colorectal-cancer: A preliminar study

A. Laghi, C. Catalano, I. Baeli, J. Carbone, R. Iannaccone, V. Panebianco, R. Passariello; *Rome/IT*

Purpose: To assess the role of spiral CT colonography in the postoperatory follow-up of patients with colorectal cancer.
Materials and methods: 15 patients, 7 women and 8 men, aged between 49 and 76 years, one with total colectomy and 14 with emicolectomy were selected. Multislice spiral CT (Somatom Plus 4 Volume Zoom, Siemens, G) examination of the abdomen and pelvis after regular colonoscopy bowel preparation and colonic distension with air was performed. Patients were scanned in supine and prone position with the following parameters: 1 mm collimation, 1 mm reconstruction index, 8 mm/s rotation feed, and mAs 80. Supine scans were acquired after administration of iodine contrast medium for liver evaluation. Images were elaborated and examined on a dedicated workstation. Correlation with conventional colonoscopy was obtained in all patients.
Results: Thirteen patients presented with negative findings at both spiral CT colonography and conventional colonoscopy. In one case a recurrence at the level of the anastomosis was observed. In one patient 8 mm polyp in the descending colon was detected and removed at conventional colonoscopy. In three cases liver metastases were detected.
Conclusion: In patients who have undergone surgical removal of a colorectal cancer, virtual CT colonoscopy could be an effective method of surveillance alternative to conventional colonoscopy. The use of contrast medium injection can be useful in order to evaluate liver metastases which are the main cause of death in patients with surgically treated colorectal cancer.

B-0590 11:35

Virtual colonoscopy as a screening post-operative method: Work-in-progress

P. Leonardou, V. Maniatis, S. Kavadias, N. Tsavaris, A. Papadopoulos, K. Stringaris, G. Zois, G. Zois; *Athens/GR*

Purpose: To evaluate virtual colonoscopy (VC) as a screening method in patients who have been operated for colon cancer.
Materials and methods: VC has been performed in 18 patients during post-operative screening. Six of them had permanent colostomy, 3 had underwent right hemicolectomy, 4 low-anterior colon resection and 5 sigmoidectomy. They were 7 women and 11 men (29 – 84 years old). 17/18 patients were examined during regular follow-up while in one case there was a strong suspicion for relapse. All these patients could not have a complete follow-up study by other methods because of post-operative adhesions/permanent colostomy or patient's refusal to have a conventional colonoscopy. CT protocol consisted of: slice thickness: 5 mm, table feed: 10 mm/s, reconstruction index: 5 mm, in both supine and prone position after distending the colon with air. VC images were created in an Easy Vision (Philips) workstation.
Results: Relapse was confirmed with VC in the suspicious case. In the rest of our cases no findings of relapsing were depicted and that came to agreement with the clinical/laboratory evaluation and the course of the disease.
Conclusion: VC is a well-tolerated imaging method for the evaluation of the colon. The absence of false negative results in our study leads to the conclusion that VC can be a reliable diagnostic tool for screening patients who have underwent an operation for colon cancer.

B-0591 11:40

CT colonography in Crohn's disease

Z. Tarjan, T. Zágoni, Z. Éles, E.K. Makó; *Budapest/HU*

Purpose: To evaluate CT colonography in patients with colonic Crohn's disease.
Material and methods: Five patients with known (4) or suspected (1) Crohn's disease of the colon underwent fiberoptic colonoscopy and CT colonography in the same day or in a weeks period. The images were evaluated with zoomed axial slice movie technique and in some region intra- and extraluminal surface shaded and volume rendered images were generated on a separate workstation. The results were compared to those of colonoscopy.
Results: The final diagnosis was Crohn's disease in four patients and Colitis ulcerosa in one. Total examination was possible by colonoscopy in two cases, with CT colonography in all the five cases. The wall of those segments severely affected by the disease were depicted by the axial CT scans to be thickened. The thick walled, segments with narrow lumen seen on CT colonography corresponded to the regions where colonoscopy was failed to pass. Air filled sinus tracts, thickening of the wall of the terminal ileum, loss of haustration pseudopolyps and deep ulcers were seen in CT colonography. Three dimensional endoluminal views demonstrated pseudopolyps similar to endoscopic images None of the colonoscopically reported shallow ulcerations or aphtoid ulcerations or granular mucosal surface were observed on two- or three-dimensional CT colonographic images.
Conclusion: CT colonography by depicting colonic wall thickening seems to be a useful tool in the diagnosis of Crohn's colitis, which could be a single examination depicting the intraluminal, and transmural extent of the disease.

B-0592 11:50

Virtual colonography. Space resolution vs. radiation dose in search for polyps: An experimental study

P. Fencl, M. Zavoral, J. Lacman, P. Kubikova, M. Vasicek, M. Heissler; *Prague/CZ*

Purpose: The aim of this study was to experimentally evaluate the space resolution of CT virtual colonography (CTC) using different scan parameters and calculate the accordant skin dose.
Material and methods: Ten artificial polyps of a diameter from 2 to 7 mm have been investigated by CTC using Somatom Plus 4. Power with single slice Ultra Fast Ceramic detectors and workstation VIRTUOSO. Constant parameters of the protocol were: 120 kV; 50 mA; kernel 4.5 and 2 mm increment of reconstruction. Variable parameters were: slice 5 mm, pitch from 1 to 1.5; slice 3 mm, pitch from 1 to 2.33; slice 2 mm, pitch from 1.5 to 2.5. The space resolution has been assessed and skin dose has been calculated.
Results: The increase of the slice thickness results in the increase of mAs. The decrease of the slice thickness improves the shape of polyp's surface. The increase of pitch reduces the radiation dose. The average skin dose of CTC was 7.2 mSv, the range of the observed values based on different parameters of both the slice and the pitch was from 94.9 to 157.08 per cent.
Conclusion: Our CTC protocol made by 5 mm slice, pitch 1.4 is associated with very low radiation dose. The decrease of slice thickness improves the space resolution. The increase of pitch allows further reduction of skin dose. The practical benefits of this experiment will have to be proved by clinical trial.

B-0593 11:55

The accuracy of computed tomographic colography (CTC) in polyp and cancer detection

D.A. Nicholson[1], R. Mehan[1], H. Burnett[1], C. Summerton[2]; [1]*Salford/GB*, [2]*Manchester/GB*

Purpose: CTC is a new technique allowing minimally invasive imaging of the colon. We are conducting a clinical trial which has been funded by the North West R&D NHS scheme to determine the accuracy of CTC compared to fibreoptic colonoscopy (FC) in detecting colonic polyps and cancer

Methods: To date, 96 patients of 200 have been recruited. Patients undergo CTC on the same day as FC. Standard bowel cleansing is given to patients. CTC is performed in both supine and prone positions using a single breath hold, spiral CT following intravenous Buscopan and air Insufflation. The findings of CTC are being correlated with the findings of FC in each patient.

Results: To date 76 patients have been analysed, A total of 37 polyps in 28 patients were detected by FC (28 of these polyps were < 1 cm in diameter). CTC detected all polyps greater than 1 cm but only 15 of the 28 polyps < 1 cm in diameter. In addition 4 false positives on CT were identified. 4 cancers seen at FC were all detected by CTC. Additionally CTC detected a further cancer in the right side of the colon not reached at FC and a renal cell carcinoma in another patient. FC was completed to the ceacum in only 65 patients (84 %) whereas CTC was completed in all.

Discussion: Initial results show that CTC is a sensitive method of detecting colonic cancer and polyps > 1 cm in size. This abstract will present the up to date figures of this on-going trial.

10:30–12:00 **Room K**

Pediatric

SS 1012

Genitourinary and central nervous system

Chairpersons:
G. Enriquez (Barcelona/ES)
R. Fotter (Graz/AT)

B-0594 10:30

MR-urography in neonates and infants with dilated upper urinary tract: Preliminary experience

M. Riccabona, J. Simmbrunner, E. Ring, R. Fotter; *Graz/AT*

Purpose: To evaluate the feasibility and diagnostic potential of dynamic MR-urography (MRU) in neonates and infants with sonographically detected dilatation of the upper urinary tract.

Patients and methods: 20 infants (age: 5 days – 18 months, mean: 1.5 months, male:female = 16:4) underwent MRU after oral sedation using T2 and contrast enhanced dynamic T1 weighted sequences. The results were compared to the findings of ultrasound (US, 20), intravenous urography (IVU, 12) and/or scintigraphy (16) based on the criteria suggestive of obstructive uropathy.

Results: Oral sedation was sufficient to perform MRU with diagnostic image quality in 19 patients. Diagnosis of the 40 kidneys included: normal system (7), duplex system (6), vesicoureteral reflux (8), megaureter (7), uretero-pelvic junction obstruction of various degrees (15), and dysplastic/cystic kidney (4), with complex pathology in 7 kidneys. MRU demonstrated anatomy better than by IVU, particularly concerning the parenchyma, the ureter, and pelvic dilatation – on T2 weighted sequences in 3 patients with non- or poorly functioning systems. MRU was superior to ultrasound in showing ureteral pathology. Tiny cysts in dysplastic kidneys were better shown by US. Gadolinium enhanced dynamic MRU allowed assessment of obstruction applying IVU criteria with equal quality. The results matched IVU results and/or scintigraphic findings.

Conclusion: MRU can be performed in infants and neonates with sufficient image quality using oral sedation. MRU properly depicts anatomy and allows assessment of urinary tract obstruction better than US and IVU. It additionally provides functional information and therefore has the potential to replace IVU.

B-0595 10:40

Gadolinium enhanced T1-weighted vs. T2-weighted MR urography in children with abnormalities of the upper urinary tract

G. Staatz, C.C.A. Nolte-Ernsting, D. Rohrmann, C. Stollbrink, P. Haage, J. Tacke, R.W. Günther; *Aachen/DE*

Purpose: To evaluate gadolinium enhanced T1-weighted MR urography (GMRU) versus T2-weighted MR urography in children with upper urinary tract abnormalities.

Methods and materials: 65 children, aged 3 weeks to 15 years, with upper urinary tract disorders underwent MR urography in a 1.5 T scanner. After an i.v. injection of low dose furosemide (0.05 mg/kg/bw), GMRU was performed with respiratory-gated, coronal 3D-gradient-echo sequences, using maximum-intensity projections for postprocessing. Respiratory-triggered Half-Fourier RARE images (HASTE) were obtained for T2-weighted MR-urography. MR-urography findings were compared to the final consensus diagnosis.

Results: MR urography was successfully performed in all cases, with only 3 of 65 children needing sedation. Gd-enhanced MR urography revealed a superior diagnostic accuracy compared to T2-weighted MR urography in non-dilated collecting systems (horseshoe kidneys, ectopic kidneys, duplex systems, single ectopic ureters, ureteroceles). GMRU and T2-weighted MRU were equivalent in the assessment of an obstructed but normal functioning urinary tract (UPJ-obstructions, megaureters). Non-functioning dilated collecting systems and multicystic dysplastic kidneys were best visualized by T2-weighted MR urography.

Conclusion: Respiratory-gated T1-weighted MRU allows accurate and sufficient evaluation of urinary tract abnormalities. T2-weighted MRU complements GMRU in the evaluation of non-functioning renal units and cystic diseases of the kidney.

B-0596 10:50

Radiological monitoring of tumor response to medical treatment in children with Wilm's tumor

A. Abramyuk, V. Zhelow, Z. Stadnyk; *Lviv/UA*

Purpose: It is well known, assessment of treatment efficacy is of great importance to patient management. The aim of our study was to analyse dynamics of US, CT findings in children with Wilm's tumor during preoperative chemotherapy (PCT).

Methods and materials: 21 children with Wilm's tumor in late stages of disease (9 boys and 12 girls) were examined by ultrasonography and computed tomography with bolus contrast-enhancement (CE) (Ultravist, 2 ml/kg) before and 24 – 48 hours after course of PCT. All children were considered good respondents to treatment, confirmed by the pathologic examination. The evaluation of tumor volume, tumor composition, vascularity and contrast-enhancement was made.

Results: 17 patients (81 %) showed gradual decrease of tumor volume, increase of heterogeneity with some growth of Resistive index (RI) in 2 of them and reduced CE in 6 of them. In the 3 patients (14 %) tumor volume remained unchanged, but there was some increase internal heterogeneity in all of them, growth of Resistive index and reduction of CE in 1 of them. 1 patient (4 %) demonstrated slight enlargement of tumor volume with marked cystic degeneration without measurable change of RI, patchy CE.

Conclusion: Although volume is most significant indicator of tumor response, other criteria such as tumor composition and vascularity also can be used in assessing tumor sensitivity to medical treatment.

B-0597 10:55

Echo-enhanced color Doppler sonography of vesico-ureteral reflux in children

M. Riccabona, E. Ring, F. Lindbichler; *Graz/AT*

Purpose: To evaluate the potential of echo-enhanced color Doppler sonography (ee-CDS) in the diagnosis of vesicoureteral reflux (VUR) in children in a prospective study.

Patients and method: 30 children (0 – 10 years) with suspicion of or known VUR were submitted for echo-enhanced ultrasound (ee-US), ee-CDS and conventional voiding cystourethrography (VCU). Ee-CDS was performed after instillation of Leveovist into the catheterized urinary bladder that had been filled with saline solution. Thereafter VCU was performed in the same session. The results of ee-US and ee-CDS were compared to VCU findings.

Results: Levovist was safe and easy to administer. Sonography detected VUR into 2 renal units (grade II and III) not seen by VCU, but missed VUR grade I in all 3 cases. Demonstration of VUR grade II and III was better by ee-CDS than ee-US.

Conclusion: Levovist is a safe sonographic contrast material for use in the pediatric bladder. It enables relaible visualization of VUR into the renal collecting system. Ee-CDS enhances contrast reflux, particularly in non-dilative or minimal dila-

tive VUR that is sometimes difficult to depict with ee-US. Ee-CDS therefore improves the sonographic visualization of VUR. However, echo-enhanced VUR-sonography cannot replace VCU.

B-0598 11:05

Ganglioneuroma and ganglioneuroblastoma in the differential diagnosis of adrenal tumours in childhood: MR imaging appearances

G.K. Schneider, K. Altmeyer, S. Aliani, N. Graf, M. Takahashi, R. Seidel, B. Kramann; *Homburg a. d. Saar/DE*

Purpose: The most frequent tumours found in the region of the adrenal gland in childhood are neuroblastomas and as a nonadrenal differential diagnosis nephroblastomas. Beside this tumours there are several rare tumours in childhood like adrenal adenomas, adrenal carcinomas or ganglioneuromas which have to be considered in DDX.

Materials and methods: Between 1995 and 1999 47 children with suspicion of a renal or adrenal tumour have been admitted to our hospital for further diagnostics and therapy. All patients underwent unenhanced and contrast-enhanced MRI for further work-up of differential diagnosis. MRI examinations were performed on a 1.5 T scanner applying T1w, T1w fs and T2w sequences unenhanced and after injection of 0.1 mmol/kg Gd-DTPA.

Results: Among the studied patients, 3 children presented with the histologically proven diagnosis of ganglioneuroma, in one patient ganglioneuroblastoma was diagnosed. In contrast to the patients suffering from neuroblastoma, MRI in these patients showed clearly delineated tumours of the adrenal gland without encasement of vessels of the upper abdomen.

Conclusion: Although malignant tumours like neuroblastoma and nephroblastoma account for the majority of lesions in the upper retroperitoneum in children, benign lesions like ganglioneuroma have to be considered in DDX to avoid unnecessary overtreatement. Since imaging features of these benign lesions in MRI are distinguishable from malignant tumours, the awareness of this diagnosis is of high clinical importance.

B-0599 11:15

Non-accidental injury: A retrospective analysis of a large cohort of patients

H.M.L. Carty, A. Pierce; *Liverpool/GB*

Purpose: To highlight the way in which the diagnosis of child abuse is made, provide a detailed analysis of the radiologically detectable injuries, and an analysis of the outcome of the effect of abuse on the children.

Method: The cohort of 467 children represented 285 males and 182 females.

Results: The diagnosis of NAI was based on admission of assault, agreed medical evidence, or a decision of the Court in cases of disputed medical evidence. There were 37 deaths in the cohort. Twenty six of these children died from head injury due to shaking and 3 from head injury without radiological evidence of shaking. A total of 408 children sustained 1689 fractures, of which 268 children had multiple fractures and 140 had a solitary fracture. One hundred and forty eight children had a diagnosis of a shaking or a shaking impact injury, of whom 99 had skeletal injury.

Conclusion: This presentation represents a very large series and demonstrates the spectrum of injury, the spectrum of the way in which the diagnosis is made, which is usually based on agreed medical evidence and seldom on admission of guilt, and provides for radiologists some outcome data which is rarely available for such a large cohort.

B-0600 11:25

Pattern analysis of periventricular blood flow using power Doppler US in newborns

H. Goo, J.-W. Kim, C. Yoon; *Seoul/KR*

Purpose: To evaluate pattern of periventricular blood flow on power Doppler ultrasound (US) in newborns according to gestational age at US examination and the presence of intracranial hemorrhage.

Materials and methods: In 42 newborns, 71 coronal and sagittal power Doppler US examinations were performed. The newborns were divided into three groups according to their gestational age at US examination: group 1, less than 32 weeks; group 2, between 32 and 38 weeks; group 3, above 38 weeks. Setting of imaging parameters was fixed in all examinations. Among them, pulse repetition frequency was set to 500 Hz for the optimal visualization of periventricular blood flow. Visual grading analysis was used for evaluation of periventricular blood flow. Three patterns of periventricular blood flow were graded according to the extent of color signal. Effects of both the gestational age at US examination on periventricular blood flow and periventricular blood flow on development of intracranial hemorrhage were analyzed.

Results: Pattern of periventricular blood flow on power Doppler US was significantly different among three groups ($p < 0.001$), but not between the newborns with and without intracranial hemorrhage. The smaller the gestational age at US examination, the more prominent the periventricular blood flow.

Conclusion: Periventricular blood flow on power Doppler US appears to be inversely related to gestational age at US examination of newborns. In addition, periventricular blood flow visible on power Doppler US may not be useful for the prediction of intracranial hemorrhage in newborns.

B-0601 11:35

MRI of the brain: Findings after bone marrow transplantation in children

H.-J. Mentzel, D. Fuchs, J. Taut, C. Fitzek, B. Gruhn, W. Behrendt, F. Zintl, W.A. Kaiser; *Jena/DE*

Purpose: Bone marrow transplantation (BMT) is increasingly used in the treatment of malignant diseases in childhood. The aim of this presentation was to evaluate possible morphologic alterations in the brain of children and adolescents after BMT.

Subjects & methods: Cranial MRI before BMT was performed in all patients (age < 18 a) who received BMT since 1994 (n = 74) on a 1.5 T MR-scanner with standard sequences (axial T1w SE, coronal T2w TSE). In cases of abnormalities further sequences were added. 37 patients were examined by cranial MRI before and after successful BMT. The time between BMT and follow-up MRI was over 3 months.

Results: Serious brain changes (arteriovenous malformation, aspergilloma) were detected in 2/74 patients (2.7 %) before BMT which allowed prompt therapy. Further findings before BMT: enlargement of CSF spaces (n = 16), unspecific white matter lesions (n = 7), dysplasia (n = 2), venous angioma (n = 3), cysts (n = 8), heterotopia (n = 1), neurinoma (n = 1). After BMT CSF spaces were enlarged in 9/37 patients (24 %) and smaller in 1 patient (2.7 %). Unspecific white matter lesions were seen increasingly in 3 and reduced in 3 patients. In 2 asymptomatic patients aspergilloma was detected; 1 patient showed signs of old infarction; hemosiderin was detected in 2 patients, 1 patient showed signs of vasculitis.

Conclusion: The detection of brain changes before BMT allow prompt therapy. So, possible complications during and after BMT could be prevent. Brain changes following BMT were predominantly enlarged CSF spaces. Many kind of further CNS complications were reported.

B-0602 11:40

Narrowing of the vertebral arteries at the cranio-cervical junction. A potential risk factor for sudden infant death syndrome (SIDS): Preliminary results of a postmortem study

S. Puig, K. Heimberger, M. Wald, N. Klupp, O. Ipsiroglu, C. Reiter, A. Pollak, E. Schindler; *Vienna/AT*

Purpose: To evaluate the influence of head rotation with or without neck extension on the vertebral arteries in children who died of sudden infants death syndrome (SIDS) compared with infants who died for other reasons in postmortem angiograms.

Method and materials: The vertebral arteries of six children (age: 9 days – 15 months) were studied using digital substraction angiography. Contrast-media was injected directly in the vertebral arteries after removing the intrathoracic organs and the brain. Angiograms were performed in neutral and rotated position of the head, with and without neck extension. Our results were compared with the final diagnosis established by the Institute of Forensic Medicine.

Results: The final diagnosis was SIDS in three and trauma in three children. 5/6 children showed a relative narrowing of the vertebral artery in the atlantoaxial region in neutral position of the head. In children who died of SIDS the narrowing of the vertebral arteries increased after head rotation with or without neck extension.

Conclusion: In children who died of SIDS, anatomic variations maybe responsible for increased narrowing of the vertebral arteries during head rotation and/or neck extension as it occurs, for example, in prone sleeping.

B-0603 11:45

Idiopathic external hydrocephalus: MRI differentiation from cerebral atrophy

H. Ilaslan, E.N. Faerber, D. White; *Philadelphia, PA/US*

Purpose: To determine the MRI criteria for diagnosing idiopathic external hydrocephalus (IEH) and differentiation from cerebral atrophy (CA).

Materials and methods: Retrospective review of 55 cranial MRIs of children under 2 years of age, diagnosed with IEH and CA from January 1998 through August 2000, was performed. Children with a history of systemic or CNS insults were excluded. Size of ventricles, sulci and interhemispheric fissures, as well as myelination patterns were evaluated.
Results: There were 37 EIH and 18 CA cases. Ventricles were normal size in 32 (86 %) cases of IEH compared to 2 (11 %) cases of atrophy. Dilatation of subarachonoid space was confined to the frontal area in 34 (92 %) cases of IEH and appeared diffuse in 15 (83 %) cases of infants with atrophy. Interhemispheric fissure dilatation was limited to the frontal area in 30 (81 %) cases of IEH whereas it was diffuse in 11 (61 %) cases of atrophy. Myelination was appropriate for the age in all cases of IEH but delayed in 2 (11 %) cases of CA.
Conclusions: Radiologic similarities between IEH and cerebral atrophy may create diagnostic challenges. MRI findings of IEH include: dilated frontal subarachnoid space and minimal or no ventricular dilatation in contrast to CA, where there is diffuse dilatation of sulci and enlarged ventricles. These findings are usually helpful to differentate these two conditions, even without clinical information.

B-0604 11:50

High resolution ultrasound of the cranial vault: A complementary tool in the diagnostic approach to head trauma in the paediatric population
E.A. Gallardo sr., I.M. Barber jr., X. Codina sr., X.C. Serres sr., N.G. Roson sr., V.F. Garriga sr.; *Granollers/ES*

Purpose: Despite the little value in obtaining skull films in the setting of head trauma, this continues to be a current practice at many centres. In cases of suspicion of fracture a CT examination is derived because of the medico legal implications even without neurological symptoms. Our purpose is to demonstrate that HRUS is a complementary tool in evaluating the cranial vault fracture when other techniques (X-Ray or CT) are not conclusive.
Methods and material: 10 patients under the age of 2 years, 6 boys and 4 girls, with head trauma were evaluated during the last 2 years. All of them had a clinical suspicious of cefalohematoma and/or conventional X-Ray suspicious of fracture. We performed HRUS in all of them and correlation with plain film and CT images was assessed. A multifrequency linear probe 10 – 12 MHz was used (Logiq 700 GE).
Results: CT and US demonstrated a cranial vault fracture in 6 patients. In one patient CT failed in the detection of the fracture but US was able to demonstrate it. In the other three patients no fracture was demonstrated by both techniques although there were linear images in the cranial X-Ray that suggested this diagnosis. In two of these patients a cefalohematoma was visualized in the US study.
Conclusion: HRUS is an excellent technique in the evaluation of cranial vault fractures in paediatric population. The absence of fracture in US may avoid a CT examination in children with doubtful images in the skull radiography and without neurological symptoms.

B-0605 11:55

MRI assessment of cavum septi pellucidi and cavum vergae in newborn with hydrocephalus internus
S.P.G. Mantke[1], M. Riccabona[2], J. Simbrunner[2], F. Anderhuber[2], F. Ebner[2]; *[1]Hartlepool/GB, [2]Graz/AT*

Subject: Comparison between newborns with hydrocephalus internus (hi) and non hydrocephalus (nh) concerning the primitive midline structures cavum septi pellucidi (csp) and cavum vergae (cav) in mri scans.
Introduction: Csp and cav are physiological midline structures of the perinatal and neonatal period. In the newborn the obliteration commences from the posterior part (cav, splenium corporis callosi) to the anterior part (genu corporis callosi, csp). In neurological disorders (epilepsy, juvenile brain tumours, hydrocephalus, ...) or retardation of the myelinisation the obliteration is delayed.
Material and methods: Approximately 663 mri scans of newborns (< 1 year) are retrospectively reevaluated for the appearance of csp and cav. The mri scans are subdivided in newborns with hi (n = 52) and nh (n = 621).
Results: In the mri scans of nh newborns there are 18 csp (2.9 %) seen, also 15 of these newborns have a cav (2.4 %). In comparison to the population of hi newborns 18 csp (34.6 %) are detected, 14 of these have also a cav (27 %).
Conclusion: In mri scans of newborns with hydrocephalus internus show a 10 times higher relative rate of midline caves like the csp and cav. The causes for this findings are unknown. Maybe a obstruction of the foramen monroi could be discussed. Cystic csp and cav rupture if the coronar diameter will be bigger than 10 mm.

10:30–12:00 **Room L/M**

Head and Neck

SS 1008

Larynx and pharynx

Chairpersons:
R. Hermans (Leuven/BE)
A. Wuttge-Hannig (Munich/DE)

B-0606 10:30

Role of spiral computed tomography in patients with cricothyroid approximation
D. Pickuth, S. Brandt, K. Neumann, A. Berghaus, R. Spielmann, S. Heywang-Köbrunner; *Halle a. d. Saale/DE*

Purpose: Cricothyroid approximation raises the vocal pitch by simulating the contraction of the cricothyroid muscle with sutures. The aim of this study was to determine the role of spiral computed tomography (CT) in patients scheduled for cricothyroid approximation.
Patients and methods: 29 transsexual patients were examined with spiral CT before and after laryngoplastic surgery. CT findings were correlated with phoniatric findings in all patients.
Results: The average reduction of the cricothyroid distance was 6 mm (range 2 – 10 mm). The vocal pitch elevation was more remarkable in the patient group with great reduction of the cricothyroid distance ($p < 0.01$).
Conclusion: CT accurately determines the cricothyroid distance before and after surgery and is an ideal method for follow-up purposes, especially when there is a postoperative reversion towards a lower pitch. In addition, CT provides important data as to the most appropriate extent and site of intracordal intervention to be done for a desired pitch elevation.

B-0607 10:40

Laryngo-pharyngeal trauma: Imaging findings and clinical scenarios
M. Scaglione, A. Pinto, R. Grassi, F. Pinto, F. Lassandro, G. Rossi, E. Bove, L. Romano; *Naples/IT*

Purpose: To show the usefulness of CT in the assessment of laryngo-pharyngeal injuries following blunt trauma, by reviewing our 10 years' experience.
Material and method: Between January 1990 and April 2000, 250 consecutive patients with cervical blunt trauma were referred at our Emergency Department. Based on the physical examination findings, 87/250 patients were excluded from any diagnostic test. The remaining 163 patients were submitted to both CT scanning of the neck and to laryngoscopic evaluation.
Findings at CT and laryngoscopy were indipendently evaluated before classifying patients as having grade 1 or grade 2 lesions: grade 1 included the presence of minor injuries (mild edema, laryngeal hematomas or minor laryngeal lacerations); grade 2 included evidence of major injuries (subcutaneous emphysema, mucosal disruption and/or laryngeal fractures without exposed cartilages).
Results: Laryngo-pharyngeal injuries were identified in 137/250 patients submitted to CT evaluation. Findings at CT included: 85 laryngeal hematomas, 37 laryngeal fractures, and 3 laryngo-tracheal avulsion and 12 pharyngeal disruption; moreover, three post-traumatic arterial pseudoaneurysms were shown.
Conclusion: Fast dynamic or helical CT are a good adjunct to physical examination, especially when physical findings are equivocal. CT permits quick and reliable evaluation of the upper airways as well of the soft tissue and the fascial planes and it is helpful in deciding whether injuries are to be managed conservatively or need surgical treatment.

B-0608 10:45

A new approach to single-bolus spiral-CT of laryngopharyngeal carcinomas: Comparison of different contrast volumes, flow rates, and start delays
M. Keberle, A. Tschammler, D. Hahn; *Würzburg/DE*

Purpose: To evaluate the impact of different protocols on the contrast performance of neck structures, including squamous cel carcinoma (SSC) in Spiral-CT with single-bolus technique.
Method and materials: 70 patients with SCC (larynx/hypopharynx n = 32, oropharynx n = 38) were prospectively randomized into four groups using different protocols (125 ml at a flow of 2.5 ml/s, 100 ml at 2.0 ml/s, 90 ml at 1.5 ml/s, or 70 ml at 1.0 ml/s). Dynamic series of the tumors were performed. In all relevant anatomical neck structures and in the boundary and center of tumors, time-density curves

were obtained. The protocols were compared regarding time and level of maximum tumor enhancement (MTE), and time of carotid artery enhancement (CAE) of > 150 HU; one selected protocol was tested in 20 consecutive routine-examinations (rotation-time 1.0 s) at start-delays of 40 s (for laryngeal/hypopharyngeal tumors; 3/4.5/3) and 45 s (for oropharyngeal tumors; 5/7.5/5).
Results: In contrast to 70 ml at 1.0 ml/s, the other protocols performed similarly well yielding a comparable MTE at 52 s and later. In spite of the smaller volume of 90 ml, due to the prolonged flow-time of 60 s at 1.5 ml/s, the CAE of > 150 HU was prolonged (compared to 100 or 125 ml). Due to these circumstances, 90 ml at 1.5 ml/s was considered more effective and, therefore, tested in routine providing MTE and good CAE.
Conclusion: Using the aforementioned start-delays, a single bolus of 90 ml at 1.5 ml/s appears to reliably provide both, excellent tumor contrast and good vessel enhancement.

B-0609 10:55

Multidetector spiral CT in the preoperative workup of small laryngeal tumors

R. Brüning, C. Sturm, C. Hong, B. Wollenberg, M. Reiser; *Munich/DE*

Purpose: For the preoperative evaluation of larynx tumors the detection of spread into the glottic fat, crossing the anterior commissure, infiltration of the arythnoids and the extension along the vocal cords are crucial to determine the adequate treatment. Purpose of the study was to determine the predictive values of multislice helical CT (MSCT) for the infiltration of deep laryngeal structures.
Material/methods: Thirty patients with suspected laryngeal cancer (mean age 63 ± 11 years) were investigated on a MSCT scanner (Siemens) with 1 mm collimation, 0.5 seconds rotation time and a coverage of the entire larynx in a single breathhold. Multiplanar reconstruction's (MPR) in sagittal and coronal plane were reconstructed. All findings were compared to surgery and histology.
Results: The sensitivity, specificity, positive and negative predictive value of MSCT regarding the infiltration of the glottic region were 93 %, 85 %, 88 % and 92 % and regarding infiltration of the anterior commissure were 85 %, 94 %, 92 % and 88 %, respectively. Sensitivity, specificity, positive and negative predictive value of MSCT regarding the infiltration of the anterior part of the vocal cords were 89 %, 92 %, 94 % and 85 % and regarding the infiltration of the arythnoids were 83 %, 96 %, 83 % and 96 %, respectively.
Conclusion: Multislice-CT has a high predictive value to determine deep extension of laryngeal tumors and is recommended for the preoperative evaluation.

B-0610 11:05

Multiplanar imaging of the larynx and hypopharynx: Analyis of 40 cases

M. Lell, U. Baum, H. Greess, A. Noemayr, W.A. Bautz; *Erlangen/DE*

Purpose: To evaluate the potential of functional multiplanar imaging of the larynx and hypopharynx.
Material: 40 patients with tumors of the larynx and hypopharynx were examined with multislice spiral CT during quiet breathing, e-phonation and modified Valsalva maneuver (4 × 1 mm slice collimation). 2 investigators analyzed axial, sagittal and coronal plane orientation for delineation of anatomical structures and tumor margins.
Results: Sufficient image quality was achieved in each examination except 2 examinations with Valsalva maneuver and 1 examination with e-phonation. Both Valsalva maneuver and e-phonation showed best results in demonstrating the piriform sinuses, e-phonation was optimal to delineate the vocal cords (axial plane) and especially the sinus Morgagnii (coronal plane). Tumor delineation was best on axial images, but sagittal and coronal images provided additional information about tumor margins.
Conclusion: MSCT with multiplanar reformations is a valuable tool for exact tumor staging in tumors of the larynx and hypopharynx. Functional studies add valuable additional information.

B-0611 11:15

Virtual laryngoscopy in the evaluation of laryngeal cancer. Does it really help? Work in progress

A. Fotinos, V. Maniatis, A. Michaelides, A. Papadopoulos, S. Kavadias, G. Zois, K. Stringaris; *Athens/GR*

Purpose: To estimate the usefulness of virtual laryngoscopy in the evaluation of laryngeal cancer.
Materials and methods: We conducted a) spiral CT (axial level) of the neck after i.v.injection of contrast medium (slice thickness: 3 mm, table feed: 5 mm, reconstruction index: 3 mm) and b) virtual laryngoscopy (reconstruction of axial raw data-slice thickness: 1.5 mm, table feed: 3 mm, reconstruction index: 1 mm) in 11 patients (age: 40 – 72 a) with an endoscopic diagnosis of laryngeal tumor. Each patient's spiral CT and virtual laryngoscopic images were assessed in order to estimate the presence and extension of the tumor. We compare the results of spiral CT and virtual laryngoscopy. We also compare the conventional endoscopy results, concerning tumor extension, with virtual laryngoscopy.
Results: In 11/11 patients spiral CT and virtual laryngoscopy demonstrated the presence of a laryngeal tumor. Histological diagnosis was laryngeal cancer in all patients. In 8/11 patients virtual laryngoscopy was superior compared to conventional endoscopy in estimating the tumor extension, while in 3/11 patients the results of the two methods were equivalent. However in every patient spiral CT of the neck provides all the information offered by virtual laryngoscopy, giving also additional information (infiltration of cartilages, adjacent soft tissues, lymph nodes) useful in the staging and therapeutic planning.
Conclusion: According to our results virtual laryngoscopy represents a simple non-invasive method for the accurate diagnosis of laryngeal cancer, but spiral CT of the neck seems to offer a more useful and comprehensive evaluation of this entity.

B-0612 11:25

Value of volume rendering in the evaluation of laryngeal cancer

F. Cademartiri, N. Piazza, G. Luccichenti, V. Lucidi, M. Squarcia, P. Pavone; *Parma/IT*

Purpose: To determine the usefulness of three-dimensional volume rendering technique for evaluation of laryngeal cancer.
Materials and methods: 14 patients with diagnosed laryngeal cancer underwent spiral-CT scan. Images were obtained at 2 mm collimation and 1 mm reconstruction interval through the neck after contrast media injection. Reconstructed images were sent to a workstation running on a NT platform equipped with post-processing software (Vitrea 2.0 – Vital Images, USA) allowing 3D reconstructions in order to generate virtual laryngographic images and virtual laryngoscopic examinations. Axial, MPR and 3D reconstructed images were reviewed by two independent radiologists.
Results: All lesions above 6 mm in diameter were demonstrated. 3D evaluation was better in qualitative evaluation of extension the lesions. Multiplanar reformatted images were particularly useful for the evaluation of extension and spatial relationships of the lesions. Invasion of structures were not visible at all on volume rendered images.
Conclusion: This preliminary experience on 3D laryngoscopy shows the potential of this tecnique in the evaluation of laryngeal cancer.

B-0613 11:30

Functional SONO-CT real-time compound imaging of the larynx: Technique, preliminary results in normal subjects and potential applications

C.H. Buitrago-Téllez, M. Reimers, U. Witte, D. Wruck, U. Otto, G.M. Bongartz; *Basle/CH*

Purpose: To assess the functional SONO-CT real-time compound imaging technique to evaluate vocal cord mobility.
Methods and materials: The real-time compound imaging technique obtaining images acquired with nine different incidence angle of the ultrasound beam was evaluated concerning its ability to detect vocal cord mobility in respiration, deglution, valsalva maneuvre and a-phonation in 10 normal subjects. Moreover, a patient with cricoid fracture and tracheotomy was evaluated for vocal fold mobility. The movements were documented by video.
Results: Real-time compound imaging allowed the visualisation of vocal cord mobility in all normal volunteers with marked reduction of artifacts. In the patient with cricoid fracture a bilateral movement integrity could be demonstrated, in spite of severe swelling.
Conclusion: Functional real-time compound ultrasound imaging seems to be a promising technique without radiation exposure to evaluate vocal cord mobility/fixation and may be potential clinically relevant in staging of laryngeal cancer.

B-0614 11:40

Helical CT of the upper airway with three-dimensional
Techniques and clinical applications

D. Wang, W.S. Zhang, J.X. Xu; *Beijing*

Purpose: To evaluate [illegible] application of helical CT three-dimensional [illegible] upper airway.
Ma[illegible] [illegible]lical CT was performed with 3.0 mm slice thickness a[illegible] 0 normal subjects and 60 patients with upper airway diseases. In [illegible]ealthy group, the upper airway shaded surface display (SSD) was pro-

cessed by using different reconstruction interval (1.0~3.0 mm) and upper threshold (ranged from 0 to -900 HU), and in the patient group, SSD, RaySum and integrated 3D images were done respectively.
Results: The optimal upper airway SSD image could be obtained using reconstruction interval 1.0 mm and upper threshold –500 HU. SSD could display the normal shape of the upper airway, and provide panoramic view of the airway compression by lesion from multiple views. It was better to investigate the internal margin of the narrowed airway. Airway appeared normal in 25 % cases. The involved extents detected on SSD image was significantly smaller than that of axial images. The integrated 3D image could clearly demonstrate the relationship between the tumor and adjacent structures such as vessels and airway.
Conclusion: Spiral CT 3D reconstruction can provide a three-dimensional image of the airway diseases, and is a good complementary method of axial and MPR images.

B-0615 11:50

Dynamic MRI of the pharynx during swallowing and for assessment of velopharyngeal closure in comparison to videofluoroscopy
A.J. Beer, C. Hannig, P. Hellerhoff, M. Settles, A. Wuttge-Hannig, R. Sader, E.J. Rummeny; *Munich/DE*

Purpose: Evaluation of the value of dynamic MRI in the assessment of swallowing and velopharyngeal closure in comparison to videofluoroscopy.
Materials and methods: 5 healthy volunteers and 5 patients suffering from velopharyngeal dysfunction or disorders of tongue movement underwent videofluoroscopy and dynamic MRI, using a T1-FFE fast gradient echo sequence (TR 3.2, TE 0.9, fa 10, slice thickness 1.5 cm) with 6 images per second. Images were acquired in the midsagittal plane and in the coronal and/or axial plane during swallowing of diluted magnevist-enteral and during phonation of several test phrases for the assessment of velopharyngeal closure.
Results: In all cases, dynamic MRI was able to show the important oral and pharyngeal stages of swallowing, including velopharyngeal closure, elevation and anterior movement of the larynx and closure of the epiglottis. In healthy subjects, complete velopharyngeal closure and full backward and upward movement of the soft palate was observed during phonation. Velopharyngeal dysfunction was successfully detected by dynamic MRI. The axial plane was acquired at the position af maximal velopharyngeal closure, so that objective measurements of the velopharyngeal area in square millimeters could be made. No discrepancies between videofluoroscopy and dynamic MRI were observed. Concerning the detection of tongue movement disorders, dynamic MRI seemed superior to videofluoroscopy due to higher soft tissue contrast.
Conclusion: Dynamic MRI has the potential to accurately evaluate deglutition, velopharyngeal function and tongue movement while avoiding the disadvantages of naso-endoscopy and videofluoroscopy in being non-invasive and free of radiation exposure.

10:30–12:00 **Room N/O**

Cardiac

SS 1003

Heart: CT/MRI/MRS

Chairpersons:
M. Oudkerk (Groningen/NL)
A.E. van Voorthuisen (Oegstgeest/NL)

B-0616 10:30

Troponin vs. functional determinants of the heart in patients during non cardiac vascular surgery
R. Rienmüller, E. Mahla, H. Metzler, H. Metzler, H. Metzler, H. Metzler, P. Tiesenhausen, B. Schröttner, M. Töpker; *Graz/AT*

Purpose: TroponinT is reported as a sensitive marker of myocardial damage (positive up to 30 %) in patients referred for non cardiac vascular surgery. The goal of this prospective study was to compare TroponinT values with ECG findings and cardiac determinants as assessed by Electron Beam Tomography (EBT).
Methods and materials: 45 patients were studied – 14 with aneurysm of the abdominal aorta, 20 with infrainquinal and 11 with carotis interna occlusive diseases – one day before, 2nd and 5th day after surgery by EBT determining following cardiac determinants: Coronary Calcium Score (CCS), Left Ventricular Muscle Mass (LVMM), Myocardial Blood Flow (MBF), Ejection Fraction (EF) and Stroke Volume (SV) and Heart Rate (HR). TroponinT values above 0.01 ng/ml were regarded as pathologic. "Hard events" were myocardial infarction, severe arhythmia and cardiac failure.
Results: Mean values and standard deviations were calculated as: CCS (3188 ± 1296), HR (73 ± 14 bpm), MBF (68 ± 18 ml/100 g/min), EF (68 ± 11 %) and LVMM (148 ± 33 g). Six of 45 patients (2.7 %) showed elevated TroponinT values. Only 2/6 had ECG characteristics of myocardial infarction. 4/6 did not reveal any "hard events". These six patients with elevated TroponinT values differed significantly from the remaining 39 either by LVMM, SV, MBF, HR or CCS from calculated mean values. However, 3/39 patients had "hard events" with normal TroponinT values.
Conclusion: Our data suggest that TroponinT-test is a more sensitive and less specific marker of myocardial damage with respect to ECG changes. Reduced MBF is not necessarily correlated with elevated TroponinT.

B-0617 10:40

Evaluation of left ventricular function by retrospectively ECG-gated multislice spiral CT: Initial experiences
K.U. Jürgens[1], R. Fischbach[1], E.M. Fallenberg[1], M. Grude[1], C. Opitz[1], B. Ohnesorge[2], T. Wichter[1], W. Heindel[1]; *[1]Münster/DE, [2]Forchheim/DE*

Purpose: Multislice spiral computed tomography (MSCT) with retrospective ECG-gating enables image reconstruction in any phase of the cardiac cycle. Left ventricular (LV) function measurements thus can be performed.
Materials and methods: Ten male patients (62.7 ± 7.1 a, heart rate 56 – 88 bpm) with CAD underwent a MSCT coronary angiography (Somatom Volume Zoom, Siemens, Forchheim: 1 mm slice thickness, pitch 1.5, 120 kV, 300 mA; nonionic CM 300 mgI/ml, flow 2.8 ml/s). Retrospectively ECG-gated images were obtained in systolic and enddiastolic phase (ACV reconstruction algorithm). LV volumes, LV ejection fraction (LV-EF) and stroke volume were determined from multiplanar reformations (SLT 6 mm) in short and long axis orientation and compared to biplane levocardiography.
Results: Multiplanar reformations allowed excellent delineation of endo- and epicardial contours in diastolic images. Due to the temporal resolution of 125 through 250 ms systolic images had motion artifacts in patients with heart rates above 75 bpm. LV-EF ranged between 56 and 78 %. Volume measurements and LV-EF had a close correlation (LV-EF: r = 0.79) with levocardiography.
Conclusion: In patients evaluated for CAD MSCT angiography with retrospective gating allows noninvasive assessment of coronary artery morphology and can also provide functional data. Even regional wall motion analysis seems feasible.

B-0618 10:50

Assessment of atrial function with MRI after Maze procedure
G.F. Bachmann, T. Dill, A. John, S. Szalay, A. Kluge, C. Hamm; *Bad Nauheim/DE*

Purpose: To compare Doppler ultrasound (US) and magnetic resonance imaging (MRI) in detection and quantification of active atrial contraction after Maze procedure (multiple incisions through the left atrium to regain active atrial contraction).
Methods: Thirty patients underwent maze procedure for treatment of atrial fibrillation. All patients were monitored by Doppler-US and MRI in an early (3 – 6 months after surgery) and a late post-therapeutic interval (11 – 22 months). On MRI (1.5 T unit, Vision and Sonata, Siemens), flow measurement was performed through the mitral valve using a ECG-triggered segmented velocity encoded GE sequence in breath-hold. Acquisition was repeated three times to calculate a velocity-time-curve on 18 points during the cardiac cycle and to assess the e- and a-wave. Doppler US demonstrated the e- and a-wave in a similar way.
Results: All patients showed sinus rhythm. Active atrial contraction was demonstrated on MRI by a proper a-wave in the early postoperative period in 23/30 patients, and on Doppler US in 20/30 patients. In the late controls, active contraction of the left atrium was demonstrated in all cases and on US in only 27/30 cases.
Conclusion: Despite the evidence of sinus rhythm active atrial contraction needs some time to recover which can be assessed individually by flow measurement on MRI and US, and MRI is advantageous to US in definition of the e-wave.

B-0619 11:00

Characterization of right and left ventricular function and pulmonary flow in the presence of endovascular stents in the right ventricular outflowtract using magnetic resonance imaging

T. Kuehne, M. Saeed, G. Reddy, H. Akbari, M. Vranicar, P. Moore, C.B. Higgins; *San Francisco, CA/US*

Purpose: Endovascular stent implantation for the treatment of right ventricular outflow tract obstruction often results in incomplete relief of the stenosis and significant insufficiency. The purpose of this study was to quantify ventricular function and pulmonary artery flow in the presence of an intravascular stent across the pulmonary valve, using MRI.

Methods and materials: Under conventional fluoroscopic guidance, endovascular stents were placed across the pulmonary valve in 6 pigs to induce acute pulmonary insufficiency (stainless steel in 1 animal and nitinol in 5). Two sham-operated pigs served as controls. Left and right ventricular volumes, as well as pulmonary flow profiles through and next to the stent, were assessed 2 to 3 days later with cine and velocity-encoded cine phase contrast MRI (VEC-MRI), before and after gadolinium administration.

Results: Regurgitant fraction could be accurately quantified in all animals with cine and VEC-MRI. Data analysis disclosed no systematic measurement bias between cine and VEC-MRI measurements distal to the stent (mean difference 8 ± 4 %). Mean regurgitant fraction was 36 ± 5 % next to the stent and 20 ± 4 %, $p < 0.05$) through the stent. Administration of gadolinium improved the definition of the vascular wall on the phase contrast sequences, which allowed accurate determination of the diameter of the stented vessel.

Conclusion: MRI has the potential to (1) assess stent morphology and patency, (2) quantify flow across stents in the right ventricular outflow tract, and (3) demonstrate the acute effect of pulmonary insufficiency on ventricular function.

B-0620 11:10

Intravascular ultrasound in the diagnosis of pulmonary hypertension

A. Ivanitsky, V. Kriukov, A. Sobolev, I. Lepikhova, R. Serov; *Moscow/RU*

Purpose: To study the value of intravascular ultrasound imaging (IVUS) for assessment of vascular morphology in congenital heart disease with pulmonary hypertension.

Methods and materials: We investigated 145 pulmonary artery segments by means of IVUS from 42 patients with pulmonary hypertension. In group 1, we compared IVUS and histologic findings in 23 pulmonary artery segments from 6 autopsy stadies in patients with pulmonary hypertension. In group 2, we investigated 122 pulmonary segments in 36 patients with different stage of pulmonary hypertension.

Results: All segments of pulmonary arteries from patients with pulmonary hypertension showed a three-layered appearance. In patients with mild pulmonary hypertension, IVUS demonstrated increased thickness of the echolucent zone due to medial hypertrophy without intimal reaction. Patients with severe pulmonary hypertension had a thick inner layer because of intimal hyperplasia. For these patients operation was contraindicated.

Conclusion: IVUS findings have good correlation with histopathologic grades of vascular lesions. The assessment of the pulmonary arteries with IVUS allows to improve the diagnosis and management in pulmonary hypertensive patients with congenital heart disease.

B-0621 11:20

Myocardial MRI to assess iron content: A qualitative and quantitative multi-observer analysis

A. Sias, V. Alvino, F. Lecca, C. Politi, R. Galanello, A. Cao, G. Mallarini; *Cagliari/IT*

Introduction: The purpose of this work is to determine whether MR of the myocardium can provide a more accurate diagnostic tool in evaluating the myocardial level of iron and thus in predicting the outcome of patients affected by β thalassemia major.

Materials and methods: We performed MR examination of the myocardium in 40 patients affected by β thalassemia major. The study was performed with a 1.5 T magnet. The examination was performed with axial images through the myocardium, to evaluate qualitatively and quantitatively the iron content of the myocardium. Three observers assessed the levels visually, and graded the images according to a pre-determined table; observers also traced ROIs and the signal intensities measured in these areas, and averages calculated. All patients underwent liver biopsy, serum ferritine and iron and these data were compared with the myocardial iron content.

Results: The inter-observers agreement was very high, thus it seems not needed to involve several radiologists as examiners of this examination. The ROIs chosen by the radiologist were also very similar. The myocardial MR examination did not necessarily correlate with the patient status, as patient with higher iron content had a poorer outcome then expected by liver biopsy and/or blood tests results alone.

Conclusion: Myocardial MRI is a valuable diagnostic tool in the assessment of myocardial iron overload in patients with β thalassemia major: since congestive heart failure is the main cause of death in these subjects, it should be performed as a screening examination to avoid adverse outcome of the disease.

B-0622 11:30

Impairment of energy metabolism in intact myocardium after acute myocardial infarction assessed non-invasively by ^{31}P-MR spectroscopy in human

M. Beer[1], J.J.W. Sandstede[1], C. Lipke[1], H. Köstler[1], T. Pabst[1], W. Kenn[1], W. Landschütz[2], S. Neubauer[3], D. Hahn[1]; *[1]Würzburg/DE, [2]Erlangen/DE, [3]Oxford/GB*

Objective: Experimental studies have demonstrated that acute myocardial infarction (MI) alters energy metabolism even in non-infarcted adjacent tissue. Using cine MRI and ^{31}P-Magnetic resonance spectroscopy (MRS), the influence of a regional ischemic insult on energy metabolism of intact adjacent myocardium was analyzed.

Patients and methods: 30 patients (mean age 59 ± 11) with wall motion abnormalities in the anterior wall were studied 23 ± 9 days after MI. Using breath-hold cine MRI (Flash-2D) size and location of the MI was determined. ^{31}P-MR spectra were obtained from non-infarcted adjacent septal myocardium (voxel size 25 cm^3) using a 3D-CSI technique. 6 months after revascularization MRI was repeated. According to recovery of regional function, patients were separated into two groups: viable versus non-viable infarctions. 15 age-matched healthy volunteers served as control group.

Results: No significant differences were found between both patients groups concerning age, infarct size, interval between MI and examination. The phosphocreatine to adenosintriphosphate (PCr/ATP) ratio of all patients was significantly decreased (1.00 ± 0.30 versus 1.58 ± 0.42). Patients with viable anterior myocardium had a PCr/ATP-ratio of 1.12 ± 0.30, whereas patients with non-viable anterior myocardium, showed a ratio of 0.88 ± 0.24 (significantly lower than patients with viable anterior myocardium).

Discussion: Even non-infarcted myocardium shows depression of energy metabolism after myocardial infarction. Metabolism is significantly more depressed in patients with non-viable myocardium in the infarcted area compared to patients with viable anterior myocardium.

B-0623 11:40

Influence of exercise training on myocardial metabolism in patients with impaired left ventricular function: Analysis with ^{31}P-MR-spectroscopy

M. Beer[1], D. Wagner[2], J.J.W. Sandstede[1], H. Köstler[1], T. Pabst[1], W. Kenn[1], S. Neubauer[3], P. Dubach[2], D. Hahn[1]; *[1]Würzburg/DE, [2]Chur/CH, [3]Oxford/GB*

Purpose: Physical capacity (PC) is known to be increased by exercise training (ET) in patients with chronic heart failure. However, a possible negative influence of ET on the myocardium itself has not yet been excluded. Using SLOOP ^{31}P-MR-spectroscopy (MRS), the influence of ET on cardiac energy metabolism was determined.

Method/materials: 20 patients with DCM (ejection fraction: 33 ± 3 %) were randomized to an exercise and to a control group ($n = 10$ each). Training consisted in 5 supervised trainings/week during 40 min. Before and after the two months study period exercise testing with respiratory gas exchange and analysis of the myocardial phosphate metabolism with 3D-CSI-MRS was performed. 10 healthy, age-matched volunteers served as control group.

Results: At study entry both groups showed no significant differences concerning cardiac or pulmonary function. In both groups absolute values of PCr and ATP were evenly significantly reduced compared to healthy volunteers (5.81 ± 1.63 vs 8.52 ± 1.54 for PCr; 4.51 ± 0.91 vs 5.73 ± 1.11 for ATP). PCr and ATP levels remained unchanged in the control group 2 months later. VO_2 max, minute ventilation, CO_2 production ml/min, exercise time and watts increased significantly in the training group. Here, no significant changes were observed concerning absolute values of PCr and ATP too.

Conclusions: ET improves significantly PC of patients with DCM. There is no evidence for a negative influence of ET in these patients on cardiac metabolism. Follow-up studies are necessary to determine whether there may be even a positive effect of ET on myocardial energy metabolism.

B-0624 11:50

^{23}Na MRI for the assessment of myocardial infarction in humans

J.J.W. Sandstede[1], T. Pabst[1], M. Beer[1], K. Bäurle[1], C. Lipke[1], W. Kenn[1], W. Völker[1], S. Neubauer[2], D. Hahn[1]; *[1]Würzburg/DE, [2]Oxford/GB*

Objective: Increase of total sodium content in myocardial infarction (MI) is due to breakdown of ion homeostasis with accumulation of intracellular Na, extracellular edema formation and, during scar formation, increase of extracellular vs. intracellular space as cardiomyocytes are replaced by connective tissue. In an animal model, ^{23}Na MRI was shown to have the potential to measure infarct size. Aim of this study was to demonstrate the feasibility of ^{23}Na MRI to assess subacute as well as chronic MI in humans.

Subjects and methods: The study group consisted of 15 patients after subacute MI (3 – 17 days; mean 8) and 10 patients with chronic MI (7 – 204 months; mean 66). Double angulated short axis ^{23}Na images of the heart were obtained in prone position using a ^{23}Na surface coil and an ECG-triggered 3d-FLASH-sequence with 32 acquisitions (FOV 450 mm; matrix 64 × 128; in-plane resolution 3.5 × 7 mm^2; slice thickness 16 mm). Wall motion abnormalities were detected by cine MRI.

Results: All patients with subacute MI showed an area of elevated ^{23}Na signal intensity correlating with the areas of dysfunctional myocardium. In chronic MI, 2/10 patients had no wall motion abnormalities or areas of higher ^{23}Na signal intensity. An elevated ^{23}Na signal was only detected in the 8/10 patients that also showed wall motion abnormalities, indicating scar formation.

Conclusions: Elevated ^{23}Na MR image signal intensity demonstrates subacute and chronic MI in humans, but chronic MI can only be imaged in the case of scar formation.

10:30–12:00 **Room P**

Vascular

SS 1015

Supraaortic and renal vessels

Chairpersons:
D.A. Kelekis (Athens/GR)
E. Mousseaux (Paris/FR)

B-0625 10:30

Ultrafast time-resolved contrast-enhanced MR angiography of supraaortic vessels

J. Scheidler, B.J. Wintersperger, A.M. Huber, A. Billing, T.K. Helmberger, M.F. Reiser; *Munich/DE*

Purpose: To evaluate whether time-resolved contrast-enhanced MR angiography (TR-MRA) provides additional information on stenoses related flow restrictions and cerebral perfusion changes compared to high-resolution (HR-MRA) in patients with carotid artery stenosis.

Method/materials: 22 patients underwent TR-MRA and HR-MRA on a 1.5 T system with a combined coil system (Symphony Quantum, Siemens). For TR-MRA, 20 consecutive single-slab acquisitions ranging from the aortic arch to the middle cerebral artery (MCA) were acquired within a breathhold (TR/TE 2.36/0.88 ms, 256 matrix, 20 partitions/slab, acquisition time 1.6 s/slab) after Gd-DTPA injection. Dynamic ROI measurements in the intracavernous section of the internal carotid arteries (ICA) were compared to the arterial contrast agent input function measured in the aortic arch. The input function corrected ICA SI-time-curves were correlated to the degree of stenoses which was graded according to NASCET criteria on HR-MRA. Additionally, TR-MRA data was screened for additional information on supraaortic or cerebral blood flow dynamics.

Results: In all patients with high grade (> 70 %) common or internal carotid artery (ICA) stenosis delayed ICA contrast inflow was apparent on TR-MRA. Additionally, TR-MRA revealed ipsilateral middle cerebral artery (MCA) opacification via the Circle of Willis in two patients. Retrograde vertebral artery contrast enhancement was found in two patients with subclavian steal.

Conclusions: Although temporal resolution is less than DSA, noninvasive TR-MRA with a 1.6 s acquisition time provides important information on blood flow dynamics in patients with carotid artery stenoses.

B-0626 10:40

Multislice spiral CT angiography in the evaluation of carotid artery stenosis: Optimization of the technique and early clinical results

F. Fraioli, C. Catalano, A. Laghi, A. Grossi, F. Pediconi, A. Napoli, R. Passariello; *Rome/IT*

Purpose: To optimize multislice spiral CT Angiography in the assessment of patients with suspected carotid artery stenosis and to evaluate early clinical results.

Material and methods: 21 patients with suspected carotid artery stenosis were examined with multislice spiral CTA after bolus administration of 60 – 100 ml of nonionic contrast agent at a concentration of 350 mgI/ml at a flow rate of 3.5 – 4.5 ml/s. Four 1.5 mm thick slices were acquired per rotation covering a volume from the jugular fossa to the sella. Due to the absence of a means for calculation of the delay time, a fixed delay time of 15 seconds was used. Images were reconstructed using volume rendering algorithm on dedicated consoles. Evaluation was performed on axial and reconstructed images. In all patients DSA was also performed and considered the standard of reference.

Results: A dosage of 100 ml of contrast agent at 4.5 ml/s was considered optimal for carotid artery imaging. Good correlation with DSA was obtained if axial and reconstructed images were analyzed, while overestimation of the degree of stenosis in 3 carotids due to calcified plaques was present when only reconstructed images were utilized. CTA was considered superior to DSA in assessing plaque morphology.

Conclusion: Multislice spiral CTA overpasses all the limitations of single slice spiral CTA regarding venous overprojection and volume coverage. Reconstructions are still time consuming to eliminate calcifications that may determine overestimation of the degree of stenosis.

B-0627 10:50

Diagnostic value of simultaneous carotid and cerebral arteries angio CT in selection of patients for carotid endarterectomy

K. Gruszczynska[1], J. Gniadek[1], J. Baron[1], Z. Zieliński[2], K. Czernicki[1], I. Biowska-Kurkowska[2], L. Kurkowski[2]; *[1]Katowice/PL, [2]Tychy/PL*

Purpose: To evaluate the diagnostic value of angioCT in patients with internal carotid arteries stenosis, prepared for carotid endarterectomy.

Material and method: Between January 1999 and September 2000, 58 carotid arteries in 28 patients suffering from brain ischaemia underwent carotid arteries CTA in search of carotid stenosis.

CTA were performed in private CT department, using HeliCAT – Elscint CT unit, collimation 2.5 mm, pitch 1:1.5, 100 ml of CM. MIP, MPR and 3D reconstructions were created.

The degree of stenosis was measured according to NASCET method. To avoid intracranial lesions which could be the contraindication for endarterectomy, angioCT of cerebral arteries was performed in each patient simultaneously.

Results: In 24 cases of carotid CTA was normal. In 29 cases carotid artery stenosis (30 % to 90 %), in 6 complete carotid occlusion and in 1 carotid aplasia were found. Residual artery lumen was clearly visible after rotation and calcifications removal. Diagnostic value of CTA was established comparing to Doppler US results. Intracranial critical stenosis or carotid occlusion were depicted in cerebral CTA in 5 cases. In 2 patients multiple intracranial aneurysms were diagnosed. Those patients were excluded from carotid endarterectomy.

Conclusion: Carotid and cerebral arteries CTA performed simultaneously enables visualisation of entire extra- and intracranial cerebral circulation, helping to select patients for carotid endarterectomy.

B-0628 10:55

Occlusive stenotic lesions of the extracranial carotid vessels in patients with different cerebrovascular pathology

S.G. Mazur, I.I. Glazovskaya; *Kiev/UA*

Purpose: Occlusive-stenotic lesions of extracranial segments of cerebral arteries are considered as a substantial cause of cerebral blood flow impairment. The main goal of the study is the comparison of the structure of arterial lesion in patients with different types of cerebral atherosclerosis.

Materials and methods: We examined 62 patients with cerebral arterial atherosclerosis (males 35, females 27) in age from 45 to 79 years old (mean – 58 years old). Of those 32 patients experienced ischemic stroke and 30 patients had atherosclerotic encephalopathy. Control group consisted of 16 healthy persons (males 8, females 8) in age 45 – 70 years old (mean age 58 years old). For examination of principle cerebral arteries we used sonography system "Sonoline-Elegra" (Siemens, Germany), transducers with the frequency mode 7.5 MHz. We evaluated morphology of arterial wall, presence of arterial deformation, obstacles for laminar blood flow.

Results: We found similar frequency of structural alterations in extracranial cerebral arteries in patients with ischemic stroke and in patients with atherosclerotic encephalopathy, however they were more distinct in the stroke group of patients: mean value of intima-media complex thickness had statistically significant difference (1.36 + 0.14 in patients after ischemic stroke and 1.15 + 0.12 in patients with atherosclerotic encephalopathy, $p < 0.05$).
Conclusions: High prevalence of atherosclerotic lesions was revealed in all patients with cerebral atherosclerosis. However in poststroke group those changes were more significant. They lead to exhaustion of collateral blood flow reserve and contributed to decompensation of cerebral haemodynamic.

B-0629 11:00

Color Doppler (CD) and power Doppler (PD) imaging of orbital arteries pre- and post-carotid endarterectomy

M. Venturini, A. Dossena, L. Pierro, E. Angeli, R. Chiesa, A. Del Maschio; *Milan/IT*

Purpose: Hemodynamically significant internal carotid artery (ICA) stenoses can cause ocular complications (transient monocular blindness, central retinal artery occlusion, ocular ischemic syndrome). Our purpose was to evaluate the effect of carotid endarterectomy on blood flow of the main orbital arteries.
Materials and methods: Ipsilateral and controlateral eyes of 60 consecutive patients with significant ICA stenosis (> 75 %) were studied by CD and PD (ATL HDI 5000/5 – 10 MHz linear probe) pre-and post-operatively (one month): ICA stenosis was also determined by CD pre- and post-surgery (means 84 % and 9 % respectively). Flow direction, peak systolic velocity (psv), end diastolic velocities (edv) and resistive index (ri) of Ophthalmic (OA), Central Retinal (CRA) and Posterior Ciliary Arteries (PCA) were evaluated for comparison. PD was used to analyze the presence of collateral vessels.
Results: We found a significant postoperative improvement of blood flow velocities in all orbital ispilateral arteries (pre-surgery: psvOA = 24.56 cm/s; psvCRA = 8.24 cm/s; psvPCA = 11.9 cm/s. Post-surgery: psvOA = 32.93 cm/s; psvCRA = 10.84 cm/s; psvPCA = 13.97 cm/s), also in those patients with OA flow direction reversed (20 % post-operatively/12 % pre-operatively) where PD showed a rich number of collateral vessels. Only one patient showed a marked reduction of CRA flow velocities (CRA occlusion), probably due to perioperative embolism. No significant changes we found in controlateral arteries.
Conclusion: CD and PD allowed an accurate evaluation of the orbital haemodynamics, showing an increased arterial blood flow post carotid endarterectomy: this orbital flow improvement can determine a reduction of ocular complications.

B-0630 11:10

Three-dimensional gadolinium-enhanced MR angiography of carotid and renal arteries: A comparative study with intra-arterial angiography

D. Brisbois, P. Reginster, E. Donkers, P. Magotteaux, A. Jadot; *Liege/BE*

Purpose: Digitalized arteriography remains an objective step after Doppler examination in assesment of carotid and renal artery stenosis. Contrast-enhanced MRA is a non-invasive procedure that could replace arteriography in those indications if demonstrated feasible, easy, reliable and reproducible.
Materials and methods: 49 patients underwent digitalized arteriograhy of carotid (n = 18) or renal (n = 31) arteries and were examined in 3D contrast enhanced MRA, using only MIP (maximum intensity projections) reformations. Stenosis were classified in five classes (1: 0 %, 2: < 50 %, 3: 50 – 79 %, 4: 80 – 99 %, 5: 100 %) and, in a second step analysis, 50 % was taken as a determinant threshold for clinical outcome. A statistical analysis was performed.
To simplify and accelerate our MRA technique we triggered the acquisition with a real-time estimation of gadolinium arrival ("care bolus technique").
Results: All complete occlusions were correctly classified (n = 4).
Observed correlation with arteriography (gold standard) considering 50 % stenosis as threshold: 0.93 (κ: 0.68); sensitivity: 0.961 (95 % confidence interval is 0.948 to 0.973); specificity: 0.724 (95 % confidence interval is 0.694 to 0.753).
Conclusion: In our experience, 3D MRA is an easy, reproducible and non invasive technique to planify treatment of carotid and renal stenosis in replacement of intra-arterial arteriography. Stenosis can be estimated with MIP reformations. The limits of the technique are those of MRI, collaboration is mandatory for renal arteries examination (in this technique), but others are available.

B-0631 11:20

Projection MRA of the renal arteries with a 2D pencil beam aortic labeling pulse and a navigator-gated free-breathing 3D True-FISP imaging sequence

E. Spuentrup[1,2], M. Stuber[1], K.V. Kissinger[1], R.W. Guenther[2], W.J. Manning[1]; *[1]Boston, MA/US, [2]Aachen/DE*

Purpose: To develop a free-breathing, cardiac-triggered projection MRA imaging technique which selectively visualizes the renal arteries and completely suppresses the surrounding static tissue and the venous signal without contrast media application.
Materials and methods: A projection MRA technique with a 2D pencil beam for aortic spin-labeling was investigated on a 1.5 T clinical MR scanner in 8 healthy adult volunteers. For selective visualization of the renal arteries, a cardiac triggered, segmented-k-space 3D balanced gradient-echo sequence (3D True-FISP, TE 1.2 ms, FA 80°, 20 start-up-cycles/R-R interval followed by 32 imaging excitations, 2 mm slice thickness, 1.1 × 1.1 mm in-plane resolution) was acquired with and without aortic spin-labeling. Subsequently, both data sets were complex subtracted. The time delay between labeling pulse and imaging part of the sequence was 150 – 200 ms, which allowed for inflow of the blood into the renal arteries. Projection MRA in a double-oblique transverse and a coronal slice orientation were obtained in late diastole (ECG) and during free-breathing at end-expiration utilizing a diaphragmatic navigator. Contrast-to-noise ratio (CNR) was calculated.
Results: In 8/8 volunteers, renal arteries including segmental branches were selectively visualized on the projection MRA images with a high CNR (> 120). Signal from static tissue and renal veins was completely suppressed. No or minor motion artifacts were seen in the projection MRA images.
Conclusion: The presented projection MRA techniques allows for the selective (high-contrast) visualization of the renal arteries including segmental branches during free-breathing and without contrast media. Patient studies are needed to investigate the potential for detecting and classifying renal artery stenoses.

B-0632 11:30

Multislice spiral CT angiography in the assessment of renal artery stenosis

F. Fraioli, C. Catalano, A. Laghi, A. Grossi, V. Panebianco, A. Napoli, R. Passariello; *Rome/IT*

Purpose: To evaluate the possible role of multislice spiral CT Angiography (CTA) in the assessment of patients with suspected renal artery stenosis.
Material and methods: Twenty-eight patients with suspected renal artery stenosis were examined with multislice spiral CTA, after bolus injection of 100 ml of nonionic contrast agent at 4 ml/s. Four 1.5 mm thick slices per rotation were acquired with a volume coverage from the origin of the celiac trunk down to the aortic bifurcation, and a scanning time of approximately 25 seconds. Images were reconstructed using a volume rendering algorithm either on a Virtuoso (Siemens) or on a Vitrea console (Vital Images). Image evaluation was performed either on axial images or 3D reconstructions. In all patients DSA was performed within 72 hours from CTA and considered the standard of reference. Sensitivity and specificity for presence of polar arteries and stenosis were calculated.
Results: CTA was considered diagnostic in all cases. All 9 renal polar arteries were correctly demonstrated; in 2 patients with ostial calcified plaque the stenosis, discrete at DSA, was overestimated with 3D reconstructions of CTA, while were correctly detected on axial images. CTA was considered decisive prior to angioplasty and stenting in demonstrating the morphology of the plaque. The degree of stenosis was correctly obtained in 21/24 cases.
Conclusion: Multislice spiral CTA, due to the high spatial and temporal resolution, provides optimal images in patients with suspected renal artery stenosis. Low contrast agent dosage suggests its use also in patients with partially impaired renal function.

B-0633 11:40

Comparison of color Doppler ultrasound and gadolinium-enhanced 3D MR angiography in evaluation of renal artery stenosis due to fibromuscular dysplasia

F. De Cobelli, C. Trentin, M. Venturini, A. Zanello, A. De Gaspari, A. Del Maschio; *Milan/IT*

Purpose: Aim of this prospective study was to compare CDU and ultrafast breathhold 3D gadolinium-enhanced MRA in patients with suspected renal artery stenosis (RAS) due to fibro-muscular dysplasia (FMD).
Materials and methods: 19 hypertensive patients with suspected FMD RAS (4 males, 15 females; age 21 – 51, mean 37) were examined with CDU and with MRA. CDU examinations were performed in both main artery (morphologic evalu-

ation and peak systolic velocity) and intrarenal vessels (acceleration time). MRA examinations were performed with a 1.5 T system with high performance gradients with a phased-array multicoil using fast 3D SPGR (TR/TE 7.0/1.4, FA 40°) or efgre 3D (TR/TE/TI 5.4/1.3/30, FA 30°) sequences with gadolinium injection (0.1 mmol/kg) by a Power injector. Patients were assessed in a blinded and prospective manner. CDU and MRA findings were correlated with IADSA (standard of reference) in all cases.

Results: At IADSA 21 stenoses were found in 41 arteries. Compared with IADSA, MRA permitted the detection of 18 out of 21 stenoses (sensitivity, 85 %), whereas CDU detected 17 of 21 (sensitivity, 81 %). Specificities and accuracies were 80 % and 83 % for MRA and 83 % and 82 % for CDU, respectively. With the combination of MRA and CDU findings, the sensitivity rose to 90 %, although the specificity was only 70 %.

Conclusion: MRA and CDU have shown comparable results in detecting fibromuscular dysplasia of the renal arteries. The combination of the two techniques has shown the highest sensitivity.

B-0634 11:50

CT angiography in the assessment of carotid artery atherosclerosis: A comparative analysis with MR angiography with reference to contrast angiography and intravascular ultrasound

M.H. Berg, H.I. Manninen, H.T. Räsänen, R.L. Vanninen, P.A. Jaakkola;
Kuopio/FI

Purpose: The aim of the study was to evaluate the ability of CT angiography (CTA) to detect even minor atherosclerosis of the carotid arteries in comparison with three-dimensional time-of-flight magnetic resonance angiography (3D TOF MRA).

Methods: The ability of CTA to detect minor atherosclerosis in comparison with that of 3D TOF MRA was evaluated using quantitative measurements from 29 atherosclerotic lesions (mean diameter stenosis 35 %, range 4 – 40 %) verified with intravascular ultrasound (IVUS). Digital subtraction angiography (DSA) of 31 patients (mean age 65 years, range 45 to 79) was used as a reference for detection of advanced atherosclerosis (51 lesions; mean diameter stenosis 50 %, range 10 – 100 %). The results of interpretations of CTA and 3D TOF MRA axial images (21 patients)were compared.

Results: CTA yielded a sensitivity of 87 % to 100 % (diameter stenosis less than or equal to 10 %/20 % regarded as normal) for the detection of lesions with reference to IVUS. Measurements of diameter stenosis ($n = 45$) from CTA correlated better with measurements from IVUS ($r = 0.7$, $P < 0.001$) than did those from 3D TOF MRA ($r = 0.53$, $P < 0.001$). CTA detected all lesions verified on DSA providing better consistency of image interpretation than 3D TOF MRA.

Conclusion: CTA seems feasible and accurate for the detection of atherosclerosis in carotid arteries.

Monday, March 5

Scientific Sessions

	room A 2nd level	room B 2nd level	room C 2nd level	room E1 entr. level	room E2 entr. level	room F1 entr. level	room F2 entr. level	room G lower level	room H lower level	
08:30										08:30
09:00	**CC 1316**	**SF 13a**	**CC 1317a**	**SF 13b**	**CC 1317b**	**SF 13c**	**RC 1311**	**RC 1305**	**RC 1307**	09:00
09:30										09:30
10:00										10:00
10:30										10:30
11:00	**CC 1417**	**SS 1410** **Musculoskeletal** Imaging in arthritis *(p. 237)*	**SS 1401** **Abdominal and Gastrointestinal** Liver: MRI *(p. 239)*		**SS 1402** **Breast** Breast intervention *(p. 241)*	**SS 1404** **Chest** Thoracic interventions and lung disease *(p. 243)*	**SS 1411** **Neuro** Stroke (1) Diffusion/ Perfusion *(p. 245)*	**SS 1405** **Computer Applications** Web and information systems *(p. 247)*	**SS 1409** **Interventional Radiology** Non-vascular intervention *(p. 249)*	11:00
11:30										11:30
12:00										12:00
12:30	**HL 3**									12:30
13:00	Scientific Exhibits Awards									13:00
13:30										13:30
14:00				**SS 1514** **Radiographers** Current work in radiography *(p. 265)*						14:00
14:30	**SA 15**	**SS 1510** **Musculoskeletal** Tumor imaging *(p. 261)*	**SS 1501a** **Abdominal and Gastrointestinal** Liver: MRI, US *(p. 263)*		**SS 1502** **Breast** Breast imaging - New developments *(p. 265)*		**SS 1511** **Neuro** Stroke (2) *(p. 267)*	**SS 1505** **Computer Applications** Teleradiology and digital report generation *(p. 269)*	**SS 1509a** **Interventional Radiology** Arterial intervention (2) *(p. 271)*	14:30
15:00				**MS 1514**						15:00
15:30										15:30
16:00										16:00
16:30	**CC 1616**	**RC 1610**	**CC 1617**	**RC 1601**	**RC 1602**	**RC 1604**	**RC 1611**	**RC 1607**	**WS 1609**	16:30
17:00										17:00
17:30										17:30

	room I lower level	room K lower level	room L/M 1st level	room N/O 1st level	room P lower level	room X entr. level	room Y 1st level	room Z lower level	
08:30									08:30
09:00	WS 1318	RC 1312	RC 1313	RC 1314	**SS 1315 Vascular** Peripheral arteries (2) *(p. 236)*				09:00
09:30									09:30
10:00							WS 20E1		10:00
10:30								WS 19D1	10:30
11:00	**SS 1407 Genitourinary** Kidney *(p. 251)*	**SS 1412 Pediatric** Gastrointestinal tract *(p. 253)*	**SS 1408 Head and Neck** Orbit/Temporal bone/Skull base *(p. 255)*	**SS 1403 Cardiac** Heart function: MRI *(p. 257)*	**SS 1413 Physics in Radiology** CT, MR imaging and more *(p. 259)*	WS 19D2	WS 20E2		11:00
11:30									11:30
12:00							WS 20E3		12:00
12:30									12:30
13:00									13:00
13:30									13:30
14:00	**SS 1501b Abdominal and Gastrointestinal** Small bowel and colon *(p. 273)*	**SS 1509b Interventional Radiology** Technological developments *(p. 275)*		**SS 1507 Genitourinary** Female genital tract *(p. 276)*	**SS 1513 Physics in Radiology** Dose and image quality in digital imaging *(p. 278)*	WS 19D3	WS 20F1		14:00
14:30									14:30
15:00							WS 20F2		15:00
15:30									15:30
16:00							WS 20F3		16:00
16:30	WS 1615	RC 1612	RC 1613	RC 1608	**SS 1607 Genitourinary** Renal and adrenal masses *(p. 280)*				16:30
17:00									17:00
17:30									17:30

08:30–10:00 **Room P**

Vascular

SS 1315

Peripheral arteries (2)

Chairpersons:
P. Rossi (Rome/IT)
L. Vlahos (Athens/GR)

B-0635 08:30

Diagnostic value of contrast-enhanced MR angiography in detecting high-grade stenoses in lower limb peripheral occlusive disease

J.T. Winterer[1], P. Uhrmeister[1], O. Schäfer[1], G. Paul[2], S. Lehnhardt[1], J. Laubenberger[1], M. Langer[1]; *[1]Freiburg/DE, [2]Bonn/DE*

Purpose: Contrast-enhanced MRA (ce-MRA) provides reliable basic assessment of peripheral arterial occlusive disease. As a replacement of conventional angiography the detection of severe stenoses (> 70 %) is critical for planning vascular interventions. The purpose of this study was to evaluate this topic using a two-step body-coil-based MRA protocol.
Methods and materials: 46 patients with at least one iliac or peripheral artery stenosis > 50 % received both, conventional DSA and ce-MRA angiography, the latter using a fast contrast enhanced high resolution 3D technique covering the pelvic and peripheral vascular tree in two examination steps. Multi-angulated subtraction MIP's were assessed by 5 observers with varying experience distinguishing moderate (50 – 70 %) from severe stenoses (> 70 %).
Results: Maximal accuracy was 69 % for all vessels, 70 % in the pelvic area, 77 % femoropopliteal and 67 % in the crural vessels. For all segments Cohen's Kappa was 0.61 in the experienced readers and 0.24 to 0.49 in the less experienced readers.
Conclusions:
Planning vascular interventions the diagnostic quality of above mentioned MRA protocol as an exclusive imaging approach does not allow reliable assessment of critical stenoses in peripheral occlusive disease. The use of contrast agents with maximal relaxivity combined with dedicated surface coils may provide sufficient contrast-to-noise and spatial resolution for eventual replacement of conventional angiography in the future.

B-0636 08:40

Realtime interactive duplex flow quantitation: MRI vs. ultrasound

M. Braunschweig[1], I. Gal[1], O. Heid[2]; *[1]Biel/CH, [2]Erlangen/DE*

Purpose: We introduce a novel duplex ultrasound – like realtime interactive MRI flow measurement technique and report on an in vivo comparison study between this method and duplex ultrasound.
Methods and materials: The MRI sequence consists of a EPI sequence augmented by a 2D RF excitation pulse to avoid foldover with extremely rectangular field of views. Thus, a local spatial resolution can be achieved at frame rates up to 35 Hz. Bipolar gradient pulses intoduce flow sensitivity in slice direction, thus reducing the flow velocity angle dependency compared to ultrasound. MRI and US measurements were performed in the large abdominal vessels of 25 healthy volunteers.
Results: The MRI and US flow spectra looked very similar. The R-indices ranged from 0.65 to 0.82 for MRI and from 0.67 to 0.78 for US, with a correlation of 81 %, apparently limited by physiological fluctuations.
Conclusion: Due to unrestricted scan plane and flow sensitization orientations and the absence of sound propagation limitations, the proposed MRI method avoids the most dominant problems of US, but allows similar realtime control, ease of application and instantaneous data evaluation. Initial results point to comparable diagnostic value.

B-0637 08:50

Automated vessel detection at lower extremity multislice CTA

A. Kanitsar[1], R. Wegenkittl[2], P. Felkel[2], D. Sandner[1], E. Gröller[1], D. Fleischmann[1]; *[1]Vienna/AT, [2]Brunn am Gebirge/AT*

Purpose: To date multislice CT angiography (CTA) of the lower extremity arteries is technically feasible, but substantially limited by the need for time-consuming manual image editing and manipulation before the datasets can be effectively interpreted. We present a new computer-assisted vessel tracking and segmentation method, yielding curved planar reformations (CPR) through the central axes of the vascular tree with a minimum of user interaction.
Materials and methods: A new algorithm based on a minimal cost search over the gradient cost space was applied to three multislice CTA datasets (1070 – 1134 transverse slices from the suprarenal aorta to the mid-foot) obtained from patients with occlusive arterial disease. Acquisition parameters were: 4 × 2.5 mm or 4 × 1 mm detector configuration, 3 mm/1 mm section thickness/spacing. The total time needed for the generation of CPRs through the automatically traced centerline of the vessels, and the imaging features of occlusive disease (stenosis, hard- and soft plaques) were directly compared to manually generated sagittal and coronal CPRs – with digital subtraction angiography (DSA) as the standard of reference.
Results: Automated CPRs through the lower extremity arteries were obtained with minimal user interaction in less than 15 minutes in all datasets. Manual generation of CPRs required between 90 and 120 minutes per case. The automated alogrithm caused less "pseudostenosis" due to an eccentric course of the CPRs compared to the manual CPRs.
Conclusion: The presented algorithm is fast and simple enough to become a routinely applicable tool for effective interpretation of lower extremity CTA.

B-0638 09:00

Whole body MR-angiography with AngioSURF

M. Goyen, H.H. Quick, M.E. Ladd, H. Kuehl, J. Barkhausen, J.F. Debatin, S.G. Rühm; *Essen/DE*

Purpose: To assess the performance of a rolling table platform (AngioSURF) which integrates the torso phased-array coil for whole body MRA.
Patients and methods: The platform is mounted on top of the original patient table of a commercially available scanner (Sonata, Siemens). A series of MR-compatible rollers at the lower side of the platform permit patient positioning at pre-defined increments for acquisition of up to 5 contiguous 40 cm image volumes. Data is collected with the standard CP body array coil which remains fixed on a coil holder. The coil adapts to the patient contour and slides smoothly over the patient during table translation. The system was tested on 5 volunteers and 5 patients referred for DSA of the peripheral arteries. Five contiguous 40 cm volumes, offset by 36 cm (4 cm overlap) were prescribed. Craniocaudal coverage thus extended over 180 cm. The applied 3D FLASH sequence was collected over 12 s and table repositioning required 3 s. The total scan time amounted to 72 s. Gd-BOPTA (BRACCO) was administered using a biphasic injection protocol at a dose of 0.2 mmol/kg BW using an automated injector.
Results: The rolling platform allowed effortless and precise translation between imaging stations covering 180 cm in merely 72 s and provided image quality sufficient to display even the distal trifurcation and pedal arteries, resulting in complete correlation with DSA.
Conclusion: The presented table platform permits diagnostic whole body MRA. It can also be used for alternative multistation imaging protocols.

B-0639 09:10

Multislice spiral CT angiography in peripheral arterial disease: Optimization of the technique and early clinical results

C. Catalano, A. Laghi, V. Panebianco, F. Pediconi, R. Brillo, A. Napoli, R. Passariello; *Rome/IT*

Purpose: To optimize multislice spiral CT angiography (CTA) and to evaluate early clinical results in patients with obstructive disease of peripheral arteries.
Material and methods: 43 patients with peripheral arterial disease were examined with CTA after bolus administration of 90 – 140 ml of nonionic contrast agent. Four 2.5 mm thick slices per rotation were acquired (rotation time: 0.5 seconds) from the origin of the renal arteries down to the distal; the maximum volume coverage was 120 cm in 30 to 34 seconds. A fixed delay time of 25 seconds was used, being not available a means to determine the delay time. In all patients DSA was also performed. Images were reconstructed using the volume rendering algorithm on two different dedicated consoles (Virtuoso, Siemens, and Vitrea, Vital Images). Evaluation was performed either on axial or 3D reconstructed images.
Results: 140 ml of contrast agent at 4 ml/s proved to be the optimal contrast agent dosage for this purpose. Reduced dosages determined a poor opacification of trifurcation vessels. Using a 25 seconds delay time a good arterial opacification was obtained in all patients. Good correlation with DSA, regarding degree of stenosis, was obtained; CTA provided superior information in patients with aneurysm and ulcerated plaques in demonstrating parietal thrombus and plaque morphology. Sensitivity of multislice CTA was 97 %, specificity of 95 %. CTA appeared particularly accurate in the assessment of distal trifurcation vessels.
Conclusion: Multislice spiral CTA appears particularly suited for the assessment of peripheral vascular disease.

B-0640 09:20

Whole-body MR-angiography with a rolling table platform (AngioSURF): Determination of optimum dose assessment

M. Goyen, S. Bosk, J.F. Debatin, S.G. Rühm; *Essen/DE*

Purpose: To determine the optimal dosage Gd-BOPTA (BRACCO) to provide diagnostic whole-body MR Angiograms.

Patients and methods: 3D data sets were acquired with a rolling table platform (AngioSURF) which integrates the body array surface coil. It can be mounted on top of the original MR table and allows the acquisition of 5 successive data sets. Thus the craniocaudal coverage extends over 180 cm. Data collection was performed with a 3D FLASH sequence at five station covering the arterial tree from carotid arteries to the trifurcation vessels. The total scan time amounted to 72 s. 12 healthy volunteers were examined. Each volunteer was examined three times with an ascending dose of Gd-BOPTA (0.1/0.2/0.3 mmol/kg BW). Contrast injection was performed with an automated injector employing a biphasic injection protocol. For image analysis, the vascular system was divided into different segments. For quantitative assessment, SNR- and CNR-values were calculated, for qualitative evaluation, a 4-point-scale (4 ... very good 3 ... good, 2 ... sufficient for diagnosis, 1 ... non-diagnostic) was used.

Results: Overall, significantly ($p < 0.05$) higher SNRs and CNRs were present for Gd-BOPTA at a dose of 0.2 and 0.3 mmol/kg compared to the lowest tested dose of 0.1 mmol/kg. According to the quantitative data, image quality was graded superior with 0.2 and 0.3 mmol/kg compared to 0.1 mmol/kg ($p < 0.05$). There was no statistically significant difference ($p > 0.05$) between 0.2 and 0.3 mmol/kg for both qualitative and quantitative data.

Conclusion: A weight-adjusted dosage of 0.2 mmol/kg BW Gd-BOPTA is sufficient for whole-body MRA using AngioSURF.

B-0641 09:30

MIP, SSD, volume rendering reconstructions vs. axial images in the assessment of arterial vasculature using multislice spiral CT angiography

C. Catalano, A. Laghi, F. Fraioli, A. Grossi, F. Pediconi, A. Napoli, R. Passariello; *Rome/IT*

Purpose: Multislice acquisition is the latest technical development in spiral CT which appears particularly useful in the assessment of vascular pathologies. Purpose of this study is to determine which reconstruction algorithm is optimal for multislice spiral CTA.

Material and methods: 124 patients with vascular pathologies were examined during the last 9 months using a multidetector CT scanner. In all cases were performed MIP (Maximum Intensity Projection), SSD (Surface Shaded Display) and VR (Volume Rendering) reconstructions, with and without bony structures elimination. Reconstructions were performed either on a Vitrea (Vital Images) or Virtuoso (Siemens) console. Images were reviewed by two readers, who examined either reconstruction algorithms and axial images.

Results: VR was considered the best reconstruction algorithm, providing all the information needed. With MIP and SSD reconstructions improved results were obtained by elimination of bone structures, which was not considered necessary for VR. Reconstruction time (independent from the reconstruction algorithm used) varied between 3 (carotid arteries) and 10 minutes (peripheral arteries). Segmentation of bone structures resulted time consuming (approximately 15 minutes for a peripheral study). VR allowed correct determination of the degree of stenosis also in presence of calcified plaques, which impaired the diagnosis, in most instances, with MIP and SSD.

Conclusion: VR reconstructions appear to provide the best results in all vascular districts, even if bone structures are not segmented. In our institution multislice spiral CTA studies are now routinely reported using axial images and VR reconstructions.

B-0642 09:40

Contrast-enhanced MR-angiography vs. digital subtraction angiography in the evaluation of patients immediately after peripheral distal bypass surgery

M. Salcuni, B. Merlino, R. Iezzi, F. Spigonardo, L. Bonomo; *Chieti/IT*

Purpose: To evaluate the feasibility and possible clinical use of CE-MRA in the assessment of peripheral distal bypasses.

Method and materials: Twenty-one consecutive patients underwent CE-MRA after three days from peripheral distal bypass surgery (3D GRE, FoV 450 mm, 1.5 mm voxel resolution, 27 – 34 s, body coil), including both lower limbs from the common femoral artery to the calf by acquiring two sequential Fovs in a caudo-cranial direction during two separate CM administrations. All patients underwent DSA within 48 h after CE-MRA. CE-MRA and DSA images were blind interpreted each set by one observer with regard to bypass patency, morphologic evaluation of proximal and distal anastomoses, presence/absence of lesions and collateral vessels.

Results: CE-MRA provided good visualization of the grafts in all cases of patent bypass (18/21, 85.7 %), including proximal and distal anastomoses. In three patients bypass occlusion was correctly assessed by CE-MRA and confirmed at DSA (14.3 %). Diagnostic accuracy in the evaluation of associated lesions was 98 %, in the assessment of collateral vessels was about 80 %.

Conclusions: In our experience CE-MRA was equal to DSA in the evaluation of patients after peripheral distal bypass surgery and could be preferable especially in the follow-up of those patients due to its non-invasiveness.

B-0643 09:50

Contrast-enhanced MR-angiography with a two-step protocol in the assessment of lower limb arteries in diabetic patients

B. Merlino, M. Salcuni, R. Fossaceca, L. Salute, L. Bonomo; *Chieti/IT*

Purpose: To assess the role of contrast enhanced MRA (CE-MRA) vs. DSA in the evaluation of peripheral artery disease in diabetic patients with moderate-severe arterial occlusive disease.

Method and materials: 21 consecutive diabetic patients with vascular disease were prospectively imaged using CE-MRA (3D spoiled GRE on the coronal plane, FoV 450 mm, ≤ 1.5 mm voxel resolution, 27 – 34 s, body coil) including both lower limbs from the aortoiliac bifurcation to the calf. Two caudo-cranial sequential acquisitions during two separate CM injections (Gadobenate Dimeglumine 0.1 mmol/kg each, 2 ml/s flow rate via power injector) have been performed, each step including a double consecutive acquisition, the first before and the second during CM arrival. All patients underwent DSA within 48 – 72 h. CE-MRA and DSA image sets were blind interpreted each by one observer as to visualization (diagnostic-not diagnostic) and grading of vessel segments (16 segments for each lower limb, judged as patent, stenotic or occluded).

Results: In 16 of 21 patients CE-MRA provided satisfactory visualization of the vascular tree in comparison to DSA. Diagnostic visualization rate was 100 % for aortoiliac and proximal femoral, 98 % for distal femoral and popliteal, 83 % for more distal segments. Diagnostic accuracy was 99 %, 91 % e 81 % respectively.

Conclusions: CE-MRA without automated table translation and surface coils provide satisfactory imaging of lower limbs arteries in diabetic patients, with only some limitations in the assessment of distal segments, especially in severely-ill arteries.

10:30–12:00 **Room B**

Musculoskeletal

SS 1410

Imaging in arthritis

Chairpersons:
A. Vieira (Porto/PT)
I. Watt (Bristol/GB)

B-0644 10:30

Dynamic panoramic-ultrasound of the radio-lunato-capitate transition in patients with rheumatoid arthritis

H. Braun, M. Jenett, A. Trusen, G. Wittenberg, D. Hahn; *Würzburg/DE*

Aim: Detecting movement-disorders in the carpal transition in patients with rheumatoid arthritis (RA). The mixture of carpal-osseus defects and soft-tissue defects in patients with RA lead to complex movement-deficits and pain. The aim of our study was to develop a method that helps to give additional information of the osseous alignment of the wrist in flexing and extending movements.

Materials and methods: In 68 patients with RA, after making radiographs of the hand, determing the Larsen-score, evaluating the motion-scale, we performed panorama-ultrasound of the radio-lunato-capitate tansition. In maximal extension and dorsiflexion of the wrist we made longitudinal standard scans along the distal radius, the lunate, the capitate, to the base of the metacarpal III. At a control group consisting of 20 healthy persons, the normal alignment was defined: the carpal silhouette forms an harmonic curve, no erosions are present. We used Siemens sonoline Ellegra, 7.5 MHz linear transducer. Statistics: Interindividual testing between control group and study group. Also intraindividual testing, to see if alignment-disorders of the wrist are dominant in a Larsen-group, was performed

Results: 14.8 % of the rheuma patients had alignment disorders consisting in carpal instability, erosion, scapholunate dissociation, fragment-transposition. Soft tissue-findings were 18.9 % joint effusion, 5 % synovial hyperplasia, 2.5 % pannus formation. There were, excluding larsen score 1 and 5, no statistical significant accumulation of alignment disorders in the larsen groups 2 – 4.
Conclusion: The method is a valuable supplementing to routinally performed radiographs of the hand.

B-0645 10:40

The role of MRI in the assessment of rheumatic joint pathology
M. Mastantuono, E. Bassetti, L. Lobina, L. D'Aviera, R. Passariello; *Rome/IT*

Purpose: MRI evaluation of rheumatic pathologies, performed after administration of contrast medium (Gd-DTPA).
Materials and methods: We studied 98 patients with documented or suspected rheumatic disease; in 53 patients we administered Gd-DTPA. The acquisitions have been performed with an high field MRI unit (1.5 T Vision Plus Siemens) and with a low field dedicated magnet (0.2 T E-Scan Esaote). All the patients were previously evaluated with high resolution X-Rays examination and ultrasound.
Results: The images showed that MR examinations, performed with administration of contrast medium clearly document the evolution of rheumatic disease. Particularly, it has been possible to study the changes of the synovial membrane both in the initial and in the late stages. In particular in 28 patients MR showed the presence of a pathology that otherwise was hidden at X Ray examination and in 19 patients was impossible to evaluate with ultrasound.
Discussion and conclusions: MRI, with the administration of contrast media, is very useful in the clinical evaluation and in monitoring the earliest changes of the pathologic signs in patients with rheumatic diseases and gives a notable contribution in the correct diagnostic framing of rheumatic diseases superior to other radiological techniques. The administration of contrast media permitted also the evaluation of the grade of activity of the synovial pannus.

B-0646 10:50

Diagnostic value of dynamic contrast-enhanced magnetic resonance imaging compared to conventional radiography in rheumatoid arthritis of the shoulder
K.-G. Hermann, M. Backhaus, D. Loreck, B.B. Hamm, M. Bollow; *Berlin/DE*

Objective: To prospectively compare precontrast and dynamic postcontrast magnetic resonance imaging (MRI) with conventional radiography (CR) in detecting erosions of the shoulder joints in rheumatoid arthritis.
Methods/material: Forty-four patients (age 55.6 ± 12 years) with rheumatoid arthritis were examined by CR and MRI. Precontrast MRI was performed in transverse and oblique coronal planes applying T1-weighted SE, STIR and T2-weighted GRE sequences followed by a dynamic T1-weighted GRE sequence after administering 0.1 mmol/kg body weight of Gd-DTPA. The percent enhancement per minute (enhancement slope) in the glenohumeral joint space was calculated. Two groups were formed on the basis of the CR findings: Group A included 30 patients with nonerosive rheumatic disease, group B 14 patients with erosions.
Results: All patients in group B showed erosions at MRI. In group A, 15 patients (50 percent) showed erosions at MRI not detected by CR. Enhancement slopes within this group differed significantly between the 15 patients with erosions and the 15 patients without erosions ($p < 0.05$). Enhancement slopes in all 29 patients with erosions at MRI also differed significantly from those in the 15 patients without erosions at MRI ($p < 0.005$).
Conclusion: Magnetic resonance imaging is superior to conventional radiography in detecting erosions of the glenohumeral joint. Especially dynamic contrast-enhanced MRI enables the reliable and early detection of humeral head erosions.

B-0647 11:00

US and MRI correlation of synovitis of wrist and ankle joint disease (role of contrast enhancement) in childhood arthritis
A.K. Karpenko, L.N. Perezhogina, V.I. Purin; *St. Petersburg/RU*

Purpose: In cases JRA and JChrA by US we are unsuccessful in detecting moderate amounts of fluid in wrist and ankle, sometimes the imaging information is false. MRI data are also unclear. Purpose was to find some diagnostic peculiar features in visualization of wrist and ankle synovitis in children with JRA and JChrA in comparison of two modern diagnostic methods.
Materials and methods: 23 children (about 60 joints) with clinical signs of joint effusion and periarticular thickening of wrist or/and ankle were examined by US with Power Doppler without/with contrast enhancement by Levovist (Shering) in proper age dosage. In cases when US data were unclear or in order to compare two diagnostic methods MRI with contrast enhancement (Omniscan, Magnevist) was performed.
Results: In 16 cases of known JRA we found joint effusion and signs of tenosynovitis in points of local soft tissue thickening. Tenosynovitis was registrated as fluid collection in tendon shifts with color (Power) doppler signals before and after contrast enhancement. These symptoms were detected by both methods. In 25 joints by US with color (Power) doppler we found only tenosynovitis (12 ankles and 13 wrists), but by US and MRI with contrast enhancement in 18 cases we found also joint synovitis. In 8 cases our US data about local tenosynovitis were confirmed by contrast MRI.
Conclusion: The only combination of two methods of US and MRI with contrast enhancement can give clear information of wrist and ankle synovitis and tenosynovitis in patients with JRA and JChrA.

B-0648 11:05

MRI of the wrist in patients with early rheumatoid arthritis
G. Alexiadis, N.G. Galanopoulos, S. Deftereos, J. Manavis; *Alexandroupolis/GR*

Purpose: To evaluate the ability of magnetic resonance imaging (MRI) of the wrist in detecting early joint's damage in hands of patients with early rheumatoid arthritis (RA).
Method: Plain x-rays and MRI was performed in 30 patients with early RA (ACR 1987) of less than 6 months duration (mean 4.2 months). In MRI the field of view was covering the area from the distal radioulnar joint to the proximal interphalageal joints. Anterior-posterior radiographs of both hands and wrists were scored separately by two radiologists blinded to the clinical pattern. MRI findings were compared with plain radiography.
Results: Bone erosions were found by MRI in 14 patients (46 %) compared with 6 (20 %) on plain x-rays. Synovitis was found in 26 patients (86 %), bone marrow edema in 17 (57 %) and tendonitis in 19 (63 %). The most frequent site for erosions was the capitate (70 %), for synovitis the recess of the distal ulnar (60 %), for bone marrow edema the capitate (40 %) and for tendonitis the flexor carpi radialis (40 %). MR imaging detected all erosions seen on conventional radiographs.
Conclusion: We suggest that MRI with Gd-DTPA is a sensitive method to reveal the involvement of wrists and hands (erosions, synovitis, bone marrow edema, tendonitis) of patients with early RA. Because of these, maybe MRI will be the first method to evaluate early RA.

B-0649 11:10

Radiological diagnosis of bone and joint changes in patients with rheumatoid arthritis
O.V. Kotlubey, M.S. Kamenetsky, O.V. Sinyachenko, N.V. Momot, L.A. Krasnaya, M.S. Litvinova; *Donetsk/UA*

Purpose: To study possibilities of radiograms photodensitometry and CT with histographical analysis for revealing the osteoporosis, possibility of sonography for detection of joint changes in patients with RA; to evaluate state of calcium metabolism in RA.
Methods and materials: Densitometry of the standardized radiograms of hands and feet together with aluminium stendwedges was conducted in 120 patients with RA. The serum concentration of total and ionized calcium, phosphorus and their regulating hormones was determined by radioimmunological analysis. 25 subjects were examined by CT with histographical analysis of lumbar vertebrae density, 30 by ultrasonography of genu joints.
Results: The reduced bone density was revealed in 108 patients with RA, including 34 persons without evident radiological sings of disease. Decreasing of ionized calcium level and increasing parathyroid hormone, calcitonine levels in plasma were detected. The histograms of lumbar vertebrae density in-patients with RA had a 1.5 – 2 times wider base than those of healthy persons. The articular slit narrowing, the bone erosion and the liquid in articular cavity were revealed using genu joints ultrasonography.
Conclusion: Radiograms photodensitometry and CT with histographical analysis enable the osteoporosis to be revealed at RA early stages. Impairments of calcium metabolism are determined in RA.

B-0650 11:15

MRI in the assessment of early and advanced sacroiliitis
R. Arkun[1], A. Yesildag[2], Y. Kabasakal[2], M. Argin[2], A. Memis[2]; *[1]Bornova/TR, [2]Izmir/TR*

Purpose: To evaluate the role of magnetic resonance imaging (MRI) and dynamic MRI in the diagnosis of acute and chronic sacroiliitis among patients with spondylarthropathy.

Methods: Sixteen patients with inflammatory back pain and normal or suspicious changes of sacroiliitis (New York criteria: 0 – 1) on conventional radiography (group 1), and 12 patients with definite ankylosing spondylitis (group 2) and 6 control subjects were studied (group3). Radiographs were evaluated on the basis of the modified New York criteria. Dynamic MRI (dMRI) and MRI were evaluated according to published criteria allowing for differantiation between acute and chronic changes in sacroiliac (SI) joints.
Result: By using dMRI, acute sacroiliitis was detected in 19 of 32 SI joints in group1 patients, and 21 of 24 SI joints in group 2 patients, and no sacroiliitis in group 3 patients. By using MRI, chronic sacroiliitis was detected 8 of 32 SI joints in group 1, 23 of 24 in group 2, and none SI joint in group 3 patients.
Conclusion: DMRI and MRI are useful to detect acute and chronic sacroiliitis in patients with spondylarthropathy. The main advantages in comparison with conventional radiographs are the ability to detect early and acute changes in the SI joints, the higher sensitivity to detect chronic changes, and the absence of radiation exposure.

B-0651 11:25

Comparison of radiographic and MRI findings in detection of non-traumatic spinal fractures in ankylosing spondylitis

L. Cyrylowski, H. Przepiera - Bêdzak, M. Brzosko, Z. Domański; *Szczecin/PL*

Purpose: To compare plain radiographic and MRI findings in evaluation of spinal fractures in non-traumatic patients with ankylosing spondylitis (AS).
Materials and methods: Plain X-ray films in lateral projection of spine were performed in 49 males with AS; mean age, 49.4 years. Fractures were diagnosed on the basis of measured ratios of vertebral body heights. The MRI examinations were performed in 13 of 22 patients with spinal fractures diagnosed on the basis of radiographic findings.
Results: Total 23 fractures in 13 patients were found with the X-ray method. The MRI examinations revealed 33 fractures. MRI examination confirmed only 9 of 23 (39.1 %) fractures revealed by radiographs. Positive correlations between disease duration and number of fractures, as well as between age of patients and number of fractures were found in patients with fractures detected with the MRI. We also found positive correlation between time of diagnosis and number of fractures. No such correlation was found in patients with fractures found with X-rays.
Conclusion: This significant discrepancy between radiographic and MRI findings may suggest less usefulness of plain X-ray films in evaluation of spinal fracture in AS patients. Radiographs seemed to underestimate the spinal fractures, what may result from difficulties in detailed outline and measurements of vertebral bodies.

B-0652 11:35

Trauma of cervicodorsal vertebral column in ankylosing spondylitis

J. Beran; *Liberec/CZ*

Purpose: To show value of radiologic methods in diagnosis of fractures in pathologic area of "bamboo spine" in ankylosing spondylitis (AS).
Methods and materials: 6 patients (all men), aged 42 to 60 years, with advanced AS and acute, severe trauma of cervicodorsal junction, underwent plain radiography, conventional tomography, CT and in the last year MRI.
Results: Most common site of injury was the region of D 1 vertebra. The fractures are not situated in vertebral bodies but are fractures-dislocations in the region of discovertebral junction, compromising spinal cord. These conditions were present in 4 of our patients and represent lifethreatening conditions for them. The role of radiology is to define the level of traumatic changes for following treatment. From optimal algorithm we usually exclude CT examination, nowadays, because of difficult evaluation of axial scans.
Conclusions: Cervicodorsal region is together with lumbar spine the most common site of trauma in AS. The mechanism of fracture-dislocation is caused by pathologic changes in ligamentous structures and the spinal cord is often affected. Diagnosis is based on plain radiography, conventional tomography and MRI.

B-0653 11:45

Ultrasound and MRI contrast enhancement in the differential diagnosis of hip-arthritis in children

A.K. Karpenko, O.V. Dumanovskaya, A.J. Okunev; *St. Petersburg/RU*

Purpose: Hip arthritis may be associated with a number of conditions We tried to follow up the behavior of US and MRI contrast agents in order to differentiate the type of hip disease in children.
Methods and materials: We examined 43 patients with mono- and oligo variants of arthritis in children of 6 months 15 years of age in about 2 weeks from the beginning of hip pain. We used US unit – Acuson 128XP and MRI of 0.15 T. Dynamic contrast enhancement of Levovist (Shering) and salts of Gadolinium was performed. In 15 cases we used only US contrast enhancement, in 17 patients both methods and in 11 cases only MRI contrast enhancement. All patients had X-ray and sometimes CT control, 14 were surgically operated.
Results: In all cases we detected joint effusion, periarticular soft-tissue swelling. In cases of JRA and JChrA contrast enhancement of irregular thickened synovium was very clear by both methods. In this group US contrast enhancement we could registrate only after 3 – 4 minutes after injection, while in MRI images in first 4 – 5 minutes synovium was enhanced. In patients with pyogenic arthritis color doppler signals were detected in periarticular tissues and synovium during first 1 – 1.5 minutes, MRI contrast in 4 – 5 minutes after injection was in joint fluid. In cases of osteomyelitis contrast was in periarticular septa of accumulated pyogenic fluid and in suffered bone areas (registered by MRI).
Conclusion: US and MRI contrast enhancement can give more clear information in radiological differentiation of different types of hip inflammation in children.

B-0654 11:50

Camurati-Engelmann disease: Genetic, clinical and radiological features

F.M.H.M. Vanhoenacker[1], K. Janssens[2], W. Van Hul[2], R. Gershoni-Baruch[3], R. Brik[4], A.M.A. De Schepper[1]; *[1]Edegem/BE, [2]Antwerp/BE, [3]Technion/IL, [4]Haifa/IL*

Purpose: To present a comprehensive overview of the genetic and radioclinical features of Camurati-Engelmann Disease (Progressive Diaphyseal Dysplasia).
Methods and materials: To identify the disease causing gene of this rare autosomal dominant disease, a genetic linkage study was done in a large Jewish-Iraqi family with 18 affected subjects in four generations. The age of the patients ranged between 3 and 64. Ten patients were female and eight male. Clinical features and imaging studies of those 18 patients were reviewed.
Results and conclusions: (1) The gene defect was mapped to Chromosome 19q13. (2) The most frequent symptoms were muscle weakness and a waddling gait, exophthalmos, and thickening of the long bones. Four patients were asymptomatic. (3) Radiologically, the disease can be classified as a craniotubular hyperostosis. Typically, fusiform thickening of the diaphyseal portions of the long bones is seen, but metaphyseal involvement was seen in 1 patient. Distribution of the lesions in the skeleton is symmetric. Hyperostosis of the skull usually involves the skull base, with occasional involvement of the calvaria and facial bones. (4) Radioclinical abnormalities are mostly detected before the age of 30, but may be present in the first decade of life. (5) Radiological examination is more sensitive than clinical symptomatology, as two of the asymptomatic patients had radiological abnormalities. (6) Two patients had no visible radiological abnormalities.

10:30–12:00 **Room C**

Abdominal and Gastrointestinal

SS 1401

Liver: MRI

Chairpersons:
B. Fornet (Budapest/HU)
S. Yarmenitis (Patras/GR)

B-0655 10:30

Characterization of hepatocellular lesions: Value of mangafodipir-enhanced MR images

M. Scharitzer, W. Schima, E. Schober, A. Ba-Ssalamah, F. Wrba; *Vienna/AT*

Purpose: To assess the additional value of mangafodipir-enhanced MRI for characterization of hepatocellular tumors.
Materials and methods: MR images of 35 patients with a total of 40 hepatocellular lesions (9 FNH, 3 adenomas, 18 HCC, 7 regenerative nodules, 3 other) were retrospectively studied. MR imaging was performed on a 1.5 T unit (Vision, Siemens or ACS-NT, Philips), using T2w TSE with fat saturation and T1w GRE (FLASH or TFE) before and 20 min after iv infusion of 5 µmol/kg mangafodipir (Teslascan, Nycomed Amersham). Images were assessed by 2 readers, who were unaware of the histo-pathological diagnosis.
Results: Enhancement after mangafodipir was observed in all hepatocellular lesions. However, enhancement was stronger in FNH than in HCC in cirrhotic livers ($P < 0.05$). FNH were homogeneously isointense or slightly hyperintense post-contrast in 77 %. Although HCC demonstrated enhancement, conspicuity of le-

sions was improved post-contrast in 83 %. In HCC, enhancement was typically inhomogenous with less/no enhancement within internal areas, which helped in the differentiation from regenerative nodules.
Conclusion: Characterization of hepatocellular lesions is improved by evaluation of unenhanced and mangafodipir-enhanced MR images.

B-0656 10:40

Can contrast-enhanced MRA replace selective DSA for the preoperative work-up before upper abdominal surgery: Results of a prospective intraindividual comparative study with blinded reading

P. Reimer[1], S. Korsawe[1], B. Tombach[2], K. Wörtler[3], T. Vestring[4]; [1]*Karlsruhe/DE,* [2]*Münster/DE,* [3]*Munich/DE,* [4]*Rotenburg a. d. Wümme/DE*

Purpose: To study the potential value of CE-MRA for the preoperative work-up prior to upper abdominal surgery.
Method/materials: CE-MRA was performed in 30 patients following selective DSA with overview runs of the upper abdominal aorta and selective runs of the celiac trunk and SMA. A dose of 0.2 mmol Gd-DTPA/kg bw was injected (3 ml/s) following measurement of individual circulation times. CE-MRA was performed with a 3D-GRE sequence (Magnetom Vision) yielding isotropic in-plane resolution with three separate acquisitions (plain, arterial and venous phase) and subsequent image subtraction. Imaging data was arranged for blinded review by two investigators. Three blinded readers independently reviewed CE-MRA, DSA, and finally all modalities together according to the classification of Lippert, Papst, and Cheng. The combined analysis and the surgical reports formed the gold standard.
Results: The celiac trunk was correctly classified in 78.2 % with DSA and 85.9 % with CE-MRA with a better definition of vessel pathology by CE-MRA. Hepatic arteries were correctly classified in 80.7 % with DSA and 71.8 % with CE-MRA with a better definition of vessel pathology by DSA. The portal venous system was correctly classified in 80.2 % with DSA and 85.2 % with CE-MRA with a better definition of vessel pathology and significantly better diagnostic quality by CE-MRA.
Conclusions: CE-MRA is comparable with selective DSA for the celiac trunk and superior for the portal venous system. DSA demonstrates a more detailed view of intrahepatic branches of the hepatic artery. CE-MRA can replace selective DSA for the preoperative work-up of upper abdominal vessels.

B-0657 10:50

Hepatic lesion detection with i.v. Gadolinium (Gd)-DTPA enhanced VIBE sequence vs. SPIO enhanced T2w sequences

P. Heim, V. Schoder, C. Dieckmann, R. Kuhlencordt, C. Weise, G. Krupski, P. Steiner, G. Adam; *Hamburg/DE*

Purpose: To compare the accuracy of Gd-enhanced VIBE sequence with three different T2-w sequences before and after SPIO enhancement in the detection of hepatic lesions in non cirrhotic livers at 1.5 T.
Materials and methods: 24 patients, 10 of which underwent surgery, with hepatic lesions in non-cirrhotic livers were preoperatively examined. All patients underwent portal CT. Three different T2-w sequences were obtained before and following superparamagnetic iron oxide (SPIO) enhancement. In between a Gd-enhanced volumetric interpolated breath-hold examination (VIBE) was performed (TR/TE 4.5 ms/1.9; 5 mm slice thickness). All images were reviewed by two readers blinded to the results of the portal CT and surgery. Analysis included qualitative (alternative free response receiver operating characteristic) and quantitative methods (CNR).
Results: The accuracy of all T2-w sequences increases significantly after SPIO enhancement. No significant difference was found between the three different T2-w sequences with regard to image quality, diagnostic accuracy and CNR. Irrespective of lesion size, the VIBE sequence tends to be as accurate as the SPIO-enhanced T2-w sequences. However, anatomical details are better displayed adopting the VIBE sequence.
Conclusion: The Gd-enhanced VIBE sequence shows promise to be an alternative to SPIO-enhanced T2-w technique for visualising liver tumors. Adding one native breathhold T2-w sequence for cyst detection would offer a conclusive, fast and accurate MR algorithm for this disease entity.

B-0658 11:00

Evaluation of a comprehensive MR protocol for assessing potential living related liver donors

M. Goyen, S.G. Rühm, J. Barkhausen, M. Malagó, G. Testa, J.F. Debatin; *Essen/DE*

Purpose: To determine the diagnostic accuracy of an all in one-MR-based-approach replacing CT, DSA and ERCP in living liver donors prior to harvesting.
Materials and methods: MR imaging was performed on a 1.5 T scanner (Sonata, Siemens, phased-array coil). Sequence parameters: T1 FLASH 2D axial, T2 HASTE axial, MRCP HASTE cor, FLASH 3D Angio (TR/TE/TA: 2.1/0.7/15), ce-T1 FLASH. The MRA data set was collected following iv administration of a Gd-chelate (Gd-DTPA, or Gd-BOPTA) at a dosage of 0.2 mmol/kg BW, using an automated injector over 12 s at a volume adjusted rate ranging between 2.5 and 3.5 ml/s. A second 3D data set for display of the portal and venous phase was collected after 10 s of free breathing. 43 potential liver donors were assessed with MRI. 24 patients also underwent DSA. Of these, 17 patients actually underwent liver harvesting. The MRA data sets were correlated with DSA. MRCP results were correlated intra-operative findings.
Results: Patients were excluded as potential donors based on the detection of hepatic hemangiomas (n = 6), as well as unfavorable hepatic morphology (n = 10), as documented on T1- and T2-weighted images. MRCP displayed the biliary system to the level of the first hepatic side branch. MRA depiction of the hepatic arterial morphology correlated with catheter angiography in all 24 patients: 5 aberrant right hepatic arteries originating from the SMA, 6 left hepatic arteries originating from the left gastric artery, and one common hepatic artery originating from the SMA. Similarly, the portal venous system was fully assessed on MRA.

B-0659 11:10

Absolute values of phosphorous metabolites in human liver determined by SLOOP ^{31}P-MR-spectroscopy

M. Beer[1], H. Köstler[1], V. Winkelmann[1], T. Pabst[1], W. Kenn[1], W. Landschütz[2], M. von Kienlin[3], D. Hahn[1]; [1]*Würzburg/DE,* [2]*Erlangen/DE,* [3]*Basle/CH*

Purpose: Quantitative ^{31}P-MR-spectroscopic (MRS) studies reported discrepancies in liver metabolite concentrations. Recently the SLOOP (Spectral Localization with Optimal Pointspread Function) postprocessing program allowed determination of absolute values of phosphorous metabolites in human myocardium with minimal contamination and reduced data deviation. Aim of our work was to establish quantification of metabolite concentrations in human liver with SLOOP ^{31}P-MRS.
Subjects & methods: The examinations were performed on a 1.5 T Magnetom VISION scanner. 10 healthy volunteers (mean age 25.6 ± 3.7 years; 5 male, 5 female) were studied in prone position. ^{31}P-spectra were obtained using a 3D-CSI technique (16 × 16 × 8 step encoding phases, FOV 400 × 400 × 320 mm^3). For determination of absolute concentrations ^{1}H-images acquired in transversal orientation through the whole liver were divided into 5 compartments. Using a concentration of 2.5 mmol for ATP as internal standard, we determined absolute values for phosphorous metabolites (PM) PME, Pi, and PDE. SLOOP included corrections for inhomogenous B1 fields, T1 relaxation.
Results: All acquired ^{31}P-spectra had sufficient signal to noise ratios for all analyzed PM. Pi was detectable in all examined volunteers. Absolute concentrations for PME, Pi and PDE were 2.4 ± 0.6, 1.6 ± 0.5 and 14.2 ± 5.5 mmol respectively. The calculated PME/PDE ratio was 0.16 ± 0.06, calculated Pi/ATP ratio was 0.81 ± 0.22 and the PDE/ATP-ratio was 8.03 ± 3.28.
Conclusion: SLOOP ^{31}P-MRS allows quantification of phosphorous metabolites in human liver. SLOOP allows to use anatomically matched compartments. Therefore, the complete liver parenchyma can contribute to the acquired signal.

B-0660 11:20

Whole body MR scanning in 30 seconds using real-time TrueFISP and a continuously rolling table platform

J. Barkhausen[1], H.H. Quick[1], T. Lauenstein[1], M. Goyen[1], S.G. Rühm[1], G. Laub[2], J.F. Debatin[1], M.E. Ladd[1]; [1]*Essen/DE,* [2]*Erlangen/DE*

Purpose: Development of a technique for a whole body MR scan, from head to knees in 30 seconds based on a rolling table platform and real-time TrueFISP imaging.
Material and methods: The developed rolling table platform BodySURF (System for Unlimited Rolling Field-of-view) with integrated surface coil was mounted on top of the original patient table of a Sonata MR-System (Siemens Medical Systems, Erlangen, Germany). During a 30 second scan, the patient was manually swept through the isocenter of the magnet and 390 continuous axial slices of the entire body are acquired. Data acquisition was performed with a real-time TrueFISP sequence (TR/TE 2.2/1.1 ms, FA 45°, matrix 63 × 128). The system was tested on three volunteers and five patients with metastatic cancer.
Results: The system performed well in all eight cases. All hepatic (19/19) und pulmonary lesions (17/17) with a diameter exceeding 8 mm, detected on thoracic and abdominal helical CT were correctly identified on the TrueFISP images. In one patient multiple small pulmonary nodules (< 5 mm) were missed. Compared to bone scintigraphy 11/15 osseous lesions were detected on the real-time TrueFISP images. Lesions in ribs were missed.

Conclusion: Whole body MRI with real-time TrueFISP and BodySURF is feasible in 30 seconds and can be used for tumor screening and staging.

B-0661 11:30

Regenerative nodules of the liver in Budd–Chiari syndrome: CT and MR findings with pathologic correlation

G. Brancatelli, M.P. Federle; *Pittsburgh, CA/US*

Purpose: To determine the CT and MR imaging appearance of regenerative nodules of the liver in Budd–Chiari syndrome.

Materials and methods: We studied five patients (all women, average age 35, range 28 – 50) with Budd–Chiari syndrome and benign regenerative nodules. CT (n = 4) and MR images (n = 2) were retrospectively reviewed. Diagnosis was based on explantation of the liver (n = 2), surgical (n = 2) or percutaneous biopsy (n = 1). The number, sizes, enhancement pattern, homogeneity of the lesions and the presence of surgical shunts were evaluated.

Results: 51 lesions were identified. The size ranged from 0.6 cm to 3 cm. On unhenanced CT, the tumors were isoattenuating (n = 33, 94 %) or hyperattenuating (n = 2, 6 %). On HAP imaging the lesions were all hyperattenuating (n = 35, 100 %). On PVP the nodules were all hyperattenuating (n = 38, 100 %). In one patient 10 tumors had an hypoattenuating ring on both HAP and PVP. On MR, the lesions were hyperintense (n = 21, 81 %) or isointense (n = 5, 19 %) on T1-WI. One isointense 3 cm nodule had an hyperintense ring. All tumors were hyperintense on T1-WI gadolinium enhanced HAP (n = 26, 100 %). The lesions were hyperintense (n = 16, 62 %) or isointense (n = 10, 38 %) on T1-WI gadolinium enhanced PVP. The nodules were hypointense (n = 11, 42 %), isointense (n = 9, 35 % %) or hyperintense (n = 6, 23 %) on T2-WI. All tumors enhanced homogeneously in all patients both on CT and MR. Three patients had a surgical mesocaval shunt.

Conclusion: Regenerative nodules in Budd–Chiari syndrome are small, multiple, hypervascular on HAP and PVP on both CT and MR imaging, and enhance homogeneously.

B-0662 11:40

Intraindividual comparison of a volumetric interpolated body exam (VIBE) with a 2D GRE sequence in patients with suspicion of focal liver lesions

A. Huppertz, J. Scheidler, A. Kraus, B.J. Wintersperger, T. Balzer, M.F. Reiser; *Munich/DE*

Purpose: To compare intraindividually a three-dimensional (3D) VIBE sequence (volumetric interpolated body exam) for MRI with a 2D GRE breath-hold, non fat-saturated equivalent in the detection and characterization of focal liver lesions.

Materials and methods: 13 patients with known or suspected focal liver lesions underwent 1.5 T MRI at two different timepoints with an interval of 24 – 72 hours. In a first examination pre- and postcontrast (0.1 mmol/kg gadopentetate dimeglumine) 2D GRE imaging (TR/TE/Flip 141/4.1/75) before, after 10 s, 50 s, 120 s and 8 minutes was performed. In a second examination 3D VIBE (5.2/2.6/25) at the same timepoints using the same dose of contrast was performed. All images were compared independently by three blinded readers. Additionally, the image quality was assessed (overall image quality, SNR, CNR and Enhancement).

Results: The total number of lesions detected was identical (n = 33) in both examinations. The VIBE technique allowed for an improved characterization of focal liver lesions by increased confidence in classification, higher spatial resolution and possibility of multiplanar reconstruction. The liver/lesion contrast was higher for the VIBE sequence (not statistically significant $p > 0.05$). SNR was lower in the VIBE sequence for all examined structures. Enhancement in liver parenchyma, lesions and aorta was equal in both sequences. Small vascular structures show higher enhancement in the VIBE sequence ($p < 0.01$).

Conclusion: VIBE technique is superior to conventional 2D GRE images in characterization of focal liver lesions during dynamic evaluation. VIBE images combine comparable liver/lesion contrast with better delineation of small vascular structures and multiplanar reconstruction possibilities.

B-0663 11:50

Liver metastases and MRI: Value of opposed-phase and water excitation sequences

B.J. Op de Beeck, P. Verbeek, F. Grignard, R. Luypaert, F. De Ridder, M. Osteaux; *Brussels/BE*

Purpose: To evaluate the value of opposed-phase and water excitation MR sequences compared to the classical standard MR sequences for detection of liver metastases.

Materials and methods: 20 patients with proven liver metastases underwent MRI examination on a 1.5 T system (Vision, Siemens). The study protocol included a T2-weighted HASTE sequence with and without fat suppression, a T1-weighted SGE sequence in-phase and opposed-phase and a water excitation sequence. Dynamic gadolinium-enhanced imaging was performed with the T1-weighted in-phase SGE sequence during the arterial and portal-parenchymal phase, water excitation sequence in the portal-parenchymal phase and a delayed T1-weighted SGE in-phase sequence with fat suppression.

Results: The best sequence for liver metastases detection was the T1-weighted in-phase SGE sequence during the arterial gadolinium-enhanced phase (213 metastases, 100 %). No significant difference in lesion detection was noticed on the T2-weighted HASTE sequence (99.5 %) nor on the pre-contrast in-phase SGE (98.1 %), portal-parenchymal gadolinium-enhanced SGE (92.0 %) and delayed T1 SGE with fat suppression (95.3 %) sequences. The detection rate on the pre-contrast T1 opposed-phase SGE sequence was lower (86.8 %), especially in patients with liver steatosis. The T1-weighted water excitation sequence before and after gadolinium shows the worst results (respectively 55.7 % and 59.6 %) despite the excellent extrahepatic soft tissue contrast.

Conclusion: T1-weighted water excitation imaging of the liver is not suitable for detection of liver metastases. In patients with liver steatosis, detection of metastases should not be done by opposed-phase T1-weighted SGE sequences.

10:30–12:00 **Room E2**

Breast

SS 1402

Breast intervention

Chairpersons:
E. Salomonowitz (St. Pölten/AT)
R.M.L. Warren (Cambridge/GB)

B-0664 10:30

Delta 16 breast device: Advantages of its use in performing breast FNA

L. Grinyte, V. Mamontovas; *Vilnius/LT*

If suspicious focus in the breast is seen, FNA or core biopsy has to follow. Delta 16 biopsy system allows to perform FNA without preliminary target point spot compression and magnification.

Purpose:

1. To perform FNA with Delta 16 without preliminary compression of suspicious focus.
2. To perform FNA without spot compression repetition.
3. To put into practice Delta 16 view correction program to emphasize important mammography signs.

Materials and methods: 2500 accidental women have been examined during 1998 – 2000. 110 FNA were done with digital Delta 16 system and Alpha RT mammography unit.

Results: 70 of 110 performed FNA were done without preliminary spot compression. 30 FNA were done after accurate spot compression and view magnification of target point. In 10 cases FNA were done without spot compression repetition when it was performed inaccurately. In all cases digital view correction system helped to reveal important mammography signs and to perform precise FNA.

Conclusions:

1. Digital Delta 16 system is excellent for FNA.
2. Spot compression and magnification is not necessary before FNA with Delta 16.
3. Computerized view correction is indispensable for making clearer mammography signs.

B-0665 10:35

Long-term follow-up of nonpalpable breast lesions diagnosed as benign with stereotactic needle localized open biopsy

C. Riedl, T.H. Helbich, M. Memarsadeghi, T. Wagner, S. Taucher, G. Pfarl, G. Wolf; *Vienna/AT*

Purpose: To assess the false-negative rate of nonpalpable breast lesions diagnosed as benign with stereotactic localized open biopsy (SLOB).

Materials and methods: From January 1994 through December 1997, 1123 SLOBs were performed in 1075 consecutive female patients. 472 cases (42 %) yielded malignant results and 651 cases (58 %) benign results. Mammographic follow-up (mean 42 months) was available (until now) for 458 of the 651 benign cases (70 %). When further abnormalities in the operated breast were reported, pre- and postbiopsy mammograms, pathology reports, and results of subsequent mammographic follow-up were reviewed.

Results: Twenty-two (5.4 %) of the 458 cases, for which follow-up was available, required further histological clarification. 5/22 cases had immediate repeat open biopsy within 3 months. 3/5 cases proved to be cancer. In 17/22 cases repeat open biopsy was performed within 8 to 53 months. Malignancy was diagnosed in 4/17 cases. This represented a false-negative rate of 1.3 % (six out of 458).
Conclusion: A small percentage of cases diagnosed as benign with SLOB will change and necessitate repeat biopsy. The data suggest that immediate repeat open biopsy is necessary in cases with a discordant result between histology and mammography. Cases that yield nonspecific benign results 6-month follow-up is a reasonable management strategy.

B-0666 10:45

Comparison of 11-g versus 14-g directional, vacuum-assisted breast biopsy: Quality of harvested tissue, false-negative rate and complication rate

G. Pfarl, T.H. Helbich, M. Rudas, F. Lomoschitz, C. Riedl, G. Wolf; *Vienna/AT*

Purpose: To compare quality of harvested tissue, false-negative rate, and complication rate of 11 gauge and 14 gauge directional, vacuum-assisted breast biopsy (DVABB).
Patients and methods: From July 1994 to October 1999, 412 female patients (age range: 25 – 88 years) underwent DVABB. 11 gauge DVABB was performed in 134 patients (32.5 %), 14 gauge DVABB in 278 patients (67.5 %). Following DVABB, patients underwent either surgical excision (n = 390; 94.7 %) or mammographical follow-up (n = 22; 5.3 %). Histological results of DVABB, surgical breast biopsy and follow-up results were compared and scored for their tissue quality on a three point scale (1 ... disagreement between DVABB and surgery; 2 ... partial agreement; 3 ... complete agreement). In addition, we determined the false negative and complication rate for both systems.
Results: Histological examination after surgery and follow-up proved 183 (44.4 %) to be benign, 18 (4.4 %) to be high-risk-lesions and 211 (51.2 %) to be malign. In the tissue quality 11 gauge DVABB scored better (score 2.92) than the 14 gauge system (score 2.91) ($p > 0.05$). Particularly, in calcifications 11 gauge DVABB scored better (score 2.92) than the 14 gauge system (score 2.88) ($p > 0.05$). The 11 gauge DVABB had a lower false negative rate (2.9 %) than the 14 gauge system (3.6 %) ($p > 0.05$). There was no difference in the complication rate between both systems.
Conclusion: Our results indicate that both DVABB systems are reliable and safe techniques in the diagnosis of non-palpable breast lesions. However, the use of 11 gauge DVABB seems to be advantageous particularly in calcifications.

B-0667 10:55

Stereotactic vacuum-assisted breast biopsy: BI-RADS-classified results of 74 lesions

K.C. Siegmann, M. Müller-Schimpfle, A. Wersebe, N. Fersis, U. Vogel, C.D. Claussen; *Tübingen/DE*

Purpose: Standardization of indication for stereotactic vacuum-assisted breast biopsy by BI-RADS categorization.
Materials and methods: We performed 74 vacuum-assisted breast biopsies in 53 patients, aged 30 – 78 years (mean 52.3) with mammographically detected lesions, sized 3 to 110 mm (mean 20 mm). Most of the lesions consisted of microcalcifications alone or within a mass (97 %; 72/74). They were classified according to the BI-RADS categories (12 BI-RADS 3; 52 BI-RADS 4; 10 BI-RADS 5).
Results: Histology revealed malignancy in 26 % (19/74) of the cases. Ductal in situ carcinomas (n = 13) were the most common findings in this group. From each lesion 8 to 72 cores (mean 26) were taken in a mean time of 60 (25 – 135) minutes. A complete/partial/insufficient removal of the lesion was achieved in 21/51/2 cases (total = 74). No BI-RADS 3 lesion (0/12), 19 % (10/52) of BI-RADS 4 lesions and 90 % (9/10) BI-RADS 5 lesions were malignant. In 4/19 cases (21 %) specimen histology underestimated the lesions pathology which was obtained after operation (in situ instead of invasive carcinoma).
Conclusion: Vacuum-assisted breast biopsy is a reliable procedure that can avoid open surgical biopsy in cases of BI-RADS 4 microcalcifications with typically low positive breast biopsy rates. Moreover it is useful in BI-RADS 5 lesions to assess the lesion extent if complete surgical removal is questionable and in BI-RADS 3 lesions if additional factors exist (e.g. patient wishs biopsy).

B-0668 11:05

Stereotactic biopsy of DCIS of the breast: Underestimation of disease

P. Crystal[1], S. Strano[2], J. Goldshtein[1], M. Koretz[1]; [1]*Beer-Sheva/IL*, [2]*Jerusalem/IL*

Purpose: The goal of this study was to assess the diagnostic accuracy of vacuum-assisted stereotactic biopsy (VASB) in the diagnosis of ductal carcinoma in situ (DCIS) of the breast.
Materials and methods: We retrospectively reviewed 337 VASB performed at our institution. DCIS was diagnosed in 57 cases. Surgical histopathologic results of DCIS patients were available in 48 women and compared with the findings at VASB. We defined the results as concordant, when only DCIS was evident at surgery, or discordant, when invasive carcinoma was found at surgery.
Results: Concordance between VASB and surgical histopathologic results was found in 37 (77 %) cases. No residual tumor was found at surgery in 3 (6 %) cases. Invasive carcinoma was found at surgery in 8 (17 %) cases. Nine patients with DCIS were lost to follow-up because unavailable surgical reports or lack of surgical treatment.
We evaluate the influence of the different factors on the accuracy of DCIS diagnosis. We did not find statistically significant difference between the results of VASB in 3 physicians. The average number of specimens in overall group and in discordant cases was similar. We used various device for VASB, but DCIS underestimation rate has not been statistically different.
Conclusion: Our results confirms that despite the fact that VASB is an accurate technique for diagnosis of DCIS, underestimation of invasive disease is still common.

B-0669 11:15

Results of reexcision after stereotactic vacuum biopsies (VB): 210 cases

K. Rotter, L. Götz, D. Köthe, G. Häntschel, D. Lampe, J. Buchmann, S.H. Heywang-Köbrunner; *Halle a. d. Saale/DE*

Purpose: Compared to core needle biopsy VB allows to remove a much larger volume of tissue. Thus sampling error can be reduced significantly and a benign diagnosis is much more reliable after VB than after needle biopsy.
By correlating the histopathologic results of VB and reexcision, which is performed in all malignant or borderline (ADH) lesions, the number of underestimates (change of ADH to DCIS or invasive carcinoma and change of DCIS to invasive carcinoma) was evaluated. Furthermore correlation of imaging assessment of complete versus partial removal was compared with histopathologis outcome.
Methods and materials: 210 reexcisions after VB (using 11 G probes) were evaluated. Final diagnosis was invasive carcinoma (76), DCIS (105), LCIS 5, ADH (24).
Results: A change from ADH to DCIS (12.5 %), DCIS to invasive carcinoma (6.7 %) and DCIS with suspected invasion to invasive carcinoma occurred in 17 cases (8 %). Radiologically incomplete removal (48.5 %) proved histologically complete in 3 %, incomplete in 45 %. Radiologically complete removal (51.5 %) proved complete in 31 %, incomplete in 20.5 %.
Conclusion: Undersestimates cannot be completely avoided. Radiologic assessment concerning complete removal is unreliable in at least 40 % of cases. Therefore reexcision remains necessary after VB with malignant or borderline histology.

B-0670 11:20

Results of a multicenter evaluation of stereotactic vacuum biopsies (VB) for work-up of mammographically detected indeterminate lesions

K. Rotter[1], U. Kettritz[2], M. Murauer[3], I. Schreer[4]; [1]*Halle a. d. Saale/DE*, [2]*Deggendorf/DE*, [3]*Berlin/DE*, [4]*Kiel/DE*

Purpose: First reports indicated that VB may allow improved accuracy over core biopsy. Purpose of this study was to check reproducibility of the results in a multicenter evaluation.
Methods and materials: Prerequisites for participation were experience with > 100 procedures, dedicated interdiciplinary breast center. In the 5 centers data of > 1500 VB studies had been accumulated and were evalueted retrospectively. Indications: mainly indeterminate or moderately suspicious (95 %) or suspicious lesions (5 %). Approximately 60 % of the lesions were < 1 cm. For VB > 20 cores were acquired using 11 g probes. All malignancies are verified by reexcision, benign lesions are followed at 6 – 12 months to check complete or partial removal.
Results: 23 % lesions proved malignant, 4 % ADH. Among malignant lesions early malignancy strongly prevailed (60 %). 50 % of all lesions and approximately 85 % of lesions < 1 cm were completely removed (imaging assessment), as proof of representative removal. So far no false negative diagnoses occurred. Repeat procedures due to technical problems: 1 %; complications requiring surgery: 0.3 %, requiring 1 night stay: 0.3 %, requiring termination of VB 0.5 %.
Conclusion: VB proves a very accurate and a safe procedure in dedicated breast centers.

B-0671 11:25

Indications for and accuracy of a localization clip in breast diagnosis and breast therapy

R.W.S. Schulz-Wendtland, U.G. Aichinger, N. Lang, W.A. Bautz; *Erlangen/DE*

Purpose: To assess indications and accuracy of a localization clip after ultrasound core cut breast biopsy and vacuum-assisted breast biopsy.
Materials and methods: Retrospective review was performed of 22 lesions that underwent placement of a localizing clip directly into the lesions after ultrasound core cut breast biopsy of lesions with the classification BI-RADS 4 (n = 7) (group 1), stereotactic vacuum-assisted breast biopsy with suspicion of mastopathy DD DCIS (BI-RADS 4/5) (n = 10) (group 2) and before undergoing preoperative chemotherapy (BI-RADS 5) (n = 5) (group 3). The localization and possible divergence of the tissue markers were compared with the follow-up mammograms by a x-y grid. Mammography and histology findings have been compared.
Results: The divergence of the tissue markers of the group 1 and 2 (n = 17) amounts to the follow-up mammograms 3 months later less than 0.5 mm, after 12 months at 16 patients less than 0.5 cm, at one patient less than 1.0 cm in both planes in comparison with the initial images. At all patients of the group 3 (n = 5) the tissue marker clip were the only possibility of the localization of the primary tumor after neoadjuvant chemotherapy and negative results by all diagnostic methods (clinical examination, mammography, ultrasound, MRI).
Conclusion: Tissue marker clip should be placed after all interventions except an operation follows at once after localization by wire in breast cancer.

B-0672 11:35

Galactoscopy: A new method in breast diagnosis?

R.W.S. Schulz-Wendtland[1], U.G. Aichinger[1], S. Kraemer[1], H. Schaaf[2], N. Lang[1], W.A. Bautz[1]; [1]*Erlangen/DE*, [2]*Pfaffenhofen/DE*

Purpose: Cytology, ultrasound and galactography are the important methods in the diagnosis of pathological nipple discharge. Our aim was to evaluate the new possibilities of the microendoscopic examination of lactiferous ducts (galactoscopy).
Materials and methods: From 12/99 to 08/00 we examined 11 patients with pathological (bloody) nipple discharge by cytology, ultrasound, galactography and the new developed method galactoscopy: after local anesthesia we used the endoscopic-system Endo Gnost® (Poly Diagnost). The ducts cannula has an outer/inner diameter of 0.45 mm/0.36 mm, working length 30 mm, the endoscope an outer diameter of 0.30 mm, 1600 pixel, integrated light fibers for illumination, adapted to a CCD-camera.
Results: The examination was possible at all 11 patients. The visual and galactographical diagnosis intraductal papilloma (11 patients) and intraductal cancerin two cases.
Conclusion: The present pilot study confirm the possibility of lactiferouss duct visualization endoscopically using fiberoptics (galactoscopy).

B-0673 11:40

Radio-frequency-breast-electro-biopsy (RF-BEB): A new diagnostic and therapeutic interventional method in breast disease?

R.W.S. Schulz-Wendtland[1], H. Sittek[2], N. Heske[3], S.H. Heywang-Köbrunner[4]; [1]*Erlangen/DE*, [2]*Munich/DE*, [3]*Türkenfeld/DE*, [4]*Halle a. d. Saale/DE*

Purpose: Core cut biopsy, vacuum-assisted breast biopsy and ABBI are standard interventional methods in breast diagnosis. Our aim was to evaluate the possibilities of the Radio-Frequency-Breast-Electro-Biopsy (RF-BEB).
Material and method: From 7/00 until 9/00 we examined 14 patients with suspicious lesions (BI-RADS 4) by clinic, sonography, mammography and the RF-BEB: after local anaesthesia we placed a coaxial system sonographically guided direct at the lesion. Through this a high frequency double walled (saline solution) microtome could be pushed forward. After turning around the microtome under high frequency the specimen and cell rests will be taken out completely by a vacuum adapter. Changing the angle of the coaxial system allows multiple biopsies. After the procedure and retraction of the coaxial system steristrips close the site of puncture.
Results: The examination was possible at all 14 patients. At 8 patients the lesions could be resected completely and at 6 patients of more than 50 %. The histological diagnosis was fibroadenoma in all cases.
Conclusion: The present pilot study confirm the possibilities of RF-BEB as an interventional method for diagnostic and therapeutic indications in breast disease.

B-0674 11:45

MR-guided vacuum-assisted biopsy of breast lesions: A multicenter study

H. Sittek[1], C. Perlet[1], A. Heinig[2], B. Amaya[2], D. Lampe[2], J. Buchmann[2], P. Schneider[1], S.H. Heywang-Köbrunner[2]; [1]*Munich/DE*, [2]*Halle a. d. Saale/DE*

Purpose: To determine the accuracy and clinical application of MR-guided vacuum biopsy (VB) of contrast enhancing lesions.
Material and methods: MR-guided vacuum-assisted breast biopsy with an 11 gauge device was performed in 129 lesions. Verification included re-excision of malignancies as well as correlation of histology and follow-up imaging in benign lesions.
Results: Of 129 lesions 37 were diagnosed as malignant, 3 as atypical ductal hyperplasia (ADH) and 89 as benign. Diagnosis of all malignancies proved correct with re-excision histology. 16 % of malignant lesions were removed completely by VB. One invasive ductal carcinoma was underestimated as ADH. Of benign lesions, one was found with no change, in all other cases MR-follow-up proved partial or complete removal of the lesion.
Conclusion: MR-guided vacuum biopsy offers good posibility in estimating small lesions which are not visible by any other modality.

B-0675 11:50

Cryotherapy of breast cancer under ultrasound-guidance: Initial results

S.O.R. Pfleiderer, A. Schneider, W.A. Kaiser; *Jena/DE*

Purpose: The aim of our study was to investigate the feasibility and potential of cryosurgery in the therapy of breast cancer.
Materials and methods: 14 patients (58.5 ± 10.4 a) with breast cancer underwent cryotherapy. After ultrasound-guided placement of the cryo probe in the tumor two freeze/thaw cycles with a duration of 7 and 5 minutes respectively were carried out. The diameters of the occuring iceballs were measured sonographically. The patients were operated within 2 to 5 days later. The operation specimen were evaluated histologically.
Results: The maximum diameters of the iceballs were between 21 and 31.8 mm. The surface of the iceballs was well definable in ultrasound. 5 tumors with a diameter below 16 mm did not show rests of invasive cancer after treatment. 3 of them had DCIS in the surrounding. Subtotal necrosis was observed in 11 tumors which had a diameter of 16 mm and more.
Conclusions: After these first cases cryotherapy seems to be promising in the treatment of small breast cancers. The remaining DCIS may be due to the short period of time between cryotherapy and histological evaluation. In larger breast cancers two or more cryo probes should be used to achieve larger iceballs.

10:30–12:00 **Room F1**

Chest

SS 1404

Thoracic interventions and lung disease

Chairpersons:
J. Cáceres (Barcelona/ES)
C. Düber (Mannheim/DE)

B-0676 10:30

Utility of polymerase chain reaction (PCR) for detecting mycobacterium tuberculosis (TB) in specimens from transthoracic lung aspiration

E.-Y. Kang, J.-A. Choi, B. Suh, Y.-W. Oh, C. Lee, J. Shim; *Seoul/KR*

Purpose: To determine the clinical utility of PCR in detecting TB in specimens from transthoracic lung aspiration.
Materials and methods: PCR for detecting TB from lung aspirates was performed prospectively in addition to cytologic and/or histologic study in 45 patients in whom CT diagnosis was difficult. Transthoracic lung aspiration was performed with 21 gauge needle by a radiologist by CT (n = 25), US (n = 5) and fluoroscopic guidance (n = 15). Final diagnoses were primary malignant neoplasm (n = 18), metastasis (n = 1), hamartoma (n = 1), TB (n = 17), and pneumonia (n = 8), including actinomycosis and aspergillosis.
Results: In 17 TB patients, PCR was positive in 11 and negative in 6. Among 11 with positive PCR, 7 included malignancy at CT diagnosis, 8 showed negative sputum AFB, and only 1 was diagnosed histologically as TB from lung aspirates. In 19 malignancy cases, PCR was negative in all. 7 of 19 included TB and 8 showed associated TB lesions at CT diagnosis. PCR was negative in hamartoma and pneumonia. Sensitivity and specificity of PCR in detecting TB from percutaneous lung aspirates were 64.7 % and 100 %.

Conclusion: PCR for detecting TB from percutaneous lung aspirates would be a good adjuvant to histologic and cytologic diagnosis for the definitive and differential diagnosis of tuberculosis.

B-0677 10:40

Atypical extrapulmonary tuberculosis: Is biopsy essential?

L. Thanos, A. Patsalides, S. Mylona, S. Arapostathi, A. Papatheodorou, N. Batakis; *Athens/GR*

Purpose: Diagnosis of extrapulmonary tuberculosis (TB) has proved to be particularly difficult. The aim of our presentation is to present our experience with atypical cases of extrapulmonary TB and show that culture or histologic analysis of biopsy specimens is still required in many patients for definitive diagnosis.
Methods and materials: We present the computed tomography (CT) findings of seven patients that were referred to our department with clinical evidence of TB. CT reveiled granulomas in atypical extrapulmonary sites. These findings could not verify extrapulmonary TB because their location was not usual and the radiologic findings could be attributed to many other diseases.
Results: The granuloma sites identified with CT are the following: symphysis pubis 1, paravertebral without vertebra involvement 1, ischium 2, porta hepatis 1, pelvis 1, thoracic wall 1. CT guided biopsy was performed in all patients and histologic specimens were obtained successfully in all cases. No complications were observed. The culture, staining and histologic findings were typical of TB in all cases and the patients were treated accordingly.
Conclusions: The correct diagnosis of extrapulmonary tuberculosis can take months. A high level of suspicion is required when dealing with high risk patients. The staining culture and the histologic analysis of the biopsy specimens is essential for definitive diagnosis, especially in atypical cases.

B-0678 10:50

Outpatient treatment of iatrogenic pneumothorax with small-bore catheter: Experience in 45 cases

L. Pancione; *Turin/IT*

Purpose: The use of small-bore catheters to treat patients with symptomatic and/or higher than 30 % iatrogenic pneumothorax (PNX), following upon lung biopsy was assessed. This study describes the procedure and the possibility of patient follow-up in an outpatients department.
Materials and methods: 45 patients with iatrogenic pneumothorax, which was not resolved by suction, were studied. Under fluoroscopic or CT guidance a 6.3 French intrathoracic pig-tail catheter (Cook), using the trocar technique, at a point corresponding to the third or fourth intercostal space on the midclavicular line was placed. After suction of intrathoracic air the catheter was connected to a Heimlich valve. If at the x-ray examination after two hours no recurrence of the PNX emerged, the patient was discharged and underwent x-ray follow-up every 24 hours in the outpatients department. If PNX recurred, or if pain and/or dyspnoea persisted, the patient was readmitted for at least one week.
Results: All cases were cured successfully. Only 9 patients were readmitted of which in 4 cases 8 – 10 French catheters were used.
Conclusions: The procedure is easy to perform, with few risk, good tolerance, and low costs. In most cases follow-up can be performed in the outpatients department. Finally, the possibility of treating an iatrogenic PNX complicating an interventional technique under radiological guidance further promotes the acceptability of this procedure by colleagues from other medical disciplines.

B-0679 11:00

US-guided percutaneous aspiration of pleural fluid

E. Testempassi, A. Attard, V. Sotiropoulou, D. Kazos, C. Artinopoulos; *Athens/GR*

Purpose: The purpose of our study is to assess the role of Ultrasound (US) in the accurate diagnosis of pleural effusions and to compare the success rate of blind and under US guidance aspiration of pleural fluid collections.
Materials and methods: A total of 556 patients were examined by Ultrasound for the investigation of known or suspected pleural effusion. All the above patients had performed unsuccessful blind thoracentesis of pleural effusion.
Results: The cause of pleural fluid was neoplastic in 221 cases, inflammatory in 198 patients, tuberculosis in 52 patients and no evidence of pleural fluid was in 85 patients. 113 patients had bilateral pleural effusions. Aspiration was performed in all patients with pleural fluid and the overall success rate was 92 %. There was no complication of pneumothorax in all above patients after the aspiration.
Conclusions: US is a useful and cost-effective examination in the investigation of pleural fluid and it is significantly helpful in the definition of the exact location of the fluid and precise point of puncture. It is also useful in the assessment of fluid morphology, the presence of loculations and pleural thickening.

B-0680 11:10

CT guided FNA of mediastinal masses

M. Stassinopoulou, E. Tavernaraki, M. Mitropoulou, K. Deliveliotis, A. Tavernaraki, D. Daskalopoulou, S. Markidou; *Athens/GR*

Purpose: To evaluate the efficiency of the CT guided FNA as a safe and quick method for the diagnosis of the mediastinal masses in out- and inpatiens.
Materials and methods: We performed FNA on 46 patients aged 21 – 82 years (15 F, 31 M) with mediastinal masses. During the preliminary CT scan, the entry site of the needle (20 – 22 G) was determined and the safest route to the lesion was chosen. A scan confirmed the location of the needle tip. We used negative pressure on the syringe to obtain material through the needle. It is important to allow the pressure to equalize before removing the needle. The taken cytological specimen was examined by the cytopathologist. A post biopsy CT scan was performed.
Results: The following results were obtained: 2 nodular hyperplasias of thyroid, 1 thymic cyst, 2 Hürthle cells tumors, 4 thymomas, 1 reactive lymphadenitis, 1 tb lymphadenitis, 1 cat scratch disease, 2 HD, 10 NHD, 11 metastatic adeno Ca, 3 small cell Ca, 1 malignant thymoma, 1 anaplastic thymic seminoma, 1 myeloma, 1 malignant fibrous histiocytoma, 2 malignant schwannoma, 1 chondrosarcoma, 1 myxoid liposarcoma. Forty out of 46 (86.9 %) cases were histologically confirmed by surgical biopsy.
Conclusion: CT-guided FNA is a safe, fast and low cost method to determine a precise diagnosis of mediastinal masses.

B-0681 11:20

Low-dose digital radiography detection of tuberculous lung lesions

I.B. Belova, V.M. Kitaev; *Moscow/RU*

Purpose: Prophylactic fluorographic examination has been the main method for detecting lung tuberculosis in Russia. It is expected that the countrywide installation of low-dose digital radiographic devices (LDRD) "Siberia" will improve radiological screening. The purpose was to determine the potential role of LDRD in the prophylaxis of lung tbc and to study the presentation of tbc on these digital images.
Materials and methods: LDRD is a digital X-ray imaging device with a multiwire proportional chamber used as the detector. LDRD has high contrast sensitivity (less than 1.5 %) and wide dynamic range (over 130), the dose for lung examination is 3 – 5 mR. Digital chest images of 30 925 high-risk patients were analysed.
Results: In 1.9 % of the patients additional examinations were necessary. In 265 patients undiagnosed lung disease was detected. There were 9 cancer cases, 36 tuberculosis, 189 acute pneumonia, 31 others. Unlike X-ray film digital images showed much better destruction, nodules, caverns, etc.
Conclusion: The LDRD screening was highly efficient in detecting lung disease. The use of "Siberia" can be recommended especially because of its low dose.

B-0682 11:30

MRI follow-up of pulmonary manifestations in patients with Wegener's disease

J. Biederer[1], M. Reuter[1], C. Winkler[1], M. Both[1], C. Richter[2], A. Schnabel[2], W.-L. Gross[2], M. Heller[1]; *[1]Kiel/DE, [2]Lübeck/DE*

Purpose: To evaluate if MRI using a specially adapted protocol could replace CT/HRCT for monitoring pulmonary manifestations of systemic Wegener's disease.
Methods and materials: Nine chest MRI of 6 patients with different stages of pulmonary Wegener's disease were evaluated blinded to CT findings and then compared with recent CT/HRCT examinations (two observers/judgement by consensus). MRI sequences: T1-GRE breath-hold (TR/TE 129/2.2 ms, matrix 173 × 256), T2-haste breath-hold/cardiac gating (TR/TE 2000/43 ms, matrix 192 × 256), T2-TSE respiration gating (TR/TE 3000 – 4000/120 ms, Matrix 270 × 512), 6 – 10 mm slices, pulsation artefacts on T1-GRE compensated by presaturation.

Results: Granulomas were detected when 5 mm or larger, reticular/linear opacities when 0.5 mm or thicker. Detection of mediastinal lymph nodes and reticular patterns in the lung periphery were superior on T2-TSE. In 2/9 examinations high signal intensity of lung parenchyma on T2-weighted MRI correlated well with recent ground glass opacities seen on follow-up HRCT. High T2-signal of granulomas may indicate inflammatory activity, but the number is too small for correct statistical evaluation. Advantages of MRI are free choice of imaging plains, excellent soft tissue contrast and absence of ionising radiation.
Conclusion: MRI has the potential to replace CT for follow up in patients with pulmonary Wegener's disease, as the combined sequence protocol offers high spatial resolution and excellent soft tissue contrast. The study will be continued.

B-0683 11:35

Radiologic-histologic correlation of the lung: Experimental quantification of lung tissue shrinkage during histologic preparation of fixed lung tissue

J. Kemper[1], C. Müller-Leisse[2], A. Prescher[3], P. Fuchs[3], U. Mödder[1]; *[1]Düsseldorf/DE, [2]Mönchengladbach/DE, [3]Aachen/DE*

Purpose: Radiologic-histologic correlations of lung tissue have revealed a shrinkage of unknown degree during histologic preparation. The aim of this study was to experimentally quantify the degree of lung tissue shrinkage and establish a possible correction factor allowing a precise morphometric correlation between radiologic and histologic morphology.
Material and methods: Porcine lungs were fixated in a glykol-formalin solution for radiologic in-vitro examination. We determined via photoplanimetric method the bronchial wall thickness, the diameter, the luminal area of 30 bronchi of varying sizes, and the area of 13 parenchymal lung samples. All specimens were then histologically embedded in paraffin by standard procedures. The histologic specimens were examined by photoplanimetry for the same parameters as mentioned above. Correlational and significance analyses were calculated for analogous measurements in both groups.
Results: All parameters showed a significant degree of shrinkage ($p < 0.0001$). The degree of shrinkage of the bronchial wall after histologic preparation was on average 4.8 ± 1.4 %. The diameter, the luminal area of the brochi, and the parenchyma shrink an average of 12 ± 1.7 %, 22.7 ± 1.9 %, 33.9 ± 1.5 %. Corresponding correction factors could thus be calculated (histology-fixation).
Conclusion: To our knowledge, we introduce for the first time correction factors p which allow the elimination of shrinkage artefacts in fixated lung tissue during histologic preparation. These factors constitute the base for exact morphometry and establish a model for reliable radiologic-histologic correlation of the lung.

B-0684 11:40

Computed tomography investigation of chest gunshot wounds

A. Salzano, V. Nocera, M. Amitrano, A. Nunziata; *Naples/IT*

Purpose: To evaluate the role of CT in detecting chest gunshot wounds, especially the complex pleural and poulmonary associated lesions, important for the surgical approach, intensive care or conservative treatment.
Methods and materials: We report our experience of 34 cases (33 males and 1 woman; mean age: 34 years, range 17 – 49 years) of chest firearms wounds observed in the last five years and studied by CT investigation. CT was carried out in emergency by dynamic scans and directly with i.v. contrast agent injection.
Results: CT assessed lung comptusive-laceration areas in 27 cases, hemothorax in 20, soft tissue chest wall enphysema in 14, pneumothorax in 9 (combined with hemothorax in 8) and pneumomediastinum in 5. The rupture of diaphragm was diagnosed in 5 cases and poulmonary atelectasia in 4; CT showed vertebral injuries of thorax in 14 cases with spinal damage in 8 cases; D3 and D5 involvement resulted most frequent.
Conclusion: CT is the method of choise to diagnose in emergency the main chest gunshot wounds, permetting rapidly the diagnosis of radiological features due to the impact and damages of bullet of the thorax and other body districts. Besides, it provides to the surgeon an accurate approach and therapeutical planning.

B-0685

withdrawn by author

10:30–12:00 **Room F2**

Neuro

SS 1411

Stroke (1) Diffusion/Perfusion

Chairpersons:
S.E. Ekholm (Gothenburg/SE)
A. Thron (Aachen/DE)

B-0686 10:30

Quantitative assessment of regional cerebral blood flow by perfusion CT: A validation study in human patients by simultaneous cerebral stable Xenon-CT

M. Wintermark, J.-P. Thiran, P. Maeder, P. Schnyder, R. Meuli; *Lausanne/CH*

Purpose: Demonstration of the validity of perfusion CT examinations for quantitative measurement of rCBF by comparison with the results of stable Xenon-CT, considered as a gold standard\CRLF
Materials and methods: Twelve stable Xenon and perfusion cerebral CT were achieved within a few minute interval in patients with various cerebrovascular diseases. Perfusion CT studies were performed with a multidetector spiral CT unit, using the following protocol: 25 successive 10 mm CT sections obtained every 2 seconds, 80 kVp, 200 mAs, CT acquisition beginning 2 seconds prior to intravenous administration of iodinated contrast material at a rate of 5 cc per second. rCBF maps were calculated from CT data according the central volume principle, by singular value decomposition (SVD) and least mean square (LMS) deconvolutions. They were compared to the stable Xenon-CT values in 20 regions of interest (ROI) at each section level in all patients, through bilateral T-tests for matched variables and linear regression analysis.
Results: Linear regression analysis demonstrated an overall strong correlation between perfusion and stable Xenon rCBF values (r: 0.89 and slope: 0.87 for SVD and r: 0.82 and slope: 0.83 for LMS). No significant difference ($p > 0.1$) could be observed between perfusion and stable Xenon-CT results on the one side and between both deconvolution methods on the other.
Conclusion: Cerebral perfusion CT studies allow for accurate and reliable quantitative measurement of rCBF in a large range of rCBF values. Perfusion CT is thus meant to afford new opportunities in the management of acute stroke patients.

B-0687 10:40

MRI and electrophysiology in lateral medullary infarction (Wallenberg's syndrom) predicting central poststroke pain

C. Fitzek[1], S. Fitzek[1], U. Baumgärtner[2], W. Magerl[2], R.D. Treede[2], H.C. Hopf[2], P.P. Urban[2], P. Stoeter[2]; *[1]Jena/DE, [2]Mainz/DE*

Purpose: To identify clinical, electrophysiological and MRI predictors of central poststroke pain in patients with medullary infarctions.
Methods and materials: Clinical findings, frequency of post stroke pain, high resolution MRI, blink reflex, and quantitative sensory testing (QST) were investigated in 12 patients with medullary infarction.
Results: Of the 12 patients with medullary infarction, 8 (67 %) developed central poststroke pain within days to 24 month after acute infarction. Facial pain correlated significantly with MRI lesions in the lower parts of the medulla and with contact of the lesion with the trigemial spinal tract and nucleus (TSTN). Although there was one patient who had a small lesion projecting on the spinothalamic tract (ST) and developed contralateral pain of the limbs, only, we found no statistical correlation between pain syndromes and contact of lesions with ST.
Conclusion: Electronic matching of high resolution MRI in combination with electrophysiological and clinical data is a qualified approach to validate current understanding of functional structures and pathways in brainstem.

B-0688 10:50

Hyperacute ischemic stroke within 6 hours of stroke onset evaluated by diffusion-weighted MR imaging and fast fluid-attenuated inversion-recovery MR imaging: The value of arterial hyperintensity in diffusion-negative stroke

M. Maeda, T. Ishii, H. Sakuma, K. Takeda; *Tsu/JP*

Purpose: Our purpose of this study was to evaluate the value of fast fluid-attenuated inversion-recovery (FLAIR) imaging in comparison to Diffusion-weighted (DW) imaging in patients with hyperacute stroke.

Methods and materials: We reviewed cerebral MR images in a 13-month period in whom DW imaging and fast FLAIR imaging were performed within 6 hours after onset (n = 11). Special attention was paid to the presence or absence of arterial hyperintensity (AH) on FLAIR images and abnormal high signal regions on DW images in the affected vascular territories.
Results: AH was positive in 8 of the 11 patients, all of whom had embolic- or thrombotic-type infarctions with middle cerebral arterial (MCA) distribution. AH was negative in the remaining 3 patients. The regions of high signal diffusion abnormalities were found in 10 of the 11 patients. A single patient showed an absence of diffusion abnormality but the presence of AH in the affected MCA territory on the initial MR examination, in whom embolic infarction was later found.
Conclusion: Although DW imaging is highly sensitive in stroke, DW imaging alone may not rule out possible infarction. AH can precede diffusion abnormality and may provide a clue to early detection of impending infarction.

B-0689 11:00

Diffusion weighted MRI at 0.5 T: Comparison with the turboFLAIR sequence in stroke patients

A. Maubon[1], M.-P. Boncoeur-Martel[1], M. DeGraef[2], P.-Y. Daclin[2], J.-P. Rouanet de Lavit[2]; *[1]Limoges/FR, [2]Montpellier/FR*

Purpose: Evaluate the feasibility and diagnostic value at low field MRI of a diffusion weighted multishot echo-planar sequence (DW) for detection of acute stroke.
Methods and materials: Eighty eight patients (36 male, 52 female, mean age 66 ± 9 year) referred for acute neurological disturbance. Cranial MRI on a 0.5 T imager with 15 mT/m gradients and echo planar capabilitites. Sequences included turboFLAIR (TR/TE/TI 8000/300/2000, TSE factoe 20, NSA 4, 256 × 256, 16 6 mm slices, 4:56 minutes) and Diffusion weighted multishot echoplanar sequence (spectral fat saturation, TR/TE 3327/140, EPI factor 13, NSA 2, 128 × 128, 16 7 mm slices, phase, measure and slice gradients activation, b = 0 and 775 s/mm^2, 2:23 minutes). Prospective double blind comparison of DW and FLAIR for the detection of stroke.
Results: A stroke was found in 60/88 patients (68 %) with 102 locations altogether. Patient motion severely degraded the sequences making them non diagnostic in 13/88 (15 %) and 5/88 (6 %) for DW and FLAIR respectively ($p < 0.05$). Acute lesions, not detected on the FLAIR sequence, were detected in 12 patients (20 locations) with the DW sequence ($p < 0.02$). No statistically significant difference was found for lesions at the acute or late phase.
Conclusion: A diagnostic quality DW sequence is routinely feasible on a commercial low field magnet. DW proved specialy useful to differentiate between acute and older lesions that all appear as high signal on the FLAIR sequence.

B-0690 11:10

Diffusion and perfusion in subregions of ischemia: A magnetic resonance imaging study in acute ischemic stroke

Y. Liu[1], J.O. Karonen[1], R.L. Vanninen[1], J. Perkiö[2], M. Könönen[1], P.A. Vainio[1], S. Soimakallio[1], H.J. Aronen[1]; *[1]Kuopio/FI, [2]Helsinki/FI*

Purpose: To study the apparent diffusion coefficient (ADC) and perfusion changes in subregions of acute (< 24 h) cerebral ischemia.
Materials and methods: We retrospectively studied 14 stroke patients who were imaged with diffusion and perfusion MR imaging on day 1 (< 24 h) and day 8 and whose infarcts showed clear enlargement in diffusion MR images during the week. Maps of ADC, cerebral blood flow (CBF), cerebral blood volume (CBV), and mean transit time (MTT) were generated from diffusion and perfusion MR images. ADC, CBF, and CBV were measured on day 1 in the area of infarct growth, ultimately surviving ischemic tissue (tissue with prolonged MTT on day 1 but which did not proceed to infarction by day 8), and their contralateral normal regions.
Results: The CBF in the area of infarct growth (46 % of normal) was significantly ($p = 0.005$) lower than in the surviving tissue (66 % of normal). The CBV in the area of infarct growth (81 % of normal) was significantly ($p < 0.001$) lower than in the surviving tissue (112 % of normal, compensatory vasodilatation). The ADC in the area of infarct growth ($0.76 \cdot 10^{-3}$ mm^2/s) was significantly ($p = 0.001$) lower than in the surviving tissue ($0.83 \cdot 10^{-3}$ mm^2/s).
Conclusion: Measurement of ADC, CBF, and CBV may help distinguish between the surviving tissue and the tissue proceeding to infarction.

B-0691 11:20

Diffusion-weighted MR imaging in acute cerebral infarction: Something more than ischaemic penumbra

J.A. Villanua[1], J.A. Recondo[1], E. Fernández[1], A. Cabrera[2], J. Massó[1], J.A. Larrea[1]; *[1]San Sebastian/ES, [2]Vitoria/ES*

Purpose: To demonstrate the Diffusion-Weighted imaging (DWI) as a valid MR technique in the study of acute cerebral infarction (ACI) in young adults, subacute arteriosclerotic encephalopaty (SAE) in elderly patients and in the differential diagnosis (DD) with tumors.
Material and methods: 40 patients clinically suspicious of ACI were consecutively submitted to MR evaluation. 4 young adults (under 40 years). 9 adults in vasculopathic age (mean 64 a). 25 patients with clinical diagnosis of SAE (mean 72 a), and 2 patients with doubtful diagnosis on the cranial CT of cerebral infarction (DD with tumor). In all of these patients we performed SE T1W, T2W, Flair and DWI MR sequences.
Results: After DWI MR the four young adults were diagnosed without doubt to have ACI. In two of them a clinical and Conventional MR presumption of Multiple sclerosis (MS) was made. In the two patients with a DD between tumor and infarction, DWI MR images clearly verified the presence of ischaemia distributed along deep perforating branches territories. In all of the 25 patients with suspicious SAE, the DWI MR studies differentiated between the acute ischaemic lesions and the chronic ones.
Conclusion: DWI MR images provide useful clinical information (not sufficiently obtained with only conventional MR studies) in cases of ACI when a consideration between tumor, MS and infarction arose, as well as in elderly patients with a clinical picture of SAE (differentiation between acute and chronic lesions).

B-0692 11:30

MR diffusion tensor imaging of early stroke at 3 T: A possible marker of outcome?

J.H. Gillard, N.G. Papadakis, K. Martin, C. Price, L. Warburton, N. Antoun, C. Huang, A.T. Carpenter, J.D. Pickard; *Cambridge/GB*

Purpose: MR diffusion weighted imaging (DWI) enables the identification of early ischaemia in acute stroke. Recent advances in DWI allow the identification of anisotropic white matter tracts with diffusion tensor imaging (DTI). We used DTI to study patients with recent stroke in a high field (3 T) MR machine specifically to determine whether DTI could produce an alternative predictor of clinical outcome and disability.
Methods and materials: Eleven patients presenting with recent stroke were imaged. Imaging was performed on a 3 T whole body system. DTI was performed using a standard single-shot spin-echo echo planar imaging pulse sequence. The DTI sequence took approximately 5 minutes, with minimal post-processing.
Results: DTI was successfully performed in ten patients. All patients demonstrated DWI changes on the b 1000 image. DTI imaging was initially abnormal in eight patients. The abnormalities consisted of actual disruption of white matter tracts in seven patients. One patient without tract disruption initially had progressed to tract disruption when reimaged six days from stroke onset. A further patient had distortion of white matter tracts around an infarct. Five months after stroke onset there had been significant recovery in motor and speech function.
Conclusion: DTI is readily performed at 3 T and produces images of high quality. The extent or lack of tract destruction may be prognostically important as it provides information that is not available with conventional diffusion or perfusion weighted imaging. Distortion of white matter tracts may be associated with improved recovery and clinical outcome.

B-0693 11:40

Diffusion-weighted MRI reliably identifies brainstem and thalamic infarctions

W. Küker, J. Weise, H. Krapf, F. Schmidt, S. Friese, M. Bähr; *Tübingen/DE*

Background and purpose: Diffusion-weighted MRI (DW-MRI) has demonstrated its high sensitivity to acute supratentorial ischemic lesions. We examined the sensitivity of DW-MRI for acute brainstem and isolated thalamic infarctions.
Methods: We performed diffusion- and T2-weighted MRI in 45 patients with clinical symptoms of infratentorial infarction between 6/1997 and 1/2000. The time between the onset of symptoms and the first MRI was 2 hours to 7 days with a median of 2 days. MRI repeats were performed in 4 cases. Lesion detectability and size were evaluated for different brainstem and thalamic localizations in appreciation of the clinical symptoms.
Results: A brainstem or thalamic infarction could be identified in all patients by comparison of DW-MRI, T2-weighted images and clinical symptoms. Pons infarctions were the largest, followed by midbrain and thalamic lesions. Medulla

oblongata infarctions were small in comparison. Pons, midbrain and thalamic infarctions were reliably identified beginning 12 hours after the onset of symptoms. In contrast, detectability of medulla oblongata infarctions varied within the first 24 hours and their overall visibilty was worse than that of other brainstem infarctions corresponding to their small size. Two medulla oblongata infarctions and one pontine infarction examined within the first 5 hours after the onset of symptoms were not identified but could be demonstrated in follow-up examinations.
Conclusion: Acute pons, midbrain and thalamic infarctions can reliably be visualized by a combination of DW-MRI and T2-weighted images beginning 12 hours after ischemia. However, sensitivity seems to be lower during the first hours and for medulla oblongata lesions.

B-0694 11:50

The value of diffusion-weighted imaging and cerebral perfusion studies in the management of patients with unclear pathology in the intensive care unit

P.C. Maly Sundgren, P. Reinstrup, B. Romner, S.L. Holtås; *Lund/SE*

Purpose: To describe the use and the clinical value of conventional MRI included diffusion-weighted (DWI) and perfusion-weighted (PWI) images in patients at the Intensive Care Unit.
Material and methods: Diffusion-weighted EPI sequences and perfusion-weighted images have been performed as a part of the evaluation in 20 intensive care patients with unclear pathology (14 men and 6 women, aged 1.5 – 70 years, mean 43 years) during a two-year period.
Results: In four cases the DWI and PWI images demonstrated changes consistent with global ischemia, which was an unexpected finding in two of the cases and contributed to the decision to close down the respiratory support. In five cases of trauma the MR images were helpful in determining the patients' final outcome. In three cases the findings were helpful in predicting the outcome after an ischemic event. The clinical history, MR images including DWI and PWI sequences, and, in some of the cases, follow-up will be presented in selected cases.
Conclusion: The use of diffusion- and perfusion-weighted images in combination with conventional MR can be very helpful in the evaluation and management of unclear cases at the intensive care unit. The obtained information can, especially if the examination can be performed early in the work-up of the patient, be helpful in predicting the clinical outcome, in suggesting further examinations and can therefore facilitate a clinical decision. In spite of their condition, these patients can be examined with MR, which, however, requires good cooperation with the staff of the Intensive Care Unit.

10:30–12:00 **Room G**

Computer Applications

SS 1405

Web and information systems

Chairpersons:
J.-C. Kurdziel (Luxembourg/LU)
B.B. Wein (Aachen/DE)

B-0695 10:30

Integrated RIS/PACS and WEB image distribution throughout the whole institution in the clinic of Erfurt/Germany

H. Grell[1], S. Basche[1], E. Kitzig[1], T.-H. Osswald[2]; *[1]Erfurt/DE, [2]Neu-Isenburg/DE*

Purpose: Fully integrated RIS (Medora) and PACS (Pathspeed) from GE Medical Systems Information Technologies in the radiology department and connection of 12 modalities, 24 PACS-Viewing Stations and WEB-based image distribution for 100 concurrent users.
Integrated RIS/PACS into one grafical user interface allows a more workflow driven handling of these systems and leads to a higher efficiency in the radiology reporting process.
Default display procedures and configurable worklists depending on different examinations and user preferences allowing a fast and easy presentation of images in the wards.
Conclusion: High acceptance of the fully integrated RIS/PACS within the whole institution due to higher efficiency and faster reporting leads to a totally filmless hospital.

B-0696 10:35

Computer applications developed by the CBT/WBT medical edutainment group

M. Grunewald[1], E. Wenkel[1], G. Bischoff[2], A. Sarikas[1], M. Wagner[1], W.A. Bautz[1]; *[1]Erlangen/DE, [2]Munich/DE*

Purpose: To increase the expertise of students and doctors in developing individual computer-based training (CBT) and web-based training (WBT) programs at the medical school of Erlangen University.
Methods and materials: The CBT/WBT medical edutainment (education and entertainment) group was founded in 1997 and consists of medical students and doctors qualified in computer science, medicine, and education. It offers the possibility to develop individual CBT and WBT programs for all departments of the medical school at Erlangen University. New members in the CBT/WBT medical edutainment group are equipped with hard- and software. Additionally they are trained in desktop and web publishing. In return, these novices provide manpower for the CBT and WBT projects. No-name publishing and selling of the developed programs provides the group's funding.
Results: Since 1997 individual CBT and WBT projects were developed for the Anatomy Institute, the Pathology Institute and the Institute of Diagnostic Radiology of our University. These programs are regularly updated and peer-reviewed. The CBT/WBT medical edutainment group members benefit from free equipment and additional qualification in desktop and web publishing. No-name publishing of the programs reduces the price for the students.
Conclusion: The CBT/WBT medical edutainment group project may be extended to other national and international universities. Thus co-operating medical students, doctors and institutes all over the world may profit from the CBT/WBT medical edutainment group project as well.
For further information contact our Website (http://www.idr.med.uni-erlangen.de/CBT-WBT-medical-edutainment-group/index.html).

B-0697 10:40

RIS/PACS: Cost effectiveness

I. Kaden[1], J. Schwarzer[1], C. Sprengel[1], D. Tolksdorf[2], R. Braunschweig[1]; *[1]Halle a. d. Saale/DE, [2]Köln/DE*

Purpose: In the last 5 years, RIS/PACS have become of paramount clinical interest. We would like to present details on cost effectiveness one year after installation.
Materials and methods: In our hospital we use all types of acquisition equipment, e.g. digital direct radiography. For image data archiving we use an Agfa IMPAX system and a RIS manufactured by GAP. An activity-based cost method was used to clarify cost effectiveness, qualitative and quantitative effects on the workflow and on the integrated health care enterprises.
Results: By the end of the installation we are completely filmless in our hospital. More than DEM 750 000 p.a. has been saved. The diagnostic and therapeutic process has been reduced by about 25 % on an average. New job profiles have been created and refinanced through these savings.
Conclusions: From the clinical point of view RIS/PACS helps to intensify our workflow. From the economical point of view RIS/PACS is able to refinance itself.

B-0698 10:50

Integrated healthcare information system in the design of a new filmless and paperless hospital

O. Ratib, H. Kho, R. Yu, W. Yang, M. McCoy; *Los Angeles, CA/US*

UCLA is in the process of building a new acute-care hospital due to open in 2005 with the intent to operate fully digitally. The strategic planning for this hospital is based on a set of new paradigms: wider and more efficient access to all information sources, enterprise-wide data repository, usage of thin-client technology and wide usage generic information-appliances and wireless devices allowing access to information from anywhere in the hospital.
These new paradigms required significant changes in architecture. We elected to adopt an enterprise-wide data repository strategy where images would reside in local PACS archive storage for limited time and then migrate to generic data archive that can be decentralized or outsourced to data-warehousing companies. The other technical innovation is the adoption of display devices that will be available across the enterprise allowing users to review patient records as well as other types of medical and technical information from a variety of sources using a similar paradigm as today's web-based technology. The emerging technology of "information appliances" consisting of devices that can be portable or wall-mounted and will allow to navigate though different clinical data.

The new infrastructure design is based on emerging technologies in networking, flat panel displays and data warehousing. Compliance with the IHE guidelines in a multi-vendor environment will be discussed. A particular attention will be given to describe foreseen changes in radiologist practice using electronic communication, special workstations and projection devices for clinical conferences, and facilitated access to images from remote locations with teleconsultation capability.

B-0699 11:00

Mediconomia: An online tutorial for radiology including cost effectiveness of diagnostic procedures

M. Pech, J. Braun, T. Tolxdorff, U.K.M. Teichgräber, J. Ricke; *Berlin/DE*

Purpose: Implementation of a multimodal, case-based teaching program for workflow and cost-effectiveness in radiology.
Materials and methods: A program was designed combining features of the software authoring tool Director from Macromedia and those of a relational database (VI2). On a virtual basis, the program presents the entire spectrum of diagnostic decision-making to the user. During the workup of cases, any diagnostic decision is followed, its clinical consequences are recorded and a cost calculation is made. During the workup of a case, the program follows not only the accuracy of the final diagnosis but also the costs generated. Based on these algorithms, the user is forced to analyse and define an appropriate and cost effective diagnostic pathway. All features of the new media are integrated in the software which supports the most recent pedagogic methods. The program is based on an open source tool. It is modifiable and expandible to meet varying future requirements. For validation of the program, a survey was conducted employing an online questionnaire.
Results: The questionnaire was returned by 26 registered online users. The system reached high acceptance among medical students as well as physicians. Modern screen layout, schematic representations and individual supplementary functions were rated as appropriate.
Conclusions: The multi-modality software program MEDICONOMIA meets the demands for teaching precise diagnoses as well as for cost effective workflows in radiology. It targets medical students as well as radiologists or physicians from other disciplines.

B-0700 11:10

RIS/PACS: User's definition and concept

R. Braunschweig[1], I. Kaden[1], W. Loch[1], H. Schenk[2]; [1]*Halle a. d. Saale/DE*, [2]*Cologne/DE*

Purpose: The technology of PACS has recently reached such a sophisticated standard that now individual needs of application have become of paramount interest. We would like to present a clinical orientated solution for our installation.
Methods and material: RIS controls the demands of the ward or those of other clients to the Diagnostic Imaging Department, the work and data flow to and from the modalities, the performance account, image distribution, reports and demonstrations and short and long time image archiving. Our hospital features espeally as a traumatological center on one hand and a center for patients with cerebral/spinal cord and burn injuries on the other.
Results: For image archiving we use two subordinate systems: a RAID system of approximately 180 Gbyte as a short-time archive and a juke box system with DLT's at a capacity of 2 Tbyte per year as the long-time archive system. The images of the people in care are in the RAID system. Patients not being in care at present are in the long-time archive system. The prefetching ist determined by three characteristics: patient data, time of investigation and the examined organ. Image distribution is organized with respect to the addressee: operation theater, intensive-care and emergency unit, ward and ambulance. We use desktop computers, flat panels and laptops, for demonstrations we apply beamers. Image quality is described by 1 k up to 2.0 k matrix and a brightness of about 400 cd.
Conclusion: A successful PACS installation requires user-oriented flexibility of the applied technology.

B-0701 11:20

On a straight way to a RIS

U. Sous, C. Müller-Leisse; *Mönchengladbach/DE*

Purpose: To report our own experience on the way towards installation of a RIS.
Concern: RIS-systems are installed in an increasing number of institutions. Difficulties from planning to running of the system however are multiple. A new workflow has to be defined, the possibilities of a RIS are hardly known. Provider of the RIS tend to glorify there products and present features broadminded and often without critical approach. Presentations and visits of reference installations take a lot of time and still it is difficult to make up one's mind. Furthermore, as information technology is hardly present in some institutions, already little simplification of procedures pretends great progress, which is wrong from an objective point of view. Moreover institutions with reference installations are not representative, because they are intensely looked after by the provider and other users will hardly get a comparable support.
Conclusion: From our experience we like to consider:

1. Constitution of a team consisting of employees of the radiological and data-processing department with know-how in IT-technology
2. Visiting of multiple reference installations in order to get an idea of the state of IT-technology and of what is possible.
3. Defining procedure steps considering the complete new work-flow as detailed as possible.
4. Precise documentation of own requirements and provider's affirmation.
5. Assurance of support in particular during and after installation of the system.

In fact, certainly, keeping in mind the above mentioned items do not guarantee proper functioning of a RIS. However, they are basics to be considered.

B-0702 11:30

The role of RIS/PACS integration in developing a PACS system

C. Saccavini, P. Mosca, S. Puggina, R. Stramare, G.P. Feltrin; *Padova/IT*

Purpose: To integrate our RIS system with a PACS. The patient data duplication (RIS/PACS) makes it impossible to associate images and reports.
Materials and methods: In our Department we use a home RIS based on a Linux Server (RedHat 6.2) with Interbase 6.0 as the database engine, front-end developed by Delphi, and a home developed PACS based on Linux Server (RedHat 6.2) with Interbase 6.0 and a DICOM server application developed starting from OFFIS library (Oldenburg, Germany). We have connected to our PACS one CT (Emotion by Siemens), one MR (Armony by Siemens), two CR (AC3 by Fuji), and one digital radiography unit (Advantix by GE). Only the Siemens devices can use DICOM worklists to connect to our RIS. The CR is connected by a Fuji proprietary protocol.
Results: Before the RIS/PACS integration there were about 5 % of patients appeared with typographical errors. By introducing the worklist integration we have avoided these patient data errors due to the multiple typed data entries (first into to the RIS, and then into the PACS). In this way the images are tightly linked to the report.
Conclusions: In our experience of developing a PACS system it is very importatnt to plan the integration between the RIS and the PACS, especially using DICOM worklist protocols. This is very difficult because only the last generation of radiological devices have the DICOM worklist capability. Sometimes the integration with non-DICOM devices have many technical problems and it is a very expensive undertaking.

B-0703 11:40

Radiology and intensive care: Comparative workflow analysis in a PACS based and film based environment

S. Peer[1], H. Sander[2], I. Marsolek[2], W. Koller[1], J. Hierholzer[3], D. Pappert[3], R. Peer[1], W. Friesdorf[2]; [1]*Innsbruck/AT*, [2]*Berlin/DE*, [3]*Potsdam/DE*

Purpose: To evaluate the joined workflow of the radiology department and the department for intensive care, with special attention for the changes in the workflow introduced by introduction of a PACS.
Materials and methods: Interactive workflow analysis was perfomed in a fully digital hospital and a conventional, film based hospital. Comparable workflow aspects were defined and differences in the two systems were evaluated.
Results: Obvious benefits of PACS are realized in the common problem areas in the film based environment concerning administration of patient and exam data, archival and distribution of images for clinical purposes and the organisation of radiological demonstrations. On the other hand difficulties in the digital environment are realized dealing with the high interconnection of various information systems – especially electronic errors occuring in one system are distributed throughout the network and may disable clinically important PACS features like prefetching or image/report distribution.
Conclusion: In the fully digital department common problems in the joined workflow of radiology and intensive care are easily improved by introduction of a PACS. However these benefits are only achieved with high availability of all digital components and a system tailored to the special needs of the departments.

B-0704 11:50

Webbased dynamic medical image database using high-effective, platform independant, no-cost common software: An approach for a standardized, flexible and future-proofed solution

J. Hohmann, T. Schaaf, K.-J. Wolf; *Berlin/DE*

Purpose: The aim of the project is to create an easy to use, all-purpose and fast medical image database with common software. The database should be flexible, platform independant and available via intra- or internet technology.
Materials and methods: By using the MySQL (http://www.mysql.com) relational database management system the fundament of the system consists of an open source software which is fast, reliable and easy to use. Access to databases is done via SQL (Structured Query Language), the most common standardized database query language. To achieve an access with familiar 'look and feel', implementation of webbased technology is needed. Using the Apache webserver (http://www.apache.org) gives the opportunity to use the PHP ("PHP: Hypertext Preprocessor", http://www.php.net) server-sided HTML-embedded scripting language. PHP generates dynamic webpages on the databaseserver by request and send it to the client. According to this technique there is no safety risk on the client-side. In addition PHP comes with integrated MySQL support.
Results: The base design of the database system represents a medical image database with 108 different cases. The biological datas are as well available as the clinical findings and the images themselves. Different pre-casted querys are available to make the operation as convenient as possible.
Conclusion: First installation of the system fullfills the expectations on a fast database mangement system which uses modern web technique and common, no-cost, platform indepedant software components. Next steps should be the extension of the database structure, the development of more complex queries and the implementation of more demanding image applications.

10:30–12:00 **Room H**

Interventional Radiology

SS 1409

Non-vascular intervention

Chairpersons:
J.-M. Bruel (Montpellier/FR)
M. Sato (Wakayama/JP)

B-0705 10:30

CT fluoroscopic guidance of transbronchial biopsy: Early clinical experiences

R. Kickuth, J. Kirchner, U. Laufer, D. Liermann; *Herne/DE*

Purpose: Computed tomography fluoroscopy (CTF) provides the ability of continuous CT imaging and has been increasingly used in interventional procedures. Our objective was to assess the usefulness of CTF in the monitoring of transbronchial biopsy procedures.
Material and methods: We evaluated 15 patients in which yield of 'conventional' transbronchial biopsies had failed. CTF was performed on a Somatom Plus 4 Power scanner (C.A.R.E. Vision© CT, Siemens Medical Systems, Forchheim, Germany) using 120 kVp, 50 mA at a frame rate of 8 images/s on a matrix of 256 × 256. Target parameters were number of biopsies, total procedure time, applied radiation dosage and histopathological outcome.
Results: CTF guidance improved yield of transbronchial biopsy. In 13 patients biopsy yielded bronchiogenic cancer, in one patient histopathologic examination showed tuberculosis. Only in one patient CTF guided transbronchial biopsy was insufficient. The mean fluoroscopy time was 145 ± 82 s, the mean procedure time was 765 ± 277 s. The surface irradiation dosage ranged between 450 and 1224 mSv with a mean of 720 mSv. Immediate complications were not encountered.
Conclusion: CTF facilitates visualization of transbronchial biopsy procedures with a drawback in increased radiation exposure. In order to compare the 'conventional' method versus CTF a randomized prospective study is necessary.

B-0706 10:40

Biopsy guidance in 4D CT fluoroscopy: A simulation study based on cone-beam CT data

C. Bontus, T. Köhler, R. Proksa, M. Graß; *Hamburg/DE*

Purpose: With the advent of multi-line CT scanners fluoroscopy will reach a new dimension. The purpose of this study is to demonstrate the application of cone-beam reconstruction methods and sliding window techniques to obtain time series of images on planes perpendicular to the biopsy needle direction.
Materials and methods: In this simulation study a pelvis phantom was constructed using mathematical objects. A 14 Gauge biopsy needle was approximated by a cylinder built of titanium. While the gantry rotated around the object the needle was pushed into the pelvis phantom. In different scenarios the needle was either in the central plane of rotation or passed through this plane with a specified angle. The reconstruction has been performed using a standard Feldkamp method and an angular weighted T-FDK method in combination with a sliding window technique. Multi-planar reconstruction can easily be applied in order to achieve data on perpendicular planes containing the needle.
Results: The simulation study leads to time series of images showing the advance of the needle in the pelvis phantom for tilted slices. Images of perpendicular planes improve the orientation for the radiologist during the intervention since three-dimensional information is displayed. Artifacts resulting from the fact that projections of a moving object were taken vary in the displayed slices depending on their orientation.
Conclusion: Using the third spatial dimension within cone-beam CT fluoroscopy will lead to new ways for tracking the biopsy needle. This approach will be helpful for an improved orientation during interventions.

B-0707 10:50

Radiology day case unit for ultrasound guided liver biopsy: A 20 month experience

R.T. Dhawan, M. Anodu, P. Rizzi, M. Ong, P.S. Sidhu; *London/GB*

Purpose: A prospective study to determine the clinical utility, safety and feasibility of a Radiology Day Case Unit (RDCU) for ultrasound (US) guided liver biopsy.
Method/materials: Patients suitable for day case biopsy were seen by a Radiology Specialist Nurse (RSN), responsible for patient care during the procedure and for 24 hour follow up. Biopsies were performed by a Radiologist, using a 16 G needle, following US site selection. The incidence of complications and US findings at 5 – 7 hours after the biopsy were recorded. Patient acceptability of the RDCU was assessed by a random survey using a questionnaire of patient satisfaction.
Results: 362 patients underwent the procedure over a 20 month period. All but 2 specimens were satisfactory for histological analyses. 94 patients experienced pain controlled by oral analgesia and 6 required parenteral analgesia. Follow-up US in 354 patients, revealed no procedure related complications in 348, subcapsular hematomas in 5, and a pericholecystic collection in 1. 358 patients remained stable and were discharged at 6 – 7 hours post procedure. Three patients had vasovagal episodes and were admitted. Of the 95 patients surveyed at discharge, 90 were satisfied with the day care concept, five expressed a preference for an in-patient procedure.
Conclusions: The performance of day case liver biopsies translates into substantial cost savings, and the RDCU achieves a level of safety comparable to in-patient care, with a high level of patient satisfaction. Imaging guidance is contributory in obtaining an adequate core using a single pass.

B-0708 11:00

CT-fluoroscopy guided transthoracic needle biopsies: Specificity and complication rate in 105 procedures

R.D. Brüning, M. Mühlstädt, U.J. Schöpf, T.K. Helmberger, A. Müller, J. Diebold, M.F. Reiser; *Munich/DE*

Purpose: To evaluate the diagnostic accuracy of CT-fluoroscopy guided core needle biopsy and to assess safety and complication rates.
Methods: One hundred and five prospective biopsies on 102 patients (mean age 59 ± 13 a) were performed using a spiral CT scanner and CT-guided fluoroscopy. The biopsies were obtained using a core biopsy needle (18 G) and a spring-driven device. All results were compared to surgery and histology or clinical follow-up for more than 12 month. Sensitivity, specificity and predictive values were calculated. Complications were assessed in the control scans.
Results: Sensitivity for intrapulmonary node biopsies was 94 %, specificity 100 % and the negative and positive predictive values (NPV, PPV) were 73 % and 100 % respectively. For biopsies of the mediastinum and the pleura the sensitivity was

87 % and 80 % respectively, specificity was 100 %. A pneumothorax appeared in 23 %, a severe pneumothorax in 1.9 %, other subclinical events like focal bleeding at an average of 6 %.
Conclusion: CT-fluoroscopy guided core needle biopsy is a reliable means to biopsy thoracic lesions. The rate of severe complications was as low as 1.9 %.

B-0709 11:05

Interventional procedures under CT-guidance: Tips and hints for safe needle placement
B.A.C. Kastler, C. Clair, J. Litzler, R. Allal, Z. Boulahdour, B. Fergane; *Besançon/FR*

Aim: CT, displaying an excellent contrast between soft tissues, bones, vessels and nerves, is an excellent method of guidance. Since 1995 we have had a dedicated CT scanner for performing percutaneous interventions. This study is an anlysis of its our experience with this equipment.
Patients and methods: 120 interventions per year were carried out for pain relief, (including stellate and spheno-palatine ganglion neurolysis, thoracic and lumbar sympathetic chain neurolysis, splanchnic and coeliac plexus neurolysis, pudental nerve and periradicular infiltrations), ablation of hepatic and bone metastases with ethanol or radiofrequency, and for acrylic glue injections.
Results: We have encountered various complications (from simple hematomas to neural injuries) in 16 out of 612 interventions (2.6 %). We will analyze the possible causes of complications and suggest methods of preventing them, including appropriate patient positioning, gantry tilting, control of the respiratory cycle, appropriate choice of pathway, use of a stack of three slices centered on the needle tip, "tutor needle guidance" and needle "steering".
Conclusion: Mastering simple methods of optimizing needle tip advancement and positioning reduces the number of complications encountered during CT-guided procedures.

B-0710 11:15

Diagnostic utility and effective accuracy of CT-guided automated coaxial core biopsy in patients with suspected malignant lesions
R. Wutke, A. Schmid, F.A. Fellner, T. Horbach, T. Papadopoulos, W.A. Bautz; *Erlangen/DE*

Purpose: The aim of this study was to investigate the diagnostic utility and effective accuracy of CT-guided automated coaxial core biopsy in 125 consecutive patients.
Materials and methods: 125 consecutive patients with suspected malignoma were included. We analysed the histological diagnosis of CT-guided biopsy, the results of open biopsy or surgery, if performed, and the final pathologic or clinical outcome with follow up for 6 months or more. We determined accuracy, sensitivity and specificity on the basis of definitive clinical outcome. To calculate effective accuracy and diagnostic utility we categorized results, that were not accepted and that required additional open or percutaneous biopsies, as equivocal-positiv and equivocal-negativ.
Results: Overall sensitivity, specificity and accuracy was 92.4 %, 100 % and 94.4 %. Effective accuracy and diagnostic utility for all biopsies were 79.2 % and 58.4 %. Reduced diagnostic utility and effective accuracy we found for needle size smaller than 16 gauge and for less than 4 obtained cores. Best results were achieved for mediastinal and osseous lesions, whereas pulmonary and hepatic biopsies produced a lower effective accuracy.
Conclusion: Utility of biopsy depends not only on its accuracy but also on its effect to the clinical management. Coaxial biopsy with more than 3 obtained cores has a high diagnostic utility and effective accuracy.

B-0711 11:25

Lung nodules 1.5 cm or smaller in size: Efficacy of percutaneous transthoracic fine needle aspiration biopsy
V.D. Souftas, D. Melidis, I. Tsitouridis; *Thessaloniki/GR*

Purpose: Lung nodules with diameter 1.5 cm or smaller are difficult to biopsy with conventional CT-guidance, because of patient respiratory variation. The objective or our study was to assess the safety and diagnostic accuracy of fine needle aspiration biopsy (FNAB), using helical CT-guidance and FNA.
Material and methods: In a period of one year, seventeen patients, 12 men and 5 women, with ages from 52 to 68 years (mean 58.2) underwent CT-guided FNAB of small lung parenchymal nodules, 1.5 cm or smaller in size, using a 20 – 22 gauge Chiba needle and a PICKER PQ5000 Hellical CT-system. The needle was inserted into the nodule and aspirates (ave 3 to 5 FNA's) were obtained. Immediate post-procedural CT scans were obtained. Patients were further monitored clinically until next morning.
Results: 14 out of 17 patients (82.3 %) were asymptomatic after FNAB, with no evidence fo pneumothorax. 3 patients (17.6 %) were noted to have minimal pneumothorax. One of them was asymptomatic and in the other two a 12 F chest tube was required for the iatrogenic pnemothorax, that was subsequently removed 24 hours later. Thus, no patients required prolonged hospitalization as a result of FNAB. Adequate material for diagnosis was obtained in 14 out of 17 patients (82.3 %), prevalence of malignant (88.2 %). The sensitinity of the method was 82.3 % and the specificity 100 %.
Conclusion: Hellical CT-FNAB is effective and diagnostic on small lung modules, with a low rate of complication.

B-0712 11:30

MR-guided biopsies of the liver: First experience with 0.2 T
S. Zangos, M. Mack, R. Straub, K. Hochmuth, N. Abolmaali, K. Eichler, D. Woitaschek, T.J. Vogl; *Frankfurt a. Main/DE*

Purpose: To evaluate the safety and precision of liver tumour biopsy of in an open, low-field MR system.
Materials and methods: MR-guided biopsies were performed with the Magnetom OPEN (0.2 T) in 14 patients with a variety of liver tumours. Nineteen biopsy specimens were obtained with 14 – 18 G cutting needles. T1 w GRE sequences were used for guidance in all patients, with additional use of fluoroscopic FISP or PSIF sequences.
Results: Adequate specimens for histological interpretation were obtained in 12 cases. In one patient the biopsy result was non-specific and and in one patient the lesion was missed. T1 w GRE images were useful for confirming needle-tip placement during the biopsy. Lesion and needle visibility are significantly affected by user-defined parameters which must be considered during procedure planning.
Conclusion: MR-guided liver biopsy can be performed with acceptable safety and accurracy in an open, low-field MR system.

B-0713 11:35

Percutaneous US guided biopsy of focal splenic lesions: A safe and valuable procedure?
P. Cabassa, L. Matricardi, L. Grazioli, R. Cuomo, A. Di Gaspare, F. Simeone; *Brescia/IT*

Purpose: The aim of this study was to investigate the safety and effectiveness of Ultrasound (US) guided biopsy in the diagnosis of splenic lesions.
Materials and methods: 34 US-guided biopsies of focal splenic masses were performed on 34 patients (19 male, age range 14 – 87 years). Patients had a history of extra-splenic malignancy (n = 15), immunosuppression (n = 8), fever of unknown origin (n = 4), anemia (n = 2) or incidentally discovered masses (n = 5). Lesions range in size was between 6 and 55 mm. by 2 radiologists. All of the biopsies were performed with the use of sonographic guidance via intercostal approach with 21 G cutting needles. Patients were observed for 2 – 4 hours and released from 6 to 24 hours after the procedure.
Results: No complication occurred. 33/34 (97.1 %) specimens obtained were sufficient for diagnosis. Definite diagnosis was made in 29/33 (87.9 %) cases. Histology revealed various types of primary and secondary malignant tumors (n = 17) or benign conditions (n = 12) including infections, angioma, granuloma. Non evidence of disease was found in 4 biopsies, follow-up of these last cases was performed by CT.
Conclusions: Percutaneous biopsy under US control is a safe, fast and accurate method in most patients with focal splenic lesions.

B-0714 11:40

Basic US guided core biopsy and interventional drainage procedures
V.B. Jadhav; *Islampur/IN*

Purpose: To assess the value of standard ultrasound-guided core biopsy and drainage procedures.
Materials & methods: Over a four year period 560 patients were referred for interventional ultrasonographic procedures. They underwent core biopsy of various masses (in the thyroid, mediastinum, lung, pleura, liver, gallbladder, spleen, pancreas, stomach, duodenum, oesophagus, small and large intestines, genitourinary tract, lymph nodes, soft tissues and bone) and drainage procedures, including drainage and irrigation of abscess cavities and cysts, thoracocentesis and paracentesis. A free-hand technique was employed for ultrasound guidance in all cases. The BARD Monopty 18 G needle was used for core biopsy. An 18 G lumbar puncture needle used for drainage procedures.
Results: In all 560 patients the procedures performed had a positive diagnostic and/or therapeutic value, except in one patient, who required core biopsy guided by colour Doppler as the mass was located at the porta hepatis.

Conclusions: Sonographic guidance offers many advantages such as real time imaging combined with excellent cross sectional anatomic orientation, speed, portability and low cost. Optimization of sonographic imaging parameters and use of appropriate transducers and techniques increase the likelihood of success.

B-0715 11:50

Celiac plexus block under real time colour ultrasound guidance (USCPB)

P.Y.R. Marcy, N. Magné, K. Benezery, A. Bleuse, B. Descamps; *Nice/FR*

Purpose: To demonstrate the feasibility and efficacy of USCPB.

Methods and materials: USCPB was attempted under local anesthesia in 15 cancer patients (mean age: 55 a). All patients had an excruciating epigastric and generalized abdominal pain caused by a carcinoma of the pancreas (n = 6), a malignancy of the upper abdominal viscera (n = 3) or extra- digestive origin. One case was an endoscopic technique failure.

Results: The technical success rate was 93 %. The target route was transhepatic in 7/14 cases. the mean length of the needle was 60 mm (range: 3 – 12 cm). 29 cc of Ethyl Alcohol (20 – 38 cc) were administered percutaneously, through a 21 – 23 G Chiba-needle. Echogenic foci appeared close to the aortic anterior wall, between the celiac trunk and the superior mesenteric artery. Pain relief was obtained in 73 % of the cases. The minor complications (13 %) included transient hypotension and left shoulder pain. Colonic interposition did not allow any visualization of the retroperitoneum (n = 1).

Conclusion: Power- and Colour-Doppler Imaging improved the visualization of the Chiba-needle when the shaft vibrated. USCPB should be attempted at first for painful cancer patients.

10:30–12:00 **Room I**

Genitourinary

SS 1407

Kidney

Chairpersons:
N. Grenier (Bordeaux/FR)
H. Schreyer (Graz/AT)

B-0716 10:30

Renal ultrasonographic findings in patients with sickle-cell disease

M.G. Papadaki, I.S. Kaskarelis, A.C. Kattamis, C.G. Hatjigiorgi, I.G. Papadaki, N.E. Malliaraki, C.A. Kattamis; *Athens/GR*

Purpose: It is a well known observation that the kidney is an organ commonly affected during the course of sickling disorders. The high metabolic activity of the renal tubules, leading to a high oxygen consumption rate, promotes HbS polymerization with subsequent focal vaso-occlusive and tissue destruction. The aim of this study is to present the renal ultrasonographic findings in patients with sickle cell disease.

Methods and materials: The study included 68 Greek patients with sickle cell disease, 13 homozygous for sickle cell anaemia (S/S) and 55 with sickle β thalassemia (Th/S). The patients' age ranged from 1 to 40 years (mean 16 years), with 33 males and 35 females.

Results: Renal abnormalities were detected in 21/68 (30.9 %) patients. Increased echogenicity of renal parenchyma was the most frequent finding observed in 20.6 % of patients, 13/55 patients with Th/S and one patients with S/S. Three different echo patterns were observed. Mild hyperechogenicity on the perimedullary spaces (type 1) was found in 4/68 (5.8 %) patients. Mild or moderate hyperechogenicity in the inter- and intramedullary spaces (type 2) was present in 8/68 (11.8 %) and marked hyperechogenicity of renal medulla (type 3) in 2/68 (3 %) cases. Enlarged kidneys had 2/13 (15.4 %) patients and three had nephrolithiasis One patient with S/S had polycystic kidney disease.

Conclusions: Ultrasonography is a readily accessible and non-invasive method for the evaluation of renal complications in sickle cell syndromes. Combined with other simple laboratory tests it can be used for screening and routine follow-up of sickle cell patients.

B-0717 10:40

Evaluation of kidney volume with 3D-sonography

B. Partik, A. Stadler, S. Schamp, A. Koller, M. Hörmann, P. Pokieser; *Vienna/AT*

Purpose: To evaluate 3D-sonography for the measurement of the kidney volume.

Material and methods: Two radiologists prospectively examined 22 human cadaver kidneys in situ with 3D-ultrasound using a 3.5 MHz probe. Each observer acquired a 3D-volume data-set and additionally calculated the volume with B-mode measurements based on a three-dimensional ellipsoid formula. Afterwards three observers evaluated the kidney volume by 3D-volumetry of each data-set and again by calculation based on a three-dimensional ellipsoid formula, this time using the 3D-data-set. Renal volume measured by water-displacement served as gold standard.

Results: Measurements by water-displacement revealed a mean kidney volume of 168 ml (range 48 – 240 ml). In comparison to those measurements conventional B-mode measurements showed a mean error of 42 ml, calculation by the ellipsoid formula from the 3D data-set showed a mean error of 37 ml, and measurements by 3D-volumetry showed a mean error of 31 ml.

Conclusion: From all sonographic methods used in our study, 3D-volumetry revealed the best results. However, with a mean measurement error of 18.5 % in comparison to the mean volume, the clinical impact of this method has to be further evaluated.

B-0718 10:45

Accuracy of duplex intrarenal velocity indices in the diagnosis of bilateral atherosclerotic renal artery stenosis

V. Napoli, S. Lodovigi, I. Bargellini, P. Petruzzi, R. Cioni, C. Vignali, S. Pinto, C. Bartolozzi; *Pisa/IT*

Purpose: To evaluate accuracy of duplex intrarenal velocimetric indexes in the diagnosis of haemodinamically (> 60 %) significant bilateral atherosclerotic stenoses of the renal arteries.

Materials and methods: Doppler velocimetric indexes obtained from the intrarenal arteries of 89 patients (71 male, mean age 62 ± 12), with hypertension and bilateral atherosclerotic renal artery stenosis, were retrospectively analyzed. A state-of-the-art device was used (3.5 MHz probe, PRF < 1 kHz). Acceleration time (T), peak systolic acceleration (A), pulsatility (PI) and resistivity (RI) indexes were obtained. All patients underwent selective renal arteriography, that represented the gold standard.

Results: Arteriography showed a significant (> 70 %) bilateral stenosis in 51/89 patients (57 %) and a significant monolateral stenosis with non-significant contralateral lesion in 2/89 cases (2 %). Laboratory specific duplex threshold values were determined through ROC curves: 144 ms (A), 205 cm/s^2 (T), 1.17 (PI) and 0.67 (RI). Diagnosis of bilateral significant (> 60 %) renal artery stenosis with intrarenal velocimetric indexes was obtained in 21/51 (T), 18/51 (A), 14/51 (PI), 12/51 (RI) patients, with sensitivity rates of 41, 35, 27, 23 %, respectively. In patients (n = 2) with monolateral significant stenosis and contra-lateral non-significant lesion, velocimetric indexes overestimated the contra-lateral stenosis, leading to the diagnosis of significant bilateral stenosis.

Conclusion: Intrarenal velocimetric indexes do not represent reliable parameters in the diagnosis of significant bilateral renal artery stenosis in patients with bilateral atherosclerotic lesions, since the comparison between the kidneys is not always significant.

B-0719 10:55

Role of Losartan scintigraphy in evaluation of patients with a unilateral small kidney for bilateral renal artery disease

J. Bharathi Dasan, M. Atul, K.S. Agarwal, D.N. Srivastava, R. Kumar, G.P. Bandopadhyaya, A. Malhotra; *New Delhi/IN*

Purpose: To evaluate the role of Losartan (AT1 blocker) DTPA renal scintigraphy in the diagnosis of bilateral renal artery stenosis (RAS) in patients with unilateral small kidneys.

Materials and methods: Ten patients (6 males and 4 females) with renal artery stenosis (9 unilateral and 1 bilateral) and unilateral small kidneys were included in the study. All patients underwent sonography, DMSA scintigraphy and baseline DTPA study which showed unilateral small poorly functioning kidneys with no evidence of renal scarring or parenchymal disease. Subsequently they all underwent captopril DTPA renal scintigraphy (CRS), followed by Losartan DTPA renal scintigraphy (LRS) on different days.

Results: Of the patients with unilateral RAS, in 5 both LRS and CRS studies had high probability for hemodynamically significant stenosis on the affected side. In 2 other patients who had elevated serum creatinine both studies were of intermediate probability for the same. In the remaining 2 patients with unilateral significant RAS, LRS and CRS were intermediate probability for stenosis on the affected side, whereas in the contralateral normal side LRS was true negative but CRS was false positive suggesting bilateral renal aretery stenosis. In the single patient

with bilateral RAS both CRS and LRS were intermediate probabilty positive on the side with the small kidney, however on the contralateral side CRS was false negative whereas LRS was high probability for hemodynamically significant stenosis.
Conclusion: Losartan renal scintigraphy seems to be superior to captopril renal scintigraphy in ruling out bilateral renal artery disease in patients with unilateral small kidneys.

B-0720 11:00

Role of duplex intrarenal velocity indices in the diagnosis and follow-up of fibrodysplastic renal artery stenosis before and after angioplasty
V. Napoli, I. Bargellini, S. Lodovigi, P. Petruzzi, S. Pinto, R. Cioni, C. Vignali, C. Bartolozzi; *Pisa/IT*

Purpose: To evaluate the role of pulsatility (PI) and resistivity (RI) indexes in the evaluation of vascular patency in hypertensive patients with fibrodysplastic renal artery stenosis, before and after percutaneous angioplasty (PTRA).
Materials and methods: From 1990 to 1999, 45 hypertensive patients (42 female, mean age 35) with fibrodysplastic renal artery stenosis were evaluated by means of duplex sonography. Among these, 2 had a solitary functioning kidney and 20 a bilateral stenosis. A total number of 65 stenoses was studied. Forty-three stenoses were treated by PTRA. Restenosis occurred in 10/43 cases. Ultrasonographic examinations were performed via a posterior lumbar approach, by a single operator, with a state-of-the-art device and a 3.5 MHz probe. Mean values ± SD of PI and RI, obtained from the intrarenal arteries, were calculated before PTRA and 24 – 72 hours, 3, 6, 12 months after the procedure. Results were compared by means of Student t-test.
Results: Mean values ± SD of PI and RI before PTRA were 0.87 ± 0.2 and 0.54 ± 0.11, respectively. A significant modification ($p < 0.01$) was observed 24 – 72 hours after successful PTRA. On follow-up, PI and RI settled (PI 0.96 ± 0.21, RI 0.59 ± 0.07), maintaining a significant difference in respect to the values calculated before treatment. In case of restenosis, PI and RI decreased, returning to the values calculated before PTRA ($p > 0.05$).
Conclusion: In young hypertensive patients with fibrodysplastic renal artery stenosis, PI and RI represent reliable parameters to evaluate renal vascular resistance and monitor vascular patency, before and after PTRA.

B-0721 11:10

Evaluation of renal artery stenosis: Combined multiphase MR angiography and MR renography performed after single Gd-DTPA injection
A. Cieszanowski, M. Golebiowski, B. Symonides, Z. Gaciong; *Warsaw/PL*

Purpose: To assess the quality of CE 3D multiphase MR angiography and MR renography performed after single-dose Gd-DTPA injection.
Methods and materials: In 24 patients suspected of having renal artery stenosis, 3D MRA sequence was performed multiple times during suspended respiration (from 10 to 360 seconds after the beginning of power-injection of Gd-DTPA). Acquisition time of single phase of MR examination was 8 s (TR of 5 ms, TE of 1.6 ms, 30 – 35 partitions, 164 × 512 matrix). First three phases, performed during single breath-hold, were used to obtain angiographic images. All phases were used to obtain curves of cortical, medullary and calyceal enhancement. Maximum number of acquisitions per minute was 4 – 5. The peak intensity values and the time to peak of the cortex, medulla and excretory system were evaluated.
Results: 21 of 24 MRA examinations were of good, 3 of fair and none of poor quality. Quality of enhancement curves was good in 22 cases and suboptimal in 2 cases because of irregular breath-holding. MRA visualized 11 stenosed and 7 accessory renal arteries. Renographic curves were abnormal in 8 patients.
Conclusions: Multiphase 3D MRA sequence with short acquisition time enables simultaneous acquisition of angiographic images and renographic curves of good quality.

B-0722 11:15

Renal artery stenting in ostial atherosclerotic stenoses: Technical and clinical outcomes
C. Vignali, F. Donati, R. Cioni, P. Petruzzi, I. Bargellini, S. Pinto, V. Napoli, C. Bartolozzi; *Pisa/IT*

Purpose: To assess efficacy and safety of renal artery stenting in patients with atherosclerotic renovascular disease.
Materials and methods: From July 1995 to Aug 2000, 129 stents were implanted in 110 patients with atherosclerotic ostial renal artery stenosis. Preprocedurally, patients were evaluated by means of duplex sonography and MR or CT Angiography. All patients were hypertensive (mean diastolic blood pressure, DBP, 109 mmHg) and 72 had impaired renal function (mean serum creatinine level 1.6 mg/dl). Stenting was performed either as primary procedure (n = 17) or after PTRA, because of persistent stenosis > 30 % (n = 77) or arterial dissection (n = 35). On follow-up, duplex sonography was performed to assess stent patency, whereas clinical conditions were monitored through periodic measurements of DBP and serum creatinine level.
Results: Technical success was achieved in 109/110 (99.1 %) patients (1 case of stent protrusion within the aortic lumen). At immediate follow-up, complications occurred in 5 patients (1 patient required nephrectomy). At 1 month, reduction/cure of DBP was obtained in 94.5 % of patients and improvement/stabilization of renal funcion (RF) in 79.2 %. At 6 months (88 patients), restenosis occurred in 10/97 stents (10.3 %); reduction/cure of DBP was obtained in 86.3 % and improvement/stabilization of RF in 85.2 %. At 24 months (54 patients), restenosis occurred in 6/64 stents (9.4 %); reduction/cure of DBP was achieved in 88.9 % of patients and improvement/stabilization of RF in 73.1 %.
Conclusion: Encouraging clinical results and low rate of complications, obtained in a large series, confirm the primary role of renal artery stenting in the treatment of ostial atherosclerotic stenoses.

B-0723 11:25

Preoperative assessment of vascular anatomy of life related renal donors with gadolinium-enhanced 3D-magnetic resonance angiography
C. Fink, R.C. Ott, P.J. Hallscheidt, W. Hosch, M. Düx, G.W. Kauffmann; *Heidelberg/DE*

Purpose: Preoperative assessment of the vascular anatomy of potential living renal donors using Gadolineum-enhanced 3D Magnetic Resonance Angiography compared to standard intra-arterial Digital Subtraction Angiography.
Method and materials: Eleven potential living renal donors were examined with standard intra-arterial Digital Subtraction Angiography (DSA) and Gadolineum-enhanced 3D Magnetic Resonance Angiography (3D-MRA). Both modalities were evaluated in a blinded manner by two radiologists. The results were correlated with the intraoperative findings.
Results: In all donors equivalent accuracies of DSA and 3D-MRA in the visualisation of the renal arteries were assessed. In 10 patients single renal arteries were depicted by both modalities. In one patient a one-sided accessory renal artery was detected by both DSA and 3D-MRA. No vascular pathology was found.
Conclusions: Gadolineum-enhanced 3D Magnetic Resonance Angiography may be an accurate non-invasive method for the preoperative assessment of the vascular anatomy of potential living renal donors.

B-0724 11:30

Live renal transplant donor assessment: Can combined gadolinium MRA and MRU replace conventional DSA and IVU?
B. Wittkop, S. Cooper, P. Guest; *Birmingham/GB*

Objectives: To investigate the accuracy of combined gadolinium-enhanced MRA and MRU in the investigation of potential live renal transplant donors and to compare with conventional DSA and IVU.
Method: A prospective study in which all potential live renal transplant donors undergo both the combined MRA/MRU investigation and DSA/IVU. MR Urography is performed using a coronal 2 second HASTE sequence, immediately followed by MR Angiography using a gadolinium-enhanced 3-D breath hold volume acquisition. DSA and IVU performed using conventional techniques.
Results: 20 patients have been currently investigated of which 15 have undergone all three tests. A total of 40 renal arteries (30 main and 10 accessory arteries) were identified. MRA correctly identified 37 of 40 renal arteries. DSA correctly identified 36 of 40 renal arteries. MRA as well as DSA results were correct in 12 out of 15 patients. MRA and DSA both reported one result as equivocal. Both MRA and DSA missed 3 accessory arteries. Review of all examinations revealed that one accessory artery was apparent but not initially reported on DSA. Similarly two accessory arteries were apparent on review of MRA data that were not reported initially. MRU identified small renal cysts in 3 patients; all IVUs were reported as normal.
Conclusions: These results for the combined MRA/MRU investigations are good. In this series the accuracy of MRA and DSA results are similar. The benefits of MRA/MRU are the avoidance of an invasive procedure and ionising radiation and added convenience of a one-stop investigation.

B-0725 11:40

US color Doppler with contrast agent vs. scintigraphy with ^{99}Tc sulphur colloid in the evaluation of renal transplant diseases

F.M. Drudi, R. Massa, F. Cascone, P. Marziale, A. Righi, F. Trippa, R. Passariello; *Rome/IT*

Purpose: Aim of our study was to compare the results of wash-in wash-out curves obtained with US Color Doppler using contrast agent and with scintigraphy ^{99}Tc sulphur colloid in the differentiation of normal grafts and renal transplant diseases.
Method/materials: From March 1999 to February 2000 thirty-three renal transplanted patients (mean age 39 years), of whom 12 from living donors, underwent US Color Doppler with contrast agent and scintigraphy with ^{99}Tc sulphur colloid. Ten of these patients presented a normal post transplant evolution (control group), 23 presented a clinical suspicion of renal transplant disease. Control parameters were creatinine serum level, diuresis, blood pressure and FNAB or biopsy which was considered the gold standard. We evaluated the following US Color Doppler parameters: morphology of the curves and wash-in wash-out quantitative values. Scintigraphy parameters were: double counting considering kidney vs iliac bone and increase of signal in different quantitative parameters which were divided in 3 different positive degrees.
Results: The comparison of US Color Doppler and scintigraphy showed sensitivity 95 ± 2 %, specificity 77 ± 3 % and accuracy 90.9 ± 1.2 % in accordance with clinical values.
Conclusions: Our study permitted to determine the correlation between US Color Doppler and scintigraphy parameters and differentiation of normal grafts and renal transplant diseases.

B-0726 11:50

Acute post-renal transplant rejection: Sonographic and power Doppler features

A.A. Daawood, T.A. El-Diasty, A.E. El-Agroudy, H.M. Gad, M.A. Ghoneim; *Mansoura/EG*

Purpose: To evaluate the effect of various acute tansplant dysfunction, particularly acute rejection, on the graft size, renovascular resistance and power Doppler appearance of cortical vascular perfusion (CVP).
Material and methods: Fourty consecutive patients undergoing transplantation from living related kidney donors were included in the study. Transplanted kidneys were examined daily during the immediate post-operative period and at frequent intervals after that. Graft CVP, cross-sectional area (CSA), as an indicator for kidney size, and resistive index (RI) as an indication for renovascular resistance, were measured. CVP was graded into G0 (normal), G1 (reduced) and G2 (markdely reduced).
Results: All normally functioning transplants had G0 CVP. CVp was reduced in all cases of acute rejection but one (22 of 23; 96 %). RI was elevated in 13 of 23 (57 %). Borderline changes (n = 6), acute cyclosporine nephrotoxicity (n = 2) and acute F.K.506 nephrotoxicity (n = 2) had no obvious changes in CVP, RI nor CSA.
Conclusion: The reduction of CVP is more accurate sign of acute renal transplant rejection than the increase of CSA and the elevation of RI. Borderline changes, acute cyclosporine and F.K.506 nephrotoxicity have no obvious effect on these parameters.

10:30–12:00 **Room K**

Pediatric

SS 1412

Gastrointestinal tract

Chairpersons:
C. Fliegel (Basle/CH)
F. Papadopoulou (Thessaloniki/GR)

B-0727 10:30

Iodixanol in paediatric gastrointestinal examinations

N. Wright[1], H.M.L. Carty[1], M. Friis[2], K. Kastberg Petersen[3], G. Stake[4], A. Klaveness[4]; *[1]Liverpool/GB, [2]Copenhagen/DK, [3]Århus/DK, [4]Oslo/NO*

Purpose: The use of a water-soluble contrast medium is sometimes indicated for radiological examination of the paediatric gastrointestinal tract. This study was designed to document the suitability of the dimer, iodixanol, for GI examinations, with respect to efficacy and safety.
Method and material: In a prospective randomized, double-blind study 152 patients received either iodixanol (Visipaque®) or iohexol (Omnipaque®). Stratification was used for entry into high or low concentration groups (Visipaque® concentrations 150 mg I/ml and 320 mg I/ml, Omnipaque® concentrations 140 mg I/ml and 300 mg I/ml). The diagnostic quality was rated as excellent, good or poor. A visual-analogue scale (VAS) was used for evaluation of overall quality of radiographic visualization and for overall quality of diagnostic information. Adverse events for 48 hours post-examination were recorded. Taste acceptance was evaluated as good, acceptable, unpleasant or bad.
Results: The VAS showed similar distribution of the quality assessments. For the various regions of interest most ratings were excellent or good. Adverse events were experienced by 12 patients (16.2 %) in the iodixanol group and 28 patients (35.9 %) in the iohexol group (p = 0.006). The difference was mainly in the occurrence of diarrhoea (5 iodixanol and 23 iohexol patients). The taste acceptance was similar and good for both contrast media.
Conclusion: Iodixanol is a contrast medium well suited for examinations of the gastrointestinal tract in children. Both contrast media provided equally high diagnostic quality. The frequency of adverse events observed in this trial was significantly lower for patients receiving iodixanol compared to those receiving iohexol.

B-0728 10:40

The reliability and effect on management of limited helical CT in children with clinical suspicion of acute appendicitis

D. Zebedin, A.J. Ruppert-Kohlmayr, E. Sorantin, J. Mayr, J. Schalamon, R. Fotter; *Graz/AT*

Purpose: To determine the diagnostic and therapeutic thinking efficacy of limited computed tomography (CT) in children with the clinical suspicion of appendicitis.
Materials and methods: Surgical staff completed questionaires before and after limited CT with rectal contrast (CTRX) was performed in 100 children aged 5 to 16 a with equivocal clinical findings for appendicitis. Number (percentage) of children in which CT was helpful to making the diagnosis appendicitis and the gain in percentage diagnostic confidence with the CT information was estimated. Further we evaluated the percentage of times CT was helpful in planning patient's further management and how often CT information changed initial management and avoided surgical procedure.
Results: CT information changed the surgeons' initial diagnoses in 75 % of the cases. (95 % CI = 70 %, 89 %). The mean gain in diagnostic confidence with CT was 50 % (95 % CI = 42 %, 57 %). CT information changed initial management decision in 80 % of the children. The level of intensity care decreased in 35 % and increased in 65 % of the cases.
Conclusion: In our institution CT information had a strong effect on surgeons' clinical diagnoses and initial management plans in children with the clinical suspicion of appendicitis. CT information enabled surgeons to safely estimate the level of intensity care and to reduce surgical procedure.

B-0729 10:50

Imaging of choledochal cysts in children

K. Gjoreski, A. Gligorievski, Z. Trajkovski, J. Joseva, L. Gjoreska; *Skopje/MK*

Purpose: The choledochal cyst constitutes idiopathic dilatation of the common billiary duct – usually of the supraduodenal portion.
Material and methods: We present 3 cases in children with cyst on the choledochal duct, 2 of them male and 1 female at the age of 15 months, 2.5 years and 3 years old. US, CT and MRCP have been done to all of them.
Results: All 3 have Choledochal cyst and we came to the precise localization and size. We have shown the morphology of the billiary trank with i.v. cholangiography; MRCP shown morphology and topography of the intrahepatic billiary paths, level of the choledochal cyst, precize location and its size.
At all 3 cases diagnosis was confirmed postoperative.
Conclusion: Choledochal cyst as a rare disease that follows autocompression on the billiary and pancreatic trunk, requires a fast and precise diagnosis.
US, CT and MR represent a true choice in the diagnostic imaging.

B-0730 10:55

Nesidioblastosis: Diagnosis and follow-up

T. Berrocal, S. Puente, C. Prieto, N. Gómez-León, P. Hidalgo, I. Pastor; *Madrid/ES*

Purpose: To examine the sonographic findings of nesidioblastosis, and demonstrate pancreatic regeneration several years after resection of 90 % of the pancreas.

Material and methods: Nesidioblastosis is a disorder consisting of a fetal condition of the pancreas in newborns characterized by diffuse proliferation of nesidioblasts, cells that differentiate from ductal epithelium. The main symptoms result from the hypoglycemia caused by abnormal insulin secretion by these embryonary cells. The hypoglycemia makes subtotal pancreatic resection necessary. Sixteen cases of nesidioblastosis have been treated in our hospital over the last twelve years. These patients were followed-up with laboratory tests and serial ultrasounds.
Results: The five cases diagnosed in neonates showed diffusely elevated echogenicity and increased size of the head, body and tail of the pancreas. The other cases, which were diagnosed in older children, showed no sonographic alterations. After resecting of 90 % of the pancreas, there was pancreatic regeneration in four cases (25 %). In three of these the size of the pancreatic head, body and tail were normal for the child's age in control studies performed at 7, 8 and 11 years of age. In one patient partial pancreatic regeneration was observed at five years of age. All had normal blood glucose levels.
Conclusion: Complete or partial pancreatic regeneration after subtotal pancreatectomy for nesidiblastosis occurs without recurrence of the disease, and can be adequately assessed with serial ultrasounds.

B-0731 11:05

Pancreatic cysts in children with cystic fibrosis: US, CT and MR imaging
T. Berrocal, S. Novo, J. Fernández-Cuadrado, C. Prieto, M. Molina, N. Gómez-León; *Madrid/ES*

Purpose: To analyze the radiologic features of pancreatic cystosis, an unusual form of pancreatic alteration in cystic fibrosis, characterized by macrocysts of different sizes distributed all over the gland.
Material and methods: Pancreatic sonographies of 194 patients diagnosed with cystic fibrosis were reviewed. Six of these patients, aged between 12 and 16 years, showed macroscopic cystic lesions in the pancreas. All of them were asymptomatic. We prospectively studied these patients with CT and MR to evaluate the number, size, shape, distribution and characteristics of the lesions.
Results: All patients showed an enlarged pancreas. A complete cystic transformation of the gland was observed in two patients with cyst sizes ranging from 2 mm to 2 cm. One patient only had a rounded, well out lined, fluid-dilled lesion in the tail of the pancreas, and three showed various multiloculated cystic lesions of different sizes with normal pancreatic tissue around the cysts. On sonography all lesions were anechoic masses; on CT they showed los attenuation and homogeneous texture, and MRI demonstrated a high signal on the T2-weighted images and markedly hypointense signal in pancreatic tissue on the T1-weighted images.
Conclusion: Pancreatic cystosis is thought to represent the extreme end of the spectrum of cystic changes secondary to ductal obstruction. Macrocysts are thought to develop when functional secretory capacity is maintained despite ductal obstruction. CT and MRI are able to provide valuable information about the nature and content of the cysts, and help to differentiate this rare condition from other pancreatic cystic lesions.

B-0732 11:15

Ultrasound diagnosis in suspect meconium ileus
G. Belfiore, G. Moggio, A. Mazzacca, A. Bencivenga, G. Panascì; *Caserta/IT*

Purpose: To evaluate the diagnostic role of abdominal examination with ultrasound (US) in the clinical suspect of meconial ileum (MI), a disease due to non-evacuation of the meconium after birth, which conventional radiology cannot easily differentiate from other causes of ileum such as intestinal atresia.
Materials and methods: Over a 3-year period, 14 newborns (6 M/8 F, age range: 6 – 30 days) with no meconium evacuation were studied with abdominal US using a 5 MHz probe for an average observation time of 15 – 20 minutes on different acquisition planes. When cystic fibrosis was suspected, Sweat-Test was also performed, showing positive values in only 3 cases.
Results: The most frequent US pattern was dilatation of small bowel loops with little gas in the colon, matched by X-ray evidence of microcolia. In 9 cases several loops with enlarged diameter and hyperechoic content due to meconium were observed, 3 of whom showing abnormal Sweat-Test results. In 3 cases without hyperechoic luminal enlargement, intestinal atresia was found at surgery.
Conclusions: When meconial ileum is clinically suspected, abdominal US represents the first-choice examination, providing ther necessary information for the subsequent therapeutic approach in these patients.

B-0733 11:25

Omental cake: Omental metastases in children
W.A. Bhatti[1], K.R. Shankar[2], H.M.L. Carty[2]; *[1]Cheadle/GB, [2]Liverpool/GB*

Aim: We present the imaging features of four children with omental metastases. The primary in two of these cases were serous papillary adenocarcinoma, one case of primary cystadenocarcinoma and one case of non specific round cell tumour of unknown origin.
Method: The children were identified retrospectively from a code index in our oncology department. There were four children whose age ranged from five to eleven years. The imaging findings including CT appearances. The MRI appearance in one of the cases will be described.
Discussion: Omental metastases in children are rare. As in adults ovarian pathology is most likely. We present four cases which show the typical image finding in childhood. The differential diagnosis will be discussed.

B-0734 11:35

Imaging methods in paediatric oncology
I. Dykan, V.V. Medvedev, T. Golovko, O. Tykhonenko, G. Lavryk, A. Begenar; *Kiev/UA*

Purpose: To improve the results of treatment of malignant tumours in children a protocol of imaging investigative modalities was developed for early detection, staging and monitoring of efficiency of treatment in paediatric oncology.
Methods and materials: 284 children aged 6 months to 14 years with nephroblastoma (58), neuroblastoma (34), lymphoma (82), osteosarcoma (64), soft tissue tumours (46) were examined using a spectrum of imaging modalities (X-ray, CT, MRI, US, osteoscintigraphy).
Results: The most informative methods for primary diagnosis and staging of soft tissue tumours and retroabdominal tumours (including lymphoma) are US CT and MRI (accuracy 94 – 98 %). To monitor early efficiency of treatment the use of US, X-ray and osteoscintigraphy is advisable. CT and MRI are indicated in cases when the results of preliminary investigations are ambiguous or clinical data do not match their respective data. Osteoscintigraphy is useful in the primary diagnosis of osteosarcoma (accuracy 92 – 97 %), bone metastasis (accuracy 91 – 96 %) and in the determination of efficiency of treatment of bone malignant lesions (accuracy 80 – 89 %).
Conclusion: A protocol of investigative imaging modalities can be used for primary diagnosis, staging and determination of effectiveness of treatment in paediatric oncology with accuracy near 98 %.

B-0735 11:45

MR signs of gastrointestinal graft-versus host disease
H.-J. Mentzel, K. Kentouche, S. Vogt, C. Fitzek, B. Gruhn, F. Zintl, W.A. Kaiser; *Jena/DE*

Purpose: The MRI findings of intestinal involvement in gastrointestinal graft-versus-host disease (GvHD) after bone marrow transplantation (BMT) are described and correlated with histopathologic findings.
Subjects & methods: An 8-year-old boy underwent allogenic BMT for severe aplastic anemia. On day 26 he developed grade I acute GvHD. With intensified immunosuppressive therapy he recovered until day 50. A rectal biopsy specimen revealed a transitory pattern between acute and chronic GvHD. Because of persistent voluminous diarrhea and increasing abdominal pain imaging was performed. MRI was performed on a 1.5 T scanner to exclude development of an abscess. T1w and T2w sequences were obtained before and after application of GdDTPA (0.1 mmol/kg).
Results: Contrast-enhanced T1w sequences showed especially after subtraction abnormal mucosal enhancement of the whole gastrointestinal tract. Three layers of the wall could be differentiated in fat saturated contrast enhanced T1w axial images. Bowel dilation was present in T2w sequences. An abscess could be excluded.
Conclusion: The MR signs of gastrointestinal GvHD were demonstrated. The intensively enhancing inner zone of the bowel wall seems to represent the pathological thickened mucosa and submucosa, and the outer less-enhancing zone the edematous muscular layer. Differentiation beween intestinal GvHD and intestinal infection seems to be not possible by MRI, but exclusion of complications like abscesses or an estimation of the degree of inflammation is possible.

B-0736 11:50

US-guided reduction of intussusception: Experience enhances it!

P. Crystal, B. Farber, V. Tsodikov, Y. Barki; *Beer-Sheva/IL*

Purpose: Intussusception is the most common abdominal emergency in the infancy. The aim of this study was to assess an efficacy of ultrasound in the treatment of childhood intussusception and predictive value of different factors on success of reduction.

Materials and methods: Over two years, 67 consecutive cases of ileocolic intussusception were diagnosed sonographically in 54 patients. In 63 cases, reduction was attempted under sonography guidance. We analyzed influence of duration of symptoms, initial location of intussusception, presence of intraperitoneal fluid, and sonologist experience on success of reduction.

Results: In 57 (90 %) cases reduction was successful. Complications did not occur. Reduction rate of staff sonologists was 95 % (53 from 56) and this is significantly higher ($p < 0.03$) than success rate (57 %, 4 from 7) in general radiologists. Initial location of intussusception (right and mid abdomen versus left abdomen) also was significant predictor success ($p = 0.04$). Presence of the peritoneal fluid and duration of symptoms were not be found as a significant predictors of success.

Conclusion: We found that skill of physician that performing reduction and initial location of intussusception are main predictors of successful reduction. US-guided hydrostatic reduction of intussusception is a safe and effective technique. The principal advantages of this technique are the lack of radiation exposure and high reduction rate. A solely disadvantage is that the presence of experienced sonographer is required on a 24-hour basis.

B-0737 11:55

Thyroid volume in pre-school children from the Warsaw area assessed by ultrasound: The norm and the role in clinical diagnosis

M. Brzewski, J. Madzik, D. Janczarska, A. Jakubowska, A. Marcinski, B. Rymkiewicz-Kluczynska; *Warsaw/PL*

Purpose: The absence of the thyroid volume proper norm in pre-school children limits the diagnosis of goiter and delay in the start of treatment. The norms of volume measurements of the thyroid based on ultrasound examinations in this group of children are introduced.

Material and methods: 182 children from 4 up to 7 years old were examined. For future assessment the group of 159 healthy children were selected (pathology was excluded on basis of clinical examinations, iodine excretion and US exams). The volume of each lobe was calculated according to Brunn's formula ($V = a \times b \times c \times 0.479$) and the total volume of both were summed up.

Results: The average volume of the thyroid growing with age, although in our group 5-years old boys had greater volume than 6-years old. Good correlation with age, height, weight and body surface was statistically characteristic in all analysed groups. The best correlation was obtained with body surface, the worst with age. There was no characteristic sex dependence difference. The 50th and 97th centile of thyroid volume was determined.

Conclusion: The review of the thyroid volume norm in European children shows big regional variation. It is necessarily to use the norms described scientifically for each population, also in Poland. The goiter in clinical exam is usually overestimated – it is the next reason for thyroid volume assessment in ultrasound. The upper normal range for thyroid volume norm was accepted on to 97th centile.

10:30–12:00 **Room L/M**

Head and Neck

SS 1408

Orbit/Temporal bone/Skull base

Chairpersons:
N. Besenski (Zagreb/HR)
M.M. Lemmerling (Gent/BE)

B-0738 10:30

Colour Doppler flow imaging and computed tomography of orbital cysticercosis

R. Mithalal IV, V. Chowdhury sr.; *New Delhi/IN*

Purpose: Seventy-five cases of ocular cysticercosis presenting with proptosis and painful eye evaluated with high resolution ultrasound (HRS), colour Doppler flow imaging (CDFI) and contrast enhanced computed tomography (CECT) were studied retrospectively for orbital and ocular presentations of cysticercosis.

Material and methods: Seventy-five patients of orbital cysticercosis were evaluated during the period of May 1998 to Feb 2000 by HRS using 7 – 12 MHz probes, CDFI followed by CECT orbit (3 mm axial and coronal sections).

Results: In 70 of 75 cases involvement of the ocular muscles by the cysticercus larva was found on HRS. Localized thickening of the muscle belly, commonly medial and inferior rectus with an anechoic cyst containing peripheral echogenic scolex was seen in 45 cases. On CDFI there was low resistance perilesional flow of frequency shift less than 2.5 MHz. In 11 of these cases there was peripheral radiating vessels from the cyst giving a "corona rubra" appearance. In twelve of these 45 cases, CECT could not define the scolex accurately. Twenty-five cases represented as ill-defined thickening of one or more extraocular muscles with heterogeneity of retroocular fat, focal increase in vascularity and streakiness on CT. These cases were better evaluated on CECT. Twenty-two cases had coexistent neurocysticercosis. Two cases presented as retroretinal mass with retinal detachment misdiagnosed as choroidal masses and 2 had orbital apex syndrome. Sixty-three cases showed regression on ultrasound after albendazole therapy.

Conclusion: HRS and CDFI is the investigation of choice in the initial evaluation of orbital cysticercosis reserving CECT for equivocal cases.

B-0739 10:40

Improved imaging of the orbit based on highly accurate image fusion of SPECT and CT/MRI

R. Moncayo, E. Donnemiller, R.A. Sweeney, M. Rieger, K. Seydl, W. Jaschke, G. Riccabona, P. Lukas, R.J. Bale; *Innsbruck/AT*

Purpose: To provide both functional and anatomical imaging of the retroorbital space using ^{99}Tc-Octreotide SPECT and CT.

Materials and methods: Patients: (1) 32 year-old woman with thyroid associated ophthalmopathy (TAO) showing clinical improvement after conservative therapy. (2) 52 year-old woman with a bilateral meningeoma of the optic nerve, before and after external radiation. The patients were studied using a newly developed ^{99}Tc-Octreotide tracer (Eur.J.Nucl.Med. 2000; 28:1318). CT studies were done using a GE CT-High Speed Advantage scanner. Positioning of the head was done using the VBH head holder adapted to the SIP Lab Innsbruck frame. Image fusion was done using spezialized had- and software from Immerge (Sofamore-Danek Inc).

Results: Case 1: Contrasting with the pre-treatment scan, the retroorbital space did not show any uptake after therapy whereas the lacrimal glands showed a faint tracer accumulation. CT could not show alterations in the lacrimal glands. Case 2: Prior to therapy ^{99}Tc-Octreotide uptake was documented on both meningeal sheets (SPECT and CT/MRI). The intensity of the uptake decreased significantly after radiation therapy, corresponding to clinical improvement.

Conclusion: Using this combined imaging approach we can clearly delineate the retroorbital structures involved in each distinct disease. Image fusion of functional and anatomical data provide clear objective criteria as to disease activity.

B-0740 10:45

Cavernous hemangioma of the retrobulbar space: CT, MRI and Doppler investigations

D. Miminoshvili, D. Gachechiladze, N. Shapatava; *Tbilisi/GE*

Purpose: To describe the CT, MRI and Dopplerographic signs of cavernous hemangioma of the orbits.

Materials and methods: CT, MRI and Dopplerography were performed in 17 patients (9 men, 8 women; age 32 – 53 years) with cavernous hemangioma of retrobulbar space.

Results: On CT cavernous hemangiomas were visible as tissue density formations with pronounced contrast enhancement, localized inside the muscular cone. On Dopplerography ($n = 14$) tumor was revealed as hypervascular formation. In 6 cases punctate arterial blood flow around the cavernous hemangioma and in 7 cases compression of upper orbital vein was noted. The indices of venous blood flow and punctate arterial blood flow were increased. Orbital main vessels had blood flow parameters within the normal range. On MRI in T1-weighted images with fat saturation the cavernous hemangioma was visible as a hypointensive formation which enhanced significantly after contrast administration, in T2-weighted image as a hyperintensive formation. 14 patients with cavernous hemangioma out of 17 were operated and the diagnosis was confirmed histomorphologicaly in all cases.

Conclusion: CT and MRI along with Dopplerography of retrobulbar space hemangiomas with evaluation of the general vascularization and hemodynamic indices allow to determine the treatment tactics and plan out the scales for operative interventions that decreases the intraoperative and postoperative complications.

B-0741 10:50

Multidetector CT scanning of the temporal bone in patients with cholesteatoma

T.F. Gotwald, C. Cihak, B. Oefner, A. Stoeger, A. Schuster, D. zur Nedden; *Innsbruck/AT*

Purpose: Near isotropic CT data acquistion of the temporal bone may obviate the need for additional radiation for coronal CT data acquisition in patients with cholesteatoma.

Materials and methods: We compared multidetector spiral CT scanning and axial and coronal image reconstruction with conventional CT data acquistion in two planes in a group of 23 patients for imaging work-up in cholesteatoma. All patients underwent multidetector CT scanning in axial orientation with coronal and axial image reconstruction as well as conventional coronary CT scanning. The comparison was made by two radiologists and one otolaryngologist who were not aware of the imaging modality at the time of the evaluation.

Results: Multidetector CT clearly surpasses conventional CT scanning in terms of patient comfort, time efficacy and radiation dose needed to obtain the patient's data. In addition, image quality was found to be equal to conventional technique. The delineation of some particular anatomic structures (e.g. of thin bony septa, the ossicles, sinus tympani) could even be improved.

Conclusion: In our institution multidetector CT scanning has replaced conventional 2-plane CT scanning and has become the standard procedure for evaluation of the temporal bone in cholesteatoma.

B-0742 11:00

High resolution computed tomography in patients with vertigo following stapes surgery

D. Pickuth, S. Brandt, A. Berghaus, R. Spielmann, S. Heywang-Köbrunner; *Halle a. d. Saale/DE*

Purpose: The role of high resolution computed tomography (CT) in patients with persistent or recurrent vertigo after stapes surgery is still unclear.

Patients and methods: 10/30 patients, who had a postoperative CT of the temporal bone between January 1993 – June 2000, presented with vertigo.

Results: In 8/10 patients, the underlying cause for postoperative vertigo could be established with CT. The CT findings included a prosthesis shaft entering the vestibule and compressing the saccule in four patients, a complete dislocation of the stapes prosthesis in one patient, air bubbles and fluid collections within the vestibule and outside the oval window indicating a perilymphatic fistula in two patients, and bony fragments leading to a compression of the basal saccule in one patient.

Conclusion: Although immediate postoperative vertigo is often transient, with persistent or recurrent vertigo the patient should be imaged, as high resolution CT will determine the underlying cause in the majority of patients.

B-0743 11:10

Outcome of cochlear implantation: Assessment by volume rendered spiral CT

E. Neri, S. Berrettini, S. Sellari Franceschini, M. Panconi, F. Forli, C. Spinelli, G. Campori, D. Caramella, C. Bartolozzi; *Pisa/IT*

Purpose: We aimed to assess the outcome of cochlear implantation with CT volume rendering.

Materials and methods: A series of 16 patients that underwent unilateral cochlear implantation were evaluated with high resolution spiral CT within 1 month after the surgical procedure. Image acquisition included axial and coronal scans of the temporal bone with 1 mm collimation and 0.5 mm reconstruction spacing. Native images were reviewed on independent workstation (Advantage Windows 3.1) and interactive volume rendering was performed with a dedicated software tool. Image analysis was aimed to exclude complications in the tympanic cavity and to assess the position of the electrode within the cochlea turns. Volume rendering was used to reconstruct in three-dimensions the electrode and the bony canal of the cochlea. Agreement between native images and volume rendering for assessing the position of the electrode within the cochlea was determined with k statistic.

Results: No major complications occurred in the tympanic cavity. The electrode was correctly positioned within the oval window, the basal and middle turns of the cochlea. The middle turn was entirely occupied by the electrode in 13 cases, and partially in 3 cases (2/3 of the middle turn). No kinking or interruption of the electrode were observed. Agreement between native images and volume rendering was good ($k = 0.56$); in some difficult cases the integration of native images with volume rendering allowed to determine the precise path of the electrode within the cochlea.

Conclusions: CT with volume rendering represents an effective method to assess the outcome of cochlear implants.

B-0744 11:20

CT virtual endoscopy of the auditory ossicular chain: Technique and clinical applications

D. Wang, W.S. Zhang, J.X. Xu; *Beijing/CN*

Purpose: To evaluate the methodology and clinical applications of CT virtual endoscopy (CTVE) in the evaluation of the auditory ossicular chain.

Materials and methods: CTVE of auditory ossicular chain w... 1.0 mm collimation at pitch 1.0, bone algorithm, 9.6 cm F... reconstruction interval in 10 normal subjects and 50 pati... ear diseases proved by operation. The threshold values fo... normal auditory ossicular chain were –600 – –200 HU and ... spectively.

Results: On CTVE images, the ... of normal malleus, incus and incudomalleal articulation ... was 32 % for the stapedial footplate. However, in only 21 %... nor and posterior crura of stapes be distinguished. The s... y and accuracy of CTVE for detecting the ossicular destru... c otitis media were 92.8 %, 92 % and 92.5 % respectiv... congenital anomaly, auditory dysplasia was seen.

C... TVE being a new, non-invasive method for demonstrating the three-di... onal image of auditory ossicular chain is useful in evaluating diseases of the ear especially the auditory ossicles.

B-0745 11:30

Diffusion weighted MR imaging of cholesteatomas of the temporal bone

T. Kittner, G. Hahn, V. Hietschold; *Dresden/DE*

Purpose: To evaluate the sensitivity and specificity of diffusion weighted imaging MRI, in the assessment of cholesteatoma recurrence.

Material/method: In this prospective study we investigated 25 patients with clinically suspected cholesteatomas of the tympanic cavity or mastoid. Imaging studies were obtained at an 1.5 T Siemens Vision scanner. Our imaging protocol included: T2-weighted DWI axial sequences (TR 3900 ms; TE 100 ms; TA 20 s; b 1000; SL 3 mm); T1-weighted SE (TR 513 ms; TE 16 ms; SL 3 mm) in coronal and axial plaine before and after single-dose Gadolinium i.v. injection.

Results: MR imaging yielded an sensitivity of 83 %; specificity of 85 % an accuracy of 84 %.

Conclusion: Diffusion weighted MR imaging is reliable and helpful particulary in patients with an intact tympanic membrane scheduled for an second look surgical resection. One should be aware that thin layers of cholesteatoma tissue will not be detected with above mentioned method.

B-0746 11:40

MR imaging of the inner ear: Comparison of a 3D-high resolution fast spin echo sequence with a Gd-enhanced T1-spin echo sequence

A.H. Karantanas, V. Sandris; *Larissa/GR*

Purpose: To prospectively evaluate the diagnostic value of MR imaging in the inner ear with a 3D-T2 weighted (w) fast spin echo (FSE) sequence in patients with clinical indication of vestibular schwannoma.

Materials/methods: In 47 patients with ear symptoms, 1.0 T MR imaging was performed with unenhanced 3D-asymmetric FSE and gadolinium enhanced T1-w spin echo (SE) with use of a head quadrature coil. The FSE images were reviewed by one radiologist with the enhanced sequence used as the standard of reference.

Results: Seven lesions were detected in the 94 ears by both sequences. All lesions were smaller that 25 mm and 1 lesion smaller than 5 mm. In the latter, the 3D unenhanced sequence overestimated (8 mm) the size of the lesion. The linear regression analysis showed a statistically significant coefficient for the maximum diameter of the lesions ($p < 0.001$). All lesions were established by surgery.

Conclusion: The unenhanced high-resolution 3D T2-w sequence allows the reliable detection of vestibular schwannoma and can be used alone as a screen. When a lesion is obvious, then the enhanced images are helpful, particularly for the intracanalicular location where there is no CSF surrounding the lesions and the actual size can not be accurately estimated preoperatively.

B-0747 11:45

Chordomas of the skull base: An otoradiologic classification

B.F. Schuknecht, A. Schade, U. Fisch; *Zürich/CH*

Purpose: Classify skull base chordomas with respect to tumor origin, type of surgical infratemporal approach and histology

Patients and methods: Multiplanar MR and CT examinations were retrospectively assessed in 12 patients with skull base chordomas with respect to tumor origin, type of otosurgical approach, degree of tumor resection and histology.

Results: Midline and paramedian chordomas were present in 6 patients each. Midline chordomas showed a close relationship to the spheno-occipital synchondrosis, while paramedian lesions were oriented along the petro-occipital synchondrosis. The origin of midline chordomas could be further subdivided into a supero-, infero-, and centroclival location that was recognized in 2 patients each.
The infratemporal approach Fisch type B allowed total or subtotal resection of midline chordomas in 4 of 6 pateints, the type C approach provided access to paraclival tumors with total or subtotal resection in 5 of 6 cases. Histologically midline chordomas belonged to the "conventional" type in 5/6 tumors, paraclival chordomas consisted of conventional and chondroid type tumors in 3 lesions each.
Conclusion: MR and CT findings indicate two separate sites of origin of skull base chordomas that are related to the spheno-occipital and petro-occipital synchondrosis respectively. These two sites require a different otosurgical access for removal and may represent two different types of histology.

B-0748 11:55

Meningiomas in patients with extracranial malignant tumors
G.T. Petkovic, L. Markovic, S. Cirkovic, A. Radosavljevic, B. Putnik; *Belgrade/YU*

Purpose: To describe the possible coincidental finding of intracranial meningeomas in patients with extracranial malignancy during staging of tumors.
Patients and methods: Five patients (2 women, 3 man; aged 56 – 71 years; two with lung cancer, one with malignant melanoma, one with breast Ca and one with adeno Ca of the rectum), with different neurological symptoms, during the staging, underwent CT of the head. After positive finding for the intracranial expansion, all of patients were examined with MRI and DSA, and finally, underwent a craniotomy.
Results: CT detected 8 expansive lesions in all patients, 3 patients had two lesions. 5 of lesions were located peripherally, with limited edema, and with good and homogenous contrast enchancement. Two lesions had an intracerebral and 1 an intracerebelar location with marked edema, and pronounced ring shaped contrast enhancement. Five peripheral lesions were recognized as meningeomas, and other 3 lesions as metastasis. All patients had meningeomas, and 3 of them had metastasis as well. All findings were confirmed by MRI, DSA and histologically confirmed.
Conclusion: The finding of an intracranial expansile lesion in patients with a malignancy is almost certain a sign of metastasis. However, there is the possibility of coincidental meningeomas with extracranial malignancy that can cause misinterpretation. CT features of CNS metastasis enable its accurate characterization and differentiation from meningeomas, and therefore, appropriate staging of the extracranial malignancies.

10:30–12:00 **Room N/O**

Cardiac

SS 1403

Heart function: MRI

Chairpersons:
M.R. Rees (Bristol/GB)
G.A. Wegenius (Uppsala/SE)

B-0749 10:30

Comparison of Cine-TrueFISP and Cine-FLASH in the assessment of myocardial function
J. Barkhausen[1], S.G. Rühm[1], M. Goyen[1], G. Laub[2], J.F. Debatin[1]; *[1]Essen/DE, [2]Erlangen/DE*

Purpose: To compare a recently developed TrueFISP with a standard 2D-FLASH sequence regarding their ability to assess myocardial function using manual and semi-automatic segmentation.
Material and methods: Examinations were performed on a 1.5 T scanner (Magnetom Sonata, Siemens, Erlangen, Germany). Following informed consent, 10 healthy volunteers and 10 patients were enrolled in the study. Short axis and long axis Cine images were collected with the standard FLASH sequence (TR 11; TE 6; FI 20°) as well as the new TrueFISP sequence (TR 3.2; TE 1.6; FI 60°). Contrast to noise ratios (CNRs) measurements were made from regions of interest (ROI) placed within the myocardium, and the left ventricular cavity. In addition, we compared the performance of manually obtained volumetric measurements with semi-automatically calculated data.
Results: Compared to FLASH the calculated CNRs of the TrueFISP sequence were improved by 46 % on short axis and 100 % on long axis images. The semi-automatic image analysis resulted in the following systematic and random differences (mean ± SD) compared to manual segmentation: TrueFISP end-diastolic volume –4.8 ± 9.7 ml; TrueFISP end-systolic volume –3.8 ± 6.9 ml; FLASH end-diastolic volume –3.7 ± 16.9 ml; FLASH end-systolic volume 11.0 ± 22.1 ml.
Discussion: The TrueFISP sequence provides Cine images with excellent contrast between the myocardium and the intraventricular cavity. Automated segmentation software provided more reliable results when analysis was based on TrueFISP-Cine images as compared to standard FLASH-Cine images.

B-0750 10:40

Assessment of ventricular function in a single breath-hold using real-time TrueFISP cine imaging
J. Barkhausen[1], S.G. Rühm[1], M. Goyen[1], G. Laub[2], J.F. Debatin[1]; *[1]Essen/DE, [2]Erlangen/DE*

Purpose: To evaluate the ability of a recently developed real-time TrueFISP sequence to assess left ventricular function within a single breath-hold.
Material and methods: Examinations were performed on a 1.5 T scanner (Magnetom Sonata, Siemens Medical Systems, Erlangen, Germany). 15 patients were enrolled in the study. Short axis Cine images (8 mm section thickness) were collected with a single-slice segmented TrueFISP sequence (TR 2.4, TE 1.2, FA 60°, matrix 120 × 256, 36 ms/frame), as well as a real-time TrueFISP sequence (TR 2.2, TE 1.1, FA 45°, matrix 63 × 128, 77 ms/frame) which collects 7 sections over 14 RR-intervals in a single breath-hold. Contrast-to-noise ratios (CNR) of both sequences were compared. Cardiodynamic parameters were determined based on the different image sets.
Results: Cardiodynamic measurements based on the real-time TrueFISP showed the following systematic and random differences (mean ± SD) compared to segmented TrueFISP: end-diastolic volume –3.1 ± 6.0 ml; end-systolic volume 2.4 ± 4.7 ml; ejection fraction –3.7 ± 2.0 %; stroke volume –5.6 ± 2.8 ml. CNR values of real-time images exceeded those of segmented TrueFISP by more than 240 % ($p < 0.01$).
Conclusion: Real-time TrueFISP permits accurate assessment of the left ventricular function within a single breath-hold. The lower temporal resolution resulted in a slight overestimation of the end-systolic volumes, and an underestimation of ejection fraction and stroke volumes.

B-0751 10:50

Influence of spatial and temporal resolution on left ventricular functional parameters derived from trueFISP Cine MR images of the heart
S. Miller[1], O. Simonetti[2], J.P. Finn[2], U. Kramer[1], J. Carr[2], G. Laub[2], C.D. Claussen[1]; *[1]Tübingen/DE, [2]Chicago, IL/US*

Purpose: To investigate the influence of spatial (S) and temporal (T) resolution on left ventricular (LV) functional parameters using TrueFISP cine MR imaging of the heart.
Material and methods: Consecutive MR examinations with continuous short axis imaging of the heart were performed in 12 healthy volunteers using a 1.5 T Magnetom Sonata MR scanner (Siemens). A segmented TrueFISP 2D pulse sequence (TR 3.0 ms, TE 1.5 ms) was modified to provide different temporal resolutions with a frame duration (T) of 21, 45, 60 and 90 ms. In-plane spatial resolution (S) was stepwise varied from 1 – 3 mm. Using interactive evaluation software (ARGUS, Siemens) the following LV functional parameters were determined: end diastolic volume (EDV), EDVindex, mass, massindex, cardiac output (CO), cardiac index (CI), ejection fraction (EF) as well as ejection and filling flow rates. Inter-study, intra- and interobserver variability were determined.
Results: With decreasing T there was a significant reduction of EF, CO, CI, ejection and filling rates (p0.05). The remaining parameters did not change, significantly. Variability results were in a range of 0 – 6 %.
Conclusion: A significant influence of S and T on LV functional parameters determined by TrueFISP cine MR imaging was observed. The influence of T can be considered more relevant than the influence of S. Serial follow-up studies should use consistent settings of S and T.

B-0752 11:00

Comparison of single-slice true-fisp cine, multi-slice true fisp cine and segmented flash cine sequences for volumetry
A. Kluge, T. Dill, C. Müller, W. Ricken, C. Hamm, G.F. Bachmann; *Bad Nauheim/DE*

Purpose: To evaluate the influence of different cine sequences with various anatomic resolutions on manual segmentation of blood pool and myocardial mass for left and right ventricular volumetry. Segmented turbo-flash cine sequences are hampered by low contrast and difficult differentiation of myocardial mass and blood pool especially in the basal and apical sections. The inherently higher contrast of

true-fisp sequences allows faster and more accurate volumetric analysis. Multi-slice true-fisp-sequences reduce examination time, but anatomical resolution is impaired.
Materials and methods: We performed volumetry on a 1.5 T MR scanner (Sonata, Siemens) and compared mean volumes and standard errors in the following three sequences: true-fisp cine sequences in single slice and multi-slice technique, and conventional turbo-flash sequences. 5 healthy volunteers and 19 patients with proven coronary heart disease, atrial and ventricular shunts and aquired valvular disease were examined.
Results: True-fisp-sequences facilitated volumetric measurements by greater contrast between blood and myocardium. The average standard deviation of volumetric results of different slices was 3.5 % vs. 5.3 % vs. 5.1 % using true-fisp single slice vs. turbo-flash-sequences vs. true-fisp multi-slice sequences. Absolute values of left and right ventricular volume did not show significant differences.
Conclusion: True-fisp sequences reduce analysis time and facilitate postprocessing. Despite the relatively lower spatial resolution, true fisp multi slice sequences permit adaequate volumetry if correct in-group standardization is performed.

B-0753 11:10

Assessment of genotype-phenotype correlation with cardiac MRI in subjects with hypertrophic cardiomyopathy

P. Sipola[1], J. Kuusisto[1], K. Peuhkurinen[1], P. Jääskeläinen[1], M. Laakso[1], K. Lauerma[2], H.I. Manninen[1], H.J. Aronen[1,2]; *[1]Kuopio/FI, [2]Helsinki/FI*

Purpose: To evaluate anatomic features associated to specific gene mutation causing hypertrophic cardiomyopathy with cardiac MRI.
Methods and materials: Cardiac MRI (Siemens Vision 1.5 T imager) was performed for three index patients with hypertrophic cardiomyopathy and gene mutation in sarcomere protein alphatropomyosin (Asp175Asn) and their 15 family members (age over 16 years) with same gene defect. Left ventricular (LV) wall thickness and mass were measured from short axis slices encompassed whole left ventricle by using breath hold gradient echo sequence (slice thickness 10 mm, TR 60, TE 4.8, FA 20). Apical myocardial thickness was assessed on long axis images.
Results: LV mass varied greatly between the patients from 79 to 262 g. At least one segment with greater than or equal to 13 mm was found in 11 of 13 patients, resulting in hypertrophic penetrance of 82 %. Anterior left ventricular free wall at mitral tendon level was the thickest segment (15.2 ± 6.4 mm; mean ± 1 standard deviation). The most normal sector was lateral LV free wall at the papillary muscle level that was hypertrophied none of the patients (8.7 ± 2.1 mm).
Conclusion: Cardiac MRI is the method of choice for evaluating genotype-phenotype correlations in different forms of genotyped cardiomyopathies. Hypertrophy at the anterior free wall at mitral tendon level and normal lateral free wall at papillary muscle level of LV suggest the diagnosis of hypertrophic cardiomyopathy caused by gene defect in alphatropomyosin gene Asp175Asn.

B-0754 11:20

Evaluation of true left ventricular aneurysms before and after aneurysmectomy with cine-magnetic-resonance imaging (Cine-MRI)

O.K. Mohrs[1], K.-F. Kreitner[1], G.F. Bachmann[2], N. Oesingmann[3], M. Thelen[1]; *[1]Mainz/DE, [2]Bad Nauheim/DE, [3]Erlangen/DE*

Purpose: To demonstrate the usefulness of Cine-MRI for evaluation of true left ventricular aneurysms (TLVA) and for prediction of surgical outcome.
Methods and materials: We investigated 15 patients with TLVA before and 13 patients before and after aneurysmectomy at 1.5 T. 15 healthy volunteers served as normal controls. For Cine-MRI, k-space segmented FI-2D GE-sequences were used. Functional analysis comprised the calculation of endsystolic and enddiastolic volumes (LV-EDVs and LV-ESVs), cardic index (CIs), ejection fractions (EFs), and prediction of cardiac volumes after aneurysmectomy.
Results: LV-EDVs and LV-ESVs were higher in patients with TLVA (240.2 ± 62.1 and 183.1 ± 65.6 ml) than in volunteers (148.5 ± 34.4 and 47.7 ± 13.5 ml) ($p < 0.001$). CIs and EFs were significantly lower in patients (2.2 ± 0.8 vs. 3.9 ± 0.9 l×m²/min, 26.0 ± 9.7 vs 67.9 ± 4.5 %, respectively) ($p < 0.001$). After aneurysmectomy, there were a significant decrease of LV-EDVs and LV-ESVs ($p < 0.001$), and a significant increase of CIs and EFs ($p < 0.001$). There was a good correlation between the preoperatively calculated and the measured left-ventricular volumes after aneurysmectomy ($r = 0.70$; $p = 0.035$).
Results: Cine-MRI allows for accurate evaluation of TLVA, and enables preoperative estimation of left-ventricular volumes after surgery.

B-0755 11:30

Myocardial function of stunned and infarcted myocardium evaluated by Cine and Tagged magnetic resonance imaging

K.U. Jürgens[1], P. Reimer[1], T. Weber[1], B. Tombach[1], J. Bankert[1], C. Bremer[2], B. Renger[1], T. Filler[1], W. Heindel[1]; *[1]Münster/DE, [2]Boston, MA/US*

Purpose: To evaluate regional and global left ventricular myocardial function (ischemic vs. remote area) by means of Cine and Tagged MRI in an experimental animal model following short-term and persistent occlusion of LAD based on histopathological analysis.
Materials and methods: 10 open-chest anesthetized dogs underwent reversible (15 min; $n = 5$) and permanent ($n = 4$) pneumatic occlusion of the left anterior artery (LAD) to induce myocardial stunning and myocardial infarction, respectively (one animal as reference). MR imaging was performed at 1.5 T (Magnetom Vision, Siemens Medical Systems) obtaining an ECG-triggered breath-hold Cine GE-sequence (Flash 2D) and a breath-hold Tagging GE-sequence with spatial modulation of magnetization (SPAMM) 60 to 90 minutes following occlusion. Postmortem, needle biopsies were taken each from the LAD-perfused and a remote area. Ex vivo, MR imaging (T1-w TSE) and TTC staining were performed.
Results: Induction of infarction was confirmed by histopathology correlating with TTC staining. LAD perfused myocardial segments demonstrated reduced systolic wall thickening ($p < 0.05$) resulting in impaired global function (EF, SV, CO; $p < 0.05$), regardless of underlying etiology. MR Tagging showed reduced minimal principal strain (I2) in infarcted areas, but no significant change in stunned myocardium compared to remote regions.
Conclusion: Cine and Tagged MRI enable the determination of global LV function and regional wall motion in stunned and infarcted myocardium based on histopathology.

B-0756 11:40

Measurement of left and right diastolic filling parameters in 42 patients with cardiomyopathy and coronary heart disease using fast MRI with breath-hold

G.F. Bachmann, M. Rominger, T. Dill, A. Kluge, C. Müller, C. Hamm; *Bad Nauheim/DE*

Purpose: Assessment of left and right diastolic filling in localized and diffuse heart diseases using fast cine MR imaging.
Methods: 15 patients with coronary artery disease (CAD), 14 patients with dilated cardiomyopathies (DCM), 13 patients with hypertrophic cardiomyopathies (HCM), and 10 healthy volunteers were examined using a segmented fast cine MR technique in breath-hold and the Argus software (1.5 T unit, Siemens). Time-volume-curves on three slices through the left ventricle (LV) and one slice through the right ventricle (RV) allowed calculation of peak filling rate (PFR, in EDV/s), time to peak filling rate (TPFR in ms) and time of end-systole (TSYS in % of RR-interval).
Results: In DCM the PFR of LV was reduced (3.1 EDV/s compared to 4.9 EDV/s of volunteers) and TSYS was prolonged (DCM 50.1 %, volunteers 35.4 %). HCM showed a lengthening of the endsystole. In CAD we found localized decreased fillings rates when PFR of basal, central and apical slices were compared to normal values.
Conclusion: Cardiac MRI in breath-hold technique permits accurate measurement of relaxation disturbances of the right and left ventricle in diffuse or localised heart disease. The definition of filling volume indices on only four slices is an acceptable compromise to the time-consuming imaging of entire ventricles.

B-0757 11:50

Quantification of aortic regurgitation by MRI

P. Kalden, K.-F. Kreitner, H. Brinkmann, T. Wittlinger, T. Voigtländer, M. Thelen; *Mainz/DE*

Purpose: Determination of the degree of aortic regurgitation by using a velocity-encoded, phase-difference magnetic resonance (MR) sequence in comparison to cardiac angiography.
Materials and methods: 25 patients with known aortic regurgitation were investigated at a 1.5 T Siemens Vision system. First the regurgitation jet was shown using a gradient-echo-sequence (cine). Then cine measurements for calculating the left ventricular function indixes were performed. For flow measurements a velocity-encoded, breath-hold phase-difference MR sequence was used ('through plane', FLASH 2D-sequence, TR/TE 110/5 ms, 'velocity encoding' 250 cm/s). Flow measurements were performed in the ascending aorta approximately 1 cm above the aortic valve. Mean flow (ml/R–R interval), stroke volume and regurgitant flow were determined and regurgitation fraction was calculated. The MRI results were compared with cardiac angiography.

Results: Correlation between the calculated stroke volumes by cine and flow measurements were very good ($r > 0.9$). In 18 of 25 (72 %) patients the assessed degree of aortic regurgitation determined by MRI and angiography were equal. In two patients the degree of regurgitation was overestimated and in 5 patients regurgitation fractions were underestimated by MRI. In all cases the indication for an aortic valve operation determined by MRI flow measurements was confirmed by angiography.
Conclusion: Using the velocity-encoded, phase-difference MR technique, a reliable non-invasive evaluation of the degree of aortic regurgitation is possible.

10:30–12:00 **Room P**

Physics in Radiology

SS 1413

CT, MR imaging and more

Chairpersons:
J. Garrido (Porto/PT)
R. Nowotny (Vienna/AT)

B-0758 10:30

Motion and beam hardening artifacts in rapid CT scanning: Electron-beam tomography vs. multislice CT

E. Hein[1], P. Rogalla[1], T.H. Wiese[1], A. Adachi[2], Y. Nobuta[2], B.B. Hamm[1];
[1]Berlin/DE, [2]Tokyo/JP

Purpose: To compare both rapid scanning modalities, electron-beam tomography (EBT) and multi-slice CT (MS-CT), with respect to suppression of motion and beam hardening artifacts.
Materials & methods: A round water phantom containing two pipes filled with contrast material (620 HU) was scanned with EBT and MS-CT without and during motion simulating in-plane breathing excursions. Similar parameters were used for the EBT/MS-CT: 130/120 kV, 0.4/0.5 s exposure per slice, 250/250 mAs, 3/2 (thin slice) and 6/8 mm (thick slice) collimation. Images were obtained using the highest and 50 % of the highest pitch possible on each system. A second series on the EBT was obtained using a cone-beam algorithm. 50 ROIs were drawn in rows parallel and perpendicular to the direction of motion. The average pixel values, the SD in each ROI, and ratios between SDs of ROIs with/without motion and beam hardening artifacts were calculated and statistically compared.
Results: No difference was seen between both scanners with respect to beam hardening artifacts in the still phantom. During motion, the MS-CT showed less increase in SDs than EBT (thin slice: 1.9 vs 1.8, $p = 0.17$, thick slice: 2.1 vs 1.5, $p = 0.012$). With the higher pitch, the SDs increased less than with the lower pitch (EBT: 1.8 vs 2.2, $p = 0.04$, MS-CT: 1.4 vs 1.8, $p = 0.03$). The cone-beam algorithm (EBT) had no measurable effect on both artifacts.
Conclusion: With the motion phantom, CT scanners can be objectively compared with respect to their susceptibility to motion and beam hardening artifacts. Being up to 3 times faster than the EBT, MS-CT scanning carries the potential to further reduce motion artifacts in patients.

B-0759 10:40

Dose reduction in subsecond multislice spiral CT by online tube current modulation

H. Greess[1], U. Baum[1], H. Wolf[2], C. Suess[2], W.A. Kalender[1], W.A. Bautz[1];
[1]Erlangen/DE, [2]Forchheim/DE

Purpose: To investigate in a controlled patient study the potential of online tube current modulation in subsecond multi-slice spiral CT (MSCT) examinations to reduce patient dose without loss in image quality.
Method/materials: Dose can be reduced for non-circular patient cross-sections without an increase in noise if tube current is reduced at those angular positions where the patient diameter and, consequently, attenuation is small. We investigated a pre-release product version of an online control for the tube current integrated in a SOMATOM VZ (Siemens AG, Erlangen/Germany) with improved technical performance.
We evaluated image quality, noise and dose reduction for examinations with online tube current modulation in a group of 75 patients (25 MSCT of the thorax, 25 MSCT of the abdomen and 25 of the thorax and abdomen). We evaluated total mAs for tube current modulation and compared it to the mAs product in standard protocols. Image quality was rated as very good, good and poor in a consensus by three radiologists.
Results: Dose was reduced typically by 23.6 to 39.4 %, depending on the patient geometry and anatomical regions (thorax mean 36.4 %, abdomen mean 34.8 %, thorax and abdomen mean 35.7 %). In general, no loss of image quality was observed. In some cases the noise pattern was improved by increasing the current in the direction of maximum attenuation, while reducing it strongly in other directions.
Conclusions: Dose in multi-slice spiral CT examinations can be reduced significantly in routine examinations by online tube current modulation without a loss of image quality.

B-0760 10:50

Effect of focal spot size on image quality in multi-detector CT

T. Azhari, M.E. Bellemann, M. Herzau, W.A. Kaiser; *Jena/DE*

Purpose: To realise the highest possible spatial resolution in CT, the acquisition parameters have to be selected carefully. The purpose of this study was to investigate the effect of the focal spot size on image quality at a multi-detector CT scanner.
Materials and methods: Due to automatic filament selection of our CT scanner (LightSpeed QX/i, GE Medical Systems), the size of the focal spot is switched from small (0.9 mm × 0.7 mm) to large (1.2 mm × 1.2 mm) when the tube power exceeds 24 kW. The GE performance phantom was scanned using different axial and helical acquisition protocols with a slice thickness of 1.25 mm and a tube voltage of 120 kV. The tube current was chosen to obtain an approximately constant mAs-product at both focal spot sizes.
Results: In the axial (helical) mode, the spatial resolution as determined from the modulation transfer function was 10.8 ± 0.1 (10.9 ± 1.0) lp/cm and 9.3 ± 0.2 (9.1 ± 0.4) lp/cm for the small and the large focal spot, respectively. At both modes, the improvement in spatial resolution was statistically significant ($P < 0.001$) while the image contrast-to-noise ratio remained unchanged. The corresponding radiation doses were 94 mGy and 107 mGy for the small and the large focal spot, respectively.
Conclusion: The small focal spot leads to a significantly higher spatial resolution at the same image contrast and at an even lower radiation dose. When choosing the tube current, the user should be aware of the focus switching point in order to achieve optimum image quality in high-resolution CT.

B-0761 11:00

Weighted CTDI dose data in two phantom materials for different CT scanners

K.A. Jessen, J. Hansen; *Århus/DK*

Purpose: Diagnostic reference levels for CT are based on the weighted CTDI values measured in dosimetry phantoms of PMMA of standard sizes for head and body according to European Guidelines on Quality Criteria for Computed Tomography (EUR 16262) and the IEC 60601-2-44 on partricular requirements for the safety of X-ray equipment for computed tomography, which also recommends that this factor be displayed on the operator's console for the actual scanner settings. Reliable measurements are therefore important.
Methods and materials: Recently water-equivalent head and body phantoms have been manufactured based on a polyurethane resin technology (QRM, Germany). Measurements of the weighted CTDI values have been performed with a pencil ionization chamber with an active length of 10 cm in both PMMA and solid water phantom materials for four different CT systems with different slice thicknesses and tube voltages.
Results: The weighted CTDI values measured in the PMMA phantoms are significantly higher (up to 20 %) than in the water-equivalent phantoms for the different beam qualities. The consequences for assessments of patient doses will be discussed.
Conclusions: The selection of appropriate diagnostic reference dose quantities has proved particularly challenging since they are required to provide a meaningful indication of patient exposure for all types of scanner and technique, whilst being simple to assess.

B-0762 11:10

Real-time interactive single shot fast spin-echo imaging

S.J. Riederer, R.F. Busse; *Rochester, MN/US*

Purpose: The purpose of this work was to develop a technique for performing single shot fast spin-echo imaging (SSFSE) in a continuous, real-time manner.
Materials and methods: SSFSE imaging is generally done using a single repetition and a net infinite repetition time. It was hypothesized that a continuously operable SSFSE sequence would further facilitate direct diagnosis. This was developed by incorporating several techniques. Driven equilibrium accelerated magne-

tization recovery, allowing reduced TR times. Wiener demodulation provided restoration of spatial resolution due to T2 decay. Interactive parameter control allowed real-time modification of the plane of section. The net sequence was tested in studies of pelvic floor motion, fetal MRI, and MR cholangiopancreatography.
Results: With driven equilibrium a 1000 ms TR time provided signal recovery matching that of a standard sequence at TR 2000 ms, allowing a 1 Hz SSFSE frame rate. Wiener demodulation restored edge definition. In each of the applications the interactive SSFSE sequence permitted tracking of the moving object or facilitated definition of the plane of section while still providing high quality images.
Conclusion: SSFSE imaging can be done on an interactive basis. The clinical feasibility studies suggest that real-time diagnostic imaging may be possible for specific applications.

B-0763 11:20

The development and optimisation of fast recovery SSFSE

M.I. Makki, M.J. Graves, R.R. Sood, D.J. Lomas; *Cambridge/GB*

Purpose: Single shot fast spin echo (SSFSE) offers a number of advantages in imaging the abdomen. However, a major problem is the poor SNR due to the short time available for signal recovery between excitations. We have developed and optimised a fast-recovery SSFSE sequence for improving image quality in abdominal MRI.
Materials and methods: The Fast-Recovery modification involves adding a (-90_x) pulse at half the inter-echo spacing to the end of the SSFSE echo-train. This pulse returns the remaining transverse magnetisation M_{xy} back to its initial position along the Z-axis thereby increasing the available longitudinal magnetisation M_z for subsequent excitations. The effect of this modification on SNR was quantified using a water and oil phantom and applied in vivo. Images were acquired using multi-phase and multi-slice sequential acquisition over a range of effective TR values. Further reductions in TR were achieved by using 110° refocusing pulses instead of the standard 155° pulses.
Results: In multi-phase imaging the Fast-Recovery modifications improved the water SNR by a factor of 1.7 – 2.0 compared with the standard SSFSE sequence depending on slice thickness. For multi-slice acquisitions the improvement in SNR was by a factor of 1.1 – 1.2. There was no significant improvement in the SNR for oil.
Conclusion: The fast recovery modification is likely to be of particular value for dynamic imaging of the small bowel using water as an exogenous contrast media.

B-0764 11:25

MR microimaging on a whole body high field MR system: Methods and applications

A. Berg, T. Singer, J. Sailer, T. Rand, J. Szeles, E. Moser; *Vienna/AT*

Purpose: Within the frame of routine NMR diagnostic imaging pathological degenerations with a spatial structural size of about 0.5 mm may be detected. We wish to outline strategies concerning additional hardware and software equipment and MR-protocols for obtaining high resolution, contrast rich parameter weighted MR images below 0.250 mm for the visualization of fine structures in the human body (e.g. inner structure of vessels, bone structure, cartilage, skin etc.).
Materials/methods: A whole body high field (3 T) MR-system is upgraded by strong, actively shielded gradient systems, either a "head system" at 28 mT/m for human extremities (i.d. 33 cm) or a "MR-microscopy insert" at 200 mT/m. For obtaining high sensitivity for the small voxel sizes object size adapted detectors are used: surface coils at i.d. 30 mm and a birdcage resonator (i.d. 35 mm). Parameter weighing is achieved by multi-slice multi echo imaging (CPMG-sequences) and stimulated echo detection with pulsed gradients for diffusion weighing.
Results: In order to quantitatively document the achieved spatial resolution beyond simple voxel size indication, grid structures at 200 µm size are visualized and quantitatively evaluated. Images of human arteries and their inner structure including arteriosclerotic plaques are visualized at VS: 0.047 × 0.047 × 0.600 mm^3 in vitro. The fine structure of trabecular bone is resolved in the human calcaneus in vivo at pixel size 0.156 × 0.156 mm^2 for osteoporosis.
Conclusion: High resolution MR-microimaging may help to open new diagnostic windows for the detection and quantification of arteriosclerosis, osteoporosis and arthritis.

B-0765 11:35

Spatial resolution of electrical impedance scanning (EIS) determined by using an animal based model of tumor detection

A. Malich[1], T. Böhm[2], M. Facius[1], M. Fleck[1], W.A. Kaiser[1]; *[1]Jena/DE, [2]Zürich/CH*

Purpose: Malignancies exhibit altered local dielectric properties. Increased conductance is measurable using EIS. Minimal detectable tumor size was determined.
Material and methods: First the tumor detectability of implanted VX 2 tumors was tested in 15 VX-2-tumors (mean size 25 mm) implanted in lower leg musculature using TS 2000, Siemens, Germany) of white New Zealand rabbits.
In a second step ten VX2-tumor-cells (highly malignant squamous cell carcinoma) were implanted at a depth of 4 – 8 mm into the lower leg musculature of five white New Zealand rabbits. The region of implantation was examined using ultrasound (HDI 5000T, ATL, USA) and EIS before, immediately following injection of tumor cells, and on every second day thereafter.
Results: 14/15 VX2-tumors revealed a positive signal in EIS. No immediate focal increase in conductance was visible at the site of injection of the five rabbits. 1/10 tumor implantation failed. In one case neither ultrasound nor EIS performances were possible due to severe skin alterations. Smallest detectable tumor size using EIS was 3 × 3 × 2 mm (9 mm^3), 6 days after implantation. The mean tumor size at the time of first EIS detectability was 8.7 × 6.6 × 4.1 mm at 4.4 mm depth. In one case the tumor was first seen by US, in all other cases detection was concurrent for US and EIS.
Conclusion: VX2-tumors are a feasable model for EIS. EIS is capable of detecting malignancies with a size of at least 9 mm^3 in vivo. The spatial resolution of EIS was shown to be similar to high-resolution ultrasound.

B-0766 11:45

DIMOND European protocol for constancy checks in interventional radiology systems

E. Vano[1], K. Faulkner[2], J.M. Fernandez[1], L. Gonzalez[1], E. Guibelalde[1], J.I. Ten[1], J. Zoetelief[3], M. Toivonnen[4]; *[1]Madrid/ES, [2]Newcastle upon Tyne/GB, [3]Delft/NL, [4]Helsinki/FI*

Purpose: To present the protocol for constancy checks in fluoroscopy systems used for interventional radiology (IR), agreed between the members of the European DIMOND research consortium.
Materials and methods: The protocol has been designed to harmonise the evaluation of complex fluoroscopy systems used in IR. Simplicity in the required experimental approach and the short time necessary to carry out the test (30 – 60 minutes) were two objectives of the protocol. The approach requires a calibrated ionisation chamber, copper filters, a lead absorber, and an image quality test object. Dose rate and dose per image at the entrance surface of the image intensifier (II) and at the entrance surface of Cu filters are measured. The image quality of the test object is evaluated on the TV monitor. In addition, the maximum skin dose rate is measured.
Results: Dose rates at the entrance of the II for 2 mm Cu, range from 0.2 to several µGy/s. Dose rates at the entrance of the 2 mm Cu filter, at 55 cm focus surface distance ranged from 5 until more than 50 mGy/min. Maximum skin dose range from 50 until more than 200 mGy/min. Dose per image had a wide range for similar conditions. Image quality also varied from excellent to poor depending on the system evaluated.
Conclusion: The initial application of the DIMOND protocol has demonstrated its validity as a simple and effective constancy check for IR systems. The test protocol permits the detection of systems in poor condition which require urgent corrective actions.

B-0767 11:55

Determination and visualisation of the propagation of contrast agents in three-dimensional cerebral vessel trees based on rotational X-ray angiography

H. Schmitt[1], V. Rasche[2], M. Graß[2], O. Jansen[3]; *[1]Heilbronn/DE, [2]Hamburg/DE, [3]Heidelberg/DE*

Purpose: Information on the three-dimensional propagation path and time dependent distribution of contrast agent injected via a catheter into cerebral vessel trees can support accurate diagnoses for aneurysms and AVMs. A new method for the determination of the contrast agent inflow in 4D is presented.
Materials and methods: 3D images of the vessel tree are reconstructed during a standard 3D-RA procedure. After segmentation of the vessels, a symbolic structure tree is built up which contains anatomy adapted vessel pieces obtained by a region growing algorithm. For the vessel pieces, time stamps are calculated from an additional fluoroscopy projection time series. A decrease of the grey value in the projection area which is associated with a vessel piece is taken as the bolus arrival time. The symbolic tree facilitates plausibility checks and filtering procedures.
Results: The accuracy of the method is analysed based on mathematical and real phantom studies. The straightforward application to a clinical case yields results which support the analysis of complex three-dimensional vessel structures. For a patient with an AVM, the feeding and the draining vessels are determined reliably.

Conclusion: A step towards 4D X-ray angiography is achieved. The visualization of the contrast agent wave propagation together with the 3D vessel morphology gives novel insight in pathological structures. Intervention planning is simplified as the vessels supplying the malformation can be depicted easily.

14:00–15:30 **Room B**

Musculoskeletal

SS 1510

Tumor imaging

Chairpersons:
J.L. Bloem (Leiden/NL)
J.R. Jiménez (Oviedo/ES)

B-0768 14:00

Chondroblastoma and clear-cell chondrosarcoma: Radiographic and MR characteristics with histopathological correlation

A. Kaim, R. Hügli, W. Steinbrich, G. Jundt; *Basle/CH*

Purpose: To analyze and compare radiologic and MRI (magnetic resonance tomography) patterns of chondroblastoma and clear cell chondrosarcorma (CCC).
Patients and methods: Group 1 included twelve patients with histological proven chondroblastoma, and Group 2 consisted of 4 patients with CCC, that all had been investigated by X-ray and MRI (T1-, T2-weighted sequences, intravenous Gd-application). Moreover, the clinical and radiologic data were considered in seven cases of CCC without available MRI. Analysis of localization, calcification of tumor matrix, periostal reaction, cortical bone, pattern of bone destruction (Lodwick radiologic grading system, LRGS), signal intensity (SI) in T1- and T2-weighted sequences, contrast enhancement, bone marrow edema and soft tissue reaction was performed.
Results: The mean age of patients with chondroblastoma (22.3 a) was lower than of CCC (36.6 a), and the lesions were smaller in group 1 (mean 2.3 cm) than in patients with CCC (mean 5.2 cm). All tumors except one were classified to grade 1A or 1B (LRGS), one CCC was defined to grade 3. High SI on T2-weighted MRI corresponded to areas with aneurysmal bone cyst or rarely to islands with hyaline cartilage in chondroblastoma and in CCC. Chondroblastoma was frequently associated with bone marrow edema (11/12), periostal reaction (10/12) and soft tissue reaction (7/12).
Conclusion: Chondroblastoma occurs in a younger patient group and with a smaller size than CCC. The overlap of SI and contrast enhancement patterns does not allow a reliable differentiation with MRI. Chondroblastoma are typically associated with bone marrow edema, periostal reaction and soft tissue reaction.

B-0769 14:10

Primary and recurrent aggressive fibromatosis: MRI Imaging

R. Arkun[1], A. Memis[2], M. Argin[2], D. Sabah[2], T. Akalin[2], B. Guney[2]; *[1]Bornova/TR, [2]Izmir/TR*

Purpose: In this study, we had two aims. The first is to describe MR imaging characteristics of both primary and recurrent aggressive fibromatosis. The second is to determine the contrast enhancement pattern of the tumor on dynamic contrast enhanced images.
Materials/methods: The MR images of 22 cases pathologically proven aggressive fibromatosis were reviewed retrospectively. There were 14 primary and 8 recurrent cases. For 6 patients, there were also follow-up images. A total of 34 scans on 22 patients were reviewed. The size, margin and signal characteristics of tumors were evaluated and correlated with pathological findings. Dynamic contrast enhanced images were obtained to define the contrast enhancement pattern, followed by substraction images.
Results: The size of tumor was under 5 cm in 9 cases and above in 13. For primary tumors, signal intensity (SI) was hypointense (9 cases), or isointense (5 cases) on T1-W images. For recurrent cases SI was mostly isointense and contained partly signal void areas. On T2-W images both primary and recurrent cases mostly had high SI. On dynamic contrast enhanced images, for primary tumors 3 cases showed no enhancement, 2 cases showed mildly late enhancement and 5 cases mildly early and strongly late enhancement and 1 no enhancement.
Conclusion: The lesion of aggressive fibromatosis showed various MR appearances. Recurrent tumors showed more inhomogenous SI and had signal void areas. The differences in SI and contrast enhancement pattern were related to the cellularity and the collagen content of the tumor.

B-0770 14:20

Osteoradionecrosis of the iliosacral joint and the iliac bone after irradiation of gynecological tumors: MRI characteristics

J. Schmitt[1], N. Abolmaali[1], U. Höller[2], R. Straub[1], W. Schwarz[1], J. Balzer[1], V. Jakobi[1], T. Vogl[1]; *[1]Frankfurt a. Main/DE, [2]Hamburg/DE*

Purpose: To describe characteristics of osteoradionecrosis of the pelvis in patients with gynecological tumors in MR-imaging.
Material and methods: 9 women with gynecological tumors received radiation therapy using opponing fields with 18 MeV photons; single doses were applied with 2 to 46 Gy. During close clinical follow-up development of an osteoradionecrosis was suspected. Multiplanar MRI was performed with a 1.5 T clinical MR-system with T2-weighted and T1-w pre- and post-contrast spin-echo sequences with and without FAT-SAT. Additionally computed tomography was performed in three patients. Final evaluation criterias were morphology, enhancement and demarcation of the iliosacral joint and surrounding soft tissue. Clinical and radiological findings were correlated.
Results: Osteoradionecrosis revealed inhomogeneous low signal-intensity in T1-w sequences with a low enhancement. In the T2-w sequences osteoradionecrosis showed high signal-intensities. Best visualization of regions with even low contrast enhancement was achieved with FAT-SAT sequences. Computed tomography showed increased density in the affected regions corresponding to osteosclerosis. In all cases at least one iliosacral joint was affected with different topographies in sacral and iliac bone.
Conclusion: MR imaging allows a clear delineation of osseous changes due to osteoradionecrosis.

B-0771 14:25

Whole-body magnetic resonance imaging vs. bone scintigraphy for the detection of prostate cancer metastatic to bone: Initial experience

T.H. Helbich, M. Funovics, A. Kurtaran, G. Kramer, B. Djavan, A. Becherer, M.J. Breitenseher; *Vienna/AT*

Purpose: To compare the accuracies of whole-body MR imaging (MRI) and bone scintigraphy for the detection of prostate cancer metastatic to bone.
Materials and methods: 20 male patients, aged 86 – 56 years, with biopsy proven prostate cancer and suspected metastatic disease underwent whole-body MRI and bone scintigraphy (with ^{99}Tc-MDP i.v.). A turbo short tau inversion recovery (STIR) sequence and T1-weighted Spin-Echo (SE) sequences before and after gadopentetate dimeglumine application were performed of the whole-body at a 1 T magnet (Gyroscan T10-NT, Philips). Both imaging procedures were performed within two weeks. MRI and bone scintigraphy were independently evaluated by four readers to determine the number and location of bone metastases. Data were compared with biopsy and/or clinical follow-up.
Results: Bone metastases were diagnosed in 10 patients. MRI detected more metastases than bone scintigraphy. Bone scintigraphy was more often false-positive due to degenerative bone diseases. However, the detection of metastases in small bones (ribs and flat bones) was limited with whole-body MRI. In addition to bone marrow metastases, whole-body MRI detected soft tissue metastases in five patients.
Conclusion: Whole-body MRI seems to be more accurate than bone scintigraphy in the detection of bone metastases in patients with prostate cancer. The detection of metastases in small bones seems to be limited with whole-body MRI. However, whole-body MRI enables the detection of soft tissue metastases.

B-0772 14:35

Whole body MR bone imaging with a rolling table platform compared to scintigraphy

T. Lauenstein, J. Barkhausen, L. Freudenberg, S.G. Rühm, J.F. Debatin; *Essen/DE*

Purpose: At present radionuclide scintigraphy is the gold standard for detecting bone metastases. The aim of this study was to compare the results of rapid whole-body MRI of the skeletal system with findings of nuclear scintigraphy in patients with bone metastases.
Materials and methods: Ten patients with known bone metastases who had undergone radionuclide scintigraphy were examined by MRI. Patients were placed on a rolling table platform (BodySURF) capable of pulling the patient through the magnet bore as well as through a phased array surface coil. Three different image sets (T1-GRE, HASTE, TIRM LOTA) were collected in the coronal plane. In addition, the spine was imaged in the sagital plane. Five stations were imaged in 45 min. MRI findings were compared to the results obtained by scintigraphy.

Results: MRI revealed excellent correlation with scintigraphy regarding metastatic lesions. A total of 28 metastatic lesions were identified on bone scintigraphy. 24 lesions were detected in identical locations with MRI. Four lesions, all located in ribs of 2 patients were missed on MRI. Both patients had lesions in other locations which were identified with MRI. MR did reveal 4 lesions not suspected on bone scintigraphy of which one was confirmed at biopsy.
Conclusion: MRI screening for bone metastases correlated well with bone scintigraphy. Use of the rolling table platform permits rapid imaging based on three different contrast mechanisms of the entire skeletal system in a short time.

B-0773 14:45

The role of diffusion-weighted MRI in the evaluation of vertebral metastasis

A.M. Herneth, M. Philipp, J. Naude, B. Bachtiary, A. Ba-Ssalamah, S. Trattnig, H. Imhof; *Vienna/AT*

Purpose: Quantification of the tissue specific apparent diffusion coefficient (ADC) in vertebral metastasis and unaffected vertebral bodies.
Materials and methods: The ADC from the vertebral metastasis and of an unaffected vertebral body was measured in 7 patients with an 1.0 T scanner and with a Phased Array Body Coil. A diffusion weighted-EPI sequence was used in the sagittal plane (TR/TE/EPI 2055/22/13; flip angle 90°; diffusion tensor: TE 80; b1: 0 s/mm^2; b2: 440 s/mm^2, b3: 880 s/mm^2; NSA 2; FOV 250 mm; slice thickness 6 mm). The ADC was calculated voxel by voxel with the following equation: ADC = log(S1/S2/(b2–b1) (LeBihan; Radiology, 1988 168:497–505).
Results: The mean ADC of vertebral metastasis ($0.45 \pm 0.21 \cdot 10^{-3}$ s/mm^2) was significantly ($p < 0.0007$) lower compared to the mean ADC of unaffected vertebral bodies ($1.4 \pm 0.47 \cdot 10^{-3}$ s/mm^2). The intra-individual difference of the ADCs was at least $0.7 \cdot 10^{-3}$ s/mm^2 (mean $1.02 \pm 0.43 \cdot 10^{-3}$ s/mm^2).
Conclusion:

1. The ADC can be reliably measured in vertebral tissue
2. The ADC is significantly different in vertebral metastasis and unaffected vertebral bodies, and thus, it seems to be an objective and comparable parameter for differentiating malign from benign vertebral tissue.

B-0774 14:55

Serial dynamic MR evaluation of radiation-induced changes of lumbosacral vertebrae: Do changes occur only inside the radiation therapy field?

S. Otake[1], N.A. Mayr[2], T. Ueda[2], V.A. Magnotta[2], W.T.C. Yuh[2]; [1]*Toki/JP,* [2]*Iowa City, IA/US*

Purpose: To evaluate the temporal changes in signal intensity (SI) and the degree of contrast enhancement (CE) of the bone marrow in the lumbosacral vertebrae inside and outside the radiation therapy (RT) field.
Methods and materials: Twenty-three patients with advanced cervical cancer who were treated with primary RT were prospectively evaluated. Each patient underwent four MR (magnetic resonance) studies: before RT, 2 and 4 weeks after the initiation of RT, and 4 weeks after the completion of RT. Quantitative analyses of precontrast SI on T1-weighted images and the degree of CE of the bone marrow were performed in all four studies of each patient.
Results: The bone marrow inside the RT field showed a steady and marked increase in precontrast SI and an early and transient increase in CE at 2 weeks after the initiation of RT followed by a progressive and marked decrease in CE at 4 weeks of RT, and 4 weeks after the completion of RT. The bone marrow outside the RT field showed a slight increase in precontrast SI, and a steady and moderate decrease in CE to a lesser degree without an early increase as seen in the bone marrow inside the RT field.
Conclusion: Our limited data suggest that RT causes an increase in precontrast SI presumably representing fatty replacement predominantly in the bone marrow inside the RT field. However, a decrease in CE is seen in the bone marrow not only inside but also outside the RT field.

B-0775 15:05

The importance of MRI for the diagnosis of and for a correct surgical planning of osteoid osteoma of the foot

E. Bassetti, M. Mastantuono, A. Scala, M. Kvasnova, R. Passariello; *Rome/IT*

Purpose: Diagnosis of intraarticular and cancellous lesions may be difficult with conventional X-ray and CT due to absent or limited reactive osteosclerosis. The location of the lesions before surgery or other treatment methods is very important to avoid recurrence due to incomplete excision. We report our experience in differential diagnosis with MRI of these kind of lesions.
Materials and methods: We studied with MRI 35 patients with persistent pain, not related to a trauma, localized in the ankle or foot. The MRI examinations have been performed with a high field (1.5 T Vision Plus Siemens) and with a small bore dedicated equipment to the studying of the limbs (0.2 T Artoscan Esaote), using T1, T2, GE and Fat Suppression.
Results: In 10 patients an osteoid osteoma was present and 1 patient had undergone previous surgical treatment. The other patients represented RSD (Reflex Sympathetic Dystrophy), osteonecrosis, stress fractures, osteochondritis dissecans, villonodular synovitis, sinus tarsi inflammation, impingement syndromes and infective process.
Discussion and conclusions: In our experience MRI permitted clear depiction of the nidus of osteoid osteoma within the lesion. It is very important to choose the right sequences because the reactive marrow edema may obscure the lesion. MRI permitted a correct differential diagnosis ahead of the other conditions with clinical symptoms similar to that of osteoid osteoma.

B-0776 15:10

Evaluation of bone allografts with MRI

M. Mastantuono, E. Bassetti, L. Di Giorgio, A. Scala, A. Napoli, R. Passariello; *Rome/IT*

Purpose: The behaviour of allograft in the reconstruction of bone loss is still a subject of intense debate in the literature. The purpose of this study is to analyze the behaviour of Tutoplast bone allograft to fill cavities produced by the removal of benign or low grade malignant lesions.
Materials and methods: We studied with X-Rays and MRI 29 patients (15 M, 14 F) affected with benign or low grade malignancy bone lesions treated by marginal resection or curettage and successive filled with bone allograft (human bone that had been sterilized and renedered inert by dehydratation with solvents – Tutoplast). We use for the MRI study a low field equipment (E-Scan Esaote Biomedica) and high field MRI unit (Vision Plus, Siemens). All patients were submitted to X-Ray and MRI follow-up.
Results: Increase in the signal intensity in all of the S.E. sequences within the graft, indicates the adipose cellular repopulation of the grafted area and thus its cancellization (22 patients). Persistence of low signal intensity in T1 and high signal intensity in T2 during the follow-up incated complication or recurrence of the tumours (6 patients).
Discussion and conclusions: MRI appears to be the technique of choise in studying the graft incorporation.

B-0777 15:20

Contrast enhanced dynamic MRI in patients with multiple myeloma and diffuse bone marrow infiltration of vertebra during thalidomide therapy or thalidomide and chemotherapy

K. Wasser, S. Delorme, T. Moehler, K. Neben, I. Zuna, H. Goldschmidt, G. van Kaick; *Heidelberg/DE*

Purpose: To assess changes in diffuse bone marrow infiltration in multiple myeloma (MM) during thalidomide therapy or thalidomide/chemotherapy using contrast enhanced dynamic MRI and to compare this with clinical response.
Methods: In an ongoing study 21 patients with refractory MM underwent a 1.5 T MRI scan of the lumbar spine prior to and following thalidomid therapy (14 patients) or thalidomide/chemotherapy (7 patients). The contrast uptake was quantified using a two compartment model with the output parameters Amplitude (a.U.) and k21 (distribution rate constant; min-1) and color-mapped. Parameters were analysed and followed up in three selected vertebral bodies.
Results: Out of 14 patients treated with thalidomide alone, 6 responded clinically, and 8 were non-responders. In neither group there was a significant change in parameters. All patients with thalidomide plus chemotherapy responded to treatment; the median change in amplitude was -16 % ($p < 0.02$), and -15 % in k21 (n.s.). A decrease in amplitude was mainly seen in vertebral bodies with Amplitude > 0.5 before treatment.
Conclusion: With dynamic MRI, a significant decrease in enhancement amplitude is seen during treatment with thalidomide plus chemotherapy if the values are highly increased before traetment. No changes, however, are found during thalidomide monotherapy, irreespective of the clinical response.

14:00–15:30 Room C

Abdominal and Gastrointestinal

SS 1501a

Liver: MRI, US

Chairpersons:
P. Leander (Malmö/SE)
C. L'Herminé (Lille/FR)

B-0778 14:00

Late phase imaging with Levovist in detection of metastatic liver lesions

B. Brkljacic, L. Patrlj, B. Kocman, A. Hebrang; *Zagreb/HR*

Purpose: To evaluate whether late phase imaging with Levovist increases the detection rate of metastatic liver lesions when compared to conventional ultrasonography of the liver.

Materials and methods: 21 patients (M:F = 11:10; mean age 61.5, range 36 – 76) were examined, using a Siemens Sonoline Elegra US scanner with a 3.5C40 scanhead and Ensemble Contrast Imaging software. After the baseline scan, 2.5 g of Levovist was injected intravenously as a bolus, in a concentration of 300 – 400 mg/ml. As a rule, after 2.5 minutes delay, two sweeps with the probe were made to image the right lobe of the liver, and one sweep to image the left lobe. Images were reviewed in cine-loop. 16 patients had colon cancer, 3 pts had rectal cancer, 1 patient had cholangiocarcinoma and 1 had a Klatskin tumour.

Results: On the baseline scan metastatic liver lesions were visualized clearly in 10/21 patients. After late-phase imaging, metastatic liver leasons were visualized in 18/21 pts. FNAC confirmation was obtained in 14/18 pts. More liver lesions were seen in 15/18 pts. on late-phase imaging after Levovist when compared to conventional.

Conclusion: Initial results indicate that late phase imaging with Levovist significantly increases visualisation of liver metastasis.

B-0779 14:10

Focal nodular hyperplasia of the liver: Lesion characterization by using nonspecific and liver-specific MR contrast agents

A. Ba-Ssalamah[1], W. Schima[1], P. Reimer[2], T.H. Helbich[1], M.T. Schmook[1], N. Schibany[1], A. Kurtaran[1], F. Wrba[1]; *[1]Vienna/AT, [2]Münster/DE*

Purpose: The goal of this study is to evaluate the efficacy of different MR contrast agents in characterization of focal nodular hyperplasia (FNH).

Materials and methods: The unenhanced and contrast enhanced MR examinations of 47 patients with 86 FNHs, who had histological or scintigraphic proof or radiological follow-up, were retrospectively reviewed. Contrast agents were used as follows: gadolinium-chelates in 16 patients (46 lesions), mangafodipir in 29 patients (48 lesions), ferumoxide in 6 patients (16 lesions), and SHU 555 A in 6 patients (6 lesions). More than one contrast agent was used in most of the patients. The lesions were quantitatively and qualitatively assessed.

Results: On unenhanced images 33 % of the lesions were homogeneously isointense on T1w and T2w images, a central T2 hyperintense scar was present in 42 %. FNH showed enhancement equal to or superior to surrounding liver parenchyma following administration of mangafodipir in 94 %. With ferumoxide or SHU 555 A, there was lesion uptake of the contrast agent but less than surrounding liver parenchyma. Dynamic Gd-chelates-enhanced MRI typically demonstrated early and vigorous enhancement of FNH with rapid wash-out. The central scar took up contrast agent in 8 cases.

Conclusion: The MR imaging features of isointensity, a central T2 hyperintense scar and homogeneous enhancement after liver-specific contrast agents allow a reliable diagnosis of FNH.

B-0780 14:20

Preoperative detection and characterization of focal liver lesions using iron oxide-enhanced MR imaging in comparison to CTAP, intraoperative ultrasound and histopathological correlation

W. Schwarz[1], R. Hammerstingl[1], S. Blume[1], T. Balzer[2], T. Diebold[1], T.J. Vogl[1]; *[1]Frankfurt a. Main/DE, [2]Berlin/DE*

Purpose: To compare the diagnostic efficacy of iron oxide-enhanced MRI to CT arterioportography (CTAP) for preoperative evaluation of liver tumors using intraoperative ultrasound and pathologic findings as a gold standard.

Materials and methods: 23 patients with focal hepatic lesions (HCC n = 14, metastases n = 7, CCC n = 2) were examined using 1.5 T scanner. The sequence protocol included T1- and T2-weigthed SE/TSE sequences before, during, and post iv bolus administration of Resovist. CTAP was performed as well. Studies were evaluated by two reviewers (R) for the type, number, and location of liver lesions. 17 patients underwent surgery with intraoperative ultrasound.

Results: 239/237 liver lesions were detected in CTAP, 123/122 lesions using T2-weighted sequence after injection of iron oxides. From a total of 80 liver lesions proven by intraoperative ultrasound 70 lesions were detected on CTAP (sensitivity 87 %), 47 lesions on unenhanced MRI (58 %), and 69 lesions on enhanced MRI (86 %).

Conclusion: Resovist enhanced MR imaging is a sensitive technique for the detection and characterization of hepatic neoplasms, with a sensitivity greater than or equal to CTAP and unenhanced MR imaging.

B-0781 14:30

Focal nodular hyperplasia (FNH): MR imaging with Gd-BOPTA

L. Grazioli[1], G. Morana[2], K. Menni[1], M. Testoni[2], M. Kirchin[3], C. Procacci[2], A. Chiesa[1]; *[1]Brescia/IT, [2]Verona/IT, [3]Milan/IT*

Purpose: To evaluate the efficacy of MR imaging with Gd-BOPTA in characterizing FNH.

Material & methods: 63 Patients with 100 FNH were studied. MR imaging was performed with 1.5 T before (TSET2w and GET1w images) then (GET1w) during the dynamic and the delayed phase (1 h, 2 h, 3 h) after Gd-BOPTA administration (0.1 mmol/kg). Criteria for FNH characterization during dynamic phase were homogeneously hyper-intensity during arterial phase with iso-intensity in portal and distribution phase and typical scar aspect (if lesion diameter > 3 cm), such dividing FNH in typical and atypical aspect.

Results: During dynamic phase 79/100 FNH showed typical aspect, whereas 21/100 were atypical. On late phase, 19/21 atypical FNH were hyper (16) or isointense (3) to the surrounding parenchyma, whereas only 2 were slightly hypointense. For FNH ≤ 3 cm (49/100) scar detection passed from 5/49 on pre-Gd-BOPTA to 15/49 on late phase; all these lesions were hyper (33/49) or isointense (16/49) in the late phase.

Conclusion: Gd-BOPTA during dynamic and delayed phase has an overall accuracy of 98 % in FNH characterization; FNH ≤ 3 cm were all characterized in the late phase as the delayed iso- or hyper-intensity reflects the characteristic abnormal biliary excretion of FNH.

B-0782 14:40

Evaluation of pre-and postoperative MRI using Gadobenate dimeglumine-enhanced dynamic imaging of focal liver lesions in patients with malignant liver tumors undergoing cryotherapy

G.K. Schneider, R. Seidel, G. Pistorius, G. Feifel, K. Altmeyer, B. Kramann; *Homburg a. d. Saar/DE*

Purpose: To evaluate the clinical value of Gadobenate dimeglumine-enhanced MRI in preoperative detection and postoperative follow-up of patients undergoing cryotherapy.

Materials and methods: 21 patients with malignant liver tumors who underwent liver cryosurgery were pre-and postoperatively examined by abdominal MRI. Imaging protocol included T1w, T2w and dynamic contrast enhanced scans after injection of 0.05 mmol/kg bodyweight Gd-BOPTA including a scan in the hepatobiliary phase. Intraoperative ultrasound (IU) was rated as goldstandard. Postoperative MRI was performed up to 18 months following cryotherapy.

Results: In 21 patients 48 malignant liver lesions could be detected. Mean lesion diameter was 2.6 cm (range 0.5 to 9 cm). IU revealed 53 lesions with mean diameter of 2.9 cm (range 0.3 to 10 cm). 5 focal tumors in 3 patients diagnosed by IU could not be previously detected by MRI. Mean diameter of these tumors was 0.5 (range 0.3 to 0.7) and localization near the liver surface. In 9 of 53 tumors treated by cryotherapy local residual tumor was detected by MRI 10 days after treatment in which after 3 months local tumor progress was observed in 7 lesions. At the site of complete tumor destruction local recurrence was found in 4 lesions after 3 months and further follow up.

Conclusion: Gadobenate dimeglumine-enhanced MRI is a useful technique in pre-and postoperative assessment of focal liver lesions undergoing cryosurgery. Compared to IU reliable tumor detection is possible for lesion diameter above 8 mm, detection of subcapsular lesions and of lesions on the liver surface is still problematic.

B-0783 14:50

Tri-phasic helical-CT vs. MR with super-paramagnetic iron oxide (endorem) in the detection of hepato-cellular carcinoma in patients with liver cirrhosis

L. Camera, E. Soscia, M. Imbriaco, C. Lambiase, M. Bresciani, M. Salvatore; *Naples/IT*

Purpose: To compare helical-CT and MR with super-paramagnetic iron oxide (SPIO) in the detection of hepato-cellular carcinoma (HCC) in patients with liver cirrhosis.
Materials and methods: 21 patients (16 M, 5 F; aged 63.4 ± 10.8 years) with liver cirrhosis underwent both tri-phasic helical-CT and MR with SPIO within 2 weeks. Helical-CT scans (10 mm beam collimation, 7 mm recon. intervals, pitch 1.0, 120 kV, 200 – 250 mAs) were performed at 25, 60 and 300 s after i.v. bolus injection of 120 cc of an iodinated contrast agent (I 300 mg/ml) at 4 ml/s. MR was performed at 0.5 T with axial scans (8 mm; 2 mm gap; matrix 224 x 190) acquired using conventional SE T1 (TR/TE 420/12 ms) and DP-T2 weighted (TR/TE 2800/35/120 ms) sequences. 60 – 90 minutes after i.v. infusion of 0.075 ml/kg of SPIO (Endorem) both SE DP-T2 weighted and GRE T2* sequences (TR/TE/FA 520/20/20°) were performed. Final diagnosis was obtained by either aspiration biopsy (8 pts) or follow-up data (13 pts).
Results: Helical-CT identified a total of 26 nodules (0.8 – 4.2 cm) in 18 patients. Most (21/26 80 %) were hyper-vascularized. Four out of 21 (19 %) were not shown by MR-SPIO and proved not to be HCC at final diagnosis. MR-SPIO showed 17 (1.5 – 4.2 cm) hyper-intense nodules in 14 patients. Overall, helical-CT showed a better sensitivity (86 vs 77 %) but a lower specificity (76 % vs 94 %) than MR-SPIO.
Conclusion: These preliminary results indicate that helical-CT and MR-SPIO are complementary in the evaluation of patients with liver cirrhosis.

B-0784 15:00

Non-traumatic hemorrhagic lesions of the liver: CT, MR features

F. Ferrozzi, G. Tognini, E. Spaggiari, S. Armaroli, P. Pavone; *Parma/IT*

Purpose: Spontaneous bleeding is a rare complication of liver lesions especially in patients not treated with oral anticoagulant therapy. The aim of our study was to evaluate the role of CT and MRI in diagnosing and characterizing non-traumatic hemorrhagic lesions of the liver.
Materials and methods: We evaluated CT and MR scans from 28 patients (12 M, 16 F, mean age 56 years) between 1993 and 2000. All patients underwent a CT examination, 11 had MR performed.
Results: In all patients, hemorrhage was demonstrated by CT and MR. Hemorrhagic metastases were demonstrated in 10 patients (3 melanomas, 4 leiomyosarcomas, 2 adenocarcinomas of the kidney, 1 carcinoma of the colon), hemorrhagic HCC (9), hemangiosarcoma (1), hemangioma (2), adenoma (3), peliosis (1), amyloidosis (1), Osler-Weber-Rendu (1). Hemoperitoneum was demonstrated in 8 patients, subcapsular hematoma in (5) and multiple lesions in (8). Anamnestic (metastatic disease, oral contraceptives therapies, cirrhosis) structural and morphological criteria helped in characterization.
Conclusions: CT and MRI are useful in the diagnosis and characterization of non-traumatic hemorrhagic lesions of the liver.

B-0785 15:10

Ultrasonographic findings of the spleen in patients with sickle-cell disease

M.G. Papadaki, I.S. Kaskarelis, A.C. Kattamis, I.G. Papadaki, N.E. Malliaraki, V. Ladis, C.A. Kattamis; *Athens/GR*

Purpose: The aim of this study is to investigate the spectrum and prevalence of ultrasonographic findings of the spleen in Greek patients with sickle cell disease.
Methods and materials: The study included 68 Greek patients with sickle cell disease, 13 homozygous for sickle cell anaemia (S/S) and 55 with sickle β thalassemia (Th/S). The patients' age ranged from 1 to 40 years (mean 16 years), with 33 males and 35 females. At the time of ultrasonographic examination 32 (47 %) patients had already undergone splenectomy (4/13 with S/S and 28/55 with Th/S).
Results: Splenomegaly was present in 26 patients (24 with Th/S and 2 with S/S) with detectable infarcts in 10/26 patients. Mild, moderate and marked splenomegaly shared equal percentages (33 %) among patients with Th/S and splenomegaly. Marked splenomegaly was present in two patients with S/S. A small-sized, calcified spleen was visualized in 4 patients with S/S.
Conclusions: Several studies have underscored the value of ultrasound imaging in detecting complications of sickle cell syndromes. New therapeutic interventions gaining credence over the last few years have and will undoubtedly change the natural history of sickle cell disease with subsequent alteration in ultrasound imaging findings.

B-0786 15:20

MRI with dynamic contrast enhancement in evaluation of vascularisation of various types of liver hemangiomas

S.V. Kourotchkine, R.F. Bakhtiozin, I.R. Tchuvashaev; *Kazan/RU*

Purpose: To evaluate the MRI possibility with Dynamic Contrast Enhancement (DCMRI) in deter-mination of subtypes of liver hemangiomas.
Materials and methods: 17 patients with liver hemangiomas, found on US, were examined by MRI. Using a 0.28 T Tomicon MR system (Bruker, Germany) T1-weighted images were performed before and after i.v. administration of contrast medium (Magnevist, Schering, Germany and Omnyscan, Nycomed, Norway). Dynamic contrast enhancement by bolus administration was done within 20 s and axial T1-weighted images in arterial, portal and parenchimatous phases were obtained.
Results: Local (spot) periphery enhancement of lesion before 20 s after injection of contrast agent were detected in 15 patients. During next 25 – 60 s (in portal and parenchimatous phases) typically full enhancement of lesion was found, except 2/17 cases hemangiomas of large volume where we found later (from 25 – 45 s) enhancement in 1 patient; and fast filling and wash out effect in other 1 case.
Conclusion: Using DCMRI we have a good possibility for simultaneous: detection, evaluation and determination of various types vascularity of liver hemangiomas.

B-0787 15:25

Study of pulse inversion mode with the late phase of Levovist to detect hepatocellular carcinoma (HCC) in diffuse liver disease: Work in progress

E. Quaia[1], C.J. Harvey[2], M.J.K. Blomley[2], D.O. Cosgrove[2], W. Gedroyc[2]; [1]*Trieste/IT*, [2]*London/GB*

Purpose: To evaluate if Pulse Inversion Mode (PIM) with the late phase of Levovist can improve HCC conspicuity and detection, using MR with Gd-DTPA or spiral-CT as reference examination.
Materials and methods: To date, 10 consecutive patients known or suspected of having HCC have been scanned with PIM 3 minutes after intravenous injection of Levovist (2 g, 300 mg/ml). Subjective and objective conspicuity of HCC was compared to baseline US and each lesion suspected to be an HCC was counted.
Results: In each case a strong gray-scale enhancement of the liver parenchyma was noticed with an improved conspicuity of HCC which appeared hypoechoic. In comparison to reference examination, PIM revealed the same number of lesions reported as HCC in 5 patients, an higher number in 1 patient and a lower number in 1 patient. In 3 patients no lesions were detected both by PIM and reference examination.
Conclusions: PIM with Levovist is a sensitive method in HCC detection. This has to be confirmed with an increased number of patients.

14:00–14:50 **Room E1**

Radiographers

SS 1514

Current work in radiography

Chairpersons:
D.A. Cunningham (London/GB)
S. Geers-van Gemeren (Haarlem/NL)

B-0788 14:00

Digitalization: Does it give us an opportunity to develop our professional role?

M.K. Selim; *Örebro/SE*

Purpose: In 1992 the governing body of Örebro Medical Centre Hospital decided to build a new radiology department that would be the center of a regional patient archiving and communication system involving the country's five different X-ray departments. I will present the experiences from the first four years of work in a filmfree digital department and how the radiographer have developed their professional role.

Methods and materials: My material is taken from discussions with radiographers where they compare working in a filmfree digital environment with working in a traditional analog department.
Results: For some years, radiographers have worked with digital techniques for procedures such as computer tomography, magnetic resonance imaging and digital fluorography. However, these examinations were presented and viewed on hardcopy films which were then archived. With the new technique, all images and patient information, including X-ray request forms, are saved in a digital archive. The areas in which most changes take place for the radiographer in conjunction with digitalization are viewing and post processing of general radiographic examinations. With the new digital system, the radiographer has adapted her/his way of working and developed her/his professional role immensely.
Conclusion: This improved method gives the radiographer a better patient contact and increased responsibility for both image production and nursing care during the whole examination.

B-0789 14:12

Clinical commissioning of diagnostic X-ray equipment
S.N.A. Wells; *London/GB*

Purpose: Determining whether an X-ray unit is usable at commissioning.
Methods and materials: In the UK, the commissioning of diagnostic X-ray equipment follows the critical examination and acceptance tests at installation. Commissioning is designed to ensure equipment is ready for clinical use and guidance given in IPEM report no.77 suggests a range of tests that should be carried out by the 'purchasers representative'. Normally this is the local medical physics department, not the end user. These tests are primarily designed to check the performance of the system and to establish baseline values for routine performance tests. However, they do not consider how the unit will be moved, positioned and used in the clinical environment. Therefore while a system appears to function correctly, ergonomically it may not be ready for use. European Directives and National legislation has been introduced to avoid manual handling injuries to workers. Therefore these need to be considered when the degree of patient and equipment handling associated with X-ray equipment is considered.
Results: Currently, there are no guidelines or protocols for clinical commissioning in order to assess whether the unit is ready for the use.
Conclusion: This presentation will focus on the importance of clinical commissioning and put forward suggestions for those parameters that should be considered. These could form the basis of a protocol in order to formalise this stage in the installation process.

B-0790 14:24

The role of user assessment
S.N.A. Wells; *London/GB*

Purpose: In the United Kingdom, the Kings Centre for the Assessment of Radiological Equipment (KCARE) undertakes the evaluation of diagnostic X-ray equipment on behalf of the Medical Devices Agency. The evaluation programme is designed to protect public health, safeguard the interests of patients and staff, and ensure equipment conforms to national and international standards.
Methods and materials: A user evaluation consists of both technical and clinical assessment. Clinical assessment involves the use of radiological/anatomical phantoms to assess image quality, an ergonomic assessment of the system and user questionnaires. KCARE also organises regular liaison meeting with users from within the UK to focus evaluations and refine its assessment protocols. Information is available directly from the centre and is also published in both single product and comparative formats.
Results: The importance of user/clinical assessment is that it evaluates working equipment in the clinical environment for which it was designed, in order to demonstrate fitness for purpose.
Conclusion: The presentation will consider the benefits and future development of user assessment.

B-0791

withdrawn by author

B-0792 14:36

Prediction of osteoporosis based on mammographic pattern analysis
N.N. Kizimenko, E.E. Karachentseva, J.N. Kizimenko, I.V. Glushkova; *Krasnodar/RU*

Purpose: To evaluate the relationship between osteoporosis and mammographic density in a screened population based on the evaluation of the condition of the glandular tissue of the breast.
Methods and materials: The mammograms of 2765 women in the age range 12 to 83 years were reviewed. We paid special attention to 69 patients aged between 22 and 31 whose mammography showed an absence of glandular tissue with fatty involution. This group of patients was further assessed with hormonal levels in the blood and bone mineral density.
Results: 34 women (49.2 %) had reduced oestrogen levels in the blood. At bone densitometry, 17 women (24.6 %) had > 30 % reduction in bone mineral density. 23 women (33.3 %) had a moderate reduction in bone mineral density (between 15 – 30 % reduction). 18 women (26 %) had bone mineral density which was reduced by less than 14 % and the remaining 11 patients had normal bone mineral density.
Conclusion: This study indicates a correlation between reduced density on mammography and reduced bone mineral density and blood hormone levels and may be of use in selecting at risk patients who should undergo bone densitometry for further assessment.

This scientific session is followed by a mini symposium on MR applications (MS 1514: presentations A-0269, A-0270 – printed in part A)

14:00–15:30 **Room E2**

Breast

SS 1502

Breast imaging - New developments

Chairpersons:
R.M. Pijnappel (Groningen/NL)
G. Rizzatto (Gorizia/IT)

B-0793 14:00

Correlation of the type of vascularisation of breast cancer with lymph node metastases
T. Changelia, L. Kvachantiradze; *Tbilisi/GE*

Purpose: Determination of correlation of breast cancer vascularisation type with lymph nodes metastatic damage.
Material and methods: We've studied 258 patients with suspected breast cancer. Breast cancer was detected by US in 251 patients, in 248 out of them diagnosis was morphologically proved. Examination was performed on apparatus "Philips-SD 800" with 7.5 MHz transducer.
Results: In 189 patients out of 248 neovascularisation was detected. Mean size of tumor with neovascularisation was 1.5 cm, minimal size 1.1 cm. 84.1 % of vascularised tumors were hypervascular.
Enlarged lymph nodes were detected in 136 patients out of 248; in 58.7 % out of 136 nodes could be palpated. minimal sizes of lymph node was 0.6 cm. Axillary metastases were mostly seen in patients with hypervascular breast cancer. In 115 cases (72.3 %) out of 159 hypervascular tumors lymph node metastatic damage was detected by US. Morphologically lymph nodes metastasis was subsequently proved in 113 cases.
Conclusion: Based on received, results could be thought to represent direct relation between regional metastatic spread and tumor vascularisation degree.

B-0794 14:10

Characterization of axillary lymph nodes in breast cancer: MRI evaluation using a superparamagnetic contrast medium
A. Di Credico, E. Cianchetti, D. Angelucci, A. Carriero, L. Bonomo; *Chieti/IT*

Purpose: To evaluate the role of Magnetic Resonance Imaging (MRI) using a superparamagnetic Contrast Medium (SCM) in the characterization of axillary lymph nodes in patients with breast cancer.

Method and materials: Four women with breast cancer and suspected pathological axillary lymph nodes, candidate to surgical intervention that foresead axillary lymphadenectomy were studied. MRI was performed with a 1.5 T magnet before and after the injection of a superparamagnetic CM (Stabilized Ferric Oxide Nanoparticles with Low Molecular Weight Dextran). MRI protocol included T1 W and T2* W sequences. Two radiologists, in blind, evaluated images according to the following criteria: on unenhanced MRI, suspect lymph nodes were those having diameter ≥ 1 cm (dimensional criteria); on post-contrast MRI, suspect lymph nodes were those showing no enhancement.
Results: Twenty-eight lymph nodes were identified and characterized. At pathology the involvement of 6 lymph nodes was documented. Unenhanced MRI showed 15 lymph nodes as true negative, 4 as true positive, 9 as false positive. CM-MRI indicated 22 lymph nodes as true negative, 4 as true positive, and 2 as false negative.
Conclusions: The integration of unenhanced and post-contrast MRI with SCM allowed to decrease the number of false positives. Our preliminary data suggest MRI with SCM to be highly specific and useful in characterizing pathologic axillary lymph nodes.

B-0795 14:20

Lymph node staging with a lymph node-specific contrast agent (USPIO) in patients with breast cancer

S.C.A. Michel, B. Marincek, J. Fröhlich, D. Nanz, D. Fink, R. Caduff, R.A. Kubik-Huch; *Zürich/CH*

Purpose: To evaluate the value of Sinerem-enhanced MRI for lymph node staging in patients with breast cancer using histopathology as standard of reference.
Methods: MRI of the axilla was performed on a 1.5 T system (GE) 24 – 48 h post Sinerem infusion (2.6 mg Fe/kg) in 9 patients with breast cancer scheduled for surgery. Axial, coronal T1w SE (TR/TE 175/1.5), axial T2w FSE (TR/TE 4500/36, with/without FatSat), GRE (TR/TE 120/15, flip angle 25°) and FSPGR (TR/TE 23/9.2, flip angle 40°) sequences were performed in supine position. Subsequently, gadolinium-enhanced MR mammography was performed in prone position. Size, form and signal intensity reflecting Sinerem uptake of nodes were evaluated; results correlated with histopathology.
Results: Sinerem was well tolerated and an integrated imaging approach including MR mammography was feasible in all patients. Results of Sinerem-enhanced MRI were true positive in 4, true negative in 4, false positive in 0, false negative in 1/9 patients (sensitivity of 80 %, specificity of 100 %). Exact node-to-node correlation was difficult. 135 lymph nodes were detected by MRI (5 malignant); 158 surgically removed (9 malignant). Inhomogeneous (rim) uptake (n = 11) of Sinerem was seen in benign and malignant nodes, thus a combination of criteria was used for distinction in these cases. Sinerem as intravascular contrast agent could not replace gadolinium for evaluation of the primary tumor.
Conclusion: Our preliminary results indicate that Sinerem-enhanced MRI might become an important adjunct to MR mammography for preoperative staging of axillary lymph nodes. Sinerem cannot replace gadolinium for assessment of the primary tumor.

B-0796 14:30

Contrast enhanced optical mammography: Feasibility tested in vitro and in MX1- tumor bearing mice

T. Böhm[1], S. Ullrich[2], A. Malich[2], W. Ecke[2], M. Fleck[2], W.A. Kaiser[2]; [1]*Zürich/CH*, [2]*Jena/DE*

Purpose: To test the feasibility of contrast enhanced near infrared (CENIR) optical mammography using a prototype optical breast scanner in vitro and in animal trials.
Method/materials: The NIR contrast agent NIR69010 (Schering AG, Berlin, Germany) is a newly synthesized hydrophilic contrast agent for use in NIR mammography. The absorption spectrum was determined using a single beam spectrometer MCS400 (Zeiss, Oberkochen, Germany). Tissue phantoms consisting milk powder and Gelatin were made. A central part of 2 × 2 cm^2 of phantoms without contrast material was replaced by phantom material containing contrast agent (0.025 nmol/l to 5 µmol/l). Optical transmission was determined using a prototype NIR breast scanner (l1 785 nm and l2 850 nm). Intensities and signal-to-noise ratios were calculated. Additionally, CENIR-imaging was performed in three MX1 breast carcinoma bearing mice.
Results: The absorption maximum was at 755 nm. No spectral shifts occurred in protein containing solutions. Spatial analysis of transmission intensity showed the following results: Signal-to-noise ratio differed between 2.4 at 40 nmol/l contrast agent concentration to 790 at 5 µmol/l. Concentrations lower than 40 nmol/l were not detectable. In vivo CENIR imaging showed enhancement of 280 % with contrasts between tumor and normal tissue of 30 %.
Conclusions: The laser wavelength l1 of the Siemens prototype laser mammography device is not situated at maximum absorption of NIR 96010, but on the descending shoulder of the spectrum resulting in a 20 % signal loss. Despite these non-ideal measurement conditions concentrations down to 40 nmol/l were detectable. In vivo CENIR imaging of experimental tumors was feasible.

B-0797 14:40

Electrical impedance scanning of breast lesions: A report of the experience, current clinical value and limitations in 240 histologically proven cases

A. Malich[1], T. Böhm[2], M. Facius[1], M.G. Freesmeyer[1], M. Fleck[1], W.A. Kaiser[1], R. Anderson[3]; [1]*Jena/DE*, [2]*Zürich/CH*, [3]*Solna/SE*

Objective: Cancer cells exhibit altered local dielectric properties compared to normal cells. Consequently, different electrical conductivity and capacitance are measurable in malignant versus normal tissues. In this study, we evaluated the reliability of electrical impedance scanning (EIS), for the classification of suspicious lesions – differentiating benign from malignant, and as a primary means of detection of breast cancer. The technical limitations of the system are observed in order to find out ist clinical relevance.
Subjects and methods: 210 women with 240 sonographically and/or mammographically suspicious findings were examined using electrical impedance scanning (EIS). Finally all lesions were biopsied or surgically treated.
Results: With respect to the histopathological findings (103 malignant and 137 benign lesions) 86 malignant lesions were correctly identified using EIS (83.5 % sensitivity), while 91 benign lesions were correctly identified as benign (66.4 % specificity; 46 benign lesions false positive). Negative and positive predictive values of 84.3 % and 65.2 % were observed, respectively. Excluding all lesions located deeper than 35 mm, retroareolar or larger than 35 mm in size the system reaches a sensitivity of 91.3 % in the detection of invasive cancers whereas the detection rate of CIS is poor (57.1 %, n = 14).
Conclusion: EIS appears to be a promising new technology providing a relatively high sensitivity for the verification of suspicious mammographic and/or sonographic lesions. Further investigations on histomorphological charateristics of false negative findings are essential to improve the current knowledge of bioelectricity of breast lesions abnd probably the detection rate of EIS.

B-0798 14:50

Eletrical impedance scanning in the evaluation of breast cancer: Comparison with mammography

M.H. Fuchsjäger, H. Ringl, T.H. Helbich, M. Funovics, M. Rudas, G. Wolf; *Vienna/AT*

Purpose: The aim of this study was to assess the value of EIS in the detection of breast cancer in comparison to mammography (MG).
Material and methods: Targeted EIS (TransScanTS2000, Siemens, Erlangen, Germany) was performed in 80 female patients (mean age 53 ± 12 years) with 80 suspicious findings at MG. Standard criteria were used for MG and EIS (focal spot diagnosis) to differentiate benign from malignant lesions. Histopathologic proof was obtained in all cases.
Results: Of 80 lesions, 41 were benign and 39 malignant. EIS was true positive in 22 (56 %), false negative in 17 (44 %) of 39 malignant lesions. MG was true positive in 34 (87 %), false negative in 5 (13 %) of malignant lesions. EIS was true negative in 38 (93 %), false positive in 3 (7 %) of 41 benign lesions, MG was true negative in 25 (61 %), false positive in 16 (39 %) of the 41 benign cases. Median size of malignant lesions was 13.2 mm. For malignant lesions with a size from 0 – 13 mm EIS showed a sensitivity of 71 %. In invasive histology sensitivity of EIS was 67 %.
Conclusion: EIS seems to have a lower sensitivity but a higher specificity in the characterization of suspect breast lesions in comparison to MG. EIS is more accurate in detection of smaller lesions and invasive breast cancer.

B-0799 15:00

Targeted electrical impedance scanning (EIS) of suspicious breast lesions: Preliminary results

A. Wersebe, K.C. Siegmann, N. Fersis, U. Vogel, C.D. Claussen, M. Müller-Schimpfle; *Tübingen/DE*

Purpose: Electrical impedance scanning is a non-invasive imaging modality for breast lesions, based on increased electrical conductivity of malignant breast tissue. Aim of our study was to evaluate the accuracy of targeted EIS to distinguish between benign and malignant breast lesions. Furthermore we investigated the influence of tumor size on sensitivity of EIS.

Material and methods: 50 patients with suspicious findings in clinical examination, mammography a./o. sonography were examined by TS2000 (Siemens, Erlangen, Germany). All patients underwent breast biopsies for histopathological correlation. The malignant lesions were subdivided into three groups depending on their size: group 1: x < 1 cm, group 2: 1 < x < 2 cm, group 3: x > 2 cm.
Results: With respect to histology there were 21 benign and 29 malignant lesions. 13/21 benign and 19/29 malignant lesions were classified correctly by EIS. Overall sensitivity of EIS was 65.5 %, specificity 61.9 %, and PPV 70.4 %. EIS had a sensitivity of 72.7 % (8/11) for group 1, 77.8 % (7/9) for group 2 and 44.4 % (4/9) for group 3. Skin irregularities and technical artifacts deteriorated the diagnostic accuracy in 21/50 cases.
Conclusion: The sensitivity of targeted EIS depends on tumor size. There may be a benefit for the additional use of EIS in detecting small breast malignancies (< 2 cm). Reduction of false positive results due to skin irregularities or technical artifacts could improve specificity of this imaging modality.

B-0800 15:05

Positron emission tomography (PET) with ^{18}F-fluoro-deoxy-glucose (fdg) and magnetic resonance imaging (MRI) for the follow-up of women with breast cancer

G.W. Goerres, S. Michel, R.A. Kubik-Huch, M. Fehr, H. Steinert; *Zürich/CH*

Purpose: To prospectively compare the accuracy of FDG PET with MRI for the detection of locoregional breast cancer recurrence and to evaluate if PET provides additional information.
Materials and methods: 30 women with a history of breast cancer and suspected recurrence or indeterminate mammographic findings underwent MRI using a dynamic contrast-enhanced 3D gradient echo sequence. In 17 patients (mean age 57 years, 32 – 72 years) FDG PET (5.7 MBq/kg BW) was performed within 4 weeks to the MRI. Breasts and axillary regions were examined with attenuation correction in prone position and images from head to pelvis were acquired in supine position. Histology or – if unavailable – follow-up examinations served as standard of reference.
Results: At present, a final diagnosis is established in 12/17 patients. MRI was true negative (TN) for the presence of malignancy (recurrence/secondary tumor) and/or metastases in 8 women, indeterminate in 1, true positive (TP) in 1, false negative in 1 and false positive (FP) in 1. PET was TN in 7, TP in 2, and FP in 3. In 2 patients, PET found additional distant metastases not examined with MRI. In 1 case, both MRI and PET detected recurrent tumor. The patient with indeterminate MRI was TN using PET. All FP PET results were due to non-specific lymph node uptake.
Conclusion: PET may provide additional information in the follow-up of women with breast cancer due to its ability to detect distant metastases. It further may help to characterize breast lesions indeterminate at MRI.

B-0801 15:15

High frequency breast electro biopsy (HF-BEB). A new technique in minimal breast intervention: First results of a phantom study

H. Sittek[1], P. Schneider[1], C. Perlet[1], A. Lebeau[1], N.J. Heske[2], M.F. Reiser[1]; *[1]Munich/DE, [2]Türkenfeld/DE*

Purpose: To develop a gentle, low-risk method of high-volume diagnostic breast biopsy.
Method/materials: High frequency electrobiopsy (HF-BEB) was developed and tested. The principle of HF-BEB (BIP Co., Türkenfeld, Germany) consists of tissue resection and coagulation with a high frequency electric current from a generator (Erbotom ICC 350, ERBE Co., Tübingen, Germany). Phantom studies were performed under ultrasound guidance (Sonoline Elegra, Siemens Co., Erlangen, Germany) in porcine striated muscle specimens (n = 10). Specimens, including biopsy samples and post-biopsy tissue lesions, underwent histologic analysis after staining with H&E and EvG. Zones of high frequency current artifact, including cell vacuolization, coagulation, and carbonization, were measured under the microscope. The HFEB instrument applied had an outer diameter of 14 mm and provided biopsy samples with maximum diameters of 10 mm.
Results: Average duration of biopsy sampling procedure was 10 minutes per specimen. Biopsy specimens averaged 1.191 mm^3, with a tissue core length of 23.6 mm, and a diameter of 8 mm. Mean volume of unusable tissue due to high frequency current artifact was 230.5 mm^3. Mean diagnostic sample volume was 871.4 mm^3.
Conclusions: The HF-BEB method reliably provides large volume biopsies within short time. Tissue loss due to HF-BEB artifact was minor and did not impair histologic analysis. Due to coagulation of resection margins, hemorrhage from post-biopsy tissue lesions is expected to be insignificant in vivo.

B-0802 15:20

Mammography in men: A retrospective analysis of 362 patients

C. Dorbritz; *Dresden/DE*

Purpose: Retrospective analysis of 362 men with abnormalities of breast, there mammograhic and sonografic features, histology.
Method and materials: The retrospective analysis based on the examination of 362 men during 1/90 and 8/00. A clinical examination, mammography (Mamma-Diagnost UC Release 1 Fa. Philipps) and additional sonography (US SSA 240A/2F730-074EXA Fa. Toshiba; 7.5 MHz) were performed.
Results: The most common mammogrphic feature was gynecomastia (about 80 %). There were a difference in the apperance of pseudogynecomastia and the "true" gynecomastia. Gynecomastia was in one (about 70 %) or in both sides.
Biopsy results in about 5 % were negative for cancer. About 1.5 % had breast cancer. The patients with breast cancer had a age of 50 years and olders. The invasive dutal carcinom was the main tumor entity.
The mammographic sign of cancer were similar apperance like in woman breast. No cancer had the mammograhic features of gynecomastia. More aggressive monitoring in patients with breast cancer by clinical exam and mammography is necessary.
Conclusion: Breast cancer in men is a rare diagnosis. Clinical exam, mammography and selected biopsie is necessary in male patient, which are older than 50 years and with suspect clinical sign. A more agressive postoperative monitoring in this group of patients is useful.

14:00–15:30 **Room F2**

Neuro

SS 1511

Stroke (2)

Chairpersons:
E.C. Kirsch (Basle/CH)
P. Svendsen (Gothenburg/SE)

B-0803 14:00

Cerebral CT angiography in acute ischemic stroke management

T. Azhari, C. Fitzek, M. Herzau, R. Bartunek, H.-J. Mentzel, S. Fitzek, U. Sliwka, W.A. Kaiser; *Jena/DE*

Purpose: The acute stroke management changed in support of penumbra/mismatch identification. The purpose of the present study was to evaluate the impact of the additional information of the cerebral CT-angiography and 3D-reconstruction in comparison to native CCT and perfusion CT.
Materials and methods: A native CCT, perfusion CCT and cerebral CT-angiography (CTA) were performed in 36 patients with clinical symptoms of acute ischemic hemispheral stroke, using a multislice CT scanner (Light Speed Qxi, General Electrics). The examinations were analysed by 2 neuroradiologically experienced radiologists in a blinded retrospective study.
Results: In 14 cases the cerebral CT angiography showed pathologic findings of the intracerebral arteries according to the infarct area while in 22 patients the intracerebral arteries were found to be correct.
An exact analysis of the arterial vessels was feasible of the ACI, MRA (M1/M2), ACA (A1/A2), PCA (P1/P2), vertebral and basilar arteries. Variations such as a carotid origin of PCA or a hypoplastic AI were identified easily. In 4 cases side effects (mild itchiness, latent hyperthyreosis) occured. 2 examinations were aborted due to technical problems.
Conclusion: Cerebral CT angiography in addition to the native CCT and perfusion CT is a simple, useful and fast technique in acute stroke evaluation that leads to relevant information for further treatment.

B-0804 14:10

Differential diagnosis of acute ischemic stroke with modern and fast imaging methods

R. Bartunek[1], C. Fitzek[1], T. Azhari[1], S. Fitzek[1], H.-J. Mentzel[1], D. Sauner[2], W.A. Kaiser[1]; *[1]Jena/DE, [2]London/GB*

Purpose: The list of differential diagnosis in an acute stroke is large. It could be caused by ischemic territorial infarction, lakunar stroke, TIA, brainstem infarction, basilary thrombosis, venous thrombosis, tumor, encephalitis, seizure and bleeding. Furthermore, hemiplegia could be also caused by hemiplegic migraine or

neurotic disturbance. The aim of this presentation is to describe ten different different patterns of these differential diagnoses in CT with CT and CT-perfusion and in MRI with DWI, MRA, and MR-perfusion.
Patients and method: 54 patients with ischemic and non-ischemic stroke were retrospective analyzed. CT: GE LightSpeed QXI; MR: Siemens Vision Plus 1.5 T. Imaging of early infarction were compared to clinical data and stroke outcome.
Results: The different patterns and the pros and cons for discrimination of differential diagnosis with acute CT and MRI are shown.
Conclusion: Differential diagnosis of acute ischemic stroke is fast and secure with modern imaging methods and clear schema of decisions.

B-0805 14:20

Dolichoectatic intracranial vertebrobasilar artery dissection: Clinical and neuroradiological features

D.A. Stojanov, P. Bosnjakovic, M. Zivkovic, S. Petrovic, N. Stojanovic, S. Ristic; *Nis/YU*

Purpose: To determine the clinical and neuroradiological features of dolichoectatic intracranial vertebrobasilar artery dissection.
Methods and materials: The clinical features, native and post-contrast CT scans of 5 patients (4 men and 1 woman; age range from 25 to 68 years) with dolichoectatic intracranial vertebrobasilar artery dissection were analyzed retrospectively for a period of 3 years. Diagnosis was confirmed by vertebral angiography.
Results: Clinical symptoms due to ischemic cerebellar and/or brain stem lesions were present in 4 patients, two of them had Wallenberg syndrome. Occipital and/or posterior neck pains were found in 4 patients. Subarachnoid hemorrhage was shown in one patient. The incidence of previously documented hypertension was 60 % (3 of 5 patients). The prognosis was relatively good. Dolichoectasia was detected by native, post-contrast CT scans and reconstructions in all patients. Intimal flap was visualized with post-contrast CT scans in on patient. Extension of the basilar artery tip into the third ventricle was detected in 3 patients. Ischemic low-density lesions were detected in 3 patients and subarachnoid hemorrhage in one patient. Vertebral angiography disclosed elongation and dilatation of the vertebral and basilar arteries, double lumen sign – the presence of a true and false lumen and an intimal flap, double density and retention of contrast medium.
Conclusion: Ischemic symptoms and head and/or neck pain were the most common clinical findings. The double lumen sign, considered as the only pathognomonic angiographic finding of arterial dissection, was found in all patients.

B-0806 14:25

Cortical laminar necrosis (CLN): MRI findings

A. Lefkopoulos, A. Charitandi, N. Siskas, I. Ioannidis, A. Kelekis, A. Drevelengas, I. Sofroniadis, A.S. Dimitriadis; *Thessaloniki/GR*

Purpose: To study MRimaging features of cortical laminar necrosis (C.L.N.)
Materials and methods: We examined 10 patients, 7 males and 3 females ranging from 55 – 83 years with a mean age of 68 years. The cause of CLN in all our patients was caused by ischemic stroke. Our examinations occured a week after the first incident and lasted up to 4 months. We used T1WI, T2WI and post contrast T1WI sequences on axial and coronal plains.
Results: MRI findings showed hyperintence lesions in the cerebral cortex on T1WI abd T2WI which correspond to a neuronal ischemic region abd represent a gliotic reaction and laminar deposition of macrophages, which are rich in lipids. The high intensity signal was still observed 3 to 10 months after the insult. CT and MR studies did not demonstrate hemorrhage in the lesions of C.L.N.
Conclusion: MRI assisted the detection of C.L.N. and the differentiation from hemorrhagic lesions in patients with ischemic stroke.

B-0807 14:35

Infarction of the corpus callosum mimicking neoplastic lesions: Atypical MR imaging findings in four patients

J. Chong, P.-S. Goh, J.S.L. Wong, S.-C. Wang; *Singapore/SG*

Purpose: To present the MR imaging findings of four patients with atypical diffuse infarction of the corpus callosum and mass-like appearance, mimicking neoplastic lesions.
Methods and materials: At our institution, a total of 1092 patients were diagnosed with acute infarcts between January 1999 and September 2000. Of these, 4 patients had atypical diffuse infarction of the corpus callosum. The diagnosis was confirmed by clinical and imaging follow-up. The MR imaging features were reviewed.
Results: All 4 patients had mass-like diffuse signal abnormality, with no significant enhancement. Three were predominantly unilateral, and 1 bilateral. One was haemorrhagic. Follow-up demonstrated encephalomalacia, progressive atrophy and decreased extent of signal abnormality, consistent with resolving infarcts.
Conclusion: Infarction of the corpus callosum can involve the entire corpus callosum, with a mass-like appearance. Awareness of this atypical presentation and knowledge of the normal vascular supply of the corpus callosum and the variants are important for patient management so as to avoid unnecessary surgical intervention. MR imaging is superior to CT scan in the evaluation of corpus callosal lesions. Certain MR imaging features such as unilaterality, lack of enhancement in the acute phase, haemorrhagic changes and other ischaemic lesions, as well as serial imaging are invaluable for reaching the final diagnosis.

B-0808 14:40

Chronic brain ischemia: White matter abnormalities in MRI and DSA parenchymography

K.S. Minkner[1], B. Jean[2], D. San Millán[1], J.-B. Martin[1], R. Sztajzel[1], J. Delavelle[1], D. Rüfenacht[1]; *[1]Geneva/CH, [2]Montpellier/FR*

Purpose: To correlate occurrence of white matter abnormalities seen in MRI with DSA parenchymography for patients with signs of chronic cerebro-vascular insufficiency.
Materials and methods: MRI T2 weighted axial or FLAIR coronal images were compared with DSA parenchymography in 50 patients. DSA parenchymography was used to identify a cerebro-vascular insufficiency of watershed areas in this retrospective study. Parenchymography of the brain was obtained during DSA with a pigtail catheter delivering a 40 cc bolus of contrast material at the level of the ascending aorta and DSA imaging of the head in a.p. projection. The capillary stain of the brain parenchyma was visualised by adapting window/level values accordingly. Reduced and/or prolonged vascular stain in the watershed areas during DSA was correlated with the presence of white matter lesions as seen in MRI using the Marconi Eclipse (1.5 T) or Marconi Nordstar Outlook (0.23 T). Three regions were defined in MRI in order to divide the white matter in (a) the watershed-territories between the medial and anterior cerebral artery, (b) the immediate periventricular zone and (c) the remaining non-a and non-b white matter areas.
Results: In patients with signs of chronic cerebro-vascular insufficiency, a good correlation was found between abnormal parenchymography of the watershed area and MRI lesions in zone (a) and (b).
Conclusions: Dynamic DSA parenchymography reliably visualise areas of diminished perfusion of the watershed area. Our findings suggest that white matter abnormalities in hemispheric watershed areas correlate with signs of chronic insufficiency of cerebro-vascular supply.

B-0809 14:50

Preliminary evaluation of brain relaxometry and lesion quantification in CADASIL patients

B. Alfano[1], M. Quarantelli[1], S. Pappata[2], H. Chabriat[2], M. Larobina[1], E. Tedeschi[1], A. Brunetti[1], M. Salvatore[1]; *[1]Naples/IT, [2]Orsay/FR*

Purpose: To assess the possibility of automatically quantifying ischemic changes occuring in the cerebral parenchyma of patients with CADASIL (Cerebral Autosomal Dominant Arteriopathy with Subcortical Infarcts and Leukoencephalopathy), a syndrome characterized by migraine attacks, recurrent strokes and cognitive and behavioural disturbances.
Materials and methods: Using a segmentation algorithm based on relaxation rate maps obtained from conventional Spin-Echo sequences (Magn Reson Med 37:84–93, 1997), brain MR studies from 6 CADASIL patients (3 females, 3 males, age range 50 – 56) were analyzed and compared with data from 50 normal subjects covering a wide age range (31 females, 19 males, age range 16 – 76). Normal (white matter, WM; gray matter, GM; cerebrospinal fluid, CSF) and pathologic tissues (infarcts) were automatically segmented based on their relaxation properties, providing corresponding tissue volumes.
Results: Quantitative automated estimation of pathologic tissue yielded less then 1 ml in normal subject, 138 ml in CADASIL patients (range 74 – 204 ml). Only two patients presented significant atrophy as measured by age-corrected fractional (percentage of total intracranial volume) CSF volume.
Conclusions: Relaxometric analysis of conventional MR studies in CADASIL patients allows operator-independent quantitative assessment of abnormal tissues and normal tissue modifications. Further work is needed to define criteria for pathologic tissue subdivision and to clarify the relationship between these results and clinical data.

B-0810 15:00

Magnetic resonance imaging and histologic findings of experimental cerebral fat embolism

H.-J. Kim, C.-H. Lee, B.-R. Park, S.-H. Lee; *Pusan/KR*

Purpose: To experimentally evaluate the MRI appearance and natural history of cerebral fat embolism in a cat model and correlate the MRI and histologic findings.
Materials/methods: Eleven cats were injected with 0.05 ml of triolein into the internal carotid artery. T2WI and Gd-T1WI images were obtained serially at 2 hours, 1 day, 4 days, 1 week, 2 weeks and 3 weeks after embolization. Abnormal signal intensity (SI) was evaluated. Brain tissues were obtained for light (LM) and electron microscopic (EM) examinations. Histologic and MRI findings were correlated.
Results: On T2WI at 2 hours, high SI was found in all cats. The high SI were increased (n = 4) or decreased (n = 7) at 1 day, decreased in all cats thereafter. Most of the lesions became iso-intense, however small focal high signal intensities were seen in eight cats at 3 weeks. On Gd-T1WI, marked enhancement was seen in all cats at 2 hours. The enhancement continued to decrease thereafter. On LM examination, eight cats showed single or multiple foci cystic necrosis at the cortex and sporadic ischemic change at the white matter in all cats. On EM examination of the cortex showing normalized SI on MRI, intracapillary fat vacuoles (n = 11) and disruption of the blood-brain barrier (n = 4) were seen. Mild perivascular edema was sporadically seen in four cats.
Conclusions: Experimental cerebral fat embolism was well-detected on T2WI and Gd-T1WI from 2 hours. Small foci necroses were seen at 3 weeks on MRI and histologic examinations.

B-0811 15:10

FLAIR-sequence in cortical infarcts

V.K. Katsaros, P. Spathi, E. Georgiadis, V. Vantali, A. Nikolaou, C. Drossos; *Athens/GR*

Purpose: To demonstrate the contribution of FLAIR-sequence in the diagnosis of cortical infarcts.
Patients and method: 692 brain MRI examinations were performed with a 1.5 T unit (Magnetom, Vision) over an 18 month period, March 1999 to September 2000. Stroke was the clinical diagnosis in 365 patients. In 61, at least one cortical infarct was shown. In addition to the standard protocol for brain MRI-examination (transverse SE T1-W, tSE PD and T2-W, coronal tGSE T2-W and sagittal SE T1-W sequences), a FLAIR (Dark Fluid) sequence (TIRM, TR 9000 ms, TE 110 ms, TI 2500 ms, TA 5 min 10 s, FA 180, FOV 230, matrix 220 × 256, acq 2) was included in transverse and/or coronal plane.
Results: The diagnostic accuracy of FLAIR (Dark Fluid) sequence was evaluated in imaging the cortical infarcts. The findings were reviewed with the clinical history patient and the other sequences, especially the PD and T2-W images. The findings were compared with the history of the patients defined as acute cortical infarct (n = 5), subacute (n = 22), chronic (n = 61) and/or haemorrhagic infarct (n = 15). The FLAIR sequence showed all suspected cortical infarcts (n = 88), suspected by PD and T2-W images, due to the higher resolution and contrast between grey matter and the subarachnoid space. Additionally, the FLAIR sequence better demonstrated the haemorrhagic components in the patients with haemorrhagic infarcts.
Conclusion: FLAIR (Dark Fluid) sequence significantly improves the diagnostic accuracy of imaging stroke, especially when cortical infarction or haemorrhagic infarct is suspected.

B-0812 15:20

Acute lacunar infarctions: Comparison of detectability between brain stem and basal ganglia/thalamus on magnetic resonance T2-weighted and FLAIR images

J. Lee, H. Choi; *Seoul/KR*

Purpose: To evaluate the diagnostic value of T2-weighted image (T2WI) and FLAIR images for detection of acute lacunar infarctions in the brain-stem and basal ganglia/thalamus which were consistent with clinical symptoms.
Material and methods: 60 lesions of 36 patients who were admitted with a clinical diagnosis of acute infarction were retrospectively reviewed. The patients were clinically diagnosed as having brain-stem infarction 16, brain-stem and basal ganglia/thalamic infarction 14 and based ganglia/thalemic infarction 29. On imaging there were 31 brain-stem infarctions and 29 basal ganglia/thalemic infarctions. Two radiologists evaluated the images and decided whether the lesions were seen better on T2WI or FLAIR images, they considered signal intensity, extent and detection of the lesions. The difference of detection of the lesions in the brain-stem and basal ganglia/thalamus were analyzed statistically.
Results: Of the 31 lesions in the brain-stem, 19 lesions were seen equally or better on T2WI and 12 lesions were seen better on the FLAIR image. Of the 29 lesions in basal ganglia/thalamus, 8 lesions were seen equally or better on T2WI and 21 lesions were seen better on FLAIR image. The difference of detectability by the two different imaging methods was statistically significant (p = 0.000).
Conclusion: FLAIR imaging has been believed to be more reliable in diagnosing acute infarction than T2WI. But, this study revealed that the lesions in brain-stem are better visualized on T2WI and the lesions in basal ganglia/thalamus on FLAIR imaging. For accurate diagnosis of acute brain-stem infarction T2WI is more helpful rather than FLAIR imaging.

14:00–15:30 **Room G**

Computer Applications

SS 1505

Teleradiology and digital report generation

Chairpersons:
D. Caramella (Pisa/IT)
M. Osteaux (Brussels/BE)

B-0813 14:00

GP link: Telemedicine solution for establishing links between radiology and general practices

N.-M. Shastry, M.R. Rees; *Bristol/GB*

Purpose: To establish a PC-based, inexpensive telemedical link between our radiology department and a general practice (GP) for a specialist clinic.
Methods & materials: We established a telemedical link between the department of radiology and a GP clinic using a Windows 98 based 350 MHz Pentium PC with a 56 k modem and an ISDN2 adapter card. We used the video conferencing software which came with the card, Paintshop Pro, for imaging and PC Anywhere for remote control. X-rays of patients for the specialist orthopaedic clinic at the GP practice were digitised and transmitted over ISDN2 telephone lines. The end users were guided into using the system through the remote control software link which would communicate with the PC through the normal telephone connection in parallel to the ISDN2, digital communication. The remote control software allowed the radiology experts to control and demonstrate the telemedical, image display and manipulation functions whenever necessary.
Results: We have used this telemedical link for more than a year for the orthopaedic clinic and are now being asked to facilitate cardiology and dermatology links. The very small learning curve for the end user helped establish the telemedical technology quite easily in an IT novice user base.
Conclusion: We have been able to demonstrate the possibility of using standard off-the-shelf computing hardware and software for sophisticated medical applications. This telemedical facility cost the GP clinic less than £ 3 000 to setup.

B-0814 14:10

TeleInViVo project: Clinical evaluation of a telematic system for viewing 3D US images

P.D.H. Gil Agostinho, L. Teixeira, F. Caseiro Alves, M. Martins, A. Gil Agostinho, P. Avidago, F. Mascarenhas Gaivão; *Coimbra/PT*

Purpose: To evaluate the feasibility and the diagnostic value of a new telematic system devoted to remote teleconsulting in ultrasound applications.
Material and methods: A home-built light weighted prototype ultrasound scanner incorporating the proprietary TeleInViVo software system was used to produce two-dimensional images of abdomino-pelvic and obstetrical examinations in 162 patients. Images were acquired with 3 – 5 MHz probes generating a stalk of 2D images that were converted in 3D imaging volumes. A total of 283 volumes were generated and sent via Internet (n = 166) or ISDN (n = 117) to the remote site for expert consultation. Images were read by two radiologists and evaluated for several parameters, namely the time of transmission, overall quality of the images and ability to produce a specific diagnosis.
Results: The transmission time of imaging volumes (about 1.5 MB) was significantly quicker via ISDN (mean 3 minutes 10 seconds) than by Internet (mean 10 minutes 33 seconds). The mean time used to review images, discuss and produce a final diagnosis was about 13 minutes. Overall quality of images was considered good or fair in 88.5 % of cases. A specific diagnosis could be produced in 87.5 % of the cases, determining a sensitivity of 83 %, specificity of 59 % and accuracy of 81 %.

Conclusions: TeleInViVo is a reliable tool to produce remote ultrasound diagnosis with the present transmission technological facilities. Short 3D files, weighting about 1.5 MB, proved accurate enough for diagnostic purposes.

B-0815 14:20

A European ultrasound network for teleconsultation and teletraining in new ultrasound techniques

Y. Koumpouros[1], P. Zoumpoulis[1], S.T. Prapavesis[2], I. Theotokas[1], A. Plagou[1]; *[1]Athens/GR, [2]Thessaloniki/GR*

Purpose: This paper deals with a network for distance education of physicians using ultrasound for diagnostic purposes. This is achieved by combining the latest information and telecommunication technologies.
Materials and methods: All the necessary information concerning brief clinical, and biochemical data, as well as a resume of the various sonographic findings for specific patient cases are effectively transferred via the WWW. Trainees are able to analyze real-life case studies on a continuous and bi-directional way, ask questions and receive answers. A multimedia database has been developed for storing images, video, sound, speech, and files containing selected cases.
Results: Physicians, by using their password, obtain access to a specific area of the database in accordance to their interest. The system has a lossy to lossless wavelet compression-decompression scheme integrated for the faster transmission of the required data. A custom-made e-mailer is used by the members of the Ultrasound Network when communicating via the WWW for security purposes. Moreover, when it is necessary the expert "side" to consult another physician in terms of using new ultrasound techniques, two videocameras, an appropriate PC-videoconferencing card, and a simple video-mixer are installed in each location.
Conclusion: All the prerequisites have been taken into account in order to end up with a secure environment, with great confidentiality and sensibility in the private patient data as well as the non time-consuming operation for the transmission of the required medical data. The ease-of-use is the key for the successful operation of the system.

B-0816 14:30

Implementation of an integrated digital imaging and telemedical solution for the early management of lung cancer

N.-M. Shastry, A.P. Morgan, P. Richardson, M.R. Rees; *Bristol/GB*

Purpose: Digital Radiography (DR) systems lend themselves to integrated imaging solutions and telemedicine. The aim of this work was to integrate Radiology & Cardiothoracic Surgical processes to enhance the quality of care to the patient, save valuable decision time and resources.
Methods & materials: A conventional chest X-ray system was used as the source while the DR system replaced the conventional film. The chest images from patients were "captured" in a DICOM3 format and transmitted over Ethernet links to the radiologist and to the surgeon, simultaneously. While waiting for the radiologist's report, the surgeon immediately instigated the necessary admission and treatment protocols for the patient.
Results: Since implementation, 210 patients have been imaged with this facility. The digital image transfer times ranged from 45 – 75 s depending upon the imaging parameters. This facility has resulted in savings of between 10 – 15 days in terms of response time enhancing the early implementation of the patient management protocols while also alleviating the patient's distress and anxiety.
Conclusion: This is the tip of an iceberg; this model can be applied inexpensively in most specialities throughout the Health Services and could also extend expert medical care to underserved, remote areas.

B-0817 14:40

Secure DICOM-communication over insecure networks

D. Emmel, J. Ricke, W. Schauer, A. Haderer, R. Felix; *Berlin/DE*

Purpose: Implementation of a transparent encryption solution for secure DICOM communication over insecure networks like ISDN for Teleradiology.
Materials and methods: To fulfil the legal requirements of data security only encrypted data is allowed to be exchanged between remote DICOM nodes over the internet or public networks. As more and more CT and MRI scanners are installed at peripheral hospitals, the needs for image communication rises. Typically, these scanners are connected to a public network via Modem or ISDN without any encryption facilities. The introduction of a PC-based system solves this problem, as it offers a transparent encryption tunnel between the communication partners. It is placed in between the existing network routers and the sending and receiving communication partners. This systems uses OpenSource components with an integrated IPSEC implementation. Without any changes of the software at the sender or receiver side it will encrypt the data before it is sent over the network. The decryption takes place at the receiver side and is forwarded to the DICOM receiver.
Results: To provide encryption facilities for DICOM communication partners a simple and open solution was developed. The OpenSource facilitates the reuse of non-Up-To-Date hardware and enables the deployment of inexpensive hardware from PC mass market.
Conclusion: A reasonable system was introduced which can be integrated into existing commercial encryption systems. The system is flexible and can be easily adapted at the time a standard solution for data security becomes available.

B-0818 14:50

Decentral biosignal processing on personal digital assistants (PDAs)

M. Kroll[1], K. Annacker[2], J. Holstein[1], K. Kleber[1], A. Schröter[1], H.-G. Lipinski[2], D.H.W. Grönemeyer[1]; *[1]Bochum/DE, [2]Dortmund/DE*

Purpose: In the clinic routine as well in medical research the tendency to mobile information systems is growing rapidly. Using organizers physicans and scientists will gain the ability to have access to patient-dependent data e.g. ECGs and EEGs whereever they want.
Methods and materials: The Java 2 Microedition Technology (J2ME) which is currently available for PDAs and cellphones as well offers the possibility to create applications which are able to display and process biosignals on mobile devices using Java's platform independency.
Results: Using J2ME specific and third party libraries like kAWT it was actual possible to create an application called "KBiosig". This application runs on the Palm Connected Organizer and the Desktop as well, without changing the application source code. The application offers useful algorithms like creating amplitude histograms or signal correlations on the mobile device, but it can also communicate with servers on the internet to delegate even more calculation power extensive algorithms to those machines. Additionally the application could be extended using so called PlugIns written by third parties.
Conclusion: The new J2ME Technology makes graphical related applications like biosignal processing using small devices like PDAs and cellphones actual possible.

B-0819 15:00

Report generation and distribution via complete digital systems

B.B. Wein, M.W. Kilbinger, F. Vogelsang; *Aachen/DE*

Purpose: Radiological reports most often are dictated on tape, transcribed by typists, printed and corrected on paper, rewritten into digital systems and then signed and distributed to the referring physician. Lost reports have to be re-authorized by the authors. To reduce the time between reporting and distribution to the referring physician, to abandon the necessity of multiple signatures, and to reduce unnessary telephone based communication, a system for digital recording, signing and distribution of reports was created and tested in clinical use.
Materials and methods: Perl- and PHP3-scripts were used to generate HTML-based report-acquisition, -correction and -signature modules from a relational SQL-driven database. Report distribution is performed via electronic transfer to printers on the wards throughout the hospital and via direct HTML-based personalized access to the SQL-database. Digital signature is achieved using the gnu-pgp crypting system, ensuring (using 1024 bit keys) an extremely high security for encryption.
Results: The report generation system has been operational since December 1998 and digital signature as well as distribution has been provided since May 2000. In total more than 179 500 reports have been generated and more than 35 600 have been digitally signed and distributed. The overall time of reports could be reduced remarkably in conventional radiology cases. For more complex modalities, with three signing radiologists, the reduction of delivery was more moderate. The frequency of user access for the digital version of the reports increases weekly.
Conclusion: Complete digital support of medical reporting provides timely delivery, gives acceptable service; and reduces unnessessary communication.

B-0820 15:10

Digital signature of radiologic reports: Impact on the radiology department

C. Saccavini, R. Stramare, S. Puggina, R. Pasini, A. Ramelli, G. Feltrin; *Padova/IT*

Purpose: To analyze the use of digital signature of radiological reports. In fact to achieve the totally digital report archive in conformity with Italian Law it is necessary to replace the autograph signature at the foot of the report with a digital signature.

Materials and methods: The radiologist visualizes the text of the report, makes changes, and then signs it introducing his smart-card with a private key. The text and the signing are encrypted by a public key and stored on optical disk (CD-ROM). In this way only an authorized addressee having a smart-card with the corresponding public key can read the report. We use intranet techology to send the report and the digital signature to referring physicians.

Results: The most encouraging results are radiologists' and physicians' acceptability of the digital signature and of electronic report distribution. We have tested, with good results, the system security level to access control and electronic data trasmission. The smart-cards have been shown to be very suitable to protect the private key and the public one, but we have found some difficulties due to the lack of standards.

Conclusions: Due to the digital signature it has been possible to store the reports only in electronic format, with unquestionable medical and organizational benefits. A final important aspect is the digital signature's role in PACS development: due to the axxociation of images and with their reports, the real "multimedial report" will be possible. In this way RIS and PACS will no longer be considered as two different and separate systems but as a single logically and legally integrated one.

B-0821 15:20

Fully automated segmentation and recognition of spine radiographs by a knowledge-based shape model

M. Kohnen, A.H. Mahnken, S. Steinberg, B.B. Wein, R.W. Günther; *Aachen/DE*

Purpose: A shape model for the segmentation and recognition of lateral lumbar spine radiographs has been developed. A robust fully automated computation process allows to acquire objective and accurate results on this image material.

Materials and methods: A knowledge based approach is used to achieve a good segmentation accuracy. The shape model is capable of learning the characteristic shape variations from a training set of spine shapes by a principal component analysis of the shape information. The spine shape model has been computed from a training set consisting of 20 manually segmented lumbar spines. The segmentation results have been computed by an optimization of the shape models based on an energy image derived from the original image by edge detection algorithms.

Results: Fully automated spine recognition is possible. By now we tested the shape model on unknown images achieving a good segmentation accuracy in more than 75 % and a lower one in less than 20 % of today 50 images. About 5 % could not be detected sufficiently. The results are highly reproducible and essential for further automated analysis of spine radiographs. Recent analysis of specific errors in the detection are currently used to refine the algorithms.

Conclusion: To overcome the problems segmenting organic structures using arbitrary methods, a knowledge-based shape model has been successfully introduced. Furthermore, computation of global orientation landmarks from the images will be computed, to actually improve the segmentation accuracy of the shape model.

14:00–15:30 **Room H**

Interventional Radiology

SS 1509a

Arterial intervention (2)

Chairpersons:
K.D. Mathias (Dortmund/DE)
R. Yamada (Osaka/JP)

B-0822 14:00

Percutaneous intraarterial thrombolysis with tissue-plasminogen activator in iliofemoral arterial thrombosis after cardiac catheterization

D.K. Tsetis, G.E. Kochiadakis, A.A. Hatzidakis, E.I. Skalidis, E.G. Chryssou, I. Tritou, P.E. Vardas, N. Gourtsoyiannis; *Iraklion/GR*

Purpose: To evaluate the efficacy of transcatheter thrombolysis with high-dose bolus recombinant tissue-plasminogen activator (rt-PA) in patients with acute limb ischemia due to arterial thrombosis after cardiac catheterization.

Materials and methods: We treated eight patients (7 men; mean age 56 a) with thrombotic occlusion of both common femoral artery (CFA) and external iliac artery (EIA) in six patients and of the CFA only in two patients. Two 5 mg boluses of rt-PA were injected into the proximal clot through a 5 F end-hole catheter and subsequently two additional boluses of 5 mg rt-PA were given through a catheter with multiple side holes. In case of residual thrombus, a continuous infusion of 2.5 mg/h rt-PA was started.

Results: Successful lysis was achieved in all patients. The mean duration of lysis was 2 hours and 41 minutes. The mean total volume of rt-PA was 23.16 mg. In four patients flow-limited dissections were managed by prolonged balloon dilatation, while in the remaining four, Wallstents were implanted. There was prompt relief of lower-limb ischemic symptoms and signs in all patients. Two groin hematomas were conservatively treated. Clinical and Color Doppler Flow Imaging follow-up with a mean duration of 15 months, showed no reappearance of ischemic symptoms or development of restenosis in all but one patient who died 6 months after thrombolysis.

Conclusion: Percutaneous intraarterial thrombolysis with high-dose bolus rt-PA is a safe and effective treatment in patients with iatrogenic iliofemoral arterial occlusion after cardiac catheterization. Prolonged balloon dilatation should be performed, but in half of the cases there is need for stent implantation.

B-0823 14:10

Treatment of femoropopliteal chronic arterial occlusions by vibrational angioplasty: Preliminary experience

D.K. Tsetis[1], L.K. Michalis[2], A.N. Katsamouris[1], M.R. Rees[3], A.A. Hatzidakis[1], A.D. Giannoukas[1], I. Tritou[1], D.A. Sideris[2], N. Gourtsoyiannis[1]; *[1]Iraklion/GR, [2]Ioannina/GR, [3]Bristol/GB*

Purpose: To determine the safety and efficacy of vibrational angioplasty in conjuction with coronary guidewires in chronic femoropopliteal occlusions.

Materials and methods: Five patients (male 4, age range: 52 – 84 years) with femoropopliteal chronic occlusions were treated. Two had superficial femoral artery (SFA) occlusions (occlusion length: 11 and 15 cm, duration of occlusion: 6 and 24 months, symptoms: SVS/ISCVS category 3) and 3 diffusely diseased popliteal artery occluded in its distal part (occlusion length ranged from 3.5 to 4.5 cm, duration of occlusion ranged from 3 to 6 months, symptoms: SVS/ISCVS category 5). In all cases vibrational angioplasty using coronary equipment (over the wire ballon catheters and a variety of 0.014" guidewires) was utilized for the lesion to be crossed. Following wire passage conventional angioplasty was performed.

Results: In all five cases, the recanalization of the occlusions with the vibrational angioplasty technique was successful and no complications were observed. In the popliteal cases the wire crossed the lesion without the necessity of inflating the coronary ballon in order to facilitate the advance of guidewire-balloon catheter system, while in the 2 SFA occlusions balloon inflations were necessary at several stages of the procedure. The times for crossing the occlusions with the guidewire were 20 and 25 minutes for the 2 SFA occlusions and from 4 to 10 minutes for the popliteal lesions.

Conclusion: Vibrational angioplasty using coronary guidewires appears to be a promising technique for managing chronic occlusions of the femoropopliteal arterial segment.

B-0824 14:20

Long-term follow-up of the subclavian artery PTA

T. Jargiello, M. Janczarek, M. Rzeszowska, M. Szczerbo-Trojanowska; *Lublin/PL*

Aim: To establish the safety and efficacy of percutaneous transluminal angioplasty (PTA) of the subclavian artery.

Methods: PTA was carried out in 66 patients: 41 had left subclavian artery stenosis, 16 had brachio-cephalic trunk stenosis and 9 had right subclavian artery stenosis. The decision to perform the procedure was reached in consultation with a vascular surgeon after careful evaluation of duplex US and angiographic findings. Patients were followed up with Doppler ultrasound immediately after PTA, at 3, 6, and 12 months, and at yearly intervals thereafter. The procedure was technically successfulin 64 out of 66 patients (97 %). Complete recanalization was achieved in 58 cases. The remaining patients had mild residual stenosis. Blood flow normalisation on duplex US after PTA was used as a criterion of success.

Results: Follow-up Doppler US after 3 and 6 months did not show any recurrent stenoses. The maximum follow-up was 74 months (mean 46) and the overall patency rate was 79 %. Twelve months after PTA normal flow was maintained in 59 patients. In four patients there was a small decrease of blood flow suggesting low-grade restenosis. One patient was lost to follow-up. After 24 months PTA was repeated in one patient with high-grade restenosis. Four patients were lost to follow-up. In the remaining 58 patients there was no evidence of restenosis. 44 patients were followed-up for 36 months: 4 had low-grade stenoses and 40 patients had normal flow.

Conclusion: PTA is a useful method of treatment of subclavian artery stenosis. Good results are achieved with appropriate selection of patients and use of good equipment by experienced staff.

B-0825 14:30

Placement of Hemobahn-covered stent-graft in femoropopliteal arteries: Early experiences and midterm results in 18 patients

H.A. Deutschmann, P. Schedlbauer, V. Berczi, J. Tauss, K.A. Hausegger; *Graz/AT*

Purpose: To determine the outcome of a new PTFE-covered stent-graft in the treatment of occlusive femoropopliteal artery lesions.

Materials and methods: Eighteen claudicants (Fontaine stages 2b – IV) with occlusive lesions (mean length 7.95 ± 2.9 cm) in the superficial femoral and/or popliteal artery were treated with a PTFE-covered stent-graft (Hemobahn).

Results: Successful stent-graft placement was achieved in 17 (94 %) patients. In one patient additional insertion of a Palmaz-stent was necessary. Mean ankle-brachial index increased from 0.72 to 0.94 (P = 0.028). Fifteen patients (79 %) reported initial clinical improvement of at least one Fontaine stage. Primary patency was 39 ± 0.14 % at 1 year and 20 ± 0.12 % at 2 years (mean patency 10 ± 2 months). Stent-graft occlusion was observed in 13 (72 %) patients after 1 to 15 months and was reopened in four patients. Thus secondary patency was 50 ± 0.25 % at 1 year and 25 ± 0.22 % at 2 years (mean 15 ± 3 months). The length of the inserted stent-grafts and the presence of severe atherosclerosis were inversely related to stent-graft patency (P = 0.03, P = 0.026 resp.). Intimal hyperplasia was observed in 7 patients (39 %) after a mean period of 7.6 ± 8 months. Complications: access site hematoma (n = 4), distal thromboembolism (n = 2), abscess around stent-graft (n = 1).

Conclusion: The placement of Hemobahn stent-grafts was of limited success. The endoprosthesis should not be used for treatment of lesions requiring stent-grafts of more than 10 cm length, or when the adjacent vessel segments show significant atherosclerotic stenosis.

B-0826 14:40

Early experience and midterm follow-up results with a new, rotational thrombectomy catheter

V. Berczi, H.A. Deutschmann, P. Schedlbauer, J. Tauss, K.A. Hausegger; *Graz/AT*

Purpose: To assess the efficacy and safety of Rotarex rotational thrombectomy catheter in treating occlusions of the femoro-popliteal arteries.

Methods: The Rotarex catheter (Straub Medical, Switzerland) is a new, rotational thrombectomy device. Indications were acut or subacut (less than 12 weeks) occlusions of the middle or distal third of the superficial femoral artery or the popliteal artery. Eighteen patients (10 females, 8 males, mean age 72.7 ± 7.2 years) with occlusions of 3 – 20 cm length were treated on 19 limbs.

Results: Primary technical success rate was 94.4 %. Additional PTA and/or stent-graft installment was performed in 17 patients. Ankle-brachial-index improved from 0.40 to 0.79 (p = 0.012) (two days postprocedure). Clinical symtoms shifted to at least one Fontaine stage lower in 13 limbs. Complications: 2 perforations (arteries showing heavily calcified plaques), 1 AV-fistula, 1 flow-limiting intima-tear (1 perforation, the fistula and the intima-tear were treated with covered-stent), 3 distal embolisations (all treated successfully with aspiration or by Rotarex). None of the complications needed surgical treatment. Follow-up studies showed 3 early (3 – 11 days) and 6 late (1 – 6 months) reocclusions, primary patency rate is 50.0 % at a mean time of 9.33 ± 2.09 months.

Conclusion: The Rotarex thrombectomy catheter is primarily effective and quick in treating acute and subacute occlusions of the superficial femoral artery. It should not be used in arteries with heavily calcified plaques. Limited long-term patency is mainly due to the complexity of the underlying lesion.

B-0827 14:50

Distal percutaneous transluminal angioplasty through an infrainguinal bypass graft

A.-M. Löfberg, C. Ljungman, T.A. Ulus, A. Boström, A. Hellberg, G. Östholm, S. Karacagil; *Uppsala/SE*

Purpose: The aim of the study was to evaluate the results of transluminal angioplasty (PTA) performed through infrainguinal bypass grafts for stenotic or occlusive lesions at the distal anastomosis and/or in the runoff arteries.

Material and methods: Fourty-one patients underwent 57 procedures at the distal anastomis (n = 13), in the runoff arteries (n = 32) or at both locations (n = 12) following a mean interval of 15.8 months after infrainguinal bypass grafting. Nineteen procedures were on the popliteal artery and the remaining were on the crural arteries. Eleven procedures were due to occlusions less than 5 cm in length.

Results: A technically successful PTA was achieved in 91 %. Primary, primary assisted and secondary patency rates at 3-years were 32 %, 53 % and 62 % respectively. There were no significant differences in regard to the graft material, the type of lesion, the level of PTA, the status of runoff and the use of thrombolysis before PTA.

Conclusions: PTA at the distal anastomosis and/or in the runoff arteries in limbs with infrainguinal bypass is technically feasible and offers satisfactory results. It might be considered as the initial choice of treatment in selected patients.

B-0828 15:00

Phase I study of intra-arterial infusion with cremophore-free paclitaxel/albumin nanoparticles (ABI-007) in 31 patients with squamous cell carcinoma of the head, neck and anal canal

G. Patelli, G. Di Tolla, L. Frigerio, F. Garbagnati, R. Lanocita, A. Marchianò, C. Spreafico, V. Tichà, C. Valsecchi; *Milan/IT*

Purpose: To assess the feasibility, the maximum tolerated dose (MTD) and the toxicity of Intra-arterial chemotherapy by using ABI-007 in patients with advanced squamous cells carcinoma of the head and neck and the anal canal.

Material and method: 31 pts with head and neck cancer (25 m, 6 f; age 6 – 75, median 63); 12 pts (2 m, 10 f; age 41 – 75, median 56) with anal canal carcinoma were treated with ABI-007 every 4 weeks without premedication. A total of 120 cycles were given by percutaneous catheterization of external carotid or hypogastric artery.

Results: Neutropenia was the dose limiting toxicity (grade 4, 3 pts). Non haematological toxicity consisted in: total alopecia (30 pts), gastrointestinal (II) 3 pts, cutaneous (II) 5 pts, neurological (II) 5 pts, ocular (II) 1 pt, flu syndrome (II) 7 pts, (III) 1 pt. Procedural complications occurred in 2.5 % cycles (2 TIA, 1 hemiparesis), fully recovered. The MTD was 270 mg/m^2. Therapeutic responses (CR and PR) was observed in 80.9 %.

Conclusions: ABI-007 intra-arterial infusion without premedication is easy and reproducible. MTD was 270 mg/m^2.

B-0829 15:10

Embolization of external carotid artery branches for paragangliomas of the head and neck

V.V. Akinfeyev, I.V. Belotserkovsky, V.S. Dudarev, E.M. Zholnerovich, L.B. Vashkevich; *Minsk/BY*

Purpose: To report our first experiences of embolization in management of head and neck paragangliomas.

Materials and methods: Five patients with paragangliomas underwent embolization of the external carotid artery branches. CT and DSA immediatly before embolization were perfomed in all patients. The embolization was preoperative in 3 cases and as a single modality in 2. Three patients had multiply tumors (one of them bilateral). The lesions were carotid body tumor (n = 3), glomus vagale tumor (n = 5), glomus jugulare tumor (n = 3) and glomus tympanicum tumor (n = 2). External carotid artery was catheterized using 5 – 6 F Headhunter catheters. For

catheterization of small feeding vessels we use Microferret-18 coaxial catheter (William Cook Europe, Bjæverskov, Denmark). Embolizing agents were gelatin sponge particles and metalic coils.
Results: Technical success was achieved in all cases. Pharingeal ascendens artery was main supplying vessel. In 3 patients embolized preoperatively a reduced blood loss (100 – 150 ml) during surgery was detected. Two unresectable patients reported noticeable resolution of symptoms in 3 and 15 months follow-up.
Conclusion: Our preliminary experience supports the use of external carotid artery branches embolization for management of paragangliomas of head and neck both in candidates for surgery and inoperable patients.

B-0830 15:20

Intratumoral CT-guided administration of Cisplatin/Epinephrine gel for the treatment of malignant liver tumors
K. Engelmann, M.G. Mack, R. Straub, K.E. Eichler, S. Zangos, T.J. Vogl; *Frankfurt a. Main/DE*

Objective: To evaluate prospectively the clinical effectiveness and the associated parenchymal changes of CT-guided direct intratumoral injection of cisplatin/epinephrine gel in malignant liver tumours.
Patients and methods: CT-guided local applications of a novel cisplatin/epinephrine gel were used to treat eight patients with 17 colorectal liver metastases (mean of 5.1 injections) and nine patients with 13 hepatocellular carcinoma (HCC) nodules (mean of 3.1 treatments). Computer-generated volumetric analysis was used to assess the tumour volume and the amount of necrosis before and after treatment.
Results: Contrast-enhanced studies demonstated pretherapeutic tumour necrosis of 12.6 % in the metastases and 1.6 % in the HCC nodules. Intratumoral drug application resulted in a necrotic volume of 110 % in metastases and 109.7 % in HCC. Local tumour control rates at 6 months follow up to was 38 % in patients with metastases and 71 % in patients with HCC.
Conclusion: Direct intratumoral injection of cisplatin/epinephrine gel is an effective and well tolerated treatment method, which results in the development of a substantial necrosis in malignant liver tumours. In patients with HCC it achieves a higher degree of local tumour control than in patients colorectal metastases.

14:00–15:30 **Room I**

Abdominal and Gastrointestinal

SS 1501b

Small bowel and colon

Chairpersons:
G. Lechner (Vienna/AT)
P.-J. Valette (Lyon/FR)

B-0831 14:00

MRI small bowel: Comparison of water and a polyethylene glycol preparation as oral contrast media
R.R. Sood, H. Franklin, I. Joubert, T. Doyle, D.J. Lomas; *Cambridge/GB*

Purpose: To assess whether a commercial oral PEG preparation (Kleenprep), currently licensed as a bowel cleansing agent, is better than water for demonstrating the small bowel using a breath-hold T2w MRI technique.
Materials and methods: 22 volunteers (12 M, 10 F, age range 21 – 55 a) were recruited and examined on two separate occasions a week apart. The fasted volunteers were asked to drink up to 2 litres of water or a commercial PEG preparation They were then imaged serially every 10 minutes with coronal projection and multi-section breath-hold single shot RARE images. The paired datasets were anonymised, randomised and analysed by two radiologists in consensus for (1) transit time to the terminal ileum and (2) adequate visualisation of small bowel segments.
Results: The PEG preparation reached the terminal ileum in 21/22 volunteers whereas water reached the terminal ileum in only 14/22 ($p = 0.04$). Mean transit time for water was 50.6 min (± 48 min) and PEG 37.7 (± 22 min) but this was not significant ($p = 0.28$). The PEG preparation was found to be significantly better at demonstration of the ileum ($p = 0.05$) and terminal ileum ($p = 0.002$) than water.
Conclusion: A non-absorbable oral preparation (PEG) provides significantly better demonstration of the small bowel in volunteers than water on T2w MRI. This preparation may prove a useful oral contrast medium for MRI "small bowel meal" studies in patients.

B-0832 14:10

MR small bowel follow through: Choice of bowel contrast agent using HASTE sequence
A.K.P. Lim, S. Redla, C. Todd, A.W.M. Mitchell, M.E. Roddie; *London/GB*

Purpose: To evaluate the effectiveness of various water based oral contrast preparations in delineating small bowel using the HASTE sequence.
Method: Four subjects were starved overnight on five different occasions, one week apart. On each occasion, a different contrast agent which consisted either of: (a) Control (nothing); (b) Water (1 l); (c) Gastrografin (15 ml made up to 1 l with water); (d) Sorbitol (70 ml 70 %w/v made up to 1 l of water); (e) Mannitol (25 g of powder dissolved in 1 l of water) was administered orally one hour prior to imaging. Coronal and paracoronal 6 mm HASTE sequences were performed through the abdomen and pelvis using a Magnetom (Siemens) 1.5 T MR scanner. The films were randomised and two independent readers each reviewed the images and scored each preparation (1 – 5) for the assessment of small bowel anatomy, distension and mucosal delineation.
Results: The most severe side effect which consisted of diarrhoea was experienced with the Mannitol preparation and the most unpleasant tasting preparation was that containing Gastrografin. Sorbitol had the highest mean with a score of 3.56 (max = 5) for all categories. Scheffe analysis showed a difference when comparing Gastrografin, Mannitol and Sorbitol individually to the control ($p < 0.05$) and also to water ($p < 0.05$). No significant difference was found when these agents were compared with each other.
Conclusion: With some refinement, this technique can be employed as a method for imaging small bowel which is quick, cheap and incurs no radiation to the patient.

B-0833 14:20

Non-invasive distension and signal optimization for MR imaging of the small bowel
M.A. Patak[1,2], J.M. Froehlich[1], M.A. Ritz[1], C. von Weymarn[1], C.L. Zollikofer[1], K.U. Wentz[1]; *[1]Winterthur/CH, [2]Zürich/CH*

Purpose: Nasogastric intubation for diagnostic imaging of the small bowel is painful and traumatizing. We present a non-invasive method for bowel distension, which can be used with either positive or negative contrast.
Material and methods: 10 volunteers ingested between 1 and 1.5 l of water over 4 hours containing either Metamucil (0.8 g/kg body weight) alone (4 volunteers) or in combination with 20 ml Gd-DOTA (10 volunteers). Series of 120 contiguous single slices (540 ms/slice) were acquired using a 1.5 T MR system (Philips ACS-NT PT6000), followed by 3D data sets. Segmental evaluation was done in each volunteer looking at distension, degree of filling, signal homogeneity, bowel wall depiction and artifacts. Data analysis was performed in static, cine and real time multiplanar display modes. The 3D data sets were post-processed in order to perform virtual endoscopy.
Results: By adding Metamucil to oral contrast, bowel distension, filling, signal homogeneity and contrast are constant and of excellent quality. Positive contrast with cine imaging allows to monitor bowel motility, while negative contrast permits optimal visualization of the bowel wall. All 3D data sets allowed to perform virtual endoscopy. No adverse events occurred.
Conclusion: The combination of Metamucil with oral contrast agents permits a reliable, easy to use non invasive distension method for MR imaging of the small bowel.

B-0834 14:30

Angioedema of the small bowel: CT appearance
A.I.B. De Backer[1], J.E. Vandevenne[2]; *[1]Edegem/BE, [2]Genk/BE*

Purpose: To describe the findings on CT scan of the abdomen in patients with angioedema of the small bowel.
Materials & methods: We reviewed the files of four patients with angioedema of the small bowel. Helical CT scan after intravenous contrast administration was performed in all patients. In only one patient iodinated contrast was administered perorally.
Results: Clinical symptoms consisted of crampy abdominal pain accompanied by distension, nausea and diarrhea without blood or mucus since several hours (n = 3) or one month (n = 1). Vomiting was noted in three patients. In one patient life-threatening hypovolemic shock secondary to fluid sequestration in the gastrointestinal tract occured 1 hour after onset of symptoms. Intestinal wall and mesenteric edema resulted on CT scan in thickening of the small bowel wall and mucosa with increased contrast enhancement and prominent mesenteric vessels. Fluid disten-

sion of the small bowel was present in all patients. Fluid accumulation in the colon was only present in two patients with acute onset of symptoms. There was ascites in three patients.
Conclusion: Visceral angioedema has been associated with a variety of causes including congenital or acquired C1 esterase inhibitor deficiency and drugs or can be idiopathic. Awareness of the clinical and CT features enables to suggest the diagnosis of visceral angioedema and may dictate further diagnostic strategy and consequent therapy.

B-0835 14:40

Preoperative assessment of Crohn's disease: Enteroclysis vs. CT-enteroclysis

E. Schober, K. Turetschek, G.R. Strasser, W. Schima, F. Herbst, G. Oberhuber, J. Karner-Hanusch, H. Vogelsang; *Vienna/AT*

Purpose: This retrospective study compares the diagnostic yield of CT-enteroclysis (CT-E) and conventional enteroclysis (CE) in the preoperative assessment of Crohn disease.
Materials and methods: 20 consecutive patients (evaluated for elective operation) were studied with both modalities. All CE and CT-E studies were performed in a standardised fashion. CE: duodenal intubation, 300 ml barium suspension, 0.5 % metylcellulose solution (800 – 1600 ml), standarised documentation. CT-E: jejunal intubation, up to 2000 ml 0.5 % methylcellulose, spiral-CT series (collimation 5, table feed 7, reconstruction index 3), i.v. contrast administration (flow 4 ml/s, delay 35 s). Results of both imaging modalities were correlated with surgery and histology. Imaging and surgery were performed within 40 days.
Results: For the assessment of inflammation at the terminal or neoterminal ileum we calculated a sensitivity of 95 % for CT-E compared to 80 % for CE. CT-E was superior to CE in correct detection of inflammatory skip lesions (sensitivity: CT-E = 85 %, CE = 71 %, specificity: CT-E = CE = 93 %). With regard to stenoses sensitivity was 96 % for CT-E and 73 % for CE with a specificity of 93 % for both modalities. CT-E correctly diagnosed all abscesses, whereas CE missed all of them. Reliable detection of fistulae is not possible by means of CE (sensitivity 42 % compared to 84 % for CT-E).
Conclusion: CT-E is superior to CE in the preoperative assessment of Crohn disease.

B-0836 14:50

Value of T2 weighted fat suppressed and non suppressed sequences after oral administration of a superparamagnetic contrast agent in the assessment of Crohn's disease activity

F. Maccioni, A. Ascarelli, A. Grossi, V. Panebianco, J. Carbone, A. Viscido, P. Rossi; *Rome/IT*

Introduction: To assess the value of plain and fat-suppressed orally contrasted T2W images, by comparing them with T1W Gd-enhanced images, in the assessment of Crohn's Disease Activity (CDA). T2 weighted images in CD are very sensitive for detecting wall inflammation; however they are associated with low contrast resolution due to the hyperintensity of the wall, of the fat tissue and of the intraluminal fluid. To improve contrast and diagnostic value of T2-weighted images we associated fat suppression with the oral administration of a superparamagnetic contrast agent.
Subjects and methods: Fifty patients with CD underwent MRI at 1.5 T after oral administration of iron oxide particles (Lumirem, Guerbet). HASTE and fat-suppressed SPIR T2-weighted, and TFE or FLASH T1-weighted images pre and post Gd-DTPA were acquired through the abdomen and pelvis. TheT2-signal and Gd-enhancement of the affected wall and perivisceral fat, the degree of wall thickening and of fibrofatty proliferation on both T2 and T1-weighted images were compared with clinical signs of activity.
Results: Increased wall T2-signal on fat-suppressed images was statistically correlated with increased wall Gd-enhancement ($p < 0.00001$) and with active disease. High signal of the perivisceral fat on T2 fat-suppressed images was strongly related with active disease ($p < 0.00001$).
Discussion: T2-weighted plain and fat-suppressed images are extremely sensitive in the evaluation of bowel inflammation and, when associated, they are comparable to T1-weighted contrast-enhanced ones in the assessment of CD activity. They can be used alone, with reduction of costs and time of the MRI examination.

B-0837 15:00

MRI in Crohn's disease: Assessment of treatment response or relapse

F. Maccioni, V. Panebianco, A. Ascarelli, A. Viscido, A. Grossi, R. Brillo, P. Rossi; *Rome/IT*

Purpose: Our purpose is to assess MRI efficacy in monitoring the effects of a new pharmacological treatment.
Methods and materials: Fourteen selected patients with active perforative CD underwent pharmacological treatment with a new drug, the anti-TNF (tumor necrosing factor). All these patients were monitorized with clinical indexes and diagnostic tests. Disease activity was assessed with clinical indexes (CDAI) and diagnostic laboratory tests. MRI was performed at time 0 and at 1 months after treatment. HASTE and fat-suppressed SPIR T2-weighted, after oral administration of iron oxide particles (Lumirem, Guerbet), and TFE or FLASH T1-weighted breath-hold sequences pre and post Gd-DTPA injection were acquired at 1.5 T. The following MRI findings were considered signs of disease activity and scored with a 0 – 2 system: (1) bowel wall signal on T2-weighted Fat-suppessed images, (2) bowel wall contrast enhancement, (3) fibro-fat signal on T2-weghted fat suppressed images.
Results: Patients with biological and clinical signs of response to the new treatment showed marked decrease of wall thickening, decrease of wall Gd-enhancement and decrease of wall T2-signal on fat-suppressed images at the level of the affected segments. The differences with the pre-treatment findings were statistically significant. The finding of stronger signal intensity and higher contrast enhancement before treatment was associated to prompt response to treatment.
Conclusions: MRI can be periodically used to monitor drugs effects in CD. It is valuable in detecting disease activity at the level of the affected wall, easily repeatible and not associated with radiation exposure.

B-0838 15:10

Activity assessment in Crohn's disease: A comparison between hydro-MRI and endoscopy

K. Schunk, S. Reiter, K. Oberholzer, P. Kalden, T. Orth; *Mainz/DE*

Purpose: To assess the accuracy of hydro-MRI in the assessment of the activity in Crohn's disease (CD).
Material and methods: After an oral bowel opacification using 1000 ml of a 2.5 % mannitol solution and a rectal bowel opacification using 250 – 500 ml of an 0.9 % saline solution, axial and coronal breathhold sequences (T2W HASTE ± FS, contrast-enhanced T1W FLASH ± FS) were acquired in 15 patients with CD. The enhancement of the bowel wall as well as morphological MRI findings were correlated with the results of colonoscopy including biopsy specimens.
Results: According to dynamic MRI studies, a significant correlation between the contrast enhancement of the inflamed bowel wall (D signal intensity) and the endoscopic/histopathologic indices could be established ($r = 0.52$; $p = 0.02$ and $r = 0.72$; $p = 0.001$). A moderate correlation between the maximal bowel wall thickness (MRI) and the histopathologic index was found ($r = 0.46$; $p = 0.04$). D signal intensity and the maximal bowel wall thickness were closely correlated ($r = 0.83$, $p = 0.0001$).
Conclusions: MRI of the small and large bowel is an alternative to endoscopic and histopathologic assessment of disease activity in CD. The lack of invasiveness and of radiation, the transmural assessment and cross – sectional imaging are clear advantages of MRI in comparison to endoscopy.

B-0839 15:20

Extra-intestinal findings at CT-colonography

M. Hellström[1], M.H. Svensson[1], A. Lasson[2]; [1]*Gothenburg/SE*, [2]*Borås/SE*

Purpose: To evaluate the frequency and types of extra-intestinal findings at CT-colonography.
Methods and materials: Patients referred for colonoscopy because of symtoms suggestive of a colon disorder were subjected to a CT-colonography in the same setting (n = 111). CT-colonography was perormed without the use of oral or intravenous contrast media. The patients were examined in the supine as well as prone position, using 5 mm collimation and 2 mm image reconstruction. All analyses were made on a work station. Extra-intestinal findings were classified according their clinical importance as minor, intermediate or major. In case of positive findings, chart review was made to determine the impact of the finding.
Results: Major findings, such as aortic aneurysm (n = 6), adrenal mass (n = 10) or suspected solid lesions in the liver (n = 10), kidney (n = 6) or pancreas (n = 2) were found in 29 % of the patients.
Conclusion: CT-colonography reveals a large number of minor, but also a considerable number of clinically important extra-intestinal findings. This has to be taken into consideration in the evaluation of CT-colonography.

14:00–15:30 Room K

Interventional Radiology

SS 1509b

Technological developments

Chairpersons:
L. Ekelund (Abu Dhabi/UAE)
A. Hatzidakis (Iraklion/GR)

B-0840 14:00

Hemolytic and hemodilution effect of mechanical and hydrodynamic thrombectomy catheters in vitro

J. Grimm, S. Müller-Hülsbeck, A. Oberle, M. Heller; *Kiel/DE*

Purpose: To evaluate the hemolytic and hemodilution effect of different thrombectomy catheter systems in an in vitro flow model.
Material and methods: A flow model consisting of silicone tubings in a waterbath (37 °C) was used with fresh human blood (150 ml), pulsatile flow was delivered at 1000 ml/min. The catheters were inserted into the system via a 7 or 8 F sheath. The 7 F Amplatz (ATD), the Hydrolyser (HL), Oasis (OA) and Angiojet (AJ) System were tested so far (n = 10 each). Blood samples were drawn distal from the catheter at 0.5, 1, 1.5, 2, 2.5, 3, 5, 8, and 12 minutes activation time. Hemolytic and hematologic parameters (LDH, GOT, K, Hct, Hb) were evaluated. As control goup the flow model without inserted catheter was used.
Results: Compared to the control without catheter a significant increase of hemolytic parameters during the course of time could be evaluated with all systems. The Angiojet caused significant more hemolysis and hemodilution than the Amplatz and the Hydrolyser/Oasis System (ranking: AJ > ATD > HL/OA). The Amplatz caused more hemodilution than the Oasis and the Hydrolyser (ranking: ATD > OA > HL).
Discussion: The Angiojet produced the most hemolysis and dilution whereas the Hydrolyser showed (compared to the other systems) only slight hemolysis and dilution.

B-0841 14:10

Endovascular irradiation to prevent restenosis after percutanous transluminal angioplasty of peripheral arteries: Preliminary results of a randomized, prospective study

K. Krueger, P. Landwehr, M. Bendel, M. Zaehringer, M. Nolte, R. Bongartz, R.-P. Mueller, K. Lackner; *Cologne/DE*

Purpose: Restenosis after percutanous transluminal angioplasty (PTA) limits the long term results in femoropopliteal arteries. In first studies endovascular irradiation has proved to reduce the occurence of restenosis.
Methods and materials: 28 patients with claudication were randomized into two groups. Patients in group I (n = 14) received endovascular γ irradiation (^{192}Iridium, 14 Gy in 2 mm depth of the vessel wall) immediately after PTA using a centering catheter (PARIS catheter, lenght 10 cm). The whole lenght of the centering catheter was irradiated. Patients of group II (n = 14) were treated by PTA alone. Follow up angiography was performed 6 and 12 month after randomization.
Results: Today the time of follow-up is 1 – 18 month (mean time: 7.6 ± 5.2) in group I and 1 – 12 month (7.8 ± 4.6) in group II. In 2 patients asymptomatic thromboembolic complications requiring local thrombolysis occured during the procedure of irradiation. The reduction of vessel diameter in group I vs. group II was determined as follows: before PTA 55.3 ± 28 % vs. 67.1 ± 13 % (n.s.), after PTA – 0.9 ± 24 vs. –8.5 ± 31 (n.s.), after 6 months –7.7 ± 25 (n = 8) vs. 30.4 ± 23 (n = 9), p = 0.005, after 12 months –8.9 ± 27 (n = 5) vs. 50.0 ± 19 (n = 5), p = 0.004.
Conclusion: Our preliminary results suggest that endovascular irradiation may reduce the frequency of restenosis following PTA in femoropopliteal vessels.

B-0842 14:15

A new mechanical method of abrasion and isolation of human vascular endothelial cells for quantitative sufficient culture and coating of intravascular stents in vitro

M. Priebe, T. Jahnke, A. Mohr, S. Müller-Hülsbeck, M. Heller; *Kiel/DE*

Purpose: A new mechanical method of abrasion of human vascular endothelial cells for a quantitative sufficient culture and coating of intravascular stents.
Materials and methods: Newborns umbilical cord were used to isolate vein endothelial cells (EC). The umbilical vein was rinsed clot-free of blood, dilated up to 5 mm diameter with phosphate buffered saline (PBS) and divided in 10 cm segments. A 6 French Cragg thrombolytic brush catheter was inserted by mechanical hand rotating and pushed back. The brush was put in sterile tube filled with 15 ml cell medium (RPMI 1640) containing 20 % fetal calf serum and shaked out about 5 seconds by the highest engine performance of the connected catheter motor drive. This procedure was repeated 5 times for each segment. Then the tube was centrifugated 15 min by 200 g. The cells were resuspended in 5 ml RPMI as described without additional cell growth factor in a fibronectin-coated culture flask (50 µg/ml).
Results: The nylon brush catheter is able to abrate viable human umbilical endothelial cells (up to 2 – 5 × 100.000 EC/10 cm). The cell-viability is time-dependent (1 – 3 h) of the age of the umbilical cord. The EC grew to confluence after 2 – 3 weeks.
Conclusions: The new mechanical catheter abrasion is an effective method to isolate viable human umbilical vein endothelial cells and to culture these cells. Probably we can use this method in vivo to isolate patients (autologous) endothelial cells for e.g. stent-coating.

B-0843 14:25

Early results of in vitro-comparison of central embolization during PTA and stent implantation in human carotids in vitro with morphometric and histopathologic correlation

R. Wenke, A. Mohr, A. Paulsen, M. Heller, S. Müller-Hülsbeck; *Kiel/DE*

Purpose: To evaluate a model for embolization in experimental PTA and stent implantation in human carotids from cadavers in vitro in correlation of angiographic, sonographic and histopathologic findings.
Material and methods: Human carotids from cadavers were excised. Intervention was performed within 24 hours after excision. For intervention carotids were stored in saline and perfused with saline by means of a pulsatile pump. After DSA over a 9 French introducer sheath a guiding wire was introduced and intravascular sonography and B-mode sonography (ATL HDI 5000) with saline as transmission medium and a 12 Megahertz transducer was performed. Carotids were randomized for PTA and Stent implantation and after the procedure intravascular and B-mode sonography and DSA was repeated. The calcifications of the plaques and postinterventional changes were additional observed by Micro-CT examination of the specimen. During the interventions the perfusing solution was filtered with a 100 µm and 30 µm mesh to comparise central embolization. Filtered material was weighted and histopathologic examination for embolization material (intimal parts, foam cells, other cell material) was performed. 3 determined histopathologic sections for plaque morphology were obtained in each specimen.
Results: The experimental model delivers reliable and well reproducible results in image morphometry and allows correlation of detected plaque morphology of sonography, conventional angiography and Micro-CT with histpathologic findings. Further data and statistics will be presented at the meeting.
Conclusion: By means of this model comparison of embolization during intervention according to plaque consistence can be evaluated.

B-0844 14:35

Self-expanding radioactive nitinol stent

J.M.A. Meyer, T. Görgen, B. Nowak, A. Bücker, K. Schürmann, D. Klee, H. Höcker, U. Büll, R.W. Günther; *Aachen/DE*

Purpose: To develop a method that allows on demand activation of a self expanding nitinol stent with ^{188}Rhenium.
Materials and methods: A self-expanding Memotherm nitinol stent (8 mm diameter, 30 mm length, Bard-Angiomed) was first coated with a functionalized polymer layer. Radiolabeling of the stent with radioactive ^{188}Rh was achieved by chelate forming reaction between the polymer and ^{188}Rh. The mechanical integrity of 15 coated stents was analyzed using electron microscopy. The dose distribution of 6 radioactive stents was determined using a high-precision, high-resolution dosimetry system allowing direct measurement of the absorbed dose.
Results: We manufactured stents with a range of activity from 2 to 100 MBq corresponding to a dose of 1 to 50 Gy in a depth of 1 mm outside the stent strut. The mechanical integrity of the coated stent and a homogeneous dosimetry along the length of the stent was achieved. This technique allows activation of the stent directly before implantation.
Conclusion: We developed an easily applicable technique to activate a self-expanding stent, creating a radioactive β-emitting stent for endovascular implantation on demand.

B-0845 14:45

Interventional methods, intraluminal irradiation and hyperthermic treatment for lumen restricting GI tumors

Z. Vígváry, E.K. Makó, Z. Tarján, G. Tóth, Z. Dömötöri; *Budapest/HU*

Purpose: To improve survival and quality of life, lumen restricting, mostly inoperatively GI tumors were treated with LDR irradiation, local electro-hyperthermy, chemotherapy, embolization, cryotherapy and metallic stenting.

Materials and methods: 219 patients, plus 72 patients preoperatively and 29 patients with recidive esophageal tumors were treated between 1982 and 1996. The dose delivered in 3 fractions was 50 Gy, protected by 24 h, from a 5 mm distance to the mucosal layer. 124 patients with inoperable rectum tumors were treated with chemoembolisation and cryotherapy and intraluminal irradiation. Survival times and quality of life and complications were assessed.

Results: Esophageal tumors: Survival preoperative (72 pts), 39.6 months, recidive (15 pts), 25.1 months, inoperable (219 pts) 11.6 months. Quality of life: decreasing of dysphagia 69 %; increasing of body weight 54 %; diminishing of pain 74 %. Rectal tumors: Complete remission: 1; partial remission: 73; minimal response: 46; progression: 4.

Conclusion: LDR ^{137}Cs after-loading method combined with chemotherapy and locoregional hyperthermy proved to be an efficient in preoperative and recidive cases of esophageal and inoperable rectal tumors.

Learning objectives: ^{137}Cs AL method combined with chemotherapy, metallic stenting and hyperthermy proved to be an efficient treatment in GI tumors.

B-0846 14:50

Intraportal transplantation of isolated fetal liver cells

A.D. Zubov, V.G. Mykhalskyy; *Donetsk/UA*

Purpose: Search for new effective method of hepatic failure complex treatment in patients with liver cirrhosis in a stage of subcompensation.

Materials and methods: The fetal liver cells were isolated, purified and cultured according to standard technique. There were performed viability, morphology and bacteriological tests. The purified cells were transplanted into the portal vein by percutaneous approach under ultrasound control with color dopplerographic monitoring of portal venous flow. After the transplantation these patients were administrated hepatoprotective, trophic, antiviral and infusion therapy. The follow-up was performed with US examination and biopsy under US control, biochemical and immunological examination.

Results: 9 patients underwent this therapy. In all these cases we achieved considerable reducing of intoxication syndrome proved with EEG, improvement of biochemical and immunological status and hystological picture for a 12 month period. Except a short-term hyperthermic reaction there were no other side effects or rejection complications. We continue this research and collection of results.

Conclusion: Our experience demonstrates one of the possible new ways of supplement complex therapy and stimulation of hepatic function with methods of minimally invasive therapy.

B-0847 15:00

Influence of general anxiety states on periinterventional complaints related to percutaneous procedures

M. Blaum[1], G. Adam[2], R.W. Günther[1]; *[1]Aachen/DE, [2]Hamburg/DE*

Purpose: Evaluation of periinterventional complaints in unselected patients treated with a percutaneous radiological procedure. Objectifying short-term changes at the time of intervention as related to patients general anxiety state.

Patients and method: Seven forms containing different self-rating scales measuring general and actual anxiety and multiple kinds of complaints or discomfort were given to 558 patients suffering from benign and malignant diseases. They were asked to fill out before, directly after and five days after a radiological intervention.

Results: Most of the used scales showed a decreased quality of life before the intervention, especially complaints with focus on emotional reactions and phsychosomatic discomfort. The observed changes in quality of life were significant and mostly seen in patients undergoing an intervention for the first time. The complaints were more excessive in patients who showed higher level of general anxiety as measured with the State Trait Anxiety Inventory STAI (Trait version). The reported troubles were decreasing in periinterventional sequel with a residual reduction of quality of life after 5 days, which was more extensive in malignant underlying diseases.

Conclusion: The complaints of patients undergoing percutaneous procedures depend strongly on their general anxiety state. An accompanying psychological support or pharmacotherapy may be helpful in anxious patients.

B-0848 15:10

Evaluation of a new magnetic field navigation system for CT-guided biopsies and interventions

N. Holzknecht[1], T.K. Helmberger[1], U.J. Schöpf[1], M.A. Kessler[1], G. Ezekiel[2], M.F. Reiser[1]; *[1]Munich/DE, [2]Tirat Hacarmel/IL*

Purpose: To evaluate the accuracy of a new electromagnetic navigation system for CT-guided interventions.

Material and methods: CT-Guide1010 (UltraGuide, Tirat Hacarmel, Israel) is an FDA-approved navigation tool for previously acquired image datasets comprising a transmitter unit and magnetic sensors. In 36 patients 43 interventions (17 thermoablations and 17 diagnostic liver biopsies, 8 other abdominal biopsies) were performed using Plus 4 or VolumeZoom CT (Siemens, Forchheim, Germany). Spiral datasets of the target area were acquired with localizing sensors fixed on the patients skin. Image data was transferred via frame grabbing. Another magnetic sensor was placed at the base of the interventional tool. The systems allows for real-time navigation including respiratory gating in the acquired spiral dataset giving the guiding information overlaid in the specified CT-slice.

Results: 17 thermoablations of liver lesions, 17 diagnostic liver biopsies, 3 pancreatic, 2 abdominal lymphnode biopsies and 3 nerve blockades were performed succesfully without complications. The deviation between the needle tip specified by the target system and true position (control scan or CT-fluoroscopy) was 2.12 ± 2.50 mm. The mean procedure time was 18.3 minutes. Problems occurred only in less cooperative patients and in needle positions very close to the patient table due to electromagnetic interactions.

Conclusion: CT-guide is a safe and accurate system for CT-guided interventions.

B-0849 15:20

Modality based navigation (MBN): A precise multi-purpose instrument for image guided therapy

H.G. Staedele, A.L. Jacob, N. Suhm, W. Steinbrich, P. Regazzoni, P. Messmer; *Basle/CH*

Purpose: To apply the combination of a navigation system developed in-house with a helical-CT unit to deliver a broad spectrum of highly precise minimally invasive interventions.

Methods and materials: MBN supports visually interactive real-time image guidance in 3 dimensions with essentially arbitrary reconstructed views. Since the patient remains in the 3D coordinate system of the modality no registration is necessary. Navigation can thus be performed without delay after image acquisition. Intra-operative image control or update is possible anytime during the intervention. The newly aquired images can in turn be used immediately for navigation. While MBN can be used with essentially any modality, at our institution it is performed in a special CT-suite with laminar air flow and a lead glass protected zone for the interventionalists.

Results: 95 pelvic fractures, 16 acetabulum fractures, 3 ISG-Arthrodeses, 4 acetabular cyst plombs, 6 osteoid osteomas, 2 neurosurgical interventions and 1 vertebroplasty and multiple biopsies were navigated intra-operatively. The intra-operative precision was ± 2 mm.

Conclusion: MBN is a precise multifaceted interventional tool. It enables interactive visual feedback and requires a minimum of intra-operative setup.

14:00–15:30 **Room N/O**

Genitourinary

SS 1507

Female genital tract

Chairpersons:
N. Naumov (Sofia/BG)
R. Salvador (Barcelona/ES)

B-0850 14:00

Assessment of pelvic endometriosis: Correlation of unenhanced MR with laparoscopic findings

A. Guarise, G.M. Carbognin, I. Vitale, G. Schenal, C. Procacci; *Verona/IT*

Purpose: To evaluate the ability of MR in diagnosing endometriosis, and correctly defining the site and number of endometrial implants, comparing the results with the laparoscopic findings.

Material and methods: 25 young female patients with a clinical diagnosis of pelvic endometriosis underwent unenhanced MR examination of the pelvis in order to evaluate the presence, number, site and size of the endometrial foci eventually present. The results were prospectively compared with the laparoscopic findings.
Results: At laparoscopy, 106 lesion were detected (rectovaginal septum, 28; ovary, 25; broad ligaments, 12; uterosacral ligaments, 8; rectal wall, 9; vagina & posterior fornix, 5; others, 19). MR examination demonstrated a total of 65 lesions (61 %) (rectovaginal septum, 22; ovary, 28; broad ligaments, 2; rectal wall, 3; vagina & posterior fornix, 4; others, 6). The following aspects were encountered at MR: 35 small nodules (3 – 15 mm); 3 large nodules (15 – 30 mm); 3 laminar lesions; 19 cystic lesions; 5 complex (i.e. associated with solid component) lesions. All the lesions showed high signal intensity on T1WI. The best results were obtained in the identification of endometrial foci in the recto-vaginal septum. The sensitivity of MR was high in identifying the disease (100 %). It was much lower in correctly defining the number and site of the lesions (i.e. grading the disease: 54 %). The poorest results were achieved in the identification of endometrial deposits in either the broad and uterosacral ligaments.
Conclusions: MRI enables the recognition of pelvic endometriosis, leading surgical decisions, even if it underestimates the grading of the disease.

B-0851 14:10

Fat-saturation MRI vs. ultrasound in the diagnosis of pelvic endometriosis
J. Iwinska-Zelder, K. Bock, V.F. Duda, K. Goerke, J.T. Heverhagen, A. Ramaswamy, L. Zwiorek, E. Genss, H.-J. Wagner; *Marburg/DE*

Purpose: Endometriosis is a condition in which tissues similiar to the endometrium occur aberrantly in various locations of the pelvic cavity, thus often causing cyclic pain, adhesions and infertility. The aim of our prospective investigation was the comparison of the MRI- and ultrasound results in the evaluation of endometriosis.
Materials and methods: 10 female patients with an age range of 21 – 42 years (mean 34 years) underwent clinical examination, transvaginal ultrasound and MRI (standard protocol with T2- and T1-weighted fat-suppressed images was obtained using 1.0 T Magnetom Expert with a body array-coil) during the luteal phase of the menstrual cycle.
Laparoscopy was performed 1 – 2 days after sonography and MRI. In a prospective analysis MRI- and ultrasound-diagnoses were compared with the results of histopathology.
Results: Both diagnostic methods detected correctly endometriomas bigger than 1 cm and classified all patients properly. In 1 case MRI excluded endometriosis and allowed correct diagnosis of a dermoid tumor. In 1 case sonography did not detect small parametrial endometriomas.
Conclusion: Laparoscopy remains the method of choice in the initial diagnosis of endometriosis. MRI as a non-invasive imaging method should be complementary used for the monitoring of treatment. MRI is especially reliable in the diagnosis of endometriomas bigger than 1 cm. Pelvic endometriosis shows variable signal appearance on MRI (different features will be discussed).

B-0852 14:20

The role of MRI in the management of uterine cervical carcinoma
T. Belšan, L. Rob, J. Neuwirth, J. Lisý jr.; *Prague/CZ*

Purpose: To define the position of MRI in staging of the cervical carcinoma.
Subject and methods: We performed 112 MRI in a group of 85 patients with proven cervical carcinoma. Two different classifications were used to stage tumors. The decission about the surgical therapy was done by the FIGO classification, that describes the uterine and pelvic extent of tumors. A new volumetry classification describes the rate of the tumor volume and cervix diameters. The decision about the preoperative chemotherapy was based on the volumetry. In 27 patients who undergo chemotherapy we performed another MRI.
Results: The cervical carcinoma stage was based on the FIGO and volumetry classifications. In 27 patients we classified the stage Ib1 or Ib2 by FIGO (bulky tumors without parametria infiltration) and the stage Ib2 by the volumetry (infiltration of more than 2/3 of the cervix). These patients undergo the chemotherapy. By control MR imaging we proved the tumor volume reduction for 70 % in an average. Results were confirmed by an operation and histology. The tumor volume reduction improved the operability of bulky tumors.
Conclusion: MRI is the basic imaging method for correct staging of cervical carcinoma in stages Ia – IIb by FIGO. MRI does not bring a new information in stages III and IV. The main role of MRI is in depicting of the tumor volume and parametria infiltration. There is a very good response of bulky tumors to chemotherapy. MRI is ideal for the volumetry, which is used for the chemotherapy indication.

B-0853 14:30

Sonography vs. MRI in the evaluation of cervical cancer
J. Iwinska-Zelder, V.F. Duda, K. Bock, T. Hardt, A. Ramaswamy, K.-D. Schulz, K.J. Klose; *Marburg/DE*

Purpose: The therapy of the different stages of cervical carcinoma is based on the FIGO-Classification. Besides from clinical examination ultrasound and MRI are the technical methods predominantly used to define the pre-operative stages, especially in the determination of parametrial infiltration. Which of both imaging methods gives the most accurate assessment?
Materials and methods: Data of 16 female patients (29 – 66 years of age) with cervical carcinoma, diagnosed with sonography (Elegra Fa. Siemens, 128 XP/10 Fa. Akuson) and MRI (1.0 T Magnetom Expert Fa. Siemens) and surgically treated between 1993 and 1998 at the Philipps University of Marburg, were retrospectively evaluated. Intra-operative situs and histopathological examination were used as gold standard.
Results: Using sonography 8 cases out of 15 were classified correctly, 4 patients were under- and 4 were over-staged. Concerning parametrial infiltration MRI obtained 5 false-positive diagnoses. Using sonography 2 cases of parametrial infiltration (correctly diagnosed at MRI) were not detected.
Conclusion: Although MRI has a high sensitivity in the detecting of parametrial infiltration, the specificity (64 %) in our small caseload was nevertheless unsatisfactory. A combination of both imaging methods with clinical findings achieves the highest diagnostic safety.

B-0854 14:40

Usefulness of magnetic resonance imaging before and after presurgical chemotheraphy in locally advanced cervical cancer: A review of 25 cases
G.M. Favagrossa, G. Superti, E.M. Martin, M. Amato, P.R. Biondetti; *Brescia/IT*

Purpose: To evaluate the usefulness of Magnetic Resonance Imaging (MRI) of the pelvis, before and after neoadjuvant chemiotheraphy (NAC) in patients with locally advanced cervical carcinoma (LACC), FIGO stages I B – IV A, larger than 4 cm.
Methods and materials: 25 patients, 33 – 58 years old, with LACC histologically confirmed (20 squamous cell carcinomas, 4 adenocarcinomas) – FIGO Stage: I B (8), II A (8), II B (7), III A (1), IV A (1) – underwent NAC including in all patients cisplatin, combined with Taxol (9) and other drug associations (16). MRI exam was performed with a 1.5 T superconducting magnet, using T1 and T2 weighted sequences; images were acquired in both sagittal and axial planes. A radical isterectomy was performed in 20 cases; in 1 patient only a surgical exploration was possible; 4 patients underwent radiotheraphy because they didn't responde to NAC.
Results: The evaluation of the two MRI exams in surgical treated patients showed that tumor disappeared (5 cases), decreased (13), didn't decrese (1). Parametrial involvement disappeared (5 cases) and decreased (2), with surgical confirmation in 6 cases. Nodal involvement disappeared in 5 out of 7 patients, with surgical confirmation in 6.
Conclusions: MRI has been excellent to show disappearance or reduction both of tumor and parametrial/nodal involvement. MRI made radical surgery easier and increased the operability rate.

B-0855 14:50

Tumor volume as a predictive factor of longterm prognosis in cervical cancer
R. Forstner, M. Trattner, C.F. Weismann, A. Graf; *Salzburg/AT*

Purpose: To assess the tumor volume as prognostic factor for the overall survival in cervical cancer and to compare MRI and histopathologic volumetric measurements.
Materials and methods: Between 1988 – 1999 in 122 patients with cervical cancer histopathologic volume measurements were performed. In 99 patients MRI was performed with a 1.5 T or a 1 T unit using sagittal and axial T2WI and axial T1WI. In all patients the tumor volume was calculated by the three maximum tumor diameters, furthermore, in 67 patients 3D analysis volumetry was also performed. A correlation between the tumor volumes by MRI, and at histopathology was performed.
Results: Overall survival was significantly influenced by the tumor volume, lymphnode status, and tumor stage. Overall survival for tumor volumes (cm^3): < 2.5 cm: 94 %; 2.5 – 10: 78 %, 11 – 25: 69 %; > 25: 65 %. The two volume measurements assessed with MRI as well as at histopathology correlated significantly. However, a difference was seen between the mean volumes in each method of volume assessment, and MRI volumes tended to be larger than at histopathology.

Conclusion: MRI contributes to the preoperative prediction of the long term survival by assessing the tumor volume. However, volumes tend to be larger than at histopathology.

B-0856 15:00

Preoperative staging of endometrial carcinoma: Accuracy of T2-weighted fast spin echo sequence and dynamic gadolinium-enhanced MR imaging

R. Manfredi, P. Mirk, T. Meloni, P. Margariti, G. Scambia, P. Marano; *Rome/IT*

Purpose: Determination of accuracy of T2-weighted images and dynamic MRI during gadolinium injection in staging endometrial carcinoma.
Materials/methods: 29 consecutive patients with biopsy proven endometrial carcinoma were included in this prospective study. Quantitative image analysis included tumor/myometrium contrast-to-noise ratio during the different phases of the dynamic study. Qualitative image analysis included: Signal intensity on T2WI; visibility of the junctional zone; signal enhancement during the dynamic study; grade of myometrial infiltration; presence/absence of infiltration of the uterine cervix. The sensitivity, specificity and diagnostic accuracy values were calculated for myometrial and cervical invasion of endometrial carcinoma. All patients underwent surgical procedure; surgical-pathologic findings represented the standard of reference.
Results: CNR values were 0.2 pre-contrast, 2.1 arterial phase, 4.9 venous phase, 5.8 equilibrium phase. Endometrial neoplasm appeared hyperintense on T2-WI in 83 % patients, isointense in 14 %, and hypointense in 3 % patient. The junctional zone was visualized in 90 % patients. Subendometrial enhancement, was detected in 41 % patients; early, thick myometrial enhancement in 24 % patients; and enhancement of the whole uterus in 34 % patients. Myometrial infiltration was correctly assessed in 86 % patients; downstaged in 10 % patients and overstaged in 3 % patient. The sensitivity was 89 % and overall diagnostic accuracy 86 %. In the assessment of cervical invasion, we had 10 % true positives, 72 % true negatives, 3 % false positive and 14 % false negatives. The corresponding sensitivity, specificity and diagnostic accuracy of MR imaging in evaluating cervical invasion was 43 %, 95 %, 83 %, respectively.
Conclusion: MR imaging accurately assess endometrial carcinoma before surgery.

B-0857 15:10

Diagnosis of ovarian cancer: Sonography vs. MRI

K. Bock, J. Iwinska-Zelder, V.F. Duda, T. Hardt, K.J. Klose, K.-D. Schulz; *Marburg/DE*

Purpose: The diagnosis of ovarian cancer is often delayed, thus leading to a poorer prognosis. Transvaginal sonography and MRT of the pelvis are preferred methods for further investigation of clinically suspected tumors of the ovaries. Which method or procedure is more appropriate for the prediction and the staging of malignancies?
Materials and methods: We re-evaluated the data of 39 patients with tumors of the adnexes, diagnosed and treated in the women's hospital of the Philipps-University of Marburg during 1993 – 1998. MRT and sonographic images in combination with written interpretations of former investigators were compared to histopathologic diagnoses. Evaluation was performed using defined scoring systems (Mainz-score for sonography, Yamashita-score for MRT).
Results: In 13 malignant and 26 benign tumors we recognised no difference in sensitivity of detection of malignancy (0.92) but reached a higher specificity with MRT than with sonography (0.8 vs 0.48). Staging was more accurate with MRT than with sonography (accuracy 0.62 vs 0.38).
Conclusion: Our results strengthen the indication for multimodal diagnosis, but are in some contradiction to the ACR's "appropriateness criteria" for technical evaluation of clinical suspected adnexal masses, which suggest a higher value of sonography than of MRT (2:1).

B-0858 15:20

Endovaginal ultrasound examination with contrast in the detection of the recurrent ovarian cancer

R.I. Badea, A. Cojocaru, C. Ganea, T. Ciuleanu, M.E. Badea; *Cluj-Napoca/RO*

Aim of the paper: evaluation of transabdominal and endovaginal sonography (EEV) in women with recurrence of operated and chemo treated ovarian cancer (OCOC).
Material: 35 patients (age between 32 – 67 years) with OCOC and clinical and biological suspicion of recurrence.
Method: Complex ultrasound examination (transabdominal and endovaginal) (General Electric LogiQ 500; Siemens Elegra machines); preparation with Macrogol 4 000 with oral administration; basal endovaginal examination followed by a low hydrosonography; administration of Levovist – 2.5 gr i.v. (5 cases).
Results: 34 recurrences were detected by means of ultrasound examination based on the following signs: pelvian tumor (15 cases); peritoneal (7) and liver metastases (1); pelvic (8) and abdominal (5) metastatic lymph nodes; ascitis (8). In 14 cases the CA antigen 125 had normal values. Operation (10 cases) identified the recurrence in 9 cases (1 false positive case).
Discussion and conclusions: (1) Transabdominal songraphy detects large tumors, ascitis and retroperitoneal lymph nodes; (2) EEV identifies small pelvic tumors and lymph nodes under 10 mm; (3) EEV performed in time of the hydrosonography is superior to the conventional EEV examination for the exclusion of the false positive images and for depiction of local tumoral extension; (4) EEV with hydric and intravenous contrast identifies with precision the delimitation and vascularisation of the tumor.

14:00–15:30 **Room P**

Physics in Radiology

SS 1513

Dose and image quality in digital imaging

Chairpersons:
P.P. Dendy (Cambridge/GB)
P. Vittay (Budapest/HU)

B-0859 14:00

Dose and image quality considerations for small field digital imaging systems in mammography

C.P. Lawinski, D. Smith, D.S. Evans, A. Mackenzie, N.S.A. Wells; *London/GB*

Purpose: Recent developments in diagnostic imaging technology have resulted in the gradual replacement of film screen imaging systems by digital devices. One area in which this new technology has been successfully implemented is small field mammography imaging. This presentation reviews the dose and imaging performance of a number of systems. Comparison is also made to film screen imaging.
Materials and methods: Four small field digital imaging systems are currently offered in the UK, all are based on CCD (charge coupled device) technology. Breast dose was assessed using a standard breast phantom. Image quality data was initially obtained using existing full field mammography test objects. However, their use is made difficult by the limited field size. Thus, a small field test object, based on a contrast detail format, was developed. In addition, several numerical parameters, including MTF (modulation transfer function) and DQE (detective quantum efficiency) were derived.
Results: The results showed that when compared to film screen imaging, low contrast sensitivity is improved and limiting resolution is poorer. Dose levels were generally slightly higher for the digital imaging systems. The numerical measurements highlighted certain differences in performance between the four systems.
Conclusions: The use of small field digital imaging for mammography appears a viable alternative to film screen imaging with acceptable dose levels and image quality. Savings of up to 50 % in examination time can result. Recently, in the UK, nearly all mammography X-ray units purchased with a stereotactic attachment have been supplied with a digital imaging option.

B-0860 14:10

A comparative evaluation of breast dose and image quality on full field digital mammography units

D. Smith, C.P. Lawinski; *London/GB*

Purpose: Full field digital imaging systems for mammography have recently been developed and introduced by a number of manufacturers. At the present time there are two such units available to the UK market: GE Senographe 2000D, Trex LoRad Digital Mammography System (DMS)
This project assessed digital imaging to compare its performance to conventional film/screen imaging and to establish its effectiveness within a breast screening programme.
Materials and methods: For each unit, an estimation of the mean glandular dose to the breast was made. This was derived from the measured air kerma and the mAs required to image a Perspex phantom. Image quality was evaluated using a range of test objects including TOR MAX, TOR MAM and RMI 180 contrast-detail phantom. Identical measurements were made on a film/screen system.
Results: The mean glandular dose to the breast using the digital systems was measured as between 1.5 and 2.5 mGy. Images of TOR MAX indicated that digital devices provide an improved small detail detectability, comparable low contrast resolution but poorer high contrast resolution when compared to film. Images of

TOR MAM, indicated that digital imaging was significantly better at displaying circular details than film. Images of particles and filaments were similar for both techniques.
Conclusion: The mean glandular dose to the breast using digital imaging is similar to that received with a film/screen system. Image quality measurements showed that there was a significant increase in low contrast sensitivity but a reduction in the high contrast limiting (spatial) resolution.

B-0861 14:20

Digitization requirements in mammography: A phantom study using ROC analysis
K. Perisinakis, J. Damilakis, J. Stratakis, N. Gourtsoyiannis; *Iraklion/GR*

Purpose: To evaluate the dependence of the detection accuracy of breast lesions on pixel size and pixel depth of the digitized mammograms.
Materials and methods: An ALVIM mammographic statistical phantom based on the modern signal theory and receiver operating characteristic (ROC) analysis was used to acquire images on a GE Senographe DMR mammographic unit. The phantom simulates microcalcifications and fiber lesions of various dimensions. Phantom images simulating breast with thickness 2.4, 3.3 and 4.2 cm were obtained. All films obtained were digitized using a Mikrotek Scanmaker 9600XL film scanner with various combinations of pixel size and pixel depth. Pixel size range was 20 – 250 µm. Pixel depth range was 8 – 12 bit. Digitized images were displayed to 3 observers on the computer monitor and also presented as laser film hard copies on a film viewing box for comparison. Window and level, zoom and pan capabilities were the only digital manipulations allowed during review of the digitized images. Images were evaluated with respect to identification of lesions.
Results: For a given pixel size, the detection accuracy of images digitized at 8 bit was significantly lower than in higher pixel depth ($p < 0.05$). Lesion detectability increased with decreased pixel size down to 40 µm and remained the same for smaller pixel sizes.
Conclusion: Pixel depth of more than 8 bits and pixel size of not higher than 40 µm are required in mammogram digitization to preserve lesion detectability.

B-0862 14:30

Comparison of charge coupled devices and amorphous silicon based technology for full field digital mammography
D.S. Evans[1], A. Mackenzie[1], A. Workman[2]; *[1]London/GB, [2]Belfast/GB*

Purpose: To objectively compare the properties of two technologies used for full field digital mammography; charge coupled devices (CCD) and amorphous-silicon based systems.
Materials and methods: The imaging properties of technologies used for full field digital mammography have been compared in terms of pre-sampled modulation transfer function (MTF) and noise power spectrum, which were used to calculate detective quantum efficiency (DQE).
Results: Film-screen systems demonstrate better MTF response compared with digital systems, especially at those frequencies above the Nyquist frequencies of the digital detectors. This was also demonstrated by the limiting resolution measurements of 11 lp·mm^{-1} and 6 lp·mm^{-1} for the CCD and amorphous-silicon systems and 18 lp·mm^{-1} for the film-screen system. The DQE of the digital detectors are superior to published film-screen data in terms of both the low frequency peak DQE and the exposure latitude over which it is maintained. The digital detectors demonstrated peak DQE of up to approximately 60 % and maintained low frequency DQE above 40 % for a large range of air kerma to the detector. The DQE for film-screen systems peaks at approximately 35 % and is only maintained across a short exposure range.
Conclusion: The objective measures of imaging performance indicate that the peak DQE of the digital detectors compares well with film-screen systems and that it is maintained across a wider range of air kerma. This, coupled with the MTF results, show that the digital systems should be able to visualise small details but that film-screen systems will provide improved shape differentiation of small details.

B-0863 14:40

Grid usefulness in direct digital mammography
W.J.H. Veldkamp, M.A.O. Thijssen, N. Karssemeijer; *Nijmegen/NL*

Purpose: The objective in this study was to determine if and when an anti-scatter grid is needed when a flat panel full field digital mammography detector is used.
Materials and methods: We carried out phantom measurements under various conditions with and without using a grid. The system we used was a GE Senograph 2000D mammography machine. Furthermore, we used a new version of the CDMAM phantom. The phantom covers a range of object sizes and thicknesses representing microcalcifications and small masses. In this version the range of the smallest object diameters has been extended to 60 µm. Breast thickness was simulated by a homogeneous layer of perspex in the range of 1 to 7 cm. Series of images were recorded for different KeV and target-filter combinations depending on the simulated thickness. Software was developed for automatic readout of the direct digital (raw) phantom images.
Results: Preliminary results suggest that for compressed breasts thicker than 5 cm usage of a grid is beneficial. Below 5 cm a grid seems not necessary.
Conclusion: Below a breast thickness of 5 cm the grid can be omitted which may allow lower dose to the patient.

B-0864 14:50

Performance of a digital flat panel detector in the detection of artificial osseous lesions: A comparison with conventional screen-film radiography and phosphor-storage radiography
K. Ludwig[1], H. Lenzen[1], K.-F. Kamm[2], T.M. Link[1], S. Diederich[1], D. Wormanns[1], W. Heindel[1]; *[1]Münster/DE, [2]Hamburg/DE*

Purpose: To compare a digital flat-panel detector in the detection of artificial lesions simulating small osteolyses with a conventional screen-film and a phosphor-storage system at different levels of exposure.
Method/materials: Artificial lesions of varying size (0.5 – 3.0 mm) were created in 100 of 200 predefined regions in 20 porcine femoral specimens. Specimens were enclosed in cylindrical containers filled with water to obtain absorption conditions comparable to a human extremity. Imaging was performed using a flat-panel detector, a conventional screen-film and a phosphor-storage system. Exposure settings identical to those used clinically were used (70 kVp, S = 400). For the flat-panel and the phosphor-storage system additional imaging was performed at lower exposure levels (S = 800, S = 1600, S = 3200). For each predefined region the presence or absence of a lesion was assessed independently by three radiologists according to a five level confidence scale. ROC-analysis was performed for a total of 4 800 observations (600 for each imaging modality/exposure level) and diagnostic performance estimated by the area under the ROC-curve (AUC). Student's paired t-test was used to compare AUC-values.
Results: ROC-analysis showed AUC-values of 0.820 (S = 400), 0.780 (S = 800), 0.758 (S = 1600) and 0.676 (S = 3200) for the flat panel detector, 0.761 (S = 400), 0.725 (S = 800) and 0.662 (S = 1600) for the phosphor-storage system and 0.788 for the conventional screen-film system (S = 400). T-test showed statistical significance of differences between all imaging modality/exposure level combinations ($p < 0.05$).
Conclusions: The flat-panel detector system is superior to conventional screen-film and phophor-storage radiography at clinical exposure settings. It offers the same diagnostic performance with a lower exposure.

B-0865 15:00

Optimisation of the relationship of the dose-image quality for a new direct digital detector
J.R.G. Persliden, K.W. Beckman, H. Geijer, T. Andersson; *Örebro/SE*

Purpose: An easy method for optimisation of digital radiographic images for noise versus image quality is presented. We optimised a pelvis examination using a newly installed direct digital detector (Philips Digital Diagnost) and compared to the existing CR image plates (PCR Philips Medical Systems).
Materials and methods: An Alderson-phantom was radiographed using the new detector at 77 kVp and a wide range of mAs levels. Radiation dose was recorded as Entrance Surface Dose (ESD). In each image, a Region of Interest (ROI) was marked. The standard deviation of pixel values in the ROI (the noise) was plotted as a function of dose. Images at different dose levels were then scored by radiologists according to EU diagnostic criteria for a pelvis examination.
Results: The ESD ranged from about 0.026 mGy to 0.95 mGy at 77 kVp for this pelvic phantom. The noise expressed as standard deviation in the ROI fell rapidly up to about 0.12 mGy but was then relatively constant. The image quality was scored as acceptable from 0.24 mGy. This level was then judged to be the new default dose-value for this type of examination. The dose was reduced from 1.4 mGy as used with the images plates, to 0.24 mGy, a reduction with 83 %.
Conclusions: The method used here was applied to the new direct digital detector but works for all digital radiography. For the pelvis examination we were able to reduce the dose to 17 % of the previously setting with clinically accepted image quality.

B-0866 15:10

Radiation dose and image quality with a flat-panel amorphous silicon digital detector

H. Geijer, K.-W. Beckman, T. Andersson, J. Persliden; *Örebro/SE*

Purpose: The recently introduced flat-panel amorphous silicon digital detectors promise reduced radiation dose for a given image quality. The aim of this study was to investigate the image quality for a flat-panel detector at different radiation dose settings compared to storage phosphor plates and a screen-film system.
Methods and materials: A CDRAD 2.0 contrast-detail phantom was imaged with a flat-panel detector at three different dose levels. Fifteen cm of acrylic was used to simulate the scattering conditions of a human body. The same phantom was also imaged with storage phosphor plates and a 160 speed screen-film system. Entrance surface dose (ESD) was recorded for all images. Four independent observers read three images for each setting.
Results: The flat-panel detector had slightly better image quality at less than half the radiation dose compared to storage phosphor plates (ESD 0.30 mGy versus 0.64 mGy). The difference was even larger when compared to film with the flat-panel detector having almost equal image quality at 18 % of the dose (ESD 0.30 mGy versus 1.7 mGy). With ANOVA, the flat-panel detector had significantly better image quality scores at 70 % of the dose compared to storage phosphor plates.
Conclusion: The flat-panel detector has a very favourable combination of image quality versus radiation dose compared to storage phosphor plates and screen-film. If the promising results of this phantom study can be realised in clinical images, a considerable dose reduction would be achieved in a large proportion of general radiology.

B-0867 15:20

Comparison of image quality for digital chest systems with traditional film/screen combinations

A. Mackenzie, D.S. Evans; *London/GB*

Purpose: A variety of technologies are currently being used or developed for digital chest systems. The imaging properties of the detectors must be quantified to allow comparison of the technologies.
Materials and method: Both film/screen and a range of digital detectors used in chest imaging were tested using a contrast detail test object (CDRAD) in a low scatter configuration for a range of exposure and kV. The high contrast spatial resolution was measured using a Huttner line pair test object.
Results: The film/screen system showed superior high contrast spatial resolution of 7.5 lp·mm^{-1} compared to digital systems which varied from 3.9 to 4.5 lp·mm^{-1}, with CR having the highest resolution. However, the improved signal to noise ratio for digital systems allowed the same visualisation of the smallest low contrast detail sizes. The amorphous-silicon detector showed the best contrast detail, while the 400 speed film and charged selenium drum were similar and the 200 speed CR system was significantly lower. Chest imaging covers a large range of attenuation (lungs and mediastinum), for the higher and lower detector doses using the digital systems performed better due to window and levelling and linear response.
Conclusion: The amorphous-silicon detector showed better image quality. The digital systems have the advantage of window and levelling compared to film/screen combinations and is therefore highly suitable for chest image. There is scope for optimisation of dose and image quality, as the digital systems were operating at higher exposure levels than for film/screen.

16:00–17:30 **Room P**

Genitourinary

SS 1607

Renal and adrenal masses

Chairpersons:
O.M. Al-Shamam (Tripoli/LY)
H. Nishitani (Tokushima/JP)

B-0868

withdrawn by author

B-0869 16:00

Variation of renal cancer vascularization demonstrated by color Doppler sonography

I.I. Dugan, V.V. Medvedev; *Kiev/UA*

Aim: To study distinctive feature of vascularization of various renal cancer histological variants according to the findings of color Doppler sonography.
Material and methods: The results of color Doppler mapping (CDM), power Doppler mapping (PDM) and pulsed Doppler sonography (PD) of kidneys in 133 patients with surgically verified diagnosis were retrospectively studied.
Results: The patients were divided into three groups. The first group included 96 patients with ckear cell renal cell carcinoma (RCC) and 21 with granular cell RCC, the second group 11 patients with spindle cell or sarcoma-like variant of RCC and the third group 5 patients with epithelial carcinoma of renal pelvis (ECRP). In the first group the tumor contained a newly formed vascular network in 78.6 % of observations. Its blood flow was characterized by chaotic state: variety of linear blood flow velocities (from 7 to 155 cm/s), absence of gradient of reducing resistance indices (RI) from large to small blood vesseks. In 48 observation arteriovenous shunting (RI < 0.4) was revealed, in 37 – highly resistants blood vessels (RI < 0.7). In 12.8 % of patients of the first group the tumoral blood vessels were multiple, but separate, in 8.5 % of the blood flow in tumor was absent. The intratumoral blood flow was absent in patients of the second and the third group.
Conclusion: Clear cell and granular cell RCC had a developed vascular network or multiple seps]arate intratumoral blood vessels in 91.4 % of cases. Sarcoma-like RCC and ECRP were avascular in all cases.

B-0870 16:05

Contrast-enhanced power Doppler sonography in the diagnosis of solid renal tumors

J.M. Esteban, L.V. Maldonado, P. Chuan, M. Gil, J.M. Santamaria, F. Ferrando; *Valencia/ES*

Purpose: The objective of this study was to investigate the potential usefulness of contrast-enhanced power Doppler sonography in the differentiation of solid renal lesions.
Materials and methods: Gray-scale and contrast-enhanced power Doppler sonography were performed prospectively in 34 solid renal lesions (15 renal cell carcinomas, 11 angiomyolipomas, two oncocytomas, 6 pseudotumors). The vascularization of the renal masses was investigated by means of power Doppler sonography before and after intravenous injection of ultrasound contrast agent, on the basis of blood flow patterns within and around the lesions and compared them with contrast-enhanced CT scans and pathologic results.
Results: At precontrast scanning, low colour Doppler signal at the periphery or within the lesion was observed in 18/34 patients only. After contrast administration, the signal-to-noise ratio increased, which allowed the visualization of tumor vessels in 28/34 patients, that is to say in all the renal neoplasms. In the cases of pseudotumor contrast-enhaced exam showed normal vascular distribution in the fetal lobations and columns of Bertin and no vascularization was detected in the cases of lobar nephronia.
Conclusion: Our experience suggests that the use of contrast agent improves power Doppler sensitivity in depicting the tumor vessels which were missed at baseline exam.

B-0871 16:10

US and CT findings of xanthogranulomatous pyelonephritis

J. Kim, D. Yu; *Daejeon/KR*

Purpose: To define the US and CT patterns of xanthogranulomatous pyelonephritis (XGP).
Materials and methods: The US and CT findings 21 cases of pathologically proven XGP in 20 patients (bilateral in one patient) were evaluated. The imaging findings, in comparison with pathology, were retrospectively evaluated with regard to extent of the disease, kidney size, the presence of calculi, hydronephrosis, and renal function, by two radiologists, who established a consensus.
Results: Sixteen of the 20 patients were female, and 19 were adult. The age ranged from 3 to 61 years (mean 45). In all patients except one, the disease was unilateral. In one patient, XGP was bilateral, and there were thus 21 cases. Seventeen (81 %) of these were diffuse, four (19 %) were focal; extrarenal extension occurred in 13 cases (62 %), among which ipsilateral pleural effusion was noted in two. The kidney was enlarged diffusely in 12 cases (57 %), and focally in three (14 %); urinary calculi were present in 16 cases (76 %), with staghorn calculi in four of these; and hydronephrosis occurred in 17 (81 %). Impairment of ipsilateral renal function was noted in 13 cases (62 %). Clinical findings of inflammation were noted in all patients.

Conclusion: In addition to nephromegaly, renal function impairment, urinary obstruction due to calculi, which are typical features of XGP, the condition may also show variable US and CT findings. If the images obtained in a middle-aged woman with clinical findings of urinary infection show atypical findings, we believe that XGP should be included in the differential diagnosis.

B-0872 16:20

Diagnostic significant tags of determination of abundance of tumors of kidneys

K.P. Gordiyenko; *Kiev/UA*

Purpose: The definition of abundance of tumoural process is necessary for selection of treatment tactics.

Materials and methods: There were 58 adult patients with the renal-cell carcinoma. Investigation were carried out on the: CT "Somatom HQ" Siemens (Germany); MRI "Bruker R-23" (Germany).

Results: The tumors of kidneys more often met in the age of 50 – 80 years. Constitution of tumors depends on stage and sizes of formation by CT and MRI is determined. It is conditioned by change of a histological constitution of a tumor. The tumors of the small sizes were homogeneous. The complexities at definition of the I St stage of tumors of a kidney were not. The advantage MRI before CT was in definition of tumoural thromboses in a renal vein and vein cave inferior. Yardstick of an estimation of a defeat of lymphatic nodes was increase of their sizes, formation of conglomerates, density change and signal strength. There were two pseudopositive conclusions at single packed lymphatic nodes. The high specificity MRI has resulted in pseudo-positive outcomes at an estimation of a germination of tumors in adjacent organs; (the perifocal edema was valued as germination in adjacent organs).

Conclusion: MRI, like as CT, are useful as a method of selection, which one is independently capable to determine a degree of abundance of tumoural process with accuracy 91.4 – 100.0 %.

B-0873 16:25

Evaluation of patients with hematuria: Value of multislice-CT

M.M. Uggowitzer, A.J. Ruppert-Kohlmayr, T. Meissnitzer, S. Alziebler, T. Colombo; *Graz/AT*

Purpose: To assess advantages of MS-CT in the evaluation of patients with painless hematuria and to assess the diagnostic value of 2D/3D-reconstruction methods.

Methods and materials: A selected group of patients with hematuria of unknown origin were examined with MS-CT. 10 patients underwent unenhanced CT and 32 patients underwent four-phasic CT with small collimation (2.5 mm), including an unenhanced phase, a corticomedullar and a nephrographic phase and an excretory phase using a compression device. Patients with acute flank pain were not included into the study.

Results: 8 transitional cell carcinomas (TCC) of the renal pelvis or ureter, in 6 renal cell carcinomas and 4 angiomyelolipomas have been revealed by MS-CT. In 12 patients non-obstructive calculi have been encountered. Other entities as the probable cause of hematuria included renal infarcts, pyelonephritis and ureteritis. No cause has been revealed in 10 % of patients. 4-phasic CT proved to be very valuable in the diagnosis of renal cell carcinoma. The corticomedullar phase added no additional information in patients with TCC and inflammatory diseases. MPR depicted the extension of intraureteral and intrapelvic masses more clearly whereas volume rendered techniques (VR) showed the relationship between masses, collecting system and vasculature more distinctly than axial slices.

Conclusion: Although radiation dose is considerably high, MS-CT is highly valuable in the detection of morphologic causes of hematuria and may avoid the time-consuming combined use of additional imaging modalities.

B-0874 16:35

Imaging features of cystic renal cell carcinoma

P.R. Biondetti, F. Franco, S. Gianpaolo; *Brescia/IT*

Purpose: The aim of our exhibit is to illustrate the spectrum of imaging features of Cystic Renal Cell Carcinoma (CRCC).

Materials and methods: We report 44 patients (33 males, 11 females; age ranging between 20 and 76 years, mean 52 years) with histologically proved CRCC. The indication for imaging was haematuria (12 cases), flank pain (10 cases), recurrent urinary infections (7 cases); in 15 cases imaging was performed because of symptoms unrelated to the upper urinary tract (incidental detection). All patients had US and CT; 18 patients had also MR; in 8 cases percutaneous needle-biopsy was performed, wich was positive in 2 cases.

Results: According to Bosniak classification, we found a malignant pattern in 26 cases (59 %): irregular or nodular thickening of the cyst wall or of the septa with contrast enhancement. In 15 patients (34 %) the findings were in accordancy with Bosniak type 3 lesion: irregular or nodular thickening of the cyst wall, thick septa, multiloculated aspect without contrast enhancement. In 3 cases (7 %) the main feature was a high density cystic content, indicating a Bosniak type 2 lesion; these patients underwent surgery because symptomatic. In 1 case the lesion failed to be characterised (indeterminate mass).

Conclusions: In our series 47 % of cystic tumors missed a frankly malignant pattern; in these cases Gagolinium-enhanced MR proved the most useful diagnostic tool.

B-0875 16:45

CT and US findings of multilocular cystic renal cell carcinoma

J. Kim[1], K. Kim[2], J. Lee[3]; *[1]Daejeon/KR, [2]Seoul/KR, [3]Pusan/KR*

Purpose: To analyze the imaging findings of multilocular cystic renal cell carcinoma (MCRCC), a recently described variety of renal cell carcinoma with characteristic pathologic and clinical features.

Materials and methods: Ten adult patients with pathologically proven unilateral MCRCC who underwent ultrasonography (US) and computed tomography (CT) were included. Their radiologic findings were retrospectively evaluated for the cystic content, wall, septa, nodularity, and solid portion, by three radiologists who established a consensus. Imaging and pathologic findings were compared.

Results: All patients were adults with age ranging from 33 to 68 (mean 46) years. On US and CT images, all tumors appeared as well-defined multilocular cystic masses composed of serous or complicated fluid. In all patients, unenhanced CT scans revealed hypodense cystic portions, and in four tumors, due to the presence of hemorrhage or gelatinous fluid, some hyperdense areas were also noted. In no tumor was an expansile solid nodule seen in the thin septa. Small areas of solid portion constituting less than 10 % of the entire lesion were found in six of the ten tumors, and these areas were slightly enhanced on contrast-enhanced CT scans.

Conclusion: On US and CT images, MCRCC appeared as a well-defined multilocular cystic mass with serous, proteinaceous or hemorrhagic fluid, with no expansile solid nodules in the thin septa, and sometimes with small slightly enhancing solid area. Where radiologic examinations demonstrates a cystic renal mass of this kind in adult males, MCRCC should be included in the differential diagnosis.

B-0876 16:55

CT guided biopsy in the assessment of renal lesions (Bosinak 3+2 F)

E.K. Lang[1], R. Macchia[2], B. Gayle[2], F. Richter[3]; *[1]New Orleans, LA/US, [2]Brooklyn, NY/US, [3]Newark, NJ/US*

Purpose: Establish efficacy of CT guided biopsy of renal lesions (Bosniak 3) with progression on follow-up versus surgical exploration.

Methods and materials: 60 patients with diagnosis of cystic renal mass (Bosniak 3) by CT and ultrasound showed progressive changes on follow-up imaging examination. (Age 32 – 93, 34 males, 24 females) Underlying medical conditions or age established perference for minimal invasive follow-up in 42. CT guided biopsies and aspirations through a 19 gauge coaxial sheath with a 20 or 21 gauge Chiba or Franseen needle were performed. Specimens were assessed by cytopathology, flow cytometry, and for LDH, amylase, lipids, protein and creatinine. Cultures were performed on all.

Results: A definitive diagnosis was established in 60 patients (abscess 11, haemorrhage 11, cystic renal cell carcinoma 6, other malignancies 1, benign neoplasms 4, complex haemorrhagic and inflammatory cysts 27). 2 lesions misdiagnosed as renal cell carcinoma proved to be a xantogranulomatous pyelonephritis, without calculus, in one and parenchymal haemorrhage in the other.

Conclusion: CT guided biopsy of indeterminate renal masses showing progression on follow-up imaging examination is recommended as minimally invasive, cost effective, low complication rate and reasonably effective procedure.

B-0877 17:05

Detection of small adrenal masses: Prospective comparison of ultrasond and contrast-enhanced spiral CT

W. Schwarz, C.F. Dietrich, J. Trojan, A. Thalhammer, T.J. Vogl; *Frankfurt a. Main/DE*

Purpose: To compare the efficacy of ultrasound to contrast-enhanced spiral CT for detecting of small adrenal tumors and evaluate whether adrenal masses less than 20 mm in size could be routinely detected by sonography.

Materials and methods: 40 patients with 47 adrenal tumors (right adrenal gland masses, n = 17; left, n = 30; bilateral, n = 9; size 22 ± 16 mm; median 16 mm; range 5 ± 80 mm) underwent prospectively high-resolution ultrasound examinations. Sonography were performed unaware of detection and size of pathologic adrenal masses, as documented by contrast-enhanced CT of the adrenal gland region prior to enrollment.

Results: The sensitivity of ultrasound for the detection of adrenal tumors was 100 % for tumors of the right and 87 % for tumors of the left adrenal gland. The specificity of sonography was 89 % for tumors of the right and 90 % for tumors of the left adrenal gland. The sensitivity and specificity of ultrasound for detection of adrenal masses less than 20 mm in size were not significantly different from those of tumors > 20 mm.

Conclusion: Ultrasound is useful for evaluation of adrenal tumors, irrespectively of size. Nevertheless, small tumors of the left adrenal gland might be missed in rare cases. Thus, sonography of adrenal gland can routinely be used for screnning and following up.

B-0878 17:15

Adrenal vein sampling in primary aldosteronism with equivocal CT and MR findings: Results in 104 consecutive patients

M. Chiesura Corona, C. Fittà, G. Rossi, A.C. Pessina, G. Feltrin; *Padova/IT*

Objectives: To investigate the feasibility, sensitivity, specificity and accuracy of adrenal vein sampling in patients with inconclusive CT and MR in the identification of adenoma.

Material and methods: 1990 to 1999, 104 hypertensives were submitted to adrenal vein sampling for measurement of plasma aldosterone (A) and cortisol (C) levels. Selectivity of AVS was assessed by the ratio between C levels in each adrenal vein and in the infrarenal inferior vena cava plasma (C_{side}/C_{IVC}). ROC analysis was carried out to establish the best AVS-derived index to discriminate between patients with and without APA and the degree of selectivity that could provide an accurate diagnosis.

Results: APA (average diameter was 12.2 mm) was diagnosed in 41 patients (40 %). Adrenal vein rupture leading to partial adrenal loss occurred in one patient (0.9 % complication rate). By assuming a cutoff value of $C_{side}/C_{IVC} \geq 1.1$ AVS was selective in 85.7 % on the right and 94.1 % on the left side, and bilaterally in 80.6 % of cases. Of all AVS-derived indexes, the aldosterone/cortisol ratio (A/C) of one over the A/C controlateral side $[(A/C)_{side}/(A/C)_{contr.}]$ furnished the best diagnostic accuracy. With a bilaterally selective AVS, a cut-off value of $(A/C)_{side}/(A/C)_{contr.} \geq 2$ provided a conclusive etiologic diagnosis of PA in 79.7 % of cases.

Conclusions: AVS resulted to be feasible and safe. When bilaterally selective (i.e. $C_{side}/C_{IVS} \geq 1.1$) (80 % of cases), a ratio of $(A/C)_{side}/(A/C)_{contr.} \geq 2$ provided the best compromise of sensitivity and false positive rate for lateralization of the etiology of PA.

Tuesday, March 6

	room A 2nd level	room B 2nd level	room C 2nd level	room E1 entr. level	room E2 entr. level	room F1 entr. level	room F2 entr. level	room G lower level	room H lower level	
08:30										08:30
09:00	**SA 17**	**RC 1710**	**CC 1717**	**RC 1701**	**RC 1702**	**RC 1704**	**WS 1711**	**RC 1705**	**RC 1715**	09:00
09:30										09:30
10:00										10:00
10:30		**SS 1810a** **Musculoskeletal** Densitometry and bone marrow abnormalities *(p. 288)*	**SS 1801a** **Abdominal and Gastrointestinal** Liver: US, CT, MRI *(p. 289)*	**SS 1810b** **Musculoskeletal** Imaging of the hand and elbow *(p. 291)*	**SS 1811a** **Neuro** Spine, CSF studies *(p. 293)*	**SS 1804** **Chest** Chest CT and HRCT *(p. 295)*	**SS 1811b** **Neuro** Pediatrics - Pituitary *(p. 297)*	**SS 1805** **Computer Applications** PACS evaluation and workflow *(p. 299)*	**SS 1809** **Interventional Radiology** Arterial intervention (3) *(p. 301)*	10:30
11:00	**CC 1816**									11:00
11:30										11:30
12:00										12:00
12:30	Junior Image Interpretation Session									12:30
13:00										13:00
13:30	Image Interpretation Session/Cases of the Day Awards									13:30
14:00	Closing Ceremony									14:00
14:30										14:30
15:00										15:00
15:30										15:30
16:00										16:00
16:30										16:30
17:00										17:00
17:30										17:30

	room I lower level	room K lower level	room L/M 1st level	room N/O 1st level	room P lower level	room X entr. level	room Y 1st level	room Z lower level	
08:30									08:30
09:00	**WS 1718**	**RC 1712**	**CC 1716**	**RC 1714**	**SS 1707** **Genitourinary** Male genital tract *(p. 286)*				09:00
09:30									09:30
10:00									10:00
10:30	**SS 1801b** **Abdominal and Gastrointestinal** MRCP *(p. 303)*	**SS 1812** **Pediatric** Chest, airways, and the musculoskeletal system *(p. 304)*	**SS 1808** **Head and Neck** Salivary glands/ Temporomandibul/ r joint *(p. 306)*	**SS 1803** **Cardiac** Heart perfusion *(p. 308)*	**SS 1815** **Vascular** Aorto-iliac vessels *(p. 310)*				10:30
11:00									11:00
11:30									11:30
12:00									12:00
12:30									12:30
13:00									13:00
13:30									13:30
14:00									14:00
14:30									14:30
15:00									15:00
15:30									15:30
16:00									16:00
16:30									16:30
17:00									17:00
17:30									17:30

08:30–10:00 Room P

Genitourinary

SS 1707

Male genital tract

Chairpersons:
M.J. Kellett (London/GB)
R.A. Kubik-Huch (Zürich/CH)

B-0879 08:30

3D power Doppler TRUS in the follow-up of acute prostatitis

M. Kisliakova, V.V. Gajonova, A.V. Zoubarev; *Moscow/RU*

Purpose: To evaluate the role of 3D PD TRUS in monitoring response to treatment in acute prostatitis.
Methods and materials: 35 patients (age range 18 – 56 years) with acute prostatitis underwent TRUS examination before, during and after treatment (from 2 to 5 TRUS examinations per patient, depending on the follow-up results). Vascularity of the prostate and of all focal lesions were studied using 2D Power Doppler (2D PD) and 3D Power Doppler (3D PD). All system settings were constant in each patient throughout the follow-up study. 2D PD results were compared with 3D PD data. US-results were compared with clinical and laboratory data.
Results: Changes in echogenicity allows monitoring of the response to treatment in grey scale TRUS in 71 % of patients. 2D PD failed in 18 (51 %) cases to determine changes in vascularity. Reconstructed 3D images simplify follow-up evaluation of the vascularity in acute prostatitis. 3D PD TRUS allowed depiction of the overall vascularity of the prostate and in focal lesions and demonstrated excellent compatibility of the follow-up data. TRUS grey scale and 3D PD results were similar in monitoring response to treatment in acute prostatitis with clinical and laboratory data in all 100 % cases.
Conclusion: 3D PD TRUS was superior to 2D PD in depiction of the vascularity in acute prostatitis. Changes in echogenicity and vascularity allowed monitoring of the response to treatment in acute prostatitis. 3D PD TRUS is a useful tool in monitoring response to treatment in acute bacterial prostatitis.

B-0880 08:40

New diagnostic approach for biopsy localization of prostatic nodules using MRI-phased array coil

V. Panebianco, C. Catalano, A. Laghi, I. Sansoni, R. Alcetta, M. Ciccariello, R. Passariello; *Rome/IT*

Purpose: To determine the role of the MRI using polarized phase array coil to predict site of neoplastic nodule at transrectal ultrasound-guided biopsy.
Method and materials: 91 patients (age range 50 – 81 a) with high PSA values (7 – 84 ng/ml) and negative (28) or doubtful (63) TRUS. MRI examination were performed on 1.5 T Vision plus (Siemens), using phase-array coil. A 2D FSE sequence was used on axial, sagittal, coronal planes, with TR 4300, TE eff. 132, ETL 33, matrix 420 × 512, FOV 280, Phase oversampling 80 %. A T1 weighted GRE sequence was also used to evaluate pelvic anatomy (FLASH 2D, TR 117.3, TE 4.1, matrix 140 × 256). Total examination time was less than 20 minutes. Biopsy results were considered "gold standard" for statistical porpouse.
Results: We observed in all patients good anatomical details of the prostate gland. In all examinations, we found peripheral zone having changes with different morphology: 15 round, 13 lobular, 23 plaque (suggestive for neoplastic changes); 5 linear, 33 triangular, 40 bilateral strips (suggestive for inflammatory changes). Concerning the staging, we observed capsular involvement in 18 cases, seminal involvement in 15, lymphoadenopaties in 15 cases. Sites of cancer predicted by MRI well correlated with sites of cancer at biopsy. There were 3 false negative MRI results among patients undergoing subsequent biopsy.
Conclusions: MRI is a valid mean to value prostatic gland anatomy and to identify and "characterize" prostate cancer in patients with negative or doubtful TRUS findings. Nodule localization on MR images is well correlated to echo-guided biopsy site.

B-0881 08:50

The effects of PC SPES-therapy on prostate cancer as determined by magnetic resonance imaging and spectroscopic imaging: A preliminary report

A.E. Wefer[1], D. Vigneron[2], H. Hricak[3], M. Swanson[2], J. Wefer[1], M. Galanski[1], J. Kurhanewicz[2]; *[1]Hannover/DE, [2]San Francisco, CA/US, [3]New York, NY/US*

Purpose: To investigate the morphologic and metabolic effects of the popular PC SPES herbal therapy on prostate cancer using magnetic resonance imaging (MRI) and spectroscopic imaging (MRSI).
Materials and methods: Fifteen patients (mean age 60 years, SD 6.3) taking PC SPES for prostate cancer (mean therapy duration 7.3 months, average dose 5.2 caps/day) underwent endorectal MRI and MRSI (25 exams total). MRI and MRSI findings were reported by sextant using a standardized anatomic model of the prostate. Regions of cancer within the peripheral zone were identified based on low signal intensity on T2 weighted MR images and compared with changes in serum PSA levels. Abnormal metabolism was defined on MRSI as (choline+creatine)/citrate ratio > 2 SD above normal values, atrophy on MRSI if choline and citrate signal/noise ratios were < 5.
Results: MRI/MRSI detected regions of healthy peripheral zone tissue in 13 of 15 patients. Although a significant decrease in PSA ($p = 0.004$) was observed among the patient population, regions of cancer were detected by MRSI in all patients. Atrophic voxels were observed in 6 patients (mean: voxels 13.2 %; mean therapy 7.2 months, range 0.4 – 18), and no atrophy in 9 patients (mean therapy 7.2 months, range 2 – 13). There was no significant correlation between MRI/MRSI findings and PC SPES duration, dosage and Serum-PSA.
Conclusions: A heterogeneous morphologic and metabolic effect of PC SPES was observed, with imaging findings indicative of prostate cancer even in cases of marked PSA response to PC SPES.

B-0882 08:55

3D transrectal power Doppler sonography in the assessment of response to radiotherapy of prostate cancer

V.V. Gajonova, A.V. Zoubarev; *Moscow/RU*

Purpose: To study dynamic changes of US parameters after radiotherapy (RT) in PC and correlate them with dynamic changes of PSA data and define the value of 3D PD TRUS.
Method and materials: 100 patients with biopsy proved PC that received a combined hormonal and RT were examined by 3D PD TRUS with a 3 months interval to 24 months. Dynamic changes of PSA level and of US parameters (glandular and residual tumor volumes – R (TV), echogenicity, grey scale intensity, vascularity degree) were evaluated. Reduction time of PSA and US parameters were studied. Dynamic curves of the changes of different US parameters were modulated. Progression or regression of the disease was evaluated based on clinical, laboratory data and US results.
Results: Mean reduction time of R (TV) and PSA level were the most accurate in assessment of RT effect. Reconstructed 3-D PD images simplified the follow-up evaluation of the R (TV) and improved standardization of comparative US data. R (TV) and PSA were accurate in predictive poor outcome in 5 pts that developed clinical recurrences with distant metastasis or local tumor growth 12 to 15 months after RT. 3D PD TRUS data correlated with PSA in 95 % of cases.
Conclusions: TRUS is a useful tool in the follow-up of RT treated patients. Dynamic changes in R (TV) with PSA allowed non-invasive and accurate monitoring of the response to treatment in PC. We believe that application of 3D PD TRUS in the PC follow-up algorithm will enhance detection of the residual cancer.

B-0883 09:05

Role of MRI using phased-array coil in identification of local prostatic cancer recurrence after radical surgery

V. Panebianco, A. Laghi, C. Catalano, M. Ciccariello, I. Sansoni, A. Bartolomucci, R. Passariello; *Rome/IT*

Purpose: To assess the effectiveness of MRI using phased array coil in identifying early prostate cancer recurrences
Method and materials: 35 patients considered at risk for prostate cancer recurrence (PSA values 12 – 56 ng/ml) following total prostatectomy were referred for MRI. All patients had been submitted to radiation theraphy after surgery. MRI examinations were performed on a 1.5 T Siemens Vision plus MR imager, using a circularly polarized phased array coil, without using an endorectal coil. A 2D FSE sequence was used on axial, sagittal and coronal planes, with TR 4300, TE eff. 132, ETL 33, matrix 420 × 512, FOV 280, Phase oversampling 80 %. A T1 weighted GRE sequence was also used to evaluate the pelvic anatomy (FLASH 2D, TR

156, TE 2.3 ms, matrix 131 x 256, TA 20 s). This sequence was repeated after i.v. injection of Gd-DTPA (0.0025 mmol/kg). Total examination time was less than 20 minutes.
Results: In all patients good anatomical details of the prostatic area could be evaluated using the phased array coil. We observed cancer recurrence in 27 patients. All nodules were detected as: hypointense on T1 weigheted images and mildly hyperintense on T2 weigheted images. After Gd-DTPA injection in 19 nodules strong enhancement, in 6 moderate enhancement and in 2 nodules no enhancement were found. Confirmation of diagnosis was obtained in all positive cases at biopsy or surgical removal.
Conclusions: MRI is a valid technique to assess recurrence of prostate cancer. The use of a phased array coil, with injection of Gd-DTPA represent a non invasive and easily reproducible method in the follow up of these patients.

B-0884 09:15

Value of MR imaging and MR-urography in the differential diagnosis of prostatic and periprostatic cysts
G.M. Heinz-Peer, A. Etele-Hainz, W. Reiter, L. Zaunbauer, M. Marberger, G. Lechner; *Vienna/AT*

Purpose: To evaluate the value of MR imaging and MR-Urography in the differential diagnosis of periprostatic cysts.
Methods and materials: MR imaging and MR-Urography was performed on 12 patients with the clinical suspicion of congenital prostatic or periprostatic cysts. The admission for MR examination was based on digital rectal examination and on sonography in all patients. Patients with congenital cysts additionally underwent conventional techniques like voiding cystography and retrograde urethrography. An intravenous urography was performed on 2 patients. 6 patients underwent cystoscopy. A fine needle aspiration with histological and cytological examination was performed on 4 patients. One patient underwent surgical resection of the cyst.
Results: MR imaging showed 15 cystic lesions (mean volume 5.37 ± 1.83 cm^3) in 12 patients with congenital prostatic and periprostatic cysts. On the basis of MR-urography the diagnosis of seminal vesicle cysts was established in 7/12 patients. 3 patients presented with an utriculus cyst. On 2 patients a Müllerian duct cyst was diagnosed. All patients with seminal vesicle cysts were found to have renal agenesis. On one patient a contralateral hydroureteronephrosis was observed. In addition, in this patient an ectopic insertion of the ipsilateral ureter was suspected.
Conclusions: MR imaging allows an excellent depiction of congenital prostatic and periprostatic cysts. In addition, together with MR-urography it is of great value in the differential diagnosis of congenital cysts.

B-0885 09:25

Mumps orchitis: Ultrasound diagnosis, follow-up and clinical correlation
M.K. Sapundzieski, M. Zezoski, J.S. Jordanoski, A. Risteski; *Prilep/MK*

Aim: Mumps orchitis often lead to infertility. We like to present the most frequent ultrasound changes in this disease, and through follow up and clinical correlation to select patients for early treatment.
Materials and methods: There were 566 patients with mumps in 1996. 73 of them had also orchitis. Four years later, during 02 – 03/2000 we reviewed again 34 of them, aged among 17 – 26 years. Scrotal ultrasound examination was done using 7.5 MHz linear probe, measuring size and echogenicity of both testicles and other scrotal findings. Ultrasound was correlated with clinicians examination and with native, quantitative spermatogram.
Results: 12/34 patients had normal scrotal ultrasound examination. In 22/34 (64.7 %), there were pathologic findings: small testicular size in 20 (58.8 %), heterogeneous testicular parenchyma due to chronic orchitis in 20 (58.8 %), varicocele in 8 (23.8 %), small hydrocele in 3 (8.8 %) and parenchymal calcifications in 2 (5.9 %). Correlation with clinician was positive in 82.4 %, and with native spermatogram in 75 %. The most pathologic findings were unilateral.
Conclusion: Scrotal ultrasound is of great help in diagnosis and follows up of patients with mumps orchitis. Although patterns are not characteristic, selecting of abnormal findings is essential for prevention and early treatment.

B-0886 09:30

Iontophoresis for treatment of peyronie's disease: Assessment of high frequency ultrasonography
G. Helweg, A. Klauser, H. Madersbacher, M. Daniaux, P. Soegner, F. Frauscher, D. zur Nedden; *Innsbruck/AT*

Purpose: Peyronie's disease is a debilitating and mutilating condition. Non-surgical treatments show limited efficacy. Promising preliminary results on iontophoresis, a non-invasive method to enhance transdermal drug transport, are reported. The goal of our study was to assess the value of high-frequency ultrasonography (US) in patients with peyronie's disease treated with iontophoresis.
Method/materials: Twelve patients with peyronie's disease were investigated using high-frequency US (12 MHz probe, Siemens Elegra, Germany) before and after iontophoresis. The iontophoresis was performed 3 times a week with 5 mA for 20 minutes via 2 electrodes connected to the chamber and to an abdominal pad. In each session 10 mg verapamil and 4 mg dexamethasone are administered. The sonographically assessed plaque size and echogenicity was evaluated and compared with the clinical outcome.
Results: In 9 of 12 patients (75 %) we found a significant decrease of plaque size ($p < 0.01$). Eight patients (66 %) presenting with hyperechoic fibrous plaques showed post-treatment a substantial loss of echogenicity. Penile pain during erection disappeared in 10 patients (83 %) and recurvatum diminished in 7 patients (58 %). The sonographic findings correlated well with the clinical outcome ($r^2 = 0.85$).
Conclusions: High-frequency US provides excellent information about morphological changes resulting from iontophoresis and proved to be helpful in therapeutic follow-up of patients suffering from peyronie's disease.

B-0887 09:40

Transurethral alprostadil administration with MUSE ("Medicated Urethral System for Erection"): Assessment of hemodynamic effects by color coded Doppler ultrasound in men with erectile dysfunction
M. Daniaux, M. Studen, F. Frauscher, A. Klauser, L. Pallwein, G. Helweg, G. Bartsch, D. zur Nedden; *Innsbruck/AT*

Purpose: The goal of our study was to evaluate the hemodynamic effects of transurethral alprostadil administration with MUSE ("Medicated Urethral System for Erection") in patients with erectile dysfunction using color coded Doppler ultrasound (US).
Method/materials: Forty-eight patients (age range: 19 – 71 a) presenting with erectile dysfunction underwent color coded Doppler US examination. Peak systolic velocity (PSV), end diastolic velocity (EDV), time averaged velocity (TAV), resitive index (RI), pulsatility index (PI) and penile arterial diameter were measured in the cavernous arteries over 30 minutes (one measurement each 5 minutes). We compared the sonographic findings following transurethral administration of 1000 µg alprostadil (MUSE) and intracavernosal injection of 10 µg alprostadil. Response of vasoactive agents was classified according to the International Index of Erectile Function (IIEF).
Results: A dose of 1000 µg transurethral alprostadil resulted in significant increases in PSV, TAV, RI and PI and cavernous artery diameter in 26 of 48 patients (55 %) and in 39 of 48 patients (82 %) after intracavernosal injection of 10 µg alprostadil. The EDV was significantly higher after transurethral alprostadil (mean: 7.1 cm/s) compared with intracavernosal injections (mean: 2.6 cm/s) ($p < 0.01$). Transurethral alprostadil resulted in satisfactory reactions (IIEF score: 24 – 30) in 22 of 48 patients (46 %) and intracavernosal injections in 40 of 48 patients (83 %).
Conclusions: The advantage of the technically easy use of the transurethral alprostadil administration is confronted with a considerably lower efficacy. Therefore intracavernosal injection must be further on considered the "gold standard" in alprostadil administration to test for patient responsiveness to local vasoactive agents.

B-0888 09:50

MRI of penile fracture: Diagnosis and therapeutic follow-up
M. Uder, D. Gohl, M. Takahashi, H. Derouet, B. Kramann; *Homburg a. d. Saar/DE*

Purpose: The rupture of the corpus cavernosum is a rare injury of the erected penis. The present study describes the role of magnetic resonance imaging (MRI) for diagnosis and therapeutic follow-up of this injury.
Methods: Four patients with suspected penile fracture were examined by MRI. 1, 6 and 12 weeks after surgical repair of the penile fracture MRI examinations were performed.
Results: In all patients T1-weighted images demonstrated a rupture of the corpus cavernosum as discontinuity of low signal intensity of tunica albuginea. Concomitant subcutaneous hematoma was visualised on T1- and T2-weighted images.

Haematomas in the corpus cavernosum could be best differentiated on contrast enhanced T1-weighted images. Findings were confirmed intraoperatively. In all cases similar healing process was observed. During the healing process, the tunical suture showed an increase in signal intensity on the T1-weighted spin echo sequences. The healing tunica albuginea tissue showed a contrast enhancement. After four months the tunica showed again a low signal intensity on all SE-sequences. These findings can be explained by the formation of vascularised granulation tissue during cicatrisation.
Conclusion: Even if experiences are limited, MRI seems to be a promising imaging modality for the diagnosis and follow-up examination of penile fractures.

10:30–12:00 **Room B**

Musculoskeletal

SS 1810a

Densitometry and bone marrow abnormalities

Chairpersons:
L. Diankov (Sofia/BG)
H.K. Genant (San Francisco, CA/US)

B-0889 10:30

High resolution MRI of the calcaneus in post-menopausal females with and without osteoporotic spinal fractures
T.M. Link[1], V. Vieth[2], J. Matheis[2], W. Heindel[2], E.J. Rummeny[1], S. Majumdar[3];
[1]Munich/DE, [2]Münster/DE, [3]San Francisco, CA/US

Purpose: The purpose of this study was to compare BMD of the spine and hip with structure measures obtained from high resolution (HR) magnetic resonance (MR) images of the calcaneus in the prediction of spine fracture status.
Material and methods: The study population consisted of 20 postmenopausal female patients with osteoporotic spine fractures and 20 age-matched postmenopausal controls. Axial and sagittal HR MR images of the calcaneus were obtained in all females using a T1-weighted spin-echo sequence with a slice thickness of 1 mm and an in plane spatial resolution of 0.195 × 0.195 mm. Texture analysis was performed using morphological parameters, analogous to standard histomorphometry. Additionally, BMD of the spine was obtained using quantitative computed tomography (QCT) and of the hip with dual-energy X-ray absorptiometry (DXA).
Results: Significant differences between both patient groups were obtained using BMD of the spine (115.5 versus 62.7 mg/ml, $P < 0.01$) and hip (femur neck: 0.91 versus 0.74 mg/cm^2, $P = 0.038$) as well as using morphological parameters in the HR MR images of the calcaneus (app. BV/TV: 0.33 versus 0.23, $P < 0.01$, app. Tb.Sp 0.52 versus 0.68, $P < 0.01$).
Conclusion: In this study BMD of the spine and structure measures of the calcaneus were best suited to predict the osteoporotic fracture status of the spine while BMD of the hip showed a lower but still significant discrimination of fracture and non-fracture patients.

B-0890 10:40

Vertebral fractal analysis: A potential method for BMD and fracture risk evaluation
G. Feltrin, C. Dus, E. Tosi, C. Saccavini; *Padova/IT*

Purpose: Increased bone fragility is the base for fracture risk; and the architectural changes of sponge bone is the most important cause of fragility. While BMD evaluates the bone mass loss, it doesn't evaluate the bone elasticity or fragility. We have attempted by fractal analysis the evaluation of trabecular bone texture.
Methods and materials: In the first step we studied 45 autoptic human lumbar vertebrae with conventional radiography (CR), HRCT, QCT and vertebral section microradiography. Furthermore the images of microradiography obtained were analyzed by a computed fractal study to evaluate the cancellous structure.
In the second step we studied 150 female patients underwent to the procedure to rule out osteoporosis with lumbar spine CR, spiral CT and BMD. The spiral CT images are evaluated by fractal analysis (FA), calculated by FD3 (a program written by J. Sarraille and Peter di Falco).
Results: We observed a good correlation between BMD and Fractal dimension on autoptic vertebrae. In fact in osteoporotic patients we have found an ordered structure but a minimal structural complexity. The FA values are strictly correlated ($r = 0.94$) to the correspondent BMD.
We compared in patients BMD and FA values on vertebral cancellous structure with satisfactory correlation.
Conclusions: Fractal analysis of spiral CT images should be used to evaluate the trabecular texture, mineralization of bone and fracture risk even in living patients to obtain a supplemental parameter of BMD evaluation and possibly of scheletal deterioration.

B-0891 10:50

Impact of renal transplantation on the calcaneal trabecular bone architecture
T.M. Link[1], S. Waldt[1], O. Saborowski[2], D. Newitt[3], Y. Lu[3], S. Majumdar[3];
[1]Munich/DE, [2]Münster/DE, [3]San Francisco, CA/US

Purpose: High resolution magnetic resonance imaging (HR-MRI) of the calcaneus was performed in patients pre- and post-renal transplantation to analyze the trabecular bone structure and to compare this technique with bone mineral density (BMD) in predicting osteoporotic fracture status.
Material and methods: HR-MRI of the calcaneus was performed at 1.5 T in 48 patients post- (6 – 120 months) and 12 patients pre-renal transplantation. Structure measures analogous to bone histomorphometry were calculated. BMD of the lumbar spine was determined using quantitative computed tomography (QCT). In addition fracture status of the spine and the peripheral skeleton was assessed.
Results: Structure measures showed no significant differences between patients pre-and post-renal transplantation for both structures measures and BMD. Osteoporotic fractures were found in 3 of the 12 pre- and 16 of the 48 post-transplant patients. Structure measures and BMD were lower in patients with fractures; differences, were significant for some of the structure measures, spine BMD but not for hip BMD.
Conclusion: Differences between pre-and post-renal transplant patients were not significant for both structure measurements and BMD. However, significant differences were found in the fracture and non-fracture patients for some of the structure measures and BMD of the spine; the best results were found for a combination of both.

B-0892 11:00

The value of the STIR-sequence to rule out suspected osteomyelitis
A.H. Mahnken, A. Bücker, G.B. Adam, R.W. Günther; *Aachen/DE*

Purpose: To assess the necessity of Gd-DTPA enhanced MR-sequences after inconspicuous Short-Tau Inversion-Recovery (STIR) sequence to rule out the diagnosis of osteomyelitis.
Material and methods: Two experienced radiologists retrospectively analyzed 112 MR examinations performed for clinical suspected osteomyelitis. All examinations were performed at 0.5 T including STIR, T1-weighted spin echo sequences (T1 SE) before and after application of Gd-DTPA. T2-weighted images were obtained in 93 cases. STIR sequences were evaluated first, followed by T1 SE and T2-weigthed images. Diagnoses were established by follow-up (80), operation (22) and biopsy (10).
Results: Osteomyelitis was diagnosed in 53 cases. The remaining 59 cases yielded other diagnoses. Sensitivity and specificity of the STIR sequence were 100 % and 49.2 % respectively. Specificity reached 79.7 % by including T1 SE images and increased to 83.1 % when contrast enhanced images were considered additionally. T2-weighted images added no further information.
Conclusion: An inconspicuous STIR sequence alone sufficiently rules out the diagnosis of osteomyelitis. The STIR sequence with additional T1 SE images demonstrates a high sensitivity and specificity for osteomyelitis.

B-0893 11:10

Functional MRI in Paget's disease of bone: Correlation of bone perfusion and metabolism
M. Libicher, M. Daniels, C. Kasperk, L. Grenacher, G.W. Kauffmann;
Heidelberg/DE

Purpose: To describe bone perfusion in Paget's disease of bone with dynamic contrast enhanced MR imaging. To compare results with corresponding bone parameters.
Material/methods: 20 patients with Paget's disease (17 men, 3 women, aged 58 – 76 years) were examined with conventional and dynamic MRI at 1.5 T. For dynamic MRI, a saturation recovery TurboFLASH sequence was used with a high temporal resolution of 13 slices per ten sections. Signal time changes were analyzed using a pharmacokinetic model and computed parameter values were visualized by color-coded overlay (parametric images). Pharmacokinetic parameters (amplitude A; exchange rate constant k21) were correlated to parameters of bone metabolism.

Results: A significant association was found between amplitude A and alkaline phosphatase ($r = 0.7$, $p < 0.01$). Parametric images showed high perfusion areas in active Paget's disease whereas in treated patients perfusion was significant lower. Furthermore regional perfusion within bone could be evaluated.
Conclusion: Dynamic contrast enhanced MRI can describe bone perfusion in Paget's disease. There is a significant correlation of bone perfusion and metabolic activity. This might be a diagnostic strategy for evaluation of activity or monitoring therapy of Paget's disease of bone.

B-0894 11:20

MRSI of bone marrow in patients with leukemia
O.W. Schulte, H. Kugel, C. Jung, B. Krug, M. Jensen, K. Lackner; *Cologne/DE*

Purpose: To demonstrate the correlation between the changes in the fat-water ratio of bone marrow as a parameter for response to chemotherapy.
Method/materials: Volume selective ^1H spectroscopy was performed using a standard 1.5 T imaging system (Gyroscan ACS NT, Powertrak 6000). In 20 patients with acute myelocytic or lymphatic leukemia, T1-and T2-weighted imaging in the coronal and sagittal direction was performed, a ≤ 8 cm^3 measurement volume was positioned in the bone marrow of a lumbar vertebra. Using the PRESS sequence without water suppression (TE 40 ms, TR 2000 ms, bandwidth 1 kHz), examinations were performed before and during chemotherapy (after 1, 2, 3, 4, 5 months of treatment). Fat-water ratios were determined and correlated with bone marrow histology and peripheral blood counts. Age-related standard values for water-fat content were used as a reference.
Results: In healthy people, the fat-water ratio is ~1, while fat content increases with age. Our examinations of patients with acute leukemia revealed that their bone marrow produces very low lipid signals and a high water signals, probably due to the markedly higher cellularity of pathologic bone marrow. Shortly after chemotherapy, the water signal was found to decrease and the fat signal normalized. An increased water signal after chemotherapy proved a poor prognostic factor for recurrence.
Conclusions: Bone marrow ^1H spectroscopy is a useful and noninvasive method for determining fat-water ratios as a parameter for predicting response to chemotherapy. Further studies are required before this promising tool can be implemented in clinical routine.

B-0895 11:30

An update on the use of ultrasound in osteomyelitis
A.K. Nath, A.U. Sethu; *Muscat/OM*

Objectives: An update study with 200 patients of our previously published paper "Nath AK, Sethu AU", AUG 1992, Use of ultrasound in osteomyelitis, (BJR) Vol. 65, No. 776, 649–652 which had 25 patients.
Methods: Plain radiographs of the affected area and sonography of the affected and the opposite normal area was performed in 200 patients clinically suspected of having osteomyelitis. Sonograms were obtained using 7.5 MHz phased array linear transducer. Needle aspiration or surgery was performed to confirm diagnosis.
Results: 120 of the 200 patients had osteomyelitis, sonographically revealing fluid in contact with the bone with no intervening soft tissue. The fluid proved to be pus. 120 osteomyelitis patients had (a) radiograph and ultrasound positive – 50 patients (b) radiograph normal initially but ultrasound positive – 70 patients. 50 patients had following findings – 30 patients had soft tissue abscesses, 10 patients had cellulitis and 10 were normal. Limitations of ultrasound in suspected osteomyelitis in remaining 30 patients, will be highlighted, as seen in sickle cell disease (10 pts), septic arthritis (10 pts), epiphyseal ostomyelitis (7 pts) and Brodies abscess (3 pts).
Conclusions: Ultrasound is useful in (1) Predicting osteomyelitis (2) differentiating osteomyelitis from soft tissue abscesses (3) localizing the lesions (4) followup while on management.

B-0896 11:40

Natural history of Type 1 vertebral end plate changes on MR of the lumbar spine
I.W. McCall, D. Mitra, V. Cassar-Pullicino; *Oswestry/GB*

Purpose: To study the natural history of Type 1 vertebral lesions which have. decreased signal on T1 and increased signal on T2 and their relationship with low back pain.
Method: MR studies of patients with back pain over a 4 year period were reviewed. Those with Type 1 changes were invited for repeat MR. Sagittal T1 SE, T2 TSE and axial T2 TSE were performed. Symptoms at the two MR studies were compared.
Results: 30 patients, age range 29 – 68 (mean 46) and M:F 1:3 had repeat MR. 13 (40.6 %) Type 1 levels changed, 12 to Type 2 (increased signal on T1, T2) and 1 to Type 3 (low signal T1, T2). 6 (18.7 %) partially changed to Type 2. 1 patient remained unchanged at 3 years and 12 (37.5 %) showed increased extent and/or increased T2 signal intensity of Type 1 changes. 44 % of those that changed from type 1 to 2 were within 2 years. 10 (33.3 %) patients had significant improvement in symptoms of which 7 (70 %) showed change of Type 1 to 2 or 3 and in 3 (30 %). Type 1 changes were worse. 13 (43.3 %) had no change in symptoms and Type 1 changes fully or partially resolved in 9 (64 %) and were worse in 4 (28 %). 7 (23.3 %) patients had increased pain of which 4 (57 %) had increased Type 1 changes.
Conclusion: Most Type 1 changes convert to Type 2, many within two years. Symptoms tend to improve or remain static during this change and increase if Type 1 changes become more pronounced.

B-0897 11:50

Longitudinal evaluation of high intensity zones (HIZ) on MR of the lumbar intervertebral disc
I.W. McCall, D. Mitra, V.N. Cassar-Pullicino; *Oswestry/GB*

Purpose: The natural history of HIZ is unclear and the relationship with pain over time has not been reported. We evaluate the appearances of HIZ over time and relate any changes to back pain symptoms.
Material and method: Lumbar MR studies over a period of five years were reviewed. Those with a HIZ were invited for a further MR. Sagittal T1 SE, T2 TSE and an Axial T2 were performed. The patient compared the present symptoms with those at the time of the previous study. A disability questionnaire was also completed.
Results: 41 patients with an age range of 25 – 58 (mean 44.5) years and M: F of 1:1 were imaged. Three patients had two level involvement. There was no change in the HIZ in 17 (38.7 %), 11 (25 %) resolved, 7 (15.9 %) were larger or more intense and 9 (20.4 %) were smaller and/or less intense. There was no relationship between the changes in HIZ and the time between initial and repeat MR. 18 (43.9 %) had improved symptoms, 13 (31.7 %) were unchanged and 10 (24.3 %) were worse. There was no relationship between symptom changes and the time from the initial study or alterations in the HIZ.
Conclusion: HIZ reflect a pathological tear in the annulus which is slow to change and which has no clear relationship to changes in symptoms.

10:30–12:00 **Room C**

Abdominal and Gastrointestinal

SS 1801a

Liver: US, CT, MRI

Chairpersons:
W.R. Lees (London/GB)
H. Mori (Oita/JP)

B-0898 10:30

Detection and characterization of focal liver lesions: A diagnostic algorithm
W. Schima, E. Schober, A. Ba-Ssalamah, M. Scharitzer, F. Laengle, F. Wrba; *Vienna/AT*

Purpose: A wide range of benign and malignant focal disease processes can affect the liver. Therefore, not only tumor detection, but also reliable characterization of the lesions is an important radiologic task. A multi-modality approach for rational work-up of liver lesions is presented.
Materials and methods: Since 1996, an algorithm has been developed at our institution for detection and characterization of focal liver lesions, including US, CT, MRI, scintigraphy, and biopsy.
Results: Ultrasound is currently used as a screening tool for detection of focal liver lesions. Depending on the findings and the suspected diagnosis at US, the decision is made to use either multi-phasic contrast-enhanced helical CT, contrast-enhanced MRI, or to go straight to biopsy. Contrast-enhanced MRI using the range of liver-specific and nonspecific MR contrast agents has evolved as a problem solving tool for characterization of liver nodules. Our approach of a rational diagnostic algorithm is presented and the different diagnostic pathways are demonstrated by examples.
Conclusion: In the era of increasing cost constraints the adherence to diagnostic algorithms for detection and characterization of liver lesions provides an accurate diagnosis and avoids redundancy.

B-0899 10:40

Comparison of diagnoses made of liver lesions by B-mode and unenhanced color and power Doppler US, contrast-enhanced Doppler US and spiral-CT: Results of a multicenter study

M. Beissert[1], M. Jenett[1], S. Delorme[2], M. Bahner[2], S. Mutze[3], S. Filimonow[3], W.R. Lees[4], A.R. Gillams[4], A. Bauer[5]; *[1]Würzburg/DE, [2]Heidelberg/DE, [3]Berlin/DE, [4]London/GB, [5]Schering/DE*

Purpose: To compare diagnoses in liver lesions using B-mode and unenhanced color and power Doppler US, contrast-enhanced Doppler, and spiral-CT with the discharge diagnosis.

Materials and methods: From the records of a multicenter study including 90 liver lesions investigated with B-mode, baseline and contrast-enhanced color and power Doppler, and spiral CT, those were evaluated where diagnoses for all modalities were available, and the discharge diagnosis based upon all clinical, labaratory and imaging data, and histologic proof had been classified as at least "highly probable".

Results: 60 lesions met the criteria. 20 lesions were ultimately diagnosed as benign, and 40 as malignant. The sensitivity was 92.5 % (37/40) with B-mode US and unenhanced color and power Doppler, 97.5 % (39/40) with contrast-enhanced Doppler, and 100 % with CT. The specifity was 65 % (13/20) with B-mode and unenhanced Doppler, 85 % (17/20) with contrast-enhanced Doppler, and 80 % (16/20) with CT. 4 of 7 false positively, and 2 of 3 false negatively classified lesions (unenhanced technique) were correctly diagnosed with contrast-enhanced Doppler.

Conclusion: Contrast-enhanced Doppler improved diagnostic results in 6 of 60 cases and was not associated with additional diagnostic errors. Its accuracy was equal to the accuracy with CT.

B-0900 10:50

Contrast-enhanced phase inversion ultrasound vs. dual phase spiral CT in the detection of liver metastasis: A prospective study with intraoperative sonographic correlation

T. Albrecht, C.W. Hoffmann, S. Schettler, S.A. Schmitz, C.T. Germer, J. Ritz, A. Overberg, X. Bolze, K.-J. Wolf; *Berlin/DE*

Purpose: To compare phase/pulse inversion ultrasound (PIUS) during the late liver-specific phase of Levovist (Schering AG, Berlin, Germany) with dual phase spiral CT in the detection of hepatic metastases using IOUS as the gold standard.

Materials and methods: 20 patients undergoing abdominal surgery for malignancy were included.

US: An unenhanced baseline scan including tissue harmonic and a PIUS scan 3 min after iv injection of Levovist (2.5 – 4 g, 400 mg/ml) were performed by a blinded sonographer using Sonoline Elegra (Siemens, Issaquah, USA) or HDI 5000 (ATL, Bothell, USA) equipment.

CT: Arterial and portal venous phase scans after 150 ml iohexol (300 mgI/ml) were performed at 5 mm collimation, 4 mm reconstruction interval, pitch: 1.5 with a Somatom plus 4Q scanner (Siemens, Erlangen, Germany) and read blindedly.

US and CT findings were correlated with IOUS.

Results: IOUS showed a total of 60 metastases in 14 patients, 6 patients had no metastases. Average sensitivity to individual lesions was 74 % for unenhanced US, 83 % for contrast-enhanced PIUS and 84 % for spiral CT. Both PIUS and spiral CT produced 6 false positive lesions. Subcentimeter lesions were present in 6 patients (IOUS) of which 5 were detected with PIUS and 4 with CT.

Discussion: Contrast-enhanced PI US was as sensitive as dual phase spiral CT in the detection of liver metastases. Both modalities had a false positive rate of 10 %.

B-0901 11:00

Characterization of focal hepatic lesions: Ultrasound with a coded harmonic angio technique using a microbubble contrast agent

H.-J. Jang, H.K. Lim, W. Lee, S. Kim; *Seoul/KR*

Purpose: Coded harmonic angio (CHA) is a new ultrasound technique that provides highly sensitive images to microbubble contrast agent at medium mechanical index. The purpose of this study is to describe coded harmonic angio (CHA) findings of common focal hepatic lesions with emphasis on lesion characterization.

Materials and methods: Thirty-nine patients with 48 lesions (20 hepatocellular carcinomas (HCC), 15 metastases, and 13 hemangiomas). Ultrasound was performed on CHA (mechanical index: 0.6 – 0.8) technique with a 2 – 5 MHz probe (LogiQ 700 EXPERT; GE Medical Systems). Scans were obtained from 20 s to 5 minutes after intravenous bolus injection of 300 mg/l of SH U 508A. For first 70 s (early phase), images were obtained with continuous scan, and during the following period (late phase), with 1 minute interval delay scan.

Results: For 20 HCCs, branching intratumoral vessels were seen in 14 lesions while stippled pattern was observed in the remaining six. Stimulated acoustic emission (SAE) imaging showed strong high signals during early phase in 10 HCCs and low signals during late phase in 17. Twelve of 15 metastases showed peripheral stippled vascularity. All metastases appeared as cold lesions on emission imaging. No hemangioma shows intratumoral vascularity. On emission imaging, typical peripheral globular enhancement pattern were seen in 12 of 13 hemangiomas and centripetal progression was observed in eight of them.

Conclusion: CHA technique enabled both continuous scan during early phase to depict intratumoral vasculature and intermittent sweeping for acoustic emission imaging, and thus provided helpful characteristic findings in differentiating focal hepatic lesions.

B-0902 11:10

Characterization of unifocal liver lesions with pulse inversion harmonic imaging (PIHI)

E. Quaia, M. Bertolotto, M. Locatelli, L. Dalla Palma; *Trieste/IT*

Purpose: To evaluate if Pulse Inversion Harmonic Imaging (PIHI) could characterize unifocal liver lesions with spiral CT as gold standard.

Materials and methods: 59 consecutive patients with unifocal liver lesions identified by B-mode US [8 hepatocellular carcinomas (HCC), 2 intrahepatic cholangiocarcinomas, 7 focal nodular hyperplasias (FNH), 19 capillary hemangiomas, 8 cavernous hemangiomas and 15 metastasis] were evaluated by PIHI after bolus injection of Levovist on vascular (30 seconds) and late phase (2 – 3 minutes) and by triphasic spiral CT.

Results: On B-mode HCCs revealed different echo-patterns, while they appeared always hyperechoic on vascular phase and prevalently (6/8) hypoechoic on late phase. FNHs were hypoechoic on B-mode in most of cases (6/7), hyperechoic on vascular phase (5/7), while on late phase the pattern was variable, isoechoic (4/7), hyperechoic (2/7) or hypoechoic (1/7). Hyperechoic capillary hemangiomas (14/19) presented variable pattern on vascular phase while they were prevalently isoechoic (12/14) on late phase. Hypoechoic capillary hemangiomas (5/19) presented a variable pattern on vascular phase while they were prevalently isoechoic (4/5) on late phase. Cavernous hemangiomas revealed peripheral enhancement on 30 s scan extending centripetally on late phase. Cholangiocarcinoma revealed unhomogeneous enhancement. On B-mode, single metastasis pattern was variable, while they were hypoechoic on all scans.

Conclusions: The difference between HCC, cavernous hemangioma, cholangiocarcinoma and single metastasis is clear. Capillary hemangiomas present a typical pattern if they are hyperechoic on B-mode, while, when they appear hypoechoic, they reveal a similar pattern to FNH. The PIHI pattern versus spiral CT will be discussed.

B-0903 11:20

Detection of liver metastases: Comparison of state-of-the-art single-slice and multi-slice spiral CT

B. van Drünen, N. Kendzierski, R. Spielmann, D. Pickuth; *Halle a. d. Saale/DE*

Purpose: The purpose of this work was to compare state-of-the-art single-slice (SSCT) and multi-slice spiral CT (MSCT) in the detection and characterization of secondary liver neoplasms.

Patients and methods: 20 consecutive patients with 84 liver metastases had triphasic scans of the liver with SSCT (SOMATOM Plus 4, Siemens) and subsequently with MSCT (SOMATOM Plus 4 Volume Zoom, Siemens) using optimized protocols. The diagnostic value of SSCT and MSCT was compared intraindividually. The number of hepatic lesions, the overall lesion detection, and the characterization of liver metastases was evaluated by consensus.

Results: No statistically significant difference in the lesion detection was observed. However, in 43 % of cases lesion margins, internal structure, and vessel infiltration could be better assessed with MSCT than with SSCT, especially when multiplanar reformations and 3D shaded surface displays were used. MSCT allowed clear differentiation between vital and necrotic tumour tissue in all cases.

Conclusion: SSCT and MSCT are approximately equivalent for lesion detection. However, MSCT improves the characterization of liver metastases and the shorter data-acquisition times make the examination much better tolerated by the patient. Furthermore, MSCT provides better image reconstruction relative to SSCT.

B-0904 11:30

Color and power Doppler with contrast enhancement (US angiography) in determination of types of vascularization of liver hemangiomas

S.V. Kourotchkine, R.F. Bachtiozin, I.V. Kliouchkine, D.V. Passynkov, Y.A. Kliouchkina; *Kazan/RU*

Purpose: To estimate the US angiography possibility in determination of types vascularization of liver hemangiomas and further differential diagnosis with other liver lesions.

Methods and materials: 51 patients with different localization liver hemangiomas (34 "typical" and 17 "atypical") were examined by Color and Power Doppler before and after Levovist administration. MRI in 49 patients was the second and final step in diagnostic algorithm. Hystomorphological verification were done in 2 cases.

Results: Type I – with "feeding" arteries in large distance. Type II – we registered many color signals ("feeding" arteries and color spots). In this patients fast filling and "wash out" effect we were registered during MRI with contrast enhancement (DCMRI). Type III was characterized of single "feeding" artery with small distance and rare color spots with venous or combined blood flow. And digital angiography clearly demonstrated the "feeding" artery with contrast delay in parenchimatous phase.

Conclusion: Using US angiography we can evaluate and determinate various types of liver hemangiomas vascularization like CT and DCMRI.

B-0905 11:35

Liver metastases: New aspects in diagnosis

S.V. Kourotchkine, R.F. Bachtiozin, M. Kourotchkina; *Kazan/RU*

Purpose: To study the blood flow in livers with metastases by US Color angiography.

Materials and methods: 14 patients with liver metastases (5 with total disease) were examined using 128XP10 scanner with Color and Power Doppler with Levovist. PI of "feeding" vessel in metastatic lesion, IP (Index Perfusion of lesion as lesion vessels/cm^2 (sec)) and DPI (Doppler Index Perfusion as hepatic artery blood flow/total hepatic blood flow (ml/min)) were studied.

Results: Metastatic disease was mainly (72 %) characterized by portal hypertension (DPI 0.48 ± 0.13). In patients with total disease, hyperarterialization of the liver was noted (arterial blood flow was 1303 ± 950.9 ml/min). Low portal blood flow (some times less then 750 ml/min) was registered in patients with moderate disease. PI of "feeding" vessels was less then 0.9 (0.75 ± 0.29). We also noted unknown blood flow of "feeding" vessel (33 %) and "claw" or "nipper" symptom (vessels around the metastatic focus like crayfish claw) in 36 % patients.

Conclusion: US Color angiography is the best method for evaluating blood flow in the liver with metastases and determination of new signs in differential diagnosis from other liver lesions.

B-0906 11:40

Diagnosis and natural history of hemangioma in the cirrhotic liver

G. Brancatelli[1], M.P. Federle[1], A. Blachar[1], L. Grazioli[2], K.M. Pealer[1]; *[1]Pittsburgh, PA/US, [2]Brescia/IT*

Purpose: To report the diagnosis by computed tomography (CT) and magnetic resonance (MR) imaging and natural history of cavernous hemangioma in the cirrhotic liver.

Material and methods: The imaging and pathologic findings of 21 hemangiomas in 17 patients were retrospectively reviewed. CT of the liver was performed in all patients, and MR imaging in 4. Cirrhosis was confirmed histologically in all patients, and the diagnosis of hemangioma was based on histopathology (15 patients; 18 hemangiomas) or on strict imaging criteria (2 patients; 3 hemangiomas). Ten patients had imaging follow up. The number, sizes, location, attenuation, pattern of enhancement, exophytic growth, presence of capsular retraction and size stability were evaluated.

Results: Of the total of 21 hemangiomas, five were not detected at CT or MR. Hemangiomas were subcapsular (12 of 16, 75 %), demonstrated exophytic growth (2 of 16, 12 %), nodular peripheral enhancement (14 of 16, 87 %) and were isoattenuating to blood vessels (16 of 16, 100 %). On MR all 5 hemangiomas demonstrated nodular peripheral enhancement and hyperintensity on T2-weighted images. Seven lesions became smaller on follow-up, and five lesions developed retraction of the hepatic capsule.

Conclusion: Even within the cirrhotic liver, larger hemangiomas can usually be diagnosed confidently with CT or MR. With progressive cirrhosis, however, hemangiomas are likely to decrease in size, become more fibrotic and are difficult to diagnose radiologically and pathologically.

B-0907 11:50

US angiography in evaluation of the vascularisation and differential diagnosis of some liver lesions

S.V. Kourotchkine, R.F. Bakhtiozin, I.V. Kliouchkine, D.V. Passynkov, Y.A. Kliouchkina; *Kazan/RU*

Purpose: To define the role of US angiography in evaluating the vascularity and differential diagnosis of some liver lesions.

Materials and methods: A total of 72 patients with hemangiomas (51), HCC (11), adenoma (4), FNH (6) were examined before and after contrast (Levovist) enhancement using and Acuson 128XP10 scanner with Color and Power Doppler. The final diagnosis of liver lesions was made by CT, MRI and histologic verification.

Results: The main ultrasound signs of hemangioma were: "avascular" ("typical" hemangiomas) lesions (75 %); PI of "feeding" vessels in "atypical" hemangiomas 0.9 ± 61617; 0.18; no "mass-effect" (83 %) and no portal hypertension in "atypical" lesions (94 %). For HCC we noted rich vascularization (73 %); PI of "feeding" vessel ≤ 0.9; lesions with neoangio-genesis (27 %); IP (Index Perfusion as lesions vessels/cm^2 (s)) – 0.17 ± 0.03. Ultrasound signs for adenoma were similar to FNH: no portal hypertension (100 %); mean PI of adenoma "feeding" vessel – 1.0 ± 0.6 and for FNH – 1.07 ± 0.1; IP was 0.14 ± 0.06 ($p < 0.02$).

Conclusion: Using US angiography we have a good possibility for simultaneous: evaluation of vascularisation and differential diagnosis of some liver lesions.

B-0908 11:55

Ultrasonography in the diagnosis and treatment (low invasive interventions) of acute cholecystitis

M.V. Konkova, P.G. Kondratenko, M.B. Pervak, A.F. Elin, A.A. Vasilyev; *Donetsk/UA*

Purpose: To determine the role of ultrasonography in the diagnosis and treatment of patients with acute cholecystitis (AC).

Methods and materials: 850 patients aged 12 to 97 years were studied. Ultrasonography was performed on the apparatus "Ultramark 4 Plus", with a 3.5 MEGC convex transducer. Ultrasonographically controlled transcutaneous transhepatic microcholecystostomy (TTMCS) was performed with Chiba needles and "pig tail" catheters using a "free hand" technique.

Results: Sonographic sings of catarrhal, destructive and complicated forms of AC were determined. Accuracy of sonographically-aided preoperative diagnosis of catarrhal, phlegmonous and gangrenous forms of AC was 90, 85 and 82 %, respectively. It allowed us to amend the tactics of treating patients with AC. TTMCS was performed in 138 patients with high operative risk. Bile leakage around the drain was noted in 3 (22 %) patients who underwent laparoscopic cholecystostomy. Laparoscopic cholecystectomy was performed in 754 patients, including 42 after TTMCS. Indications and counterindications for using TTMCS in AC were determined.

Conclusions: The study results show a high efficacy for sonography in the diagnosis and treatment of patients with AC.

10:30–12:00 **Room E1**

Musculoskeletal

SS 1810b

Imaging of the hand and elbow

Chairpersons:
A. Chevrot (Paris/FR)
V.M. Metz (Vienna/AT)

B-0909 10:30

High-resolution CT of the scaphoid: Technique and results

R.R. Schmitt, S.C. Froehner, G. Coblenz, G. Christopoulos, K.-H. Kalb, U. Bartelmann, P. Hahn, H. Krimmer; *Bad Neustadt a. d. Saale/DE*

Purpose: To detect traumatic lesions of the scaphoid and degenerative changes of the periscaphoidal joints by using high-resolution CT, and to compare the results to conventional radiograms.

Method and materials: A total of 690 CT exams were done on 564 patients suffering from acute trauma or chronic wrist pain (126 control exams). Oblique sagittal scans parallel to the long axis of the scaphoid were performed: 1 mm thickness, FoV 60 mm, high-resolution reconstruction and MPR's.

Results: 68 acute fractures were detected, either exclusively with CT or in greater extension compared to X-ray's, and in 104 doubtful cases lesions could be excluded. 146 CT's were done after treatment, and 151 exams to stage the extent of non-unions. Finally, in 196 cases arthrodeses of the scapho-trapezio-trapezoidal joints were controlled. High-resolution CT was significantly superior to X-ray in detecting (a) acute fractures and their extension, (b) humpback deformity, (c) the fracture consolidation or the delayed union and nonunion, (d) precise morphology of nonunions, and (e) posttraumatic osteoarthritis in the radiocarpal or/and mediocarpal joints.
Conclusion: High-resolution CT of the wrist is highly recommended for imaging the acutely injured scaphoid, in the follow-up after therapy, in detecting and staging delayed unions and nonunions of the scaphoid, and for the early diagnosis of posttraumatic osteoarthritis.

B-0910 10:40

Computed tomography in wrist fracture evaluation: Comparison of conventional with spiral CT with multiplanar volume reconstruction
G. Superti, G.M. Favagrossa, M. Amato, F. Franco, A. Di Gaspare, E. Orlandi, D. Guidetti, P.R. Biondetti; *Brescia/IT*

Purpose: To compare wrist computed tomography (WCT) performed by conventional scanner with multiplanar volume reconstructive tecnique (MVRT).
Method and materials: We studied 90 patients with certain (59 cases) or doubtfull (31) wrist fractures. A WCT exam with direct axial, sagittal and coronal sections was performed in 27 patients, using a conventional scanner (CT Pace – General Electric), with 1 mm slice thickness and 1 mm table increment. A spiral WCT (HiSpeed – General Electric) was performed in 45 cases with direct axial sections and using slice thickness of 1 mm (pitch 1.0) and MVRT images in coronal and sagittal planes. In 18 patients we performed both multiplanar WCT with conventional scanner and spiral WCT in axial plane and MVRT.
Results: In the 27 patients studied with conventional scanner WCT showed fractures in 21 cases clearly. In the 45 patients examinated with spiral scanner and MVRT, WCT showed well defined fractures in 33 cases. In the 18 patients who were examinated both with conventional scanner and spiral scanner with MVRT we discovered fractures in the same 14 cases.
Conclusions: In our experience spiral CT of the wrist with MVRT is similar to conventional CT in diagnostic value. Spiral CT is better in decreasing global time examination and allowing an adequate exam in all patients.

B-0911 10:50

Clinical evaluation of 3-compartment wrist arthrography and arthro-CT vs. wrist arthroscopy
G. Scheurecker, M.C. Freund, M. Lutz, S. Pechlaner, W. Jaschke; *Innsbruck/AT*

Purpose: To compare the effectiveness of 3-compartment wrist-arthrography combined with arthro-CT (AG+CT) versus wrist-arthroscopy (AS) for scapho-lunate ligament (SLL), luno-triquetral ligament (LTL) and triangular fibrocartilage (TFC) defects.
Material & methods: In 58 patients (18 – 69 years) the affected wrist was examined initially by conventional 3-compartment wrist-arthrography with digital subtraction technique during injection followed by digital stress images. Afterwards spiral arthro-CT was performed in the semi-coronal and axial plane with 1 mm slice thickness and secondary true-coronal and sagittal reconstructions. Within 1 month arthroscopy was performed in general anesthesia utilizing standard joint entry points combined with routine digital picture archiving. Both examinations were evaluated for SLL, LTL and TFC defects.
Results: Following detection rates were observed for defects of the SLL, LTL and TFC (AG+CT positive – AS negative/AG+CT negativ – AS positive/AG+CT – AS positive/AG+CT – AS negative): SLL: 4/9/16/16; LTL: 10/4/13/29; TFC: 5/2/25/31. Using AS as the "gold standard" this translates into following sensitivity (%), specificity (%), and accuracy values (%) for AG+CT: SLL 59.2/76.5/92.6; LTL 76.5/75.6/75.8; TFC 92.6/76.2/70.7.
Conclusion: AG+CT detects to a moderate degree SLL, LTL and TFC defects; however defects are more reliably displayed on the ulnar than on the radial wrist side. Therefore AG+CT may represent a reliable less-invasive imaging alternative compared to AS for ulnar-sided pathology.

B-0912 11:00

Multislice CT-arthrography of the wrist: Are direct coronal slices still usefull?
T. Ludig, S. Iochum, L. Catel, F. Walter, J. Roland, A. Blum; *Nancy/FR*

Purpose: To determine the value of coronal and sagittal MPR compared to direct coronal slices in the diagnosis of wrist ligament tears.
Materials and methods: 35 patients with wrist pain underwent CT-arthrography with a multislice CT scan (Somatom VZ, Siemens) to depict ligaments tears. The CT-arthrography protocol consisted of transaxial and direct coronal slices 0.5 mm thick, completed with coronal and sagittal MPR, 1 mm thick. The final diagnosis was retained by consensus by two radiologists. Axial vs direct coronal slices and axial slices vs MPR were analysed. CT arthrographies were independently reviewed by two radiologists who assessed the wrist ligaments tears and the size of TFCC tears (< 1, 1 – 3, > 3 mm).
Results: 35 % of the patients had a scapho-lunate tear, 42 % had a luno-triquetral tear and 24 % a TFCC tear. The degree of intra and inter-observer reproducibility for the assessment of ligament tears was excellent (respectively Kappa = 0.94 and 0.89). The degree of agreement between the two groups of images was excellent for the diagnosis of ligament tear: K = 0.96 and 0.98 for the scapho-lunate ligament, K = 1 and 0.98 for the TFCC and K = 0.86 and 0.78 for the lunotriquetral ligament. However, the degree of agreement was moderate for the evaluation of the size of the TFCC tear (respectively Kappa = 0.62 and 0.47).
Conclusion: CT arthrography with 0.5 mm axial slices provides excellent MPR for assessment of wrist ligaments tears. Direct coronal views could be avoided in many situations.

B-0913 11:10

Evaluation of carpal tunnel release failure: Role of high resolution ultrasound and power Doppler
E.A. Gallardo sr., I.M. Barber jr., J. Guillén jr., X.C. Serres sr., X.C. Pruna sr., V.F. Garriga sr.; *Granollers/ES*

Purpose: To demonstrate the utility of High Resolution Ultrasound (HRUS) and Power Doppler (PD) in the assessment of the causes of carpal tunnel release failure (CTRF).
Material and methods: We studied 90 wrists in 63 patients after 2 – 36 months from the CTR. We performed axial and longitudinal scans in neutral position of the wrist, using a multifrequency linear probe, 9 – 13 MHz (Logiq 700, GE). We evaluated the median nerve (MN) echotexture, its proximal area and its vascularization. We also studied the presence of hypertrophic scar, tenosynovitis or flexor retinaculum reformation. We correlated these findings with clinical outcome and secondary surgery.
Results: 65 (72 %) wrists were asymptomatic and HRUS demonstrated a normal MN echotexture in 98 % of them. 25 (28 %) wrists were symptomatic and HRUS depicted the following findings: 13 cases of reentrapment of the MN in the distal tunnel, 6 cases of hypertrophic scar and 4 of tenosynovitis. These last 10 patients had a good outcome with conservative treatment.
Conclusions:
HRUS and PD are very useful methods in the diagnosis of CTR failure, allowing an accurate therapeutic approach.

B-0914 11:20

High resolution sonography in the assessment of carpal tunnel syndrome (CTS)
E.S. Antipa, M. Tsouroulas, A. Michaelides, G. Panagopoulos, A. Tsikkini, K. Andrianopoulos, K. Karageorgiou, K. Stringaris; *Athens/GR*

Purpose: To determine the role of high resolution sonography in the diagnosis and grading of the Carpal Tunnel Syndrome (CTS).
Materials and methods: 37 wrists of 19 patients (12 women and 7 men, age range: 28 – 72) with clinical evidence of Carpal Tunnel Syndrome underwent ultrasound examination using a 5 – 12 MHz linear transducer in an ATL-5000 HDI unit. Ultrasound findings were compared to EMG findings as well as to ultrasound findings of 40 normal wrists. EMG is considered to be a method of high sensitivity and specificity in the diagnosis of CTS. EMG and ultrasound findings were classified as mild, moderate and severe. The anteroposterior dimension of the carpal tunnel, the maximum median nerve anteroposterior and transverse diameters and cross sectional area were evaluated.
Results: In 34/37 cases both methods accurately diagnosed CTS. There were 2 false negative and 1 false positive ultrasound results. All patients had increased anteroposterior diameter of the carpal tunnel. Sensitivity was 94 % for ultrasound in comparison to EMG in the diagnosis of CTS. Finally in 4/37 wrists there was overestimation of the grading of CTS by sonography.
Conclusion: HR Sonography is a highly accurate method and it should be strongly considered as a new diagnostic modality for the evaluation and grading of Carpal Tunnel Syndrome.

B-0915 11:30

Closed rupture of the extensor tendon of the hand: Evaluation with ultrasound

C. Walch, G. Bodner; *Innsbruck/AT*

Purpose: Closed extensor tendon ruptures of the hand are clinically difficult to diagnose due to local swelling and hematoma. We performed this study to assess the feasibility and accuracy of high resolution ultrasonography in closed extensor tendon rupture.

Method/material: 18 patients were clinically suspected having a rupture of the extensot tendon of the hand. In all cases the examination was performed in using a linear array working at 12 MHz using a HDI 5000 (Advanced Technology Laboratories, Washington, USA).

Results: In more than the half of the cases (n = 10) clinically suspected extensor tendon rupture were confirmed by high resolution ultrasonography. A retraction of the proximal stump of the extensor tendon was a typical sign for complete tendon rupture. Three cases showed a capsular lesion with fliud collection surrounding the tendons. In one case we detected a complete annular pulley rupture, producing an insufficient finger extension, I n other three cases rupture of the capsular holding apparatus was found.

Conclusions: High resolution ultrasonography is a simple, fast, in expensive but significant method to diagnose extensor tendonrupture of the hand and to detect other pathologic conditions in reduced finger extension.

B-0916 11:40

MR-imaging of chronic epicondylitis: Usefulness of Gd-DTPA administration

S.C.A. Herber, P. Kalden, C. Riedel, K.-F. Kreitner; *Mainz/DE*

Purpose: To evaluate the usefulness of iv contrast administration in patients with chronic lateral epicondylitis.

Patients and methods: 42 consecutive patients with chronic epicondylitis and 10 ellbow joints of 5 healthy volunteers were evaluated retrospectively. MR-protocol at 1.0 T comprised STIR-, T2*-weighted FLASH-2D- and T2-weighted TSE-sequences in the coronal and axial plane as well as a fat-suppressed T1-weighted SE-sequence before and after iv Gd-DTPA in the coronal plane. Image assessment included the signal intensity, the integrity of the common extensor tendon, the collateral ligaments and joint capsule, as well as the presence of joint effusion or bone marrow edema.

Results: 39/42 patients showed an increased signal intensity (SI) at the insertion of the extensor tendons on STIR-images as well as on T1-weighted fat-suppressed images after iv contrast application. A partial tear of the extensor tendon was diagnosed in 17/42 and a complete tear in 3/42 patients. The lateral collateral ligament showed an increased SI in 17/42 cases. A joint effusion in 13/42 patients. 8/10 elbow joints of healthy volunteers did not reveal any pathological finiding, however, in one case each an increased SI and a bone marrow edema could be observed. Compared to unenhanced imaging, the application of iv. contrast did not provide any additional information with regard to the analyzed anatomical structures.

Conclusion: Increased SI of the extensor tendon and the lateral collateral ligament are characteristic findings in patients with epicondylitis, but can be seen in asymptomatic patients as well. The use of iv. contrast agents is not neccessary.

B-0917

withdrawn by author

B-0918 11:50

Synovial fringe of the elbow: Normal arthro-MRI findings and pathology

T. Robba, C. Faletti, G. Regis, M. Larciprete; *Turin/IT*

Introduction: A synovial fringe is physiologically present on the posterolateral side of the elbow joint. This has a fibrocartilaginous component and forms a meniscus like structure, which increase joint stability. This fringe may be involved in the elbow distorsion and in sport/work related repetitive trauma.

Methods and materials: We enrolled 9 patients with elbow pain on lateral side, functional impairment and no clinical signs of lateral epicondilytis. They underwent radiography, US, standard MRI and, if standard MRI was negative, arthroMRI. Finally we correlated the radiological results with the arthroscopic finding.

Results: In 1 patient X-rays showed a meniscus-like calcification on the lateral articular side. US was always negative. In 3 cases standard MRI showed a posterolateral synovial inflammatory reaction; in the other 7 patients the arthroMRI demonstrated the presence of pathology of the synovial fringe. 4 cases were of degenerative change and in 2 cases it was displaced posteriorly. The MRI findings were always confirmed at the arthroscopy.

Conclusions: The arthroMRI proved to be a very useful examination in cases of a suspected synovial fringe pathology and negative results of xrays, US and the standard MRI.

10:30–12:00 **Room E2**

Neuro

SS 1811a

Spine, CSF studies

Chairpersons:
C. Manelfe (Toulouse/FR)
P.M. Parizel (Antwerp/BE)

B-0919 10:30

Evolution of intevertebral disk herniation: Assessment by MRI with i.v. administration of contrast medium

G. Cerone, M. Gallucci, A. Splendiani, S. Delli Colli, M. Di Pietro, M. Sabatini, C. Masciocchi; *L'Aquila/IT*

Purpose: Disk herniation demonstrates a natural tendency toward anatomical and clinical regression in up to 70 % of cases. The aim of our study was to look for eventual predictive signs of evolution offered by MRI.

Methods and material: Fifty patients, affected by acute intervertebral disc herniation, were enrolled. A 1.5 T magnet, SE T1w and FSE T2w sequences on axial and sagittal planes, before and after contrast injection were employed. The following parameters were considered: age, sex, level and size of disc herniation, its relationship with the spinal canal, clinical onset interval, type of herniation, distinguishing focal bulge from extrusion and free fragments, disc herniation signal intensity and pattern of contrast enhancement. After 6 months all the patients underwent clinical-MRI follow up: disk herniation size and contrast enhancement pattern variations were evaluated.

Results: Spontaneous regression of disk herniation was found in 32 cases. Better clinical-anatomical results were identified from registered in free fragments (spontaneous regression in 100 % of cases), in cases with hyperintense extruded disks and in cases with peripheral enhancement at the first exam (83 % of regressions). Rest in bed for at least 15 days were a significant factor. No relationship with side, size and level was found.

Conclusion: MRI offers signs predictive of the natural history of disk herniation, thus helping in its prognostic assessment.

B-0920 10:40

Contrast-enhaced magnetic resonance in lumbar disk herniation: Does the type and pattern of enhacement have a prognostic value?

A. Ramos, M. Alcaraz, S. Sirvent, J. Gonzalez Preciado, S. Fernandez; *Getafe/ES*

Objective: The aim of our study was to demostrate that there is a correlation of intervertebral disk herniation enhacement with the course of the desease process, in patients with acute-onset of radiculopaty secondary to disk herniation.

Methods: Pattients suffering from acute sciatica and lumbar disk herniation diagnosed by Computed Tomography were included in the study, and those with another morfologic causes of sciatica were excluded. We performed a prospective study: patients underwent physical examination and Magnetic Resonanace imaging (all using GD) every four months; and enhacement and type of enhacement, size, location and type of disk herniation were measured in correlation with clinical manifestations measured.

Results: Magnetic Resonanace study demostrate enhacement of the disk herniation in 75 % of 100 patients. Disk herniation size was: 2 cm in 4 % of the cases. 37 % of disk herniations were extruded and 63 % were subligamentous disk herniations. Homogeneous enhacement was noted in 39 % of the disk herniations, heterogeneous enhacement in33 % and peripheral enhacement in 28 %. We present the results of the follow-up along one year in fifty patients.

Conclusion: The purpose of this prospective study was to define imaging criteria like type and pattern of enhacement on Magnetic Resonance correlated with clinical outcomes, with prognostic patterns might allow earlier patient selection for treatment. Disk herniation enhacement on GD-Magnetic studies seems to be a favourite prognostic factor, in correlation with clinical and radiological findings.

B-0921 10:45

MRI and electromyographic findings of para-spinal muscle changes in patients with intra-foraminal disk herniation

F. Iannessi, M. Gallucci, A. Splendiani, R. De Amicis, F. D'Emidio, C. Porto, C. Masciocchi; *L'Aquila/IT*

Purpose: This paper aims to evaluate changes in para-spinal musculature in patients with intra-foraminal disk herniation using MRI and electromyography.
Materials and method: Thirty-eight patients aging from 20 to 50 years, affected by unilateral intra-foraminal disk herniation entered this study. All the patients underwent MR examination (1.5 T unit); sequences employed were FSE T2W and FSE T1W on sagittal scan plane and FSE T2W with and without fat saturation on axial scan plane. The axial slab covered both the vertebral bodies above and below the disk herniation. Using an arbitrary visual scale 2 radiologists blinded to the presence of the disk herniation evaluated the muscular structures. Paraspinal musculature were electromyographycally successfully evaluated in 22 cases.
Results: We divided patients into two groups: group A 26 patients (clinical onset during the past three months), group B 12 patients (clinical onset before the last three months) In all the patients of group B axial scan planes revealed asymmetry of the para-spinal musculature because of diseased side atrophy with concomitant enlargement of the fat tissue regions. In the group A 10 patients revealed normality of the muscular structure and 16 showed mild asymmetry in absence of fat tissue regions enlargement. Electromyography revealed different degrees of nerve involvement in both groups of patients.
Conclusion: In case of nerve rooth compression MR is able to detect late paraspinal muscle atrophic changes related to denervation of the dorsal branch of the spinal nerve. EMG demonstrated better sensibility in earlier phases.

B-0922 10:55

Application of multidetector helical scanning to postmyelographic CT

K. Tsuchiya, S. Katase, A. Yoshino, A. Osawa, J. Hachiya; *Tokyo/JP*

Purpose: To determine the value of helical scanning by multidetector (MD) CT in postmyelographic CT.
Methods and materials: Postmyelographic CT was performed on an MD-CT scanner (Aquilion, Toshiba, Tokyo, Japan) in 26 patients. Lumbar region was examined in 21 patients (12 with disk herniation and 9 with canal stenosis) and cervical region in 5 (all with canal stenosis). Helical scanning was performed with 4 × 2 mm collimation, helical pitch of 3, 0.5 second rotation time, and coverage of 25 cm in 21 seconds. From data thus obtained, we reconstructed images in sagittal, and "coronal planes. We assessed the MD-CT images comparing with myelograms, conventional postmyelographic CT scans, and MR images.
Results: The MD-CT images demonstrated deformity of the dural sac better than other modalities in all patients. Reformatted images in the coronal plane and/or along the dural sac well depicted indentation of the nerve sleeves and roots in 12 patients with lumbar lesions. A bony spur or ossified ligament indenting the dural sac was better depicted than any other modality in 22 patients.
Conclusion: Postmyelographic CT using a helical MD-CT technique is a promising method to visualize anatomical details.

B-0923 11:05

Contrast-enhanced 3D MR-angiography of the spinal cord vasculature

S.R. Felber, A. Auer, P. Waldenberger, B. Amort, S. Golaszewski, J. Willeit; *Innsbruck/AT*

Purpose: The flow conditions of the intraspinal vessels prevent them from being consistantly visualized using time of flight and phase contrast magnetic resonance angiography (MRA) techniques. Here we exploited the potential of contrast enhanced (CE) MRA for the diagnosis of intraspinal vascular disorders.
Methods and materials: A total number of 33 patients (10 – 75 a) underwent CE-MRA as part of a spinal MRI study. For CE-MRA we used a 3D FLASH sequence (TR 4.6 ms, TE 1.8 ms, t 11 s, FOV 40 × 20 × 6.5 cm). The sequence was repeated 4 times, with the contrast agent (10 – 30 ml Gd-chelate) targeted to the second aquisition and using a 20 s delay betweeen the 3rd and 4th aquisition. Projective angiograms were calculated after subtraction of the 1st (native) aquisition.
Results: CE-MRA revealed an arteriovenous (AV) shunt in a dural AV fistula and showed shunt occlusion in 3 patients after endovascular treatment. A tumor blush was present in 3 patients with intraspinal hemangioblastomas, paraganglioma and ependymoma. Prominent leptomeningeal veins were also seen in 3 patients with inflammatory disorders.
Conclusion: As a luminography, CE-MRA is independent from flow velocities and flow directions. Although, the spatial resolution (1.4 × 0.8 × 1.4 mm) is inferior to catheter angiography, CE-MRA can display AV-shunts, dilated leptomeningeal veins and ateries and tumor blushes. CE-MRA has potential as a noninvasive means to select patients for catheter angiography, both for diagnosis and follow-up.

B-0924 11:15

RF neurolysis of the stellate ganglion in the sympathetic pain syndrome of the upper limb

B.A.C. Kastler, C. Clair, D. Michalakis, E. Delabrousse, J. Litzler, B. Fergane; *Besançon/FR*

Aim: Neurolysis or stellate ganglion block is an efficient and accepted method in the diagnosis and treatment of acute and chronic sympathetically maintained pain syndrome of the upper limb, thoracic viscera, and head and neck including causalgia, reflex sympathetic dystrophy and post herpetic neuralgia. CT guidance, displaying an excellent contrast between soft tissues, bones, vessels and nerves, is a well suited and safe mean of guidance
Methods & materials: At our institution since 1997 we have treated 17 patients with reflex sympathetic dystrophy (15) and causalgia (2) of the upper limb, resitant to specific medication. Two 22 G needle tips were positioned under CT control in contact with the stellate ganglion at two sites (C7 and T1). RF thermal ablations were performed with a Radionics generator. Patients were evaluated for pain before the procedure, immediately after and at day 8, 30 and 90, and thereafter every 3rd month.
Results: 10 patients had a significant (50 %) pain relief immediately and at 3 months. 5 patients had temporary and/or 3 no pain relief. No incidents occurred during the interventions. No patient had a Horner syndrom. 2 patients had a neuralgia of surrounding nerves (brachial plexus), 2 were temporary (inferior to 3 weeks) and two lasted 3 months.
Conclusion: Sympathetically maintained pain syndrome of the upper limb is difficult to treat even with high doses of specific medication. RF neurolysis of stellate ganglion under CT-guidance is safe and seems efficient particularly in distal (hand and wrist) pain.

B-0925 11:25

Vertebroplasty: Clinical experience and follow-up results

K.S. Minkner, J.-B. Martin, D. Rüfenacht; *Geneva/CH*

Purpose: To evaluate percutaneous vertebroplasty using polymethyl-methacrylate (PMMA) in a consecutive group of patients.
Materials and methods: Percutaneous vertebroplasty was performed in 111 patients and 206 vertebral levels. Indication was pain and included patients with metastasis (52), osteoporosis (30), hemangiomas (17), myelomas (12) and traumatic collaps (2). Under general anesthesia, direct access to the vertebral body was obtained by using needles of 2 – 3 mm O.D. Vertebral phlebography allowed for treatment planning by indicating the filling pattern. A diluted PMMA mixed with contrast was injected under fluoroscopic control and implant position was assessed by CT. Clinical evaluation included immediate and delayed follow up studies of the patient's general condition and neurological status. A questionnaire helped to assess degree of pain relief, reduction of pain medication and improvement of overall mobility.
Results: Follow-up was obtained in 105 of 111 patients. Pain relief was observed in 91 %. In a subgroup of patients, pain relief was obtained only after treatment of additonal vertebral levels. Withdrawal of pain medication was possible in 88 %. Overall mobility improved in 90 %. Clinical complications were observed (4/110) with deep venous thrombosis of the leg, aspiration pneumonia, and Two nerve root irritation due to cement leakage.
Conclusion: Vertebroplasty is a very efficient pain treatment. Treatment failure was mostly related to inaccurate pretreatment evaluation. Complications were mostly related to patient co-morbidity or excessive PMMA injection. Control of PMMA volume seems to be the most critical point for avoiding technical complications.

B-0926 11:30

3D CT technique with virtual simulation assists in planning cervical spine surgery: Posterior spinal instrumentation C1–C2–C3 segment

O. Balboa Arregui, C. Rodríguez Morejón, A. Mostaza Saavedra, E. Reimunde Seoane, M. Gutierrez Arias, L. Martínez Blanco; *León/ES*

Purpose: To show how useful 3D reconstructions can prove in the adequate planning of placement of transpedicle screws of spinal fixation in the pathology of the proximal cervical segment.

Methods: CT spiral images (1.5 pitch, 5 mm collimation, 3 mm reconstruction, 15 s delay with power injection of contrast medium) were obtained in 12 patients with a traumatic and/or inflammatory pathology of the C1–C3 cervical segment, which were in need of posterior intervertebral fixation. Later on, 3D multitissue reconstructions (spine, vertebral artery, soft tissues) were made in order to visualize and study them with a CAD 2D/3D system which enabled us to assess the following: The analysis of fracture trajectories, the assessment of the course, position, variations or anomalies of the vertebral arteries to avoid puncturing them with the screw and to calculate the entry point coordinates, the entry angle, the length and trajectory of the screws.
Results: The exact placing of the screws has been later checked with spiral CT in all the patients. The clinical progress has been good.
Conclusion: 3D reconstructions of the proximal cervical segment and their study in collaboration with a neurosurgeon represent a great help in planning treatment with transpedicle screws which must go through thin bone structures and avoid important vascular structures.

B-0927 11:40

Intrathecal gadopentetate dimeglumine (Gd)-enhanced MR-cisternography in the evaluation of clinically suspected cranial cerebrospinal fluid leaks: Preliminary report
R.J. Jinkins[1], E. Tali[2], G. Krumina[3], M.A. Rudwan[4], A. Mironov[5], D. Milosevich[6], N. Tokgöz-Ercan[2]; *[1]Omaha, NE/US, [2]Ankara/TR, [3]Riga/LV, [4]Kuwait/KW, [5]Aarau/CH, [6]Nis/YU*

Purpose: This study was designed to evaluate the utility of intrathecal gadopentetate dimeglumine (Gd)-enhanced MR-cisternography in the evaluation of patients with suspected cranial CSF leaks.
Method/materials: Eight adult patients (age range: 44 – 68 years) with clinically suspected CSF rhinorrhea were included in this study. The patients experienced cranial trauma varying from 4 to 8 years prior to the MR examination. Preceding high-resolution CT examinations showed evidence of anterior skull base fractures in each patient. Via lumbar puncture, a single dose of 0.5 ml Gd was injected into the subarachnoid space. The patients were positioned 45° Trendelenburg position for 10 – 20 min after withdrawal of the needle. Immediate and delayed T1- and T2WI were carried out utilising the identical parameters as those performed in the precontrast MRI. All patients were hospitalised for an observation period of 24 hours after the examination.
Results: No patient manifested gross behavioural changes, neurologic alterations, or seizure activity. Five patients showed leakage of Gd through the cribriform plate into the ethmoid air cells/nasal cavity. Two revealed leakage into the sphenoid sinus. No leakage was observed in one patient. Based on the information from the Gd-enhanced MR-cisternography, surgery was undertaken during which a dural patch was placed over the surgically visualised dehiscence of dura in the area of suspected CSF leakage in five patients. The CSF rhinorrhea halted after the surgery.
Conclusions: This cooperative study shows the relative safety, feasibility of low dose (1.0 ml or less) intrathecal Gd-enhanced MR-cisternography in the diagnosis of the location of CSF leaks.

B-0928 11:50

Intrathecal gadolinium (GD) enhanced MR. Evaluation of the intracranial CSF spaces in normal and pathological conditions: A cooperative study
G. Krumina[1], A. Platkajis[1], H. Ozolinsh[1], D. Apskalne[1], S. Dzelzite[1], J. Dzelzitis[1], I. Buike[1], R.J. Jinkins[2]; *[1]Riga/LV, [2]Omaha, NE/US*

Purpose: To evaluate the safety and clinical value of intrathecal Gd MRI.
Material and methods: 23 patients (age range: 17 – 78) with intracranial cysts, congenital malformations, post head trauma, post tumour resection and post meningitis were examined on 1.0 T GE Signa magnet using T1-w, T2-w, FLAIR parameters. 0.1 mmol/kg Gd by lumbar puncture was administrated. Protocol included pre-Gd; immediate and 24; 48; 96 hours delayed MRI. Pre- and post-Gd neurological, vital signs, EEG, CSF examinations were obtained. Evoluation in the dynamics of subarachnoid, ventricular and parenchymal contrast enhancement were described.
Results: The tolerance of intrathecal Gd administration was excellent. None of patients had abnormal vital signs, neurological, CSF alterations or increased seizure activity. Postcontrast-Gd MRI showed the mode of CSF circulation in patients with arachnoidal adhesions; parenchymal cavities; intracranial cysts; hydrocephalus and congenital malformations.
Conclusions: The intrathecal Gd MRI is highly sensitive for the research of CSF physiology, its dynamics in the liquor spaces and brain parenchyma – the evaluation of the time, kind and sequence of CSF contrast enhancement, its procedure and resorbtion in the normal and pathological conditions. The clinical utility is the precise demonstration of the level of obstruction in the liquor pathway and the exact control of endoscopically treated intracranial cysts.

10:30–12:00 **Room F1**

Chest

SS 1804

Chest CT and HRCT

Chairpersons:
A. Mester (Budapest/HU)
M. Rémy-Jardin (Lille/FR)

B-0929 10:30

High resolution CT (HRCT) in miliary tuberculosis (MTB) of the lung: Correlation with pulmonary function tests and gas exchange parameters
S.N.J. Pipavath, S. Mukhopadhyay, S.K. Sharma, M.S. Gulati, S. Datta Gupta, A. Kumar; *New Delhi/IN*

Purpose: To identify patterns of pulmonary MTB on HRCT and to correlate the HRCT disease extent with pulmonary function tests (PFT) and gas exchange analysis (GEA).
Method/materials: 16 immunocompetent patients with MTB underwent HRCT of chest, PFT, GEA. All investigations in each patient were completed within 20 days of each other. MTB was diagnosed by biopsy from lymph nodes (3/16), or skin, liver, bone marrow (5/13), and lung (transbronchial) (1/16). In one patient fundoscopy revealed choroid tubercles. In 6 patients, diagnosis was confirmed by clinical/radiological improvement following anti-tubercular therapy. Radiological patterns of involvement of lungs were studied and disease extent was estimated in each case by consensus between two radiologists using specially devised visual scoring system. Disease extent was correlated with PFT and GEA. Spearman rank correlation was used for statistical analysis.
Results: Findings on HRCT in MTB included miliary nodularity (16/16), alveolar lesions such as ground glass attenuation and/or consolidation (5/13), lymphadenopathy (8/13), peribronchovascular interstitial thickening (1/16), emphysema (1/16), pleural pathology (2/16), and pericardial effusion (2/16). Significant correlation was noted between disease extent score and following parameters: forced vital capacity ($r = -0.76$; $p = 0.03$), forced expiratory volume in one second ($r = -0.74$; $p = 0.005$), total lung capacity ($r = -0.66$; $p = 0.037$), oxygen saturation in arterial blood ($r = -0.69$, $p = 0.01$), diffusion capacity of the lung ($r = -0.811$; $p = 0.02$), and change in carbon dioxide minute ventilation with exercise ($r = -0.67$: $p = 0.048$).
Conclusions: HRCT reliably diagnoses MTB, and helps in predicting derangement of pulmonary function tests an d GEA in these patients.

B-0930 10:40

The role of CT in the diagnosis of different patterns of lung tuberculosis
F. Todua, N. Khutulashvili, G. Tsivtsivadze, L. Gzirishvili; *Tbilisi/GE*

Purpose: The aim of the work was to evaluate the value of CT in the diagnosis of the different types of lung tuberculosis.
Material: 139 patients with different types of lung tuberculosis were studied: fibrous-cavernous (n = 21), cavernous (n = 13), infiltrative (n = 22), focal (n = 34), disseminated (n = 13), intrathoracic lymph nodes tuberculosis (n = 6), tuberculoma (n = 14), caseous pneumonia (n = 16). Age of patients varied from 7 to 74 years, 82 males, 57 females. Localization, spread and stage of pathological process and also presence of post-tuberculosis changes were considered.
Results: Accuracy of CT in diagnosis of different types of lung tuberculosis was 95.6 %. False negative results (n = 4) were mostly related to incorrect differential diagnosis of tuberculosis and other disseminated processes in lungs: carcinomatosis (n = 3), alveolitis (n = 2). In one case the diagnosis of sarcoidosis was made because of the presence of lymph nodes. In most cases CT provided additional information on localization, spread, and also on the phase of the tuberculous process (infiltration, decay, dissemination; resolvement, pulmonary consolidation, scarring, calcification).
Conclusion: CT provides important additional information in the diagnosis of lung tuberculosis. It helps to evaluate the localization, the spread and the phase of the pathological process, which are all extremely important to determine further treatment.

B-0931 10:50

Pulmonary angioinvasive aspergillosis and mucormycosis in immunocompromised patients (bone marrow transplant recipients): Utility of chest CT and HRCT for early diagnosis

G. Carrafiello, A. Rampoldi, F. Vimercati, A. Nosari, E. Morra, A. Vanzulli; *Milan/IT*

Purpose: To evaluate the usefulness of chest CT and HRCT in the diagnosis of pulmonary angioinvasive aspergillosis and mucormycosis in immunocompromised patients.

Materials and methods: In the past 3 years, 30 patients (16 male and 14 female) underwent CT and/or HRCT of the chest; all patients were bone marrow transplant recipients and immunosuppressed with neutropenia (from 10 to 17 days) and fever.

Results: The earliest pathological findings and the course of disease were analysed. We found 26 patients affected by aspergillosis and 14 by mucormycosis. The most common findings of pulmonary infections were nodules (70 %) with or without halo sign, segmental ground-glass attenuation (45 %) and an air crescent sign (90 % of case). Chest CT and HRCT were also very useful to monitor the clinical evolution after therapy. All patients underwent bronchoalveolar lavage and CT guided fine needle biopsy.

Conclusion: Chest CT and HRCT are very helpful in early diagnosis of angioinvasive aspergillosis and mucormycosis and provide important information to the clinician for therapy and follow-up.

B-0932 10:55

CT features of round atelectasis of the lung

A. Alexopoulos, G. Tsioga, A. Petroulakis, E. Liapi, K. Dalamarinis, P. Antonopoulos; *Athens/GR*

Purpose: To illustrate the spectrum of CT findings in patients with round atelectasis.

Methods and materials: We retrospectively reviewed the CT findings in 28 patients with a known history of round atelectasis confirmed by the combination of follow-up CT exams, bronchoscopy and percutaneous needle biopsy (3 cases).

Results: All patients had CT findings of a rounded or ovoid mass located in the lung periphery. The areas of round atelectasis were mainly in a lower lobe in 24 of 28 cases, bilateral in 3 of 28 cases and multiple in one lobe in two cases. In all cases vessels and bronchi were seen curving in toward the mass (comet-tail sign). Also pleura thickening was found in all cases. Air bronchograms were seen in 19 of 28 cases. The pleura was thickest next to the mass in 17 of 28 cases. The mass formed an acute angle with the pleura in 15 of 28 cases and sharp lateral margins in 22 of 28 cases. Twelve cases showed hyperintlation of the adjacent lung and displacement of the main bronchus.

Conclusion: The presence of a rounded mass abutting the pleura in the lung periphery in association with vessels and bronch. Curving in toward the mass and pleural thickening are characteristic CT findings of round atelectasis and in most cases further diagnostic evaluation is unnecessary.

B-0933 11:00

Is visual determination of full inspiration on CT images possible?

J. Vikgren, Å. Johansson, M. Moonen, B. Bake, U. Tylén; *Gothenburg/SE*

Purpose: It is important to know in what state of inspiration the images are obtained when diagnosing disseminated lung diseases by HRCT. We wanted to find out whether it is possible to visually decide that an image is taken in full inspiration.

Material and methods: Ten healthy volunteers were examined by HRCT at spirometrically controlled degrees of inspiration, varying from TLC to TLC minus 2.0 litres. Mean HU value for the lung parenchyma in each slice was calculated. Two experienced radiologists evaluated visually a total of 100 images, in random order. They only had to answer the question: is the picture taken in full inspiration or not?

Results: For each individual there was a linear relationship between lung volume and attenuation, with a statistically significant increase of density by 20 HU for each 10 % reduction of lung volume in the calculated interval from TLC to 60 % of TLC. At TLC there was a range of 40 HU. The radiologists were expected to evaluate 20 % of the images as taken in full inspiration, but the outcome was 62 % and 71 %, respectively. In the interval 60 – 69 % of TLC the outcome was 0 – 20 %.

Conclusion: It was not possible to visually decide whether an HRCT image was taken in full inspiration. Not until the lung volume was reduced with 2 litres, i.e. approaching FRC, the radiologists were reasonably certain. When looking for specific conditions spirometric gating may be necessary.

B-0934 11:10

HRCT patterns in clinical and subclinical pulmonary involvement in systemic sclerosis

K.S. Malagari, H. Koutrouveli, E. Alexopoulou, D. Kokkinos, A. Nikita, T. Dailiana, L. Thanos, D.A. Kelekis; *Athens/GR*

Purpose: The aims of this study were: a) to evaluate the presence of interstitial lung disease as depicted on HRCT among different clinical subgroups of systemic sclerosis (SSc), and b) to study the relationship between HRCT patterns and extent with functional parameters.

Material and methods: A cohort of 127 patients with a confirmed diagnosis of SSc [57 with diffuse SSc (dSSc), 46 with limited SSc (lSSc), and six with overlap syndromes] were evaluated. Clinical suspicion for lung involvement was present in 64 (50.4 %). Examinations included high-resolution computed tomography (HRCT) and pulmonary function tests [PFTs: FVT, TLC and DLCO]. Disease extent and severity were assessed by a HRCT grading system.

Results: Twenty-eight of the 70 subclinical patients (40 %) had abnormal HRCT findings, namely isolated septal/subpleural lines, interface signs and ground-glass opacities. The prevalence of HRCT findings of fibrosis was higher in the symptomatic group (87.1 %) [$p < 0.01$] and in the dSSc group compared with the lSSc and overlap forms [$p < 0.001$]. Overall, a negative correlation between HRCT total interstitial disease scores (TID) and PFTs were found [TLC: $r = -0.31$, $p < 0.006$; DLCO: $r = -0.51$, $p < 0.001$). Lung volumes did not significantly differ among patients with ground-glass opacities and those with reticular patterns on HRCT, while the diffusing capacity for carbon monoxide was significantly lower ($p < 0.05$) in the latter.

Conclusions: HRCT is a sensitive tool in detecting interstitial lung disease even in subclinical SSc. Moreover, HRCT patterns may assist along with BAL studies in the identification of indices with different prognostic implications.

B-0935

withdrawn by author

B-0936 11:20

Monitoring of interstitial lung disease activity in polymyositis and dermatomyositis: Clinical value of HRCT

J. Biederer[1], M. Reuter[1], C. Richter[2], A. Schnabel[2], W.-L. Gross[2], M. Heller[1]; *[1]Kiel/DE, [2]Lübeck/DE*

Purpose: To determine the clinical value of HRCT for monitoring interstitial lung disease activity in patients with Polymyositis/Dermatomyositis (PM/DM).

Patients and methods: 25 Patients with PM/DM and suspected pulmonary involvement were enrolled. 18/25 underwent sequential HRCT evaluation, mean follow-up 22 months. The findings were correlated with the clinical course and data from blood and bronchoalveolar lavage (BAL) samples. In 46/62 cases (24/25 patients) BAL was performed 1 – 3 days after CT including cytologic and microbiologic assessment of the lavage fluid.

Results: 94 % of the HRCT revealed pulmonary abnormalities related to PM/DM with high variability in onset and intensity of pulmonary involvement. Between different patients lesion profusion did not correlate with duration of PM/DM, but the spectrum of lung parenchyma alterations changed with the course of disease. Ground-glass opacities predominated in patients with short duration of disease (up to 50 months), reticular/fibrotic lesion patterns in patients with long duration (over 120 months). Individual cases showed a reversibility of ground-glass opacities without development of fibrosis under intensified treatment.

Conclusions: The study confirms the clinical value of HRCT for detection of florid interstitial lung disease associated with Polymyositis/Dermatositis. Appearance of ground-glass opacities indicates early infiltrations that may be reversible under intensive therapy.

B-0937 11:30

Pneumonia: High-resolution CT findings in 114 patients

P. Reittner[1], S. Ward[2], L. Heyneman[2], N.L. Müller[2]; *[1]Graz/AT, [2]Vancouver, BC/CA*

Purpose: To assess the high-resolution CT appearances of different types of pneumonia.

Materials and methods: The high-resolution CT scans obtained in 114 patients with bacterial, Mycoplasma pneumoniae, viral, fungal, and Pneumocystis carinii pneumonias were analyzed retrospectively by two independent observers for presence, pattern, and distribution of abnormalities.

Results: Areas of air-space consolidation were not detected in patients with viral pneumonia and were less frequently seen in patients with Pneumocystis carinii pneumonia (2 of 22 patients, 9 %) than in bacterial (30 of 35, 85 %), Mycoplasma

pneumoniae (22 of 28, 79 %), and fungal pneumonias (15 of 20, 75 %) (all $p < 0.01$, Chi square test). There was no significant difference in the prevalence or distribution of consolidation between bacterial, Mycoplasma pneumoniae and fungal pneumonias. Extensive symmetric bilateral areas of ground-glass attenuation were present in 21 of 22 (95 %) patients with Pneumocystis carinii pneumonia and were not seen in other pneumonias except in association with areas of consolidation and nodules. Centrilobular nodules were present less commonly in bacterial pneumonia (6 of 35 patients) than in Mycoplasma pneumoniae (24 of 28), viral (7 of 9), or fungal (12 of 20) pneumonia ($p < 0.01$).
Conclusion: Except for Pneumocystis carinii pneumonia, which often has a characteristic appearance, high-resolution CT is of limited value in the differential diagnosis of the various types of pneumonia.

B-0938 11:40

Evaluation of portable computed tomography in intensive care units
U.K.M. Teichgräber, C. Born, J.G. Pinkernelle, R. Bittner, J. Ricke, D. Barckow, J. Rademaker, R. Felix; *Berlin/DE*

Purpose: To assess usage of portable CT in an intensive care unit (ICU)
Material and methods: Mobile CT scans were performed on 95 consecutive ICU patients from January 1 to July 30, 2000 with a Tomoscan M (Philips Medical Systems). An evaluation by ICU staff was performed on acceptance, work load, improvement of patient care and expectations of the portable CT scanner. Time measurements were performed on 25 CT examinations performed with a fixed CT scanner in the radiology department compared to 25 CT examinations performed with the portable CT used in the intervention suite within the ICU. The time measurements included preparation, transportation and throughput time. In addition, the transportation distances and time were measured for CT performed within the ICU versus the radiology department.
Results: The portable CT scanner received a high acceptance by ICU staff, and the work load was considered smaller compared to the CT examinations performed in the radiology department. There was an improvement in patient care with portable CT scanning in the ICU. The average transportation time to the ICU intervention suite was 3.1 minutes compared to 9.0 minutes to the radiology department. In contrast, the throughput time for the portable CT with 13.9 minutes was longer compared to the CT examination in the radiology department with 8.9 minutes.
Conclusions: The acceptance of mobile CT has been very positive by the ICU staff. It facilitates the work flow by reducing transportation time and assuring continuity of ICU therapy while the CT scan is performed.

B-0939

withdrawn by author

10:30–12:00 **Room F2**

Neuro

SS 1811b

Pediatrics - Pituitary

Chairpersons:
O. Flodmark (Stockholm/SE)
B. Góraj (Lódz/PL)

B-0940 10:30

Magnetic resonance imaging of the fetal brain
A. Auer, B. Amort, P. Schwaerzler, S.R. Felber; *Innsbruck/AT*

Purpose: Our intention was to evaluate the potential of magnetic resonance imaging (MRI) for the diagnosis of fetal brain abnormalities.
Methods and materials: Ten pregnant women (18^{th} – 33^{rd} weeks of gestation) unterwent MRI because of sonographically suspected fetal brain anomalies. The examinations were performed on a 1.5 T scanner (Vision, Siemens) using a phased array coil. The examination protocol included a T2 weighted HASTE sequence (TR 4.4 – 12 ms, TE 90 ms, 4 – 6 mm slice thickness, t 20 – 30 s) in 3 orthogonal orientations and a T1 weighted turbo FLASH sequence (TR 11 ms, TE 5.3 ms, 6 mm slice thickness, t 1 min 24 s) in at least 1 orientation. Flunitrazepam (1 mg) was orally administered in order to reduce fetal movements. Follow-up examinations were performed in 3 patients, including 1 postnatal MRI.
Results: MRI revealed brain anomalies in 8 (10) fetuses. Abnormalities included communicating hydrocephalus (n = 1), agnesis of the corpus callosum (n = 2), minor form of holoprosencephaly (n = 1), microcephaly (n = 1), anterior meningocele with hemispheric dysorganisation (n = 1), T2 hyperintense lesions of the white matter (n = 1), and mulifocal cerebral hemorrhages (n = 1).
Conclusion: If ultrasound findings are questionable, MRI is a safe, noninvasive and fast method for the diagnosis of fetal brain pathology.

B-0941 10:40

Optimisation of prenatal CNS magnetic resonance imaging
K. Wagiel[1], M. Bekiesinska-Figatowska[1], J. Walecki[1], K. Wermenski[1], M. Jozwik[2], A. Ceran[1]; *[1]Warsaw/PL, [2]Bialystok/PL*

Purpose: To determine the optimal strategy of fetal CNS pathology visualisation by means of MR imaging. To show the difference in image quality depending on sequence parameters.
Methods and materials: A 1.5 T Philips Gyroscan system was used to obtain fetal MR exams in 14 complicated pregnancies (mean age of gestation: 33 weeks). CNS pathology was found in all cases on ultrasound.
Results: The first studies showed poor quality because of motion artifacts resulting from the long acquisition time (30 – 90 s). T2-weighted turbo spin-echo single shot images presented the highest quality and therefore were chosen for further optimalisation. Gradual changing of repetition time, echo time, field of view, slice thickness, matrix size and number of acquisitions led us to obtain high quality images with the following parameters: TR 8300 ms, TE 100 ms, FOV 230 – 350 mm, ST 3 – 4 mm, MX 109 × 109 (reconstruction MX 256 × 256), NA 1 – 2. Acquisition time of 8 – 16 s allowed the patients to hold breath and allowed us to shorten the overall time of examination. Visualisation of the whole length of the spinal canal was possible thanks to TSE sequence (TR 1800 ms, TE 650 ms, ST 0.8 – 1 mm) with 3D MIP reconstruction.
Conclusions: Our experience shows that the time of data acquisition is the main factor influencing the fetus imaging quality. Therefore image settings that have theoretically worse parameters (smaller matrix, smaller number of acquisitions, bigger slice thickness) supply us with better images thanks to the shorter time of examination.

B-0942 10:45

MRI and MRS study of the fetal human brain
V.A. Rogozhyn, Z.Z. Rozhkova, A.P. Perfilov, S.P. Pisareva, M.A. Vasilenko, L.G. Kirillova, I.S. Luk'janova, L.I. Tkachuk; *Kiev/UA*

Purpose: Our goal is evaluating the brain anomalies in human fetus by MRI, for measurement of fetal brain structures, and ^{1}H MRS, for determination of cerebral metabolite concentrations.
Methods and materials: Two groups of 10 women with (G1) and 5 women without (G2) complicated pregnancies are studied by 1.5 T Magnetom Vision Plus System (SIEMENS). MR-images of fetal brain in utero (from 25 to 39 weeks of gestational age) were obtained with HASTE sequence. ^{1}H spectra are recorded with the STEAM and PRESS sequences. The metabolite ratios NAA/Cr, Cho/Cr, NAA/Cho and NAA/(Cho + Cr) are calculated from spectra.
Results: From MR-images of fetal brain in G2 it is found that the ratio ventricel/brain decreases, and the length of corpus collosum, and also the length, height, and area of cerebellar vermis increas with gestational age. The ratios NAA/(Cho + Cr), NAA/Cr and NAA/Cho for G1 and G2 are not significantly distinguishable. The ratio Cho/Cr decreases significantly in G1 compared to G2. Lac signal present in 4 cases in G1 and in 1 case in G2. In 3 cases in G1 the decrease of the intensities of Glu-Gln signals in comparison with G2 is observed. This occurs together with reducing the ratio Cho/Cr and appearing Lac.
Conclusion: MRI and ^{1}H MRS are very sensitive and effective methods for early detection of fetal hypoxic ischemic injury. Both the methods can be applied for assessment and understanding of intrauterine growth retardation.

B-0943 10:50

Assessment of periventricular brain movement in normal volunteers and in patients with various causes of hydrocephalus
B.B. Ertl-Wagner[1], A. Lienemann[1], R. Eymann[2], M. Kiefer[2], W. Reith[2], M.F. Reiser[1]; *[1]Munich/DE, [2]Homburg a. d. Saar/DE*

Purpose: We aimed to establish an easy and reliable method to test for periventricular brain motion as a means of distinguishing between hydrocephalus patients and healthy volunteers and to moreover assess therapeutic effects of CSF shunting.

Materials and methods: 25 healthy volunteers, 5 patients with communicating hydrocephalus, 3 children with non-communicating hydrocephalus and 5 children post CSF shunting were examined with an axial true fast imaging steady precession sequence in a 1.5 T clinical MR scanner (TR 4.8 ms, TE 2.3 ms, flip 70°, SL 5 mm, FOV 330 mm, 3 slices). Images were assessed both as dynamic images in cine mode and by measuring lateral ventricular size over time.
Results: All volunteers showed marked periventricular brain motion (mean reduction of the ventricular area under Valsalva 18 % (SD 7)). Patients with communicating and non-communicating hydrocephalus showed virtually no periventricular brain motion, while children with a well-functioning CSF shunt revealed a good mobility of the periventricular walls. All differences were statistically significant with a $p < 0.0001$.
Conclusion: Out method clearly distinguished patients with symptomatic communicating and non-communicating hydrocephalus from healthy volunteers. It may moreover aid in the evaluation of CSF shunt patency.

B-0944 11:00

Diffusion-weighted MRI in young children for prognostic evaluation of ischemic and anoxic injuries

W. Küker, S. Friese, H. Krapf, W. Grodd, I. Krägeloh-Mann; *Tübingen/DE*

Purpose: DW-MRI has been shown to differentiate between interstitial and intracellular oedema. This discrimination is used to evaluate the extent of irreversibly damaged brain parenchyma in adult stroke patients. Intracellular oedema is regarded as sign of inevitable cell death. On the other hand, the lack of diffusion abnormality in interstitial oedema may indicate the possibiltiy of reversibility. Increasing availability of diffusion sensitive echo planar sequences on state of the art MR scanners has facilitated the examintion of small children with this method. A diffusion MRI can be carried out in a few seconds and is very robust against motion artifacts.
Methods and materials: During the last 12 months we examined nine patients under the age of 10 with diffusion sensitve sequences on a 1.5 T unit (Siemens Magnetom Vision). Indications were stroke (n = 6), hypoxia (n = 2) and seizures (n = 1).
Results: Whereas in hypoxia no focal diffusion abnormality could be demonstrated, in complete focal stroke the diffusion abnormality matched the area of brain necrosis (n = 5). In a patient with a right sided infarction in the medial cerebral artery territory during birth, diffusion MRI showed a massive hyperintensity in the course of the pyramidal tract after three days, probably indicating axonal degeneration. This has not been reported before. In a case of focal oedema in the vascular territory behind a high grade medial cerebral artery stenosis, diffusion MRI was normal. This lesion was completely reversible without any permant neurologic deficit.
Conclusion: Diffusion abnormality in young childeren probably indicates intracellular oedema and hence irreversible cell damage.

B-0945 11:10

MR imaging of hypoxic ischemic encephalopathy in cerebral palsied children

N. Erdogan, A. Coskun, A.C. Durak, S. Kumandas; *Kayseri/TR*

Purpose: To find out the incidence of brain injuries detected in neuropathologic studies of children with hypoxic ischemic encephalopathy in MR images of patients with cerebral palsy.
Methods and materials: We retrospectively reviewed T1 axial, T2 axial, T1 sagittal and T2 coronal images obtained by Philips Gyroscan 1.5 T in 37 patients (mean age, 4.2 years; range, 5 months to 16 years). For each type of injury the diagnostic criteria were defined according to morphological changes required for neuropathological diagnosis. The patients were divided into two groups: Group I (Patients with MR images diagnostic for any of the injury forms) and, Group II (Patients without diagnostic images).
Results: Twentythree cases (62.1 %) were included in Group I. Most commonly encountered injury forms were periventricular leukomalacia (16.2 %) and parasagittal injury (16.2 %). In both groups, the incidence of the lesions known to have prenatal onset was 29.7 %.
Conclusion: MR studies may help to identify the events leading to cerebral palsy in a high percentage of patients. The role of birth asphyxia as a cause of cerebral palsy should be questioned because of the events which are known to have prenatal onset. However, perinatal factors still play some role, since, parasagittal injury, which is the characteristic injury for term neonates, has a relatively high incidence in our study.

B-0946 11:20

Pediatric demyelinating disorders: Clinical and neuroradiological findings in 29 cases

M. Caulo[1], M. Gallucci[1], G. Cerone[1], M. Conti[2], A. Achene[2], A. Splendiani[1], C. Masciocchi[1]; *[1]L'Aquila/IT, [2]Sassari/IT*

Purpose: This work aims to review 29 cases of demyelinating disease with onset in the pediatric age to register the main clinical and neuroradiological evidences and to establish if significant differential criteria between Multiple Sclerosis and Schilder's disease (SD) are available.
Materials and method: 29 childood patients affected by demyelinating disease have been enrolled: 26 diagnosed as typical remitting-relapsing MS and 3 as SD. Clinical presentation at the onset, CSF analysis, number and size of MRI detected palques were evaluated.
Results: In 7 of 26 cases atypical clinical presentation had been found, seizures were the clinical onset in 2 cases and lethargy in 1 case, signs of intracranial hypertension had been detected in 4 cases. In all the cases of SD and in 6 cases of MS oligoclonal band were absent. Giant plaques had been found in all SD cases and in 14/26 MS cases.
Conclusion: From this data we postulate pediatric MS to represent a wide category of disease with different clinical, laboratory and MRI findings if compared to typical adult presentations. Statistically significant differences between MS and SD groups were found suggesting SD should not to be considered a specific entity nor a MS variant. SD seems to represent the occasional combination of clinical and radiological findings mostly occuring during pediatric MS.

B-0947 11:30

Why do primary intracranial manifestations of Langerhans cell histiocytosis (LCH) prefer extraaxial structures?

D.M. Prayer, N. Grois, H. Brosch, E. Schindler, H. Gadner; *Vienna/AT*

Purpose: Intracranial manifestations of Langerhanscell Histiocytosis (LCH) have been decribed to occur in up to 20 % of cases, Cranial MR-scans of patients with histologically proved LCH were evaluated to determine the types of intracranial involvement of this disease.
Patients and methods: 352 cranial MRI-scans of 85 patients, done in 43 institutions in 12 countries, were reviewed with emphasis on the differentiation between intra-and extraaxial primary LCH lesions.
Results: Consisted of: meningeal lesions (28 %), choroid plexus manifestations (7 %), pituitary stalk pathology (69 %), hypothalamic mass lesions (27 %), empty sella (20 %), and intraaxial lesions (23 %). In most of the cases more than 1 of the mentioned localizations was involved. 4 children (5 %) with intracerebral manifestations have died, all children with extraaxial manifestations only are still alive.
Conclusion: Our results suggest a predominant LCH-involvement of extraaxial structures that do not possess a blod brain barrier (BBB). If intraaxial regions are affected, this probably means a breakdown of immunologic functions of the BBB, and worsens the further prognosis. In addition, these findings support the theory that intracranial LCH involvement might be mediated by CNS-directed immune responses in which endothelial cells of the BBB play a crucial role.

B-0948 11:40

Pituitary gland height evaluated by MR in patients with α thalassemia major: A marker of pituitary gland dysfunction

M.I. Argyropoulou, D.N. Kiortsis, Z. Metafratzi, C. Tsampoulas, S.C. Efremidis; *Ioannina/GR*

Objective: In transfussion dependent α-thalassemia major, increased iron deposition in the pituitary gland has a cytotoxic effect leading mainly to hypogonadotropic hypogonadism. Pituitary gland height, evaluated by MR, has been used in the study of pituitary gland function. The purpose of this study was to evaluate the pituitary gland height as a marker of pituitary gland dysfunction in patients with α-thalassemia major.
Subjects and methods: In 29 patients with α-thalassemia major and 40 controls the pituitary gland height was evaluated in a midline sagittal scan using a spin echo T1 weighted (500/20 TR/TE) sequence. In all patients, an extensive endocrine evaluation was performed, including measurements of spontaneous and stimulated levels of gonadotropins, thyroid hormones, growth hormone, insulin-like growth factor, and adrenal hormones.
Results: The pituitary gland height was lower in thalassemic patients (mean 4.42; SD 1.4) compared to the controls (mean 6; SD 0.98), ($p < 0.001$). The pituitary gland height was lower in thalassemic patients with hypogonadotropic hypogonadism (mean 3.5; SD 0.62) compared to those without pituitary dysfunction (mean 5.34; SD 1.5) ($p < 0.001$).

Conclusion: The pituitary gland height is a useful marker in the evaluation of thalassemic patients, being more reduced in those with hypogonadotropic hypogonadism.

B-0949 11:50

MR imaging of the pituitary gland in patients with transfusional hemosiderosis

A.S. Dimitriadis, E. Hasapopoulou, I. Ioannidis, A. Haritandi; *Thessaloniki/GR*

Purpose: To evaluate the reduction of MR signal intensity in the anterior lobe of the pituitary gland in patients with secondary hemosiderosis due to transfusion dependent thalassemia major before the onset of treatment with the oral chelator deferiprone.

Materials and methods: Thirty patients with secondary hemosiderosis (11 male, 19 female, aged 16 – 36 years) due to thalassemia major underwent MRI examination of the pituitary gland. Serum feritin levels were elevated in all patients (mean 5 863; range 789 – 12 600; normal level < 300 ng/ml). 18 patients had a diagnosis of hypogonadotropic hypogonadism established with clinical and laboratory data. MR imaging examinations were performed by using sagittal and coronal TSE T2-weighted sequences and coronal GRE T2-weighted sequence.

Results: All patients showed reduction of signal intensity of the anterior lobe of the pituitary gland. The reduction of pituitary signal intensity was greater in patients with higher feritin levels.

Conclusion: Our results confirmed that MRI is modality of choice for detecting iron overload in the pituitary gland. The reduction of signal intensity in the anterior lobe of the pituitary gland correlates with the severity of iron overload.

10:30–12:00 **Room G**

Computer Applications

SS 1805

PACS evaluation and workflow

Chairpersons:
T. Andersson (Örebro/SE)
W. Hruby (Vienna/AT)

B-0950 10:30

PACS in an almost filmless hospital: One-year experience in Taiwan

Y.-T. Kuo, G.-C. Liu, H.-C. Chu, S.-J. Hwang, C.-S. Chang, C.-S. Lai; *Kaohsiung/TW*

Purpose: To share the experience of implementation of a picture archiving and communication system (PACS) and a near filmless operation in a medium-sized general hospital.

Materials and methods: Two-stage hospital-wide implementation of PACS has been carried out in a medium-sized general hospital (428 beds) since November 1998. All the images except mammography were digitized as DICOM 3.0 format. Physicians can access current and prior images and their reports from 40 view stations distributed in the hospital. Image compression to lossless (3:1) and lossy (18:1) data for short-term and long-term storage in redundant array of inexpensive disks (RAID) of 200 gigabytes (GB) and 400 GB was done.

Results: A near filmless operation has been achieved since September 20, 1999. The mean films used per patient were 1.5 and 0.06 before and after PACS implementation. The time spent in retrieving images was reduced to few seconds. The vast majority of the preliminary radiological reports were available on PACS and hospital information system within 1 day. The costs of film-related material, file room personnel and space were significantly decreased. The capacities of RAID can offer more than 6 months of short-term lossless and estimated 5 years of long-term lossy image data available for on-line query.

Conclusion: PACS can achieve a near filmless medical environment for a medium-sized general hospital. It can meet most of the needs of both the radiologists and referring physicians and improves clinical efficiency.

B-0951 10:40

Issues arising following the installation of PACS

M.E. Hurley, A. Twair, M. O'Dowd, A. Byrne, G.D. Hurley; *Dublin/IE*

Purpose: (1) Review of experience following installation of a whole-hospital PACS in a 600 bed teaching hospital in 1998 with efficiency, cost and staff satisfaction analysis. (2) Highlight the advantages and difficulties of a "big bang" approach with PACS versus a phased approach.

Methods and materials: A turnover study of 200 patients' results pre- and post PACS installation was performed. We also reviewed the costs of materials and staffing. PACS appreciation by clinicians, radiologists and radiographers was assessed over a two-year period. Finally, we compared the advantages and limitations of the "big bang" versus a phased approach.

Results: PACS proved to induce a 70 % reduction in report generation time. Significant savings arise from the diminished costs of film and chemicals, which were however spent on updating hard- and software in the year following PACS installation. Clinicians and radiologists adjusted at first with hesitation, but with time well to PACS. An increased turnover of radiographers was however observed in the first year post installation due to educational requirements and necessary redeployment. We experienced the skipping of a phased approach in PACS installation as advantageous.

Conclusions:

1. PACS is more efficient.
2. PACS is cheaper once the system is established.
3. PACS provided a satisfactory service for most staff.
4. Taking the "big bang" approach has considerable operational advantages over a phased approach.

B-0952 10:50

Filmless hospital: Experience after 24 months

C. Capotondi, S. Sparbati, M. Minnetti, M. Clementi, G. Alessi; *Rome/IT*

Purpose: Our aim is to evaluate a complete HIS-RIS-PACS integration implemented as filmless hospital since February 1999.

Materials and methods: In our 255 beds community hospital (M.G. Vannini Hospital, Rome, Italy), the department of imaging includes 3 traditional X-ray rooms, 1 CT, 1 MRI, 2 US, 1 DSA and 2 mammography rooms and multiple portable X-ray devices. A PACS AGFA IMPAX is connected to all modalities by DICOM standard protocol. Long-term archive is realized storing on magneto optical disk (MOD) WORM type using compression factor 2 that permits to have about 12 months of images data on-line. Components are linked by a combination of switched and fast-ethernet networked over fiber optics. HIS-RIS-PACS interface is realized through a MITRA PACS-broker.

Results: There was a time reduction of 25 % in the execution of examinations and 30 % in reporting time; with no-printing of in-patients CT and MRI examinations we have 35 % of saving-time in technician's work. Other benefits are decreased in the need of archives-spaces (reduction of 95 % per year) and archivist-personell (no dedicated personell). Radiologist reports are immediately available to all clinicians.

Conclusion: This system allows optimization of workflow with shortening on global time of execution and reporting. PACS improves efficiency of data management especially in storage both economical and human resources. Filmless hospital is time saving in all departments' workflow with improvements in patient care.

B-0953 11:00

Low cost PACS system: An opensource project approach

C. Saccavini, P. Mosca, R. Stramare, S. Puggina, G.P. Feltrin; *Padova/IT*

Purpose: To realize a low-cost PACS system using opensource software and new archiving strategy.

Materials and methods: In our Department we use selfmade PACS based on Linux Server with Interbase 6.0 as database engine and a DICOM server application developed starting from OFFIS library (Oldenburg Germany). The network is a 100 Mbit/s FastEthernet. We have connected to our PACS one CT (Emotion by Siemens), one MR (Armony by Siemens), two CR (AC3 by Fuji), one digital radiography (Advantix by GE), two reporting workstation (MagicView by Siemens, HiC 655 by Fuji) and four reporting workstation PC-based. To archive the radiological images we use high capacity fast hard disks instead of optical disk jukebox: infact the cost of 500 Gb online HD archive is 7 Euro/Mbyte agaist 26 Euro/Mbyte of optical disk Jukebox. We backup all the images on CD-ROM in order to have a offline legal archive.

Results: The PACS system in these 6 months has worked very well; the users appreciate the very fast time of image retrivial due to high performance of hard disks. The high number of backup CD-ROM suggest us to change the media support to DVD in the next months.

Conclusions: The new opensource software changes the traditional approch in planning PACS system: new strategies are incoming. In the next months we plan to distribute our software on Internet as opensource project.

B-0954 11:10

Automatic transfer of exposure data from imaging modalities to the electronic patient record (RIS) in a filmless hospital

H.M. Mosser, G. Paertan, A. Maltsidis, W. Hruby; *Vienna/AT*

Introduction: On the background of increasing demands on quality assurance and radiation protection the exposure dose used for radiological examinations has to be documented in the patient medical record. According to radiation protection legislation, this documentation must include the dose area product (DAP) and alternatively also the respective kV and mAs values. We developed an automatic exposure measurement and transfer system for exposure related parameters from the modalities to the electronic patient record. For modalities, where dose data are available in the DICOM header, all information is gained directly from the image. Other modalities are equipped with a dose-area product meter (Diamentor M4) connected to a PC via a serial RS-232 interface. At this PC a number of system parameters, such as number of frames, dose-area product, mAs, kV, exposure time etc., are recorded automatically and added to the examination record in the RIS.

Results: For radiological examinations such as Fluoroscopy, Angiography, Radiography and Computertomography it could be technically achieved by a dedicated software and hardware adaptation, that exposure parameters (DAP for DR and Fluoro or DLP for CT) are automatically transferred to the electronic patient record (Radiology Information System).

Conclusion: The automatic transfer of exposure parameters from all imaging modalities to the electronic patient record is basis not only for quality assurance but also for risk assessment and check of compliance to regulatory exposure dose records. This is a further major step and a significant improvement in the integration of data from different digital sources and in radiation protection.

B-0955 11:20

A web-based concept for DICOM image storage and distribution

A. Haderer, J. Ricke, D. Emmel, W. Schauer, U.K.M. Teichgräber, T. Ehrenstein, C. Gillessen, R. Felix; *Berlin/DE*

Purpose: To design and implement an inexpensive and scalable infrastructure for distributing radiological images and reports.

Materials and methods: A distributed server farm creates a web-based storage and distribution platform for radiological images and reports. The server infrstructure is part of a radiological service portal and works with a UNIX OS. The software has been implemented employing the OpenSource components Perl, Apache, Postgres, and the DICOM Toolkit OFFIS. The DICOM protocol is used for image exchange with the imaging devices (MR, CT, DLR), access to reports is generated through HL7 protocol. Distributed hardware of the server infrastructure enables simple expansion and scalability: CPU load and Network traffic can be distributed over different machines and reduces bottlenecks. The access to datasets including icons of original image data, DICOM images and reports is protected by an authentication scheme presented through the webserver. Clients access the server data using common web browsers and visualise DICOM images with appropriate helper applications or in-page applets.

Results: Access to radiological reports and images is simple and user friendly. The scalable server farm allows easy adaption to changing requirements with respect to image storage and distribution. OpenSource Software enables the re-use of non-Up-To-Date hardware and the integration of inexpensive hardware from the PC mass market. The system has been in routine use since January 1st 2000 with just 20 minutes of system failure to date.

Conclusions: The image archive and its distribution platform have proven great reliability. Advantages are inexpensiveness and the potential for flexible expansion.

B-0956 11:30

Asena: A web based data base system for remote administration of clinical multicentre trials

J. Ricke, N. Yakan, A. Haderer, M. Pech, C. Gillessen, T. Ehrenstein, U.K.M. Teichgräber, R. Felix; *Berlin/DE*

Purpose: To design and implement software for administration and data collection of clinical multicentre trials ("Asena").

Materials and methods: A web based server infrastructure was implemented for remote acquisition and administration of medical trials data. The server infrastructure is Unix-based employing open software.

To perform a clinical trial, the service provider designs a HTML-page according to the specific study requirements of a given trial. Proprietary software automatically generates the data base structure as well as the form for data input according to the description given by the initial HTML page.

For data input, study participants use a regular web browser. Access to or visualisation of study data is role based following individual rights of study participants and the study co-ordinator.

For follow up studies, cyclic patient folders may be created. Radiographic images can be attached in multimedia or DICOM format. Data collected may be retrieved for statistical analysis in standardised format (SPSS, Excel, DIF).

Results: The system allows fully electronic clinical multicentre trials. Data base administration may be performed remotely by a service provider. Study participants submit medical data independent of their individual location via the Internet or other networks.

Conclusion: The system supports pharmaceutical companies or research institutes to perform clinical multicentre trials. The system supports existing workflows in clinical trials. Major advantages are improved quality management by advanced monitoring capabilities as well as time savings in clinical trials by efficient data handling.

B-0957 11:40

Effects of image postprocessing and monochrome monitors on the quality of image review outside the radiology department

J. Ricke, E. Lopez, U.K.M. Teichgräber, C. Gillessen, D. Emmel, A. Haderer, R. Felix; *Berlin/DE*

Objective: To assess potential advantages of a new PC-based viewing tool featuring image post-processing for viewing computed radiographs on low-cost hardware (PC) with a common display card and color monitor. To evaluate the effect of using color versus monochrome monitors.

Materials and methods: Computed radiographs of a statistical phantom were viewed on a PC with and without post-processing (spatial frequency and contrast processing) employing a monochrome or a color monitor. Findings were compared to viewing on a radiological Workstation and evaluated with ROC analysis.

Results: Image post-processing improved the perception of low-contrast details significantly irrespective of the monitor used. No significant differences of perception were observed between monochrome and color monitors. Review at the radiological Workstation was superior to review at the PC with image processing.

Conclusion: Lower quality hardware (graphic card and monitor) used in low cost PCs negatively affects perception of low-contrast details in computed radiographs. In this situation, it is highly recommended to use spatial frequency and contrast processing. No significant quality gain has been observed for the high-end monochrome monitor compared to the color display. However, the color monitor was affected stronger by high ambient illumination.

B-0958 11:50

Workflow analysis for multislice-CT

J.E. Roos, B. Marincek, P.R. Hilfiker; *Zürich/CH*

Purpose: To evaluate time management and workflow for Multislice-CT (MS-CT).

Material and methods: Time for patient and data handling was evaluated for 160 patients during a 12-days period for the following steps: (a) change of clothes/patient instruction; (b) placement/iv catheter; (c) acquisition planning and programming; (d) data acquisition; (e) reconstruction; (f) storage/printing. Imaging was performed on a Somatom Plus 4 Volume Zoom (Siemens, Erlangen, Germany). Images were reconstructed immediately after acquisition on an attached workstation (Volume Navigator). Printing, data transfer, and data storage was performed on a second workstation (Volume Wizard).

Results: 63 abdomen, 35 thorax, 22 combined thorax/abdomen, 20 spine, 11 combined neck/thorax/abdomen, 5 HRCT, and 4 CTA were acquired. Time measurements revealed the following: (a) 5.02 min (1 – 15 min); (b) 5.2 min (1 – 15 min); (c) 3.94 min (1 – 15 min); (d) 36 s (9 – 120 s); (e) 5.78 min (2 – 15 min); (f) 7.66 min (3 – 20 min). Planning CT angiograms needed most time (7.25 min), whereas thorax and abdominal CTs needed only 3.52 min and 3.57 min, respectively. Reconstruction time was highest for HRCT (11.75 min) and CTA (10.50 min). Data storage/printing was most time consuming for HRCT (13 min), followed by combined neck/thorax/abdomen data sets (11 min).

Conclusion: Acquisition time is no longer a problem with MS-CT. Patient management, data reconstruction and data storage are the most time consuming parts. Therefore, well-trained technicans and 'state-of-the-art' workstations are the most important factors to improve workflow.

B-0959 11:55

Evaluation of an automatic algorithm for the analysis of cine phase contrast velocity imaging

A.N. Priest, M.J. Graves; *Cambridge/GB*

Purpose: Evaluation of score-guided erosion (SGE) as an automated method for finding the boundaries of blood vessels in cine phase contrast (CPC) velocity imaging.

Materials and methods: A computer program was developed in IDL to automatically find and track the vessel boundary in CPC images using a modification of the SGE algorithm. CPC studies of the aorta, comprising 16 temporal phases, were acquired in three normal volunteers. The resulting 48 images were analysed using the automatic method and manually by two observers. To investigate the effect of partial volume errors the automatically determined contours were also dilated by one pixel.

Results: The automatic and dilated areas always bounded the area of each manual contour for every phase. The automatically areas also varied more smoothly with cardiac phase. The automatic stroke volume (SV) was calculated as the mean of the SGE and dilated contours. The manual measurements were expressed as the mean of the two observers. Automatic SV (ml): 73.7 ± 3.4, 96.4 ± 2.3 and 69.2 ± 4.6. The corresponding manual SV (ml): 73.2 ± 1.5, 96.5 ± 1.4 and 68.6 ± 0.5. There was no significant difference between the automatic and manually determined SVs ($P = 0.296$).

Conclusion: SGE is a robust technique for the rapid and automatic analysis of CPC velocity images.

10:30–12:00 **Room H**

Interventional Radiology

SS 1809

Arterial intervention (3)

Chairpersons:
A. Besim (Ankara/TR)
W. Jaschke (Innsbruck/AT)

B-0960 10:30

Uterine myomas embolization vs. hysterectomy: Progress report

P.C.C.H. Chimeno, H.H.G.H. Gomez, I.T.P.P. Pinto, L.L.P.P. Paul, A.A.R.A. Romo; *Madrid/ES*

Purpose:

1. To measure the efficacy of the uterine arterial embolization in vaginal bleeding control, in patients with bloody uterine myomas.
2. To compare the uterine arterial embolization with the surgical treatment of the histerectomy in hospital sojourn terms (efficiency) and safety through secondary effects valoration.

Material and methods: Trial Clinical, prospective, controled, randomized. We began the trial one year ago and the patients were recruited consecutively. The inclusion criteria are: patients with vaginal bleeding by uterine myomas and surgical candidates. The exclusion criteria are: those patients with any size myomas but asymptomatics, menometrorrhagias caused by differents disorders, or surgical contraindication. The estimated sample size to an allowance in blocks an non-equal 2:1, is 66 patients (44 embolization, 22 hysterectomies) that includes possible loss and pilot cases. The follow-up is two years.

Techniques: Puncture of femoral artery, and selective catheterization of both uterine arteries. Embolization of the uterine arteries with Ivalon particles (400 – 600). After the procedure the analgesic therapy is made with a morphine pump.

Results: We have already made the embolization to 2/3 of the patients. There has been three technic procedure failure because of imposibility of catheterization of the uterine arteries. In patients' controls, all have improved in their symptoms of bleeding and also in their analitical results. We haven't had significant postprocedure complications. The average stay in hospital has been 2 days in the embolization group.

Conclusion: Embolization of uterine arteries for treatment of uterine myomas seems to be an efficacious alternative, improving patients symptoms inmediatly.

B-0961 10:40

Uterine artery embolisation for symptomatic fibroids: Experience of a cost effective approach in a developing country using gelfoam

T.A. Rana; *Karachi/PK*

Purpose: Uterine Artery embolisation (UAE) is an emerging minimally invasive technique for alleviation of symptomatic fibroids. This study was done to assess the efficacy of this treatment modality in Pakistani women using gel foam only.

Materials and methods: During December 1998 to August 2000, 50 women underwent UAE. The mean age group was 25 – 30 years. Menorrhagia in isolation or combination was the principal indication. The procedure was carried out through a right sided femoral arterial puncture. Both uterine arteries were super selectively cannulated and complete embolisation to cessation of flow was performed using gelfoam in the form of particles and/or slurry. Adequate pre procedural antibiotics (Inj Ciproxin 0.1 mg i/v stat) and adequate pain control. The patients were followed every three months on ultrasound for a period of 1 – 18 months

Results: The procedure was technically successful in all the patients. There was complete cessation of menorrhagia in all but one patient with in 2 months. The mean decrease in the uterine volume was 30 % at 3 months, 40 % at six months and to normal level by 12 months. 3 patients had in utero sloughing of fibroid which were removed trans vaginally. One patient got pregnant 3 months after the procedure with return to normal menstrual cycle in all pre menopausal women with in 3 months.

Conclusion: UAE using gelfoam exclusively is a safe alternative to surgical treatment in symptomatic fibroids. This procedure can be done cost effectively in developing countries using simple angiographic catheter and gelfoam.

B-0962 10:50

Transcatheter arterial embolization in the treatment of symptomatic cavernous hemangiomas of the liver: A prospective study

D.N. Srivastava, D. Gandhi, A. Seth, G.K. Pandey, P. Sahni; *New Delhi/IN*

Purpose: This is a prospective study evaluating the clinical and radiological results of transcatheter arterial embolization (TAE) for the treatment of symptomatic cavernous hemangiomas (CH) of the liver.

Materials and methods: Eight patients (5 M & 3 F, mean age 47.75 a, SD: 8.59) with symptomatic CH of the liver were treated by TAE with polyvinyl alcohol particles or gelfoam and steel coils (single session) followed by supportive treatment. The tumor characterization (extent and number) was done on triple phase helical CT or gadolineum enhanced dynamic MRI.

Results: The lesions were located in the right lobe in 4 pts, left lobe in 2 pts and both lobes in 2 pts. The largest diameter of the lesion ranged from 6 to 18 cm (mean 9.28 cm, SD 5.13). The treatment response was assessed on US or CT. Embolization was the only method of treatment in seven patients, however, surgery was done in 1 patient after transcatheter arteial embolization as the symptoms were only partly relieved. Indications for the embolization included abdominal pain (8), rapid tumor enlargement (4 of 8) and recurrent jaundice (1 of 8). Symptomatic improvement was documented in all patients after the embolization. In no patient did the symptoms worsen. The mean size of the tumour did not reveal any statistically significant change on follow-up radiological examinations. However, in one patient, the tumour regressed in size after the embolization.

Conclusions: Transcatheter arterial embolization of hepatic CH is a useful procedure.

B-0963 11:00

Embolization and chemoembolization of evolving liver metastasis from adrenal cortical carcinoma

D. Haddar, B.V. Girish, M. Kardache, T. de Baère, A. Roche; *Villejuif/FR*

Purpose: The aim of our study is to evaluate the benefit of chemoembolization in patients with adrenal cortical carcinoma liver metastasis.

Methods and materials: Between February 1994 and September 1999, 9 patients, aged 31 – 69 years were treated by transcatheter arterial chemoembolization for progressive liver metastasis secondary to adrenal cortical carcinoma. Four patients presented hormonal symptomatology. The number of metastasis was 1, 2 or 3 in 7 cases, and greater in two cases. Their size ranged from 1 to 15 cm. The mean duration of the follow-up was 9 months. Fourteen treatment sessions were carried out. The treatment sessions were separated by a mean interval of 4.2 months. Embolization alone was used in 3 cases and chemoembolization was used in 11 cases. Embolization was carried out with gelatin sponge particles, Embospheres® or Ivalon. The anticancer drug used was cisplatinum emulsioned with iodized oil.

Results: Hormonal symptomatology was stable in 3 cases and increased in one case. Morphologic response was complete in 1, partial in 3, minor in 2 of evaluated patients. The metastasis were stable in one case and progressive in one case. Postembolization syndrome secondary to tissue necrosis was experienced by all patients to a variable degree for 1 day to 4 weeks. No mortality was related to chemoembolization. Four patients were alive at the end of the study.
Conclusion: Chemoembolization is safe and can be effective for clinical and morphological stabilization of progressive liver metastasis from adrenal cortical carcinoma.

B-0964 11:10

Microcatheter embolization of lower gastrointestinal bleeding

B. Funaki[1], J. Lorenz[1], D. Yip[1], G. Zaleski[2], T. Van Ha[1], J. Rosenblum[1], C. Straus[1], J. Leef[1]; *[1]Chicago, IL/US, [2]Racine, WI/US*

Purpose: To evaluate superselective therapeutic embolization for severe colonic hemorrhage.
Materials and methods: Sixteen patients with severe colonic bleeding due to diverticular disease (n = 12), angiodysplasia (n = 2) or metastases (n = 2) underwent embolization with microcoils (n = 14), polyvinyl alcohol particles (n = 1) or both (n = 1). Microcatheters were utilized in all procedures and embolization was performed at the level of the vasa recta or marginal artery of Drummond. Branches of the superior mesenteric artery were embolized in 7 patients and branches of the inferior mesenteric artery were embolized in 9 patients.
Results: Immediate hemostasis was achieved in all patients although 1 patient rebled 24 hours after embolization and required endoscopic cauterization. A second patient with severe co-morbid conditions and widespread bowel metastases continued to have intermittent melena. No patients developed bowel infarction. Two patients with severe diverticulosis had episodes of bright red blood per rectum 2 and 4 months after successful procedures that were treated conservatively.
Conclusion: Therapeutic embolization for severe colonic hemorrhage is effective and well tolerated. The risk of bowel infarction is low.

B-0965 11:20

Superselective embolization treatment of non-iatrogenic kidney trauma

H.-P. Dinkel, W. Danuser, J. Triller; *Berne/CH*

Purpose: To evaluate the feasibility and success of transarterial, superselective embolization after blunt kidney injury.
Methods: In a series of 47 patients with severe renal damage (grade 3 – 5) after non-iatrogenic kidney trauma 25 were treated conservatively, 16 surgically and 7 by radiologic interventional procedures (19 %). After selective angiography (5 F) the exact site of hemorrhage was detected and treated by superselective embolization via a coaxial catheter system (3 F) either using coils (n = 5) or polyvinyl alcohol particles (Ivalon, n = 2).
Results: In all interventionally treated patients bleeding was controlled successfully and rapidly. Additional surgical treatment was not necessary. In one patient whose renal artery stump was embolized due to a complete renal pedicle avulsion organ function was lost. In another, elderly patient with known reduced kidney function partial renal failure happened after the intervention. In all other patients renal function recovered totally. Other complications were not observed.
Conclusion: Superselective embolization is a feasible, effective, and well-tolerated modality after traumatic kidney hemorrhage. Percutaneous transarterial therapy may avoid an operation if diagnostic work-up gives no evidence for other injuries which would warrant surgery. Thus, interventional management reduces the morbidity and mortality in these often polytraumatized patients with increased surgical and anesthetic risks.

B-0966 11:30

Transcatheter embolization of biopsy-related vascular injuries in renal allografts: Technical, clinical and biochemical results

G. Maleux[1], T. Messiaen[1], L. Stockx[2], R.H. Oyen[1], G. Wilms[1]; *[1]Leuven/BE, [2]Genk/BE*

Purpose: To assess the effect of superselective embolization of biopsy-related vascular injuries in renal allografts by evaluating immediate technical and clinical success, the effect on renal function and by determining the long-term survival.
Materials and methods: Between 1993 and 2000, 12 patients were referred for selective embolization. Clinical symptoms were hypovolemic shock due to perinephric hematoma and hematuria. Selective angiography revealed an AV-fistula, a pseudoaneurysm and perinephric contrast extravasation. All lesions were treated by coils. Immediate radiological and clinical success were analyzed as well as renal function 30 and 60 days after embolization.
Results: In all patients a successful embolization could be performed. Clinical symptoms disappeared in all patients. Serum creatinine levels decreased significantly in 10 patients; a slight deterioration of the renal function was observed in 2 patients.
Conclusion: Transcatheter embolization is a safe and effective endovascular technique to treat biopsy-related vascular injuries in renal transplants. In the majority of cases an immediate and significant benefit in renal function can be obtained and longevity of the allograft after successful embolization mainly depends on his natural (medical) outcome.

B-0967 11:40

Endovascular treatment of true and false visceral artery aneurysms: Mid-term results

G. Mansueto, M. D'Onofrio, G. Morana, U. Rozzanigo, M. Valentini, C. Procacci; *Verona/IT*

Purpose: To evaluate mid-term results of endovascular treatment of visceral artery aneurysms.
Methods and materials: From October 1992 to September 2000, 17 patients – six with pseudoaneurysms and eleven with true visceral artery aneurysms (mean diameter 2.9 cm) – were treated. In three patients the aneurysm was filled with coils. In one patient a covered stent was used. In nine patients exclusion of the aneurysm was achieved using "ligation" with coils placed both up- and down-stream. In four patients with ruptured aneurysms embolization utilizing acrylic glue (in three cases) or ligation with coils (in one case) was used. All patients were followed up at 3, 6 and 12 months with Doppler ultrasound and/or CT.
Results: One patient with a ruptured aneurysm and portal hypertension died despite successful embolization. In two patients the procedure was unsuccessful. In two patients "packing" of coils with reperfusion of the aneurysm was seen at three months; definitive occlusion was achieved with a second embolization with coils. In the 14 patients treated successfully, (including those who underwent a second procedure) neither reperfusion nor rupture of the aneurysm was observed during a mean follow-up period of 20 months.
Conclusions: Visceral artery aneurysms can be treated safely and successfully with endovascular techniques.

B-0968 11:50

Embolization treatment of pulmonary arterio-venous malformations

H.-P. Dinkel, T. Dörnhöfer, J. Triller; *Berne/CH*

Purpose: To evaluate the success of superselective transarterial embolization in pulmonary arterio-venous malformations (PAVM).
Methods: A consecutive series of 9 patients (4 male, 5 female, age 18 – 74 years, mean 44 ± 21 years) with 12 PAVM underwent arterial superselective embolization treatment in n = 15 interventions. Arterial pulmonary angiograms were obtained using 5 – 6 F Grollmann type pulmonary pigtail-catheter through a femoral venous approach. Then selective angiography with a 5 F Cobra catheter was obtained, followed by superselective catheterization by means of 3 F coaxial tracker catheter system in n = 10 cases. Embolization was done in all interventions with platinum coils. Size of the PAVM varied between 6 mm and 6 cm (mean 3.2 cm), number of feeders between 1 and 3.
Results: In all patients embolization was successful. Complete primary occlusion succeeded in 8/12 lesions (67 %); in 3 lesions embolization was successful on repetition. Only in one patient (11 %) a lesion was only partially occluded. Clinical symptoms subsided and pO_2 normalized in all cases. Extrasystoles can be observed when the guide wire or catheter tip passes the right atrium. In one patients bradykardia was observed. Serious complications were not observed.
Conclusion: Superselective embolization of PAVM is highly effective and non-invasive. Percutaneous transarterial therapy is the method of choice in the treatment of PAVM and surgery is only necessary in very exceptional cases.

10:30–12:00 **Room I**

Abdominal and Gastrointestinal

SS 1801b

MRCP

Chairpersons:
M.J. Lee (Dublin/IE)
Y. Menu (Clichy/FR)

B-0969 10:30

MR-cholangiopancreaticography: A comparison of three TSE-sequences

T. Ruell, K.J. Hellerhoff, H. Helmberger, E. Rummeny; *Munich/DE*

Purpose: Intraindividual comparison of three TSE-sequences for MRCP in patients with pancreaticobiliary diseases.

Materials and methods: 52 patients with pancreaticobiliary diseases were investigated with MRCP using a 1.5 T MR scanner (ACS NT Philips). Single-shot-TSE sequences in single-slice (SS) and multi-slice (MSL) technique were compared with a 3D TSE sequence. For evaluation the biliary system was divided in ten, the pancreatic system in five sections, than image quality and the best depiction of pathologic findings were assessed by two radiologists in a blinded fashion. Agreement of diagnosis and the extent of additional information by the combination of all three sequences were analysed.

Results: The SS-sequence showed the best image quality. The differences were significant for the intrahepatic bile ducts and the middle and distal pancreatic duct ($p < 0.05$). Minor changes of the pancreatic duct were significantly better depicted with the SS-technique ($p < 0.05$). There was no difference in the final diagnosis comparing the three sequences. In 16/52 patients additional information was found with the combination of all three sequences.

Conclusion: The three techniques did not differ regarding the final diagnosis. However the combination of a projection image (SS-sequence or MIP) and a thin slice technique is recommended, since it yields additional information.

B-0970 10:40

Normal and abnormal MRI findings following cholecystectomy

K. Håkansson[1], O. Ekberg[2], H.-O. Håkansson[1], P. Leander[2]; *[1]Kalmar/SE, [2]Malmö/SE*

Purpose: To describe the normal MRI appearance after cholecystectomy and the findings in patients with postoperative complications using fast pulse sequences in abdominal MRI.

Material and methods: In a prospective study of 119 patients, 64 were examined with MRI after cholecystectomy. In total 56 patients with uncomplicated cholecystectomy were examined with MRI 1 – 5 days (mean 1.6 days) after cholecystectomy. Nine patients had an abdominal postoperative complication and 8 of these were examined with MRI after the complication commenced, 1 – 12 days after the cholecystectomy.

Results: Oedema in the gallbladder fossa was the only finding in 39 patients (61 %), all with uneventful recovery. Small fluid collections in an area consistent with the gallbladder fossa was seen in 9/64 (14 %) patients of which 3 had surgical complications; 1 bleeding and 2 bile duct leakage. Twenty-two (34 %) patients had small locally situated fluid collections adjacent to the liver, 14 were uneventful and 8 showed postoperative surgical complications. Seven patients had fluid in the rest of the abdomen of which 5 had surgical complications; 4 due to bile duct leakage and 1 acute panreatitis. One patient had a postoperative bleeding not seen on MRI.

Conclusion: MRI is very sensitive in detecting fluid collections. Early MRI findings following cholecystectomy are normally only subtle changes, mainly in the gallbladder fossa. Fluid collections diagnosed elsewhere than in the gallbladder fossa usually indicate a surgical complication while a surgical complication is unlikely if MRI fails to show a fluid collection.

B-0971 10:50

Pancreas divisum: Assessment with MR cholangiopancreatography

P. Boraschi, E. Neri, G. Braccini, R. Gigoni, M. Cossu, F. Falaschi, C. Bartolozzi; *Pisa/IT*

Purpose: To determine the usefulness of MR cholangiopancreatography (MRCP) in the diagnosis of pancreas divisum.

Materials and methods: A series of 356 patients underwent MRCP at 0.5 and 1.5 T unit (GE Medical Systems) for the evaluation of the pancreaticobiliary tract. MRCP was performed through a non-breath-hold, respiratory-triggered, fat-suppressed, two-dimensional, heavily T2-weighted fast spin-echo sequence and through a breath-hold, thick-slab, single-shot T2-weighted sequence in the coronal plane. Axial T1- and T2-weighted sequences were previously obtained. In 123 patients, correlation with endoscopic retrograde cholangiopancreatography (ERCP) was available. MRCP source images and maximum intensity projections were analysed by two experienced observers, that were asked to identify the presence and type of anatomic variants of the pancreatic ductal system. Agreement between observers was evaluated with ê statistic.

Results: MRCP identified 29 (8.1 %) cases of pancreas divisum, with an excellent interobserver agreement ($k = 0.97$). Regarding the differentiation between the type of anatomic variant (complete or incomplete pancreas divisum) the interobserver agreement was low ($K = 0.37$). Neither false positive nor false negative cases occurred at MRCP among the 10 patients with pancreatic ductal system variant that was confirmed by ERCP.

Conclusion: MRCP represents an effective imaging method for the diagnosis of pancreas divisum. In particular, in cases with unexplained abdominal pain or recurrent episodes of pancreatitis, MRCP should be performed instead of ERCP.

B-0972 11:00

Acute pancreatic-biliary disease: Can MR cholangiopancreatography influence its management?

F. Pinto, A. Ragozzino, M. Scaglione, R. De Ritis, S. Mosca; *Naples/IT*

Purpose: To assess the influence of MR Cholangiopancreatography (MRCP) on the management in patients referred with acute pancreatic-biliary disease.

Methods: Clinical and radiological records from 37 patients, with clinical diagnosis of pancreatic-biliary disease were retrospectively reviewed. All the patients had undergone evaluation with Ultrasonography (US) and MRCP. In 18/37 patients a CT evaluation had also been performed. The initially suggested therapeutic option (medical treatment, surgical treatment, or evaluation with endoscopy) based on clinical and US or on CT findings, was compared to the treatment adopted after evaluation with MRCP.

Results: In the 37 investigated patients, the following findings were revealed at MRCP evaluation: complication after hepatic transplantation ($n = 9$); retained stones ($n = 8$), leakage ($n = 7$); acute pancreatitis ($n = 7$); acute cholecystitis ($n = 3$); stricture ($n = 2$); traumatic injury ($n = 1$). Treatment based on clinical, US or CT findings was changed in 13/37 patients (35.1 %) after MRCP was performed.

Conclusion: MRCP provides a reliable assessment in patients with pancreatic-biliary disease. In about 1/3 of patients MRCP did influence the therapeutic options.

B-0973 11:10

The diagnostic accuracy of magnetic resonance cholangiopancreatography (MRCP) compared with endoscopic retrograde pancreatography (ERCP) in the evaluation of patients with suspicion of biliopancreatic disease but no obvious need for endoscopic intervention: A prospective study

K.J. Hellerhoff, H. Helmberger, T. Roesch, M. Settles, T.M. Link, M. Classen, E.J. Rummeny; *Munich/DE*

Purpose: To evaluate prospectively the diagnostic accuracy of MRCP in those patients, who need diagnostic imaging of the biliopancreatic ducts, but have no obvious need for endoscopic intervention.

Methods: 113 patients (66 female, 47 male, 56.3 a) with moderate suspicion for pancreatobiliary disease (bilirubin 2.4 mg/dl, diameter of common bile duct in ultrasonography 10 mm) scheduled for diagnostic ERCP were included. MRCP was acquired at 1.5 T (Philips ACS NT) using single shot, 2D multi slice- and 3D-TSE. MRCP diagnoses were blinded to ERCP.

Results: The following biliary diagnoses were found ($n = 84$): stones ($n = 13$), strictures ($n = 29$), normals ($n = 42$). The diagnostic accuracy (sensitivity/specificity) of MRC was demonstrated for normals (83 %/87 %), stones (77 %/95 %), and strictures (93 %/93 %). Pancreatic diagnoses were ($n = 63$): chronic pancreatitis ($n = 11$), strictures ($n = 11$), pancreas divisum ($n = 4$), other normal variants ($n = 3$) and normals ($n = 34$). Diagnostic accuracy (sensitivity/specificity) of MRP was demonstrated for normals (97 %/100 %), pancreas divisum/normal variants (86 %/98 %), chronic pancreatitis (91 %/100 %) and strictures (100 %/100 %).

Conclusion: MRP can provide comparable diagnostic information to ERP and should obviate invasive examination in most patients. Bile duct strictures are correctly detected and classified in nearly all patients. The diagnostic accuracy of MRC for choledocholithiasis is not yet sufficient.

B-0974 11:20

MR cholangiopancreatography: Optimal range of effective echo time in HASTE sequences

G.R. Strasser, W. Schima, E. Schober, M. Uffmann, S.M.M. Metz-Schimmerl; *Vienna/AT*

Purpose: The purpose of the study was to assess the diagnostic quality of different HASTE-MR pulse sequences in the assessment of biliary- and pancreatic duct pathology.
Methods and materials: 31 patients (18 male, 13 female; mean age 51 years) with suspected biliary or pancreatic abnormalities were referred for MRCP. MR-studies were performed on a 1.5 T unit (Vision, Siemens), using three breath-hold HASTE pulse sequences in the coronal plane with a TE of 95, 250, and 900 ms. The images were assessed quantitatively (SNR, CNR of biliary ducts), and qualitatively by blinded reading of two experienced readers.
Results: Quantitatively, there was no significant difference in SNR of bile ducts between the different HASTE pulse sequences. CNR of biliary ducts was highest on HASTE (TE 250) pulse sequence. Qualitatively the HASTE (TE 250) pulse sequence was rated best by two readers (excellent delineation, 48.4 %, good delineation, 45.2 %). The HASTE (TE 900) pulse sequence was read worse than the HASTE (TE 95) pulse sequence (excellent delineation 16.1 % vs. 22.6 %, good delineation 25.8 % vs. 51.6 %, fair delineation 25.8 % vs. 19.4 %, poor delineation 29.1 % vs. 6.4 %).
Conclusion: The breath-hold HASTE pulse sequence with a TE of 250 is the preferred MR pulse sequence for evaluation of biliary and pancreatic ducts.

B-0975 11:30

MR imaging and MR cholangiopancreatography assessment in hilar cholangiocarcinoma: Correlation with surgical and pathologic findings

R. Manfredi, M.G. Brizi, G. Masselli, G. Nuzzo, A. Vecchioli Scaldazza, P. Marano; *Rome/IT*

Purpose: To compare magnetic resonance cholangiopancreatography (MRC) and magnetic resonance imaging (MRI) in the evaluation of hilar cholangiocarcinomas (Klatskin's tumors) with surgical and histopathologic findings.
Materials and methods: Twelve consecutive patients (8 men, 4 women) (mean age: 58 years) with hilar cholangiocarcinomas underwent MRI and MRCP. MRI imaging was performed on 1.5 T imager using breathhold T2-weighted imaging and T1-weighted imaging before and after dynamic injection of gadolinium. All patients underwent surgical resection; the pathologic specimens were employed as standard of reference. Without knowledge of the surgical and pathologic findings three radiologists independently reviewed the MR images to assess the tumor signal pattern, bile duct involvement (according Bismuth classification), local parenchimal extension, vascular involvement and adenopathy.
Results: The neoplastic lesions on T1 images were hypointense in 10/12 patients (83 %) and isointense in 2/12 (17 %); on T2-weighted images were hyperintense in 12/12 patients (100 %). On dynamic gadolinium-enhanced images, progressive heterogeneous enhancement was seen in 11/12 patients (91 %). The MRCP demonstrated correctly the bile duct involvement in 10/12 patients (83 %). The MRI were accurate in 11/12 (91 %) for local parenchimal extension, in 8/12 (66 %) for vascular involvement, 50 % for adenopathy.
Conclusion: MR studies allowed noninvasive, accurate pretherapeutic staging of Klatskin's tumor.

B-0976 11:40

Sclerosing cholangitis: Evaluation with MR cholangiography

I. Tsitouridis, G. Kouklakis, D. Melidis, M. Emmanouilidou, F. Goutsaridou; *Thessaloniki/GR*

Purpose: To determine the clinical usefulness of MR Cholangiography in the evaluation of sclerosing cholangitis of the biliary tract.
Materials and methods: 23 patients with sclerosing cholangitis were studied by MR cholangiography. Examinations were performed on a 1 T (Expert plus, Siemens) scanner and 1.5 T (Gyroscan, Phillips) scanner using HASTE and 2D-FSE sequences. In a period of 3 years we examined 23 patients with sclerosing cholangitis (12 women and 11 men). All patients had a biopsy after the MR Cholangiography, so there was also correlation between MRI and pathology.
Results: MR Cholangiography clearly revealed pathology in all cases. The configuration of the biliary tree was clearly depicted in only 9 patients and in the others, there was only hazy and unclear imaging of the biliary tree, due to the extensive fibrosis. Characterization of the lesion was very difficult and in all cases additional axial conventional MRI scans were necessary.
Conclusion: MR Cholangiography was found to be valuable in the evaluation of sclerosing cholangitis, but both conventional MRI or biopsy are needed for accurate detection and characterization of this disease.

B-0977 11:50

Duodenal diverticulum: Evaluation with MR cholangiography

I. Tsitouridis, G. Kouklakis, N. Krokos, D. Melidis, M. Emmanouilidou, F. Goutsaridou; *Thessaloniki/GR*

Purpose: To evaluate the capabilities of MR cholangiography in patients with duodenal diverticula.
Material and methods: 31 patients with proven diverticula of the duodenum were evaluated with conventional MRI and MR Cholangiography. The examination were performed using a 1 T Siemens Expert plus scanner with a HASTE sequence, before and after the oral administration of 150 ml of water.
Results: 19 of 31 patients with duodenal diverticulosis were correctly diagnosed. In the remaining patients, 3 were suspected to have diverticula but these were not seen clearly, 5 were misintepretated as being normal and in the other 3 patients imaging was unclear but indirect evidence that something abnormal was happening near Ampulla of Vater was present.
Conclusion: MR Cholangiography was found to be valuable in the detection and characterization of duodenal diverticula. One must suspect the disease if there is deviation of the position of the common bile duct.

10:30–12:00 **Room K**

Pediatric

SS 1812

Chest, airways, and the musculoskeletal system

Chairpersons:
S. Laurin (Lund/SE)
M. Riccabona (Graz/AT)

B-0978 10:30

True FISP thick-slice MRI at low field strength: A fast and radiation free modality for paediatric chest imaging

M. Wagner, B. Böwing, W. Rascher, M. Deimling, R. Kuth, T. Rupprecht; *Erlangen/DE*

Purpose: The objective was to evaluate a new technique of fast MRI as an alternative to conventional radiography in paediatric patients.
Materials and methods: 132 investigations were performed in 113 patients (65 m, 43 w, median age 15 a). Imaging was done without cardiac or respiratory triggering in a 0.2 T MR system (Magnetom Open, Siemens, Germany). A modified true FISP sequence was used (TR 6 ms, TE 3 ms, TA 3.6 – 4.6 s, acquisition matrix 200 – 256 × 256, flip angle 90°, T1/T2-weighted image contrast, slice thickness 30 – 300 mm). The results obtained were compared with the conventional chest radiographs.
Results: The examination time per scan (3 slices) was 3.6 – 4.6 s. Lung parenchyma and intrathoracal structures were well visualised. A high signal-to-noise ratio from 4.5 – 7.3 was measured for lung parenchyma. Of 309 pathologies diagnosed on the images 80.3 % were seen on both, x-ray and MR images, 8.4 % were seen on radiographs only, 11.3 % on MRI only. Visibility was rated "equal in both modalities" in 27.2 %, better on radiographs in 31.1 % and better on MRI in 41.7 %. With a reduction of the image matrix real time MRI was made possible.
Conclusion: The true FISP lung MR technique is a promising alternative to conventional paediatric chest radiography due to its very short examination time (rapid imaging) and the large amount of diagnostic information provided by the images.

B-0979 10:40

Multidetector CT in the assessment of atelectases in newborns and infants

J.F. Schäfer, J. Vollmar, M.D. Seemann, W. Luboldt, A. Kopp, C.D. Claussen; *Tübingen/DE*

Purpose: To determine the performance of Multidetector CT (MDCT) in demonstrating the cause of atelectasis in infants.
Material and methods: 10 infants ranging in age from 1 days to 16 months presenting with atelectasis underwent contrast enhanced MDCT (Volume Zoom, Siemens) in high spatial and temporal resolution (collimation/tablefeed/increment –

1 mm/4 mm/0.5 mm). Images were interactively analyzed with the help of reformats, virtual bronchoscopy and bronchography simultaneously displaying tracheobronchial tree and vessels.
Results: Atelectases were found in eight cases including bronchial compression through dilatation of pulmonal artery, mucoid impaction by bronchopulmonary dysplasia, bronchial malacia with ventile-stenosis, complex congenital malformation with aplasia of lung lobes, horseshoe lung and tracheal agenesis. No atelectases were present in two cases with mild deformity of the trachea or a tracheal stent. Virtual bronchography with simultaneous depiction of the vessels was helpful in demonstrating or excluding a vascular genesis as reason for bronchial compression. Virtual bronchoscopy allowed assessment of the trachebronchial tree up to the segmental bronchi and thus permitted diagnosis of intrinsic causes of bronchial obstruction.
Conclusion: The high spatial and temporal resolution provided by MDCT allows comprehensive and noninvasive assessment of the tracheobronchial tree and vessels, improving the diagnostic work up for infants presenting with therapy resistant atelectases.

B-0980 10:50

Bronchopulmonary and sinus inflammatory changes in congenital immunodeficiency syndroms: CT findings in 31 patients
M.P. Bondioni, M.T. Zampedri, R. Maroldi; *Brescia/IT*

Purpose: To identify and quantify bronchopulmonary changes related to recurrent infections in patients affected by Agammaglobulinemia (AG) and Common-Variable-Hypogammaglobulinemia (CVID); to assess the incidence/degree of chronic sinusitis and their relation to bronchopulmonary changes.
Materials and methods: Between 1993 and 2000, 31 patients (23 M, 8 F) affected by AG (15) and CVID (16) underwent HRCT of the lung (42) and CT of paranasal sinuses (51). Age ranged from 4 to 42 years (avg. 21.5 a). All patients received IVIG approximately every 3 weeks, and underwent antimicrobial profilaxis at least in winter-time.
Results: Seventeen out of 31 patients (54.8 %) had bronchopulmonary changes, more frequently observed among AG (66.6 %) than CVD (43.7 %). Bronchiectasis has been detected in AG (6/15) and CVD (3/16), the difference being not significant ($p = 0.3$); bronchiolectasis was present either among AG (2/15) or CVD (7/16) ($p = 0.1$). CT findings of chronic sinusitis have been detected in 30/31 patients, mucosal thickening (29/31), nasosinusal polyposis (10/31) and bone sclerosis of sinusal walls (9/31) being the most frequent features. The mucosal thickening has been shown within the maxillary (84.3 %), sphenoid (41.1 %), ethmoid (35.3 %) and frontal (27.4 %) sinuses. There was no statistically significant difference between AG and CVD patients. CT signs of diffuse chronic sinusitis were detected in patients with (60 %) or without (50 %) bronchiectasis.
Conclusions: On CT the prevalence of bronchopulmonary changes and chronic sinusitis among patients affected by congenital immunodeficiencies is respectively of 54.8 % and 96.7 %. Type and severity of lung lesions do not correlate with the type of immunodeficiency in patients receiving IVIG and antimicrobial profilaxis.

B-0981 11:00

The use of rapid magnetic resonance imaging in the assessment of velopharyngeal dysfunction in children
R. Hanlon, R. McGennis, S. McMahon, G. Hughes, H.M.L. Carty; *Liverpool/GB*

Purpose: To evaluate the role of rapid magnetic resonance imaging in the assessment of velopharyngeal dysfunction in children.
Materials and methods: Seven children aged between 6 and 14 years with suspected velopharyngeal insufficiency were referred for assessment to Alderhey Childrens Hospital. Six of the children were initially investigated by either nasendoscopy or videofluoroscopy. One child underwent both investigations. Dynamic MR imaging of the velopharynx was then performed in all seven cases during phonation directed by a speech therapist. Dynamic T1W images were obtained in the sagittal and coronal planes using a 0.5 T Philips NT Gyroscan. The results of the MR imaging were then compared to those of the videofluoroscopy and nasendoscopy.
Results: Dynamic MR imaging was tolerated in all seven cases. Four of the seven children underwent MR imaging due to failed nasendoscopy. In three cases this was due to poor compliance and in one due to excessive mucus obscuring the field of view. The other three children were investigated by MR following an equivocal videofluoroscopy result. The causes of velopharyngeal insufficiency as shown by Dynamic MR imaging were as follows; hypoplastic palate (2), occult submucous cleft (2), previous cleft palate repair (2) and a combination of submucous cleft and hypoplastic levator muscles (1). The results of the MR imaging were comparable with nasendoscopy and videofluoroscopy where available.
Conclusion: Dynamic MR imaging is a useful adjunct to nasendoscopy and videofluoroscopy. It is well tolerated and particularly useful in those cases of failed nasendoscopy or where other investigative techniques are inconclusive.

B-0982 11:10

Value of CT angiography with MIP reconstruction in the postoperative care of aortic coarctation
G.J. Schaffler, E. Sorantin, R. Groell, A. Gamillscheg, E. Maier, H. Schoellnast, R. Fotter; *Graz/AT*

Objective: The value of CT angiography and three dimensional (3D) reconstructions were investigated in the postoperative care after surgical repair of aortic coarctation and compared with conventional angiography.
Subjects and methods: Twenty-five patients referred because of suspicion of stenosis in the area of former coarctation were prospectively studied with CT angiography and catheter angiography. The morphometric and morphological findings such as aortic diameter, stenosis, aneurysm, intimal flaps or arteriosclerotic plaques were determined with 3D reconstructions using maximum intensity projection (MIP) technique and catheter angiography. The results of both modalities were compared to each other.
Results: The former coarctation was normal in 11 patients, (44 %) [Group A], narrowed in 12 children (48 %) [Group B] and dilatated in two children (8 %) [Group C]. An intimal flap and a circumscribed pouch was delineable in 4 subjects. MIP reconstructions and catheter angiography revealed identical results regarding the classification into Group A, B, C, intimal flaps and circumscribed pouches. Statistical analysis revealed good correlation between the narrowest aortic diameters measured on MIP reconstructions and catheter angiography, whereas there was no correlation between the systolic pullback blood pressure gradient and the diameter ratio of the former coarctation and the descending aorta.
Conclusion: CT angiography and 3D reconstructions using MIP technique represent a reliable non-invasve technique to replace diagnostic catheter angiography in the postoperative care of former coarctation and provides the clinician with valuable information concerning further invasive procedures.

B-0983 11:20

MRI in the diagnosis and follow-up during treatment in children with congenital hip dysplasia and hip dislocation
J. Iwinska-Zelder, T. Wirth, M. Haake, J.T. Heverhagen, E. Walters, K.J. Klose; *Marburg/DE*

Purpose: The assessment of the correct position of the hip joint after closed or open reduction in children with congenital dislocation of the hip is very difficult. To make a correct diagnosis from the radiograph with the hips in plaster is difficult. As the delayed recognition of a recurrent hip dislocation has bad effects on the outcome of the affected hip, a safe and reliable imaging method must be established and obtained.
Materials and methods: 6 children with 8 congenital dislocations of the hip joint were examined by MRI immediately after closed or open reduction. 3 hips had to be treated by open surgery.
Results: MRI allows perfect differentiation between the bony and cartilaginous parts of the hip in plaster. Interpositioning of soft tissues which prevent reduction could be visualized clearly as well. The best sequence in order to differentiate bony from cartilaginous sturctures was a gradient echo sequence in FLASH-technique using a flip-angle of 60 degrees. In all cases the correct position of the hip in plaster after reduction could be demonstrated.
Conclusion: MRI is the imaging method of choice for evaluation and documentation of the reduced position of the hip in plaster. Radiographs are no longer needed.

B-0984 11:30

Three-dimensional-CT of hip dislocation: Qualitative criteria for preoperative planning
C.H. Buitrago-Téllez, R. Brunner, C. Pavlik, B. Mengiardi, G.M. Bongartz; *Basle/CH*

Purpose: To assess the value of qualitative analysis of standardised 3D-CT image reconstructions in children with hip luxations preoperatively.
Methods and materials: A spiral CT (3 mm slices; pitch 1.5, 1.5 mm reconstruction interval) was obtained in 47 subjects aged 3 – 22 (mean 8.85) years with a total of 62 hip luxations. 3D-CT reconstructions (surface rendering technique) were obtained in 12 standard projections. The following criteria were evaluated by a radiologist and a pediatric orthopaedic surgeon by consensus on 3D images: morphology of the femoral head, lateral head impression, head-in-neck deformity, ligamental spike and pseudoarticulation.

Results: An abnormal morphological configuration of the femoral head with loss of rounded form was detected in 37/62 luxated hip joints. A lateral head impression was observed in 30/38 hip dislocations of children with cerebral palsy (CP) and in 2 cases of myelomeningocele (MMC). A head-in-neck deformity was also seen in 14 cases of CP and 5 of MMC and 1 of trysomy. A spike at the insertion of the transverse acetabuli ligament that must be resected was diagnosed in 6 cases of hip dislocations in CP and two other hips with MMC and arthrogryposis. A pseudo-articular surface could be well identified in 52 of all 62 hip luxations.
Conclusion: 3D-CT with standard projections increases detectability of qualitative signs of hip dislocations, which otherwise are difficult to define on single axial or coronal images. Thus, 3D-CT seems to be relevant in cases where operative correction is considered, especially in the setting of cerebral palsy.

B-0985 11:40

MR-imaging in children with former hip dysplasia
S.C.A. Herber, V. Nuss, K. Kuellmer, K.-F. Kreitner; *Mainz/DE*

Purpose: CCD- and AT-ankle evaluation in children with a former hip dysplasia. Assessment of cartilage thickness and surface as well as osseous structures by the mean of MRI.
Material and methods: 90 consecutive children (5 – 14 years) with a former hip dyplasia grade 1 – 3 (Graf score) and 10 healthy children were evaluated at 1.0 T using a surface coil. The defined study protocol included T1-SE, T2*-Flash-2D and a STIR-Sequence in the coronal plane. Image analysis was performed by 2 experienced radiologists by consensus. Qualitative assessment surrounded the signal intensity of the bone marrow as well as the cartilage and the adjacent soft tissue. Quantitative assessment included the cartilage thickness and the evaluation of CCD- and AT- and CE-ankle. Statistical analysis was performed by calculating MEAN-value and SD as well as the Interobserver-variability.
Results: 5/90 children had a severe hip dysplasia that demands for further treatment. 85/90 children had normal findings or even moderate changes, that does not require for a treatment or is recommended for further observation. Cartilage thickness was rated normal in 90/90 cases. AT-, CE- and CCD-ankle measurement could be successfully performed in each case. Interobserver-Variability for ankle measurement did not significantly differ for CE, AT and CCD-ankle and showed a very good correlation with a mean difference < 5°.
Conclusion: MR-Imaging in children with a former hip dysplasia is a promising tool in the diagnostic follow up and should be recommended due to the missing radiation dose as the procedure of the selection.

B-0986 11:50

Pediatric applications of three-dimensional ultrasound (3DUS): Preliminary results
M. Riccabona[1], E. Sorantin[1], D.H. Pretorius[2], T.R. Nelson[2]; *[1]Graz/AT, [2]San Diego, CA/US*

Objective: To evaluate the feasibility of 3DUS in various pediatric conditions.
Patient and method: 60 patients (0 – 14 years) underwent 3DUS of the bladder, the kidney, the brain (including cerebral vessels), various tumors and small parts. 3DUS was performed with various systems using mechanic volume transducers or electromagnetic positioning devices. The reconstructed data were displayed in multiplanar and rendered views. The results of 3DUS were prospec-tively compared to standard 2DUS and results of other imaging (CT, MRI, IVU) when available.
Results: 3DUS was successfully performed in 56 children, in 4 patients data were inaccurate due to motion artifacts. Only incidentally 3DUS provided additional diagnostic information; no significant pathology was missed at shorter investigation time at the patient. Demonstration of complex structures was superior in spite of the poorer resolution on 3DUS (ventricles, cerebral vasculature, hydronephrosis, megaureter). 3DUS volumetry was more accurate. However, abdominal 3DUS suffered from motion artifacts in some patients.
Conclusion: 3DUS can be applied to infants and children. It offers best results in regions with little respiratory movement. It can be considered a useful adjunct to 2DUS for demonstration of complex anatomy, for standardization and documentation. It allows for virtually rescanning after the patient has left, enabling better comparison during follow up or for consulting and teaching/education. 3DUS offers increased volumetric accuracy and might be integrated in future imaging protocols.

10:30–12:00 **Room L/M**

Head and Neck

SS 1808

Salivary glands/Temporomandibular joint

Chairpersons:
E. Hofmann (Fulda/DE)
R. Maroldi (Brescia/IT)

B-0987 10:30

Prospective evaluation of MRI as a first-line investigation of salivary disease in primary care referrals
S.J. Golding, S.R. Watt-Smith; *Oxford/GB*

Purpose: To evaluate an established departmental policy of using MRI as a first-line investigation of salivary disease in primary care referrals.
Methods and materials: 36 patients (20 F, 16 M) with suspected salivary disease referred consecutively from primary care underwent MRI at 1.5 T, using a four-sequence protocol to demonstrate the major salivary glands and their ducts. Presenting symptoms were painful swelling (24), painless swelling (5) and recurrent inflammation (7). Examinations were reported by one radiologist. Additional investigations were carried out at the discretion of the radiologist or at clinical request; clinical records are continually reviewed for evaluation of the patient's course.
Results: Nine patients had normal images. Pathology consisted of sialectasis (15), calculus (4), extrinsic tumour (4), acute infection (3) and dental abcess (1). To date further investigation was requested in six patients but contributed to further management in only two; three sialograms concurred with the MRI findings and one excluded a calculus; radiographs in one patient confirmed dental abcess and one follow up MRI study confirmed reactive lymphadenopathy.
Conclusions: MRI offers a radiation-free method of obtaining information for clinical management of salivary disease in most patients. Only a minority require further investigation. The clinical scenario in which this policy operates is described.

B-0988 10:40

Post-stimulatory MR sialography: Evaluation of a new technique
W.J. Platt, S.J. Golding, S.R. Watt-Smith; *Oxford/GB*

Purpose: To determine the clinical value of adding MR sialography, before and after sialogogue stimulation, to MRI of the major salivary glands.
Methods and materials: Twenty nine patients presenting consecutively underwent sectional MRI at 1.5 T, using a four-sequence protocol to demonstrate the major salivary glands and their ducts. MR sialograms were obtained in bilateral sagittal oblique slabs, and repeated following stimulation by sipping lemon juice. Examinations were read by one radiologist, reading sectional images first and separately from MR sialograms. Objective evaluation of the effect of stimulation on MR sialography was achieved by a separate scoring exercise.
Results: Twenty-five patients completed the procedure. Sectional MRI showed lymphadenopathy (9), sialectasis (5), calculi (4), neoplasm (2), and fatty infiltration (1). Four examinations were normal. Only one MR sialogram showed additional information in a case of calculus. No post-stimulation MR sialogram added further information. Scores of post-stimulation images showed no change in score in 5, improved score in 14 and poorer score in 6. However these differences were not statistically significant (Wilcoxon signed-rate test).
Conclusions: Sectional examination of the salivary glands by MRI provides adequate information for clinical management in most patients. MR sialography provides additional information in a minority of cases and does not appear to be improved by sialogogue stimulation.

B-0989 10:50

Electrical impedance scanning (EIS) as a new additional tool for increased differentiation of parotid and submandibular lesions
M. Facius[1], A. Malich[1], R. Anderson[2], M. Fleck[1], W.A. Kaiser[1]; *[1]Jena/DE, [2]Solna/SE*

Purpose: Compared to nomal cells, cancer cells exhibit altered local dielectric properties (increased conductance). Malignant tumors of the breast and lymph nodes metastases show increased values of conductance. In this study, we tested the reliability and feasibility of (EIS) for assessment of subandibular and parotic tumors.

Method and materials: 45 patient with equivocal lesions were examined using ultrasound (HDI 5000, ATL, USA) and TransScan TS2000 (Siemens, Germany). Each focal spot representing high conductance, which was not caused by artifacts was classified as a positive finding and consequently suspicious for malignancy. The lesions were biopsied or surgically extracted.
Results: 15 of 16 lesions were correctly detected as malignant, and 14/29 were correctly detected as benign (sensitivity 94 % and specificity 48 %). Reasons causing false positive findings were discussed. Positive and negative predictive value were 50 % (15/30) and 93 % (14/15), respectively.
Conclusions: Initial results suggest usefulness of EIS as an adjunct for increased differentiation of uncertain lesions of both locations, parotic and submandibular gland.

B-0990 10:55

Benign lymphoepithelial lesions (BLL) of salivary glands in HIV positive patients: Clinical significance

F. Pretolesi, V. Del Bono, A. Collidà, C. Martinoli, M. Marturano, D. Bassetti, L.E. Derchi; *Genoa/IT*

Introduction: BLLs of salivary glands are relatively common pathological conditions in HIV+ patients, regarded as early manifestation of disease and/or a viral reservoir. Diagnosis is on clinical, US and cytologic grounds. Little is known about the natural hystory of these lesions during therapy and about their possible malignant transformation. We report the clinical and imaging follow-up of 22 patients with BLL.
Materials and methods: We followed-up (mean period 48 months) 22 pts (15 m, 7 f; age range 31 – 60, mean 38.4) with BLL. Special attention was paid to CDC classification of pts at diagnosis, efficacy of high activity antiretroviral therapy (HAAT), evolution of HIV infection, and development of neoplasms.
Results: Of the 11 pts who started HAAT after BLL diagnosis, 7 had regression of the lesions, while 3 remained unchanged. The remaining pt had poor therapy compliance and lesion regression that was considered as spontaneous. Among the 11 pts who were already on HAAT when BLL was diagnosed, 2 remained unchanged, 3 were lost to follow-up and 6 developed non-Hodgkin lymphoma (2 within affected parotid gland; 4 at other sites). On US, the BLLs that developed lymphoma changed their structure into solid and heterogeneous.
Conclusions: Disappearance of most BLLs after HAAT leads to consider such lesions as viral reservoir. Occurrence of lymphoma in pts who developed BLL during HAAT suggests that close follow-up is needed to detect early neoplastic development. The increased survival of HIV+ patients under HAAT will allow better understanding of the clinical significance of BLL.

B-0991 11:05

Fine needle aspiration biopsy in a diagnostic workup algorithm of salivary gland tumours

S. Ivanova, J. Slobodnikova, E. Janska; *Bratislava/SK*

Purpose: To evaluate the utility of fine needle aspiration biopsy (FNAB) under ultrasound control as a diagnostic method of the salivary gland diseases.
Methods and materials: 326 patients with swelling or palpable masses in salivary glands region were ultrasonographicaly examinated in the last 2.5 years period. After evaluation of initial US findings in 132 of them was performed FNAB. 88 patients were surgicaly treated and these histopatological results were compared with the sonography and cytology images (50 tumors and 38 non-tumour deseases).
Results: 34 tumours were benign and 16 malignant. The most frequent benign tumor was pleomorphic adenoma – 23 (68 %), 10 of all malignant lesions were metastatic etiology.
Conclusion: The results demonstrate that fine needle aspiration biopsy under US is usefull to distinguish between benign and malignant lesions and both from non-neoplasm deseases. FNA has proved to be very effective in evaluating the therapeutic strategy – surgery or conservative. In addition, this procedure made it possible to make differential diagnosis of salivary gland tumours without more expensive imaging methods. FNAB has important position in preoperative diagnostic algoritm.

B-0992 11:15

Three-dimensional vascular sonography in the study of cervical masses: Preliminary study

M.E. Badea, M. Baciut, A. Rotaru, R.I. Badea; *Cluj-Napoca/RO*

Aim of the paper: evaluation of three-dimensional sonography "free hand" (3D) for the study of cervical tumors.
Material: 15 patients with cervical tumors (pleomorph adenoma of the parotidian gland – 3; parotidian neoplasm – 2; submandibular neoplasm – 5; metastatic lymph nodes – 3; parotidian abscess – 2).
Methods: Sonography with high resolution (9 – 11 MHz) combined with 3D power and Doppler sonography (Siemens Elegra; General Electric LogiQ 500 devices). All the cases were operated.
Results: Vascularisation was studied only in cases of malignant tumors (11/15). In benign tumors (2) and abscesses (2) no vascular signal was detected. The identified vascular pattern in tumors was the known one: numerous, aberrant, arborescent vessels suggestive for arterio – venous fistulae.
Discussion and conclusions: (1) 3D angiographic sonography facilitates the evaluation of the vascular pattern in malignant cervical tumors; (2) The method is not able to differentiate a malignant tumor from an abscessed mass and does not give information concerning its extension; (3) 3D angiographic sonography is useful for the identification of the main tumoral vessel and for the identification of the relations with the large vessels of the neck.

B-0993 11:25

Real time cine magnetic resonance imaging of the temporomandibular joint in assessment of mobility of the disc and the mandibular condyles

N.M. Hof[1], T. Treumann[2], M. Settles[1], A. Neff[1], E.J. Rummeny[1]; [1]*Munich/DE*, [2]*Luzern/CH*

Purpose: To evaluate a new method of real time cine magnetic resonance imaging (cMRI) in imaging of internal derangement of the temporomandibular joint (tmj) and compare it to static MRI.
Method and materials: 65 patients were investigated with single slice cMRI using a fse T1-weighted sequence (TR/TE 333/23, echo train length 23) with zoom imaging using a 1.5 T MRI unit with 3 images per second during active mandibular movements. Static MRI was performed in a sagittal plane without and with i.v. contrast medium administration in closed and open mouth position. Electronic axiography (CADIAX, Fa. Gamma, Austria) recorded the movement of the mandibular condylus (mc) during active opening and closing of the mouth. MR curves of mc and disc movement were correlated with axiography curves. Visualization of mc, disc and amplitude of condylar translation were correlated with static MRI results.
Results: The relative positions of condylus to disc were visualized better, equally or worse with cine MRI compared with static MRI in 8 %, 69 % and 23 %, respectively. The mobility of the condylus was evaluated better, equal or less with cine MRI in 32 %, 53 % and 15 %, respectively. There was an excellent correlation of cine MRI and axiography ($\kappa = 0.83$).
Conclusion: Real time cMRI of tmj provides a good visualization of disc and mc in the majority of cases. It provides additional information about mobility of condylus and disc during active jaw movements. Therefore cMRI should be added to the standard MR protocol for the investigation of tmj.

B-0994 11:35

Internal derangements of the temporomandibular joint: Diagnosis with high resolution ultrasonography in comparison with magnetic resonance imaging

A.R. Rudisch, G. Bodner, R. Emshoff, W. Judmaier, C. Walch, W. Jaschke; *Innsbruck/AT*

Purpose: To prospectively evaluate high resolution ultrasonography (HR-US) as a diagnostic examination for temporomandibular joint (TMJ) disorders.
Method/materials: 180 joints of 90 patients with TMJ related pain and dysfunction were studied (closed and open mouth position). Magnetic resonance imaging (MRI) as well as HR-US were performed in order to determine the disk-condyle relationship and to detect joint effusions and lesions of the condylar articular surface. The MRI studies (1.5 T, cor. and sag. planes, SE-PD and TIRM sequence) were interpreted by two independent radiologists; an adjudicator made the final decision on discordant interpretations. Longitudinal and coronal HR-US scans along the condyle axis were performed with a linear array, working at high frequency of 12 MHz. The condyle and the articular eminence were assessed as sonogaphic landmarks. The form of the condyle, the position of the disk and the capsular structures were evaluated. The outcome of the HR-US examination was compared with the MRI-diagnosis as the reference standard.
Results: The sensitivity and specificity of HR-US for assessing TMJ effusions were 92 % and 90 %, for assessing lesions of the condylar articular surface 95 % and 97 % respectively. The sensitivity and specificity for assessing TMJ disk displacements with reduction rated 83 % and 90 %, for assessing TMJ disk displacements without reduction 84 % and 96 % respectively. With regard to the diagnosis of 'absence of disk displacement', the sensitivity and specificity rated 94 % and 96 % respectively. Some false-negative errors may be related to the fact that the

reduction of a dislocated disc is an unstable finding and depends on the way of opening the mouth, therefore it can rather be reproduced by the dynamically applicated HR-US than by the static MRI-technique.
Conclusion: High resolution ultrasonography (HR-US) showed a high accuracy for diagnosing anterior, anteromedial, anterolateral and lateral TMJ disc displacements as well as depicting TMJ effusions and lesions of the condylar articular surface. However, it was unable to depict medially or posteriorly dislocated TMJ disks.

B-0995 11:45

Dynamic ultrasound examination of bone regeneration in patients with mandible compression-distraction osteosynthesis
A. Nadtotchi, A. Shamsudinov, N. Bukatina; *Moscow/RU*

Introduction: The compression-distraction osteosynthesis is one of the surgical methods in patients with mandibular abnormalities and deformations. Ultrasound offers the opportunity to study the bone regeneration in a dynamic way. The main aim of this presentation is to show the possibility of echography in bone regeneration.
Subjects & methods: All ultrasound examinations (UE) were obtained on Philips SonoDiagnost 400. 32 patients were examined with mono- (24 cases) and bilateral (8 cases) distraction. UE were performed: the first examination 2 – 3 days after osteotomia and bone fragments compression; the second one – close before bone distraction; weekly examinations during the distraction process; one examination in 2 – 3 weeks during the fixation process.
Results: UE showed the normal compression-distraction osteosynthesis in 20 patients. In 12 cases different complications or deviations of osteosynthesis were shown (complications: 3 cases with osteoporosis development and compression-distraction apparatus (CDA) mobility appearance, 2 cases of CDA metallic construction deformation, 2 cases of mandible angular deformation; deviations: in 3 cases the early echographic finding of high osteogenesis activity made it necessary to increase the distraction speed, in 2 cases the findings of low osteogenesis activity made it necessary to stop distraction for 1 day and then to decrease the distraction speed). Thanks to UE in the last 5 cases there were not complications.
Conclusions: Dynamic UE during the whole treatment period made it possible to investigate the mandibular compression-distraction osteosynthesis and to correct this treatment according to the individual osteogenesis activity.

B-0996 11:55

Cavernoma of the temporal muscle
S. Heckl, A. Aschoff, S. Kunze; *Heidelberg/DE*

Purpose: Intramuscular cavernous haemangiomas are uncommon in the head and neck region with the masseter muscle to be the most frequent site followed by the trapezius and sternocleidomastoideus muscle. Presentation of such a lesion in the temporal muscle is an extremely unusual situation (only 2 cases in literature 1996 and 97). We want to report about a third case.
Materials: A 55 year old man suffered from intermittent headaches and swelling of the right temple region in stress situations. Swelling could be provocated by Valsalva-manoeuvre and bending forward. No tenderness to pressure, no inflammatory signs.
Results: MRI revealed a hyperintense mass in the temporal muscle on T2 without enhancement or arrosion of the bone. MRI control two years later demonstrated no growth of cavernoma. No resection was performed.
Conclusion: In planning a treatment approach one must bear in mind that the cavernomas in the temporal muscle or otherwise in muscle of head and neck stabilize over time. Complications are extremely rare (hemorrhage or functional deficits). These cavernomas should simply be followed up and only be resected in case of any problems.

10:30–12:00 **Room N/O**

Cardiac

SS 1803

Heart perfusion

Chairpersons:
N. Hosten (Berlin/DE)
M.F. Reiser (Munich/DE)

B-0997 10:30

Contrast-enhanced magnetic resonance imaging and myocardial contrast echocardiography in patients with acute myocardial infarction: Comparison with ^{99}Technetium Sestamibi SPECT for the detection of perfusion defects
L. Natale, A. Meduri, A. Lombardo, A. Giordano, L. Galiuto, A. Rebuzzi, P. Marano, A. Maseri; *Rome/IT*

Background: MRI and non-invasive Contrast Echocardiography (CE) are emerging tools in assessing regional myocardial perfusion. We validated them in patients with acute myocardial infarction (MI) comparing with resting ^{99}Tc-Sestamibi SPECT.
Method/materials: 14 consecutive patients with first acute MI (61 ± 9 a, 12 anterior, 2 inferior) underwent MRI, MCE and SPECT, within 7 days after onset. MRI was performed on short axis, with multi-slice FSE and cine, single-slice first pass (iv Gd-DTPA, Magnevist, 10 ml, 3 ml/s), and delayed T1w FGRE. CE was performed in Harmonic Power Doppler mode (iv Levovist 4 – 8 g, 400 mg/ml, 4 ml/min). Analysis was performed using a 16 segments LV model. At MRI, segments were defined as Type1 (normal first pass, delayed hyperenhancement); Type 2 (hypoenhancement at first pass, delayed hyperenhancement); Type 3 (persistent hypoenhancement). At MCE a perfusion defect was defined as absent or heterogeneous enhancement.
Results: MCE was diagnostic in 74 % of segments of infarct zones and correctly identified perfusion state in 79 % of segments (sensitivity 79 %, specificity 78 % versus SPECT). MRI correctly identified perfusion state in 75 % of the same segments. Patterns 2 and 3 had 65 % sensitivity and 78 % specificity versus SPECT. Pattern 3 alone was 100 % specific. Concordance between MCE and MRI in recognising perfusion status was 80 %.
Conclusions: In our patients, non-invasive MCE is slightly superior to MRI in identifying perfusion defects. This could be due to the single slice first pass study, available on our scanner; multi-slice first pass is mandatory to gather better accuracy.

B-0998 10:40

Combined first-pass and delayed contrast enhanced MRI in the assessment of myocardial viability after acute infarction
L. Natale, A. Meduri, A. Lombardo, A. Giordano, P. Marano, A. Maseri; *Rome/IT*

Purpose: Myocardial viability assessment is crucial in patients with acute myocardial infarction (AMI), to rule out therapy and prognosis. To define MRI role, we compared MRI, rest ^{99}Tc SESTAMIBI SPECT and Dobutamine Echocardiography (DE).
Method/materials: 12 consecutive patients with first AMI (63 ± 9 a, 10 anterior, 2 inferior, 5 primary PTCA, 5 thrombolysis) underwent MRI, DE and SPECT within one week after onset. MRI was performed on short axis with multi-slice bh FSE and bh cine, single-slice first-pass (iv 10 ml Gd-DTPA, 3 ml/s) and multi-slice delayed T1w FGRE. Image analysis was performed using a 16 segments LV model and for infarct area. Segments were classified as: (1) normal at first pass, absent or delayed hyperenhancement; (2) hypoenhancement at first-pass, delayed hyperenhancement; (3) hypoenhancement at first-pass and delayed images. Segments out of first-pass slice were classified at delayed imaging as normal, hyperenhanced and hypoenhanced. Patterns 2 and 3 and patterns hyper- and hypo- were considered non viable myocardium. Contractile reserve at DE and MIBI uptake > 50 % were considered positive for viable tissue.
Results: Infarct area approach (at least 2 viable segments per area) showed better agreement within the 3 techniques; furthermore, using MIBI SPECT as viability standard, MRI showed 77 % sensitivity, 100 % specificity and 83 % accuracy.
Conclusions: Pattern 1 and pattern 3 respectively identify viable and non viable tissue. Pattern 2 or delayed hyper-lack in specificity. Combined approach is superior to delayed images alone, but multislice first pass (at least 3 slices) is mandatory.

B-0999 10:50

MRI first-pass myocardial perfusion pre- and post percutaneous myocardial laser-revascularisation

C. Weber, P. Steiner, S. Baldus, G. Adam; *Hamburg/DE*

Purpose: Evaluation of MRI first-pass myocardial perfusion pre- and post percutaneous myocardial laser-revascularisation (PMR).
Material and methods: MRI was performed, in 10 patients with coronary heart disease grade III – IV, 1 – 4 days prior to PMR, 1 – 5 days and 6 months after PMR. Contrast enhanced (0.1 ml/kg; 4 ml/s) "first-pass" MRI imaging was obtained by breathhold, ECG-triggered, multislice Turbo-FLASH GRE. For quantitative analysis absolute and procentual signal-to-noise (S/N)-measurements were calculated. Positron Emission Tomography (PET) was regarded as gold standard for myocardial perfusion.
Results: The mean values of absolute and % S/N-increase revealed no statistical difference between pre- and immediately post-PMR imaging. Six months following PMR both values were significantly elevated (14.1 vs. 24.4 and 127 vs. 176; $p = 0.03$ and $p = 0.01$). However, the non-treated myocardial segments revealed a similar S/N pattern. Intra-individual analysis showed a significant S/N-increase post PMR in one patient, and in additional 4 patients 6 months later. PET diagnosed increased myocardial perfusion in only 2/10 patients. Following PMR 5/10 patients experienced a significant reduction of chest pain equivalent to 2 CCS grades. Two of these had significant S/N-elevations but no evidence of increased perfusion by PET.
Conclusion: S/N first-pass calculations following PMR do not well correlate with the true situation of myocardial perfusion. They seem to be more closely associated with other histological phenomena and possible explanations for the improved clinical symptomatology.

B-1000 11:00

Prediction of necrosis and regional viability after myocardial infarction by MR imaging: A one year follow-up study

S. Miller, U. Helber, U. Kramer, N.I. Stauder, J. Pflumm, H.M. Hoffmeister, C.D. Claussen; *Tübingen/DE*

Purpose: Complementary MR imaging may be helpful to determine the extend of necrosis and preserved viability in the subacute phase after myocardial infarction (MI). This study reports on a one year follow-up after acute MI using complementary techniques of MR imaging.
Methods: 32 patients were examined 7 – 14 days after acute MI using a 1.5 T Magnetom Vision (Siemens). Tissue injury was assessed with a T2-weighted fast spin echo sequence. Cine-FLASH 2D imaging was applied to determine regional myocardial wall thickening (MWT). First pass and late contrast enhancement were studied with a Turbo-FLASH 2D sequence injecting a bolus of 0.1 mmol/kg Gd-DTPA. Increased signal intensity (SI) in T2-weighted and late enhancement images was interpreted as evidence of ischemic myocardial injury and compared to segmental MWT. Regions with preserved systolic function were defined to represent preserved viability. Until September 2000 17 patients were re-examined 12.9 ± 0.5 months after the initial acute ischemic event.
Results: A high grade perfusion deficit was found to serve as a 100 % predictor of scar formation. Pathological T2 SI/late post contrast enhancement was found in 18 %/14 % of segments in acute MI and in 0 %/12 % of segments one year later. Whereas functional recovery was observed in 28 % of segments with increased T2 SI, regional function remained significantly decreased in 92 % of segments with late enhancement.
Conclusion: MRI can determine necrosis and preserved viability in the very early phase after MI using complementary imaging techniques.

B-1001 11:10

Correlation of contrast enhancement patterns after Gd-BOPTA with myocardial infarction and viability

J.J.W. Sandstede[1], M. Beer[1], C. Lipke[1], T. Pabst[1], S. Neubauer[2], D. Hahn[1]; *[1]Würzburg/DE, [2]Oxford/GB*

Introduction: Different contrast enhancement patterns (CEP) have been described for the detection of myocardial infarction (MI) and viability with various contrast agents at different time points after injection. Gd-BOPTA is known to have a higher relaxivity in the presence of serum proteins which are extravasated in acute MI. Aim of this study was to analyze CEP and their time course in subacute MI after injection of Gd-BOPTA in humans.
Subjects and methods: 7 patients with subacute MI (18 ± 9 days) and 1 patient with chronic MI (212 days) were examined at 1.5 T before and 3 and/or 6 months after revascularization of the infarct-related artery. Regional wall motion was assessed by cine MRI. Repetitive images of one representative slice with wall motion abnormalities were acquired up to 30 min after injection of 0.1 mmol/kg Gd-BOPTA using a T1-w TSE-sequence.
Results: 3 patients showed homogenous or mid-wall/subendocardial enhancement of the infarcted region associated with mechanical improvement after revascularization. 4 patients including the one with chronic MI revealed enhancement with a mid-wall hypoenhanced zone that showed unchanged wall motion abnormalities at follow-up. 1 patient presented a mixture of homogenous and mid-wall hypointense enhancement matching with a mixture of improvement and scar formation at follow-up. Depiction of this mid-wall hypoenhanced area was optimal 5 min after injection and was constant at follow-up.
Discussion: Homogenous and mid-wall/subendocardial enhancement after Gd-BOPTA indicates viable myocardium. Mid-wall hypoenhancement indicating microvascular obstruction correlates with scar formation and can be observed in the subacute and chronic state of MI.

B-1002 11:20

Validation of a three-dimensional contrast-enhanced magnetic resonance imaging technique for determination of myocardial viability

M. Regenfus, C. Schlundt, D. Ropers, S. Achenbach, M. Schmidt, N. Oesingmann, W.G. Daniel, W. Moshage; *Erlangen/DE*

Background: To validate a new three-dimensional (3D) contrast enhanced magnetic resonance (MR) imaging technique for detection of myocardial viability versus the commonly used two-dimensional (2D) MR technique.
Methods: 23 patients who had suffered myocardial infarction were examined on a 1.5 T scanner (SONATA, Siemens) with high performance gradient system (40 mT/m amplitude, 200 T/m/s slew rate) using both 2D (TR/TE 8.0/4.0 ms) and 3D (TR/TE 3.4/1.2 ms) segmented Turbo FLASH sequences. Signal of normal myocardium was suppressed by individually adapted inversion recovery magnetization preparation. Acquisition was started 15 min after intravenous injection of 0.2 mmol/kg Gd-DTPA (MAGNEVIST, Schering). Within one exspiratory breathhold 20 short axis slices were acquired by the 3D technique. For the 2D technique corresponding single slices had to be performed during repeated breath-holds. Quantitative image analysis was performed by determination of signal-to-noise (SNR) and contrast-to-noise ratio (CNR).
Results: MR images of both 3D and 2D techniques could be evaluated in all subjects and were able to depict the area of myocardial infarction. SNR showed no statistically significant difference (3D: 32.5 ± 17.4 v. 2D: 27.4 ± 20.4, $p < 0.27$) whereas CNR was better for the 3D technique (3D: 28.6 ± 17.3 v. 2D: 18.9 ± 12.6, $p < 0.02$).
Conclusion: The new 3D MR technique for detection of myocardial viability compared favourably in respect of image quality to the commonly used 2D technique. Advantages of the 3D technique might be the potential of 3D reconstruction and volumetry of nonviable myocardial areal and the uncomplicated single breath-hold approach.

B-1003 11:25

Determination of myocardial viability by three-dimensional contrast-enhanced magnetic resonance imaging: Comparison with 201-thallium scintigraphy

M. Regenfus, C. Schlundt, D. Ropers, S. Achenbach, N. Oesingmann, G. Platsch, T. Kuwert, W.G. Daniel, W. Moshage; *Erlangen/DE*

Background: Contrast enhanced magnetic resonance (MR) imaging has been validated for detection of myocardial viability. We compared a new 3D MR imaging technique to ^{201}Thallium scintigraphy (TH) in respect to detection of myocardial viability.
Methods: 11 patients who had suffered myocardial infarction were examined on a 1.5 T scanner (SONATA, Siemens) with high performance gradient system (40 mT/m amplitude, 200 T/m/s slew rate) using a 3D (TR/TE 3.4/1.2 ms) segmented Turbo FLASH sequence. Signal of normal myocardium was suppressed by inversion recovery magnetization preparation. Acquisition was started 15 min after intravenous injection of 0.2 mmol/kg Gd-DTPA (MAGNEVIST, Schering). 20 short axis slices were acquired within one exspiratory breath-hold. TH was performed according standard techniques. A 16-segment model of corresponding basal, midventricular and apical slices was analysed independently for viable and nonviable segments.
Results: All 176 segments could be evaluated by MR. By TH 10 segments of the redistribution series had to be excluded because of poor image quality whereas all 176 segments of the rest series could be evaluated. MR defined 139 segments as viable and 37 segments as nonviable compared to 129 viable and 47 nonviable segments by TH. There was a close correlation between both techniques ($p < 0.05$).

Conclusion: Delayed enhancement MR and TH show an excellent correlation for determination of myocardial viability. Potential advantages of MR are the uncomplicated single examination approach and the considerably higher spatial resolution. Therefore, MR may be able to depict directly patchy and subendocardial necroses and facilitate discrimination of patients for revascularization therapy.

B-1004 11:30

Cardiac morbidity in patients referred for non cardiac vascular surgery

R. Rienmüller, E. Mahla, H. Metzler, P. Tiesenhauser, B. Schröttner, S. Zoroufchi; *Graz/AT*

Purpose: Cardiac morbidity in patients referred for non cardiac vascular surgery was reported to be about 10 % (Mangano; 1990). The goal of this prospective study was to evaluate determinants of cardiac function which may influence cardiac morbidity.

Methods and materials: 14 patients with aneurysm of the abdominal aorta (AAA), 20 with infrainquinal (IBS) and 11 with carotis interna occlusive diseases (CIS) were studied one day before, 2nd and 5th day after surgery by Electron Beam Tomography determining following functional parameters of the heart: Coronary Calcium Score (CCS), Left Ventricular Muscle Mass (LVMM), Myocardial Blood Flow (MBF), Ejection Fraction (EF) and Stroke Volume (SV). Additionally, the blood pressure and the Heart Rate (HR) were measured.

Results: The mean values and standard deviations were calculated as: CCS (3188 ± 1296), HR (73 ± 14 bpm), MBF (68 ± 18 ml/100 g/min), EF (68 ± 11 %) and LVMM (148 ± 33 g). 5 of 45 patients (2.6 %) showed "hard events" as myocardial infarction (n = 1), cardiac heart failure (n = 3) or tachycard dysrhythmia (n = 1). These five patients differed significantly either by LVMM, HR, SV, MBF or CCS from calculated mean values from the remaining 40 patients without "hard events". The low cardiac morbidity is seen to be due to perioperative intravenous acetylsalicylic acid application.

Conclusion: The presented results suggest that it is possible to identify patients with risk of "hard cardiac events" non invasively before non cardiac vascular surgery. The LVMM, CCS and the HR seem to be more important predictive determinants of patients outcome than EF or MBF.

B-1005 11:40

MRI in acute leftventricular myocarditis for guidance of endomyocardial biopsy

G.K. Schneider, I. Janzen, K. Altmeyer, R. Seidel, B. Kramann, B. Schwaab; *Homburg a. d. Saar/DE*

Purpose: Definite diagnosis of myocarditis requires myocardial biopsy as well for histologic evaluation as to apply molecular techniques. The aim of our study was to evaluate if MRI is useful in preinterventional localisation of acute inflammatory processes to minimize sampling error in endomyocardial biopsy.

Materials and methods: In 13 patients (age 40 ± 18) showing clinical signs of myocarditis ECG-gated MR imaging of the heart was performed using as well single-shot sequences as T1w, T2w and STIR sequences in breath-hold technique unenhanced and after injection of Gd-DTPA. Images were aquired in the four chamber view as well as in the short axis view of the heart. MRI was rated positive if hyperintense myocardial areas could be detected in T2w images showing contrast enhancement after Gd injection. 4 biopsies were made in the areas depicted in MRI. Biopsies were rated positive for active myocarditis if activated T-lymphocytes and macrophages or persistent virus without myocardial fibrosis could be detected.

Results: Biopsy showed chronic myocarditis in 6 patients, in 1 patient healing up myocarditis was diagnosed. In 6 patients biopsy was negative. MRI was positive in all patients with histological proven myocarditis as well as in 2 patients with negative biopsy, thus resulting in a sensitivity of 100 % and a specificity of 67 % with a negative predictive value of 100 % and a positive predictive value of 78 %.

Conclusion: Regarding these first results, MRI seems to be useful for screening of patients with clinical signs of myocarditis for guidance of biopsy to minimize sampling error.

B-1006 11:50

Predictive value of spect with ^{123}Iodine pentadecanoic acid and ^{123}Iodine-MIBG in cardioc patients

V.Y. Soukhov, N.P. Fadeev, I.Y. Savitcheva, A.E. Kuznetsov; *St. Petersburg/RU*

The prognostic properties of cardiac imaging with ^{123}Iodine labeled 15-iodinepentadecanoic acid (^{123}I-PDA) and meta-iodobenzylguanidine (^{123}I-MIBG) for different heart disease were evaluated. While ^{123}I-PDA as the synthetic radiolabeled free fatty acid has the ability to show differences in blood supply and metabolism of myocardium, ^{123}I-MIBG allows to evaluate cardiac sympathetic innervation and function. SPECT images of the heart using "APEX SP-6" camera (Elscint, Israel) were obtained from one hundred sixty three patients with history of myocardial infarction (MI): n = 49, congestive heart failure (CHF): n = 30, cardiomyopathy: n = 11 and coronary artery disease (CAD): n = 72. All patients had undergone ^{123}I-MIBG myocardial scintigraphy: injected dose of 185 MBq and were twice examined by ^{123}I-PDA: at 3 – 5 and 35 – 40 min after i.v. injection of 400 MBq. Early ^{123}I-PDA SPECT demonstrated high specificity in diagnostics of perfusion defects (up to 85 %). The delayed images showed foci of remainig higher activity in regions of ischemic, but viable myocardium. Non uniformity of ^{123}I-PDA uptake indicated the ischemic or dilated cardiomyopathy. There were significant correlations between MIBG uptake, calculated cardiac function (average value of LVEF) and regional wall motion assessment by means of echocardiography. ^{123}I-PDA appeared excellent characteristics in detecting of perfusion/metabolic abnormalities and viability assessment of ischemic myocardium and ^{123}I-MIBG in cardiac innervation and function assessment. The combined use of these radiopharmaceuticals is suitable for prognosis of treatment efficacy, helpful for adequate therapy choice and its assessment during follow-up.

10:30–12:00 **Room P**

Vascular

SS 1815

Aorto-iliac vessels

Chairpersons:
I.P. Arlart (Stuttgart/DE)
F.P. Boudghène (Paris/FR)

B-1007 10:30

Multislice-CT angiography vs. calibrated catheter digital subtraction angiography of the abdominal aorta before endoprothetic stenting of abdominal aortic aneurysms

H.-P. Dinkel, P. Herrmann, M. Sonnenschein, T. Dörnhöfer, H. Hoppe, D. Do, J. Triller; *Berne/CH*

Purpose: Digital subtraction angiography (DSA) using a calibrated catheter is the examination of choice for planning stent-grafts in aneurysms of the abdominal aorta before endoprothetic stenting. However, CT is needed to assess the outer diameter of the vessels which are often narrowed by a thrombus. This examination is to whether multislice-CT angiography (MSCTA) can replace calibrated DSA.

Methods: In 20 patients which were to undergo endoprothetic stenting of the abdominal aorta both calibrated DSA and multislice-CT angiography were performed. MSCTA was acquired on a Asteion MS (Toshiba) with 120 kV, 200 mA, 0.75 s rotation, in 4 x 2 mm collimation, pitch 5.5, 2 mm reconstruction interval with 140 ml of 300 mg/ml I non-ionic contrast at 4 ml/s using bolus-triggering. Threedimensional maximum intensity projections were obtained on the console. DSA was performed on a Philips Integris V5000. Measurements of the length and diameter of the aneurymal body and neck and the diameter of the iliac arteries were performed on an Easy vision workstation (Philips) for DSA and MSCTA by two independent readers.

Results: MSCTA was found to be similar of equivalent to DSA with respect to the depiction of the renal arteries and the superior and inferior mesenteric artery. Measurements were reliable and reproducible with both methods within a margin of error of less than 10 % in most and 15 % in all cases.

Conclusion: Multislice CT angiography of abdominal aorta is equivalent to calibrated DSA before endoprothetic stent-graft treatment of aneurysms of the abdominal aorta.

B-1008 10:40

Evaluation of thoracic aorta with retrospective and prospective ECG-triggered multislice CT (MS-CT)

J.E. Roos, J.K. Willmann, M. Lachat, M. Turina, P.R. Hilfiker; *Zürich/CH*

Purpose: To evaluate MS-CT with prospective and retrospective ECG triggering for assessment of thoracic aorta in comparison with non triggered MS-CT.

Material and methods: In 45 patients with suspected thoracic disease either a conventional MS-CT (n = 15) or ECG-triggered (prospective n = 15, retrospective n = 15) MS-CT (Siemens Somatom Plus VolumeZoom, Erlangen, Germany) was performed. Prospective ECG triggering was performed in sequential mode with a 2.5 mm slice thickness and rotationtime of 0.5 s. Retrospective ECG gating was performed with 1 mm slice thickness in spiral mode (pitch 1.3 – 1.8). 1.25 mm

slices were reconstructed with an increment of 0.8 mm. Both acquisitions were performed during a single breath hold. Data were evaluated on axial slices and multiplanar reformations (MPR).
Results: With ECG-triggering or -gating, no motion artifacts in the ascending and descending aorta were detected. The involvement of aortic root, coronary arteries and the supraaortic vessels in aortic disease could be clearly determined, especially in cases of aortic dissection. With conventional MS-CT, motion artifacts are most evident in the aortic root and ascending aorta.
Conclusions: ECG-trigged or gated MS-CT provides, compared with conventional MS-CT, a motion free evaluation of the entire thoracic aorta and adjacent areas.

B-1009 10:50

Multislice-CT-angiography can replace catheter angiography in patients with vascular emergencies

M. Rieger, A. Mallouhi, W. Perkmann, R.J. Bale, M. Maas, A. Buchegger, A. Dessl, C. Fink, W. Jaschke; *Innsbruck/AT*

Purpose: The aim of this study was to demonstrate the feasibility of high resolution multislice-CT-reconstruction (MSCT-R) in emergency diagnosis of vascular pathologies
Materials and methods: In 89 patients with suspected vascular pathology Multislice-CT (GE, Light Speed QX/i) and 3-D reconstruction were performed instead of angiography. The possibility of large volume acquisition within seconds and the performance of high resolution reconstructions within a few minutes in patients with multiple Trauma or vascular emergency allows imaging of the injured arteries as well as aortic or cerebral aneurysms and arterial occlusive disease.
Results: In all but one patients MSCT-R was sufficient to detect pathological changes of the vessel within a few minutes. In only a few patients an additional angiography was carried out, but in the majority of the cases no further information could be obtained. Only in one case a suspected aneurysm near the base of the skull could not be detected by MSCT-R. MSCT-R gives more detailed information, as the three-dimensional visualisation allows a more exact representation of the diseased vessel than angiography.
Conclusion: MSCT-R as a first diagnostic step in emergency vascular patients can replace angiography without missing sensitivity. As a positive side-effect the saving of time, money and medical staff in these mostly critical patients ean be observed.

B-1010 11:00

Contrast-enhanced helical CT in the diagnostic work-up of acute thoracic aortic injuries

M. Scaglione, M. Tuccillo, F. Pinto, R. Niola, S. Giovine, I. Trasente, R. Grassi, A. Ragozzino, L. Romano; *Naples/IT*

Purpose: The purpose of this retrospective study was to determine the value of contrast-enhanced helical Computed Tomography (CT) for detecting and managing acute thoracic aortic injury (ATAI).
Materials and methods: 1419 consecutive chest CT examinations were performed in the setting of major blunt trauma. The following CT findings were considered indicative of ATAI: intimal flap, pseudoaneurysm, contour irregularity, lumen abnormality, extravasation of contrast material. On the basis of these direct findings no further diagnostic investigations were performed. Evidence of isolated mediastinal hematoma constituted an abnormal CT study: in these cases, thoracic aortography was performed even if CT indicated normal aorta.
Results: 77 patients had abnormal CT scans: among the 23 patients with direct CT signs, acute thoracic aortic injuries was confirmed at thoracotomy in 21. Two false-positive cases were observed. The 54 remaining patients had isolated mediastinal hematoma without aortic injuries at CT and negative angiograms. No adverse clinical sequela were observed in the 1342 patients with negative CT scans.
Conclusion: Contrast-enhanced helical CT as a critical role in the exclusion of ATAI; direct CT signs of ATAI do not require further diagnostic investigations: isolated aortic bands or contour abnormalities should be considered as possible artefacts or related to non-traumatic etiologies especially if mediastinal hematoma is absent. In cases of isolated mediastinal hematoma other sources of bleeding should be first considered before directing patients to thoracic aortography.

B-1011 11:05

Three-dimensional gadolinium-enhanced MR angiography of abdominal aorta and lower limbs: "Hybrid technique"

D. Brisbois, P. Magotteaux, A. Nchimi, J.-F. Biquet, C. Saive, A. Jadot; *Liège/BE*

Purpose: MR angiography is an elegant and non invasive technique to work-up arterial pathologies in the lower limbs. With the hybrid technique we covered aorta and peripheral vessels including the run-off. This study demonstrates the reliability and accuracy of MR angiography in this indication.
Materials and methods: 50 intra-arterial angiograms of abdominal aorta and lower limbs were followed by MR angiography in a delay of maximum 24 hours. The indications were mainly claudication (stage I to III). We used a standardized technique with a first step on abdominal aorta triggered by direct visualisation of the contrast arrival ("care bolus"), panoramic array and body phased-array were combined to cover abdominal aorta and lower limbs. MR results were retrospectively reviewed and correlated with DSA. The accuracy of the stenosis quantification and image quality were statistically estimated including interobserver correlation.
Results: All MR examinations were feasible. The degree of image quality is estimated for aorta and renal arteries, iliac arteries, femoro-popliteal arteries and run-off. Global accuracy is over ninety percent. A slight overestimation observed seems to not have clinical significance to planify treatment. Only two examinations were classified poor quality for the thigh. In every cases distal arteries were nicely shown (better than DSA in five cases).
Conclusion: MR angiography of aorta and lower limbs is in our experience an easy, quick, reliable and non invasive technique for diagnosis of atherosclerosis. It could replace DSA in the near future.

B-1012 11:15

CT and MR imaging of mycotic aneurysms and infected grafts of the aorta and pelvic vessels

P.R. Knuesel, D. Weishaupt, P.R. Hilfiker, P.R. Vogt, M.I. Turina, B. Marincek; *Zürich/CH*

Purpose: To compare the performance of CT and MR imaging in mycotic aortic aneurysms and infected grafts of the of the aorta and pelvic vessels.
Methods: Preoperative spiral CT and MR images of 21 patients with surgically and microbiologically proven infections of the aorta or the pelvic arteries (10 patients with mycotic aneurysms, 11 patients with aorto-iliac graft infections) and CT or MR images of 25 patients without clinical evidence of an vascular infections (12 patients with aortic aneurysms and 13 patients with grafts) were reviewed by two radiologists. Various imaging findings potentially associated with a vascular infections were assessed. In addition, the two readers rated their confidence independently on MR and CT images using a five point scale for the presence of vascular infection. Surgical findings served as standard of reference.
Results: Sensitivity and specificity of CT imaging and MR imaging for the presence of a mycotic aortic aneurysm was 83 % and 85 %, and 81 % and 75 %, respectively. Sensitivity and specificity of CT imaging and MR imaging for the presence of an infected graft was 88 % and 92 %, and 67 % and 80 %, respectively. The most reliable single imaging finding for both imaging modalities was the presence of an enhancing perivascular or periprosthetic mass (sensitivity, 81 %, specificity, 96 %). Receiver operating characteristics revealed a higher confidence when interpretation was based on CT images.
Conclusion: Use of CT is more useful than MR imaging in the assessment of suspected mycotic aortic aneurysms and infected grafts of the aorta and pelvic vessels.

B-1013 11:25

Aortoiliac curvature evaluation before endovascular repair of abdominal aortic aneurysms: Comparison of observer interpretation of helical CT angiography and digital subtraction angiography images relative to a quantitative standard

M. Tillich[1], G.D. Rubin[2], B.J. Betts[2], P.R. Hilfiker[2], A. Lee[2], M. Razavi[2], D. Sze[2], Y. Wolf[2], C.K. Zarins[2]; *[1]Graz/AT, [2]Stanford, CA/US*

Purpose: To determine the ability of interventional radiologists and vascular surgeons to detect and grade curvature of the aorta and iliac arteries from 3D shaded surface CTA and digital subtraction angiography (DSA) images in patients with abdominal aortic aneurysms.
Materials and methods: The median luminal centerline of the aorta and iliac arteries from helical CTA data of 22 patients with aortic aneurysms prior to stent-graft repair was extracted. Curvature was quantified every millimeter along the centerline and served as the reference standard for curvature. Three interventional radiologists and three vascular surgeons experienced in stent-graft delivery inde-

pendently reviewed CTA and DSA images in two sessions, to assess which iliac artery was more tortuous and which site in each iliac artery has the greatest tortuosity and to grade the severity of iliac curvature on a five-point scale.
Results: The observers correctly detected which iliac artery was more tortuous with CTA in 76 % (CI: 68 – 83 %) and DSA in 70 % (CI: 61 – 77 %). The most tortuous site in the left and right iliac arteries was correctly diagnosed with CTA in 65 % (CI: 56 – 73 %), and with DSA in 67 % (CI: 58 – 74 %). There were no significant differences in the performances of radiologists or vascular surgeons. There were no significant differences between CTA and DSA in grading of curvature.
Conclusion: Aortoiliac curvature cannot be determined reliably using either 3-D CTA or DSA images.

B-1014 11:35

Hybrid rendering and virtual angioscopy before and after endovascular repair

M.D. Seemann[1], F. Schmid[2], W. Luboldt[1], J. Vollmar[1], J.F. Schäfer[1], C.D. Claussen[1]; *[1]Tübingen/DE, [2]Ulm/DE*

Purpose: A shaded-surface- and volume display (hybrid rendering method) with the possibility of virtual endoscopy was developed. To give an impression of the possibilities and advantages of this rendering algorithm we have specifically highlighted the use in relation to the arterial vascular system before and after endovascular stent-graft repair.
Materials and methods: We examined 12 patients with aneurysmal changes of the thoracic aorta (n = 3), abdominal aorta (n = 8) and popliteal artery (n = 1) before and after stent-graft repair, using image data sets from thin-section spiral computed tomography (SCT). The arterial vascular system and the stent-grafts were segmented and visualized with a surface rendering method. The other surrounding bony and soft tissue structures were visualized using a transparent volume rendering method. Virtual angioscopy was performed with a shaded-surface model without color coding and with a transparent color-coded shaded-surface model.
Results: The hybrid rendering method enables a clear visualization of the pathological changes of the arterial vascular system before and after stent-graft repair by using the advantages of both rendering methods. Complications as leaks and material defects could easily be seen. Virtual angioscopy using a transparent color-coded shaded-surface model enables a faster orientation than a shaded-surface model without color coding.
Conclusions: Hybrid Rendering and virtual angioscopy with a transparent color-coded shaded-surface model support spiral computed tomographic angiography and obviate the need for time consuming detailed analysis and presentation of axial source images.

B-1015 11:45

Gadolinium-enhanced MRA for the diagnosis of thoracic vascular malformations in a very young pediatric population

P.D.H. Gil Agostinho, G. Ramalheiro, P. Gil Agostinho, C. Sanches, E. Castela, F. Caseiro Alves; *Coimbra/PT*

Purpose: To describe the use of contrast-enhanced 3D MR angiography (MRA) for the diagnosis of congenital malformations of thoracic vessels in the infant and newborn child.
Methods and materials: Fourteen patients (4 infants and 10 newborn child) with congenital thoracic vascular malformations were studied on a 1 T MRI unit, using a 3D gradient-echo (GRE) sequence with short TR/TE values, performed in the coronal plane. Image acquisition was started after a fixed delay of 6 seconds from the beginning of a hand injection of a double dose of Gd-DTPA (0.4 ml/kg b.w.) with the childs under general anaesteshia and on spontaneous breathing. The original set of 3 – 4 mm thickness slices were retrospectively reconstructed every 1 – 1.5 mm. Post-processing was performed on an independent diagnostic workstation using the maximum-intensity projection algorithm and volume rendering technique.
Results: Gd-enhanced MRA provided excellent depiction of the thoracic vasculature without any adverse event in all cases. Gd-enhanced MRA allowed the diagnosis of aortic coarctation in three cases, aortic interruption in three, total abnormal venous pulmonary return in one, double aortic arch in one, and measurement of main pulmonary arteries diameter in three cases. Suspicion of aortic coarctation raised by Doppler sonography was ruled out by Gd-enhanced MRA in three other cases.
Conclusion: Gd-enhanced 3D MRA is a reliable tool for the diagnosis of complex thoracic vascular malformations even in the very young pediatric population, potentially avoiding the more invasive intra-arterial DSA.

B-1016 11:55

MR imaging (MRI) and MR angiography (MRA) of abdominal aortic aneurysms (AAA) treated with nitinol based aortic stent-graft: Preliminary results in 10 patients

C. Gervás, M. Blas, J.M. Egaña; *San Sebastian/ES*

Purpose: To describe MRI and MRA findings in patients with AAA treated with nitinol based aortic stent-grafts and compare with other follow up imaging techniques (conventional arteriography and helical CT).
Materials and methods: 10 patients with AAA treated with nitinol based aortic stent-grafts (mean follow up 18 months) were imaged in a 1.5 T MR system. Axial T1w-TSE (TR/TE/Turbo factor, 400/11/5), axial T2w-TSE (TR/TE/Turbo factor, 4800/100/23), 3D gradient-echo gadolinium enhanced in the coronal plane (TR/TE/flip angle, 6.8 ms/2.2 ms/40°), effective slice thickness 2 mm, with MIP and MPR reconstructions. Images were analized by one radiologist, blinded to the results of the helical CT or conventional angiography, for the presence of artifacts related to the stent graft, aneurysmal leaks, aneurysmal remodelling, aneurysmal sac measurements, mural thrombus signal intensity characteristics. Findings were correlated with helical CT, and conventional angiography when available.
Results: Artifacts simulating stenosis at the junction of the iliac limb with aortic body of the stent graft in all cases. Aneurysmal leak was detected in two cases, aneurysmal remodelling in 8. Complete correlation with helical CT and arteriography. Good correlation in the measurements of the aneurysmal sac with helical CT. Partially organized thrombus in all cases.
Conclusion: AAA treated with nitinol based aortic stent-grafts can be imaged effectively with Magnetic Resonance with good results as compared to the established follow up imaging modalities (helical CT and conventional arteriography), which may benefit patients allergic to iodinated contrast material or renal insufficiency. Nevertheless, more patients need to be studied to validate the technique.